

Institut für Organische Chemie und Biochemie
der Technischen Universität München

Design, Parallel Synthesis and Biological Evaluation of Agonists for the G Protein Coupled Human Orphan Receptor BRS-3

Dirk Weber

Vollständiger Abdruck der von der Fakultät für Chemie der Technischen Universität
München zur Erlangung des akademischen Grades eines

Doktors der Naturwissenschaften

genehmigten Dissertation.

Vorsitzender: Univ.-Prof. Dr. St. J. Glaser

Prüfer der Dissertation: 1. Univ.-Prof. Dr. H. Kessler
2. apl. Prof. Dr. L. Moroder
3. Univ.-Prof. Dr. J. Buchner

Die Dissertation wurde am 23.1.2003 bei der Technischen Universität München eingereicht
und durch die Fakultät für Chemie am 7.3.2003 angenommen.

meinen Eltern

Die vorliegende Arbeit wurde am Institut für Organische Chemie und Biochemie der Technischen Universität München in der Zeit von Oktober 1999 bis Januar 2003 unter der Leitung von Prof. Dr. H. Kessler angefertigt.

Mein ganz besonderer Dank gilt Herrn Prof. Kessler für die Überlassung des Themas, das mir entgegengebrachte Vertrauen und die jederzeit vorhandene Unterstützung und Hilfsbereitschaft bei der Anfertigung dieser Arbeit. Darüber hinaus haben insbesondere die sehr gute technische Ausstattung und die große wissenschaftliche Freiheit zum Gelingen dieser Arbeit beigetragen.

Mein weiterer Dank gilt:

- Herrn Dr. J. Antel, der die Kooperation mit Solvay initiierte, und diesem Projekt fortdauernd grosses Interesse entgegenbrachte. Darüber hinaus danke ich ihm für die technische Unterstützung, die ich bei Solvay erfahren durfte.
- Allen Kollegen meines Arbeitskreises für das angenehme Arbeitsklima und die ständige Diskussions- und Hilfsbereitschaft. An die Touren in die Dolomiten denke ich gerne zurück.
- Den Solvay Mitarbeitern des Bereichs PH-FB, Medizinische Chemie und Intellectual Property. Davon insbesondere Frau Dr. Claudia Berger für die gute Zusammenarbeit und die Hilfestellung beim Erlernen des FLIPR-assays sowie Heidrun und Christiane für ihre großartige Unterstützung in der Zellkultur und am FLIPR und für ihren Humor. Weiterhin Dr. Timo Heinrich und Dr. Peter Eickelmann für das Interesse an meiner Arbeit und die Mitarbeit im BRS-3 Projekt. Ausserdem Herrn Reineke und Frau Dr. Mühlebach für die Aufnahme von hochaufgelösten Massenspektren und Frau Dr. K. Larbig für die gute Zusammenarbeit beim Verfassen der Patentschrift.
- Burghard Cordes und Herrn Krause für die professionelle Hilfe bei der Aufnahme von Massenspektren sowie Mona Wolff und meinen Praktikanten Michael, Anna und Denis bei der Unterstützung im Labor. Weiterhin Frau M. Machule und Frau

E. Bruckmaier für ihre Hilfe in bürokratischen Fragen und Dr. R. Haefßner für das Lösen von Software- und Hardwareproblemen.

- Dr. Koka Jayasimhulu (University of Cincinnati, Ohio) für die Aufnahme von hochaufgelösten Massenspektren.
- Judith und Sven für das konstruktive Korrekturlesen dieser Arbeit und Sven für die weiterhin gute, transatlantische Zusammenarbeit.
- Herrn Dr. M. Wiesner (Merck KGaA) für die gute Kooperation auf dem Gebiet der Integrinantagonisten.

Der größte Dank gilt meiner Familie, ganz besonders natürlich meinen Eltern, die mir stets helfend zur Seite standen und mich immer liebevoll begleitet haben. Genauso danke ich Judith für ihre Unterstützung, die schöne Zeit in München und ihrer Aufgeschlossenheit gegenüber der schwäbischen Mentalität.

Table of Contents

1	Introduction and Objective.....	1
2	Strategies in Medicinal Chemistry.....	4
2.1	Medicinal Chemistry in the Context of Drug Discovery.....	4
2.2	Combinatorial Chemistry.....	5
2.3	Origin and Generation of Lead Structures.....	6
2.4	Optimization of Lead Structures.....	9
3	G Protein Coupled Receptors (GPCRs) as Drug Targets.....	12
3.1	Basics about GPCRs.....	12
3.1.1	G Protein Coupled Receptors-Structure and Ligand Binding.....	12
3.1.2	G Proteins.....	16
3.1.3	Interactions of Activated GPCRs and G Proteins.....	18
3.1.4	Signal Transduction Cascades of GPCRs.....	20
3.1.5	Orphan G Protein Coupled Receptors and the Reverse Pharmacological Strategy.....	22
3.1.6	Biological Assays.....	25
3.2	The Orphan Receptor Bombesin Receptor Subtype 3 (BRS-3).....	27
3.2.1	The Bombesin-Like-Peptides and the Bombesin Receptor Family...	27
3.2.2	Peptide Bombesin Receptor Antagonists.....	29
3.2.3	Small Molecule Ligands for Bombesin Receptors and Related GPCRs.....	30
3.2.4	Discovery, Pharmacology and Ligands of the Orphan Receptor BRS-3 – Status Quo.....	33
3.2.5	Binding Sites and Selectivity at Bombesin Receptors.....	34

4	Design, Synthesis and Biological Evaluation of BRS-3 Agonists.....	36
4.1	Introductory Remarks.....	36
4.2	Biological Evaluation of the BRS-3 Agonists.....	36
4.2.1	Intracellular Calcium Measurements with the FLIPR-System.....	36
4.2.2	Characterization of the FLIPR Cell-Assays.....	40
4.3	Linear and Cyclic Peptide BRS-3 Agonists.....	43
4.3.1	General Synthetic Aspects.....	43
4.3.2	Alanine Scans of [D-Phe ⁶ ,β-Ala ¹¹ ,Phe ¹³ ,Nle ¹⁴]Bn(6-14) and [D-Phe ⁶ ,Phe ¹³] Bn(6-13) propylamide.....	46
4.3.2.1	Synthesis.....	46
4.3.2.2	Biological Evaluation.....	47
4.3.3	D-Amino Acid Scans of [D-Phe ⁶ ,β-Ala ¹¹ ,Phe ¹³ ,Nle ¹⁴]Bn(6-14) and [D-Phe ⁶ ,Phe ¹³] Bn(6-13) propylamide.....	51
4.3.4	Shortened Fragments and Substitutions.....	55
4.3.5	Cyclic Analogues of [D-Phe ⁶ ,β-Ala ¹¹ ,Phe ¹³ ,Nle ¹⁴]Bn(6-14).....	59
4.3.5.1	Introduction and Strategy.....	59
4.3.5.2	Synthesis.....	63
4.3.5.3	Biological Evaluation.....	65
4.3.6	Discovery of the Tetrapeptide Lead-Structure.....	67
4.3.7	Systematic SAR of Tetrapeptide Lead.....	68
4.3.8	C-Terminal Optimization.....	70
4.4	Peptidomimetic BRS-3 Agonists.....	72
4.4.1	General Strategy.....	72
4.4.2	Design and Scope of a Small-Molecule Library.....	72
4.4.3	N-Terminal Modification and Gln Substitution.....	77
4.4.3.1	Synthesis.....	77
4.4.3.2	Biological Evaluation.....	81
4.4.4	Probing the Necessity of the N-terminal Amide Bond.....	83
4.4.4.1	Introduction.....	83

4.4.4.2	Synthesis.....	84
4.4.4.3	Biological Evaluation.....	87
4.4.5	Azapeptides as BRS-3 Agonists.....	88
4.4.5.1	Introduction.....	88
4.4.5.2	Synthesis.....	90
4.4.5.3	Biological Evaluation.....	92
4.4.6	Semicarbazones as BRS-3 Agonists.....	93
4.4.6.1	Synthesis.....	93
4.4.6.2	Biological Evaluation.....	94
4.4.7	Semicarbazides as BRS-3 Agonists.....	95
4.4.7.1	Synthesis.....	96
4.4.7.2	Biological Evaluation.....	97
4.4.8	Piperazine- and Piperidine Derivatives.....	98
4.4.8.1	Synthesis.....	98
4.4.8.2	Biological Evaluation.....	99
4.4.9	FLIPR Antagonist Experiment.....	100
4.4.10	Do Peptide- and Small Molecule BRS-3 Agonists bind to different epitopes?.....	100
5	Integrins – An Introduction.....	102
6	Synthesis and Biological Evaluation of $\alpha\beta 3$-Antagonists.....	104
6.1	Previous Work and Objective.....	104
6.2	Synthesis.....	106
6.3	Biological Evaluation and Discussion.....	110
7	Summary	114
8	Experimental.....	118
8.1	Materials for Synthesis and General Methods.....	118

8.2	General Synthetic Methods.....	121
8.2.1	General Methods for Solid-Phase Synthesis.....	121
8.2.2	General Methods for Solution-Phase Synthesis.....	126
8.3	BRS-3 Agonists.....	132
8.3.1	Solution-Phase Synthesis of Building Blocks.....	132
8.3.2	Linear and Cyclic Peptide BRS-3 Agonists.....	161
8.3.3	Peptidomimetic BRS-3 Agonists.....	175
8.4	$\alpha v\beta 3$ Integrin Antagonists.....	209
8.4.1	Solution-Phase Synthesis of Building Blocks.....	209
8.4.2	Peptidomimetic $\alpha v\beta 3$ Integrin Antagonists.....	224
8.5	Biological Evaluation.....	233
8.5.1	Molecular Cloning, Transfection and Cell Culture.....	233
8.5.2	FLIPR (Fluorometric Imaging Plate Reader) Assay.....	234
8.5.3	FLIPR Antagonist Experiment.....	235
9	Literature.....	237
10	Appendix.....	266

Abbreviations

1D, 2D, 3D	one-, two-, three dimensional
7-TM	seven transmembrane helices
Ac	acetyl
ADME	absorption, distribution, metabolism, excretion
ADMET	absorption, distribution, metabolism, excretion, toxicity
ADP	adenosine diphosphate
AMP	adenosine monophosphate
Apa	(<i>R,S</i>)-3-amino-3-phenylpropionic acid
aq.	aqueous
arom	aromatic
ATP	adenosine triphosphate
BB-R ₄	bombesin receptor subtype 4
BLP	bombesin-like peptide
Bn	bombesin
Boc	<i>t</i> butyloxycarbonyl
BOP	Benzotriazole-1-yl-oxy-tris(dimethylamino)- phosphoniumhexafluorophosphate
(h)BRS-3	(human) bombesin receptor subtype 3
bs	broad singlett
c	concentration
°C	degree Celcius
[Ca ²⁺] _i	intracellular calcium
calcd	calculated
cAMP	cyclic AMP
CART	constitutively activating receptor technology
CCD	charge-coupled device
CCK	cholecystokinin
CHO	chinese hamster ovary

CI	chemical ionisation
CoMFA	comparative molecular field analysis
COSY	correlated spectroscopy
cLogP	calculated logarithm of the partition coefficient
CREB	cAMP-response element binding protein
δ	chemical shift
d	dublett/day
dd	double dublett
DAG	<i>sn</i> -1,2-diacylglycerol
DCC	dicyclohexylcarbodiimide
DCE	dichloroethane
decomp	decomposition
DIPEA	diisopropylethyl-amine
DMAP	4-dimethylamino pyridine
DME	dimethoxyethane
DMF	<i>N,N</i> -dimethylformamide
DMSO	dimethyl sulfoxide
EC ₅₀	concentration at which 50% of the maximum effect is reached
ECM	extracellular matrix
EDTA	ethylenediamine tetraaceticacid
EGF	epidermal growth factor
EI	electron ionisation
eq	equivalents
ESI	electrospray ionisation
EST	expressed sequence tag
FAK	focal adhesion kinase
FLIPR	Fluorometric Imaging Plate Reader TM
Fmoc	9-fluorenylmethoxycarbonyl
FMPE	2-(4-formyl-3-methoxyphenoxy)ethyl

FTIR	Fourier transform infrared spectroscopy
g	gram
GABA	γ -amino-butyrlic acid
GC	gas chromatography
GDP	guanosine diphosphate
GFP	green fluorescent protein
GPCR	G protein coupled receptor
G protein	guanine nucleotide-binding protein
GRP	gastrin-releasing peptide
GRP-R	gastrin-releasing peptide receptor
G _t	transducin
GTP	guanosine triphosphate
HATU	2-(1 <i>H</i> -9-azabenzotriazole-1-yl)-1,1,3,3-tetramethyluronium hexafluorophosphate
HEK	human embryonic kidney
HEPES	<i>N</i> 2-hydroxyethylpiperazine- <i>N</i> '2 ethanesulfonic acid
HIV	human immunodeficiency virus
HMQC	heteronuclear multiple quantum coherence
HOAt	<i>N</i> -hydroxy-9-azabenzotriazole
HOBt	<i>N</i> -hydroxybenzotriazole
HPLC	high performance/pressure liquid chromatography
HRMS	high resolution mass spectrometry
hr(s)	hour(s)
HTS	high throughput screening
Hz	Hertz
IC ₅₀	concentration at which 50% of the maximum inhibition is reached
ICAM	intracellular adhesion molecule
Inhib.	Inhibition
Ins(1,4,5) <i>P</i> ₃	Inositol (1,4,5)-triphosphate

<i>J</i>	coupling constant
K	Kelvin
λ	wavelength
LHRH	luteinizing hormone-releasing hormone
m	multiplatt/meter
M	mass/molar
MAPK	mitogen-activated protein kinase
MBHA	4-methylbenzhydrylamine
MCH	melanin-concentrating hormone
MHz	Megahertz
MIDAS	metal ion dependent adhesion site
min	minute
mL	milliliter
mmol	millimole
mp	melting point
MS	mass spectrometry
MW	molecular weight
m/z	mass-charge relation
NCE	new chemical entity
n	number of independent dose response measurements
N	normal
Nle	norleucin
NK	neurokinin
NMB	neuromedin B
NMB-R	neuromedin B receptor
NMP	<i>N</i> -methylpyrrolidinone
NMR	nuclear magnetic resonance
PCR	polymerase chain reaction
PE	polyethylene
pH	<i>pondus Hydrogenii</i>

PIP ₂	phosphatyl inositol 4,5-biphosphate
PKA	protein kinase A
PKC	protein kinase C
PLC β	phospholipase C β
PPA	polyphosphoric acid
ppm	parts per million
Propylamide	n-propylamide
PSI	plexins, semaphorins and integrins
PyBOP	Benzotriazole-1-yl-oxy-tris-pyrrolidino-phosphonium hexafluorophosphate
q	quartett
QSAR	quantitative structure activity relationship
quant	quantitative
R _f	retention factor
RP	reverse phase
rpm	rotations per minute
RSAT	Receptor Selection and Amplification Technology™
s	singlett
SAR	structure activity relationship
SCLC	small cell lung cancer
SEM	standard error of mean
SP	substance P
SPECT	single photon emission computer tomography
SPPS	solid phase peptide synthesis
sst	somatostatin
t	triplett
TBTU	2-(1 <i>H</i> -benzotriazole-1-yl)-1,1,3,3-tetramethyluronium tetrafluoroborate
THF	tetrahydrofurane
<i>t</i> Bu	tertiary butyl

TFA	trifluoroacetic acid
THP-1	human acute monocytic leukemia cell line
TIPS	triisopropylsilane
TLC	thin layer chromatography
TMOF	trimethylorthoformate
TMS	trimethylsilane
TOF	time of flight
t_R	retention time
UV/Vis	ultraviolet/visible
v/v	volume by volume
w/v	weight by volume

The nomenclature used in this work is based on the guidelines recommended by *Chemical Abstracts* (Chemical Abstracts, 'Index Guide', 77, 210) and the IUPAC-IUB commissions (IUPAC, *Eur. J. Biochem.* **1971**, *21*, 455-477; IUPAC, *Pure Appl. Chem.* **1996**, *68*, 1919; IUPAC Commission on Nomenclature of Organic Chemistry (CNOC) and IUPAC-IUB Joint Commission on Biochemical Nomenclature (JCBN), *Biochemistry* **1974**, *10*, 3983; IUPAC-IUB (JCBN), *Eur. J. Biochem.* **1984**, *138*, 9-37). Expressions derived from the latin language, names of companies and commercial names of products are written in *italic*.

1 Introduction and Objective

Today, our concept to treat physiological disorder (*i.e.* disease) mainly relies on the drug receptor theory (chapter 3.1.5) and Fischer's 'lock and key' theory,^[1] which developed into 'induced fit'. In other words, certain proteins – in many cases these are membrane receptors –, identified as being one element in a signal transduction process on a cellular level, are sought to be manipulated, preferably with small molecules, because they have the potential to be orally administrable.

In recent years, the increasing amount of biological and biochemical knowledge concerning sequence, structure and function of biopolymers and biochemical processes has provided an abundance of new potential targets to the field of drug discovery.^[2] Especially the enormous progress in the analytical techniques such as X-ray crystallography, NMR and mass spectrometry, which are able to produce structural information, and besides this, PCR-based cloning technologies and the sequencing of the (human) genome have contributed a lot to this development. The latter produced the field called functional genomics, which is the search for the physiological role of a gene for which only its primary sequence is known, and it has revolutionized pharmacological research (chapter 3.1.5).

Unfortunately, much of the obtained knowledge can still be considered as 'raw data'. So far, it did not substantially translate into 1) an enhanced understanding of complex pathophysiological processes, which mainly boils down to the understanding of protein/protein-, peptide/protein- and nucleic acid/protein interactions and 2) an increase of productivity in the drug discovery process (chapter 2.1). An important task to be solved remains to find ways to reasonably process, interpret and understand the acquired information in order to be able to identify 'drugable' targets. This and other reasons (chapter 2.1), have forced the drug discovery process to develop into a very complex research and business area and to become one of the major driving forces for the combination of the classical research disciplines, namely chemistry, biology, pharmacology, medicine and even physics.

Organic chemistry (chapter 2.1 and 2.2) is a helpful tool within this process of understanding, because it can give useful insights into the function of proteins by

providing a (large) number of differently designed molecules, which may interact with them. This work is a contribution to the ongoing attempt in medicinal chemistry to acquire information about the physiological role of receptors through the elaboration of structure activity relationships concerning their ligands.

In October 1999, a cooperation between Prof. Kessler (*TU München*) and *Solvay Pharmaceuticals GmbH* (Hannover) on the G protein coupled bombesin receptor subtype 3 (BRS-3) was initiated. BRS-3 is a product of genomic research belonging to the class of so-called ‘orphan receptors’ with yet unclear physiological role (chapter 3.1.5 and 3.2.1). It became of interest to the pharmaceutical industry because the knock-out mouse model was pointing towards an involvement in obesity (chapter 3.2.4).

The starting point for this work are structure activity relationship studies on the – at that time - only known high affinity BRS-3 agonists, which are two bombesin-derived peptides – octapeptide [D-Phe⁶,Phe¹³]Bn(6-13) propylamide and the non-selective high affinity nonapeptide [D-Phe⁶,β-Ala¹¹,Phe¹³,Nle¹⁴]Bn(6-14) (chapter 3.2.4). Although these peptides allowed previously conducted receptor pharmacology studies in cell lines expressing the cloned BRS-3 receptor, they did not prove useful for *in vivo* studies. Therefore, the final goal is to obtain useful tool-substances, preferably proteolytically more stable, potent and selective small molecules, which may help to elucidate the possible role of BRS-3 in obesity and cancer. Biological evaluation of the alanine and D-amino acid scan analogues of these peptides is carried out using their ability to mobilize intracellular calcium in BRS-3 transfected CHO α -16 cells in a Fluorometric Imaging Plate Reader (FLIPR) assay (chapter 4.2.1) combined with receptor binding studies.

In the second step, with the initial structure activity relationship (SAR) information in hand, different strategies, such as N- and C-terminal deletions (chapter 4.3.4), cyclization (chapter 4.3.5), and attaching the identified pharmacophores onto a small peptide scaffold (chapter 2.3 and 4.3.6), are applied. If these techniques would render a small molecule lead structure, systematic optimization should be possible in repeated steps comprising synthesis followed by biological evaluation. Finally, such a

lead structure should be useful for the design and parallel synthesis of compounds for 'biased libraries', pursuing the goal to obtain potent and selective small molecules.

The second and smaller part of this thesis is a continuation of G. Sulyok's work in cooperation with *Merck KGaA* (Darmstadt) on small molecule $\alpha v \beta 3$ antagonists mimicking the RGD sequence, which have been demonstrated to possess enhanced pharmacokinetic properties. A series of small molecule azapeptides bearing large aromatic systems, heteroaromatics and arylethers in the 3-position of glutaric acid, which serves as Asp mimetic, is synthesized and evaluated. Furthermore, the effect of incorporating a cyclic constrained β -amino acid as replacement for aspartic acid on the binding affinity will be investigated.

2 Strategies in Medicinal Chemistry

2.1 Medicinal Chemistry in the Context of Drug Discovery

The science of medicinal chemistry deals with the finding, identification, characterization, synthesis and optimization of chemical compounds, which are potential drug candidates. Medicinal chemistry therefore represents an important element in the process of modern drug discovery (Figure 2.1).



Figure 2.1: Schematic depiction of the drug discovery process. Medicinal chemistry is involved in lead generation and optimization.

In the last 10 years the prevailing paradigm in drug discovery was the attempt to overcome the lack of understanding complex biological systems with a massive use of high technology, which should enable universal and complete trial and error. This has changed medicinal chemistry, which used to be solely dominated by organic synthesis in former days. Today, the focus lies on the rapid, technology-supported identification – *in silico* and/or via synthesis - of new promising leads, their optimization and the provision of sufficient amounts thereof for biological testing. However despite the existence of high throughput technologies, an ever increasing speed of data processing and the huge amount of available information today, the number of new chemical entities (NCEs) is on a constant decline.^[3] The reasons for this can be found in the required high safety standards for drugs, which cause a high failure rate of drug candidates and the high existing therapeutic standards, making it difficult and often extremely costly to improve already established drugs or therapies. Moreover, despite all the high technologies available today, many steps in the overall process of drug discovery are still not predictable but instead mainly driven by serendipity.

Nevertheless, or perhaps because of this, the pharmaceutical market is extremely interesting and profitable.

The following chapters will give a very brief overview over the important issues concerning the complex field of medicinal chemistry and its tools with an emphasis on those being relevant for the design of BRS-3 agonists (chapter 4).

2.2 Combinatorial Chemistry

Combinatorial chemistry has become an important tool for medicinal chemists, because different strategies allow the rapid synthesis of large numbers of compounds. Advances in combinatorial chemistry have always been closely related with the progress in solid phase synthesis (chapter 4.3.1).^[4]

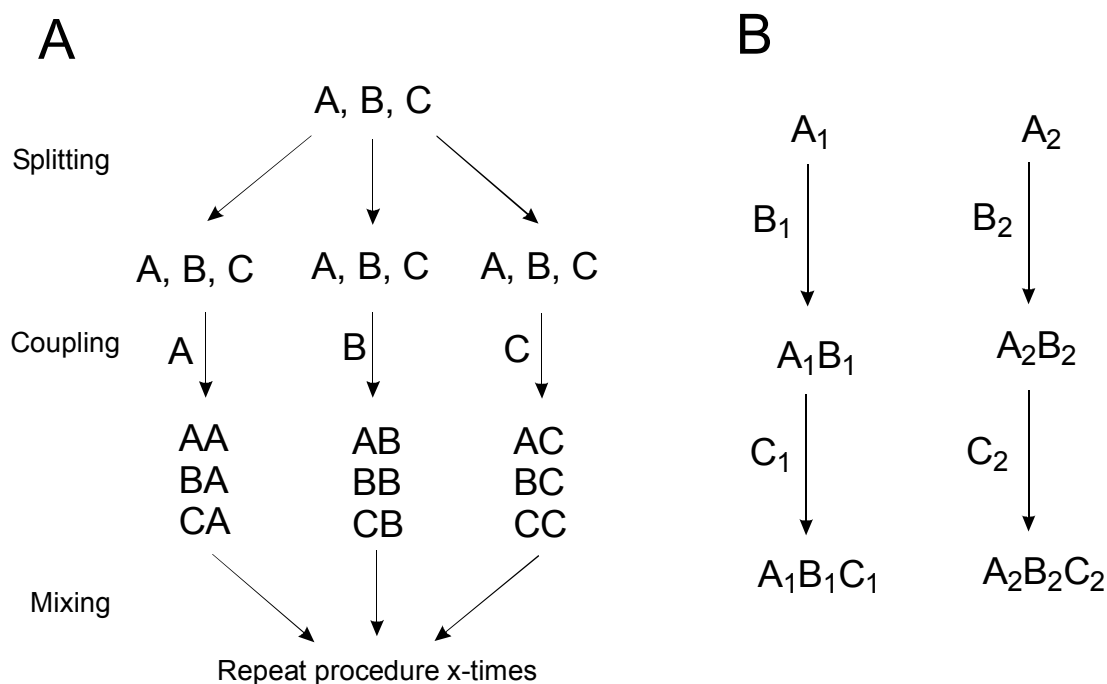


Figure 2.2: A) Single step of the 'split-mix' approach, which includes splitting, coupling and mixing. B) Parallel synthesis of two compounds in distinct reaction vessels employing similar monomers. A, B and C are monomers.

The ‘split-mix’ approach has been introduced by Furka in the early 1980s,^[5,6] Houghten *et al.* have used a similar method employing tea bags (Figure 2.2).^[7,8] A single step of this strategy comprises splitting of the solid support (polymer resin) into N equal parts (N is the number of employed monomers), coupling of each monomer to one of the created fractions and finally mixing of the divided parts. If this whole process is repeated x -times, the possible number of theoretically obtainable compounds is N^x . This approach leads to compound-mixtures, which, after biological screening, have to be deconvoluted, *i.e.* potential active compounds have to be identified. The ‘one-bead-one-compound’ concept followed from the realization that the ‘split-mix’ method generates only one distinct type of compound on each resin-bead.^[9] For large libraries a 3-fold excess of beads vs. possible compounds is necessary in order to ensure that 95% of all possible molecules are present.^[10] Biological evaluation of the compounds may be carried out ‘on bead’ using antibodies, which induce a coloring of the beads.^[11] The following techniques may be used for the identification of the ‘active’ compound: Sequencing, mass spectrometry,^[12] or tagging.^[13,14]

Different from the ‘split-mix’ approach the parallel synthesis strategy uses the combinatorial coupling of building blocks to generate single compounds in distinct reaction vessels (Figure 2.2). Although this strategy is not suitable for the synthesis of extremely large numbers of compounds, it has, compared to the synthesis of compound-mixtures, the advantages that deconvolution is not required and biological evaluation of single compounds is possible. Geysen *et al.* were the first to realize parallel peptide synthesis on polymer-coated pins.^[15,16] The recent development of resin bound reagents for organic synthesis is expected to have an impact on the synthesis of combinatorial libraries.^[17]

2.3 Origin and Generation of Lead Structures

Many drugs are derived from natural products, obtained from plants, animals and their poisons or microorganisms in an overwhelming structural diversity. However only

relatively few compounds directly became drugs, such as morphine, digitoxin, or cyclosporin,^[18] because the original compounds either had severe side effects, low bioavailability, or an antagonist was needed instead of an agonist (or vice versa). In most cases, natural products serve as a lead structure. Prominent examples for this are the antibiotic tetracyclin,^[19] the macrolides epothilone^[20] and taxol,^[21] or the dolastatin peptides,^[22] modified derivatives of which are used in cancer therapy.

Besides natural products, synthetic compounds are an important source for lead structures. Although the screening of large compound collections is not a new idea – a prominent example are Domagks' sulfonamides^[23] - the advent of the high throughput screening (HTS) technology in the 1990s revolutionized the search for lead compounds. Today, the 'ultra' HTS (uHTS) technology, based on the 1536-well plate format, allows the screening of about 100.000 compounds per day.^[24] This technology has been complemented by the combinatorial/parallel and rapid synthesis of large numbers of compounds (chapter 2.2).

As a contrast to the above-described random search, the so-called *de novo design* is purely knowledge-based.^[18] In this approach, molecules with a known (crystal)structure are 'docked' to the binding pocket of the target protein - with known 3D structure. A second, more challenging possibility is the stepwise 'building' of protein ligands. Rational design has been most successful for inhibiting enzymes - serine-, aspartyl- or metalloproteases – prominent examples for this are renin,^[25,26] or HIV-protease.^[27,28] However, this approach mainly remained limited to enzymes, because of the unavailability of 3D structures and reliable models of more complex proteins such as transmembrane receptors.^[29,30]

The so far described methods may be seen as the 'extreme' strategies for lead-finding, both having their successes and limitations. Therefore, nowadays strategies which try to combine both type of elements, random and rational search, are gaining attraction in medicinal chemistry.^[31]

Several strategies use neuropeptides as a starting point for the generation of small molecule leads. If the solution structure of a peptide is available, a 3D pharmacophore model can be generated. Then, in a virtual screening procedure, molecules with a similar 3D arrangement of identical or isosteric functional groups can be identified as

lead structures. This method has been successfully used for the identification of non-peptide small molecules as lead structures using cyclic peptides as a starting point (see also chapter 3.2.3).^[32-34]

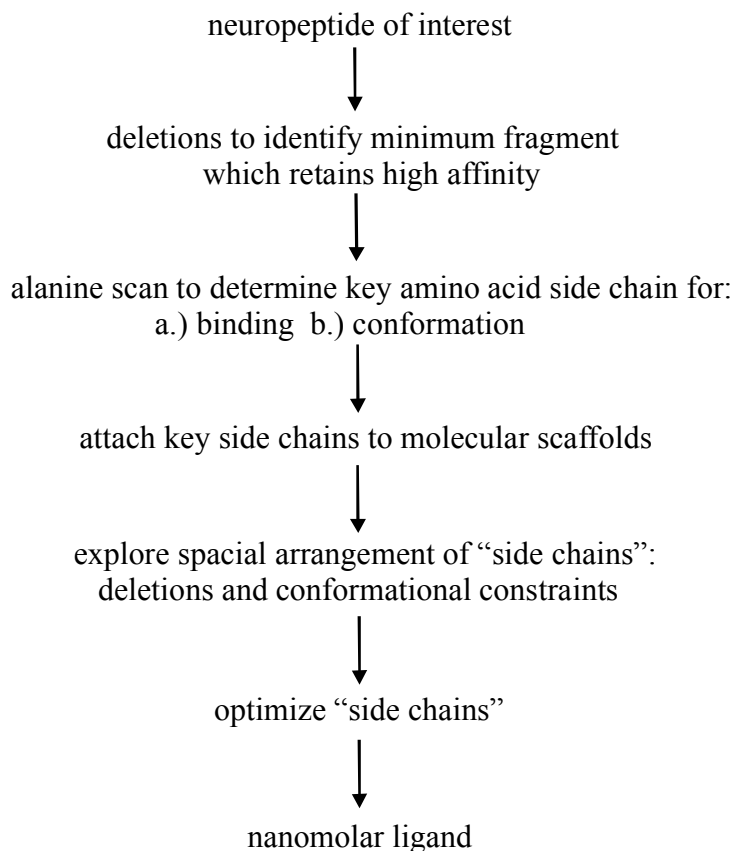


Figure 2.3: 'Peptoid' design strategy (Horwell, Howson, Rees, 1988).

Researchers at *Parke-Davis* (Cambridge, UK) developed the so-called 'peptoid design strategy' (described in Figure 2.3) as a method to design low molecular weight ligands using the chemical structure of mammalian neuropeptides as a starting point^[35,36] - the term 'peptoid' is used here, differently as in chapter 4.4.4, in the sense of 'a small molecule topographical analogue of a peptide'.^[37] This strategy is based on the 'three ligand hypothesis' by Schwyzer, Ariens and Farmer (1980).^[37-39] They argued that since a nanomolar binding affinity is represented by a binding energy of approximately $12.6 \text{ kcal.mol}^{-1}$ (Gibbs-Helmholtz equation), this could be achieved by only three appropriately orientated amino acid side-chains. Therefore, it is possible to attach the pharmacophores, which are assumed to have a certain spatial proximity, onto a molecular scaffold of small size.

Moreover, the evaluation and classification of common drug shapes^[40] has led to the identification of so-called ‘privileged scaffolds’ for specific classes of target proteins. These scaffolds represent common motives repeatedly found in known ligands, and constitute a possible starting point for the design of new libraries.^[41,42] In case of GPCRs 4-phenyl-piperazine was the most frequently occurring fragment.^[43]

2.4 Optimization of Lead Structures

In many cases a new drug has to combine many features exceeding efficacy, such as selectivity, low toxicity of the drug and its metabolites. Furthermore, oral administration is desirable and distribution/excretion parameters should be such that the drug has to be administered not more than once a day. These aspects are mainly determined by the pharmacokinetic properties of a compound, also known as ADME-parameters (absorption, distribution, metabolism, excretion).^[44] Very often toxicity is included in the term (\rightarrow ADMET), because these issues together are intensely investigated before and during the clinical phases I and II of a promising candidate. Due to the high costs of these studies and ethical aspects, they can only be carried out for a few selected compounds. Increasing attempts are made to use simple models, such as an absorption test using Caco-2 cells, toxicity tests (*e.g.* ATP measurements, enzyme release), or *in vitro* metabolism assays using liver microsomes or hepatocytes, in order to determine and predict these characteristics of a compound as soon as possible (known as ‘early ADME’ or eADME).^[45-47]

Semi-empirical methods enable a rough prediction whether compounds can be classified as so-called ‘druglike molecules’. An important parameter of a compound influencing the above-mentioned properties, especially relating to absorption, is lipophilicity. The biologically active molecule, after oral administration, needs to sufficiently dissolve in an aqueous solution (*e.g.* in the stomach, blood) and pass several lipophilic cell membranes until it reaches its target tissue. Corwin Hansch

developed a model simulating these processes.^[48] Thereby the partition coefficient P between 1-octanol and water serves as criterion for the lipophilicity of a compound:

$$P = \frac{[\text{compound}]_{\text{octanole}}}{[\text{compound}]_{\text{water}} \cdot (1 - \alpha)} \quad \alpha : \text{dissociation constant in water}$$

Because most contributions from fractions of larger molecules add up in a linear fashion in this model, the lipophilicity, which is presented as the $\log P$, of any desired molecule can be calculated (\rightarrow $c\text{LogP}$) using computer programs.^[49] Depending on the mode of action of a specific drug most cases require a bivalent character with respect to lipophilicity, because too lipophilic compounds will be easily resorbed but are quickly eliminated (first pass effect), too polar compounds will not be able to pass membranes.

The relation between lipophilicity, the number of H-bond donors and -acceptors, and molecular weight and the absorption- and permeability properties was finally summarized by Lipinski *et al.*,^[50] who analyzed 2245 compounds out of a 50.000 compound database, having superior physico-chemical properties - they managed to enter clinical phase II. Based on this analysis, a practical 'rule of five' was set up, which states that poor absorption and permeability are likely, when:

- $c\text{LogP} > 5$,
- the molecular weight > 500 g/mol,
- the number of H-bond donors (sum of NHs and OHs) > 5 ,
- the number of H-bond acceptors (sum of Ns and Os) > 10 ,
- compounds, that are substrates for biological transporters are an exception of this rule.

A very recently published evaluation of 1100 drug candidates at *GlaxoSmithKline* suggests that a high oral bioavailability in rats can be attributed to a reduced molecular flexibility, as measured by the number of rotatable bonds, and a low polar surface area.^[51] Although these latter rules do not allow a quantitative prediction either, they

offer a more sophisticated solution to the problem because now higher molecular weights can be tolerated, if rigidity is sufficient. Taken together, these rules are important for the optimization process of lead compounds because the borders between pharmacokinetics and pharmacodynamics, which is the interaction of the compound with its target, are fuzzy and the first is clearly influenced by the latter.

Optimization of these processes is pursued via structural modifications of the lead compound, as being realized in the synthesis of ‘focused’ or ‘biased libraries’. The evaluation of such a series of compounds leads to a SAR model. A statistical – *i.e.* quantitative – computer-based SAR (\rightarrow QSAR) model can guide or dominate this optimization process and may allow predictions concerning biological activity and bioavailability.^[52,53] Early QSAR models were mainly limited to explaining in the retrospective. More powerful are 3D-QSAR methods such as the comparative molecular field analysis (CoMFA), which correlates the electronic and steric field environment of a compound with its biological activity.^[43,54]

There are a lot of plausible structural modifications, including the bioisosteric replacement of functional groups through residues with similar biological properties (due to a similar electronic distribution), *e.g.* the exchange of hydrogen by fluorine, or the carboxylic acid by tetrazole. Furthermore, the variation of spacer lengths and substitution patterns, *e.g.* of aromatic systems, or the incorporation of conformational constraints, such as the insertion of alkyl chains at the C $^{\alpha}$ or cyclization (see also chapter 4.3.5). Whereas the pharmacophore groups of a lead structure usually react very sensitively against changes, other moieties may be variable. Therefore, the simple removal of residues from lead structures is an important further option. Insertion of new groups, as outlined above, is also possible. As a rule of thumb the attachment of additional polar groups is often unsuccessful. Better results are usually obtained with properly placed additionally lipophilic groups, which optimize the steric fit of the molecule in the binding pocket.

3 G Protein Coupled Receptors (GPCRs) as Drug Targets

3.1 Basics about GPCRs

G protein coupled receptors (GPCRs) represent a large superfamily of membrane proteins, which share a conserved structure composed of seven transmembrane helices (7-TM). Despite of their structural homology, a number of diverse ligands for GPCRs are known. They include peptide hormones such as bradykinin, bombesin, angiotensin, somatostatin and endothelin, biogenic (catechol)amines, which can also serve as neurotransmitters, such as epinephrine (adrenaline), dopamine, serotonin, and furthermore nucleosides and nucleotides, lipids, eicosanoids and others such as glutamate and Ca^{2+} .^[43,55] Because of their central role in cell-cell communication, GPCRs are important targets for the modulation of pathophysiological processes.

Today, GPCRs represent the largest and single most important class of all drug targets.^[56] Currently, worldwide more than 50% of all drugs are GPCR based and their annual sales exceeded 30 billion US\$ in 2001.^[57] Among the 100 top-selling drugs 25% are targeted against GPCRs. Due to this proven track of being excellent drug targets, it is commonly assumed that orphan GPCRs, which emerged from genomic research, will offer a similar aptitude in the future.^[58-60] About 1-3% of the human genome encode approximately 1000 GPCRs, a number, which, until recently, was predicted to be much larger.^[61,62] Excluding sensory (olfactory) receptors, there are presently about 200 receptors which are categorized as ‘known’ GPCRs to be activated by some 70 identified ligands, and about 100-150 orphan GPCRs with unknown ligand(s) and physiological role (see chapter 3.1.5).^[55,60,63]

3.1.1 G Protein Coupled Receptors – Structure and Ligand Binding

Despite their topological homology, mammalian GPCRs are grouped into three major families, based on their structural differences:^[64]

- Family A: The rhodopsin- or adrenergic-like receptors. This group is by far the largest. Its characteristics are a short N-terminal tail and some 20 highly conserved amino acids in the transmembrane receptor core.
- Family B: This small group of secretin- or glucagon-like receptors displays a longer N-terminal tail with six highly conserved cysteine residues.^[65]
- Family C: The metabotropic glutamate-like receptors share a very long N-terminal domain (500-600 residues), which is involved in glutamate, GABA or calcium binding.^[55,66,67]

Rhodopsin constitutes a special case among GPCRs because its ligand, the inverse agonist 11-*cis*-retinal, covalently bound by a Schiff's base to the amino group of Lys²⁹⁶ in helix 7 of the opsin, is uniquely activated by photons, which cause isomerization to all-*trans*-retinal.^[68] Nevertheless, it currently serves as a general model for GPCRs.^[29,43,69] The first high resolution structure of a prototype GPCR, which became available in 2000 with the successful crystallization of the inactivated form of bovine rhodopsin,^[29,30,70,71] shows, as expected,^[72,73] the overall structure to be dominated by seven counterclockwise oriented (as seen from the extracellular side), normally transmembrane located helices, an N-terminal extracellular and a C-terminal cytoplasmic domain (Figure 3.1). The most striking, newly found features were that 1) the helices are kinked at Pro residues located roughly around the binding site of 11-*cis* retinal, and that 2) the fourth cytoplasmic loop, which is formed through anchoring the C-terminal domain to the membrane with palmitoylated cysteins, contains a small amphiphilic helix (VIII in Figure 3.1 A), lying almost parallel to the membrane.^[29] This helix is thought to be involved in the rhodopsin-transducin interactions (see chapter 3.1.3).^[74-76] Helices 2, 3, 5 and 6 are more hydrophilic than helices 1, 4, and 7 and are therefore located towards the transmembrane core of the receptor, whereas the latter can be found peripherally.^[77-79] The extracellular domain of rhodopsin is comprised of three loops (Figure 3.1). While loops 1 and 2 are both along the periphery of the molecule, loop 2 displays some unique features: It contains two β strands, is attached to helix 3 through a disulfide bond, and deeply folds into the center of rhodopsin, thus contributing to the retinal binding pocket by forming a

lid.^[29,30] Two out of the three cytoplasmic loops of rhodopsin in the crystal structure, namely C2 and C3, which are thought to be involved in G protein interaction (see chapter 3.1.3), could not be resolved due to their flexibility.^[30]

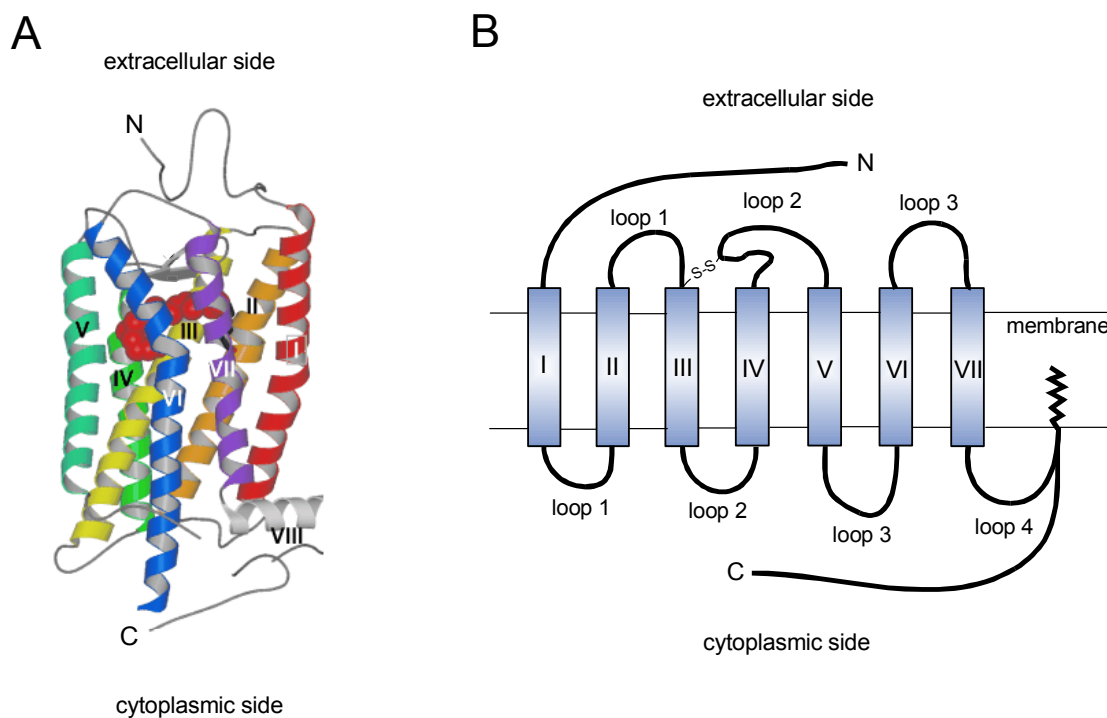


Figure 3.1: (A) Ribbon drawing of the 2.8 Å crystal structure of bovine rhodopsin^[29] showing 11-cis-retinal in red and a counterclockwise arrangement of the 7-TM helices. (B) Schematic secondary structure representation of a transmembrane GPCR. The palmitoylated C-terminal segment forms a fourth cytoplasmic loop, the disulfide bond between Cys¹¹⁰ and Cys¹⁸⁷ is conserved among most GPCRs.

As can be seen from the crystal structure, the retinal is buried deeply into the transmembrane core.^[29,30] A similar observation has been made in general for small molecule ligands of GPCRs, which are found to preferentially bind to the 7-TM region.^[55] Binding of catecholamine was studied in case of the β -adrenergic receptor and is thought to involve helices 3, 5, 6 and 7. Residues, which take part in the interactions include two serines, namely Ser²⁰⁴ and Ser²⁰⁷ on helix 5, Asp¹¹³ on helix 3, and several Phe moieties on helix 6 and 7, perhaps responsible for π -stacking.^[80-82] This binding mode can be interpreted as more or less generally valid for the

interaction between biogenic amine agonists and GPCRs, because a conserved involvement of Asp¹¹³ located on transmembrane helix 3 was observed for several biogenic amines- (*e.g.* β -adrenergic-, angiotensin-receptor) and peptide binding GPCRs (*e.g.* urotensin II-, somatostatin-, melanocyte concentrating hormone receptors).^[43] In this model Asp¹¹³ forms a salt bridge with the basic amine nitrogen. Moreover, other small ligands, *e.g.* adenosine/ATP as agonists for the purinergic receptors, or spiroperidines as agonists for the chemokine receptors, have been found to bind to the transmembrane cleft in comparable fashion as biogenic amines or retinal.^[83-85]

Based on this similar binding mode for a large number of different small ligands, it would be reasonable to speculate about a common binding pocket for all agonists. However, this greatly oversimplifies the picture,^[86] because early results from mutational mapping experiments showed, that certain peptide agonists most likely do not penetrate the transmembrane pocket but instead bind to peripheral sites.^[87-90] Furthermore, antibodies directed against extracellular loops were found to be able to activate GPCRs.^[91] In order to be able to give a possible explanation for this phenomenon, the originally developed ternary complex model,^[92] which assumes cooperative interaction among receptor, G protein and agonist, had to be extended.^[93,94] Based on the original postulation of a steady equilibrium of receptors being in the active and the inactive state by Costa and Herz,^[95] net activation of the receptor can be achieved by shifting this equilibrium through stabilization of the active state(s) caused by ligand binding, even to peripheral domains. Today, allosteric action of – even small molecule - agonists at GPCRs is widely recognized.^[96-102] However, the presence of a ligand is not necessarily a prerequisite for receptor activation. This concept was validated by experiments, which showed that mutations on extracellular loops produced an active conformation of the receptor.^[103,104] Moreover, it explains the mechanism of inverse agonism^[105] and has led to the generation of constitutively activated receptors, which may lead to a better understanding of the detailed mechanism of the action of currently used drugs or even to the discovery of ligands with high efficacy, which were not detectable by conventional drug screening methods before.^[94,104,106]

In general, it is thought, that ligand binding causes disruption of a stabilizing network of intramolecular interactions, which constrain the receptor in its inactive state.^[107,108] This leads to a conformational change of the receptor, and in the special case of rhodopsin, it was possible to dissect these conformational changes that follow photoinduced ligand activation into a series of activated states, namely bathorhodopsin, lumirhodopsin, and meta-states I and II using UV/Vis and FTIR spectroscopy.^[68] However, similar models for other GPCRs could not be obtained.^[107] At present, little is known about the formation of GPCR dimers/oligomers and their potential role in receptor activation.^[107,109,110] It is assumed, that the oligomerization of receptors may have a similar importance for signal amplification as it is known for G proteins.^[110] One of the most important observations indicating (hetero-) oligomerization came from the metabotropic γ -aminobutyric acid (GABA) receptor. So far, the concept of receptor oligomerization had little impact on the design of assays or multivalent ligands or new therapies.^[110]

3.1.2 G Proteins

Signal transduction of the GPCRs is mediated through heterotrimeric guanine nucleotide-binding proteins (G proteins).^[111,112] G proteins are made up of α , β , and γ subunits. Although there are many gene products which encode these subunits (20 α , 6 β and 12 γ gene products are known),^[112] only four main classes of G proteins are distinguished on the basis of their α -subunits due to sequence homology,^[111,113] and because these subgroups use similar second messenger pathways (see chapter 3.1.4):

- The G_q family comprises five members, namely $G\alpha_q$, $G\alpha_{11}$, $G\alpha_{14}$, $G\alpha_{15}$, and $G\alpha_{16}$, which activate phospholipase C β (PLC β).
- The G_s family ('s' stands for 'stimulatory') and the G_i family ('i' stands for 'inhibitory') stimulate or inhibit adenylate cyclase.
- G_{12} and G_{13} .^[113] Currently, little information is available about their function.^[112]

G α 15 and G α 16^[114] have received considerable attention in pharmaceutical research, especially concerning orphan receptor research, because – unlike other G α_q family members – they are able to link to a great variety of natively G $_s$ -, G $_i$ - and G $_q$ -coupled receptors^[115] and stimulate PLC β with subsequent Ca²⁺ release, which enables screening analysis using the FLIPR-technology^[116] (see chapter 3.1.6 and 4.2.1). Although G α 16 is still the most versatile known G protein,^[117] engineered chimeric G proteins are thought to substitute G α 16 in cases where coupling to the PLC β pathway fails.^[117-120] Chimeras based on the G α_q backbone with a C-terminal sequence of G α_i , and an N-terminal shortened sequence with an attached myristic acid, have proved to be more efficient in coupling G $_i$ -linked receptors (*e.g.* the somatostatin receptor) to the phospholipase C β (PLC β) pathway than G α 16 and therefore enable detection using the FLIPR-assay.^[117]

In 1996, the first crystal structure of a heterotrimeric G protein, the G $_t$ was solved with bound GDP and in absence of the receptor.^[121] The G α_t subunit has three distinct structural components:^[121]

- A Ras-like GTPase domain consisting of a six-stranded β -sheet surrounded by six helices. This GTPase domain hydrolyzes bound GTP after activation of the G protein and returns it to the inactive form.^[122]
- An entirely α helical domain consisting of a long central helix surrounded by five smaller helices.
- An N-terminal α helix that projects away from the remainder G α_t subunit.

The guanine nucleotide binds in a deep cleft between the GTPase and a helical domain. The G β_t unit starts with an N-terminal helix, and further comprises seven β -sheets with four antiparallel strands each, aligned in a propeller-like structure. The G γ_t unit consists of two helices but contains no inherent tertiary structure.

Interactions between the G α_t and the G $\beta\gamma_t$ subunits occur at two distinct locations, termed the ‘switch-interface’ and the ‘N-terminal interface’. Hereby, the α subunit has

no direct contact to the γ subunit. A comparison to previous crystal structures separately obtained for the α subunit^[123] and the $\beta\gamma$ dimer^[124] shows, that binding of $G\alpha_t$ to $G\beta\gamma_t$ results in a dramatic structural reorganization at the contact sites of the α subunit, however no significant changes on the $\beta\gamma$ unit are observed.

3.1.3 Interactions of Activated GPCRs and G Proteins

A conformational change of the receptor leads to an activation of the G protein. This causes the exchange of guanosine triphosphate (GTP) for bound guanosine diphosphate (GDP) at the α subunit, leading to the dissociation of the heterotrimer into a $G\alpha$ -GTP- and a $G\beta\gamma$ -unit,^[125-128] which triggers further signal transduction using downstream effectors^[112] as described in the following chapter.

As rhodopsin for the GPCRs, the interaction between rhodopsin and transducin (G_i) is thought to serve as a model for the understanding of the signal transduction from GPCRs to G proteins.^[68,129] Although high resolution X-ray structures are available for each single unit, the GDP bound transducin crystallized in the absence of rhodopsin^[121] and dark-state rhodopsin,^[29,30,70,71] the interactions between rhodopsin and transducin and the molecular mechanism of the catalyzed GDP release are still not understood,^[68] also because information about the complex is limited.^[74]

The particularly important role of the extreme C-terminus of the G protein^[130,131] for the receptor/G protein-interface has early been expected since the pertussis toxin-catalyzed ADP-ribosylation of a Cys, which is conserved among the G_i family and four amino acids away from its C-terminus, causes disruption of this interaction.^[120,132] This initial insight has been supported by numerous subsequent studies, which include C-terminal mutations in the α subunit of G proteins^[133,134] the generation of C-terminally chimeric G proteins,^[117,118] and the inhibition of the GPCR–G protein interactions by antibodies developed against C-terminal sequences.^[135-137] Furthermore, binding of peptides, namely one mimicking the 11 C-terminal amino acids of $G\alpha_t$ ^[138] and two peptides corresponding to C-terminal residues

of the γ subunit of G_t ^[74,139] were found to block rhodopsin/transducin interactions while stabilizing the excited meta II state of rhodopsin. Based on these results the binding of G_t to rhodopsin was roughly explained by a two-site sequential fit mechanism.^[140] NMR spectroscopical studies of the C-terminally undecapeptide $G\alpha_i(340-350)$ yielded an almost ideal α -helical conformation with an α_L -type C-capping motif in the bound state.^[129,141-144] This region was found to be unstructured in the crystal structure (unbound state).^[121] Rhodopsin/transducin complexes have also been studied by FTIR spectroscopy.^[145-147]

Out of the four loops C1-C4, which together with the carboxyl-terminal tail comprise the cytoplasmic surface of rhodopsin (Figure 3.1), three are thought to be involved in the interactions with G_t , namely C2, C3^[148] and C4.^[74-76] In case of the M_2 muscarinic receptor, the critical residues for recognizing the C-terminal end of the chimeric $G_{i/o}$ were determined in mutagenesis studies^[149] as Val³⁸⁵, Thr³⁸⁶, Ile³⁸⁹ and Leu³⁹⁰.

3.1.4 Signal Transduction Cascades of GPCRs

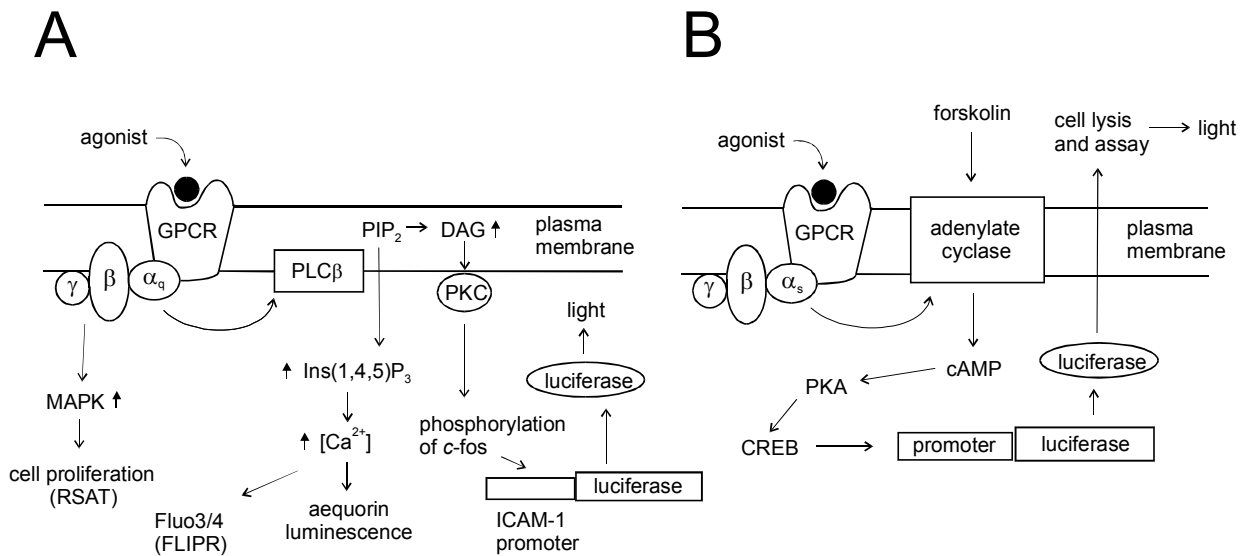


Figure 3.2: Pathways and detection possibilities of the GPCR signalling through $G\alpha_q$ via PLC- β activation (A) and through $G\alpha_s$ (or $G\alpha_i$, not shown) via activation of adenylyl cyclase (B). For details see text.

The translation of the extracellular stimulus into a biochemical intracellular signal following G protein activation and the possibilities to detect this event in a dose-dependent manner are depicted in Figure 3.2 and described in the following. Depending on the nature of the receptor and G protein, two different major pathways can be observed.^[112,120,122]

- The phosphoinositide cascade (Figure 3.2, A).^[150-52] The $G\alpha_q$ subunit, which is formed during dissociation of G_q activates the isoform 1 of PLC β , which catalyzes the cleavage of phosphatidyl inositol 4,5-bisphosphate (PIP₂) into the two separate messengers inositol (1,4,5)-triphosphate [Ins(1,4,5)P₃] and *sn*-1,2-diacylglycerol (DAG). The first one causes a rapid release of Ca²⁺ from intracellular stores such as the endoplasmic reticulum, which is used as a quantitative readout for receptor activation. The latter activates protein kinase C (PKC), which relays activation of

transcription factors, promotor based recognition elements and finally reporter gene translation. The gene product can be used as quantitative assay readout.

- The cAMP cascade (Figure 3.2, B):^[153,154] Release of the α subunit from G_s activates the membrane bound adenylate cyclase, which leads to a conversion of ATP to cyclic AMP. The second messenger cAMP activates protein kinase A (PKA), which consists of two catalytic and two regulatory chains and is inactive in absence of cAMP. Binding of cAMP to the regulatory units releases the catalytic chains, which then phosphorylate specific serine and threonine residues in target proteins. Among others, a possible target is the cAMP-response element binding protein (CREB), which in case of activation leads to an increase in the transcription of genes (*e.g.* firefly luciferase) with the CRE within their promotor sequence. As for the phosphoinositide cascade, the gene products can be used as assay readout. If the associated protein is G_i , the inhibition of the forskolin mediated cAMP production by the agonist can be detected.

Although the $G\beta\gamma$ dimer is not involved in these pathways, it can also serve as effector, *e.g.* as activator of certain ion channels or the MAP kinase pathway.^[112]

Receptor desensitization involves phosphorylation, subsequent binding of β -arrestins followed by internalization.^[155] However, this process is presently under constant revision, also because the β -arrestins are now thought to additionally play a role in the signaling pathway.^[155]

3.1.5 Orphan G Protein Coupled Receptors and the Reverse Pharmacological Strategy

In classical pharmacology, a disease state and/or the discovery, isolation and (if possible) identification of a pharmacologically active substance and its physiological characterization stood at the beginning of a research project, which eventually could lead to the development of new drugs.^[58,59]

In contrast, modern pharmacological research is based on the drug receptor theory, founded by Langley and Ehrlich,^[156] and the vast genetic data, obtained from the complete sequencing of the human genome.^[61,62]

Mass sequencing of randomly chosen expressed sequence tags (ESTs) followed by bioinformatic analysis of these sequences to identify structural characteristics of (known) GPCRs has led to the identification of about 100-150 orphan receptors in recent years.^[60,63,157] The strategies, which are applied to determine the physiological role of these receptors – the first step usually is the search for a natural ligand -, have been termed ‘reverse pharmacology’ and/or ‘orphan receptor strategy’.^[58,59,63,158-161] At present, several definitions for the term ‘reverse pharmacology’, which is somewhat broader than just covering orphan GPCRs, are given in the literature.^[58,63,161] This is because the optimal concept of how to generate drugs most efficiently is under constant debate. However, it can be generally said that biological assays employing more or less characterized receptors represent the starting point (see also chapter 2.1). The orphan receptor strategy can be considered as a special case of the reverse pharmacological principle, its first step is the transfection of the complete orphan receptor gene into appropriate cells (Figure 3.3).^[63,159-161] Because the orphan receptor strategy faces two major unknowns (Figure 3.4), namely the nature of the ligand(s) itself and the type of second messenger response, that the ligand may evoke,^[159] a variety of screening systems should be used for the search of this ligand(s) (see chapter 3.1.6).

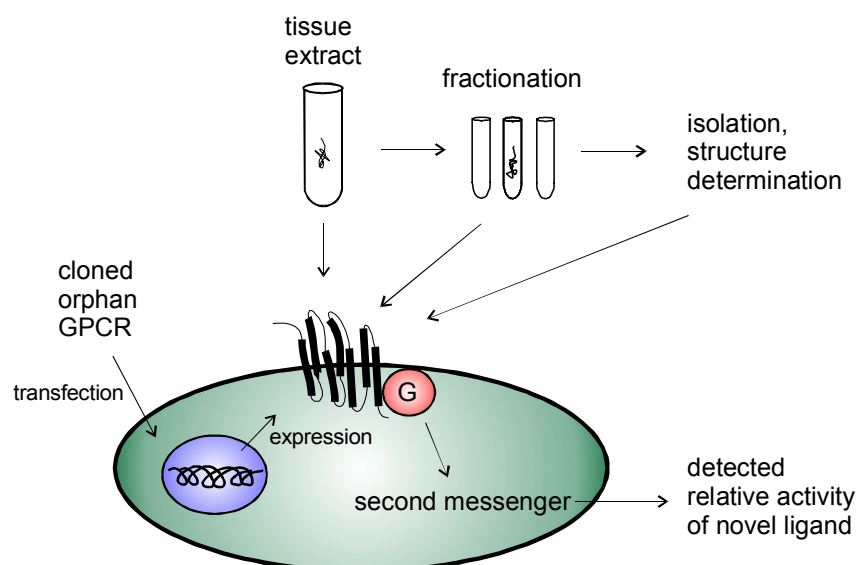


Figure 3.3: *The orphan receptor strategy involves: (1) expression of the cloned orphan GPCR in a cell line; (2) exposure of this cell line to a tissue extract that is expected to contain the natural ligand. (3) recording the second messenger response (4) fractionation of the tissue extract, isolation and structural determination of the active compound (5) resynthesis and testing of the active compound (not shown).*

So far a very helpful tool in the determination of an orphan receptors' role proved to be primary sequence homology comparisons. They allow to find out about its relationship to other known receptors, because the number of permutations caused by possible ligands and activities, would make the search for its natural ligand an almost impossible task (Figure 3.4).^[159] Furthermore, in many cases expression in chinese hamster ovary (CHO)- and human embryonic kidney (HEK) 293-cells lines^[58,59] and linking to G α 16 or related chimeras (see chapters 3.1.2 and 3.1.3) successfully enabled screening in functional assays using the PLC β pathway. As a source for the natural ligand, tissue extracts (compound mixtures) and libraries of known ligands have been used.^[63,159-161] In the absence of a ligand, receptor expression can be confirmed using northern and Western blotting.^[59]

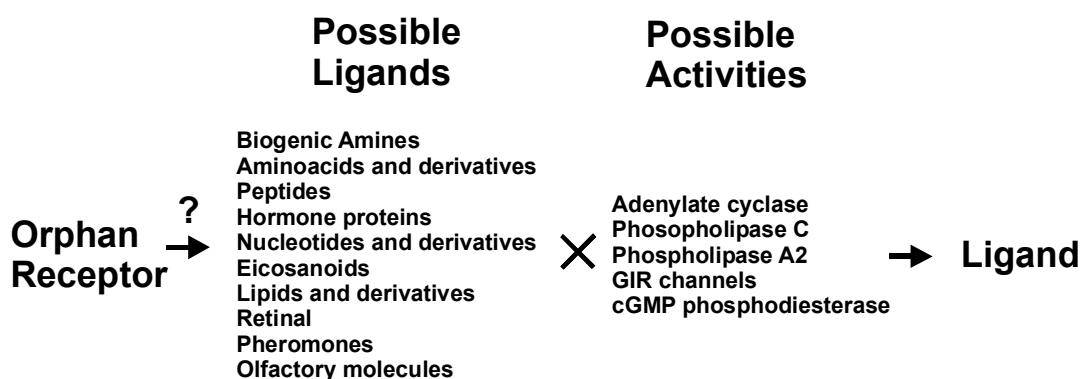


Figure 3.4: *The difficulty of the orphan receptor strategy is the vast number of possible permutations generated by possible ligands and second messenger activities, which have to be used in assays for detection. Without additional information, the search for natural ligands is therefore an extremely challenging task.*

Although the orphan receptor strategy and reverse pharmacology approach have led to the identification of many natural ligands in recent years (Table 3.1),^[63,161] the proportion of available orphan receptor sequences that have been ‘de-orphanized’ in this manner remains relatively small. New approaches like the constitutively activating receptor technology (CART) are gaining increasing attention,^[104] also because it is now a generally accepted concept that various ligands can bind to different binding sites to have different effects on GPCRs.^[86,96,104,107]

Table 3.1: *Orphan GPCRs and identified ligands.*

Receptor	Ligand	Found	Major function	Ref.
ORL-1	Nociceptin/Orphanin FQ	1995	Anxiety, Memory	162
HFGAN72	Orexins/Hypocretins	1998	Feeding, Sleeping	163,164
GPR-10	Prolactin-releasing pept.	1998	Prolactin secretion	165
APJ	Apelin	1998	Immune response	166
GHS	Ghrelin	1999	Obesity	167
SLC-1	Melanin-concentrating hormone (MCH)	1999	Obesity	168
GPR-14	Urotensin II	1999	Vasoconstriction	169-172
FM-3/4	Neuromedin U	2000	Uterine contraction	173

From the perspective of the pharmaceutical drug research, the most relevant inherent problem of the genomics-based search for new drugs using cloned orphan receptors is target validation.^[3] In contrast to that in classical pharmacology very often a fortuitously discovered ‘validated target’ constituted the origin of the development of a new drug. Target validation can be defined as the relevance of a questioned target for a disease process and the possibility of taking influence on the development of such a process by manipulating this target. In the last consequence definite proof can only be obtained from clinical trials, however early studies *e.g.* using animal models are desirable. Moreover, functional genome analysis together with proteomics can provide valuable information.^[174] However, it becomes more and more apparent, that many orphan receptors may be part of very complex biological systems void of the still prevailing and desired ‘one drug/one target/one disease’ principle.^[174-177]

3.1.6 Biological Assays

Assays for screening of ligands against GPCRs can be classified into two major categories: cell assays (functional cell-assay) and homogenous assays with membrane preparations containing the receptor (classical binding assay).^[178] Both systems are apparently different and each is limited in its possibilities. The functional cell assays such as the FLIPR-assay (described below) comprising the entire receptor/promotor/effector system allow the detection of agonism and antagonism (however competitive and non-competitive antagonism are not distinguishable) as a result of the triggered biochemical transduction cascade (see chapters 3.1.3 and 3.1.4). The classical binding assay can (only) give information about the competitive binding of a questioned compound to the agonist binding site on the receptor protein by observing the displacement of the usually radiolabelled peptide agonist. A putative intrinsic agonist activity of a compound displaying high affinity to the agonist epitope can not be detected via the binding assay. On the other hand functional assays are complex systems relying on multiple parameters and suffer from the disadvantage, that activation of the receptor - or stabilization of the activated form thereof – can only

be assumed to happen through interactions of the ligand with the receptor at the agonist epitope. However, in principle other possibilities - which complicate the situation - are thinkable, *e.g.* allosteric modulation of the receptor or intervention into the transduction cascade remote from the agonist-receptor level. The development of the orphan receptor strategy^[63,161] is closely related with the development of numerous new functional cell assay systems in the last years, some of which will briefly be introduced in the following (see also Figure 3.2 and chapter 3.1.4):

- The Fluorometric Imaging Plate ReaderTM (FLIPR) assay^[116] (a detailed description is given later in chapter 4.2.1) measures the elevation of intracellular calcium $[Ca^{2+}]_i$ upon agonist activation. This assay has found broad application because coexpression of $G\alpha_{16}$ enables coupling of most GPCRs, the simple readout (fluorescent dyes or aequorin luminescence) and a high degree of automatization allow high throughput screening.
- In reporter-gene assays^[179,180] a number of promoters (*e.g.* ICAM-1) have been used to activate the translation of reporter genes such as *e.g.* firefly luciferase^[181,182] or GFP.^[183] Luminescence is used as a readout.
- The Receptor Selection and Amplification TechnologyTM (R-SAT)^[184-186] developed by *Arcadia Pharmaceuticals* relies upon the focus (*i.e.* colony) forming and proliferative capacity of agonists acting on GPCRs in NIH 3T3 cells using the MAP kinase cascade.
- Cloned GPCR are expressed in yeast cells.^[187,188] However difficulties in demonstrating functional expression is a limitation.

More or less distant in the future lies the use of constitutively active GPCRs for drug screening^[104] (chapter 3.1.1), or a recent development of noncovalently immobilized, isolated GPCRs arranged as microarrays, which may allow the simultaneous screening of multiple receptor types.^[189,190]

3.2 The Orphan Receptor Bombesin Receptor Subtype 3 (BRS-3)

3.2.1 The Bombesin-Like-Peptides and the Bombesin Receptor Family

The family of bombesin-like peptides (BLPs) derives its name from a peptide of 14 amino acids originally isolated by Anastasi *et al.* in 1971 from the skin of the European frog *Bombina bombina*.^[191] The subsequently isolated peptides, which are structurally related to bombesin, have been classified into three subfamilies:^[192,193] the bombesin (Bn), the ranatesin and the phyllolitorin subfamilies (Table 3.2). This classification is based upon the differences of the C-terminal amidated seven/eight amino acids comprising domain, which is highly conserved among the BLPs and mainly responsible for biological activity and binding.^[194]

At present only two mammalian bombesin-like peptides are known - gastrin-releasing peptide (GRP),^[195,196] a 27-mer, which belongs to the bombesin subfamily and neuromedin B (NMB),^[197] a 10-mer, which shares similarities with the amphibian peptide ranatesin. So far no mammalian member of the phyllolitorin family has been isolated.

Table 3.2: Bombesin-like peptides share a high sequence homology at the C-terminus as highlighted through comparison of the positions respecting to positions 7 to 14 of bombesin (pE = pyroglutamic acid).

		7	8	9	10	11	12	13	14	
Bombesin	pEQRLGN	Q	W	A	V	G	H	L	M	NH ₂
Alytesin	pEGRLGT	Q	W	A	V	G	H	L	M	NH ₂
GRP	VPLPAGGGTVLTKMYPRGN	H	W	A	V	G	H	L	M	NH ₂
NMB	GN	L	W	A	T	G	H	F	M	NH ₂
Litorin	pE	Q	W	A	V	G	H	F	M	NH ₂
Ranatesin	pEVP	Q	W	A	V	G	H	F	M	NH ₂
Phyllolitorin		pE	L	W	A	V	G	F	M	NH ₂

The exogenous introduction of BLPs induces a wide range of biological activities, both, on isolated organs *in vitro* and on organisms *in vivo*.^[198] Besides other actions,

such as the control of smooth muscle contraction,^[194,199] the secretion of other gastrointestinal peptide hormones,^[200] the regulation of body temperature,^[201,202] and certain behavioral responses,^[203,204] the regulation of food intake and satiety^[205-210] has probably attracted most attention. However, such observations do not necessarily allow simple deductions for the role of the BLPs in organisms, because these effects are obtained after administration and therefore primarily represent a pharmacological effect. Furthermore, BLPs are thought to act as autocrine growth factors in human small cell lung cancer (SCLC).^[211,212]

As described above, in the beginning research on the ‘bombesin-field’ concentrated on the isolation of native peptides from different organisms and the detection of their biological activities. In the late 1980s it became apparent, that there are at least two different receptors, which account for these biological activities. Autoradiographic studies in rat brain revealed different binding affinities for radiolabelled NMB and Bn in several regions.^[213,214] This finding was later manifested using several antagonists in various tissues.^[215-217] Further investigations demonstrated that one receptor named NMB-R^[218-220] - *i.e.* neuromedin B preferring bombesin receptor, sometimes also referred to as bombesin receptor 1 - binds NMB and Bn with highest affinity (nanomolar range) and GRP with lower affinity (hundreds of nanomolar range), whereas a second receptor named GRP-R receptor^[219,221] - *i.e.* gastrin releasing peptide preferring receptor, sometimes also referred to as bombesin receptor 2 - binds GRP and Bn with high affinity (nanomolar range) and NMB with lower affinity (hundreds of nanomolar range).^[222]

Today, there is evidence for at least two more bombesin receptors besides the NMB-R and GRP-R described above, namely bombesin receptor subtype 3 (termed BRS-3),^[223,224] and the bombesin receptor subtype 4 (BB₄-R).^[225,226] Unlike the first two Bn receptors, which have been discovered and characterized employing classical pharmacological methods including their natural ligands, the latter two have been introduced on a rational basis due to sequence homologies using cloning technologies and can be classified as orphan receptors (see chapter 3.1.5). A detailed description of BRS-3 is subject of chapter 3.2.4. A gene encoding the mentioned fourth putative bombesin receptor was found in frog brain.^[225] Unlike for the other three bombesin

receptors no mammalian form of the BB₄-R could so far be identified. Studies with different Bn agonists and antagonists showed, that this receptor has a unique profile with respect to this ligands (named pharmacological profile).^[226] However, similar as for BRS-3 (see chapter 3.2.4) a severe limitation for studying the biological relevance of the BB₄-R is the lack of native cells containing the receptor on a sufficient level.

3.2.2 Peptide Bombesin Receptor Antagonists

Bn antagonists have been developed on the basis of the Bn peptide sequence or related peptides such as substance P. In order to find analogues with retained affinity but reduced agonist action, the common strategy was to alter those parts of the native structure, which are responsible for agonist action but not important for affinity. All of these compounds are selectively acting on the GRP-R. The discovered antagonists can be grouped into several different classes:^[227]

- As a first class of Bn/GRP antagonists, D-amino acid analogues of substance P (SP) such as [D-Arg¹,D-Phe⁵,D-Trp^{7,9},Leu¹¹]SP or [D-Arg¹,D-Pro²,D-Trp^{7,9},Leu¹¹]SP, which originally have been developed as substance P receptor antagonists, were described.^[228,229] Major limitations of these peptides however are their relatively low potency and their lack of selectivity.
- Secondly, insertion of D-amino acids at position 12, especially Phe, results in Bn/GRP antagonists, the most potent being [D-Phe^{6,12}]Bn.^[230] However, as for the substance P analogues, low potency is a limitation.
- Reduction of single peptide bonds in Bn proved to be successful between position 13 and 14 and resulted in the potent Bn/GRP antagonist [Leu¹³,ψCH₂NHLeu¹⁴]Bn.^[231] This class of compounds could be further optimized by insertion of D-Phe at position 6, which allowed N-terminal deletion of amino acids, resulting in the potent antagonist [D-Phe⁶,Leu¹³,ψCH₂NHPhe¹⁴]Bn(6-14).^[232,233] Furthermore, Leu¹³ and Leu¹⁴ have been successfully substituted by D-Pro-ψCH₂NH-Phe^[234,235] and different mimics.^[236]

- A fourth class of potent Bn/GRP antagonists is represented by the desMet analogues of the C-terminus of Bn^[237,238] and GRP.^[239-241] Again, insertion of D-Phe at position 6 allowed deletion of the residual N-terminal amino acids, C-terminal esters and amides proved to be especially potent. Very recently, the application of [D-Phe⁶,Leu-NHET¹³,desMet¹⁴]Bn(6-14) analogues modified with 1,4,8,11-tetraazaundecane labeled with ^{99m}Tc as a diagnostic tool in oncology using the SPECT technology was described.^[235]

Discussions about the bioactive, receptor bound conformation of bombesin analogues resulted in a type II β -bend conformation^[201,231,242-245] with Gly¹¹ in a pivotal position, not at least because of structural parallels to somatostatin analogues. More recently, for Ac-Bn(7-14) a conformation of three consecutive γ -turns followed by a bend and finishing with two γ -turns was proposed.^[246] Unfortunately, so far none of these proposals has been elaborated into a working model. However, the successful implementation of conformational constrained dipeptide mimics replacing Val¹⁰-Gly¹¹,^[247] or the agonists and antagonists obtained by covalent cyclization of Bn^[243] point at a bend conformation.

Despite the similarity of the GRP-R and NMB-R, peptide antagonists acting on the NMB-R have not been obtained by the above-described strategy.^[227,248] It was later discovered that an unrelated cyclic somatostatin analogue SS-octa has about 100-fold selectivity of NMB-R over GRP-R.^[249]

3.2.3 Small Molecule Ligands for Bombesin Receptors and Related GPCRs

The first described nonpeptide Bn/GRP antagonists displaying affinities in the micromolar range were found from screening of large compound libraries (CP-70,030 and CP-75,998, Figure 3.5),^[250] or isolated from plant extracts such as the natural products kuwanon G and H.^[251] Unlike the examples described before, more potent GRP/NMB antagonists have been developed by researchers at *Parke-Davis* (Cambridge, UK) on a rational basis using the so-called 'peptoid' design

strategy^[35,36,252] as described in chapter 2.3. In this remarkable approach, an alanine scan of the Bn peptide fragment AcBn(7-14)^[246] represented the starting point for the design of small molecule GRP/NMB antagonists.^[253,254] A focused search applied on the companies' compound collection for small molecules comprising the three most important residues for binding, namely Trp⁸, Val¹⁰ and Leu/Phe¹³, yielded the high affinity lead PD141467, a α -methyl-(*S*)-tryptophan urea bearing a C-terminal phenylserinol and an N-terminal 2,5-diisopropylphenyl moiety.^[253] Subsequent C/N-terminal optimization furnished the selective high affinity NMB antagonist PD168368 and the 'balanced' NMB/GRP antagonist PD176252 (Figure 3.5).^[254] Recently, it was demonstrated that the latter is able to treat sexual dysfunction when administered to rats.^[255] These are the only small molecule ligands described for Bn receptors to date. Neither small molecule agonists are available for any of the Bn receptors nor antagonists for the BRS-3.

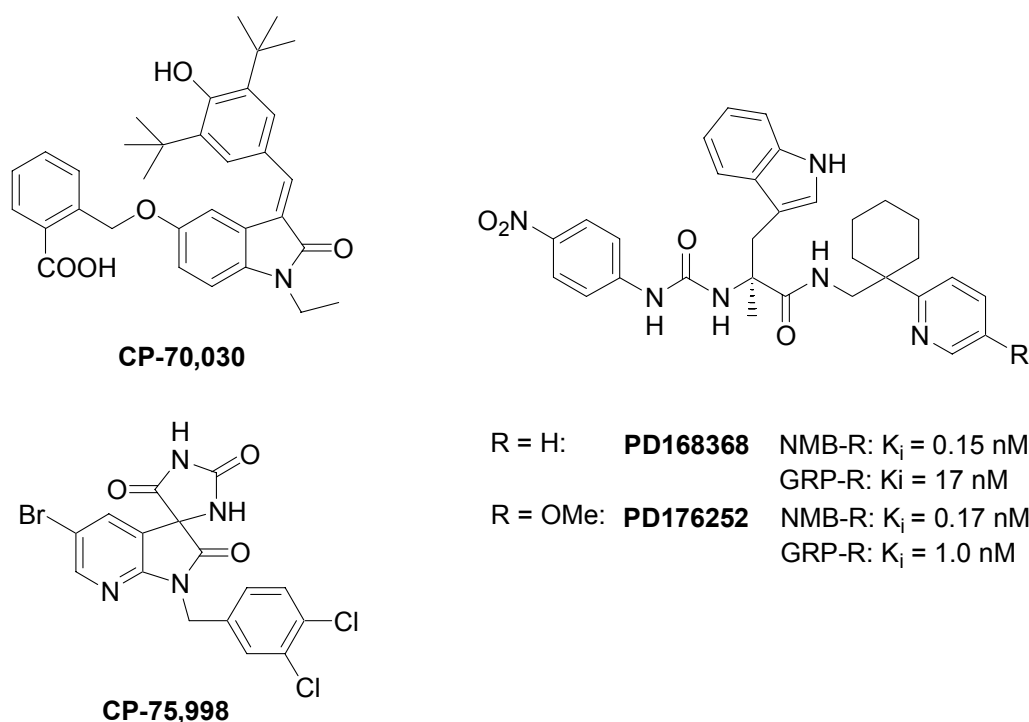


Figure 3.5: CP-70,030 and CP-75,998 are low affinity GRP-R antagonists ($IC_{50} = 1.5$ - 3 μ M). PD168368 is a selective, high affinity NMB-R antagonist, PD176252 a mixed NMB/GRP antagonist.

It is noteworthy that similar small molecule agonists/antagonists bearing a constrained tryptophan as their central unit have been obtained for related GPCRs using comparable strategies (Figure 3.6):

- Starting out with CCK-8S, a sulfated fragment of the endogenous neuropeptide cholecystokinin (CCK), the key amino acids for binding within this peptide sequence were determined in an alanine scan as Trp and Phe.^[256] Optimization of a Trp-Phe dipeptide lead yielded the selective CCK-B antagonist CI-1015, a α -methyl-(*R*)-tryptophan derivative (Figure 3.6, A).^[257-260]
- Similar as for CCK and Bn receptors, researchers at *Parke-Davis* developed selective antagonists for the neurokinin receptors NK₁,^[261,262] NK₂^[263,264] and NK₃^[265,266] (Figure 3.6, B).
- Using the Veber-Hirschmann peptide^[267] as a template, nonpeptide selective agonists for the somatostatin receptor sst2 have been obtained from a focused search for small molecules comprising the Tyr-D-Trp-Lys motif of the *Mercks'* compound collection followed by lead optimization (Figure 3.6, C).^[33,34,268]

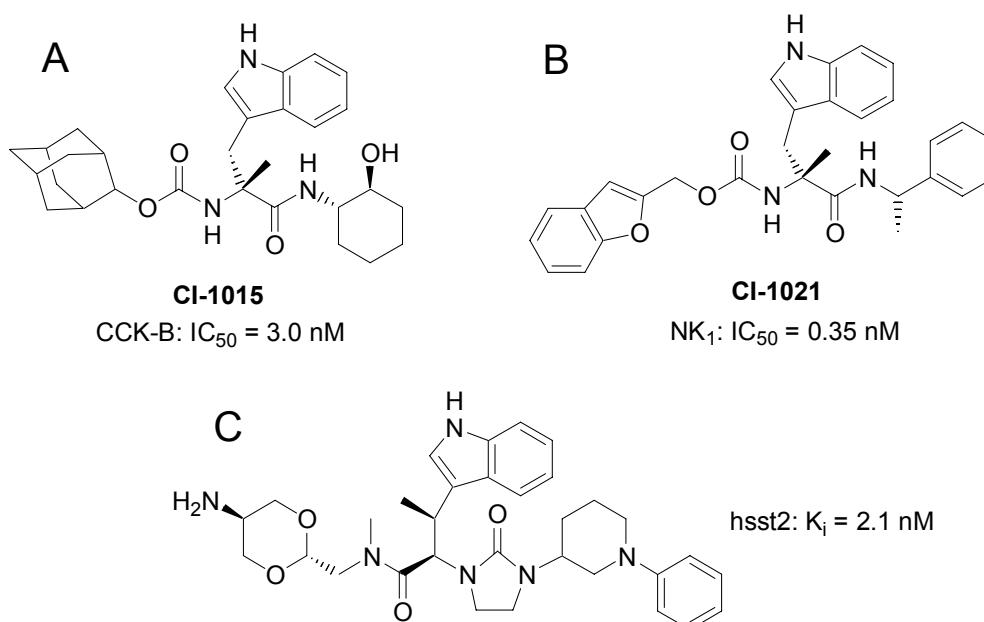


Figure 3.6: Selected ligands, all bearing constrained tryptophan as a core unit, addressing related target GPCRs: A) CCK-B antagonist (*Parke-Davis*). B) NK₁ antagonist (*Parke-Davis/Pfizer*). C) sst2 agonist (*Merck*).

3.2.4 Discovery, Pharmacology and Ligands of the Orphan Receptor BRS-3 – Status Quo

The orphan receptor, bombesin receptor subtype 3 (BRS-3) was identified as a member of the Bn receptor family since it shares 51% and 47% amino acid sequence homology with the two mammalian bombesin receptors, NMB-R and GRP-R, respectively.^[223,224]

Unlike NMB-R and GRP-R, which are widely expressed in rat brain and gastrointestinal tract,^[218-221,269] distribution of BRS-3 is much more limited. It has only been found on pregnant guinea-pig uterus, to a low degree in guinea-pig brain, on secondary spermatocytes in testis of rats, in a specific brain region of mice, and in human lung, ductal breast and epidermal carcinoma cell lines.^[223,224,270,271]

Although the orphan receptor strategy^[58,59,63,159-161] has led to the identification and assignment of several neuropeptides to orphan GPCR's, in case of BRS-3 a natural high affinity ligand still remains unknown and the physiological and pathological function is still not understood. However, very recently hemorphins, which are endogenous peptides formed during the *in vivo* hydrolysis/degradation of hemoglobin, namely LVV-hemorphin-7 and VV-hemorphin-7, could be identified as ligands for BRS-3.^[272] These ligands induce Ca^{2+} mobilization in a FLIPR-assay using CHO hBRS-3 cell lines in the micromolar range comparable to the response obtained by GRP and NMB.^[272]

In principle, although this approach may reach too short, potential (patho-) physiological roles for BRS-3 can be speculated to be of the same categories as for the more established GRP-R and NMB-R. An important hint about the biological importance of BRS-3 was obtained from BRS-3 deficient mice produced by targeted disruption. In contrast to GRP-R or NMB-R knock-out mice^[207,209] they develop mild obesity, hypertension and diabetes.^[273,274] Therefore it was concluded, that BRS-3 is important for the regulation of energy balance, body weight and blood pressure. However, a direct relation between BRS-3 and obesity is improbable, because an investigation of the BRS-3 encoding gene of humans suffering from adipositas did not show any mutations.^[275]

Like NMB-R and GRP-R, which are involved in the growth regulation of SCLC as mentioned above in chapter 3.2.1, BRS-3 was found on human lung cancer cells,^[223,276-278] and ovarian cancer,^[279] however at a lower level of expression. Very recently, BRS-3 was connected with the treatment of neurological disorders.^[280]

So far, two peptidic high affinity BRS-3 agonists have been described, [D-Phe⁶,Phe¹³]Bn(6-13) propylamide^[281] and the non-selective high affinity agonist [D-Tyr⁶,β-Ala¹¹,Phe¹³,Nle¹⁴]Bn(6-14) and its D-Phe⁶ analogue,^[222,282] which was further developed into the more selective (*R*)-Apa¹¹ and (*S*)-Apa¹¹ analogues.^[242] They were derived synthetically from BLP fragments by substitution of amino acids and C-terminal modification. These peptides allowed receptor pharmacology studies for the first time since so far no known natural agonist or antagonist of the Bn receptor family showed high affinity on BRS-3.^[222,224,226,281] Studies with the agonist [D-Tyr⁶,β-Ala¹¹,Phe¹³,Nle¹⁴]Bn(6-14) showed that the BRS-3 receptor has a unique pharmacology compared to the other bombesin receptors, NMB-R, GRP-R and BB-R₄.^[222,226,283] Additional difficulties were encountered by the fact that no natural cell line could be found to express BRS-3 in a sufficient level for study.^[281,283] Therefore BRS-3 pharmacology studies were carried out using BRS-3 transfected BALB 3T3 or NCI-H1299 non-small cell lung cancer cells.^[281,283,284] These studies,^[281,283] as well as others^[285,286] gave insight in the signaling pathway of BRS-3. Receptor activation can be measured by the increase of the level of intracellular calcium ($[Ca^{2+}]_i$) caused by phospholipase C activation. Furthermore, activation of BRS-3 leads to increases in inositol phosphates and an increase in tyrosine phosphorylation of p125^{FAK}.^[283]

3.2.5 Binding Sites and Selectivity at Bombesin Receptors

Ligand-based investigations designed to elaborate the importance of structural differences required for selectivity on these two receptor subtypes showed that when NMB, which differs from Bn in positions 3, 6 and 9 (Table 3.2), was made more GRP- or Bn-like, position 3 was most important followed by position 9.^[248,287]

Several studies addressing the receptors' molecular basis of selectivity for ligands – agonists and antagonists - have been carried out using mutants of the GRP-R, NMB-R and BRS-3 produced by site directed mutagenesis.^[284,286,288-291] As already mentioned above all known BLPs have low affinities for the BRS-3.^[222] In two different studies four amino acids, which are conserved among GRP-R and NMB-R however not at BRS-3, namely Gln¹²¹, Arg²⁸⁸, Ala³⁰⁸ and Pro¹⁹⁹, were exchanged against the corresponding residues in the BRS-3 sequence. As a result of this a drop in the affinities of GRP and Bn in case of the GRP-R,^[284] and NMB and Bn in the case of NMB-R,^[291] respectively, was observed. Conversely, affinity for Bn/GRP or Bn/NMB, respectively, could be increased when these four residues were altered in the human BRS-3 sequence, thereby placing emphasis on the importance of these residues for the selective binding of the natural ligands. Three out of these four residues are located in the transmembrane helices 3, 6 and 7, whereas one (Pro¹⁹⁹) can be found in the third extracellular loop. Further studies carried out on GRP-R identified Tyr²⁸⁵ as critical for agonist binding and Phe³¹³ for the affinity of an antagonist.^[288] It is noteworthy, that the binding of the peptidomimetic high affinity NMB-R antagonist PD168368,^[253] was not improved on BRS-3 upon exchange of the said four amino acids.^[291] The authors concluded that, although this peptidomimetic antagonist was developed employing structural features of NMB required for high affinity, both compounds “may have overlapping, but distinct structural requirements for high affinity binding”, which even would not rule out different binding sites.^[291] Further studies showed that inhibition of this antagonist is competitive, however allosteric antagonism could not be excluded.^[286] Recent results obtained from receptor mutational and modeling studies imply, similar as described above for the natural ligands,^[284,291] a small importance of the third extracellular loop for the selectivity of the antagonist PD168368 for the NMB-R over the GRP-R. Furthermore, an important role for the residues of the fifth upper transmembrane region was found.^[290] Modeling studies based on a bacteriorhodopsin homology model suggest, that Tyr²²⁰ of helix 5 interacts with the nitrophenyl-moiety of the antagonist in the transmembrane binding pocket.^[290]

4 Design, Synthesis and Biological Evaluation of BRS-3 Agonists

4.1 Introductory Remarks

The following chapter describes the development of low molecular weight BRS-3 agonists in a systematic medicinal chemistry approach with a linear nonapeptide and octapeptide, respectively, as a starting point. As already pointed out in the introduction, this work resulted from a cooperation initiated in October 1999 between Prof. Kessler (*TU München*) and *Solvay Pharmaceuticals GmbH* (Hannover). The synthesis part was carried out at the *TU München* and the biological testing in the pharmacological department of *Solvay Pharmaceuticals*. Furthermore, some selected compounds were tested in a previously described radioligand binding assay^[222] at *CEREP* (Celle L'Evescault, France).

It is important to mention that unlike *e.g.* in natural product synthesis, where the goal of a work is clearly defined, for this work neither a suitable strategy nor the outcome was known or predictable. This work is comprised of iterative steps of synthesis and biological testing. Therefore it was decided to dissect this chapter in logical units that reflect the chronological and strategic progress of this project. In each section the strategic decisions, planning, synthesis, biological results and possible structural implications of a series of compounds are described and discussed.

4.2 Biological Evaluation of the BRS-3 Agonists

4.2.1 Intracellular Calcium Measurements with the FLIPR-System

The biological evaluation of all described BRS-3 agonists at *Solvay Pharmaceuticals* was carried in a functional cell assay using the FLIPR-system (Fluorometric Imaging Plate ReaderTM, *Molecular Devices*), which is able to detect changes in the intracellular calcium concentration ($[Ca^{2+}]_i$) of cells as a result of G protein receptor activation. Originally, this system was developed for the measurement of membrane

potentials at *Pharmacia-Upjohn*. It consists of the following four components: Pentium-computer, argon-laser, 96-well-pipettor and a CCD-camera (Figure 4.1).

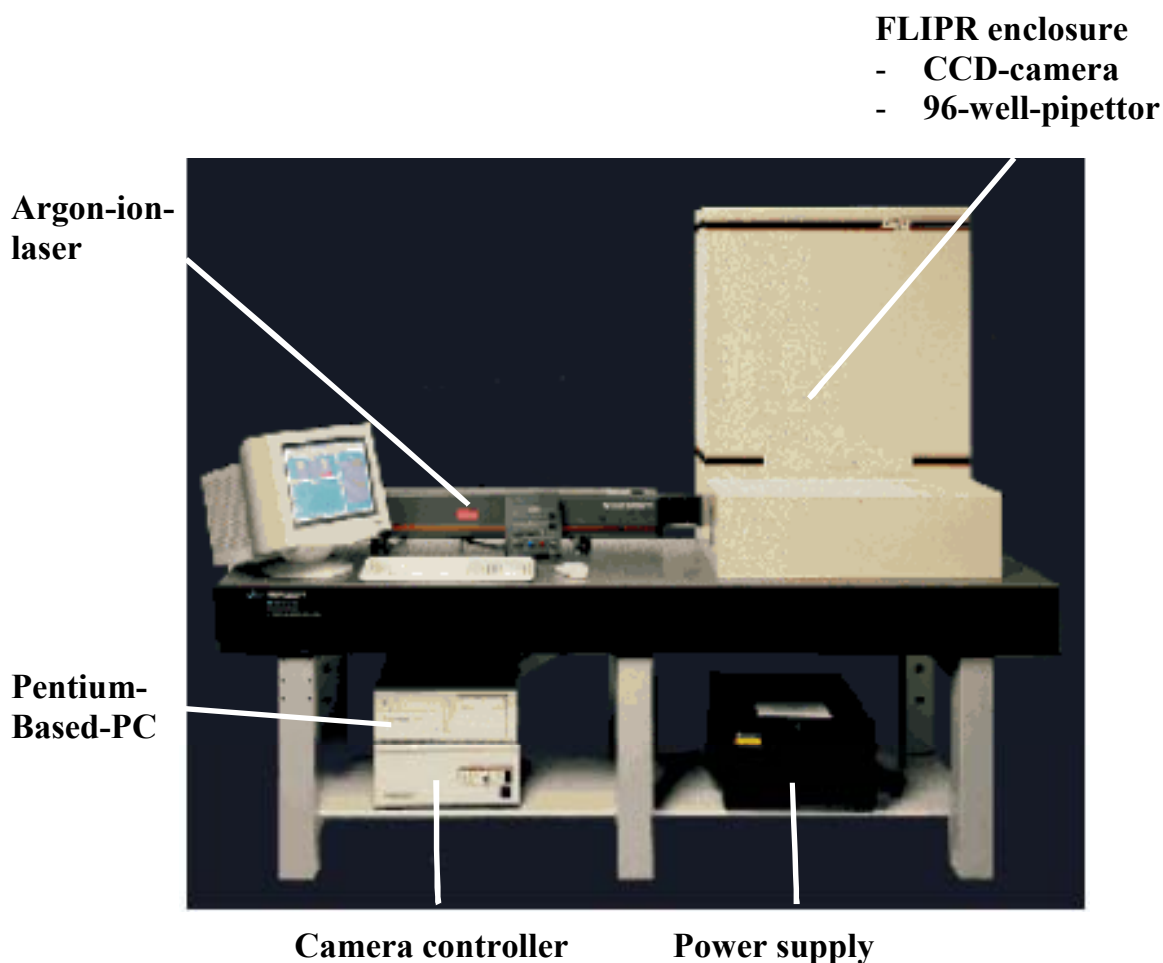


Figure 4.1: *The FLIPR²-system.*

The FLIPR-system was designed for measurements in the 96-well-plate format and is suitable for pharmacological HTS. The pipettor has three positions for 96-well plates, which makes it possible to consecutively add two different substances to a well containing the cells during any one experiment (see chapter 8.5.3). For FLIPR measurements, both adherent (*e.g.* CHO, HEK-293) and non-adherent cells (*e.g.* Jurkat, THP-1) can be used. Changes of the intracellular calcium concentration are mediated by a change in specific fluorescence, which is induced by laser-excitation of the calcium sensitive fluorescent dye Fluo-4/Fluo-3 (*Molecular Probes*) and detected by the CCD-camera. The difficult aspect of this particular assay is the strong

background component to the fluorescence data making it necessary to discriminate between the fluorescence signal from a cell monolayer and the background fluorescence from the extracellular medium. This problem has been technically solved by an angular direction of the laser from below through the clear-bottomed 96-well plates containing the cell monolayer, thereby minimizing the proportion of unspecific fluorescence. The calcium fluorescent dye Fluo-4 is present in its acetoxymethylester form (Figure 4.2), which enables permeabilization of the cell membrane. Additionally, the detergent pluronic acid F-127 facilitates the passive transport of the dye into the cell cytoplasm. Intracellular esterases cleave the ester to yield the free acid, which is able to form a complex with calcium ions. The cell membrane is almost impermeable for the free acid. A possible residual permeability via ion channels is blocked by the addition of probenecid.

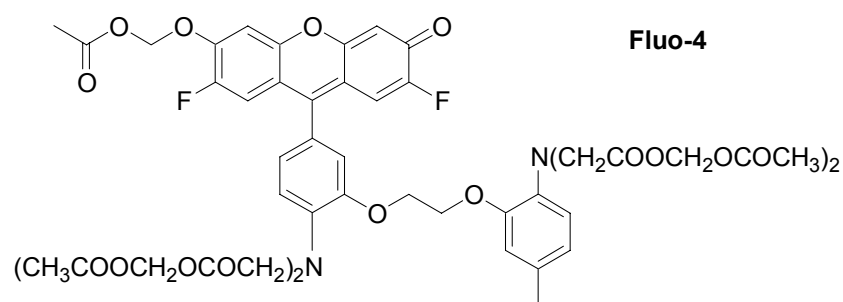


Figure 4.2: *Molecular structure of the acetoxymethylester form of fluorescent dye Fluo-4.*

The FLIPR measurement using adherent CHO cells consists of the following steps (for experimental details see chapter 8.5.2):

1. Plating of the Cells

Cultivated cells are seeded into 96-well plates one day prior to measurement and cultivated in the incubator.

2. Loading of the Cells with Fluorescent Dye

The culture medium is replaced by the loading medium. The cells are incubated for 45-60 min with the dye at 37 °C in the incubator.

3. Washing of the Cells

After loading of the cells with the dye, the residual extracellular dye is removed by washing with a Denley cell-washer (*Labsystems*).

4. Generation of the Application Plate

The substances to be tested are dissolved in DMSO and then diluted into 96-well plates. Substances are diluted into 8 or 16 different wells depending on compound and receptor. Each application plate contains one line (8 wells) of a reference compound, *i.e.* the endogenous ligand or [D-Phe⁶,β-Ala¹¹,Phe¹³,Nle¹⁴]Bn(6-14), respectively, and one line (8 wells) of buffer.

5. FLIPR Measurement

The FLIPR-system is controlled by a *Windows (Microsoft)* compatible software. Before starting the measurement, the loading of the cells is checked by recording the fluorescence in each well at a constant exposure intensity and –duration. Values are supposed to be between 3000-5000 counts.

In order to approach statistical limits, each application plate was measured on 2-3 cell plates, and additionally in most cases, experiments were repeated on different days. Measured calcium signals are obtained in counts over time. A typical FLIPR calcium signal from a single well is shown in Figure 4.3. From each well only the maximum of the signal was exported to *Excel*. There the values were normalized with the value of the reference compound at a concentration of maximal response, usually 16 μM. Values from all measurements for each compound were combined in *Excel* and for each compound one single dose-response curve was generated using Graphpad Prism (Version 3.00, *Graphpad Software*). For comparison of functional potencies of different compounds, EC₅₀-values were extracted (Figure 4.3). The EC₅₀-value (EC = Effect Concentration) represents the concentration where the half maximal relative Ca²⁺ signal for a specific compound on a certain receptor is reached. However, the EC₅₀-value does not provide any information about the maximal intensity of the functional activation of a compound, which also represents an important criterion for potency. Therefore, for some compounds, additionally, the maximal relative functional potency at a specific concentration (usually 16 μM) compared to the

endogenous ligand or [D-Phe⁶,β-Ala¹¹,Phe¹³,Nle¹⁴]Bn(6-14), respectively, is given in Tables 4.8, 4.11-16 and Figures 4.7 and 4.8.

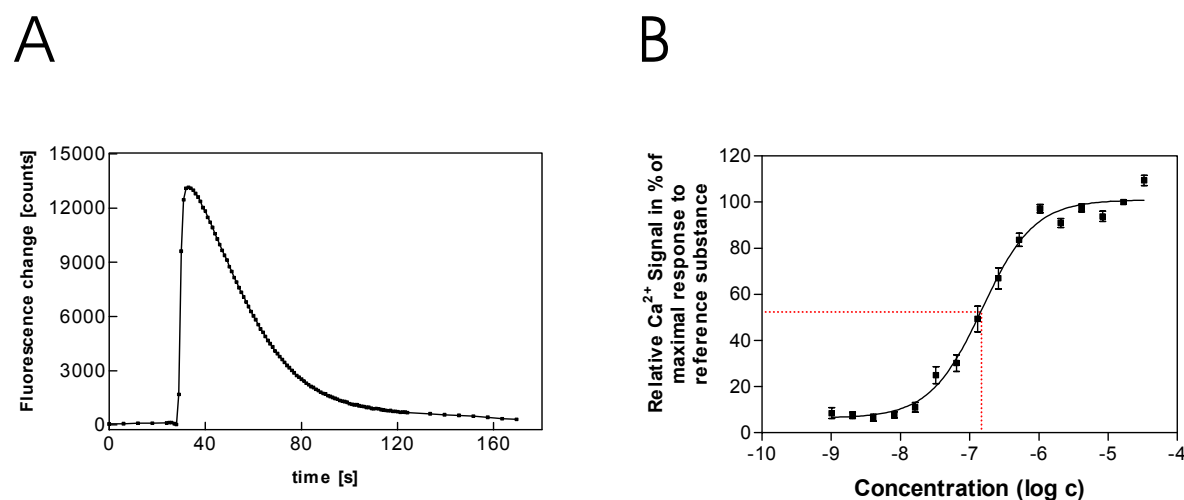


Figure 4.3: A) FLIPR calcium signal. B) Dose-response curve created with Graphpad Prism. The red dotted lines mark the concentration of half-maximal activation (= EC_{50} -value).

4.2.2 Characterization of the FLIPR Cell-Assays

In order to demonstrate the liability of the used FLIPR cell-assays, we evaluated its characteristics and compared them with literature data. Therefore, the two endogenous ligands NMB (**2**) for NMB-R and GRP (**3**) for GRP-R and the high affinity BRS-3 agonist [D-Phe⁶,β-Ala¹¹,Phe¹³,Nle¹⁴]Bn(6-14) (**1**) were used as reference compounds. Functional potencies of **1** at NMB-R, GRP-R, and BRS-3 in comparison with NMB and GRP are shown in Figure 4.4 and Table 4.1 and can be summarized as follows: NMB-R showed clear preference for NMB, GRP-R showed preference, however less clearly, for GRP. Both peptides, NMB and GRP, showed relatively low activity on BRS-3. **1** showed functional potency at all three receptors with low selectivity.

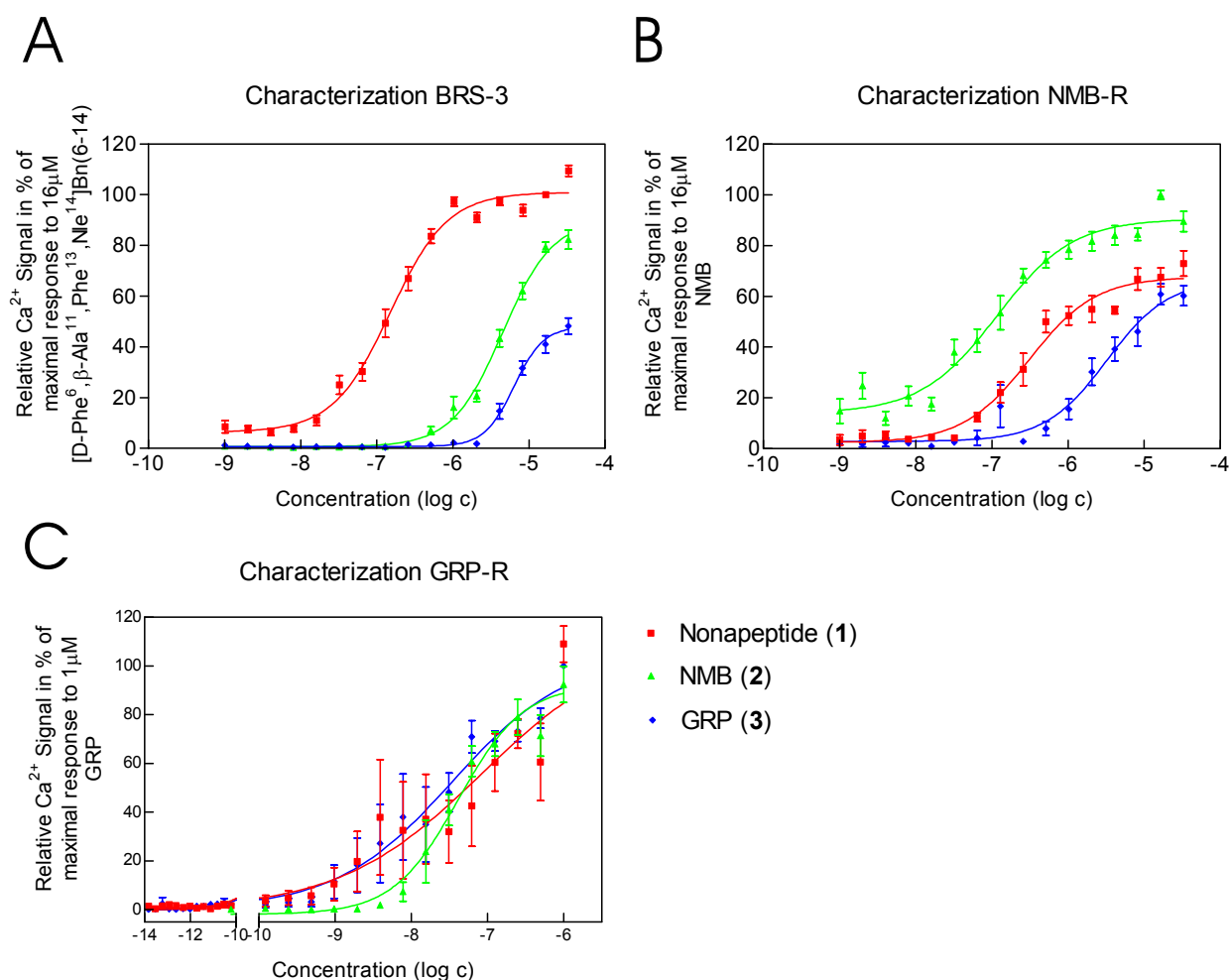


Figure 4.4: Characterization of the FLIPR cell-assays. Dose-response curves of the three peptides $[\text{D-Phe}^6, \beta\text{-Ala}^{11}, \text{Phe}^{13}, \text{Nle}^{14}]\text{Bn}(6-14)$ (1), NMB (2) and GRP (3) tested on the three receptors: A) BRS-3; B) NMB-R; C) GRP-R.

In recent studies^[222,282], the affinity of $[\text{D-Phe}^6, \beta\text{-Ala}^{11}, \text{Phe}^{13}, \text{Nle}^{14}]\text{Bn}(6-14)$ (1) towards the bombesin receptors NMB-R, GRP-R, BRS-3 and BB-R₄ has been determined in radioligand binding assays. Later, the ability of 1, NMB, GRP and Bn to induce calcium mobilization in a FLIPR-assay using HEK-293 and RBL-2H3 cells was assessed.^[292] In accordance with these studies 1 showed high functional potency on all three bombesin receptors NMB-R, GRP-R and BRS-3 in our measurements (Table 4.1).

Table 4.1: Mobilization of intracellular calcium by [D-Phe⁶,β-Ala¹¹,Phe¹³,Nle¹⁴]Bn(6-14) (**1**) and endogenous ligands NMB (**2**) and GRP (**3**) in CHO cells transfected with the human bombesin receptors NMB-R, GRP-R and BRS-3.

no.	peptide	NMB-R	GRP-R	BRS-3
		-pEC ₅₀ ^a	-pEC ₅₀ ^a	-pEC ₅₀ ^a
1	[D-Phe ⁶ ,β-Ala ¹¹ ,Phe ¹³ ,Nle ¹⁴]Bn(6-14)	6.51 ± 0.08	7.08 ± 0.09	6.82 ± 0.05
2	NMB	6.93 ± 0.11	7.38 ± 0.06	5.35 ± 0.04
3	GRP	5.49 ± 0.14	7.46 ± 0.15	5.20 ± 0.02

^a FLIPR-assay. Functional potencies are given in -pEC₅₀ ± SEM from 4-30 independent concentration-response curves. Additional experimental details are described in Table 4.2 and chapters 4.2.1 and 8.5.

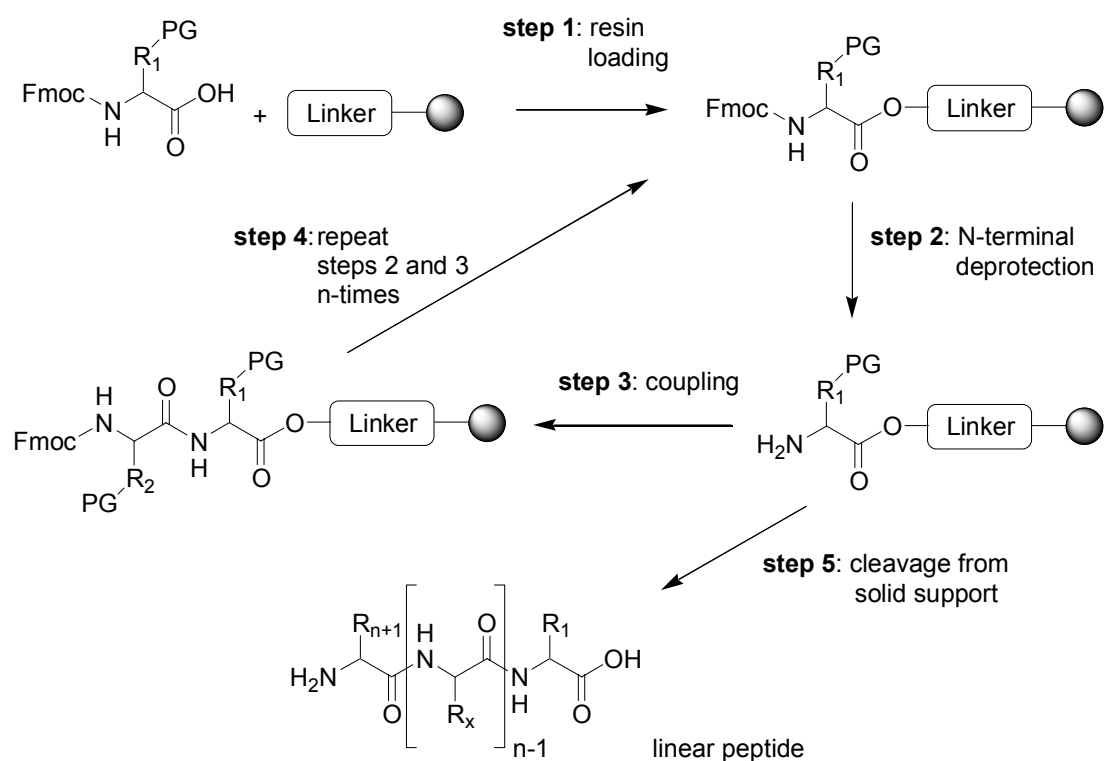
Different from others,^[292] but similar as reported for the affinity studies,^[222] we found little functional activity for NMB and GRP on BRS-3 with NMB > GRP. Relatively low functional potency of NMB on BRS-3 was also reported by Wu *et al.*^[281] In accordance with previous studies,^[292] functional selectivity of the BRS-3 receptor towards **1** was much higher than selectivity of the NMB-R receptor towards NMB and the GRP-R receptor towards GRP. However, in contrast to others^[292] we found that the functional potency of **1** > GRP on NMB-R and NMB > **1** on GRP-R. Taken together, we achieved satisfactory high, although not total correspondence with results obtained from different^[222] and identical^[292] test systems.

4.3 Linear and Cyclic Peptide BRS-3 Agonists

4.3.1 General Synthetic Aspects

Peptide chemistry and synthesis have gone through dramatic changes since Curtius^[293] and Emil Fischer^[294] have synthesized the first simple peptide derivatives. The interest in preparing these chains of amino acids linked by amide bonds stemmed from the observation made by Hofmeister^[295] and Fischer,^[296] that proteins are polymers consisting of amino acids. Although methods for the coupling of two amino acids were available, it was due to failures in the development of applicable protecting groups that substantially delayed further progress in peptide chemistry.^[294,297] A breakthrough occurred in 1932 when Bergmann introduced the benzyloxycarbonyl protecting-group.^[298]

A further milestone was marked by Merrifield in 1963 with the development of the automated peptide synthesis on solid support, a copolymer of styrene crosslinked with 1-2% divinylbenzene.^[4] The SPPS technique substantially facilitates the practical



Scheme 4.1: Peptide synthesis according to the Fmoc/tBu-strategy on solid support.

peptide synthesis procedure, because the anchoring of the C-terminal amino acid to the insoluble support allows the use of an excess of amino acids and coupling reagents, which enables almost quantitative yields for the coupling steps of small peptides. Furthermore, after reaction coupling reagents and by-products can be removed by simple filtration.

The synthesis of peptides longer than two amino acids requires the tactical utility of orthogonal temporary and permanent protecting groups.^[299] Among others,^[300,301] the Boc-strategy^[302-304] and the later developed Fmoc/*t*Bu-strategy^[303-306] are most prominent today. The Fmoc/*t*Bu-strategy, which has proved to be especially practicable in combination with SPPS (Scheme 4.1), was used for the synthesis of peptide BRS-3 agonists described in the following chapters.

In modern Fmoc SPPS, the C-terminal properties of a peptide can easily be determined by the choice of the appropriate linker. The linkers employed for the synthesis of BRS-3 agonists are summarized in Figure 4.5: The Rink MBHA linker^[307] and the Sieber amide linker^[308] have been used for the synthesis of peptide amides, the trityl chloride linker^[309] for the synthesis of peptide carboxylic acids and the FMPE-linker^[310] for the synthesis of carboxamides.

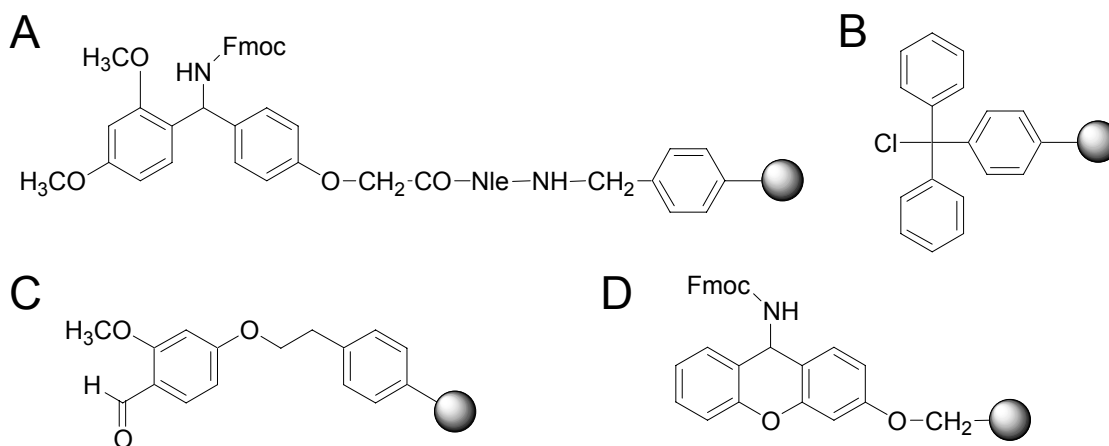


Figure 4.5: Linkers employed for the synthesis of BRS-3 agonists: A) Rink amide MBHA linker. B) Trityl chloride linker. C) 2-(4-Formyl-3-methoxyphenoxy)ethyl (FMPE) linker. D) Sieber amide linker. Product after cleavage/-conditions: A) Peptide amides/90% TFA. B) Peptide carboxylic acids/90% TFA. C) Carboxamides/90% TFA. D) Peptide amides/1% TFA.

Besides other coupling methods such as the azide process,^[293] acid chlorides,^[311] acid fluorides,^[312] mixed- and symmetrical anhydrides,^[313] or nitrophenyl- and pentafluorophenyl active esters,^[300,314] the use of in situ activated amino acids became very popular, also because this method is very compatible with automated synthesis.

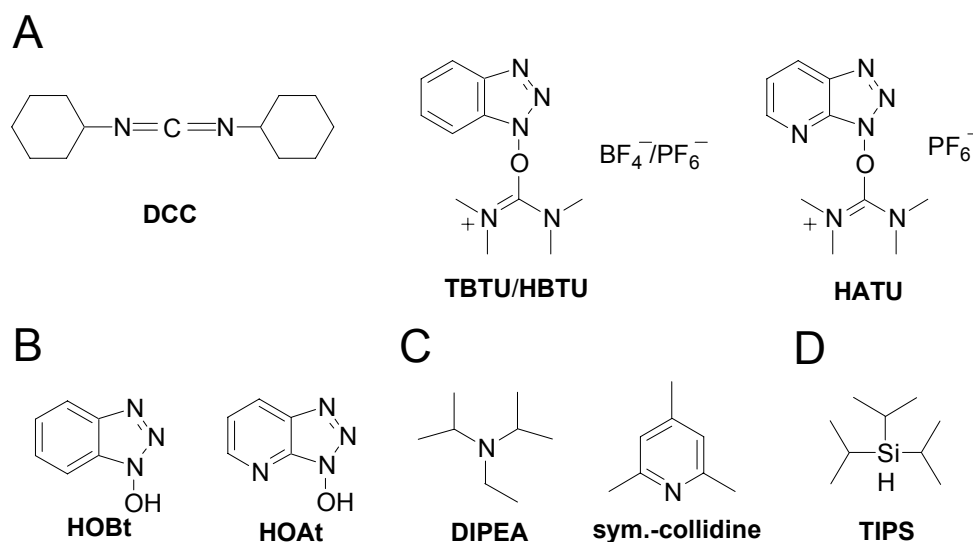


Figure 4.6: Coupling reagents (A), coupling additives (B), sterically hindered bases (C) and scavengers (D) that were employed for the synthesis of BRS-3 agonists (with the exception of DCC and HBTU).

Originally, carbodiimides such as DCC (Figure 4.6, A) have been used for activation,^[315] however due to low solubility of the formed dicyclohexylurea and because amino acids were especially prone to racemization,^[316] it has been mostly displaced by other coupling reagents^[317-323] (Figure 4.6, A). Furthermore, the use of additives^[324-326] (Figure 4.6, B) has helped to minimize the latter problem: Nucleophilic attack of the amino acid carboxylate at the coupling reagent (Figure 4.6, A), driven by the good leaving group OBt or OAt, respectively, intermediately leads to a acyluronium- or -phosphonium-derivative (precursors of the latter such as BOP,^[321] PyBOP^[320] etc. are not shown here), which is then quickly transformed to the OBt/OAt-active ester due to the presence of two moles of OBt or OAt, respectively, or anhydrides. This active ester is less susceptible to racemization than the acyluronium-species,^[316] yet still reactive enough for *N*-acylation of amino acids.

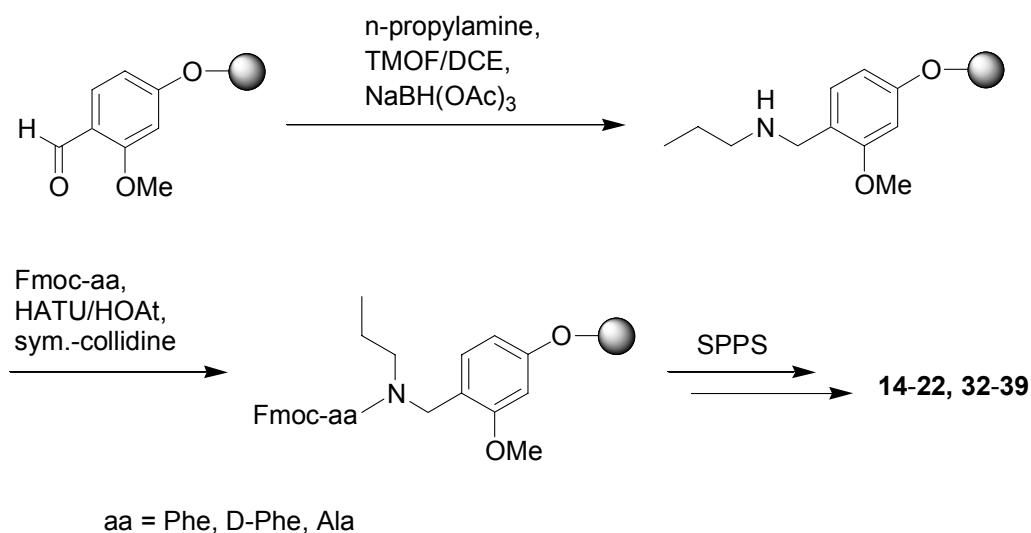
Furthermore, the use of sterically hindered and weak bases such as sym.-collidine (Figure 4.6, C) helps to prevent racemization considerably.^[327,328]

In Fmoc/*t*Bu SPPS, deprotection of the temporary protecting group Fmoc is carried out with 20% piperidine in NMP (v/v).^[306] For final cleavage of the peptide from solid support and simultaneous deprotection of the permanent protecting groups a cocktail of trifluoroacetic acid and suitable scavengers is used. For this work, the use of sidechain protecting groups was limited to triphenylmethyl- (Trt) at Gln, Cys and His and *t*butyloxycarbonyl- (Boc) at Trp. Triisopropylsilane (TIPS) has proved to be especially suitable as scavenger because it irreversibly hydrates carbocations and is easy to remove.^[329,330] Problems encountered during the deprotection of Trp(Boc)^[331] – however not necessarily observed for all the compounds that contained Trp(Boc) - are discussed below in chapters 4.3.5.2 and 4.4.4.2.

4.3.2 Alanine Scans of [D-Phe⁶,β-Ala¹¹,Phe¹³,Nle¹⁴]Bn(6-14) and [D-Phe⁶,Phe¹³]Bn(6-13) propylamide

4.3.2.1 Synthesis

C-terminal reductive amination for the synthesis of peptide-carboxamides **14-22**, **32-39**, peptides for C-terminal optimization (chapter 4.3.7) and some of the peptidomimetics as described later in chapter 4.4 has been conducted on FMPE resin.^[310] Therefore, the imine, resulting from the condensation of the appropriate amine with the aldehyde-functionalized resin in the presence of the water-withdrawing reagent TMOF (Scheme 4.2), was reduced with NaBH(OAc)₃ in a one-pot synthesis.^[332] Coupling of the first C-terminal amino acid to the resin-bound secondary amine was then carried out using HATU/HOAt/sym.-collidine activation^[318,320,326] For further chain-elongation, standard Fmoc protocols were used.



Scheme 4.2: Reductive amination on FMPE resin. Synthesis of C-terminally amidated peptides 14-22 and 32-39.

4.3.2.2 Biological Evaluation

Alanine scans of biological active polypeptides are conducted in order to acquire information about the role of a single amino acid sidechain for affinity or functional potency. Sidechains can either be directly involved in the binding to the receptor or, alternatively, they may play a major role for the intramolecular stabilization of the 'bioactive' conformation. Both can be achieved via hydrogen bonds,^[333] electrostatic or hydrophobic interactions.^[334,335] However, without further data, it is almost impossible to deduce such details of the binding mode solely from a binding- or functional assay.

The effect on calcium mobilization at NMB-R, GRP-R and BRS-3 and receptor affinity at BRS-3 of substituting an individual amino acid against Ala or D-Ala, respectively, in **1** is shown in Table 4.2 and Figure 4.7.

In the case of BRS-3, replacement of Trp⁸ or Phe¹³ reduced functional potency in **1** drastically by about 400-fold or 200-fold, respectively. This finding was consistent with a significant loss of affinity of analogues **7** and **12** towards the BRS-3 receptor as determined in the radioligand binding assay.^[222]

Table 4.2: Mobilization of intracellular calcium in CHO cells transfected with the human bombesin receptors NMB-R, GRP-R and BRS-3 and receptor affinity to the human bombesin receptor BRS-3 by analogues of [D-Phe⁶,β-Ala¹¹,Phe¹³,Nle¹⁴]Bn(6-14) (**1**) in which individual amino acids were replaced by Ala or D-Ala, respectively.

no.	peptide	NMB-R	GRP-R	BRS-3	
		-pEC ₅₀ ^a	-pEC ₅₀ ^a	-pEC ₅₀ ^a	Inhib. ^b
4	AQWAVβAHF-Nle-NH ₂	6.33 ± 0.13	8.35 ± 0.08	7.49 ± 0.13	91 ^c
5	aQWAVβAHF-Nle-NH ₂	5.12 ± 0.59	8.28 ± 0.05	7.13 ± 0.09	^d
6	fAWAVβAHF-Nle-NH ₂	5.45 ± 0.07	7.63 ± 0.05	6.51 ± 0.05	95
7	fQAAVβAHF-Nle-NH ₂	Inactive	7.25 ± 0.04	4.62 ± 0.10	47
8	fQWAVβAHF-Nle-NH ₂	6.01 ± 0.10	8.03 ± 0.07	7.21 ± 0.18	96
9	fQWAAβAHF-Nle-NH ₂	5.41 ± 0.40	8.58 ± 0.08	6.78 ± 0.06	97
10	fQWAVAHF-Nle-NH ₂	5.39 ± 0.10	7.22 ± 0.03	5.93 ± 0.02	103
11	fQWAVβAAF-Nle-NH ₂	Inactive	8.31 ± 0.06	6.32 ± 0.24	99
12	fQWAVβAHA-Nle-NH ₂	4.95 ± 0.22	8.24 ± 0.07	4.84 ± 0.07	51
13	fQWAVβAHFA-NH ₂	Inactive	8.71 ± 0.07	6.60 ± 0.09	100

^a FLIPR-assay (Solvay Pharmaceuticals GmbH, Hannover, Germany). Functional potencies are given in -pEC₅₀ ± SEM from 3-9 independent concentration-response curves. ^b Radioligand binding assay (CEREP, Celle L'Evescault, France).^[222] Values are given in percent of control specific binding of the reference compound [D-Tyr⁶,β-Ala¹¹,Phe¹³,Nle¹⁴]Bn(6-14) from two independent measurements at 10 μM. ^c Two independent measurements at 0.1 μM. ^d Not determined. Additional experimental details are described in chapters 4.2.1 and 8.5.

A smaller, but still significant drop in functional potency of about 20-fold was observed when substituting β-Ala¹¹. Negligible effects were found when other amino acids were replaced against Ala. In the case of GRP-R peptides showed smaller differences in potencies, a reduction of about 5-6 fold was found when Trp⁸ and β-Ala¹¹ were exchanged. Marginal increases of about 4-5 fold could be observed when Val¹⁰ and Nle¹⁴ were substituted. At NMB-R all replacements caused a loss of functional potency, alteration of Trp⁸, His¹² and Nle¹⁴ resulted in completely inactive peptides (analogues **7**, **11** and **13**). Smaller effects, about 4-fold loss of activity, could

be observed for Gln⁷, Val¹⁰, and β-Ala¹¹, whereas the functional potency of analogue **12** with substituted Phe¹³ dropped about 10-fold.

The results of the alanine scan of **18** concerning calcium mobilization and receptor affinity at BRS-3 are given in Table 4.3 and Figure 4.7.

Table 4.3: Functional potencies and receptor affinity of [D-Phe⁶,Phe¹³]Bn(6-13) propylamide (**18**) analogues in which individual amino acids were replaced by Ala or D-Ala, respectively.

no.	peptide	BRS-3		clogP
		-pEC ₅₀ ^a	Inhib. ^b	
14	AQWAVGHF-propylamide	5.08 ± 0.29	85 ^c	^d
15	aQWAVGHF-propylamide	5.02 ± 0.09	^d	-1.39
16	fAWAVGHF-propylamide	5.43 ± 0.07	93	^d
17	fQAAVGHF-propylamide	4.70 ± 0.16	42	^d
18	fQWAVGHF-propylamide	6.66 ± 0.18	99	^d
19	fQWAAGHF-propylamide	5.36 ± 0.10	99	^d
20	fQWAVAHF-propylamide	6.84 ± 0.08	87	^d
21	fQWAVGAF-propylamide	Inactive	89	^d
22	fQWAVGHA-propylamide	4.79 ± 0.05	85	^d

^a FLIPR-assay. Functional potencies are given in -pEC₅₀ ± SEM from 2-4 independent concentration-response curves, potencies on NMB-R and GRP-R were not determined. ^b Radioligand binding assay.^[222] Values are given in percent of control specific binding at 10 μM. ^c Two independent measurements at 0.1 μM. ^d Not determined. Additional experimental details are described in Table 4.2 and chapters 4.2.1 and 8.5.

The parent ligand **18** showed about 3-fold lower functional potency compared to **1**. Interestingly, the EC₅₀-value rose of about 1.5-fold when Gly at position 11 was substituted (**20**). All other replacements in **18** including N-terminal amino acids D-Phe⁶ and Gln⁷ led to a loss of functional potency. As in **1**, Trp⁸ and Phe¹³ are key residues for receptor activation. Upon replacement a significant drop of about 90-fold and 70-fold, respectively, was observed. However, contrary to **1**, substitution of His¹²

in **18** resulted in a completely inactive peptide. The importance of Trp⁸ is underlined by the receptor affinity data. However, no significant impact was observed when His¹² or Phe¹³ were altered.

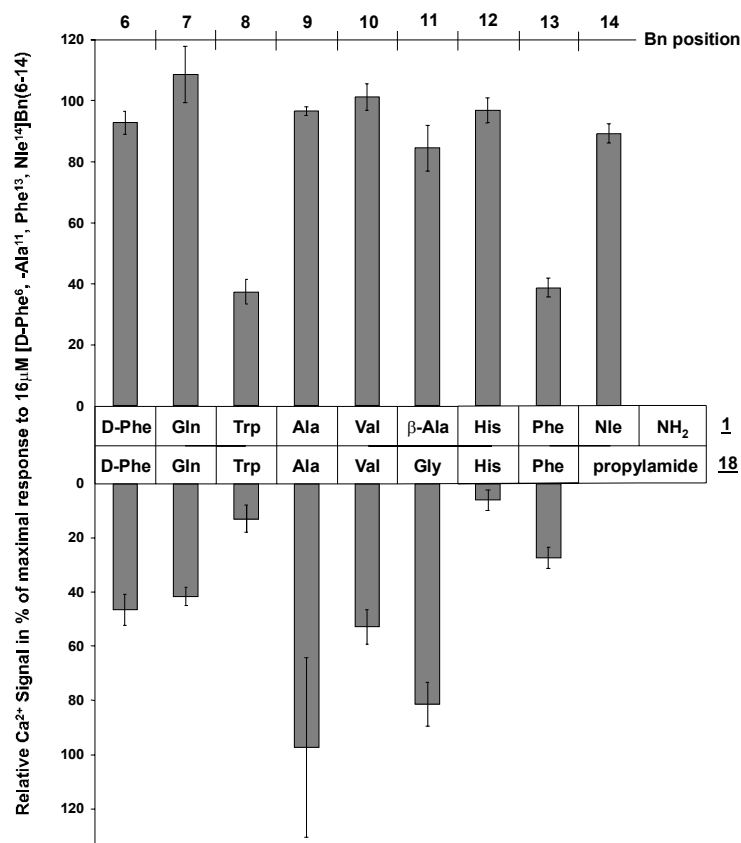


Figure 4.7: Effect on intracellular calcium mobilization of replacing single amino acids with Ala in $[D\text{-Phe}^6, \beta\text{-Ala}^{11}, \text{Phe}^{13}, \text{Nle}^{14}]\text{Bn}(6\text{-}14)$ (**1**) compared to $[D\text{-Phe}^6, \text{Phe}^{13}]\text{Bn}(6\text{-}13)$ propylamide (**18**) at 16 μM in BRS-3 transfected CHO α 16 cells. D-amino acids were substituted with D-Ala, β -Ala with Ala. Functional potencies from 2-3 independent measurements are given in percent \pm SEM relative to the Ca²⁺ response of **1**.

Structure activity studies revealed the importance of Trp⁸ and His¹² for biological activity of Bn,^[194] and Trp⁸ and Leu¹³ for the activity of Ac-Bn(7-14) on NMB-R and GRP-R,^[246] respectively. However, in a very recently published work^[292] functional potency was maintained on all three bombesin receptors when Trp⁸ was substituted by alanine in $[D\text{-Phe}^6, \beta\text{-Ala}^{11}, \text{Phe}^{13}, \text{Nle}^{14}]\text{Bn}(6\text{-}14)$ (**1**). This contradicts our

measurements, which showed in accordance with the studies mentioned above,^[194,246] that Trp⁸ in **1** as in other bombesin analogues is crucial for receptor activation and affinity (Table 4.2, Figure 4.7), although a change of its configuration did not greatly affect functional potency (Table 4.4). This result was even more confirmed by the structure activity studies performed on [D-Phe⁶,Phe¹³]Bn(6-13) propylamide (**18**) (Table 4.3, Figure 4.7). On the other hand, the reported significant reduction of the biological response on NMB-R and BRS-3 but not on GRP-R by replacement of Phe¹³ with alanine in **1**^[292] is consistent with our findings (Table 4.2, Figure 4.7). As for BRS-3, Trp⁸ and β -Ala¹¹ were found to be important for functional potency on GRP-R. Furthermore, contrary to a previous report^[292] we could not observe enhanced functional potency on GRP-R when D-Phe⁶ was replaced by alanine. However, there was a small increase when Val¹⁰ was substituted (Table 4.2).

4.3.3 D-Amino Acid Scans of [D-Phe⁶, β -Ala¹¹,Phe¹³,Nle¹⁴]Bn(6-14) and [D-Phe⁶,Phe¹³]Bn(6-13) propylamide

The effect on calcium mobilization at NMB-R, GRP-R and BRS-3 and receptor affinity at BRS-3 of substitution of an individual amino acid against its stereoisomer in **1** is shown in Table 4.4 and Figure 4.8.

In case of BRS-3 functional activity dropped about 400-fold when Phe¹³ was replaced. That the L-isomer is required at position 13 was also confirmed by radioligand binding data. Other substitutions also caused reductions in potency, especially those analogues with altered Ala⁹, Val¹⁰ and β -Ala¹¹ displayed about 50-140 fold lower EC₅₀-values. Relatively insensitive towards stereochemical changes were positions 6, 7 and, to a lesser degree also 12 and 14, where EC₅₀-values dropped about 4-6 fold and about 20-30 fold, respectively. At GRP-R functional potency dropped significantly when Trp⁸, Ala⁹, and also, to a lesser degree, the three C-terminal amino acids His¹², Phe¹³ and Nle¹⁴ were altered.

Table 4.4: Functional potencies and receptor affinity of [*D*-Phe⁶, β -Ala¹¹,Phe¹³,Nle¹⁴] Bn(6-14) (**1**) analogues in which individual amino acids were replaced by their stereoisomers.

no.	peptide	NMB-R	GRP-R	BRS-3	
		-pEC ₅₀ ^a	-pEC ₅₀ ^a	-pEC ₅₀ ^a	Inhib. ^b
23	FQWAV β AHF-Nle-NH ₂	5.54 \pm 0.09	8.17 \pm 0.06	6.60 \pm 0.31	100
24	f q WAV β AHF-Nle-NH ₂	5.17 \pm 0.07	8.44 \pm 0.07	6.46 \pm 0.10	100
25	fQ w AV β AHF-Nle-NH ₂	Inactive	6.11 \pm 0.06	5.65 \pm 0.10	80
26	fQW a v β AHF-Nle-NH ₂	Inactive	6.22 \pm 0.09	5.47 \pm 0.04	89
27	fQWAV β AHf-Nle-NH ₂	4.73 \pm 0.08	7.19 \pm 0.04	5.06 \pm 0.04	79
28	fQWAV α HF-Nle-NH ₂	5.18 \pm 0.06	7.56 \pm 0.07	5.40 \pm 0.05	74
29	fQWAV β AHf-Nle-NH ₂	4.78 \pm 0.04	6.38 \pm 0.03	5.74 \pm 0.08	94
30	fQWAV β AHF-Nle-NH ₂	Inactive	6.45 \pm 0.06	4.60 \pm 0.04	46
31	fQWAV β AHF- D -Nle-NH ₂	4.74 \pm 0.03	6.53 \pm 0.02	5.84 \pm 0.12	92

^a FLIPR-assay. Functional potencies are given in -pEC₅₀ \pm SEM from 3-6 independent concentration-response curves. ^b Radioligand binding assay.^[222] Values are given in percent of control specific binding at 10 μ M. Additional experimental details are described in Table 4.2 and chapters 4.2.1 and 8.5.

Nevertheless, as for the replacement with alanine, the importance of Phe at position 13 was much lower at GRP-R compared with BRS-3 or NMB-R. Contrary to BRS-3, at NMB-R and GRP-R position 11 showed low sensitivity concerning stereochemical changes with reductions of about 7-fold at NMB-R and approximately 3-fold at GRP-R. As for BRS-3, at both receptors NMB-R and GRP-R, N-terminal amino acids could be exchanged by their stereoisomeric counterparts without much impact on functional potency.

Table 4.5: Functional potencies and receptor affinity of [D-Phe⁶,Phe¹³]Bn(6-13) propylamide (**18**) analogues in which individual amino acids were replaced by their stereoisomers.

no.	peptide	BRS-3
		-pEC ₅₀ ^a
32	FQWAVGHF-propylamide	5.44 ± 0.06
33	fqWAVGHF-propylamide	5.35 ± 0.02
34	fQwAVGHF-propylamide	4.80 ± 0.12
35	fQWaVGHF-propylamide	Inactive
36	fQWAvGHF-propylamide	Inactive
37	fQWAVaHF-propylamide	4.96 ± 0.21
38	fQWAVGhF-propylamide	4.66 ± 0.49
39	fQWAVGHf-propylamide	Inactive

^a FLIPR-assay. Functional potencies are given in -pEC₅₀ ± SEM from 2-4 independent concentration-response curves, potencies on NMB-R and GRP-R were not determined. Additional experimental details are described in Table 4.2 and chapters 4.2.1 and 8.5.

Stereochemical changes in **18** basically resulted in inactive peptides at BRS-3 as shown in Table 4.5 and Figure 4.8. Only analogues **32** and **33** with changed D-Phe⁶ and Gln⁷ retained modest functional activity.

As already pointed out in chapter 4.3.2, the presence of the phenyl-ring at position 13 had a low significance for functional activity on GRP-R. Moreover, it could now be demonstrated, that an L-configuration at position 13 is absolutely necessary for functional potency on BRS-3 but not on GRP-R (Table 4.4, Figure 4.8). This fits very well into the picture that the sidechain of position 13 is less important for the activation of the GRP-R. A previous study^[287] already pointed out that the residue in position 13 is important for selectivity of NMB-R over GRP-R. However in Ac-Bn(7-14), Leu¹³ was approximately equally important for both, NMB-R and GRP-R.^[246]

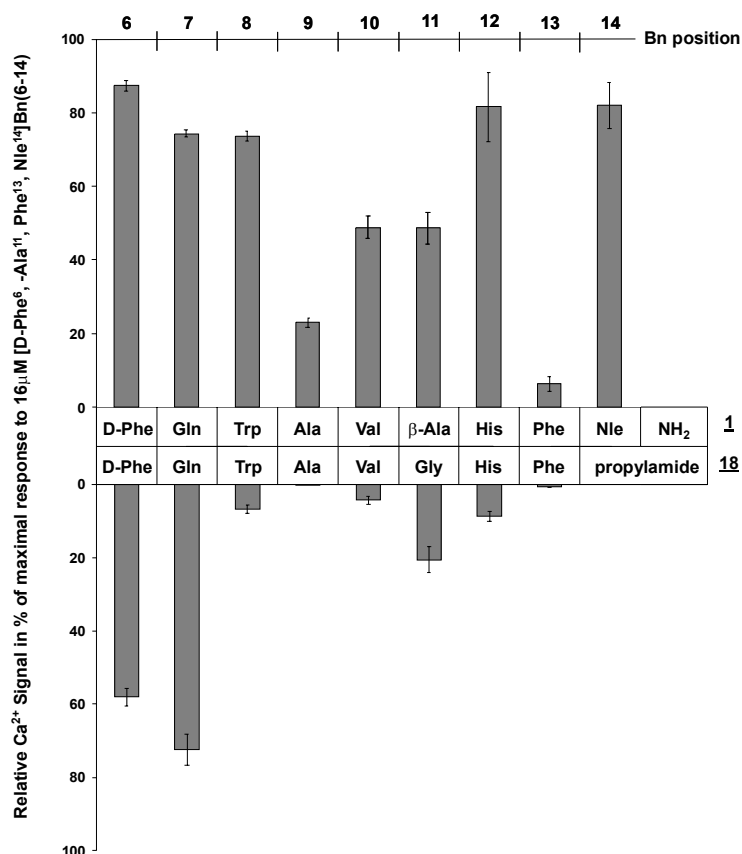


Figure 4.8: Effect on intracellular calcium mobilization of replacing individual amino acids against their stereoisomeric form in $[D\text{-Phe}^6, \beta\text{-Ala}^{11}, \text{Phe}^{13}, \text{Nle}^{14}]\text{Bn}(6\text{-}14)$ (**1**) compared to $[D\text{-Phe}^6, \text{Phe}^{13}]\text{Bn}(6\text{-}13)$ propylamide (**18**) at $16 \mu\text{M}$ in BRS-3 transfected CHO α 16 cells. Gly and β -Ala were substituted with D-Ala. Functional potencies from 3 independent measurements are given in percent \pm SEM relative to the Ca^{2+} response of **1**.

4.3.4 Shortened Fragments and Substitutions

The alanine- and D-amino acid scans of the two peptides **1** and **18** revealed a remarkable difference in their biological response. This was quite surprising because the difference in their amino acid sequence is limited and furthermore contained to two positions, namely position 11, with β -Ala in **1** and Gly in **18** and the C-terminus, where **1** bears a Nle instead of *n*-propylamide in **18**. In order to better understand this phenomenon, the two peptides **40** and **41** were prepared. They should allow a better comparison between **1** and **18** (especially **41**), and an interpretation of the results described in the previous two chapters (Table 4.6).

Table 4.6: Functional potencies and receptor affinity of [*D*-Phe⁶, β -Ala¹¹,Phe¹³,Nle¹⁴]Bn(6-14) (**1**) analogues in which Ala⁹ and β -Ala¹¹ were substituted against Gly.

no.	peptide	NMB-R	GRP-R	BRS-3		clogP
		-pEC ₅₀ ^a	-pEC ₅₀ ^a	-pEC ₅₀ ^a	Inhib. ^b	
40	fQWGV β AHF-Nle-NH ₂	4.85 \pm 0.12	7.83 \pm 0.08	5.97 \pm 0.13	^c	-0.07
41	fQWAVGHF-Nle-NH ₂	5.81 \pm 0.08	7.72 \pm 0.09	5.64 \pm 0.06	97	0.04

^a FLIPR-assay. Functional potencies are given in -pEC₅₀ \pm SEM from 3-5 independent concentration-response curves. ^b Radioligand binding assay.^[222] Values are given in percent of control specific binding at 10 μ M. ^c Not determined. Additional experimental details are described in Table 4.2 and chapter 4.2.1 and 8.5.

Peptide **40** showed a decreased functional potency especially on BRS-3 and NMB-R. Compound **41** was synthesized to further elucidate the importance of position 11 and for comparison between **1** and **18**. Replacement of β -Ala¹¹ by Gly (**41**) led to a tremendous, about 35-fold reduction of functional potency at BRS-3 but only to small, about 2-fold declines at NMB-R and GRP-R.

Interestingly, the absence of the imidazole ring at position 12 caused no major loss of functional potency on BRS-3 in **1** but, similar to the observation for Bn,^[194] in **18** (Table 4.2 and 4.3, Figure 4.7). The explanation for this shift of importance probably lies within the one carbon atom elongated backbone structure at position 11 in **1** compared to **18** (β -Ala exchanged vs. Gly). However contrary to that, Leu at position

13 was important for receptor affinity at NMB-R and GRP-R in Ac-Bn(7-14).^[246] The discovery of the highly potent BRS-3 agonist **1**^[222] and the more selective analogues, which were obtained by manipulation of position 11,^[242] also demonstrated the crucial role of this position in BLPs concerning BRS-3 activity and selectivity over the other bombesin receptors NMB-R and GRP-R. Comparison of peptide **1** with β -Ala¹¹, peptide **10** with Ala¹¹ and peptide **41** with Gly¹¹ showed that functional potency decreased drastically in the order β -Ala > Ala > Gly on BRS-3, whereas functional potency concerning NMB-R and GRP-R is less affected. This corresponds very well with previous results.^[292] Interestingly, a similar order of functional potency on BRS-3 was observed for peptides **18** and **20** with Ala > Gly. However, analogues of **18** with variation at position 11 showed higher functional potency compared with their corresponding analogues of **1**. With the exception of positions 6 and 7 a change in the stereochemistry of **18** resulted in inactive peptides (Table 4.5, Figure 4.8). When compared to the corresponding D-amino acid scan analogues of **1** this negative trend can also be at least partially attributed to the difference in backbone length at position 11, which obviously makes the bioactive conformation of peptide **18** more sensitive towards stereochemical changes.

Concluding from the results of the alanine- and D-amino acid scans, it was speculated that the easiest way to obtain shorter BRS-3 active compounds was to simply delete amino acids from the C- and especially D-Phe⁶ and Gln⁷ from the N-terminus. Therefore, in a next step N-terminal and/or C-terminal shortened fragments of **1** with acylated N-terminus and analogues, in which individual amino acids are substituted, were prepared (Table 4.7).

The effect of N-terminal deletion of D-Phe⁶ and Gln⁷ and simultaneous variation of position 11 by insertion of Gly, Ala, β -Ala and γ -amino-butyric acid was studied in a series of compounds, namely **42-49**. In order to avoid possible negative influence of an N-terminal charge each peptide analogue was additionally prepared in the N-terminal acetylated form (peptides **43**, **45**, **47** and **49**). All truncated fragments showed reduced functional activity with β -Ala > γ -amino-butyric acid > Gly > Ala on BRS-3 and interestingly also on GRP-R.

Table 4.7: Functional potencies and receptor affinity of [D-Phe⁶,β-Ala¹¹,Phe¹³,Nle¹⁴] Bn(6-14) (1) analogues in which N-terminal and/or C-terminal amino acids are deleted, individual amino acids are substituted and the N-terminus is acetylated.

no.	peptide	NMB-R	GRP-R	BRS-3		clogP
		-pEC ₅₀ ^a	-pEC ₅₀ ^a	-pEC ₅₀ ^a	Inhib. ^b	
42	WAVGHF-Nle-NH ₂	Inactive	6.02 ± 0.04	4.93 ± 0.05	60	0.94
43	Ac-WAVGHF-Nle-NH ₂	4.75 ± 0.07	6.22 ± 0.02	4.93 ± 0.02	61	0.9
44	WAVAHF-Nle-NH ₂	Inactive	5.86 ± 0.05	4.76 ± 0.04	24	1.25
45	Ac-WAVAHF-Nle-NH ₂	Inactive	5.75 ± 0.01	Inactive	40	1.21
46	WAVβAHF-Nle-NH ₂	Inactive	6.89 ± 0.13	5.29 ± 0.06	80	1.14
47	Ac-WAVβAHF-Nle-NH ₂	Inactive	7.45 ± 0.06	5.70 ± 0.10	98	1.11
48	WAVXHF-Nle-NH ₂ ^c	Inactive	6.18 ± 0.03	5.33 ± 0.05	82	1.35
49	Ac-WAVXHF-Nle-NH ₂ ^c	Inactive	6.45 ± 0.04	5.17 ± 0.06	78	1.31
50	wAVβAHF-Nle-NH ₂	Inactive	6.86 ± 0.07	4.72 ± 0.01	79	1.14
51	Ac-wAVβAHF-Nle-NH ₂	Inactive	6.70 ± 0.07	5.49 ± 0.10	95	1.11
52	WAVβAYF-Nle-NH ₂	4.88 ± 0.01	5.85 ± 0.02	4.76 ± 0.02	< 10	2.88
53	Ac-WAVβAYF-Nle-NH ₂	4.71 ± 0.12	6.17 ± 0.11	4.76 ± 0.01	< 10	2.84
54	fQWAVβAYF-Nle-NH ₂	4.74 ± 0.04	7.78 ± 0.13	5.01 ± 0.10	< 10	1.97
55	fQWAVβAHF	Inactive	Inactive	4.77 ± 0.37	92	1.21
56	WAVβAHF	Inactive	Inactive	Inactive	< 10	-1.23
57	Ac-WAVβAHF	Inactive	Inactive	Inactive	< 10	1.0

^a FLIPR-assay. Functional potencies are given in -pEC₅₀ ± SEM from 2-5 independent concentration-response curves. ^b Radioligand binding assay.^[222] Values are given in percent of control specific binding at 10 μM. ^c X = γ-amino-butyric acid. Additional experimental details are described in Table 4.2 and chapters 4.2.1 and 8.5.

Functional potency of **46** at BRS-3 with β-Ala¹¹ increased with N-terminal acetylation approximately 2.5-fold. This strategy had an opposite effect when applied to **48** with γ-amino-butyric acid at position 11, where activity dropped slightly about 1.5-fold.

Changing the stereochemistry at the N-terminal position 8 of analogues **46** and **47** resulted in peptides **50** and **51**, where functional potency was even slightly more reduced. Most interestingly, substitution of His¹² by Tyr led to a selective GRP-R agonist **54**, which showed only about 2-fold reduced activity at GRP-R but almost eradicated functional response at NMB-R and BRS-3. C-terminal modification of the amide into a carboxylic acid (compound **55**) resulted in a huge loss of functional response on all three receptors. However, receptor affinity at the BRS-3 was almost retained. Peptides **56** and **57** with truncated C-terminal Nle¹⁴-amide and N-terminal D-Phe⁶ and Gln⁷ were completely inactive.

As already observed for the comparison between **1** and **18** (Tables 4.2, 4.4 and 4.6), the series of N-terminally truncated compounds **42-49** also confirmed that position 11 is obviously optimized with β -Ala on BRS-3 and also on GRP-R (Table 4.7). However, for the truncated compounds the order for Ala and Gly was flipped to Gly > Ala.

Interestingly, high selectivity for GRP-R of the unselective agonist **1** could be achieved by a single substitution of His¹² against Tyr (Table 4.7). The reasons for this selectivity as can be concluded from the aforementioned results rather lie in the presence of the tyrosine side chain than in the absence of the imidazole-ring of the histidine. It can be speculated, that the orientation of the adjacent phenyl ring at position 13, which is crucial for selectivity at GRP-R over NMB-R and BRS-3, is unfavorably affected by this substitution.

Although residues at positions 6, 7 and, with the exception of NMB-R, also 14 seemed not to be necessary for functional potency on all three receptors as determined by the alanine- and D-amino acid scans, it was not possible to obtain equally active shorter fragments by simple deletion (Table 4.7). Therefore it can be concluded, that **1** or **18**, respectively, or their one N-terminal amino acid shortened fragments are minimum active BLP-derived fragments. This agrees well with the minimum length of the NMB sequence that is required for retention of full BRS-3 activity.^[281,292] Comparable results were also obtained in a minimal ligand analysis for GRP.^[239]

4.3.5 Cyclic Analogues of [D-Phe⁶,β-Ala¹¹,Phe¹³,Nle¹⁴]Bn(6-14)

4.3.5.1 Introduction and Strategy

Because a simple deletion of amino acids at the two termini of **1** was not a successful strategy to obtain equally active shorter fragments we pursued two different and separate attempts in order to receive functional potent and selective BRS-3 compounds with an increased activity and/or a reduction of molecular weight down to about 500 Da. The first strategy was to synthesize cyclic peptide analogues of **1**, which is described in this chapter. In a second approach, which is described in chapter 4.3.6, we attached the pharmacophores onto a molecular scaffold.

Cyclization of linear peptides has become a general approach for the generation of lead structures and for the elucidation of bioactive conformations.^[336-338]

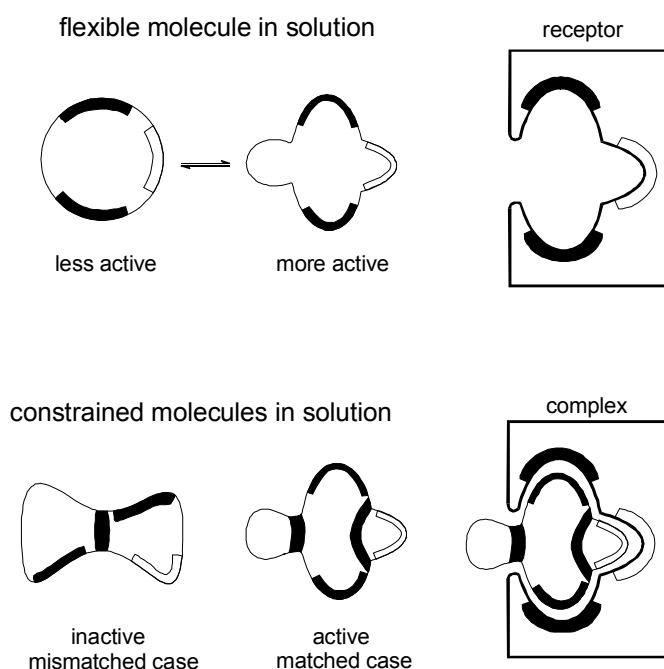


Figure 4.9: Flexible molecules (e.g. linear peptides) can have many different conformations in solution. Cyclization restricts the number of possible conformations.

Cyclization of peptides has two major implications:

- The degree of conformational freedom of the peptide backbone is drastically reduced.
- The stability against proteases of the peptide is increased.

Most linear peptides can be considered as very flexible in solution. They can adopt many different conformations, which even may be energetically relatively equally favored. Cyclization fixes the 3D structure of the peptide because it leads to a reduction of the possible number of conformations and to the preferential population of only a few thereof. In case where, by accident, the ‘bioactive’ conformation of the peptide is matched (‘matched-case’), cyclization can lead to a tremendous increase in affinity or activity at the receptor because of a decrease in entropy (Figure 4.9). Furthermore, an increase in selectivity for a certain receptor is also a possible consequence. On the other hand, if the linear peptide is forced into an unfavorable conformation (‘mismatched-case’), the introduction of such a sterical constraint can also lead to a complete loss of the biological activity (Figure 4.9). The increase in proteolytical stability is important, if the development of a drug is pursued, because the metabolic stability of linear peptides usually is very limited.

We have seen many examples where cyclization of a linear peptide has led to a dramatic increase in biological activity.^[243,337,339-344] In the ‘ideal’ case, the amino acids important for biological activity were found to be next to each other in the primary sequence of the natural ligand.^[345-355] Then, a reasonable approach usually proved to be the generation of systematic libraries of stereoisomeric cyclic penta- and hexapeptides.^[337,340] The structure of cyclic penta- and hexa- modelpeptides has been studied thoroughly in our group.^[336,356,357] The conformation of homodetic, cyclic peptides is mainly determined by the configuration of its amino acids. It is known, that D-amino acids in general and especially D-proline prefer the $i+1$ position of a β II’ and a β I-turn, respectively.^[336,356] Cyclic hexapeptides are often comprised by two β -turns,^[358] for cyclic pentapeptides, two ‘most important’ conformations, the β,γ - and the γ,γ -conformation have been proposed.^[336,359,360] The important implication for the

systematic search for new lead structures in drug design of these studies is, that due to this simple tool which, to a certain degree, enables to distinctly manipulate and ‘freeze’ the comparatively rigid conformation of cyclic penta- and hexapeptides, a systematic spatial screening by insertion of a single D-amino acid at different positions becomes possible.^[361,362]

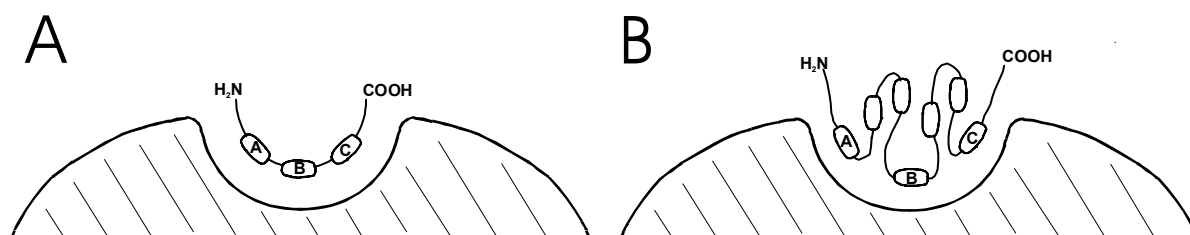


Figure 4.10: *Topography of epitopes of peptides when bound to the receptor. Amino acids A, B and C of the epitope are A) adjacent to each other-synchronous message; B) non-adjacent to each other-asynchronous message.*

Obviously, this case was more complicated: The alanine and D-amino acid scans indicated that there are four additional amino acids between the pharmacophoric important amino acids, namely Trp⁸ and Phe¹³. Although there are different suggestions about the exact bioactive conformation of bombesin and related peptides,^[201,231,242-246] it is feasible that they adopt a bend-like structure. This is supported by the fact that a β -turn mimetic could successfully replace the dipeptide Val-Gly in conformational constrained bombesin analogues.^[247] Taken together, this gave rise to the assumption that peptide **1** forms a secondary structure in which these amino acids are – although not adjacent in the primary sequence – spatially located close to each other (Figure 4.10). Consequently, a spatial screening by systematic manipulation of the configuration of single amino acids in a head-to-tail cyclized nonapeptide **1** as described above for libraries of penta- and hexapeptides^[337,340] was not considered as a promising strategy because of the following reasons:

- In case when several pharmacophoric amino acids are adjacent the conformational decisive area is usually limited to these amino acids. In this case however, the task

of accidentally fixing the bioactive conformation of a nonapeptide, which had turned out to be the minimum active fragment (see chapter 4.3.4), was pursued. In other words, besides the correct orientation of the pharmacophoric groups, their spatial distance was unknown.

- Because of the lack of spatial distance information with respect to the crucial amino acids Trp⁸ and Phe¹³, the probability to fix these residues in a wrong distance was very high. Furthermore, no information was available that allowed the assumption that a head-to-tail cyclization would provide the correct distances.

Moreover, because of the assumed high flexibility in both, the native linear and a potential cyclic nonapeptide **1**, a NMR-supported structure analysis leading to a more structure-based rational design was not feasible.^[243]

Because of the aforementioned reasons, a combinatorial approach for the introduction of a conformational constraint by means of cyclization where both, stereochemistry and spatial distances would be varied simultaneously was considered as being most promising. Recently, Liskamp *et al.* introduced the concept of the ‘rolling loop scan’ by connecting the side chains of bis-*N*-alkylated peptides by means of ring-closing metathesis.^[363] Thereby, loops of any desired size and position connecting two peptide amide bonds could be formed. Inspired by this approach we applied a similar combinatorial concept for **1** (Figure 4.11, A). Loops were introduced by oxidative connection of two inserted Cys or D-Cys, respectively.^[243,339,342,343,364-368] Therefore, all possible positions except Trp⁸, Phe¹³ and β -Ala¹¹, which were found to be important for functional activity at BRS-3 (see chapter 4.3.2 and 4.3.3), were substituted. Because our results and previous findings suggested, that β -Ala¹¹ can be considered as the pivotal point of the proposed bend-like structure of the molecule,^[201,231,242-246] not at least because of structural parallels to somatostatin analogues, each position lower than that of β -Ala¹¹, namely 6, 7, 9, and 10, was linked to one of the two higher positions 12 and 14 by cystine formation. Insertion of Cys and D-Cys, respectively, at each position generated all four possible stereoisomers for each possible loop size, which ranged from 3-9 amino acids.

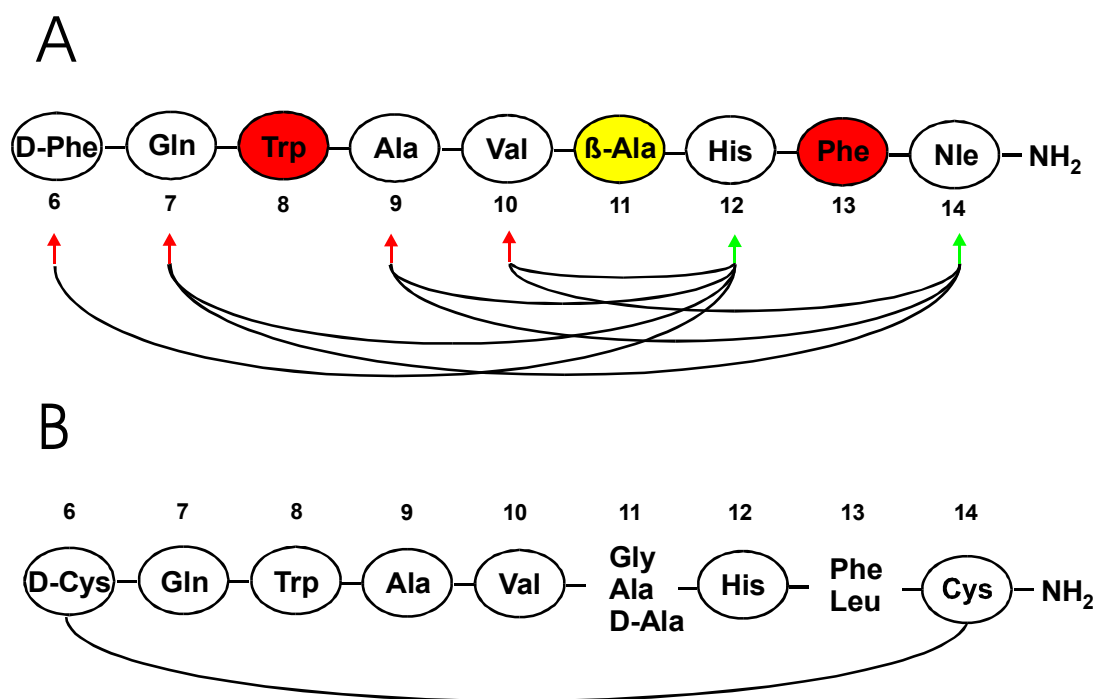


Figure 4.11: *A) Combinatorial “rolling loop-scan” of 1. Two amino acids at one time were replaced by Cys or D-Cys, respectively, except those with high (red-colored) and medium (yellow) significance for functional activity, to form disulfide-bridged cyclic peptides of varying loop size after oxidation. Arrows mark the position of the connecting disulfide-bridge. B) Published derivatives^[243] with variations at position 11 and 13 were synthesized for comparison.*

4.3.5.2 Synthesis

Parallel automated synthesis of the linear precursors of the heterodetic cystine peptides **58-94** was carried out on a multiple peptide synthesizer SyRoll using standard Fmoc/*t*Bu-strategy,^[303-306] HOBt/TBTU activation^[324,325] and Sieber amide resin^[308] as described in chapter 8.2.1 and 8.3.2. The following synthesis, which included cleavage of the linear peptide from solid support, deprotection and oxidative cyclization could efficiently be carried out as a single process, which can be characterized by repeated steps of addition/reaction/concentration and precipitation (chapter 8.2.1 and 8.3.2). This became possible because only a small amount of by-

products were formed during this process and DMSO was used as oxidative agent (see below).

It is known that especially Cys and Trp are susceptible to various side reactions during the cleavage/deprotection process including alkylation by cations produced under highly acidic conditions without appropriate quenching^[302-304] or reduction of the indole ring of the tryptophan with silanes/TFA.^[369] These problems were effectively circumvented by the use of:

- Triisopropylsilane, which is superior to other scavenger systems,^[329,330] provides irreversible quenching and furthermore has a lower reduction potential towards Trp than *e.g.* triethylsilane.^[369]
- Trp(Boc), which under strong acidic conditions forms the stable and indole-protecting *N*-carboxy indole^[331,370] resulting from the incomplete cleavage of the Boc-protecting group under highly acidic conditions.

Destruction of the *N*-carboxy indole was achieved during the oxidation process in aqueous solution^[331,370] as described below. The triphenylmethane, which was formed during deprotection of the Cys and His and quenching with triisopropylsilane, was removed by precipitation of the peptide in ice-cold ether. Thereby the triphenylmethane stayed in solution and was separated by simple decantation after centrifugation.

Among the various cystein oxidation methods, which include air oxidation in aqueous solution,^[371-373] iodine,^[374,375] thallium trifluoroacetate^[376] or $K_3Fe(CN)_6$,^[377,378] we preferred the DMSO-mediated oxidation^[379,380] because of the following advantages:^[367]

- Reagents such as the highly toxic thallium trifluoroacetate, iodine or $K_3Fe(CN)_6$ are strongly oxidative and afford careful adjustment of the reaction conditions in order to avoid overoxidation.^[381] Furthermore, sidechains such as Trp and His are susceptible to side reactions.^[375]

- Oxidation with air oxygen is equally mild as DMSO. However, unlike DMSO,^[379,382] air oxidation sometimes affords careful adjustment of the pH, otherwise the reaction proceeds very slow or incomplete.^[373,378]
- The use of strong oxidative agents such as the ones described above affords additional workup procedures.^[378,383]
- DMSO is an excellent solvent for peptides.

The oxidation process was carried out in a 50% aqueous DMSO (v/v) solution. In principle, lower DMSO concentrations can also be used without limitations.^[367] However in this case, the DMSO also served as a solvent because of the low solubility of the peptides in water. In order to prevent intermolecular dimerization and oligomerization, the reaction was carried out at peptide concentrations of approximately $c = 5 \times 10^{-4}$ M.

Furthermore, it is noteworthy that the yields of the deprotection/cyclization-step did not depend on the size of the ring - yields ranged from 44-69% after HPLC purification (data not shown).

4.3.5.3 Biological Evaluation

In a previous work, Coy *et al.* studied the effect of several covalently cyclized bombesin analogues on basal and bombesin-stimulated amylase release in rat pancreatic acini.^[243] It was found, that cyclo[6,14][D-Cys⁶,Cys¹⁴]Bn(6-14) (**90**) was an amylase releasing agonist with an EC₅₀ of 187 nM.^[243] Furthermore, the activity of this agonist could be enhanced by substituting D-Ala for Gly at position 11 (peptide **91**).^[243] These compounds as well as some more NMB-like analogues with Phe at position 13 instead of Leu (peptides **93** and **94**, Figure 4.11, B) were prepared for comparison with peptides **58-89**.

As can be taken from Table 4.8 none of the cystine-bridged peptides including the reported agonist **90** on rat pancreatic acini displayed considerable activation of the BRS-3 receptor in the FLIPR-assay.

Table 4.8: Functional potencies of disulfide-bridged cyclic analogues of [*D*-Phe⁶, β -Ala¹¹,Phe¹³,Nle¹⁴]Bn(6-14) (**1**).

no.	peptide	BRS-3		
		-pEC ₅₀ ^a	E _{max} ^a	clogP
74	cyclo[6,12][Cys ^{6,12} , β -Ala ¹¹ ,Phe ¹³ , Nle ¹⁴]Bn(6-14)	4.76 ± 0.01	10 ± 5	1.35
75	cyclo[6,12][<i>D</i> -Cys ⁶ , β -Ala ¹¹ ,Cys ¹² ,Phe ¹³ , Nle ¹⁴]Bn(6-14)	4.89 ± 0.01	23 ± 8	1.35
76	cyclo[6,12][Cys ⁶ , β -Ala ¹¹ , <i>D</i> -Cys ¹² ,Phe ¹³ , Nle ¹⁴]Bn(6-14)	4.76 ± 0.04	30 ± 3	1.35
77	cyclo[6,12][<i>D</i> -Cys ^{6,12} , β -Ala ¹¹ ,Phe ¹³ , Nle ¹⁴]Bn(6-14)	4.79 ± 0.02	23 ± 2	1.35
85	cyclo[9,12][<i>D</i> -Phe ⁶ , <i>D</i> -Cys ^{9,12} , β -Ala ¹¹ ,Phe ¹³ ,Nle ¹⁴]Bn(6-14)	4.92 ± 0.05	27 ± 5	1.88
87	cyclo[10,12][<i>D</i> -Phe ⁶ , <i>D</i> -Cys ¹⁰ , β -Ala ¹¹ ,Cys ¹² ,Phe ¹³ ,Nle ¹⁴]Bn(6-14)	4.91 ± 0.01	15 ± 4	0.63

^a FLIPR-assay. Functional potencies are given in -pEC₅₀ ± SEM from 2-3 independent concentration-response curves, potencies on NMB-R and GRP-R were not determined. E_{max} represents the Ca²⁺ signal at 16 μ M in percent of maximal response of **1**. Additional experimental details are described in Table 4.2 and chapters 4.2.1 and 8.5.

Only modest activities with EC₅₀-values of less than 10 μ M and a receptor activation of maximal 30% compared to **1** was observed for compounds **74-77**, which have been cyclized between position 6 and 12 (former *D*-Phe⁶ and His¹²). Furthermore, peptide **85** with cyclization points between position 9 and 12, and compound **87** to an even lower degree, have some residual activity. Although this approach did not render the aimed increase in activity, some conclusions can be drawn:

- The observation, that cyclic peptides can (although only moderately) activate the receptor supports the assumption that **1** is present in a kinked structure when bound to the receptor.
- The fact that peptide **90** and derivatives thereof (Figure 4.11, B) could not address the BRS-3 receptor in the FLIPR-assay although it is a reported agonist on rat pancreatic acini^[243] has its cause in the selectivity of this compound for the NMB/GRP receptors or is due to the difference of the used test-systems.

4.3.6 Discovery of the Tetrapeptide Lead-Structure

The evaluation of N- or C-terminal deleted fragments made clear that **1**, or its by D-Phe⁶ truncated fragment, already was a minimum active BLP-derived fragment concerning functional activity at BRS-3. Therefore a different approach was attempted to obtain smaller lead structures. Using the knowledge obtained from the results described above and considering the hypothesis, that the spatial distance between Trp⁸ and Phe¹³ in the bioactive conformation of **1** is small due to a turn induced around position 11, [201,231,242-246] a tetrapeptide was designed (Figure 4.12).

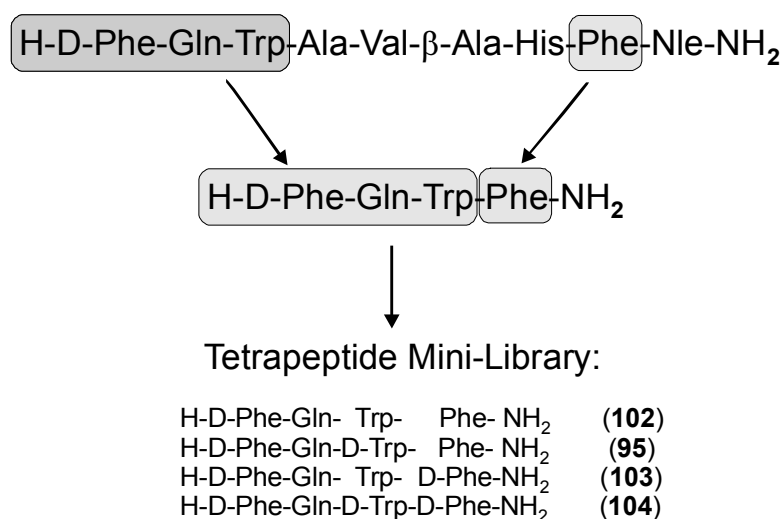


Figure 4.12: A tetrapeptide consisting of the three N-terminal amino acids of [*D*-Phe⁶,β-Ala¹¹,Phe¹³,Nle¹⁴]Bn(6-14) (**1**) and Phe-NH₂ formed the basis of a four membered mini-library. The peptides with permuted stereochemistry at the two C-terminal amino acids presented the residues Trp and Phe or their stereoisomers at two different distances.

It consisted of the three N-terminal amino acids of **1** and Phe-NH₂ (compound **102**) and formed the basis of a four-membered mini-library (compounds **95**, **102-104**). The peptides with permuted stereochemistry at the two C-terminal amino acids presented the residues Trp and Phe or their stereoisomers at two different distances.

4.3.6 Systematic SAR of Tetrapeptide Lead

Functional potency and receptor affinity at BRS-3 of the four membered mini-library (peptides **95**, **102-104**) and modified analogues are shown in Table 4.9. To our very surprise, compound **95** clearly showed residual activity with an EC₅₀-value of about 10 μM in the FLIPR-assay.

Table 4.9: Functional potencies from 2-5 independent concentration-response curves and receptor affinity of the tetrapeptide mini-library (peptides **95**, **102-104**) and analogues in which individual amino acids were substituted.

no.	peptide	BRS-3		clogP
		-pEC ₅₀ ^a	Inhib. ^b	
95	fQwF-NH ₂	5.00 ± 0.09	15	0.1
96	Ac-fQwF-NH ₂	Inactive	25	^c
97	aQwF-NH ₂	Inactive	< 10	^c
98	fAwF-NH ₂	4.82 ± 0.10	26	-0.34
99	fQaF-NH ₂	Inactive	< 10	-1.31
100	fQWA-NH ₂	Inactive	< 10	-1.32
101	FQwF-NH ₂	5.05 ± 0.03	14	0.1
102	fQWF-NH ₂	Inactive	11	0.1
103	fQWf-NH ₂	Inactive	< 10	0.1
104	fQwf-NH ₂	Inactive	19	0.1
105	fNwF-NH ₂	5.08 ± 0.08	27	0.79
106	fβAwF-NH ₂	Inactive	13	1.8
107	fQwF	Inactive	< 10	-0.95

^a FLIPR-assay. Functional potencies are given in -pEC₅₀ ± SEM from 2-5 independent concentration-response curves. All compounds are inactive on NMB-R and GRP-R except **95** with -pEC₅₀ of 4.76 ± 0.01 on GRP-R, functional activity of **96** on NMB-R and GRP-R was not determined. ^b Radioligand binding assay.^[222] Values are given in percent of control specific binding at 10 μM. ^c Not determined. Additional experimental details are described in Table 4.2 and chapters 4.2.1 and 8.5.

N-terminal acetylation resulted in a loss of functional activity (**96**), however, enhanced receptor affinity was observed. Analogues of **95**, in which amino acids were replaced by alanine (**97-100**) indicated the importance of the three aromatic residues whereas removal of the sidechain of Gln even slightly increased receptor affinity. Analogues with modified stereochemistry (compounds **101-104**) demonstrated the intolerance towards C-terminal alterations as well as the necessity of a D-conformation at the Trp-residue (**102**). On the other hand, functional potency was retained when stereochemistry was changed at the N-terminal D-Phe (**101**). As expected from the aforementioned results, Gln could be replaced by Asn (**105**). However, β -Ala was not tolerated (**106**). Again, C-terminal removal of the lipophilic amide resulted in a compound without functional response (**107**).

4.3.7 C-Terminal Optimization

In a next step C-terminally modified analogues of the discovered tetrapeptide lead-structure **95** were prepared (Table 4.10). Formally, the C-terminal Phe-NH₂ group was replaced by differently substituted arylamines.

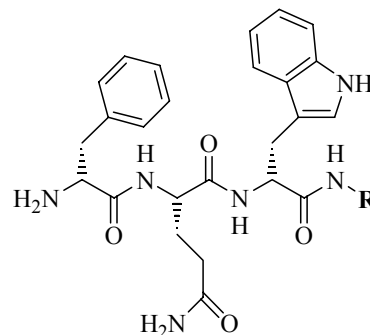


Table 4.10: Functional potencies and receptor affinity of C-terminally modified analogues of **95**.

no.	R	BRS-3		
		-pEC ₅₀ ^a	Inhib. ^b	clogP
108	Benzyl-	Inactive	49	1.09
109	1-(2-Phenylethyl)-	6.15 ± 0.08	82	1.3
110	1-[2-(3, 4-Dimethoxyphenyl)ethyl]-	Inactive	< 10	0.96
111	1-[2-(4-Bromophenyl)ethyl]-	5.68 ± 0.07	58	1.7
112	1-(Pyridine-2-ylethyl)-	5.97 ± 0.06	16	-0.19
113	1-[(<i>R</i>)-(+)-β-Methylphenylethyl]-	5.63 ± 0.05	59	1.7
114	1-[(<i>S</i>)-(-)-β-Methylphenylethyl]-	5.58 ± 0.09	51	1.7
115	1-(2,2-Diphenylethyl)-	Inactive	28	^c

^a FLIPR-assay. Functional potencies are given in -pEC₅₀ ± SEM from 2-5 independent concentration-response curves. All compounds were tested inactive on NMB-R and GRP-R. ^b Radioligand binding assay.^[222] Values are given in percent of control specific binding at 10 μM. ^c Not determined. Additional experimental details are described in Table 4.2 and chapters 4.2.1 and 8.5.

Most importantly, incorporation of a 1-(2-phenylethyl)-residue (**109**) increased functional potency about 15-fold. Insertion of a benzyl-moiety resulted in a loss of functional activity (**108**), which demonstrated that the carbon chain length is crucial. Aromatic substitutions (**110** and **111**) or replacement of phenyl- by 2-pyridyl- (**112**) did not further improve functional potency. Interestingly, compound **112** showed almost equal functional potency compared to **109** but much lower receptor affinity. Sterical constraints (**113** and **114**) reduced functional response about 2-fold compared

to **109**, incorporation of a 1-(2,2-diphenylethyl)-residue (**115**) resulted in a completely inactive compound. Compounds **108-115** did not induce calcium mobilization on the NMB-R and GRP-R.

Furthermore, compound **95** (Table 4.9) suggests that a relative proximity of the residues Trp⁸ and Phe¹³ in the bioactive conformation of **1** is very probable. The same conclusion can be drawn from the recently described antagonists for the NMB-R, GRP-R^[253,254] and related receptors (see chapter 3.2.3). Although these compounds have been developed by similar strategies,^[35,36,252] a successful shortening of the sequence required for BRS-3 activation as represented by compound **95** was very surprising. Systematic SAR of the lead structure **95** revealed that all three aromatic residues are necessary for functional potency on BRS-3 (Table 4.9). Furthermore, a D-conformation for the Trp seemed to be mandatory (Table 4.9). Our first attempts to optimize the lead structure **95** were directed towards the C-terminus (Table 4.10). As expected, the transformation of the C-terminal amide group into a free carboxylic acid was unfavorable for functional potency on BRS-3 (Table 4.7 and 4.9) because most naturally occurring peptides including the bombesin-like peptides are C-terminally amidated. Moreover, a comparison of compounds **18** and **41** showed that deletion of the C-terminal amide group even raised BRS-3 functional potency. Based on this observation we rationalized that further increased C-terminal lipophilicity by removal of the C-terminal amide group would lead to a substantial increase of functional activity of the lead structure **95**. This concept worked very well, within our studies the unsubstituted 1-(2-phenylethyl)amide (compound **109**) proved to be the most suitable C-terminal structural moiety (Table 4.10). Structural constraints did not improve functional response, too lipophilic residues were not tolerated (Table 4.10). Gln was incorporated into the structure of compound **95** because it was part of the N-terminal tripeptide sequence of peptide **1** (Figure 4.12). In addition to that the Gln served as a spacer between the Phe and the Trp. Therefore it was not very surprising that its sidechain was not necessary for functional potency on BRS-3 (Table 4.9). The fact that the Gln might be replaceable represented a promising outlook for further structural modifications towards nonpeptide ligands for BRS-3, which will be subject of the following chapters.

4.4 Peptidomimetic BRS-3 Agonists

4.4.1 General Strategy

In the previous chapters, it was described how we have been able to design the short peptide agonist H-D-Phe-Gln-D-Trp-1-(2-Phenylethyl)amide (**109**) using the linear nonapeptide [D-Phe⁶,β-Ala¹¹,Phe¹³,Nle¹⁴]Bn(6-14) (**1**) as a starting point.^[384]

Although the improvement in functional activity from D-Phe-Gln-D-Trp-Phe-NH₂ (**95**) to H-D-Phe-Gln-D-Trp-1-(2-Phenylethyl)amide (**109**) as described in chapters 4.3.6-4.3.8 was considerable with about 15-fold (Tables 4.9 and 4.10) a comparison with the activities of the nona- and octapeptides (Tables 4.2 and 4.4) made clear, that presumably all compounds would bind to the same epitope, it would be possible to further optimize the interaction of these smaller molecules with the receptor by – maybe even small - structural changes. Furthermore, we were now also aiming towards compounds with a reduced peptidic character, which would increase the proteolytical stability, and a higher lipophilicity, which would putatively improve the pharmacokinetic profile and may eventually allow oral application. However, the first goal of this further optimization was to generate new tool substances, which may help to unravel the still unclear physiological role of the human orphan receptor BRS-3 and its possible use as a drug target in obesity and cancer.

It was tried to approach these goals by means of combinatorial chemistry. In the following chapters the course from initial thoughts and planning leading to the parallel solid- and solution phase synthesis of a combinatorial library of low molecular weight peptidomimetic agonists based on the structure of the short peptide agonist **109** is described.

4.4.2 Design and Scope of a Small-Molecule Library

In the following, the prominent features of this library will be summarized. Because the same assay-system as for the peptides described in the chapters above would be

used, generation of the library-compounds would be carried out by the use of parallel synthesis. Application of the ‘split-method’^[5,6] combined with ‘on-bead screening’ technology^[12] or biological screening of compound mixtures was not considered as an option mainly because of their incompatibility with the FLIPR-assay but also because these methods are only useful for a qualitative but not quantitative determination of affinity. Moreover, they suffer from substantial drawbacks such as the need for synthetic optimization, time consuming deconvolution or a high susceptibility for artefacts in the obtained biological data due to synergistic effects.^[385,386]

As a consequence of this the C-terminal unit of agonist **109**, namely D-Trp-1-(2-Phenylethyl)amide was considered as ‘optimized’ with respect to functional potency. Although ADMET^[3,44] parameters were not taken into account in this optimization process and other structural modifications are thinkable, a limitation of the C-terminal optimization process was necessary in order to keep the synthesis of the library manageable. Parallel synthesis - which requires separate workup, compound purification and biological testing - limits the number of processable compounds in a reasonable time.

Since the knowledge obtained from our previously conducted studies was used for the design of this library, it can be considered as ‘biased’. Our attention was directed towards the N-terminal part of the molecule, because the SAR of lead-structure **95** already suggested, that the sidechain of the Gln is not essential for functional activity. However all three aromatic moieties are needed.^[384] Furthermore, a stereochemical change of the N-terminal D-Phe in **95** did not affect functional potency.^[384]

The C-terminal unit D-Trp-1-(2-Phenylethyl)amide, either attached to solid support or, represented by building block **138**, in solution phase, serves as a common basis for all members of the library (Figure 4.13). To this C-terminal building block, differently modified substitutes for the D-Phe-Gln unit would be attached. During such a fine-tuning process with no 3D structural data available it is advisable that changes at the original structure are carried out stepwise rather than several ones simultaneously. The applied structural modifications can roughly be divided into two different classes:

- The backbone of the D-Phe-Gln unit is modified by deletions and the introduction of various peptidomimetic elements.
- In this context it is reasonable to investigate modifications of the sidechains such as deletions with respect to the Gln-sidechain and the substitution pattern of the N-terminal aromatic residue of the D-Phe or the replacement with heteroaromatic- or constrained aromatic systems.

Taken together, these tools should allow the further elaboration of the structural requirements for biological activity of this part of the agonist and a reduction to a minimum fragment. Moreover, the backbone variations should mainly account for the enhanced metabolic stability of potential conformationally tolerated surrogates.

The use of different peptidomimetic backbone elements or classes automatically leads to a division of the overall library into several sublibraries. A summary of these different backbone modifications that are used for the substitution of the N-terminal D-Phe-Gln unit of **109** is given in Figures 4.13 and 4.14:

- In a first step, the N-terminal amine is deleted and the Gln sidechain is removed (chapter 4.4.3).
- Additionally, the N-terminal carbonyl is removed. Formally this corresponds to a replacement of the D-Phe-Gln unit by *N*-substituted glycines and -alanines (chapter 4.4.4).
- Alternatively to the N-terminal carbonyl removal, the Gln C^α is substituted by nitrogen, which leads to azapeptides (chapter 4.4.5).
- Replacement of the N-terminal amide bond in azapeptides by a C-N double bond leads to semicarbazones (chapter 4.4.6).
- Formal reduction of this C-N double bond of the semicarbazones leads to semicarbazides (chapter 4.4.7).
- Finally, scaffolds containing piperazine and piperidine are inserted (chapter 4.4.8).

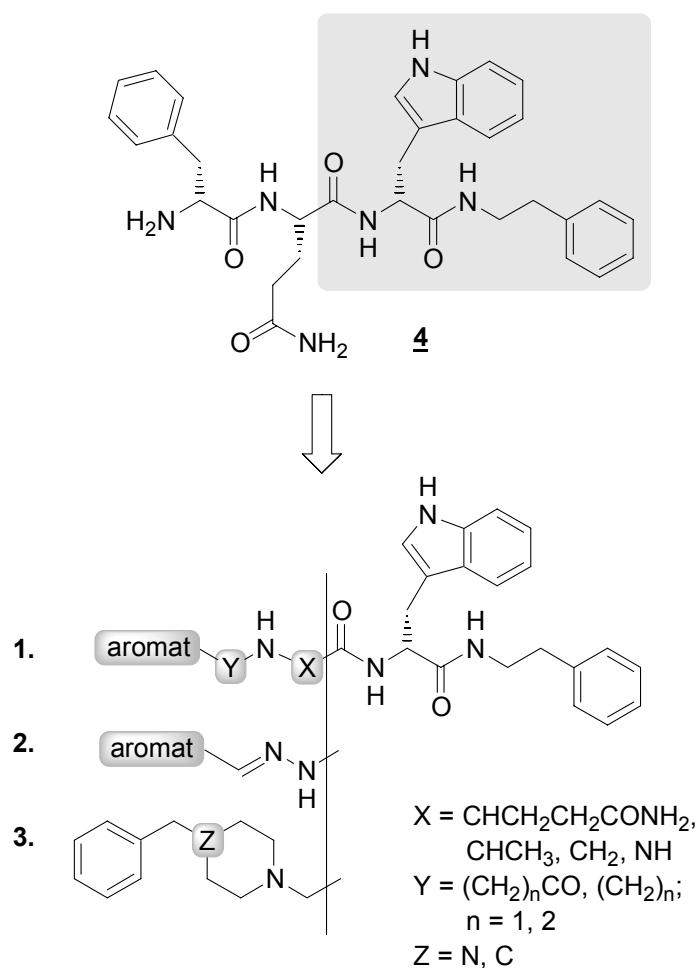


Figure 4.13: Modular design of peptidomimetic BRS-3 agonists. The marked region of structure **109** depicts the previously optimized part of the molecule, which is left unchanged for the further studies. ‘Aromat’ refers to differently substituted or heteroatoms containing aromatic residues.

It is planned that each of these sublibraries would contain several representatives, differing in their N-terminal aromatic systems. With respect to the variation of this N-terminal aromatic system two goals are pursued:

- Among each other the members within a series should contain residues of great diversity.
- By repeating identical or similar substitution patterns within each series a comparison between the different series of compounds would be possible.

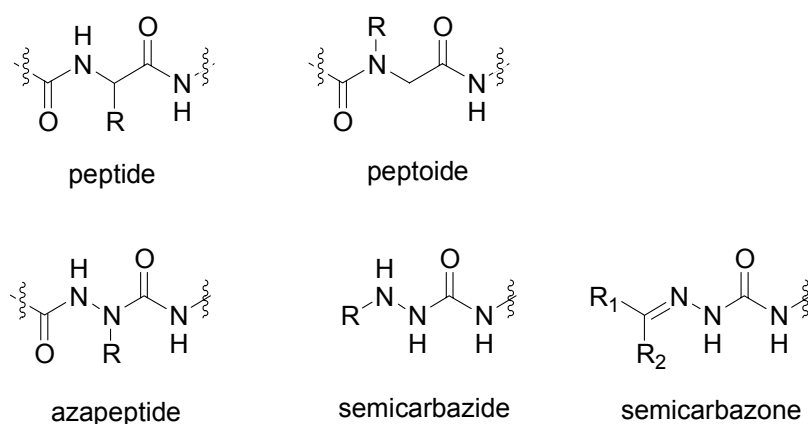


Figure 4.14: Schematic depiction of different classes of peptide mimetics/backbone modifications that are used in this work (R = substituted or functionalized alkyl- or aryl moieties; in some cases, not for peptoides, semicarbazones, $R = H$).

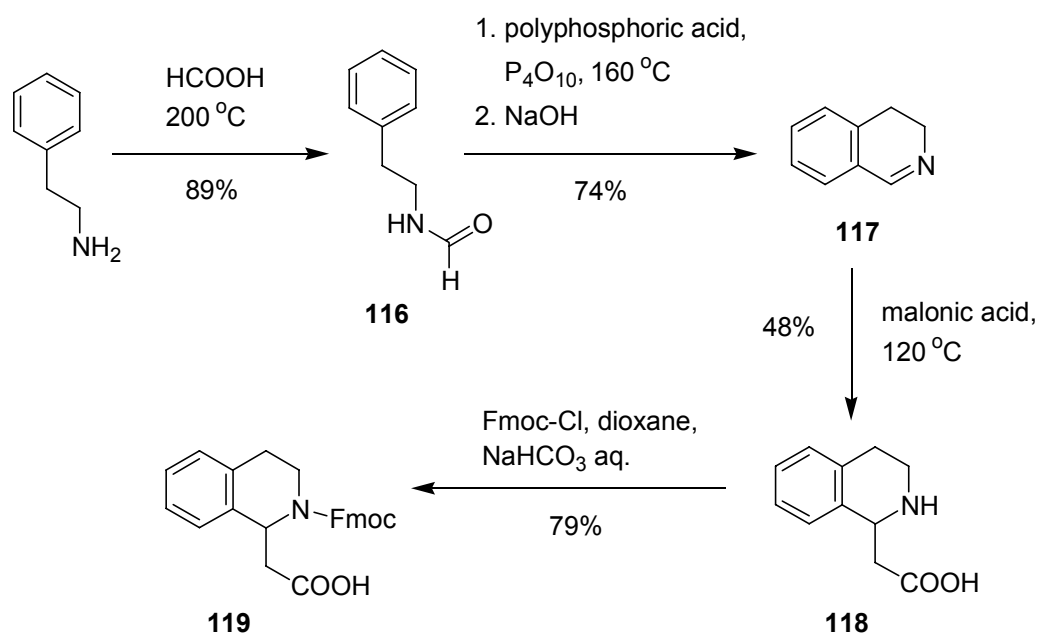
In order to obtain diversity at the N-terminus the following different aromatic systems are incorporated: (1) The unsubstituted phenyl-moiety; (2) 4-chlorophenyl- as lipophilic residue; (3) 3-pyridyl- as heteroaromatic/basic moiety; (4) 2-furyl- as heteroaromatic residues; (5) 1,3-benzodioxol-5-yl-; (6) tetrahydroisoquinolin-1-yl (**122**) as constrained/basic system; (7) 2-indolyl- (**119**) as heteroaromatic/constrained system. Furthermore, the spacer attached to the aromatic system is varied in length. Not all of these aromatic elements are used in all of the sublibraries. This is because building blocks are on the one hand chosen to generate a maximum of diversity, on the other hand quick availability is necessary, either by easy synthetic access or commercial purchase. In this context the 2-arylacetic acids, which can be obtained commercially in great diversity, prove to be advantageous as N-terminal capping element (chapter 4.4.3.1 and 4.4.5.2). The same accounts for arylaldehydes needed for the synthesis of semicarbazones (chapter 4.4.6.2). They also serve as a starting point for building blocks leading to semicarbazides (chapter 4.4.7.2). Furthermore, differently substituted benzyl- and phenylethyl-bromides were purchased as educts for *N*-substituted glycines and alanines (chapter 4.4.4.2). Synthesis of the two building blocks (**119**) and (**122**) is described in chapter 4.4.3.1.

4.4.3 N-Terminal Modification and Gln Substitution

4.4.3.1 Synthesis

Firstly, in order to remove N-terminal chirality and increase lipophilicity, peptides with a removed N-terminal aminofunction (**163-167**) were prepared (Scheme 4.6).^[310] For synthesis of the peptides, FMPE resin^[310] was reductively aminated with 1-(2-phenylethyl)amine as described above (Scheme 4.2) and loaded with Fmoc-D-Trp-OH using HATU/HOAt/sym.-collidine activation^[318,320,326] to yield resin-bound Fmoc-protected propanamide **138**.^[332] Chain extension including the coupling of the N-terminal building blocks, which were incorporated instead of the D-Phe in lead-structure **109**, namely phenylacetic acid, 4-chlorophenylacetic acid, 3-(4-chlorophenyl)propionic acid, 2-{1,2,3,4-tetrahydro-2-[(9*H*-fluoren-9-ylmethoxy)carbonyl]-1-isoquinolinyl}acetic acid (**119**)^[306,387,388] and (1*H*-indol-2-yl)acetic acid (**122**)^[389,390] was carried out using standard Fmoc protocols^[303,304] with TBTU/HOBt/DIPEA activation^[324,325] (Scheme 4.5). N-terminal building blocks except **119** and **122** – their synthesis is described below – were purchased from commercial sources.

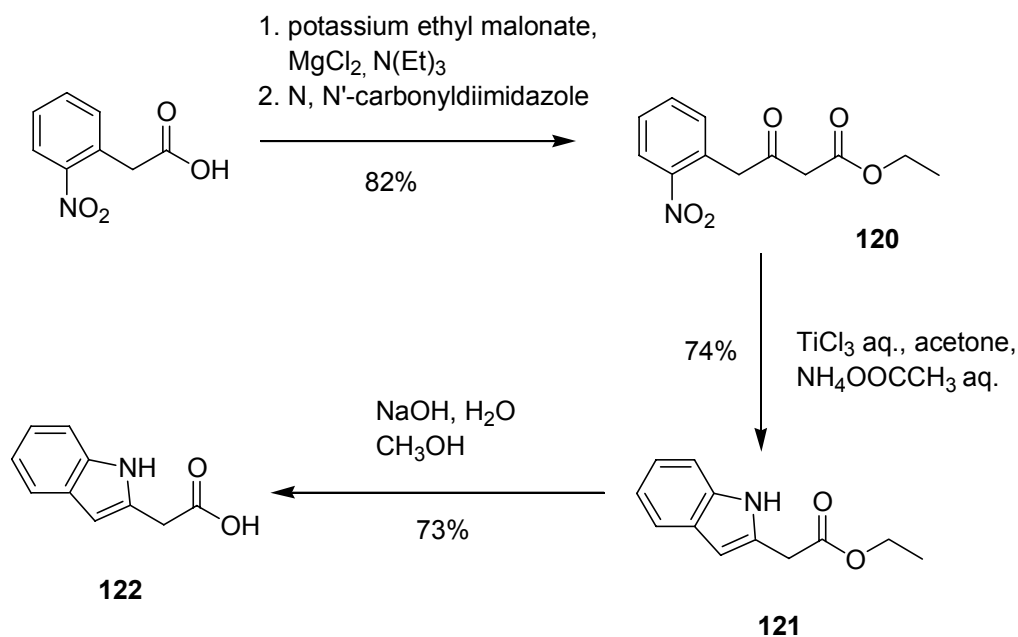
Fmoc-protected 3,4-dihydroisoquinoline acetic acid **119** was synthesized in four steps (Scheme 4.3): First, 1-(2-phenylethyl)amine was condensed with formic acid by slowly heating the reaction mixture to 200 °C and simultaneously distilling the emerging water and then the formic acid off to ensure complete reaction.^[387] A possible further (and unwanted) side-reaction of the relatively low-reactive carbonyl **116** to the Schiff-base product was suppressed by an excess of formic acid. The product was finally purified by vacuum distillation and obtained in 89% yield. In a second step, ring-closure was achieved under Bischler-Napieralski conditions, which furnished the desired 3,4-dihydroisoquinoline **117** in 74% yield.^[387] In this thermodynamically controlled process drastic reaction conditions (160 °C, 1.5 hrs) ensure the electrophilic attack at the aromatic system, a mixture of polyphosphoric acid and phosphorus pentoxide (‘super-PPA’) effects the withdrawal of water.



Scheme 4.3: Synthesis of 2-(1,2,3,4-tetrahydro-2-[(9H-fluoren-9-ylmethoxy)carbonyl]-1-isoquinoliny]acetic acid (**119**).

Workup of this reaction was somewhat tricky, because the formed product could only be extracted from the resulted brownish-black reaction mixture after complete neutralization of the acid at pH = 10. Alternatively, phosphorus oxychloride can be used for cyclization.^[391] The solvent-free conversion of the 3,4-dihydroisoquinoline **117** with malonic acid under abstraction of CO₂ was straightforward^[388] and produced the racemic cyclic constrained β -amino acid **118** in 48% yield after recrystallization, which is still capable of improvement. Final Fmoc-protection^[306] provided compatibility of this building block with the Fmoc-strategy.^[303,304,392]

As a second possible constrained phenylalanine mimetic besides **119**, (1H-indol-2-yl)acetic acid (**122**) was introduced and prepared in three steps (Scheme 4.4): First, 4-(2-nitrophenyl)acetoacetic acid ethyl ester (**120**) was prepared from (2-nitrophenylacetyl)imidazolidine as acylating agent and potassium ethyl malonate in the presence of magnesium dichloride/triethylamine with subsequent decarboxylation in 82% yield.^[389] The imidazolidine was prepared in situ from 2-nitrophenyl acetic acid and *N,N'*-carbonyldiimidazole. In principle, there are other routes, which lead to ethyl arylacetylacetates such as the Claisen-condensation – acylation of the enolate of

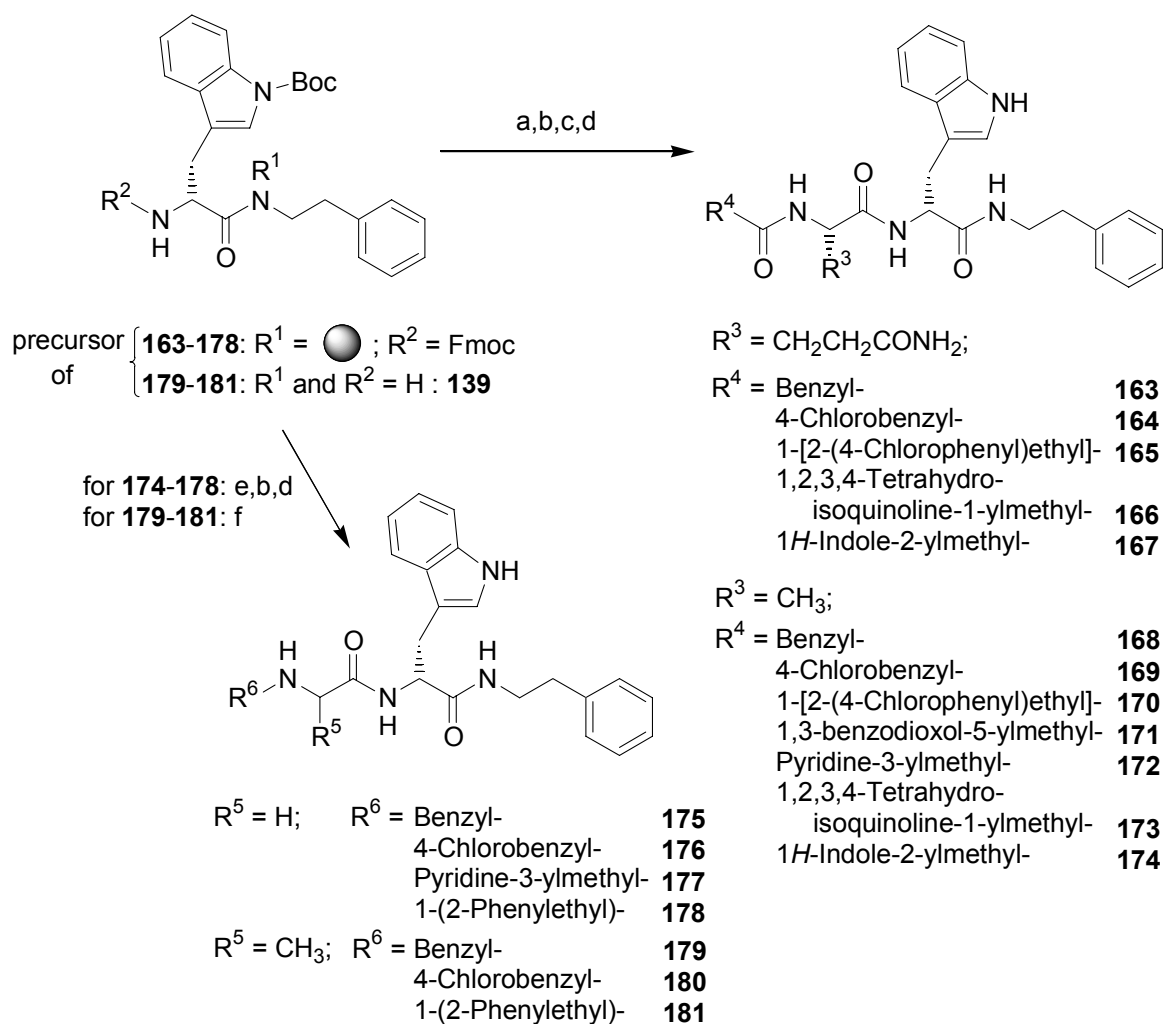


Scheme 4.4: Synthesis of (1H-indol-2-yl)acetic acid (**122**).

ethylacetate with ethyl arylacetates^[393] – or, similar to the malonic acid ester synthesis described above, the use of Meldrum's acid^[394] followed by decarboxylation. However, these methods produce lower yields or give rise to retro-condensation reactions.^[389,390] Cyclization of the β -ketoester **120** was carried out using titanium (III) chloride in aqueous acetone and yielded the indolyl acetic acid ester **121** in 74% yield (Scheme 4.4).^[390] The mechanism of this reaction can be proposed as follows: Reduction of the nitro-group to the amine is followed by an intramolecular condensation and finally by an H-shift, generating the thermodynamically more stable aromatic system.

Saponification of the ester **121** with aqueous NaOH/methanol yielded indolyl acetic acid **122** in 73% yield (Scheme 4.4).

Cleavage of the final compounds **163-167** from solid support and acidic deprotection was carried out with TFA/TIPS/H₂O (18:1:1). Stable carbaminic acids were not observed, probably due to their rapid decay under the mild acidic aqueous HPLC-conditions. The additional substitution of Gln with Ala besides the removal of the N-terminal NH₂ of lead-structure **109** led to peptides **168-174**, which were prepared similarly as **163-167** (Scheme 4.5).



Scheme 4.5: Synthesis of analogues of **109** with a removed *N*-terminal aminofunction (**163-167**) and with an additional substitution of *Gln* against *Ala* (**168-174**). Compounds **175-181** with removed *N*-terminal peptide bond are discussed in chapter 4.4.4. Reagents: (a) (for R₂ = Fmoc: 20% piperidine/NMP), Fmoc-*Gln*(Trt)-OH or Fmoc-*Ala*-OH, TBTU/HOBT/DIPEA, NMP; (b) 20% piperidine/NMP; (c) carboxylic acid building blocks,^a TBTU/HOBT/DIPEA, NMP; (d) 1.) TFA/TIPS/H₂O (18:1:1), 2.) HPLC; (e) {arylalkyl-[9*H*-fluoren-9-ylmethoxy]carbonyl}amino}acetic acid (**131-134**), TBTU/HOBT/DIPEA, NMP; (f) 1.) 2-{arylalkyl-[(9*H*-fluoren-9-ylmethoxy)carbonyl]amino}propionic acid (**135-137**), HATU/HOAt/sym.-collidine, DMF, 2.) TFA/CH₂Cl₂/TIPS (10:10:1), 3.) DMSO/HOAc/H₂O (8:1:1), 4.) 20% piperidine/DMF, 5.) HPLC (65-87%).^a Purchased from commercial sources except **119**, **122**.

4.4.3.2 Biological Evaluation

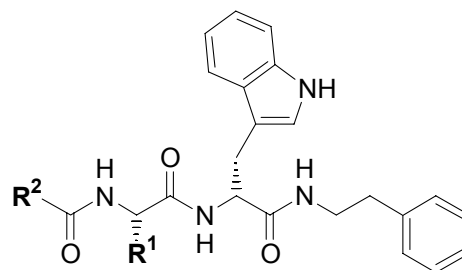
One of the most reliable methods in medicinal chemistry to improve in vitro activity is to incorporate properly positioned lipophilic groups or, as could be suggested for our case, to remove ‘unnecessary’ hydrophilic groups (chapter 2.4). Although C-terminal optimization of the aforementioned lead-structure, which resulted in the removal of the amide function, was sufficient to increase functional potency about 15-fold to generate agonist **109** with an EC_{50} of 710 nM,^[384] we expected that further improvement of functional activity could be achieved by exploiting the N-terminal SAR of this molecule. On the other hand, we were aiming at oral availability, which requires solubility. Therefore, regarding Lipinski’s ‘rule of five’,^[50] lipophilicity, which can be estimated and expressed by the *n*-octanol/water partition coefficient cLogP value, should not exceed the magnitude of five. Firstly we deleted the N-terminal aminofunction of the agonist **109** (Scheme 4.5, Figure 4.13). As a result of this, the cLogP value raised from 1.3 to 1.81 (Tables 4.10 and 4.11), as compared to the augmentation of 0.1 of H-D-Phe-Gln-D-Trp-Phe-NH₂ to 1.3 of agonist **109** (Tables 4.9 and 4.10).

As can be seen from Table 4.11 (compounds **163-167**) the effect of this increase of lipophilicity on functional potency at BRS-3 is low except for compound **167** with an increase of about 12-fold. Compounds **163** and **164** showed functional potencies on the NMB-R and GRP-R in the micromolar range.

In the second step a series of compounds were investigated where in addition to the deleted aminofunction Gln was replaced by Ala and the N-terminal aromatic residue was differently substituted or replaced by heteroaromatic moieties (Table 4.11). Although the synthetic effort to get from lead structure H-D-Phe-Gln-D-Trp-Phe-NH₂ to compounds **168-174** was relatively small, the impact on improvement of functional potency was enormous. With compounds **168** and **171**, potencies in the nanomolar range were obtained. Furthermore, all compounds showed excellent selectivity for BRS-3. As seen in the preceding series, compounds **163-167**, indole-2-yl/3-pyridyl was clearly favored as N-terminal aromatic residue over 4-chlorophenyl. On the other hand, these alterations probably do not represent much progress concerning

proteolytic stability, since these compounds still comprised three peptide bonds. Therefore, efforts now were directed towards a reduction of the peptidic character of the compounds.

Table 4.11: Functional potencies of modified analogues of **109** with N-terminally deleted aminofunction (**163-167**). Additionally, in compounds **168-174**, Gln was replaced by Ala.



no.	R ¹	R ²	BRS-3		
			-pEC ₅₀ ^a	E _{max} ^a	cLog P
163	(CH ₂) ₂ CONH ₂	Benzyl-	5.92 ± 0.25	38 ± 1	1.81
164	(CH ₂) ₂ CONH ₂	4-Chlorobenzyl-	5.85 ± 0.15	62 ± 4	2.52
165	(CH ₂) ₂ CONH ₂	1-[2-(4-Chlorophenyl)ethyl]-	6.63 ± 0.13	68 ± 6	2.91
166 ^b	(CH ₂) ₂ CONH ₂	1,2,3,4-Tetrahydroisoquinoline-1-ylmethyl-	6.15 ± 0.25	^c	^c
167	(CH ₂) ₂ CONH ₂	1 <i>H</i> -Indole-2-ylmethyl-	7.25 ± 0.34	82 ± 5	1.8
168	CH ₃	Benzyl-	8.67 ± 0.26	71 ± 5	3.62
169	CH ₃	4-Chlorobenzyl-	6.85 ± 0.28	75 ± 9	4.33
170	CH ₃	1-[2-(4-Chlorophenyl)ethyl]-	5.19 ± 0.05	30 ± 2	4.72
171	CH ₃	1,3-Benzodioxol-5-ylmethyl-	8.11 ± 0.46	75 ± 7	3.18
172	CH ₃	Pyridine-3-ylmethyl-	7.50 ± 0.14	74 ± 2	2.12
173	CH ₃	1,2,3,4-Tetrahydroisoquinoline-1-ylmethyl-	6.51 ± 0.10	69 ± 8	3.83
174	CH ₃	1 <i>H</i> -Indole-2-ylmethyl-	7.10 ± 0.20	69 ± 1	3.61

^a FLIPR-assay. Functional potencies are given in -pEC₅₀ ± SEM from 4-11 independent concentration-response curves. All compounds tested were inactive on the NMB-R and GRP-R except for **163** with EC₅₀ = 15.0 μM (13.9-16.3) on NMB-R and EC₅₀ = 19.1 μM (15.5-23.5) on GRP-R and **164** with EC₅₀ = 18.5 μM (16.6-20.7) on NMB-R and EC₅₀ = 12.2 μM (11.1-13.3) on GRP-R. ^b Compound contained impurities. ^c Not determined. Additional experimental details are described in Table 4.2 and chapters 4.2.1 and 8.5.

4.4.4 Probing the Necessity of the N-terminal Amide Bond

4.4.4.1 Introduction

An important milestone in the course from peptide to nonpeptides of a lead structure such as **109** is to find suitable surrogates, which reduce the peptidic character – *i.e.* the peptide bond, which is responsible for it – thereof. If the questioned amide bond is not directly involved in the binding to the active site of the receptor or, alternatively, in the intramolecular stabilization of the active substances' 3D structure, this strategy can lead to a success. However, it is impossible to make predictions about the outcome of such an attempt, if precise structural data of receptor and ligand are lacking. In principle there are several possibilities for the modification or removal of a peptide bond:

- The peptide bond can be replaced, *e.g.* by a sulfonamide,^[395,396] a phosphonamidate,^[397] or urea.^[398-401]
- The amide bond can be reduced, as successfully carried out *e.g.* for bombesin,^[231,244] somatostatin^[402] or substance P^[403] analogues.
- A 'shift' of the peptide sidechains from the C^α by one position along the peptide backbone to the amide nitrogen leads to so-called 'peptoids'.^[404-406]

The latter of these approaches was followed, and since we aimed to alter only the N-terminal amide bond in a first step by incorporation of one single peptoid monomer,^[407,408] it can be considered as equivalent to a reduction according to the second point and a simultaneous shortage of the backbone.

The definition of the term 'peptoid' has been coined by Zuckermann *et al.* as oligomers of *N*-substituted glycines,^[404,405] although it was also used in a different sense before^[409] (chapter 2.3). Peptoids have been successfully used as lead structures^[410,411] and offer the following advantages: Besides their metabolic stability,^[412] a great variation of functional groups is easily possible and due to their achirality and certain flexibility, they allow the probing of a large conformational space.^[404] There are two synthetic routes that lead to oligomers of *N*-substituted

glycines, both of which have been shown to be applicable to solid support automated synthesis and the generation of chemically diverse libraries.^[413-416]

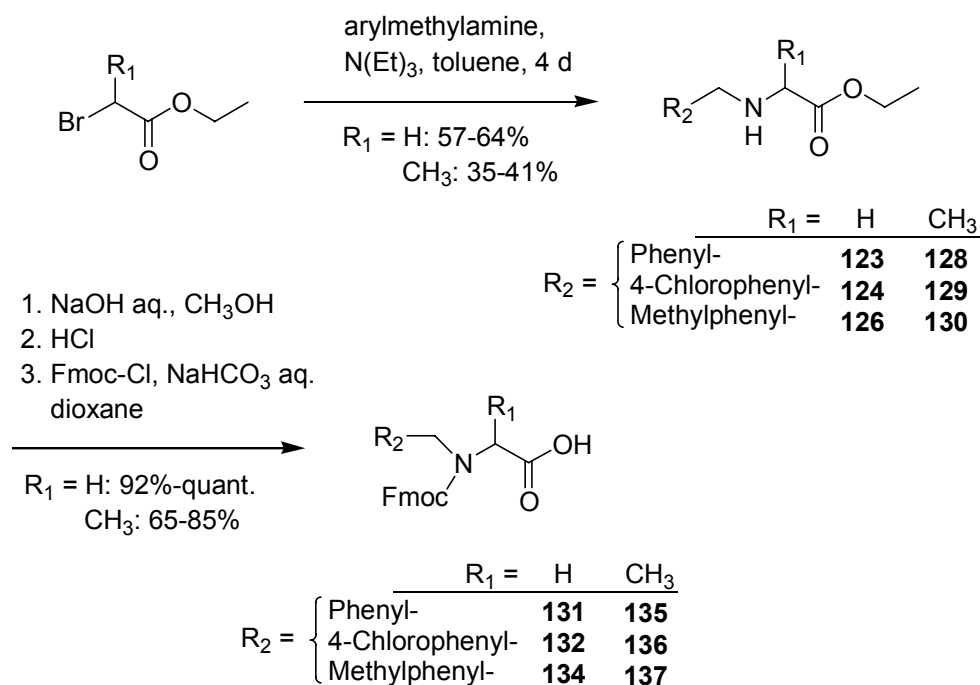
- The alignment of N-terminal Fmoc-protected *N*-substituted glycines according to the Fmoc-strategy.^[404] This route requires a previous synthesis of the monomers.
- The ‘submonomer’ synthesis, in which the (hetero-)polymer is assembled by alternated coupling of an α -haloacetic acid and nucleophilic substitution with a primary amine.^[405]

Synthesis of peptoid monomers can be carried out by direct alkylation of α -haloacetic acid esters in toluene.^[417,418] However, this method can lead to substantial side reactions such as dialkylation or aminolysis of the ester, especially if the chloroacetate is used.^[417] An alternative for water-soluble amines is the reaction with glyoxylic acid followed by reduction.^[404] Good results can also be obtained for lipophilic amines, when bromoacetic acid ethyl ester is used.^[419]

4.4.4.2 Synthesis

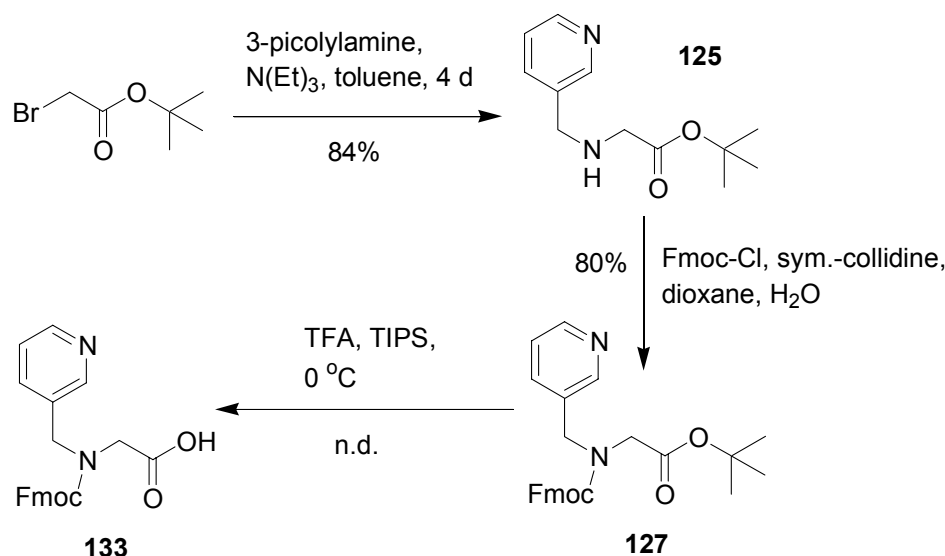
In order to probe the necessity of the N-terminal amide bond for functional activity, it was planned to replace the N-terminal unit of **109**, D-Phe-Gln against differently *N*-substituted glycines and alanines. For being able to implement these building blocks into standard Fmoc protocols,^[303,304] it was decided to furnish them with an Fmoc protecting group in order to minimize side reactions during the coupling process. All protected peptoid monomers, except **133**, were synthesized in two steps: Firstly, 2-(arylalkylamino)acetic acid ethyl esters (**123**, **124** and **126**) and 2-(arylalkylamino)propionic acid ethyl esters (**128-130**) were prepared from 2-bromoacetic acid ethyl ester and benzyl-, 4-chlorobenzyl- and 1-(2-phenylethyl)amine in toluene (Scheme 4.6).^[417,418] While yields for the glycine analogues **123**, **124** and **126** were in the range of 57-64%, only 35-41% were obtained for the alanine analogues **128-130** after column chromatography. In the second step, the esters were

hydrolyzed with aqueous NaOH and, after neutralization with 1 N HCl, Fmoc was introduced without intermediate purification to yield the Fmoc-protected *N*-alkylated glycines **131**, **132** and **134** and the corresponding alanine building blocks **135-137**, which were obtained as racemic mixtures. Again, yields for this two step transformation were higher for the glycine analogues (92% - quant) compared to the corresponding alanine analogues (65-85%). Interestingly, some of the *N*-Fmoc protected monomers showed cis-trans-isomerie about the amide bond (compounds **127** and **133-136**), as detected in the ¹H NMR-spectrum, whereas others (**131**, **132** and **137**) did not. Nevertheless, all monomers eluted in the analytical HPLC as single, well-defined peaks.



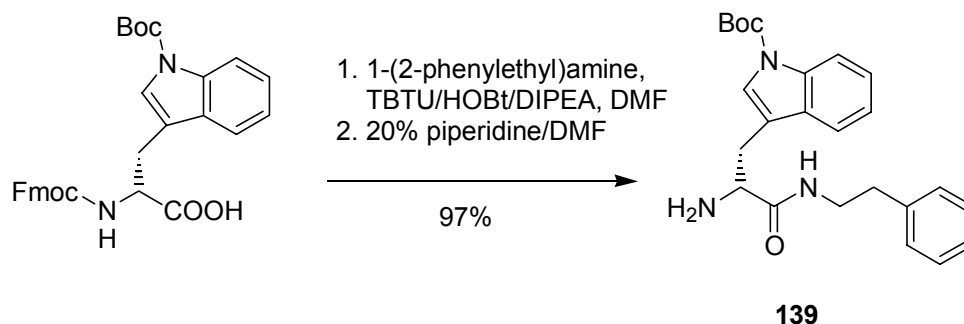
Scheme 4.6: Synthesis of {arylalkyl-[9*H*-fluoren-9-ylmethoxy]carbonyl}amino}acetic acids (**131**, **132** and **134**) and 2-{arylalkyl-[(9*H*-fluoren-9-ylmethoxy)carbonyl]amino} propionic acid derivatives (**135-137**).

Differently from the above described peptoid monomers, 2-{pyridine-3-ylmethyl-[(9*H*-fluorene-9-ylmethoxy)carbonyl]amino}acetic acid (**133**) was synthesized in three steps^[419,420] via the *tert*-butyl ester **125** (Scheme 4.7) because introducing the Fmoc group at the C-terminally unprotected monomer was found to be extremely



Scheme 4.7: Synthesis of 2-{pyridine-3-ylmethyl}-(9H-fluorene-9-ylmethoxy)carbamoyl amino}acetic acid (**133**).

difficult.^[419,420] Fmoc-protection of *tert*-butyl ester **125** was straightforward using sym.-collidine as a base as previously described.^[420] For final cleavage of the *tert*-butyl group TIPS was conveniently used as a scavenger in a 1:10 (v/v) mixture with TFA, thereby avoiding the previously used low-volatile *m*-Kresol.^[420]



Scheme 4.8: Synthesis of *tert*-Butyl-3-{(2*R*)-2-amino-2-[1-(2-phenylethyl)carbamoyl]ethyl}-1*H*-1-indole-carboxylate (**139**).

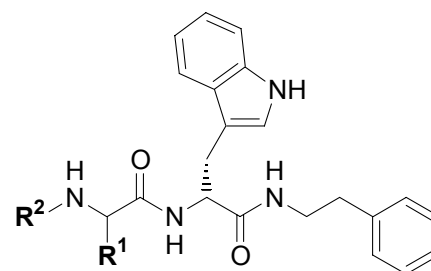
Preparation of the peptoid-peptide hybrids **175-178** was carried out on solid support^[310] using TBTU/HOBt/DIPEA activation^[324,325] (Scheme 4.5). For synthesis of compounds **179-181**, Fmoc-protected peptoid monomers **135-137** were coupled to **139** in solution with HATU/HOAt/sym.-collidine activation^[318,320,326] (Scheme 4.5). Cleavage of the Boc-protecting group from D-Trp turned out to be incomplete after

treatment with TFA/TIPS (10:1) (v/v) at 0 °C.^[331] ESI mass spectral data indicated that the carbaminic acid was stable under these highly acidolytic and water-free conditions. Destruction of the carbaminic acid was achieved by treatment with DMSO/H₂O/HOAc (8:1:1) (v/v). Compounds **179-181** were tested as racemic mixtures.

4.4.4.3 Biological Evaluation

In compounds **175-178**, the N-terminal peptide bond was removed by incorporation of *N*-substituted glycine, in compounds **179-181** by *N*-substituted alanine (Table 4.12). Thus, it is assumed that these modifications introduce a greater flexibility to the backbone accompanied with enhanced metabolic stability.^[404-406,412]

Table 4.12: Functional potencies of modified analogues of **109** containing peptoid monomer building blocks (**175-178**) and *N*-arylated 2-aminopropionic acid building blocks (**179-181**).



no.	R ¹	R ²	BRS-3		
			-pEC ₅₀ ^a	E _{max} ^a	cLog P
175	H	Benzyl-	7.68 ± 0.17	87 ± 6	3.86
176	H	4-Chlorobenzyl-	8.54 ± 0.39	81 ± 2	4.58
177	H	Pyridine-3-ylmethyl-	7.68 ± 0.23	82 ± 8	2.37
178	H	1-(2-Phenylethyl)-	7.78 ± 0.27	92 ± 16	4.08
179	CH ₃	Benzyl-	7.34 ± 0.14	86 ± 13	4.17
180	CH ₃	4-Chlorobenzyl-	8.39 ± 0.26	83 ± 13	4.89
181	CH ₃	1-(2-Phenylethyl)-	7.60 ± 0.13	82 ± 10	4.39

^a FLIPR-assay. Functional potencies are given in -pEC₅₀ ± SEM from 7-11 independent concentration-response curves. All compounds tested were inactive on the NMB-R and GRP-R. Additional experimental details are described in Table 4.2 and chapters 4.2.1 and 8.5.

Deletion of the carbonylfunction caused cLogP values to slightly increase by about 0.2-0.7. Here, in contrast to the preceding series, the 4-chloro substituted compounds **176** and **180** showed the highest functional potency with EC₅₀-values around 3-4 nM. The explanation for this shift of high functional potency could probably be that a high lipophilicity is favorable but only in the correct distance from the tryptophan. This distance is obviously too large for compounds **163-174**. Moreover a basic functionality located closer to the tryptophan seems to enhance functional activity. The overall series of compounds **175-181** demonstrated, that the carbonyl function or the planarity caused by the peptide bond was not contributing to the binding mode of the compound to the receptor or to its activation and therefore could be omitted.

4.4.5 Azapeptides as BRS-3 Agonists

4.4.5.1 Introduction

The exchange of a C^αH of an amino acid against a nitrogen atom leads to a so-called azaamino acid.^[421] Since the first systematic incorporation of azaamino acids into peptides,^[422,423] a large number of peptides incorporating these residues have been prepared and examined in the field of medicinal chemistry,^[421] mainly because of the following reasons:

- The exchange of an azaamino acid against an amino acid goes along with a loss of asymmetry and with a conformational change.^[424-427] This may lead to an increase in biological activity.
- An increase in biological activity can also be the result of the enhanced stability of azapeptides against enzymatic degradation^[421,428] which may cause a prolonged duration of action or different absorption-, distribution- and transport characteristics of azapeptides. The latter is undoubtedly influenced by the observation that the acidity of the NH which is next to the N^α is higher compared to that of the corresponding peptides.^[429]

- The relatively easy synthetic access to azapeptides.^[421,430-435]

Azaamino acids have been successfully incorporated into various peptide hormones,^[421,422,436] and comprise the scaffold of small molecules such as integrin antagonists^[12,437] and a number of different protease inhibitors.^[438-441] So far, two drugs bearing azaamino acids, namely the LHRH-agonist *Zoladex*TM ^[421] and a dipeptide isoster for the inhibition of HIV-1 protease,^[438,442] have been introduced to the market.

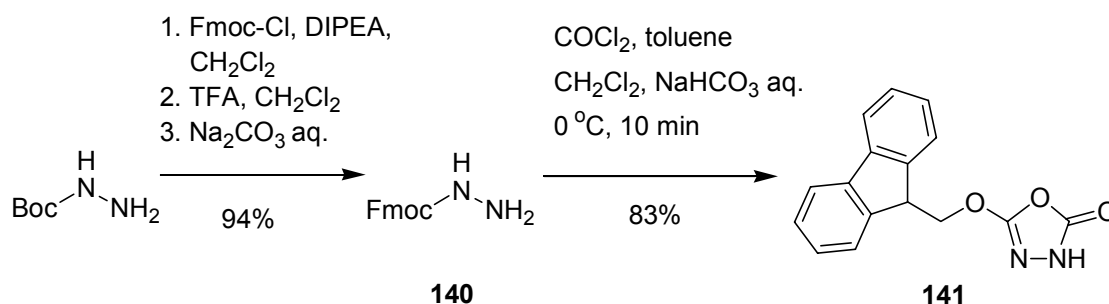
The isoelectronic C^αH→N^α replacement probably leads to a configuration, which can be described as somewhere in between the D- and the L-configuration of the corresponding amino acid.^[421,431] *Ab initio* calculations for diacylhydrazines showed that the N-N torsional angle should be twisted with a CO-N-N-CO dihedral angle of approximately 90°.^[424] While for the glycine analog the rotational barrier is relatively small, it increases significantly upon *N*-substitution of the nitrogen suggesting that azapeptides are relatively rigid. Similar structural information has been obtained from crystal structures of model-azapeptides^[425,426] and *ab initio* calculations for comparable compounds,^[427,443-445] which showed dihedral angles of about $\phi = -70^\circ$, $\psi = -20^\circ$ for the first and $\phi = \pm 90^\circ \pm 30$, $\psi = 0 \pm 30$ or 180 ± 30 for the latter.

The precursors of azaamino acids, the monoalkylated hydrazines, can either be prepared by the condensation of blocked carbazates with aldehydes and subsequent reduction^[446-449] or alternatively by the nucleophilic alkylation of hydrazines.^[450,451]

The coupling of these building blocks to the amine of the 'preceding' amino acid can be achieved by a variety of different carbonylating agents and methods,^[421,434,435] either activating the N- or the C-terminus. Despite the numerous routes and examples for the synthesis of azapeptides in solution,^[421,439,440,452] besides the synthesis of azatides,^[431] there are only a few reported for the preparation on solid support.^[430,432,434,435,453,454]

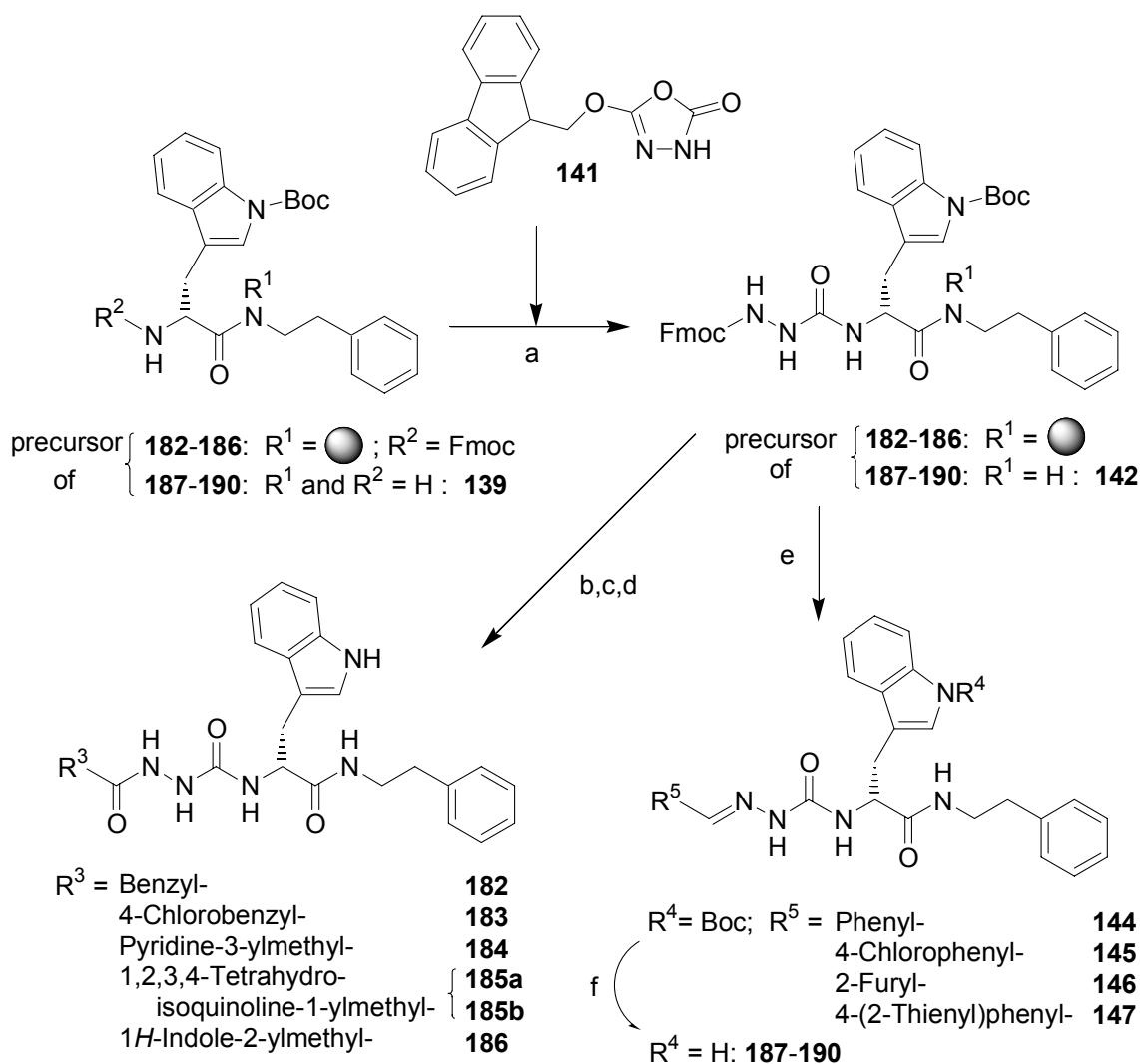
4.4.5.2 Synthesis

In order to receive azapeptides **182-186** (Scheme 4.10), formally, Gln had to be replaced in peptide **109** by azaglycine. The synthesis was planned to be carried out on FMPE resin.^[331,332] In search for a suitable solid phase method, activation of the Fmoc-protected hydrazine with phosgene was chosen^[430] because other solid phase methods suffer from major drawbacks: The N-terminal activation with bis-2,4-dinitrophenyl carbonate leads to hydantoin formation and furthermore has a reportedly slow reaction rate,^[432,433,455] the in situ activation of alkylated hydrazines with triphosgene,^[434,435] gives rise to considerable amounts of by-products when applied to Fmoc-hydrazine.^[430] Moreover, the approach used by J. Wermuth and J. S. Schmitt in our group for the synthesis of cyclic RGD peptides containing azaamino acids,^[453,454] namely the activation of the aminofunction with triphosgene leading to the isocyanate, was not favored. This method is devoid of the advantage of organic reactions carried out on solid support, namely to achieve complete conversion by the use of an excess of reagent.



Scheme 4.9: Synthesis of 5-(9H-Fluoren-9-ylmethoxy)-1,3,4-oxadiazol-2(3H)-one (**141**).

For synthesis 5-(9H-fluoren-9-ylmethoxy)-1,3,4-oxadiazol-2(3H)-one (**141**) was freshly prepared from Fmoc-hydrazine **140** using an excess of phosgene (1.89 M solution in toluene) as previously described^[12,430,437] (Scheme 4.9). Fmoc-hydrazine was easily synthesized from Boc-hydrazine in high yield in a protection step with Fmoc-Cl and DIPEA as a base followed by a Boc-deprotection step carried out with



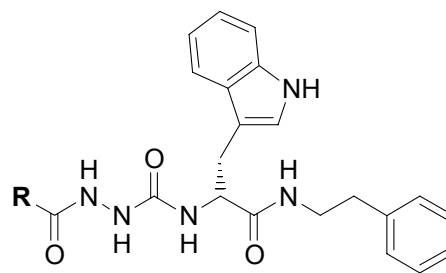
Scheme 4.10: Synthesis of azapeptides **182-186** and semicarbazones **187-190**. Reagents: (a) oxadiazolone **141**, CH_2Cl_2 (68% ^a); (b) 20% piperidine/NMP; (c) carboxylic acid building blocks, ^{b,c} TBTU/HOBt/DIPEA, NMP; (d) 1.) TFA, TIPS, H_2O (18:1:1), 2.) HPLC; (e) 1.) 20% piperidine/DMF, 2.) arylaldehydes, ^{b,d} THF (47-83%); (f) 1.) TFA/ CH_2Cl_2 /TIPS (30:30:1), 2.) DMSO/HOAc/ H_2O (8:1:1), 3.) HPLC (56-63%). ^a For $R^1 = \text{H}$. ^b Purchased from commercial sources except: ^c **119**, **122**; ^d **143**.

50% TFA (v/v) in CH_2Cl_2 at 0 °C (Scheme 4.9).^[392] Final careful neutralization caused precipitation of the product. Thereby, unwanted Fmoc-cleavage was not observed. This method was found to be superior to the one which was previously used in our group,^[456,457] namely monoprotection of aqueous hydrazine with Fmoc-Cl,^[306] because this method suffers from the drawback that a certain amount - usually about 5-10% -

of diacylated hydrazine is formed. For the incorporation of azaglycine in compounds **182-186**, resin-bound propanamide **138** was Fmoc-protected and reacted with an excess of freshly prepared oxadiazolone **141** in dry CH_2Cl_2 for 90 min^[430,457] (Scheme 4.10). Further coupling of the N-terminal carboxylic acid building blocks 2-phenylacetic acid, 2-(4-chlorophenyl)acetic acid, 2-(3-pyridyl)acetic acid and the constrained **119** and **122**, which were previously described in chapter 4.4.2, was carried out using standard Fmoc protocols^[303,304] with TBTU/HOBt/DIPEA activation.^[324,325] Azapeptides **182-185** were finally obtained after cleavage from solid support and subsequent HPLC purification in 13-31% overall yield with reference to the loaded resin. Diastereomers **185a** and **185b** have been separated by HPLC.

4.4.5.3 Biological Evaluation

As already mentioned earlier it is generally believed that a critical amount of rigidity is a prerequisite for high activity and selectivity.^[337] Although calculations showed that azaglycine, unlike other azaamino acids, has a relatively easy access to different conformations,^[424] there are examples for scaffolds bearing azaglycine as their core and structurally dominating unit, such as RGD-mimetics, which demonstrated to possess these features.^[12,430,437] Obviously the same proves true in this case. All azapeptides show excellent activities and selectivities on the BRS-3 receptor, especially compound **183** with an EC_{50} -value in the subnanomolar range (Table 4.13). It is noteworthy, that the dose-response curves of compounds **183** and **186** have relatively shallow slopes (see appendix). Although the distance to the lipophilic 4-chloro substituted moiety seems to be larger than in compounds **175-181** with the removed peptide bond, it is feasible that the azaglycine induces a bent-like structure because of the torsion of the N-N angle. Therefore the actual length of the compound in its 'bioactive' conformation could resemble that of the peptoid-peptide hybrids (chapter 4.4.4).

Table 4.13: Functional potencies of azapeptides 182-186.

		BRS-3		
no.	R	$-\text{pEC}_{50}^a$	E_{max}^a	cLog P
182	Benzyl-	8.51 ± 0.18	86 ± 10	3.61
183	4-Chlorobenzyl-	9.72 ± 0.49	89 ± 14	4.33
184	Pyridine-3-ylmethyl-	8.87 ± 0.26	102 ± 26	2.12
185a	1,2,3,4-Tetrahydroiso-	8.03 ± 0.12	95 ± 15	3.83
185b	quinoline-1-ylmethyl-	7.71 ± 0.12	91 ± 15	3.83
186	1 <i>H</i> -Indole-2-ylmethyl-	8.66 ± 0.43	84 ± 4	3.6

^a FLIPR-assay. Functional potencies are given in $-\text{pEC}_{50} \pm \text{SEM}$ from 7-14 independent concentration-response curves. All compounds tested were inactive on the NMB-R and GRP-R. Additional experimental details are described in Table 4.2 and chapters 4.2.1 and 8.5.

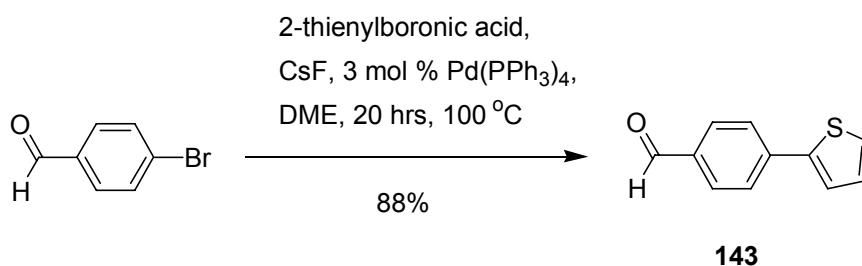
4.4.6 Semicarbazones as BRS-3 Agonists

Similar as for the preceding series of compounds described in chapters 4.4.3 and 4.4.4, a removal/substitution of the N-terminal amide bond was also tried for the azapeptides (previous chapter). Synthesis and evaluation of semicarbazones are subject of this chapter 4.4.6. The next chapter 4.4.7 deals with the synthesis and biological evaluation of semicarbazides.

4.4.6.1 Synthesis

Analogues of azapeptides **182-186**, bearing a C-N double bond instead of the N-terminal peptide bond, were prepared in solution (Scheme 4.10). Acylation of amine

139 (Scheme 4.8) with freshly prepared oxadiazolone **141** in DMF at room temperature resulted in azacompound **142** which was then Fmoc-deprotected and without intermediate purification reacted with benzaldehyde, 4-chlorobenzaldehyde, furan-2-carbaldehyde and 4-(2-thienyl)benzaldehyde (**143**) in THF at room temperature. Imine bond formation was slow probably due to residual basicity, however since the desired compounds **144-147** were obtained in acceptable yields, optimization of this process was not pursued. Benzaldehyde, 4-chlorobenzaldehyde, furan-2-carbaldehyde were purchased from commercial sources whereas 4-(2-thienyl)benzaldehyde (**143**) was synthesized from 4-bromobenzaldehyde via Suzuki-coupling (Scheme 4.11).^[458] Final Boc-deprotection under first strong and then mild acidic conditions gave semicarbazones **187-190**.



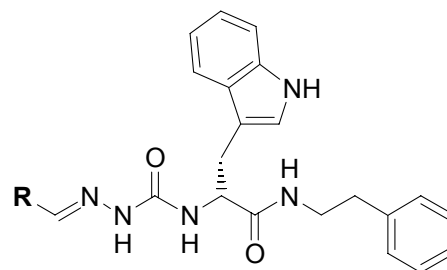
Scheme 4.11: Synthesis of 4-(2-thienyl)benzaldehyde (**143**).

4.4.6.3 Biological Evaluation

The replacement of the N-terminal peptide bond by an N-terminal C-N double bond, (semicarbazones **187-190**, Table 4.14) caused an increase of the cLogP value of about 0.6 compared to the azapeptides **182-186** (chapter 4.4.5). This increase in lipophilicity was tolerated for the 2-furyl as aromatic moiety, but not for highly lipophilic residues such as 4-chlorophenyl- (compound **188**) or 4-(2-thienyl)phenyl- (compound **190**), for which low activities were observed. This drop of functional activity correlates well with the increasing cLogP value. Because compound **189** was highly active, the low activity of the more lipophilic compounds can not be attributed to a possible conformational change. Taken together, the results confirm those obtained from the

peptide-peptide hybrids **175-181**, namely that the N-terminal peptide bond is not involved in receptor activation.

Table 4.14: Functional potencies of semicarbazones **187-190**.



no.	R	BRS-3		
		-pEC ₅₀ ^a	E _{max} ^a	cLog P
187	Phenyl-	6.63 ± 0.32	89 ± 0	4.21
188	4-Chlorophenyl-	5.56 ± 0.27	78 ± 0	4.92
189	2-Furyl-	8.83 ± 0.34	94 ± 3	3.38
190	4-(2-Thienyl)phenyl-	5.10 ± 0.31	58 ± 7	5.98

^a FLIPR-assay. Functional potencies are given in -pEC₅₀ ± SEM from 6 independent concentration-response curves. All compounds tested were inactive on the NMB-R and GRP-R. Additional experimental details are described in Table 4.2 and chapters 4.2.1 and 8.5.

4.4.7 Semicarbazides as BRS-3 Agonists

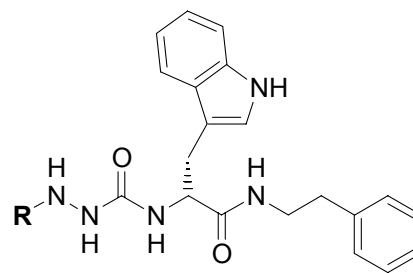
Formally, analogues of azapeptides **182-186** with a removed N-terminal peptide bond (semicarbazides) could be obtained by reduction of the semicarbazones described in chapter 4.4.6. In this case however, a different strategy was needed, avoiding the necessity to reduce the imine bond in the presence of the tryptophan moiety, which itself is susceptible towards reductive reagents as discussed earlier in chapter 4.3.5.1.^[369] Therefore suitably protected azaamino acid constituents were prepared, which then would be coupled to the amine **139** (Scheme 4.12).

steps. Because the site of acylation is dependent on the nature of the substituted hydrazine and the activation reagent and therefore was difficult to predict,^[430,431,446] Fmoc was introduced at the arylalkylated nitrogen to give building blocks **154-156**. Preliminary attempts to cleave the Boc-protecting group were carried out by careful treatment with TFA/CH₂Cl₂/TIPS/H₂O (4:14:1:1) (v/v) at 0 °C and showed approximately 70% deprotection after 1 hr as monitored by TLC and HPLC-MS. However, we observed unexpected degradation of the dried deprotected species at room temperature within 24 hrs. Surprisingly, attempts to remove the Boc with 4 N HCl in dioxane as a solvent at room temperature^[438] failed because of insufficiently low reaction rates. Therefore, it was decided to cleave the Boc-group of **154-156** under more drastic conditions than aforementioned with TFA/CH₂Cl₂/TIPS (20:20:1) (v/v). Without further workup, activated carbazic acid esters were immediately generated using bis(pentafluorophenyl)carbonate, and without isolation instantly reacted with the amine **139**.^[431,451] This method worked very well and was found to be superior to the use of a solution of phosgene in toluene,^[430] which seems to require more subtle adjustment of the reaction conditions. Direct cleavage of Boc and Fmoc without intermediate purification finally furnished the desired semicarbazides **191-193** (Scheme 4.12).

4.4.7.3 Biological Evaluation

Functional potencies of the semicarbazides **191-193** were lower than of the corresponding azapeptides **182-186**, however, as expected still excellent (Table 4.15). As for the peptoid-peptide hybrids, removal of the carbonyl group caused the cLogP values to raise about 0.3 orders of magnitude compared to azapeptides **182-186**. Unlike for the semicarbazones (chapter 4.4.6), which are more lipophilic, but similar as for the azapeptide series (chapter 4.4.5) the N-terminally 4-chloro substituted compound **192** showed highest activity.

Table 4.15: Functional potencies of semicarbazides **191-193**.



no.	R	BRS-3		
		-pEC ₅₀ ^a	E _{max} ^a	cLog P
191	Benzyl-	7.84 ± 0.23	81 ± 0	3.9
192	4-Chlorobenzyl-	8.22 ± 0.42	83 ± 5	4.62
193	Furyl-2-ylmethyl-	7.62 ± 0.14	96 ± 14	3.08

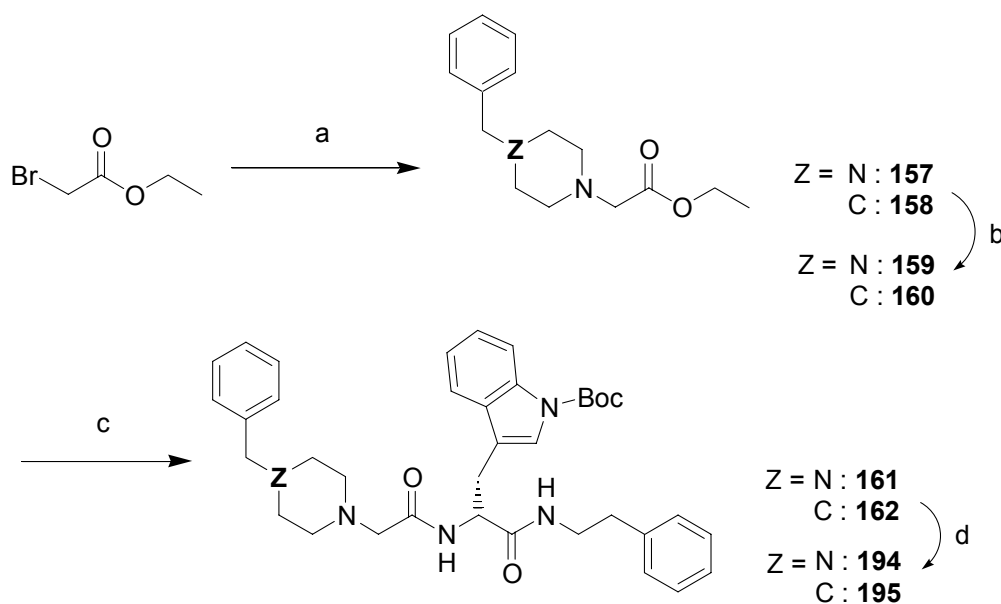
^a FLIPR-assay. Functional potencies are given in -pEC₅₀ ± SEM from 6 independent concentration-response curves. All compounds tested were inactive on the NMB-R and GRP-R. Additional experimental details are described in Table 4.2 and chapters 4.2.1 and 8.5.

4.4.8 Piperazine- and Piperidine Derivatives

We furthermore decided to incorporate benzyl-piperazine and -piperidine as N-terminal building blocks. It has not escaped our notice that this are commonly used motives for lead structures. This has been confirmed in a very recent investigation: A quantitative classification of known GPCR ligands revealed 4-phenyl-piperazine to be the most privileged substructure (chapter 2.3).

4.4.8.1 Synthesis

Building blocks (4-benzyl-piperazin-1-yl)acetic acid (**159**) and its piperidine analogue **160** were prepared in two steps similar as described for **123-126** followed by saponification (Scheme 4.6). After coupling of these building blocks to the amine **139** (Scheme 4.8) using TBTU/HOBt/DIPEA activation^[324,325] and Boc-deprotection, carried out as described above for synthesis of **179-181**, compounds **194** and **195** were obtained (Scheme 4.13).



Scheme 4.13: Synthesis of compounds **194** and **195** containing piperazine and piperidine. Reagents: (a) 4-benzyl-piperazine/-piperidine, $N(Et)_3$, toluene, 4 d (90-92%); (b) 1.) NaOH aq., CH_3OH , 2.) HCl (quant); (c) **139**, HATU/HOAt/sym.-collidine, DMF (74-79%); (d) 1.) TFA/ CH_2Cl_2 /TIPS (30:30:1), 2.) DMSO/HOAc/ H_2O (8:1:1), 3.) HPLC (68-72%).

4.4.8.2 Biological Evaluation

Table 4.16: Functional potencies of compounds containing a piperazine and piperidine scaffold.

BRS-3				
no.	Z	$-pEC_{50}^a$	E_{max}^a	cLog P
194	N	7.16 ± 0.09	90 ± 1	4.98
195	C	7.52 ± 0.79	84 ± 5	5.85

^a FLIPR-assay. Functional potencies are given in $-pEC_{50} \pm SEM$ from 6 independent concentration-response curves. Compounds tested were inactive on the NMB-R and GRP-R. Additional experimental details are described in Table 4.2 and chapters 4.2.1 and 8.5.

Table 4.16 shows functional activities of the peptidomimetics incorporating piperazine (**194**) and piperidine (**195**). As for the preceding series of compounds, high activities (EC_{50} -values of 70 nM and 30 nM) and selectivities were obtained. Similar as for compounds **183** and **186** (chapter 4.4.5.3), the dose-response curve of compound **195** was found to have a shallow slope (see appendix). The cLogP value of compound **195** clearly exceeds the suggested upper limit of five according to Lipinski *et al.* and would therefore most probably possess poor absorption and permeability properties.

4.4.9 FLIPR Antagonist Experiment

Additional FLIPR experiments were carried out to assess the selectivity of the new agonists to the BRS-3 receptor over the NMB and the GRP receptors. The ability of compounds **163-195** to inhibit receptor activation of the agonists NMB at NMB-R and GRP at GRP-R was investigated. As a reference, the known antagonists [D-Phe¹²]Bn, [D-Phe⁶,Leu¹³,p-chloro-Phe¹⁴]Bn(6-14) and [D-Phe⁶,Leu-NHEt¹³,desMet¹⁴]Bn(6-14) were used.^[232,459,460] First, a solution of the new agonists and reference antagonists at eight different concentrations were added to CHO cells transfected with the NMB or GRP receptor followed by a solution of the agonist and calcium mobilization was permanently measured. In all measurements, no reduction of the calcium emission induced by the presence of the aforementioned compounds could be observed. Thus we conclude, that the investigated compounds are not antagonists of the NMB-R and GRP-R.

4.4.10 Do Peptide- and Small Molecule BRS-3 Agonists bind to different Epitopes?

For a selection of peptidomimetic BRS-3 agonists, binding affinities were determined in the radioligand binding assay (*CEREP*).^[222] The results of these studies are shown

Table 4.17: *Binding affinities (BRS-3) for selected compounds.*

compound	Inhib. ^a	compound	Inhib. ^a
168	14	183	34
171	22	188	5
175	2	189	-1 ^b
176	6	192	5
182	25	195	56

^a Radioligand binding assay (CEREP, Celle L'Evescault, France).^[222] Values are given in percent of control specific binding of the reference compound [D-Tyr⁶,β-Ala¹¹,Phe¹³,Nle¹⁴]Bn(6-14) from two independent measurements at 1 μM. ^b Binding of reference compound slightly improved.

in Table 4.17. Except compound **195**, which showed 56% inhibition of the radioligand binding at a concentration of $c = 10^{-6}$ M, only azapeptides **183** (34%) and **182** (25%) weakly inhibited radioligand binding. If these compounds would bind to the same epitope as the BRS-3 peptide agonists/antagonists, we would have expected a greater inhibition of the radioligand binding. Assuming, that high functional activity requires high affinity to the receptor, a possible explanation for the low inhibition is that the peptides and the small molecule compounds bind to different areas of the receptor. This would be unexpected, because the small molecules were designed to contain peptide structural features critical for high functional activity. For the peptides, structural requirements for binding and functional potency were almost congruent (chapter 4.3.2 and 4.3.3). One can speculate about the parallelism seen for the binding mode of the NMB-R antagonist PD168368 as discussed in chapter 3.2.5.^[290,291] This antagonist has structural similarity to the BRS-3 agonists described in the previous chapters. Because at present, limited data concerning binding and structure is available, an explanation of this phenomenon remains to be awaited in the future.

5 Integrins – An Introduction

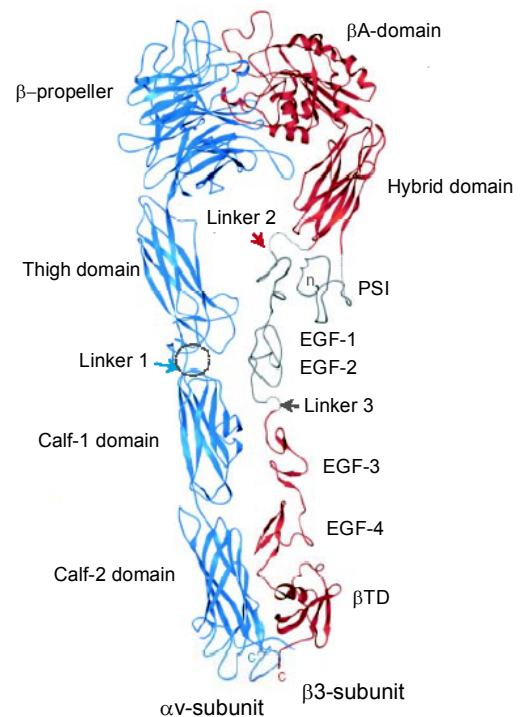
The integrins are a large family of cell adhesion receptors, which besides the cadherins, selectins and the immunoglobulins, mediate cell-cell and cell-matrix interactions.^[461] Adhesive contacts between cells or between cells and the extracellular matrix (ECM) are important for embryogenesis, cell differentiation, hemostasis, wound-healing and immune response.^[345,462-464] These interactions include cell-anchoring and the transmission of signals. The ‘outside-in signaling’ process is thought to affect migration, cell shape and proliferation.^[464,465] Unlike for other receptors, ‘inside-out signaling’ is possible, a process which regulates the status of the integrins between low- and strongly adhesive.^[466]

Integrins are heterodimeric, transmembrane glycoproteins, containing non-covalently linked α - and β -subunits. There are 18 known α - and 8 β -subunits, which make up some 24 different known combinations with the $\beta 1$ -, the $\beta 2$ - and the αv -families (5 integrins) being the largest subgroups.^[467] The most common integrin binding motif is the Arg-Gly-Asp (RGD) sequence found within many extracellular matrix proteins.^[345,468-470]

The $\alpha v \beta 3$ integrin (vitronectin receptor) binds various RGD-containing proteins including fibronectin, fibrinogen, vitronectin, as well as many disintegrins and small peptides. The $\alpha v \beta 3$ integrin is expressed on the surface of a variety of cell types including platelets, endothelial cells, vascular smooth muscle cells, osteoclasts and tumor cells.^[471] Therefore, this integrin is thought to play a major role in angiogenesis,^[472-474] apoptosis,^[475,476] and osteoclast mediated bone resorption.^[477,478]

In 2001, the crystal structure of the extracellular segment of the $\alpha v \beta 3$ integrin was solved (see Figure 5.1).^[479] The N-terminal segment of the αv -subunit contains four repeated motives (9 amino acids of lengths) within the β -hairpin loops of blades 4-7 of the β -propeller, which bind divalent cations (Ca^{2+} , Mg^{2+}) and have structural similarity to the ‘EF hand’ of calmodulin.^[479,480]

Figure 5.1: *Crystal structure of the extracellular segment of $\alpha\beta3$.^[479] The two N-terminal segments assemble into a 'head', from which two 'tails' emerge. The α -subunit (blue) consists of three β -sandwich domains (Calf-1, Calf-2 and thigh domain) and the seven-bladed β -propeller. The $\beta3$ -subunit (red) comprises two 'head' domains, the βA - and the hybrid domain, and six 'tail' domains, namely a PSI domain, four cysteine-rich epidermal growth factor (EGF) domains and a β -tail domain (βTD).*



The interface between the βA domain and the β -propeller was found to have great resemblance to the interface between the α and β subunits of G proteins (see chapter 3.1.2). Interestingly, at the core of this interface, the sidechain of Arg²⁶¹, which is part of a 3_{10} -helix of the βA domain, interacts with several aromatic sidechains of the β -propeller through cation- π bonding.^[479] The βA domain comprises a 'metal ion dependent adhesion site' (MIDAS).^[479] The divalent cation (Ca^{2+} , Mn^{2+}) is coordinated by five amino acids of the integrin and a water molecule, or an glutamate - in the presence of a ligand.^[481,482] A crystal structure of the liganded $\alpha\beta3$ integrin^[333] shows, that the Arg sidechain of the ligand pentapeptide inserts into a groove of the β -propeller forming salt bridges to Asp²¹⁸ and Asp¹⁵⁰, the Asp contacts the Mn^{2+} at MIDAS in βA , and the Gly being at the interface between the β -propeller and the βA domain.

The C-terminus of the β -subunit binds intracellular proteins such as talin,^[483] vinculin,^[484,485] and α -actinin,^[486] thereby linking the receptor to the actin-filament of the cytoskeleton.

6 Synthesis and Biological Evaluation of $\alpha\nu\beta 3$ -Antagonists

6.1 Previous Work and Objective

In recent years, the development of selective $\alpha\nu\beta 3$ integrin antagonists has attracted considerable attention in medicinal chemistry.^[487,488] Besides for small cyclic peptides,^[337,420] progress has been achieved towards nonpeptide ligands. Interestingly, a multitude of different scaffolds proved to be capable of successfully mimicking the original RGD sequence by linking together an C-terminal acidic and N-terminal basic moiety: Among others, there are benzodiazepins,^[489,490] hydantoins^[491], spirocyclic scaffolds,^[492,493] constrained glyceryl amides,^[494] acyliminothiazolines,^[495] and

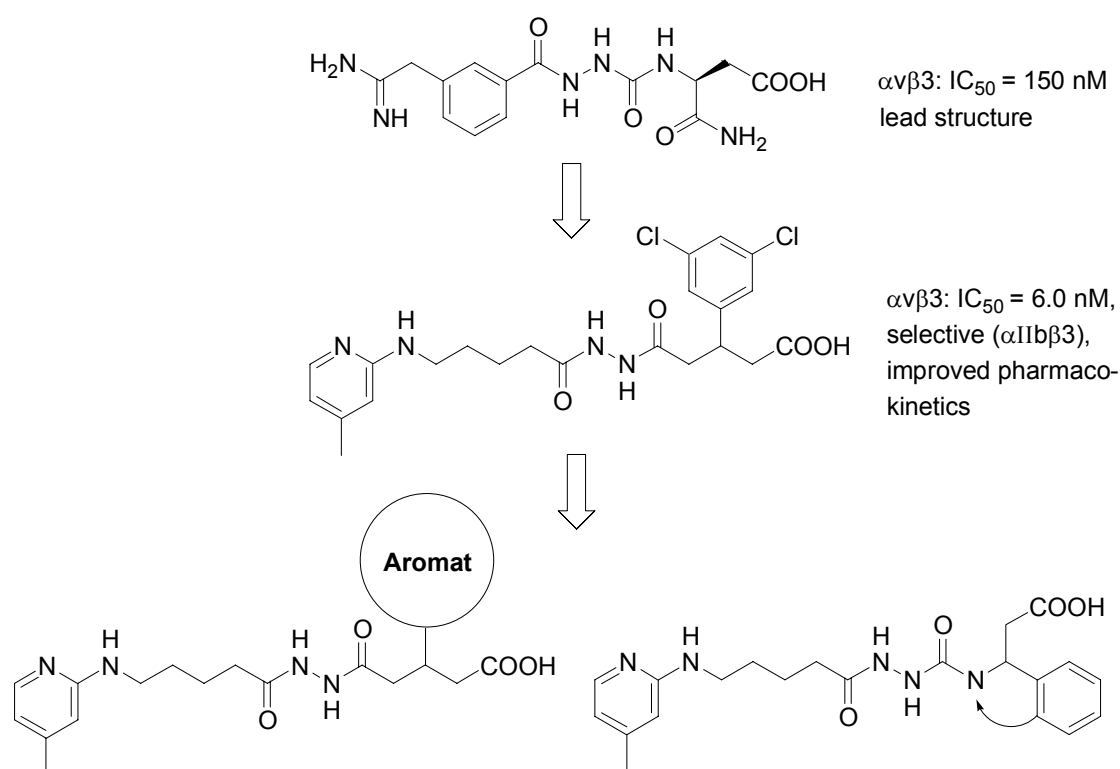


Figure 6.1: Design of $\alpha\nu\beta 3$ integrin antagonists. Previously, a azapeptide lead structure (top)^[457] has been optimized (middle)^[456] by coworkers. This work investigates the incorporation of 1) larger aromatic, heteroaromatic residues and arylethers at the 3-position of the C-terminal glutaric acid (bottom left) and 2) of a cyclic constrained β -amino acid (bottom right).

isoxazolines.^[496] In our group work has been directed towards the development of azapeptide scaffolds as peptidomimetic $\alpha\nu\beta 3$ antagonists (Figure 6.1). Based on a lead structure developed by C. Gibson,^[12,430,457] which incorporates azaglycine (Figure 6.1), a library of peptidomimetics was synthesized by G. Sulyok.^[437,456] Thereby, major improvement was achieved by increasing C-terminal lipophilicity realized through the incorporation of aromatic β -amino acids and bioisosteric glutaric acids as Asp mimetics. Furthermore, basic building blocks and spacers, constituting the arginine mimetic, have been varied. As a result of this optimization a 3,5-dichloro substituted compound bearing methylaminopyridine as guanidine mimetic^[489,490] (Figure 6.1) showed improved affinity and pharmacokinetic properties with approximately 7% oral bioavailability.

As already demonstrated by G. Sulyok in a few examples and assumed to be valid in more general case large aromatic or highly lipophilic residues are favorable for affinity at $\alpha\nu\beta 3$.^[456] In continuation of this work this question will be investigated in more detail. Secondly, heteroaromatic moieties and arylothers will be incorporated. Furthermore, an interesting issue is the tolerance towards C-terminal constraints concerning the backbone. In a previous investigation the insertion of the cyclic carboxylic acid building block nipecotinic acid resulted in an inactive compound.^[456] We assumed that 1) the lack of a C-terminal aromatic residue and 2) a too restricted flexibility of the C-terminal carboxylic acid may be responsible for this result. Since benzodiazepines^[489] and other compounds,^[490] incorporating aromatic residues and an additional methylene unit between the (seven-membered) ring and the carboxylic acid have shown to be potent $\alpha\nu\beta 3$ antagonists we expected the cyclic constrained β -amino acid 2-(1,2,3,4-tetrahydro-1-isoquinoliny)acetic acid (**118**) to be a suitable substitute for aspartic acid.

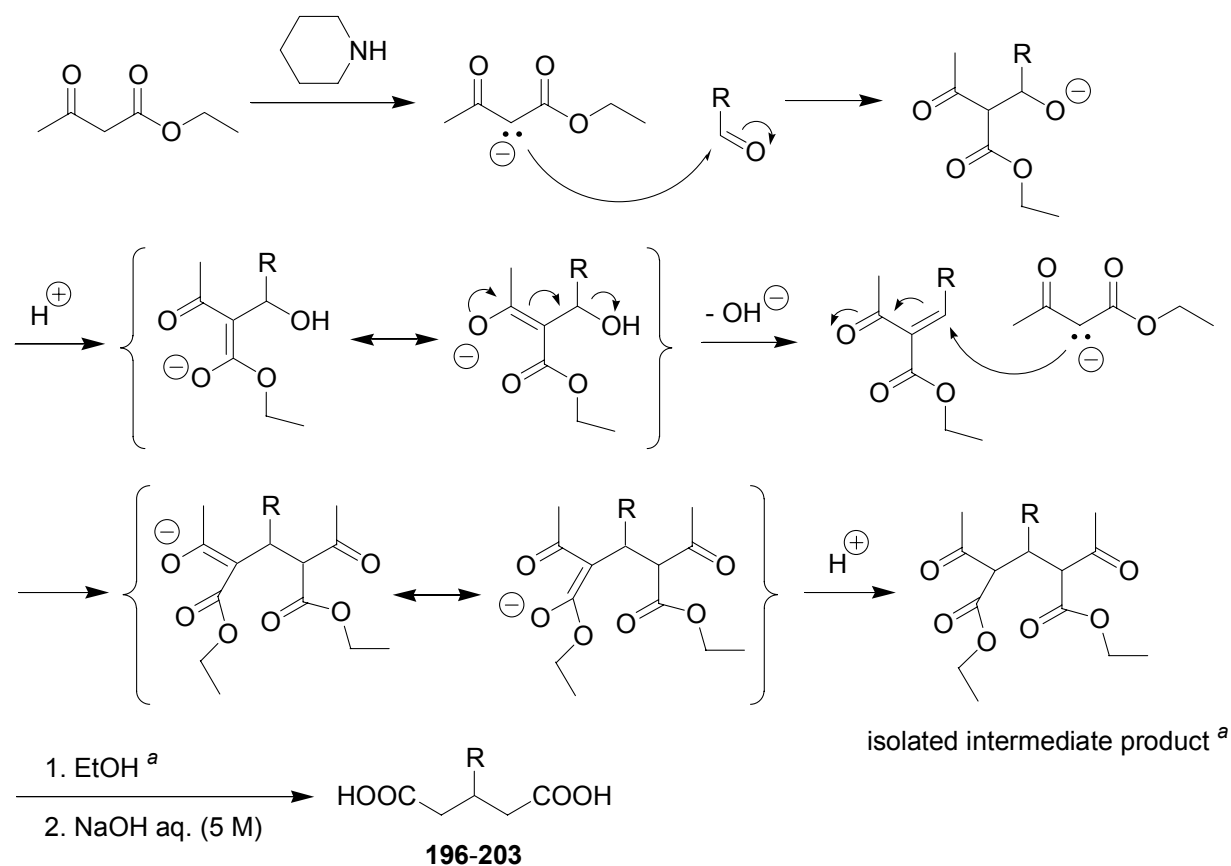
Besides the lengths of the spacer the basicity of the guanidine or of a suitable replacement is an important factor for the selectivity of $\alpha\nu\beta 3$ antagonists over $\alpha\text{IIb}\beta 3$.^[497-501] As already mentioned above (methyl-)aminopyridine in combination with alkyl spacers has a proven record of being such a suitable guanidine replacement with high selectivity for $\alpha\nu\beta 3$.^[437,456,489,490] Because it was pursued to selectively

investigate C-terminal modifications, all $\alpha\nu\beta 3$ antagonists in this series were equipped with 5-[*N*-(4-methylpyridine-2-yl)amino]pentanoic acid (**213**) as Arg mimetic.

6.2 Synthesis

In analogue manner as the parental RGD sequence the planned $\alpha\nu\beta 3$ antagonists can be retrosynthetically dissected into the following subunits: A C-terminal aspartic acid mimetic, a mimetic for the centrally located glycine and an N-terminal arginine mimetic. These individual mimetics and their precursors were synthesized in solution phase, final assembly of the azapeptide $\alpha\nu\beta 3$ antagonists was carried out partially in solution and on solid support (TCP resin^[309]) in similar fashion as previously elaborated by G. Sulyok.^[437,456]

Starting out with differently substituted arylaldehydes (Scheme 6.2) a number of glutaric acids with different substitution in the 3 position were prepared as Asp mimetics (Scheme 6.1). Similar as previously described^[456,502,503] the corresponding arylaldehyde was reacted with two equivalents of ethylacetoacetate, which simultaneously served as a solvent, and 0.136 equivalents of piperidine. Whereas for substituted benzaldehydes the reaction mixture solidifies in reaction times rarely exceeding 24 hrs aldehydes bearing heteroaromatic and large aromatic systems can afford longer reaction times and produce viscous oils (precursors of compounds **196** and **201**). A possible reaction mechanism of this reaction is depicted in Scheme 6.1: First, one equivalent of ethylacetoacetate is thought to condense with the aldehyde in a Knoevenagel-type reaction, then a second equivalent of ethylacetoacetate is consumed in a Michael-addition to yield the racemic 2,4-bisaceto-3-arylglutaric acid diethylester. After recrystallization in ethanol saponification using a 5 M aqueous solution of NaOH interestingly affords, besides the cleavage of the ester groups, a removal of the acetyl-groups in a retro-Claisen reaction. Weaker basic conditions (1 molar) would lead to decarboxylation and the corresponding diketone.^[504] The overall yields of this reaction were in the range of 15-66%.

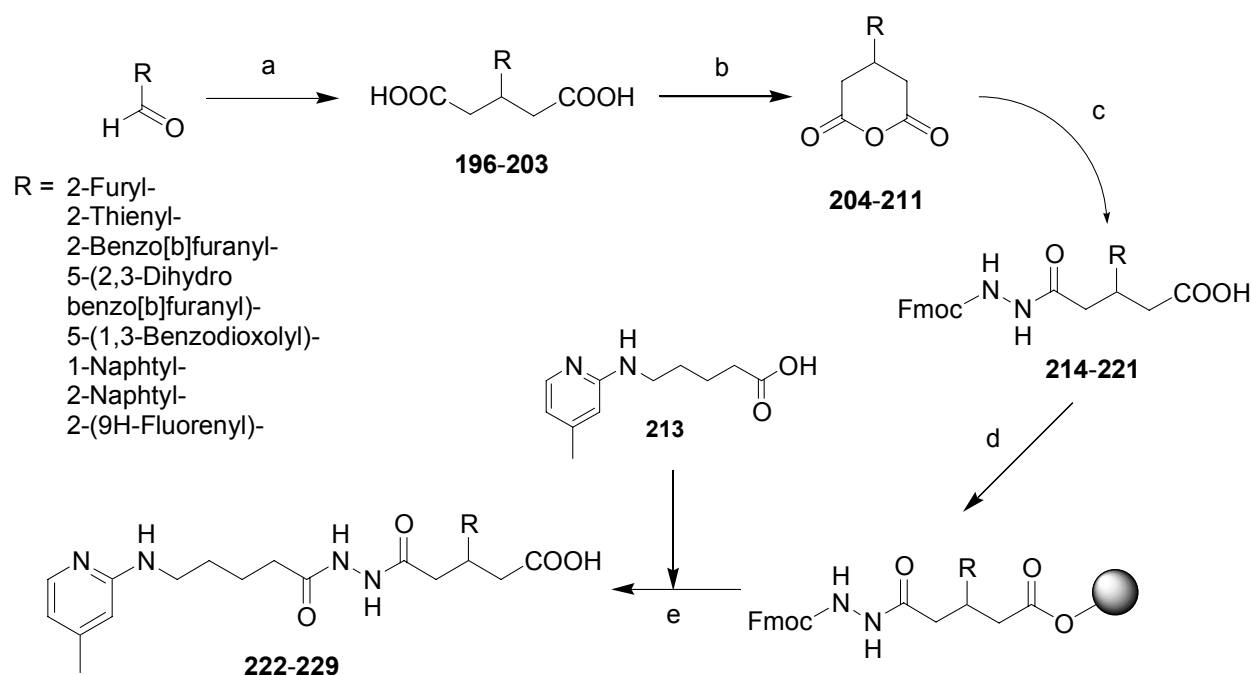


Scheme 6.1: Possible reaction mechanism for the synthesis of glutaric acid building blocks **196-203**: 1) Knoevenagel-type reaction followed by 2) Michael-addition.

^a Intermediate products of **196** and **201** have not been isolated and recrystallized (viscous oils).

As glycine mimetic azaglycine was used.^[12,437,456] The synthesis of Fmoc-hydrazine is described earlier in chapter 4.4.5.2. As already outlined in the previous chapter 5-[*N*-(4-methylpyridine-2-yl)amino]pentanoic acid (**213**) was used as Arg mimetic. It comprises an alkyl spacer, pentanoic acid, and 2-amino-4-methylpyridine as basic moiety. For synthesis a twofold excess of aminopyridine was reacted with 5-bromopentanoic acid ethyl ester over night at 130 °C.^[456,505] Separation from the side product, bisalkylated aminopyridine, was achieved using flash chromatography and yielded 5-[*N*-(4-methylpyridine-2-yl)amino]pentanoic acid ethyl ester (**212**) in 45% yield. Saponification of the ethyl ester **212** was carried out with a 2 M aqueous solution of NaOH. Problems were encountered for the isolation of the product, because the unprotected compound **213** combines a basic and acidic moiety. Although

the product could not be precipitated as previously described,^[456] extraction from the dried residue with chloroform and excess DIPEA was possible (27% yield).



Scheme 6.2: Synthesis of azapeptides **222-229**. Reagents: (a) 1.) ethylacetoacetate, piperidine, 0 °C, 2.) ethanol, reflux,^a 3.) NaOH aq., 85 °C, 4.) HCl (15-66%); (b) acetic anhydride, 140 °C (63-85%); (c) Fmoc-hydrazine (**140**), THF, reflux (64-95%); (d) DIPEA, CH₂Cl₂, TCP resin; (e) 1.) 20% piperidine/NMP, 2.) **213**, HATU/HOAt/sym.-collidine, NMP, 3.) TFA/TIPS/H₂O (18:1:1), 4.) HPLC (6-59%).

^a Intermediate products of **196** and **201** have not been isolated and recrystallized (viscous oils).

Assembly of the $\alpha\text{v}\beta\text{3}$ antagonists started with the solution phase coupling of the C-terminal glutaric acids to Fmoc-hydrazine.^[437,456] In order to achieve selective coupling to one of the two acid groups of the dicarboxylic acids, they were converted to their corresponding anhydrides using a 4.7-fold excess of acetic acid anhydride (Scheme 6.2) and obtained as crystalline solids in yields ranging from 63-85%.^[506] Then the mono-activated and -protected carboxylic anhydrides were reacted with Fmoc-hydrazine in THF under opening of the six-membered ring to give 5-[N²-(Fmoc)hydrazino]-5-oxo-3-arylpentanoic acids **214-221** in 64-95% yield (Scheme

6.2). Prior to coupling of **213** to the Fmoc-protected hydrazine moiety using HATU/HOAt/sym.-collidine activation^[318,320,326] building blocks **214-221** were attached to solid support (Scheme 6.2). Resin loading was in the range of 0.45-0.71 mmol/g. Final cleavage of the $\alpha\beta$ 3 antagonists from the resin was achieved with TFA/TIPS/H₂O (18:1:1). After HPLC purification and lyophilization the azapeptide RGD peptidomimetics **222-229** were obtained in 6-59% yield with respect to resin loading.

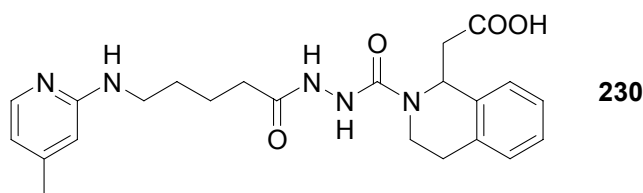


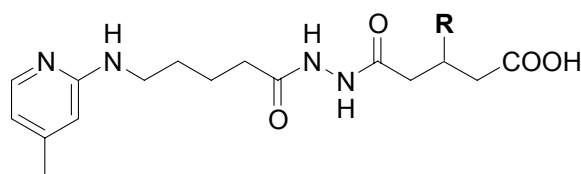
Figure 6.2: Azapeptide RGD peptidomimetic **230** incorporating the cyclic β -amino acid Asp mimetic **118**.

Synthesis of the azapeptide RGD mimetic **230** incorporating the cyclic constrained β -amino acid 2-(1,2,3,4-tetrahydro-1-isoquinolinyl)acetic acid (**118**) (Figure 6.2) was carried out in similar manner as described above for compounds **222-229**. A detailed description for the synthesis of racemic **119** - which is Fmoc-protected **118** - is given earlier in chapter 4.4.3.1 (Scheme 4.3). Whereas loading of TCP resin with **119** was sufficient with 0.426 mmol/g problems were encountered for the coupling of activated Fmoc-hydrazine **141** (chapter 4.4.5.2) to the resin-bound, Fmoc-protected secondary amine **118**. After coupling of the Arg mimetic **213** carried out as described above, cleavage from the resin and HPLC purification, **230** was obtained in only 1.3% yield with respect to resin loading. Optimization of this process was not further pursued.

6.3 Biological Evaluation and Discussion

Binding affinities on isolated integrin receptors $\alpha v\beta 3$, $\alpha v\beta 5$, $\alpha v\beta 6$ and $\alpha IIb\beta 3$ for all synthesized RGD mimetics were determined in the laboratory of Dr. S. Goodman at *Merck KGaA* (Darmstadt). The used αv -integrins were isolated from human placenta, from human thrombocytes ($\alpha IIb\beta 3$) or cloned using a baculovirus system ($\alpha v\beta 3$).^[437,456] The natural ligands vitronectin ($\alpha v\beta 3$, $\alpha v\beta 5$), fibronectin ($\alpha v\beta 6$) and fibrinogen ($\alpha IIb\beta 3$) were obtained from human plasma. Inhibitory effects of the RGD mimetics were determined by measuring their effect on the interaction between immobilized integrin and biotinylated soluble ligands. The exact determination of the IC_{50} -value was carried out only for compounds exceeding the threshold of > 50% inhibition at 10^{-7} M (Table 6.1).

Table 6.1: Azapeptide integrin antagonists incorporating heteroaromatic moieties, arylethers and larger aromatic residues.



no.	R	$\alpha v\beta 3$	$\alpha v\beta 5$	$\alpha v\beta 6$	$\alpha IIb\beta 3$
		IC_{50} [nM] ^a	IC_{50} [nM] ^a	IC_{50} [nM] ^a	IC_{50} [nM] ^a
222	2-Furyl-	78	> 10000	54% ^{b,e}	> 10000
223	2-Thienyl-	31	> 1000	95% ^{b,e}	> 10000
224	2-Benzo[<i>b</i>]furanyl-	17	> 10000	130	> 1000
225	5-(2,3-Dihydro benzo[<i>b</i>]furanyl)-	22	> 10000	52	> 10000
226	5-(1,3-Benzodioxolyl)-	1.2	91% ^{c,e}	50	81% ^{c,e}
227	1-Naphthyl-	120	> 10000	> 10000	> 10000
228	2-Naphthyl-	13	72% ^{c,e}	19	> 10000
229	2-(9 <i>H</i> -Fluorenyl)-	2.3	> 10000	13	62% ^{d,e}

^a Receptor binding assay on isolated integrin receptors (*Merck KGaA*, Darmstadt, Germany). Peptide GRGDSPK was used as a reference for $\alpha v\beta 3$ (IC_{50} = 520 nM), peptide Ac-RTDLDLRLT for $\alpha v\beta 6$ (IC_{50} = 5.7 nM). For additional experimental details see text. ^b Inhibition at 10^{-6} M. ^c Inhibition at 10^{-5} M. ^d Inhibition at 10^{-7} M. ^e IC_{50} -value was not determined.

Compounds **222-224** comprise heteroaromatic moieties, **225** and **226** arylethers, and compounds **227-229** contain larger aromatic systems (Table 6.1). For the series of heteroaromatic residues, affinity towards $\alpha\nu\beta$ 3 increases in the order 2-furyl < 2-thienyl < 2-benzo[*b*]furanyl. Compound **224**, which is bearing the largest residue benzo[*b*]furanyl, has high, however not excellent affinity. It can be speculated, that an exchange of the oxygen atom in the benzo[*b*]furanyl moiety against sulfur would lead to a similar affinity enhancement as seen for the 2-furyl moiety with the 2.5-fold increase. In similar order as observed for $\alpha\nu\beta$ 3, affinity for $\alpha\nu\beta$ 6 increases, however on a lower level. Selectivity against $\alpha\nu\beta$ 5 and α I**II** β 3 is relatively high (> 30 fold).

Interesting results are obtained from the incorporation of arylether moieties (compounds **225** and **226**). The presence of a heteroatom (oxygen) in the *para*-position of the phenyl as realized in the bicyclic 5-dihydrobenzo[*b*]furanyl moiety (compound **225**) leads to a decrease of binding affinity compared to the unsubstituted phenyl ($IC_{50} = 22$ nM compared to 7.3 nM^[456]) similar as for the *para*-methoxy substituted compound^[456] ($IC_{50} = 22$ nM). Insertion of an additional heteroatom (oxygen) in the *meta*-position leading to the 5-benzodioxolyl moiety increases affinity almost 20-fold, thus producing the most potent compound of this series. A very similar observation has been made by researchers at *Merck* (West Point, USA) in a work concerning β -amino acids as Asp mimetic,^[507-509] published during the course of this investigation.

So far the investigation of larger aromatic systems was limited to biphenyl and 1-naphthyl, the latter being incorporated into a β -amino acid.^[456] Whereas similar moderate affinity values were obtained for 1-naphthyl as incorporated in glutaric acid (compound **227**) shifting to 2-naphthyl substantially increases affinity about 10-fold (Table 6.1). The effect for $\alpha\nu\beta$ 6 is even larger: Shifting the anchoring position of naphthyl from one to two leads to an increase of affinity from $IC_{50} > 10000$ (inactive) to $IC_{50} = 19$ nM. Finally it was found, that 2-fluorenyl (compound **229**) is comparable to or slightly better than biphenyl.^[456]

Based on these results a clearer SAR model concerning the requirements of the C-terminal aromatic residue of azapeptide $\alpha\text{v}\beta\text{3}$ antagonists can be proposed (Figure 6.3). Because similar observations have been made for aromatic β -amino acids as part of RGD mimetics based on different scaffolds,^[507-509] this model is expected to be of more general value than just for this series of azacompounds.

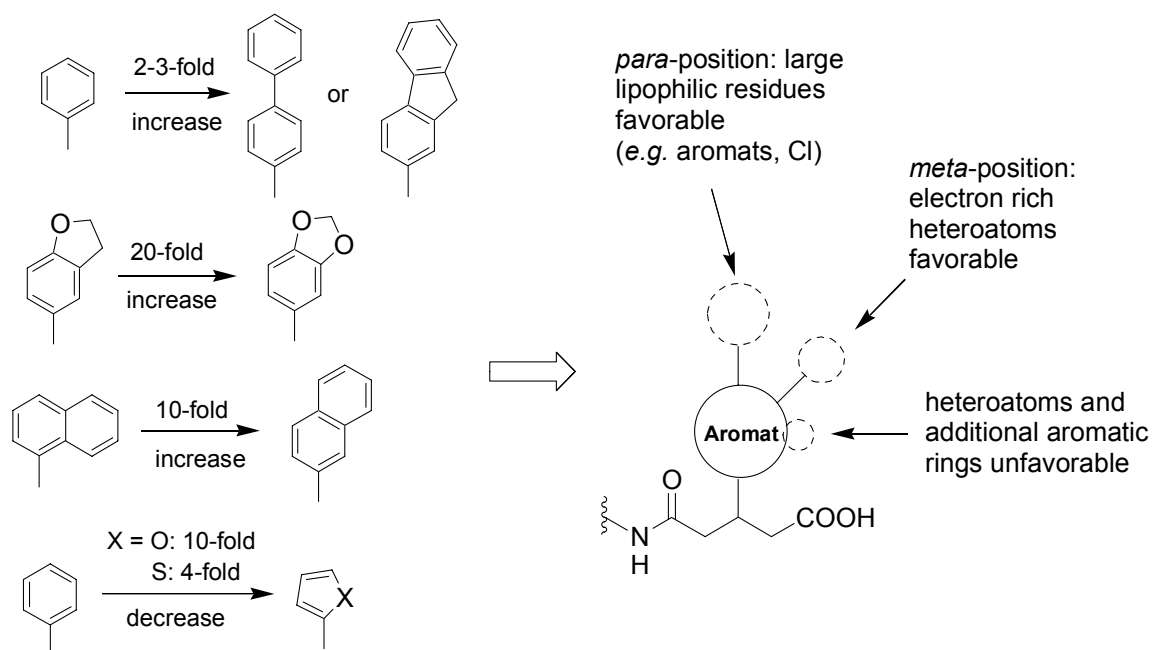


Figure 6.3: C-terminal structure activity relationship model of $\alpha\text{v}\beta\text{3}$ integrin antagonists.

In *para*-position of the aromatic system, large lipophilic residues such as phenyl or chlorine^[456] are favorable for high affinity, probably because of hydrophobic interactions with the receptor. In *meta*-position, electron rich heteroatoms are favorable, whereas electron deficient residues such as NO_2 ^[456] are unfavorable. This may be due to hydrogen bonding or polar interactions with the $\alpha\text{v}\beta\text{3}$ integrin. Finally heteroatoms in the 2-position of the aromatic system or additional aromatic rings annealed in the 2- and 3-position are unfavorable for affinity.

Summarizing the results for $\alpha\nu\beta$ 6 it has been shown in accordance with previous results,^[456] that large and preferably bicyclic aromatic residues are favorable for activity, however only if the second ring is attached or annealed in the 3-/4-position. Biological evaluation of compound **230** incorporating 2-(1,2,3,4-tetrahydro-1-isoquinolinyl)acetic acid (**118**) as Asp mimetic (Figure 6.2) gave only 15% inhibition at $\alpha\nu\beta$ 3, 11% inhibition at $\alpha\nu\beta$ 5 and 0% inhibition at $\alpha\nu\beta$ 6 and α I**1b** β 3 (all measurements were carried out at $c = 10^{-5}$ M). IC_{50} -values are therefore $> 10 \mu\text{M}$. A more systematic investigation with respect to different ring sizes and cyclization positions - as originally planned - was not further conducted. Nevertheless, the evaluation of compound **230** seems to indicate that introducing C-terminal rigidity mediated by a six-membered ring as a scaffold to which the necessary elements for affinity - an aromatic residue and an acetic acid moiety - are connected is not tolerated.

7 Summary

The first part of this work describes the development of bombesin receptor subtype 3 (BRS-3) agonists. The G protein coupled receptor BRS-3 belongs to the class of so-called ‘orphan receptors’, because it was discovered by identifying a gene sequence which shares about 50% homology to those of the more established bombesin receptors NMB-R and GRP-R.^[223] This origin explains the inherent lack of knowledge concerning the physiological function and natural ligands of BRS-3. Latest results point towards an involvement in a special form of lung cancer (SCLC),^[223,276-278] the regulation of the energy household and obesity.^[273] The presented work is the attempt to learn more about the ligand structural requirements of this receptor and to provide new small molecule tool substances for pharmacological research and the elucidation of its function.

A pictorial summary of the BRS-3 project is given in Figure 7.1 and described in the following. Detailed structure activity studies on nonapeptide [D-Phe⁶,β-Ala¹¹,Phe¹³,Nle¹⁴]Bn(6-14)^[222,282] (**1**) and octapeptide [D-Phe⁶,Phe¹³]Bn(6-13) propylamide^[281] (**18**) concerning functional potency on NMB-R, GRP-R, and BRS-3 in a FLIPR-assay were used as a starting point. We could demonstrate that for functional activity of **1** on BRS-3, the amino acids Trp⁸, Phe¹³ and also β-Ala¹¹ are important. However, in **18** the sidechain of His¹² is crucial for BRS-3 functional activity as well. This shift of importance can at least be partially attributed to the difference in backbone length at position 11. Substitution of His¹² by Tyr in **1** led to a high selectivity of GRP-R over BRS-3 and NMB-R: Functional potency on GRP-R was almost maintained whereas functional response on BRS-3 was reduced about 150-fold and about 20-fold on NMB-R.

The knowledge derived from the structure activity studies was used to develop 1) a library of disulfide bridged peptides of varying ring size, which turned out to be devoid of remarkable functional activity and 2) a small tetrapeptide library of peptides comprising the three N-terminal amino acids of **1** and a C-terminally amidated Phe. By permutating the stereochemistry of the two tetrapeptide C-terminal amino acids Trp and Phe it could be demonstrated, that only compound **95** was able to selectively

and the glutamine sidechain and the configuration of the N-terminal D-Phe being of low importance. Furthermore, BRS-3 functional potency of this lead structure could be increased markedly, *i.e.* about 15-fold, by removal of the C-terminal amide. Then efforts were directed towards using the obtained selective short peptide BRS-3 agonist H-D-Phe-Gln-D-Trp-1-(2-Phenylethyl)amide (**109**) as a structural template for the design of proteolytically more stable small molecules. A 'biased' library of peptidomimetics with conserved C-terminal D-Trp-1-(2-Phenylethyl)amide moiety and structural variations on the N-terminal H-D-Phe-Gln unit was developed. It was demonstrated that N-terminal increase of lipophilicity by simple deletion of the aminofunction combined with removal of the Gln sidechain furnished selective BRS-3 agonists in the nanomolar range. Furthermore, substitution of the H-D-Phe-Gln unit by peptide monomers showed that the N-terminal peptide bond is not required for receptor activation. Gln can further be replaced with azaglycine, leading to compounds with subnanomolar activities (**183**: $EC_{50} = 0.19$ nM). For azapeptides, too, a removal of the N-terminal peptide bond is possible (semicarbazides **191-193**). However, as shown by the semicarbazones **187-190** a too lipophilic N-terminus seems not to be tolerated. The finding, that also piperidine or piperazine can be incorporated suggests that a large number of different spacers are able to mimic the function of the former Gln at this position. From the analysis of the substitution and distance pattern for the different series of compounds it seems very likely that a lipophilicity placed at a correct distance from the tryptophan combined with a basic functionality located in between is favorable for functional potency. A further FLIPR experiment, in which the ability of the described peptidomimetics to inhibit activation of NMB-R and GRP-R by their natural ligands was investigated showed, that these compounds are not antagonists for the NMB-R and GRP-R. The fact that some selected peptidomimetics were not able to inhibit radioligand binding was unexpected and leaves open questions as to which epitope these compounds bind in order to activate the receptor as detected in the FLIPR-assay.

In summary this work describes the development of selective tool substances for BRS-3 with improved pharmacokinetic properties, which may prove to be helpful in the understanding of the physiological role of this orphan receptor. At present extended

pharmacological tests including animal tests are conducted with two selected compounds (**183** and **195**) at *MDS Panlabs Inc.* (Taiwan).

The second part of this work describes the synthesis and evaluation of a series of azapeptide RGD mimetics as $\alpha\beta3$ integrin antagonists. The inhibition of integrin receptors is currently thought to be of substantial value for the treatment of pathophysiological processes in which the migration of cells or the invasive formation of new blood vessels plays a central role. By attaching large aromatic systems, heteroaromatics and arylethers to the 3-position of glutamic acid, which serves as a substitute for aspartic acid in the RGD sequence, the prevailing picture of a C-terminal pharmacophore SAR model elaborated by G. Sulyok could be refined. Whereas large lipophilic residues are favorable in *para*-position and electron rich heteroatoms in *meta*-position, heteroatoms in 2-position or annealed aromatic rings in 2-/3-position are likely to decrease affinity. Highest affinity for the $\alpha\beta3$ receptor was achieved by placing an oxygen atom in *meta*-position of the aromatic moiety (compound **226**; $IC_{50} = 1.2$ nM). Increasing C-terminal rigidity by incorporation of the cyclic β -amino acid 2-(1,2,3,4-tetrahydro-1-isoquinoliny)acetic acid (**118**) as mimetic for aspartic acid turned out to be unsuccessful and produced an inactive compound.

8 Experimental

8.1 Materials for Synthesis and General Methods

Solvents for synthesis were either obtained ‘technical grade’ and distilled prior to use or purchased (‘absolute’ or ‘for synthesis’) from *Fluka* (Seelze) or *Merck* (Darmstadt). NMP (distilled) was a gift from *BASF* (Ludwigshafen). Solvents for column chromatography were obtained ‘technical grade’ and distilled prior to use except hexane, which usually was used undistilled. The HPLC-solvents acetonitrile (solvent B) and TFA were purchased ‘gradient grade’ from *Merck* (Darmstadt), water (solvent A) was deionized and further purified using a Milli-Q system from *Millipore* (Molsheim, France).

Fmoc-protected **amino acids** were purchased from *Novabiochem* (Darmstadt), *Advanced ChemTech* (Louisville, USA) or *MultiSynTech* (Witten), 2-(4-formyl-3-methoxyphenoxy)ethyl polystyrene (FMPE) resin, Rink Amide MBHA resin and Sieber Amide resin were purchased from *Novabiochem* (Darmstadt). Tritylchloride polystyrene resin (TCP resin) was obtained from *PepChem* (Tübingen), HATU and HOAT from *Perseptive Biosystems* (Hamburg), TBTU and HOBt from *Quantum Appligene* (Heidelberg), bis(pentafluorophenyl)carbonate from *Senn Chemicals* (Dielsdorf, Switzerland), 3-(4-chlorophenyl)propionic acid from *CPS Chemie + Service* (Düren), TFA from *Solvay* (Hannover) and 2,3-dihydrobenzo[*b*]furan-5-carbaldehyde from *Maybridge Chemicals* (UK). All other **chemicals** were purchased from *Aldrich* (Deisenhofen), *Merck* (Darmstadt), *Lancaster* (Mühlheim), or *Fluka* (Seelze).

Peptide Synthesis was carried out manually or on a multiple peptide synthesizer *SyRoll* from *MultiSynTech* (Witten). For manual synthesis, PE-syringes (2 mL, 5 mL or 20 mL) from *Becton-Dickinson* (Fraga, Spain) or *Braun* (Melsungen) equipped with PE-frits from *Roland Vetter Laborbedarf* (Ammerbuch) were used. To ensure optimal mixing conditions, the syringes were rotating at about 30 rpm. Loading of the resin was carried out in glassware equipped with glass frits.

Air or moisture sensitive reactions were carried out in dry glassware and under argon (99.996%) atmosphere. Moisture sensitive and/or absolved solvents were transferred in syringes under argon.

For **HPLC purification** compounds were dissolved in DMSO, acetonitrile or methanol ('gradient grade') and filtered using syringe filters RC 15 or RC 25 (RC-membrane, 0.45 μm) from *Sartorius* (Göttingen). Purification and analytical purity determination was carried out on RP-HPLC systems from *Amersham Pharmacia Biotech* (analytical: Äkta Basic 10F with pump system P-900, detector UV-900 and Autosampler A-900; preparative: Äkta Basic 100F with pump system P-900, detector UV-900) or *Beckman* (System Gold with solvent module 125 and detector module 166; pump system 110B, control unit 420 and detector *Knauer* Uvicord) were used equipped with columns from *Omniscrom YMC* (analytical: ODS-A C₁₈, 250 mm \times 4.6 mm, 5 μm , flow rate: 1 mL/min; semi-preparative: ODS-A C₁₈, 250 mm \times 20 mm, 5 μm or 10 μm , flow rate: 8 mL/min; preparative: ODS-A C₁₈, 250 mm \times 30 mm, 10 μm , flow rate: 25 mL/min) or *Macherey-Nagel* (preparative: Nucleosil C₁₈, 250 mm \times 40 mm, 7 μm , flow rate: 25 mL/min). Compounds were eluted with linear gradients (30 min) of acetonitrile (solvent B) in water (solvent A) and 0.1 % (v/v) TFA. For **analytical purity determination** of the compounds after semi-preparative or preparative HPLC purification the peak integrals of the analytical HPLC chromatogram at the detector wavelength of 220 nm was evaluated.

For **column chromatography** Silica Gel 60 (230-400 mesh ASTM, Korngröße 0,040-0,063 mm) from *Merck* (Darmstadt) was used in 50-100 fold excess to the raw material, for flash chromatography pressure of 1-1.2 bar was applied.

Thin layer chromatography (TLC) and the determination of the R_f-value was carried out using TLC aluminium sheets covered with Silica Gel 60 F₂₅₄ from *Merck* (Darmstadt). For detection, TLC-plates were examined under UV-light ($\lambda = 254 \text{ nm}$). If enhanced visualization was necessary, the plate was treated with aqueous molybdophosphoric acid/cer-(IV)-sulfate solution (6.25 g molybdophosphoric acid hydrate, 2.5 g cer-(IV)-sulfate, 15 mL sulfuric acid and 235 mL water) and heated.

Melting points were determined on a *Büchi* 510 melting point apparatus according to Dr. Tottoli and are uncorrected.

All $^1\text{H-NMR}$ and $^{13}\text{C-NMR}$ spectra were recorded on *Bruker* AC250 or DMX500 instruments at 300 K, spectral data was processed on *Bruker* Aspekt 1000 (AC 250) or on *Silicon Graphics Indy*-, *O2*- and *Octane*-workstations running XWIN-NMR software. Chemical shifts (δ) are given in parts per million (ppm) relative to tetramethylsilan, coupling constants are given in Hertz (Hz). As internal standard, tetramethylsilane or the solvent peak was used: DMSO- d_5 : 2.49 ppm ($^1\text{H-NMR}$) and DMSO- d_6 : 39.5 ppm ($^{13}\text{C-NMR}$); CHCl_3 : 7.24 ppm ($^1\text{H-NMR}$) and CDCl_3 : 77.0 ppm ($^{13}\text{C-NMR}$). $^{13}\text{C-NMR}$ spectra were recorded ^1H broad band decoupled. For peak assignment, HMQC- and COSY-experiments were performed in most cases.

GC-mass spectrometry (EI or CI) was carried out on a *Finnigan* MAT 8200 instrument connected to a GC-unit Serie 4160 from *Carlo Erba*. **Electrospray ionisation** (ESI)-mass spectra were recorded on a *Finnigan* LCQ mass spectrometer in combination with a *Hewlett Packard* 1100 HPLC-system equipped with a ODS-A C_{18} (125 mm \times 2 mm, 3 μm , flow rate: 0.2 mL/min) column from *Omniscrom YMC*. Compounds were eluted with linear gradients (15 min) of water (solvent A) and acetonitrile (solvent B) in 0.1% (v/v) formic acid. Low-resolution mass spectra are given in the form 'X (Y) $[\text{M}+\text{Z}]^+$ ', where 'X' is the detected mass, 'Y' the observed intensity of the mass peak, 'M' the investigated molecule and 'Z' the attached cation.

High-resolution mass spectra (HRMS) were recorded by *Solvay Pharmaceuticals GmbH* (Hannover) (BRS-3 agonists) and at the mass spectrometry facility of the *University of Cincinnati* (Cincinnati, Ohio, USA) on spectrometers using the electrospray ionisation-time of flight (ESI-TOF) technique.

Lyophilization was carried out using an Alpha 2-4 lyophilizer from *Christ* (Osterode).

cLogP-values (logarithm of the partition coefficient between n-octanole and water) were calculated by *Solvay Pharmaceuticals GmbH* (Hannover) using *Sybyl 6.8* from *Tripos Inc.*

8.2 General Synthetic Methods

8.2.1 General Methods for Solid-Phase Synthesis

General Method 1: Reductive Amination of the Formyl Resin FMPE and Coupling of the First Amino Acid^[310,332]

FMPE resin (2.378 g, maximum capacity: 0.5 mmol/g) is pre-swollen in DCE (24 mL) for 10 min. Then TMOF (12 mL), the appropriate amine (11.89 mmol) and NaBH(OAc)₃ (2.52 g, 11.89 mmol) are added and the mixture is submitted to ultrasonic for 10 min and then shaken over night at room temperature. The resin is washed with CH₂Cl₂ (3 × 20 mL, 3 min each) and NMP (3 × 20 mL, 3 min each) followed by the addition of a mixture of the Fmoc-protected amino acid (2.378 mmol), HATU (0.904 g, 2.378 mmol), HOAt (0.323 g, 2.378 mmol) and sym.-Collidine (2.882 g, 23.78 mmol) in NMP (20 mL). The resin is shaken at room temperature for 5 hrs, then washed with NMP (3 × 20 mL, 3 min each) and again treated over night with a mixture of the Fmoc-protected amino acid (2.378 mmol), HATU (0.904 g, 2.378 mmol), HOAt (0.323 g, 2.378 mmol) and sym.-collidine (2.882 g, 23.78 mmol) in NMP (20 mL) (double coupling). Finally the resin is washed with NMP (3 × 20 mL, 3 min each), CH₂Cl₂ (3 × 20 mL, 3 min each) and dried thoroughly *in vacuo*. The loading of the dry resin is determined using the following equation:

$$l = \frac{(m_2 - m_1) \times 1000}{(MW_{aa} + MW_a - 34.01) \times m_2}$$

- l loading of the resin with building block (Fmoc-protected amino acid plus amine) [mmol/g]
m₁ weight of the used resin before coupling [g]
m₂ weight of the dried polymer after coupling [g]

MW_{aa} molecular weight of the Fmoc-protected amino acid [g/mol]

MW_a molecular weight of the amine [g/mol]

General Method 2: Loading of TCP Resin

To pre-swollen TCP resin (1.16 g, maximum capacity: 0.9 mmol/g) in dry CH_2Cl_2 (6 mL, 10 min.), the appropriate Fmoc-protected amino acid or Fmoc-protected carboxylic acid building block (1.56 mmol, 1.5 eq) and DIPEA (177 μ L, 1.03 mmol) is added and the resin is left to stand for 5 min. Then DIPEA (91 μ L, 0.52 mmol) is added and the resin is shaken. After 2 hrs, for capping of unreacted trityl-groups, methanol (1.16 mL) is added and the resin is shaken for another 15 min. Finally the resin is washed with dry CH_2Cl_2 (5×20 mL, 3 min each), NMP (5×20 mL, 3 min each), dry CH_2Cl_2 (5×20 mL, 3 min each), then with a mixture of methanol/ CH_2Cl_2 (1:1, 20 ml) and methanol (20 ml). The resin is dried thoroughly *in vacuo*, and the loading of the dry resin is determined using the following equation:

$$l = \frac{(m_2 - m_1) \times 1000}{(MW - 36.45) \times m_2}$$

l loading of the resin with building block [mmol/g]

m_1 weight of the used resin before coupling [g]

m_2 weight of the dried polymer after coupling [g]

MW molecular weight of the Fmoc-protected amino acid/carboxylic acid building block [g/mol]

The error that emerges from the weight difference between Cl- and MeO- can be neglected.

General Method 3: Cleavage of the Fmoc-Protecting-Group^[306]

The resin (100 mg) is pre-swollen in NMP (5 mL, 10 min). The Fmoc-protecting-group is cleaved with a freshly prepared solution of 20% piperidine (v/v) in NMP (5 mL) for 15 min, then the resin is washed with NMP (5×5 mL, 3 min each) and again treated with 20 % piperidine (v/v) in NMP (5 mL, 15 min). Finally the resin is washed with NMP (5×5 mL, 3 min each).

General Method 4: Coupling with TBTU/HOBt^[324,325]

The resin-bound free amine (0.045 mmol) is washed with NMP (5 × 5 mL, 3 min each). Then the resin is treated with a solution of the appropriate Fmoc-protected amino acid or carboxylic acid building block (0.09 mmol, 2 eq), HOBt·H₂O (12.2 mg, 0.09 mmol, 2 eq) and TBTU (28.9 mg, 0.09 mmol, 2 eq) in NMP (2 mL). At last, DIPEA (44 μL, 0.256 mmol, 5.7 eq) is added and the resin is shaken for 45 min. After washing with NMP (5 × 5 mL, 3 min each), the coupling step is repeated using the same reagents, amounts and coupling time (double coupling). Finally the resin is washed with NMP (5 × 5 mL, 3 min each).

General Method 5: Coupling with HATU/HOAt^[318,320,326]

The resin-bound free amine or hydrazine (0.389 mmol) is washed with NMP (5 × 5 mL, 3 min each). Then the resin is treated with a solution of the appropriate Fmoc-protected amino acid or carboxylic acid building block (0.779 mmol, 2 eq), HATU (296 mg, 0.779 mmol, 2 eq) and HOAt (106 mg, 0.779 mmol, 2 eq) in NMP (5 mL). At last, sym.-collidine (1027 μL, 7.79 mmol, 20 eq) is added and the resin is shaken over night. After washing with NMP (5 × 5 mL, 3 min each), the coupling step is repeated using the same reagents, amounts and coupling time (double coupling). Finally the resin is washed with NMP (5 × 5 mL, 3 min each).

General Method 6: Acetylation of Resin-Bound Free Amines

The resin-bound free amine (100 mg resin) is washed with NMP (5 × 5 mL, 3 min each). Then a mixture of acetic acid anhydride (0.28 mL, 2.9 mmol), DIPEA (0.48 mL, 2.8 mmol) and NMP (4.2 mL) is added and the resin is shaken for 20 min. Finally the resin is washed with NMP (5 × 5 mL, 3 min each).

General Method 7: Standard Protocol for Solid Phase Synthesis

The protected amino acids or carboxylic acids are coupled according to the following general protocol:

step	reagents	operation	number	time [min]
1	NMP	washing	1	10
2	20% (v/v) piperidine/NMP	deprotecting	1	15
3	NMP	washing	5	3
4	20% (v/v) piperidine/NMP	deprotecting	1	15
5	NMP	washing	5	3
6	BB ^a /DIPEA/HOBt/TBTU/NMP	coupling	1	45
7	NMP	washing	5	3
8	BB ^a /DIPEA/HOBt/TBTU/NMP	coupling	1	45
9	NMP	washing	5	3

^a Building block = Fmoc-protected amino acids or commercially available carboxylic acids.

If the synthesis is stopped at one point over night, the resin is washed with NMP (5 times, 3 min each) and dry CH₂Cl₂ (5 times, 3 min each) and thoroughly dried *in vacuo*. Before the compound is cleaved from the resin under acidic condition, the Fmoc-group is removed according to general method 3.

General Method 8: Cleavage from FMPE, TCP or Rink Amide MBHA Resin and Deprotection

Cleavage and deprotection of the compound from the resin is achieved using the following general protocol:

step	reagents	operation	number	time [min]
1	CH ₂ Cl ₂	washing	3	10
2	TFA/TIPS/H ₂ O (18:1:1)	cleaving/deprotecting	3	30
3	CH ₂ Cl ₂	washing	3	3

For 100 mg of resin, usually 2 mL of cleaving reagent is used. The combined filtrates of the steps 2 and 3 are reduced *in vacuo* using a liquid-nitrogen-cooled rotary evaporator.

General Method 9: Cleavage from Sieber Amide Resin and Deprotection

The dried Sieber Amide resin (approx. 100 mg, 0.036-0.052 mmol) is pre-swollen in CH_2Cl_2 . The linear peptide is cleaved from the resin by continuously dropping CH_2Cl_2 (70 mL) with 1% (v/v) TFA through the resin within a time period of 3 hrs (flow-procedure). Then, water (1 mL) is added to the yellow solution and the organic solvent is removed *in vacuo*. The residue is treated with TFA (1.8 mL), water (0.1 mL) and triisopropylsilane (0.1 mL) and left to stand for 30 min. Then the solvent is evaporated using a liquid-nitrogen-cooled rotary evaporator and a freshly prepared solution of 20% piperidine (v/v) in NMP (10 mL) is added and the mixture is left to stand for another 30 min. The deprotected, linear peptide is precipitated by adding this mixture to an ice-cold solution of diethyl ether (200 mL). After 10 min, the solution with the precipitated peptide is centrifugated and the solvent is decanted.

General Method 10: Formation of Disulfide-bridged Cyclic Peptides via Cysteine Oxidation^[379,380]

The linear peptide, containing two trityl-protected cysteins, is cleaved from Sieber Amide resin and deprotected according to general method 9. Then the peptide is dissolved in DMSO (40 mL), water (40 mL) is added slowly and the solution is stirred at room temperature over night. The solution is removed *in vacuo* using a liquid-nitrogen-cooled rotary evaporator, and the residue is submitted to RP-HPLC.

General Method 11: Coupling of 5-(9*H*-Fluoren-9-ylmethoxy)-1,3,4-oxadiazol-2(3*H*)-one (141) to Resin-Bound Free Amines^[430]

FMPE resin (100 mg, 0.354 mmol/g, 0.035 mmol) is treated with 20% piperidine (v/v) in NMP (2×5 mL, 15 min each) to deprotect the resin-bound amine. Then the resin is washed with NMP (5×5 mL, 3 min each), dry CH_2Cl_2 (5×5 mL, 3 min each) and subsequently left in dry CH_2Cl_2 (5 mL) for half an hour. Then the resin is treated with a solution of 5-(9*H*-fluoren-9-ylmethoxy)-1,3,4-oxadiazol-2(3*H*)-one (**141**) (30.5 mg, 0.108 mmol, 3.1 eq) in dry CH_2Cl_2 (1 mL) and stirred for 90 min. The reaction is stopped by washing with CH_2Cl_2 (5×5 mL, 3 min each) and NMP (5×5 mL, 3 min each).

8.2.2 General Methods for Solution-Phase Synthesis

General Method 12: Synthesis of *N*-Arylalkylated Glycine or Alanine Ethyl Ester Derivatives^[417,418]

In a 250 ml flask the appropriate benzylamine or phenylethylamine (50 mmol) and triethylamine (50 mmol) are stirred in toluene (38 mL) at 0 °C. Then, the appropriate bromoacetic acid ethyl ester, bromoacetic acid tert-butyl ester or 2-bromo-propionic acid ethyl ester (50 mmol) in toluene (18 mL) is added dropwise during a period of 4 hrs and then the mixture is left stirring for 4 d at room temperature. For workup the organic phase is extracted with water (300 mL) and dried over Na₂SO₄. The solvent is removed and, if necessary, the residue is submitted to flash-chromatography (ethyl acetate/ hexane, 1:1).

General Method 13: Synthesis of *N*-Arylalkyl-*N*-[(9*H*-fluoren-9-ylmethoxy) carbonyl] Glycine or Alanine Derivatives

The appropriate *N*-arylalkylated glycine or alanine ethyl ester (5.17 mmol) is treated with 1 N NaOH (7.76 mL, 7.76 mmol) and methanol (15 mL) for 30 min at room temperature. Then, the solution is neutralized with 1 N HCl, the solvent is removed *in vacuo*, and the residue is dissolved in saturated NaHCO₃-solution (16 mL) and dioxane (4 mL). Under ice cooling Fmoc-Cl (5.3 mmol) dissolved in dioxane (10 mL) is added dropwise over 15 min. The solution is stirred for another 30 min at 0 °C and then over night at room temperature. For workup, water (20 mL) is added and the aqueous phase is washed with diethyl ether (100 mL) and then acidified with conc. HCl to pH = 1. Finally the product is extracted with ethyl acetate (3 × 100 mL), the solvent evaporated and, if necessary, the residue is chromatographed (ethyl acetate/hexane/acetic acid, 1:1:1%).

General Method 14: Synthesis of (4-Benzyl-piperazin/piperidin-1-yl)acetic acid

The appropriate ester (3.82 mmol) is treated with 1 N NaOH (5.73 mL, 5.73 mmol) and methanol (11.5 mL) at room temperature and stirred over night. For

workup, the solution is neutralized with conc. HCl and evaporated to dryness. The residue is then submitted to flash-chromatography (methanol/chloroform, 1:1).

General Method 15: Synthesis of *N'*-(Arylmethylene)hydrazinecarboxylic Acid *tert*-Butyl Ester Derivatives^[446]

In a 250 ml flask the appropriate arylaldehyde (15 mmol) in THF (5 mL) is added dropwise at room temperature over 10 min to a stirred solution of *tert*-butoxycarbonyl hydrazine (15 mmol) in THF (15 mL). The precipitated product is collected after 3 hrs and dried, or, in cases, where no precipitation occurs, the solvent is removed and the residue is submitted to flash-chromatography.

General Method 16: Synthesis of *N*-(*tert*-Butoxycarbonyl)-*N'*-arylmethyl hydrazine Derivatives^[448]

A suspension of the appropriate *N'*-(arylmethylene)-hydrazinecarboxylic acid *tert*-butyl ester (6.8 mmol) in dry THF (30 mL) is treated with NaCNBH₃ (10.2 mmol) at 0 °C under argon atmosphere. Then acetic acid (11.5 mL) is added dropwise over a period of 10 min and the resulting clear mixture is left stirring over night at room temperature. For workup, water (60 mL) and ethyl acetate (60 mL) are added, the aqueous phase is brought to pH = 8 with NaHCO₃. Then the organic layer is separated, washed with saturated NaHCO₃-solution (50 mL) and brine (50 mL), dried over Na₂SO₄ and concentrated *in vacuo*. The colourless residue is treated with methanol (40 mL) and 1 N NaOH (20 mL), stirred for 1 hr at room temperature and heated to reflux for 1 hr. Then the product is extracted with diethyl ether (3 × 100 mL), the solvent is removed and drying yields a yellow oil which, if necessary, is submitted to flash-chromatography.

General Method 17: Synthesis of *N*-Arylmethyl-*N'*-[(9*H*-fluoren-9-ylmethoxy)carbonyl]-*N'*-(*tert*-butoxycarbonyl)hydrazine Derivatives

The appropriate *N*-arylmethyl-*N'*-(*tert*-butoxycarbonyl)hydrazine (4.49 mmol) is suspended in dioxane (7 mL) and 10% NaHCO₃ (23 mL) at 0 °C. After Fmoc-Cl (4.95 mmol) in dioxane (14 mL) is added dropwise within 10 min, the mixture is allowed to stir over night at room temperature. For workup, water (70 mL) is added, the aqueous

phase is then extracted three times with diethyl ether (300 mL), the organic phase is separated and the solvent removed *in vacuo*. The residue is then submitted to flash-chromatography.

General Method 18: Coupling with TBTU/HOBt in Solution^[324,325]

The appropriate carboxylic acid (2.14 mmol), amine (2.14 mmol), HOBt (3.21 mmol) and TBTU (3.21 mmol) are dissolved in DMF (15 mL). Then DIPEA (9.2 mmol) is added dropwise over 5 min. at room temperature and the solution is allowed to stir under TLC-control for a given time. The solvent is removed using a liquid-nitrogen-cooled rotary evaporator and the residue is submitted to flash-chromatography.

General Method 19: Coupling with HATU/HOAt in Solution^[318,320,326]

The appropriate carboxylic acid (0.736 mmol), amine (0.736 mmol), HATU (1.10 mmol) and HOAT (1.10 mmol) are dissolved in DMF (7 mL). Then sym.-collidine (11.0 mmol) is added dropwise over 10 min at room temperature and the solution is allowed to stir for a given time. The solvent is removed using a liquid-nitrogen-cooled rotary evaporator and the residue is submitted to flash-chromatography.

General Method 20: Cleavage of the Fmoc-Protecting-Group in Solution^[306]

The appropriate Fmoc-protected amine (1.59 mmol) is dissolved in a solution of 20% (v/v) piperidine in DMF (6 mL) at room temperature and the solution is allowed to stir for 30 min. Then the solvent is removed *in vacuo* using a liquid-nitrogen-cooled rotary evaporator and the residue is submitted to flash-chromatography.

General Method 21: Deprotection of Boc-Protected Tryptophan-Containing Compounds in Solution^[331,370]

The appropriate Boc-protected tryptophan-containing compound (0.289 mmol) is dissolved in CH₂Cl₂ (3 mL). Triisopropylsilane (0.1 mL) is added and the solution is cooled to 0 °C. Then TFA (3 mL) is added dropwise over 5 min and the solution is allowed to stir for 1 hr. The solvent is removed *in vacuo* using a liquid-nitrogen-cooled

rotary evaporator and the residue is treated with a mixture of DMSO (8 mL), water (1 mL) and acetic acid (1 mL) and stirred over night. The solution is evaporated to dryness using a liquid-nitrogen-cooled rotary evaporator and the residue is submitted to RP-HPLC.

General Method 22: Coupling with Bis(pentafluorophenyl)carbonate in Solution^[431]

The appropriate *N*-arylmethyl-*N*-[(9*H*-fluoren-9-ylmethoxy)carbonyl]-*N'*-(*tert*-butoxycarbonyl)hydrazine (0.54 mmol) is dissolved in CH₂Cl₂ (2 mL), triisopropylsilane (0.1 mL) is added and the solution is cooled to 0 °C. Then TFA (2 mL) is added dropwise over 5 min and the solution is allowed to stir for 30 min until TLC-control showed complete cleavage of the Boc-protecting-group. The solution is evaporated to dryness using a liquid-nitrogen-cooled rotary evaporator and redissolved in a solution of dry CH₂Cl₂ (8 mL) and DMAP (0.54 mmol). This solution is added dropwise and under stirring to a solution of bis(pentafluorophenyl)carbonate (0.54 mmol) in dry CH₂Cl₂ (20 mL) over a period of 20 min. Upon completion of the addition, a solution of the amine (0.54 mmol), DMAP (0.54 mmol) and dry CH₂Cl₂ (8 mL) is added. The resulting mixture is allowed to stir for 30 min at room temperature. Then the solvent is removed *in vacuo* and the residue is redissolved in CH₂Cl₂ (4 mL) and triisopropylsilane (0.1 mL) and the solution is cooled to 0 °C. TFA (4 mL) is added dropwise over 5 min and the solution is allowed to stir for 30 min. The solution is evaporated to dryness using a liquid-nitrogen-cooled rotary evaporator and then treated with a solution of 20% (v/v) piperidine in DMF (10 mL) for 30 min. at room temperature. The solvent is removed using a liquid-nitrogen-cooled rotary evaporator and the product is purified by RP-HPLC.

General Method 23: Cleavage of the Fmoc-Protecting-Group and Hydrazone Formation in Solution

*N*1-(2-Phenylethyl)-(2*R*)-2-{[*N'*-((9*H*-fluoren-9-ylmethoxy)carbonyl)hydrazino]carboxamido}-3-[1-(*tert*-butoxycarbonyl)-3-indolyl]propanamide (**142**) (0.26 mmol) is dissolved in a solution of 20% (v/v) piperidine in DMF (2 mL) at room temperature

and the solution is allowed to stir for 30 min. Then the solvent is removed *in vacuo* using a liquid-nitrogen-cooled rotary evaporator, the residue is redissolved in THF (10 mL) and the appropriate aldehyde (0.26 mmol, 1 eq) is added. The mixture is allowed to stir at room temperature. After 2-24 hrs, another 1-2 eq of the aldehyde are added. As soon as TLC-control shows sufficient product formation, the solution is evaporated to dryness and the residue is submitted to flash-chromatography.

General Method 24: Synthesis of 3-Arylglutaric Acids^[456,502,503]

A mixture of the appropriate arylaldehyde (80 mmol) and ethylacetoacetate (159 mmol) is cooled to 0 °C and stirred. Then piperidine (1.08 mL) is added dropwise within 10 min and the mixture is allowed to warm up to room temperature and left stand for 3 days. The mixture usually solidifies after 24 to 48 hrs. To the obtained solid ethanol (70 mL) is added and the suspension is heated until a clear solution is formed. This solution is allowed to cool down to room temperature, the precipitation is collected in a funnel, washed with small amounts of ethanol and dried *in vacuo*. In some cases, the reaction mixture remains a viscous oil. In this case the intermediate product is not isolated. The intermediate product is saponified by portionwise addition to a stirred solution of NaOH (10 g, 0.25 mol) in water (50 mL) at 85 °C, and kept at this temperature for additional 3 hrs. Then the mixture is allowed to cool, and after addition of ice (100 g), it is extracted with ethyl acetate (3 × 50 mL). The aqueous phase is then carefully acidified to pH = 1 with conc. HCl. Upon acidification the product precipitates or separates as oil from the aqueous phase. The precipitation is collected, the oil is extracted with ethyl acetate, dried over MgSO₄, and evaporated to dryness. The obtained solid is dried *in vacuo*.

General Method 25: Synthesis of 3-Arylglutaric Acid Anhydrides^[506]

The appropriate 3-arylglutaric acid (10 mmol) is mixed with acetic acid anhydride (4.5 mL), heated to 140 °C (oil bath temperature) under reflux and kept at this temperature for 30 min. Then the mixture is allowed to cool to room temperature. In cases where the product crystallizes, it is separated and dried *in vacuo*. If no

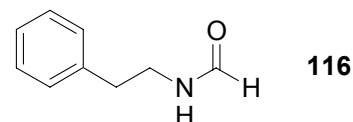
precipitation occurs the solvent is evaporated and the residue is chromatographed (CH_2Cl_2 /ethyl acetate, 20:1).

General Method 26: Synthesis of 5-[*N'*-(9*H*-Fluoren-9-ylmethoxycarbonyl)hydrazino]-5-oxo-3-arylpentanoic acids

The appropriate 3-arylglutaric acid anhydride (3.57 mmol) and an equimolar amount of *N*-[(9*H*-fluoren-9-ylmethoxy)carbonyl]hydrazine (**140**) are dissolved in dry THF (40 mL) and refluxed at 100 °C (oil bath temperature) over night under argon atmosphere. Then the solvent is evaporated and the residue is chromatographed (ethyl acetate/hexane/acetic acid, 2:1:1%).

8.3 BRS-3 Agonists

8.3.1 Solution-Phase Synthesis of Building Blocks

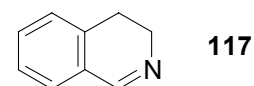


N-Phenylethyl-formamide (**116**)^[387]

A mixture of 1-(2-phenylethyl)amine (20.0 g, 0.165 mol) and formic acid (49.4 ml, 1.309 mol) was slowly heated to 200 °C, while water and formic acid were distilled off. Then the mixture was kept at 200 °C for 1 hr, distillation of the product under vacuum yielded a colourless oil (22.0 g, 0.147 mol, 89%).

¹H-NMR (250 MHz, DMSO-*d*₆, 300 K) δ = 8.06 (bs, 1H, CHO), 7.16-7.32 (m, 5H, C₆H₅), 3.32-3.42 (m, 2H, NH-CH₂), 2.77 (t, *J* = 7.2 Hz, 2H, NH-CH₂-CH₂);

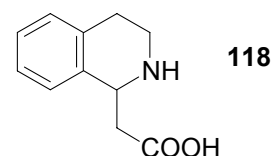
Analytical HPLC (5-90% in 30 min) *t*_R = 15.04 min.



3,4-Dihydro-isoquinoline (**117**)^[387]

Polyphosphoric acid (25 g) and phosphorus pentoxide (5.4 g, 38.0 mmol) were kept under argon while being heated to 180 °C in an oil bath for 1 hr. Then, *N*-phenylethyl-formamide (**116**) (4.3 g, 28.8 mmol) was added at 160 °C and stirring and heating were continued for 1.5 hrs before the mixture was allowed to cool down to room temperature. For workup, water (40 mL) was added, and the mixture was brought to pH = 10 through careful addition of saturated NaOH-solution. The aqueous solution was then extracted with diethyl ether (500 mL), the organic phase was separated and dried with NaOH, evaporation of the solvent yielded a brown oil (2.81 g, 21.4 mmol, 74%).

$^1\text{H-NMR}$ (250 MHz, $\text{DMSO-}d_6$, 300 K) δ = 8.32 (t, J = 2.3 Hz, 1H, N-CH), 7.16-7.40 (m, 4H, C_6H_4), 3.59-3.66 (m, 2H, N- CH_2), 2.66 (t, J = 7.3 Hz, 2H, N- CH_2 - CH_2); **Analytical HPLC** (5-90% in 30 min) t_{R} = 8.29 min.



2-(1,2,3,4-Tetrahydro-1-isoquinolinyl)acetic acid (118)^[388]

3,4-Dihydro-isoquinoline (**117**) (2.2 g, 16.77 mmol) and malonic acid (1.94 g, 16.77 mmol) were mixed at room temperature and heated in an oil bath at 120 °C for 1 hr. Then the mixture was cooled down and recrystallized from methanol (150 mL), drying yielded a colourless solid (1.52 g, 7.99 mmol, 48%).

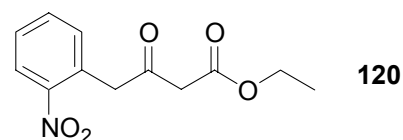
mp 230 °C decomp; **$^1\text{H-NMR}$** (250 MHz, D_2O , 300 K) δ = 7.13-7.23 (m, 4H, C_6H_4), 4.65 (t, J = 6.9 Hz, 1H, CH-NH), 3.44-3.54 (m, 1H, NH- CH_2), 3.24-3.34 (m, 1H, NH- CH_2), 2.95-3.03 (m, 2H, NH- CH_2 - CH_2), 2.79 (d, J = 6.1 Hz, 2H, CH_2 -COOH); **HRMS** (ESI-TOF) for $\text{C}_{11}\text{H}_{14}\text{NO}_2$ [$\text{M}+\text{H}$]⁺: 192.1047 (calcd 192.1025); **Analytical HPLC** (5-90% in 30 min) t_{R} = 10.15 min.



2-{1,2,3,4-Tetrahydro-2-[(9H-fluoren-9-ylmethoxy)carbonyl]-1-isoquinolinyl}acetic acid (119)

A suspension of 2-(1,2,3,4-tetrahydro-1-isoquinolinyl)acetic acid (**118**) (0.9 g, 4.73 mmol), saturated NaHCO_3 -solution (15 mL) and dioxane (5 mL) was cooled to 0 °C. Then Fmoc-Cl (1.35 g, 5.2 mmol) dissolved in dioxane (5 mL) was added dropwise over 30 min and the mixture was allowed to stir over night at room temperature. The aqueous phase was extracted with diethyl ether (30 mL) and acidified to pH = 1 with conc. HCl. The product was then extracted with ethyl acetate (50 mL), the organic phase was dried with MgSO_4 and removed *in vacuo*. The residue was chromatographed (ethyl acetate/hexane/acetic acid, 1:1:1%), drying yielded a colourless foam (1.54 g, 3.73 mmol, 79%).

mp 61-63 °C; **TLC** R_f (ethyl acetate/hexane/acetic acid, 1:1:1%) = 0.54; **$^1\text{H-NMR}$** (250 MHz, $\text{DMSO-}d_6$, 300 K) δ = 7.79-7.91 (m, 2H, $\text{CH}_2\text{-CH-C-C-CH}$), 7.63-7.66 (m, 2H, $\text{CH}_2\text{-CH-C-CH}$), 7.05-7.39 (m, 8H, $\text{CH}_2\text{-CH-C-CH-CH-CH}$ and C_6H_4), 5.40-5.52 (m, 1H, NH-CH), 4.37-4.42 (m, 1H, $\text{COO-CH}_2\text{-CH}$), 4.25-4.32 (m, 2H, COO-CH_2), 3.62-4.02 (m, 1H, N-CH_2), 3.27-3.38 (m, 1H, N-CH_2), 2.52-2.76 (m, 4H, N-CH-CH_2 and $\text{N-CH}_2\text{-CH}_2$); **MS** (ESI) m/z 179.1 (30), 414.0 (20) $[\text{M}+\text{H}]^+$, 436.2 (25) $[\text{M}+\text{Na}]^+$, 492.8 (15), 826.7 (5) $[\text{2M}+\text{H}]^+$, 849.1 (45) $[\text{2M}+\text{Na}]^+$, 865.1 (100) $[\text{2M}+\text{K}]^+$; **HRMS** (ESI-TOF) for $\text{C}_{26}\text{H}_{24}\text{NO}_4$ $[\text{M}+\text{H}]^+$: 414.1721 (calcd 414.1705); **Analytical HPLC** (5-90% in 30 min) t_R = 27.53 min.

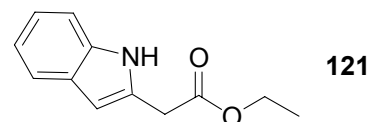


4-(2-Nitrophenyl)acetoacetic acid ethyl ester (**120**)^[389]

Triethylamine (8.7 mL, 62.4 mmol) and magnesium chloride (4.64 g, 48.7 mmol) were added to a stirred solution of potassium ethyl malonate (6.97 g, 37.8 mmol) in dry acetonitrile (70 mL), and stirring was continued for 2 hrs at room temperature. Then, a solution of 2-nitrophenyl acetic acid (3.55 g, 19.5 mmol) and *N, N'*-carbonyldiimidazole (3.47 g, 21.4 mmol) in dry acetonitrile (25 mL), which was prepared 15 min before, was added. The mixture was stirred at room temperature overnight and then heated to reflux for 2 hrs. After the mixture had cooled, 13% HCl (70 mL) was added slowly to the suspension and the temperature was kept below 25 °C. The organic phase was then separated and evaporated, the residue was treated with ethyl acetate, and the aqueous layer was extracted with ethyl acetate (100 mL). The combined organic phases were washed with saturated NaHCO_3 solution and brine, then dried with Na_2SO_4 , and finally concentrated to give yellow crystals (4.0 g, 15.8 mmol, 82%).

mp 56-57 °C; **$^1\text{H-NMR}$** (250 MHz, CDCl_3 , 300 K) δ = 8.14 (dd, J = 7.0 Hz, J = 1.0 Hz, 1H, $\text{NO}_2\text{-C-CH}$), 7.61 (ddd, J = 7.5 Hz, J = 7.5 Hz, J = 1.2 Hz, 1H, $\text{NO}_2\text{-C-CH-CH-CH}$), 7.48 (ddd, J = 7.5 Hz, J = 7.5 Hz, J = 1.2 Hz, 1H, arom), 7.31 (dd, J = 7.5

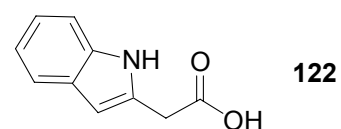
Hz, $J = 1.2$ Hz, 1H, arom), 4.26 (s, 2H, CO-CH₂-C₆H₄NO₂), 4.23 (q, $J = 7.0$ Hz, 2H, CH₂-CH₃), 3.64 (s, 2H, CO-CH₂-CO), 1.31 (t, $J = 7.0$ Hz, 3H, CH₂-CH₃); **MS** (EI) m/z 43.2 (35), 87.1 (35), 115.1 (100), 120.0 (65), 137.0 (55), 164.0 (25), 206.0 (5), 250.9 (1) [M^+]; **Analytical HPLC** (20-90% in 30 min) $t_R = 14.07$ min.



(1H-Indol-2-yl)acetic acid ethyl ester (121)^[390]

4-(2-Nitrophenyl)acetoacetic acid ethyl ester (**120**) (2.68 g, 10.7 mmol) was dissolved in acetone (30 mL) and transferred to a separating funnel. Aqueous ammonium acetate solution (4 M, 288 mL) and aqueous TiCl₃-solution (15%, 77 mL) were added. The mixture was shaken for 7 min and the resulting dark green solution was extracted with ether (4 × 100 mL) and the combined extracts were washed with brine and dried with MgSO₄. The ether was removed *in vacuo* and the residue was chromatographed (CH₂Cl₂), drying yielded orange crystals (1.6 g, 7.87 mmol, 74%).

mp 26-30 °C; **TLC** R_f (CH₂Cl₂) = 0.59; **¹H-NMR** (250 MHz, CDCl₃, 300 K) $\delta = 8.66$ (bs, 1H, NH), 7.52 (d, $J = 7.6$ Hz, 1H, NH-C-C-CH-CH), 7.25 (d, $J = 7.3$ Hz, 1H, NH-C-CH-CH), 7.03-7.15 (m, 2H, NH-C-CH-CH-CH), 6.32 (s, 1H, NH-C-CH-C), 4.16 (q, $J = 7.3$ Hz, 2H, CH₂-CH₃), 3.75 (s, 2H, CH₂-COOC₂H₅), 1.25 (t, $J = 7.3$ Hz, 3H, CH₂-CH₃); **¹³C-NMR** (62.9 MHz, CDCl₃, 300 K) $\delta = 170.57, 136.24, 130.56, 128.12, 121.56, 119.98, 119.65, 110.74, 101.64, 61.27, 33.86, 14.03$; **MS** (EI) m/z 77.1 (10), 103.1 (10), 130.0 (100), 203.0 (55) [M^+]; **Analytical HPLC** (5-90% in 30 min) $t_R = 21.91$ min.

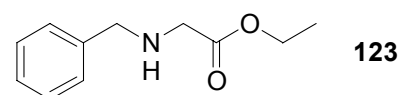


(1H-Indol-2-yl)acetic acid (122)

(1H-Indol-2-yl)acetic acid ethyl ester (**121**) (1.0 g, 4.92 mmol) was treated with NaOH (0.45 g, 11.3 mmol) in water (2.5 mL) and methanol (2.5 mL) for 30 min. Then the aqueous phase was washed with diethyl ether (25 mL) and acidified to pH = 1 with

conc. HCl. The product was then extracted with ethyl acetate (30 mL), the solvent was dried with MgSO_4 and removed *in vacuo*. The residue was chromatographed (ethyl acetate/hexane/acetic acid, 1:1:1%), drying yielded a colourless solid (0.63 g, 3.59 mmol, 73%).

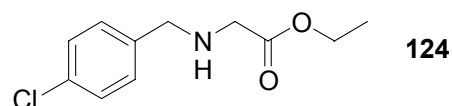
mp 103/104 °C; **TLC** R_f (ethyl acetate/hexane/acetic acid, 1:1:1%) = 0.42; **$^1\text{H-NMR}$** (250 MHz, $\text{DMSO-}d_6$, 300 K) δ = 12.49 (bs, 1H, COOH), 10.98 (bs, 1H, NH), 7.43 (d, J = 7.6 Hz, 1H, NH-C-C-CH-CH), 7.31 (d, J = 8.0 Hz, 1H, NH-C-CH-CH), 6.90-7.05 (m, 2H, NH-C-CH-CH-CH), 6.24 (s, 1H, NH-C-CH-C), 3.72 (s, 2H, $\text{CH}_2\text{-COOH}$); **Analytical HPLC** (5-90% in 30 min) t_R = 17.12 min.



2-(Benzylamino)acetic acid ethyl ester (123)

2-(Benzylamino)acetic acid ethyl ester (**123**) was prepared according to general method 12 using benzylamine (5.53 g, 51.7 mmol) and bromoacetic acid ethyl ester (8.63 g, 51.7 mmol). The residue was chromatographed, drying yielded a yellow oil (5.74 g, 29.7 mmol, 57 %).

TLC R_f (ethyl acetate/hexane, 1:1) = 0.46; **$^1\text{H-NMR}$** (250 MHz, $\text{DMSO-}d_6$, 300 K) δ = 7.22-7.30 (m, 5H, C_6H_5), 4.09 (q, J = 7.1 Hz, 2H, $\text{CH}_2\text{-CH}_3$), 3.72 (s, 2H, NH- $\text{CH}_2\text{-C}_6\text{H}_5$), 3.30 (s, 2H, NH- $\text{CH}_2\text{-CO}$), 2.54 (bs, 1H, NH), 1.19 (t, J = 7.2 Hz, 3H, $\text{CH}_2\text{-CH}_3$); **GC-MS** (EI) m/z 65.0 (30), 91.0 (100), 106.0 (80), 120.0 (85), 192.9 (5) $[\text{M}]^+$; **Analytical HPLC** (5-90% in 30 min) t_R = 10.34 min.

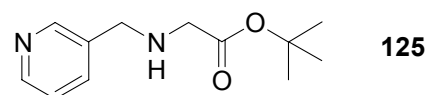


2-(4-Chlorobenzylamino)acetic acid ethyl ester (124)

2-(4-Chlorobenzylamino)acetic acid ethyl ester (**124**) was prepared according to general method 12 using 4-chlorobenzylamine (7.08 g, 50.0 mmol) and bromoacetic

acid ethyl ester (9.05 g, 50.0 mmol). The residue was chromatographed, drying yielded a yellow oil (6.55 g, 28.8 mmol, 58%).

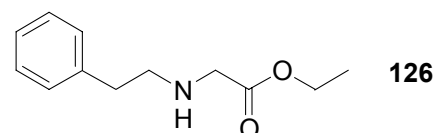
TLC R_f (ethyl acetate/hexane, 1:1) = 0.46; **$^1\text{H-NMR}$** (250 MHz, DMSO- d_6 300 K) δ = 7.34-7.36 (m, 4H, $\text{C}_6\text{H}_4\text{Cl}$), 4.10 (q, $J = 7.1$ Hz, 2H, $\text{CH}_2\text{-CH}_3$), 3.71 (s, 2H, $\text{NH-CH}_2\text{-C}_6\text{H}_4\text{Cl}$), 3.30 (s, 2H, $\text{NH-CH}_2\text{-CO}$), 2.52 (bs, 1H, NH), 1.19 (t, $J = 7.0$ Hz, 3H, $\text{CH}_2\text{-CH}_3$); **GC-MS** (EI) m/z 77.1 (15), 89.1 (40), 99.0 (15), 125.0 (100), 140.0 (80), 154.0 (85), 197.9 (1), 226.9 (5) $[\text{M}]^+$; **Analytical HPLC** (5-90% in 30 min) $t_R = 13.36$ min.



2-(Pyridine-3-ylmethylamino)acetic acid *tert*-butyl ester (125)

2-(Pyridine-3-ylmethylamino)acetic acid *tert*-butyl ester (**125**) was prepared according to general method 12 using 3-picolylamine (5.0 g, 46.2 mmol) and bromoacetic acid *tert*-butyl ester (9.02 g, 46.2 mmol). Drying yielded a brown oil (8.6 g, 38.7 mmol, 84%).

TLC R_f (acetonitrile/water, 4:1) = 0.64; **$^1\text{H-NMR}$** (250 MHz, DMSO- d_6 , 300 K) δ = 8.52 (d, $J = 1.7$ Hz, 1H, N-CH-C), 8.46 (dd, $J = 4.7$ Hz, $J = 1.7$ Hz, 1H, N-CH-CH), 7.71-7.76 (m, 1H, N-CH-C-CH), 7.31-7.37 (m, 1H, N-CH-CH), 3.75 (s, 2H, $\text{NH-CH}_2\text{-C}_5\text{H}_4\text{N}$), 3.22 (s, 2H, NH-CH), 2.52 (bs, 1H, NH), 1.44 (s, 9H, CH_3); **GC-MS** (EI) m/z 41.1 (45), 57.1 (65), 92.0 (100), 107.0 (25), 119.0 (20), 121.0 (100), 165.9 (65), 221.8 (2) $[\text{M}]^+$; **Analytical HPLC** (5-90% in 30 min) $t_R = 8.41$ min.

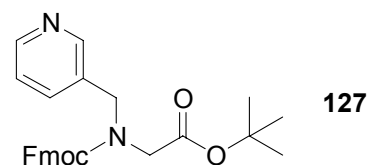


2-[1-(2-Phenylethyl)amino]acetic acid ethyl ester (126)

2-[1-(2-Phenylethyl)amino]acetic acid ethyl ester (**126**) was prepared according to general method 12 using 1-(2-phenylethyl)amine (6.79 g, 56.0 mmol) and bromoacetic

acid ethyl ester (9.35 g, 56.0 mmol). The residue was chromatographed, drying yielded a yellow oil (7.45 g, 35.9 mmol, 64%).

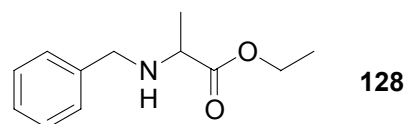
TLC R_f (ethyl acetate/hexane, 1:1) = 0.42; **$^1\text{H-NMR}$** (250 MHz, DMSO- d_6 , 300 K) δ = 7.15-7.28 (m, 5H, C_6H_5), 4.08 (q, J = 7.1 Hz, 2H, $\text{CH}_2\text{-CH}_3$), 3.33 (s, 2H, $\text{NH-CH}_2\text{-CO}$), 2.67-2.78 (m, 4H, $\text{NH-CH}_2\text{-CH}_2$), 1.91 (bs, 1H, NH), 1.18 (t, J = 7.2 Hz, 3H, $\text{CH}_2\text{-CH}_3$); **GC-MS** (EI) m/z 42.1 (80), 77.1 (20), 88.1 (35), 105.0 (75), 116.0 (100), 134.0 (70), 207.9 (2) $[\text{M}]^+$; **Analytical HPLC** (5-90% in 30 min) t_R = 11.59 min.



2-{Pyridine-3-ylmethyl-[(9H-fluorene-9-ylmethoxy)carbonyl]amino}acetic acid *tert*-butyl ester (127)^[419,420]

2-{Pyridine-3-ylmethyl-[(9H-fluorene-9-ylmethoxy)carbonyl]amino}acetic acid *tert*-butyl ester (**127**) was prepared from 2-(pyridine-3-ylmethylamino)acetic acid *tert*-butyl ester (**125**) (1.12 g, 5.04 mmol). Under ice cooling, Fmoc-Cl (1.42 g, 5.5 mmol) in dioxane (7.5 mL) was dropped in a period of 30 min to **125** and sym.-collidine (668 μL , 5.04 mmol) in water (20 mL) and dioxane (20 mL). Upon completion of the addition the mixture was stirred another 1 hr at 0 °C and then for 24 hrs at room temperature. Then the solvent was removed *in vacuo* and the residue was chromatographed (ethyl acetate/hexane, 1:1), drying yielded a colourless oil (1.8 g, 4.04 mmol, 80%). The compound shows *cis/trans*-isomerie in a ratio of approximately 1:1.

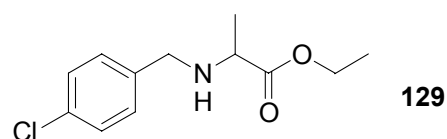
TLC R_f (ethyl acetate/hexane, 1:1) = 0.26; **$^1\text{H-NMR}$** (250 MHz, DMSO- d_6 , 300 K) δ = 8.31-8.48 (m, 2H, N-CH-C and N-CH-CH), 7.88 (t, J = 7.6 Hz, 2H, arom), 7.21-7.52 (m, 8H, arom), 4.21-4.53 (m, 3H, $\text{CH}_2\text{-CH}$), 4.23 (s, 2H, N-CH_2), 3.85 and 3.87 (s, 2H, $\text{N-CH}_2\text{-CO}$), 1.32 (s, 9H, CH_3); **MS** (ESI) m/z 179.1 (15), 211.1 (17), 389.2 (100), 445.1 (25) $[\text{M}+\text{H}]^+$, 467.1 (25) $[\text{M}+\text{Na}]^+$, 911.0 (10) $[\text{2M}+\text{Na}]^+$; **Analytical HPLC** (5-90% in 30 min) t_R = 21.91 min.



2-(Benzylamino)propionic acid ethyl ester (128)

2-(Benzylamino)propionic acid ethyl ester (**128**) was prepared according to general method 12 using benzylamine (5.36 g, 50.0 mmol) and 2-bromo-propionic acid ethyl ester (9.05 g, 50.0 mmol). The residue was chromatographed, drying yielded a yellow oil (3.7 g, 17.8 mmol, 36%).

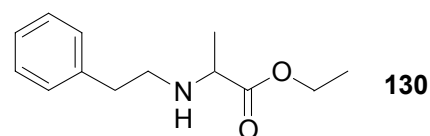
TLC R_f (ethyl acetate/hexane, 1:1) = 0.57; **$^1\text{H-NMR}$** (250 MHz, DMSO- d_6 , 300 K) δ = 7.20-7.28 (m, 5H, C_6H_5), 4.10 (q, J = 7.1 Hz, 2H, $\text{CH}_2\text{-CH}_3$), 3.66 (q, J = 13.4 Hz, 2H, $\text{NH-CH}_2\text{-C}_6\text{H}_5$), 3.25 (q, J = 6.9 Hz, 1H, NH-CH), 2.40 (bs, 1H, NH), 1.17-1.23 (m, 6H, $\text{CH}_2\text{-CH}_3$ and CH-CH_3); **GC-MS** (EI) m/z 65.1 (45), 91.1 (100), 106.1 (60), 134.1 (100), 176.0 (1), 192.0 (1), 207.0 (1) $[\text{M}]^+$; **Analytical HPLC** (5-90% in 30 min) t_R = 12.36 min.



2-(4-Chlorobenzylamino)propionic acid ethyl ester (129)

2-(4-Chlorobenzylamino)propionic acid ethyl ester (**129**) was prepared according to general method 12 using 4-chlorobenzylamine (7.08 g, 50.0 mmol) and 2-bromo-propionic acid ethyl ester (8.35 g, 50.0 mmol). The residue was chromatographed, drying yielded a yellow oil (4.25 g, 17.6 mmol, 35%).

TLC R_f (ethyl acetate/hexane, 1:1) = 0.58; **$^1\text{H-NMR}$** (250 MHz, DMSO- d_6 , 300 K) δ = 7.31-7.38 (m, 4H, $\text{C}_6\text{H}_4\text{Cl}$), 4.09 (q, J = 7.1 Hz, 2H, $\text{CH}_2\text{-CH}_3$), 3.65 (q, J = 13.9 Hz, 2H, $\text{NH-CH}_2\text{-C}_6\text{H}_4\text{Cl}$), 3.20-3.24 (m, 1H, NH-CH), 2.51 (bs, 1H, NH), 1.17-1.22 (m, 6H, $\text{CH}_2\text{-CH}_3$ and CH-CH_3); **GC-MS** (EI) m/z 84.1 (15), 89.1 (35), 99.0 (10), 125.0 (100), 140.0 (45), 168.0 (100), 209.9 (1), 225.9 (1), 241.9 (1) $[\text{M}]^+$; **Analytical HPLC** (5-90% in 30 min) t_R = 13.85 min.

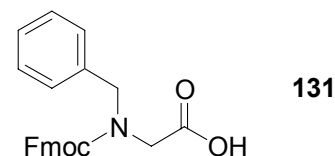


130

2-[1-(2-Phenylethyl)amino]propionic acid ethyl ester (130)

2-[1-(2-Phenylethyl)amino]propionic acid ethyl ester (**130**) was prepared according to general method 12 using 1-(2-phenylethyl)amine (6.3 g, 52.0 mmol) and 2-bromo-propionic acid ethyl ester (9.41 g, 52.0 mmol). The residue was chromatographed, drying yielded a yellow oil (4.7 g, 21.2 mmol, 41%).

TLC R_f (ethyl acetate/hexane, 1:1) = 0.48; **$^1\text{H-NMR}$** (250 MHz, DMSO- d_6 , 300 K) δ = 7.15-7.28 (m, 5H, C_6H_5), 4.08 (q, J = 7.1 Hz, 2H, $\text{CH}_2\text{-CH}_3$), 3.29 (q, J = 6.9 Hz, 1H, NH-CH), 2.62-2.78 (m, 4H, $\text{NH-CH}_2\text{-CH}_2$), 1.91 (bs, 1H, NH), 1.17 (m, 6H, $\text{CH}_2\text{-CH}_3$ and CH-CH_3); **GC-MS** (EI) m/z 56.1 (90), 77.2 (30), 91.1 (20), 105.1 (95), 130.1 (100), 148.1 (85), 190.0 (1), 221.0 (1) $[\text{M}]^+$; **Analytical HPLC** (5-90% in 30 min) t_R = 13.39 min.



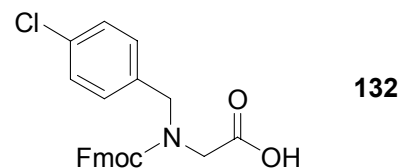
131

2-{Benzyl-[(9H-fluoren-9-ylmethoxy)carbonyl]amino}acetic acid (131)

2-{Benzyl-[(9H-fluoren-9-ylmethoxy)carbonyl]amino}acetic acid (**131**) was prepared from 2-(benzylamino)acetic acid ethyl ester (**123**) (1.0 g, 5.17 mmol) according to general method 13. The residue was chromatographed, drying yielded a colourless solid (1.85 g, 4.78 mmol, 92%).

mp 133-135 °C; **TLC** R_f (ethyl acetate/hexane/acetic acid, 1:1:1%) = 0.37; **$^1\text{H-NMR}$** (250 MHz, DMSO- d_6 , 300 K) δ = 12.73 (bs, 1H, COOH), 7.88 (t, J = 7.6 Hz, 2H, arom), 7.64 (d, J = 7.3 Hz, 1H, arom), 7.52 (d, J = 7.6 Hz, 1H, arom), 7.23-7.43 (m, 8H, arom), 7.00-7.02 (m, 1H, arom), 4.35-4.49 (m, 3H, $\text{COO-CH}_2\text{-CH}$), 4.29 (s, 2H, $\text{N-CH}_2\text{-C}_6\text{H}_5$), 3.83 (s, 2H, $\text{N-CH}_2\text{-CO}$); **HPLC-MS** (ESI) m/z 179.1 (90), 388.0 (40) $[\text{M}+\text{H}]^+$, 410.2 (35) $[\text{M}+\text{Na}]^+$, 774.9 (30) $[\text{2M}+\text{H}]^+$, 797.1 (60) $[\text{2M}+\text{Na}]^+$, 813.2 (100)

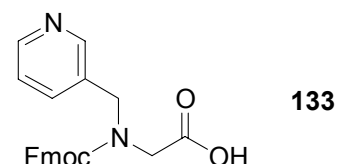
$[2M+K]^+$, 1184.1 (30) $[3M+Na]^+$; **Analytical HPLC** (5-90% in 30 min) $t_R = 25.75$ min.



2-{4-Chlorobenzyl-[(9H-fluoren-9-ylmethoxy)carbonyl]amino}acetic acid (**132**)

2-{4-Chlorobenzyl-[(9H-fluoren-9-ylmethoxy)carbonyl]amino}acetic acid (**132**) was prepared from 2-(4-chlorobenzylamino)acetic acid ethyl ester (**124**) (1.0 g, 4.4 mmol) according to general method 13. Drying yielded a colourless solid (1.85 g, 4.4 mmol, quant).

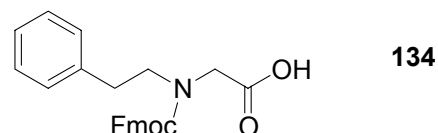
mp 145 °C; **TLC** R_f (ethyl acetate/hexane/acetic acid, 1:1:1%) = 0.32; **1H -NMR** (250 MHz, DMSO- d_6 , 300 K) $\delta = 7.88$ (t, $J = 7.8$ Hz, 2H, arom), 7.64 (d, $J = 7.3$ Hz, 1H, arom), 7.23-7.51 (m, 8H, arom), 6.99 (d, $J = 8.6$ Hz, 1H, arom), 4.34-4.50 (m, 3H, COO- CH_2 -CH), 4.22 (s, 2H, N- CH_2 -C $_6$ H $_4$ Cl), 3.84 (s, 2H, N- CH_2 -CO); **HPLC-MS** (ESI) m/z 179.1 (75), 422.0 (30) $[M+H]^+$, 842.9 (25) $[2M+H]^+$, 865.0 (50) $[2M+Na]^+$, 881.2 (100) $[2M+K]^+$; **Analytical HPLC** (5-90% in 30 min) $t_R = 28.38$ min.



2-{Pyridine-3-ylmethyl-[(9H-fluorene-9-ylmethoxy)carbonyl]amino}acetic acid (**133**)^[419,420]

2-{Pyridine-3-ylmethyl-[(9H-fluorene-9-ylmethoxy)carbonyl]amino}acetic acid (**133**) was prepared from 2-{pyridine-3-ylmethyl-[(9H-fluorene-9-ylmethoxy)carbonyl]amino}acetic acid *tert*-butyl ester (**127**) (0.4 g, 0.89 mmol) by treatment with a mixture of TFA (4 mL) and triisopropylsilane (0.4 mL) at 0 °C for 1 hr. The solvent was removed *in vacuo*, drying yielded a colourless solid (yield not determined). The compound shows *cis/trans*-isomerie in a ratio of approximately 1:1.

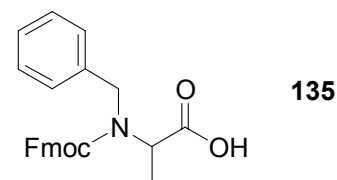
mp 166/167 °C ; **TLC** R_f (acetonitrile/water) = 0.61; **$^1\text{H-NMR}$** (250 MHz, $\text{DMSO-}d_6$, 300 K) δ = 8.47-8.71 (m, 2H, N-CH-C and N-CH-CH), 7.23-7.78 (m, 10H, arom), 4.52-4.59 (m, 2H), 4.24-4.36 (m, 3H), 3.93 and 4.02 (s, 2H, N-CH₂-CO); **HPLC-MS** (ESI) m/z 179.1 (25), 211.1 (30), 389.2 (100) $[\text{M}+\text{H}]^+$, 776.9 (50) $[\text{2M}+\text{H}]^+$; **Analytical HPLC** (5-90% in 30 min) t_R = 16.86 min.



2-{1-(2-Phenylethyl)-[(9H-fluoren-9-ylmethoxy)carbonyl]amino}acetic acid (134)

2-{1-(2-Phenylethyl)-[(9H-fluoren-9-ylmethoxy)carbonyl]amino}acetic acid (**134**) was prepared from 2-[1-(2-phenylethyl)amino]acetic acid ethyl ester (**126**) (1.0 g, 4.83 mmol) according to general method 13. The residue was chromatographed, drying yielded a colourless solid (1.86 g, 4.63 mmol, 96%). Compound shows cis/trans-isomerie in a ratio of 1:1.60.

mp 140/141 °C; **TLC** R_f (ethyl acetate/hexane/acetic acid, 1:1:1%) = 0.42; **$^1\text{H-NMR}$** (250 MHz, $\text{DMSO-}d_6$, 300 K) δ = 12.65 (bs, 1H, COOH), 7.90 (d, J = 7.0 Hz, 2H, arom), 7.66 (d, J = 7.0 Hz, 1H, arom), 7.61 (d, J = 7.6 Hz, 1H, arom), 7.17-7.45 (m, 8H, arom), 6.91-6.95 (m, 1H, arom), 4.21-4.54 (m, 3H, COO-CH₂-CH), 3.79 and 3.93 (s, 2H, N-CH₂-CO), 3.12 and 3.46 (t, J = 7.6 Hz, 2H, N-CH₂-CH₂), 2.41 and 2.79 (t, J = 7.6 Hz, 2H, N-CH₂-CH₂); **HPLC-MS** (ESI) m/z 179.1 (90), 402.0 (50) $[\text{M}+\text{H}]^+$, 424.2 (30) $[\text{M}+\text{Na}]^+$, 802.9 (40) $[\text{2M}+\text{H}]^+$, 825.1 (45) $[\text{2M}+\text{Na}]^+$, 841.3 (100) $[\text{2M}+\text{K}]^+$, 1225.9 (25) $[\text{3M}+\text{Na}]^+$; **Analytical HPLC** (5-90% in 30 min) t_R = 27.27 min.

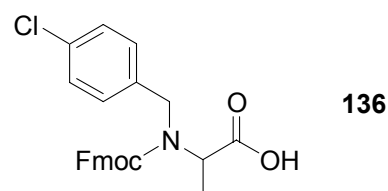


2-{Benzyl-[(9H-fluoren-9-ylmethoxy)carbonyl]amino}propionic acid (135)

2-{Benzyl-[(9H-fluoren-9-ylmethoxy)carbonyl]amino}propionic acid (**135**) was prepared from 2-(benzylamino)propionic acid ethyl ester (**128**) (1.0 g, 4.83 mmol) according to general method 13. The residue was chromatographed, drying yielded a

colourless oil (1.26 g, 3.14 mmol, 65%). Compound shows cis/trans-isomerie in an undetermined ratio.

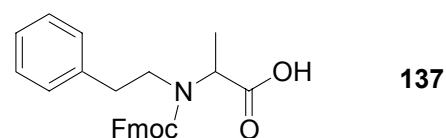
TLC R_f (ethyl acetate/hexane/acetic acid, 1:1:1%) = 0.35; **$^1\text{H-NMR}$** (250 MHz, DMSO- d_6 , 300 K) δ = 12.34 (bs, 1H, COOH), 7.83-7.91 (m, 2H, arom), 7.68 (d, J = 7.3 Hz, 1H, arom), 7.12-7.50 (m, 10H, arom), 4.21-4.46 (m, 6H, N-CH, N-CH₂, COO-CH₂-CH), 1.13 and 1.20 (d, J = 7.2 Hz, 3H, CH₃); **HPLC-MS** (ESI) m/z 179.1 (70), 402.0 (70) [M+H]⁺, 424.2 (60) [M+Na]⁺, 825.1 (55) [2M+Na]⁺, 841.2 (100) [2M+K]⁺, 1225.8 (25) [3M+Na]⁺; **Analytical HPLC** (5-90% in 30 min) t_R = 27.64 min.



2-{4-Chlorobenzyl-[(9H-fluoren-9-ylmethoxy)carbonyl]amino}propionic acid (136)

2-{4-Chlorobenzyl-[(9H-fluoren-9-ylmethoxy)carbonyl]amino}propionic acid (136) was prepared from 2-(4-chlorobenzylamino)propionic acid ethyl ester (129) (1.0 g, 4.14 mmol) according to general method 13. The residue was chromatographed, drying yielded a colourless oil (1.3 g, 2.98 mmol, 72%). Compound shows cis/trans-isomerie in an undetermined ratio.

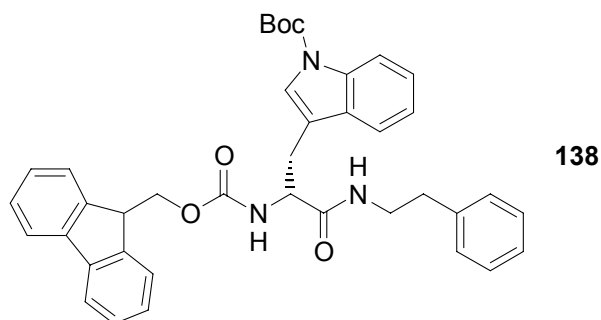
TLC R_f (ethyl acetate/hexane/acetic acid, 1:1:1%) = 0.41; **$^1\text{H-NMR}$** (250 MHz, DMSO- d_6 , 300 K) δ = 12.43 (bs, 1H, COOH), 7.82-7.90 (m, 2H, arom), 7.67 (d, J = 7.3 Hz, 1H, arom), 7.21-7.48 (m, 8H, arom), 7.08 (d, J = 8.2 Hz, 1H, arom), 4.20-4.49 (m, 6H, N-CH and N-CH₂ and COO-CH₂-CH), 1.12 and 1.20 (d, J = 7.3 Hz, 3H, CH₃); **HPLC-MS** (ESI) m/z 179.1 (95), 436.0 (75) [M+H]⁺, 458.2 (40) [M+Na]⁺, 893.0 (50) [2M+Na]⁺, 909.2 (100) [2M+K]⁺; **Analytical HPLC** (5-90% in 30 min) t_R = 29.36 min.



2-{1-(2-Phenylethyl)-[(9*H*-fluoren-9-ylmethoxy)carbonyl]amino}propionic acid (137)

2-{1-(2-Phenylethyl)-[(9*H*-fluoren-9-ylmethoxy)carbonyl]amino}propionic acid (**137**) was prepared from 2-[1-(2-phenylethyl)amino]propionic acid ethyl ester (**130**) (1.0 g, 4.52 mmol) according to general method 13. Drying yielded a colourless resin (1.6 g, 3.85 mmol, 85%).

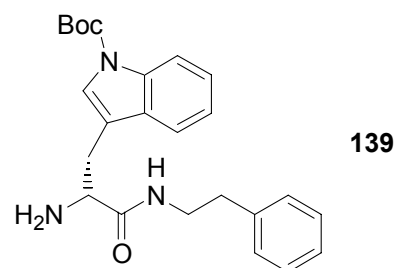
TLC R_f (ethyl acetate/hexane/acetic acid, 1:1:1%) = 0.45; **$^1\text{H-NMR}$** (250 MHz, DMSO- d_6 , 300 K) δ = 7.87 (d, J = 7.3 Hz, 2H, arom), 7.67 (d, J = 7.0 Hz, 2H, arom), 7.18-7.39 (m, 8H, arom), 6.91 (d, J = 6.7 Hz, 1H, arom), 4.33-4.64 (m, 3H, COO- CH_2 - CH), 2.80-3.47 (m, 2H, N- CH_2 - CH_2), 2.95-3.20 (m, 1H, N- CH), 2.44 (t, J = 7.8 Hz, 2H, N- CH_2 - CH_2), 1.23 (d, J = 7.9 Hz, 3H, CH- CH_3); **HPLC-MS** (ESI) m/z 179.1 (100), 194.1 (45), 416.0 (95) $[\text{M}+\text{H}]^+$, 438.2 (50) $[\text{M}+\text{Na}]^+$, 830.8 (45) $[\text{2M}+\text{H}]^+$, 869.3 (90) $[\text{2M}+\text{K}]^+$, 1267.8 (20) $[\text{3M}+\text{Na}]^+$; **Analytical HPLC** (5-90% in 30 min) t_R = 28.42 min.



***N*1-(2-Phenylethyl)-(2*R*)-2-[(9*H*-fluoren-9-ylmethoxy)carboxamido]-3-[1-(*tert*-butoxycarbonyl)-3-indolyl]propanamide (138)**

*N*1-(2-Phenylethyl)-(2*R*)-2-[(9*H*-fluoren-9-ylmethoxy)carboxamido]-3-[1-(*tert*-butoxycarbonyl)-3-indolyl]propanamide (**138**) was prepared according to general method 18 from 1-(2-phenylethyl)amine (0.26 g, 2.14 mmol) and Fmoc-D-Trp(Boc)-OH (1.13 g, 2.14 mmol) in a reaction time of 1 hr. The residue was chromatographed (ethyl acetate/ hexane, 1:1), drying yielded a colourless, waxy solid (1.33 g, 2.1 mmol, quant).

mp 140 °C; **TLC** R_f (ethyl acetate/hexane, 1:1) = 0.67; **$^1\text{H-NMR}$** (500 MHz, $\text{DMSO-}d_6$, 300 K) δ = 8.18 (t, J = 5.4 Hz, 1H, $\text{NH-CH}_2\text{-CH}_2$), 8.05 (d, J = 8.1 Hz, 1H, N-C-CH-CH), 7.86 (d, J = 7.6 Hz, 2H, $\text{CH}_2\text{-CH-C-C-CH}$), 7.74 (d, J = 7.8 Hz, 1H, N-CH-C-C-CH), 7.70 (d, J = 8.5 Hz, 1H, NH-CH-CH_2), 7.62-7.65 (m, 2H, $\text{CH}_2\text{-CH-C-CH}$), 7.59 (s, 1H, N-CH-C), 7.37-7.41 (m, 2H, $\text{CH}_2\text{-CH-C-C-CH-CH}$), 7.33 (t, J = 7.8 Hz, 1H, N-C-CH-CH), 7.21-7.29 (m, 5H, $\text{CH}_2\text{-CH-C-CH-CH}$ and $m\text{-CH}$ and N-CH-C-C-CH-CH), 7.16-7.19 (m, 3H, $o\text{-CH}$ and $p\text{-CH}$), 4.31-4.36 (m, 1H, NH-CH-CH_2), 4.16-4.24 (m, 3H, $\text{COO-CH}_2\text{-CH}$), 3.34-3.39 (m, 1H, NH-CHH-CH_2), 3.25-3.30 (m, 1H, NH-CHH-CH_2), 3.03 (dd, J = 14.6 Hz, J = 4.7 Hz, 1H, NH-CH-CHH), 2.95 (dd, J = 14.3 Hz, J = 9.8 Hz, 1H, NH-CH-CHH), 2.70 (t, J = 7.3 Hz, 2H, $\text{NH-CH}_2\text{-CH}_2$), 1.55 (s, 9H, CH_3); **HPLC-MS** (ESI) m/z 308.2 (20), 530.3 (40), 630.3 (40) $[\text{M}+\text{H}]^+$, 652.4 (10) $[\text{M}+\text{Na}]^+$, 1259.5 (100) $[\text{2M}+\text{H}]^+$, 1281.5 (30) $[\text{2M}+\text{Na}]^+$; **Analytical HPLC** (5-90% in 30 min) t_R = 32.99 min.

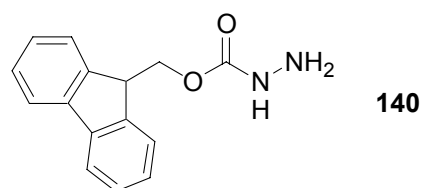


***tert*-Butyl-3-((2*R*)-2-amino-2-[1-(2-phenylethyl)carbamoyl]ethyl)-1*H*-1-indole-carboxylate (139)**

tert-Butyl-3-((2*R*)-2-amino-2-[1-(2-phenylethyl)carbamoyl]ethyl)-1*H*-1-indole-carboxylate (**139**) was prepared from *N*1-phenethyl-(2*R*)-2-(9*H*-fluoren-9-ylmethoxy)carboxamido-3-[1-(*tert*-butyloxycarbonyl)-3-indolyl]propanamide (**138**) (1.0 g, 1.59 mmol) according to general method 20. The residue was chromatographed with ethyl acetate/hexane (2:1). After the Fmoc-piperidine-complex was washed from the column, the product was eluted with chloroform/methanol (15:1), drying yielded a yellow oil (0.63 g, 1.55 mmol, 97%).

TLC R_f (chloroform/methanol, 10:1) = 0.54; **$^1\text{H-NMR}$** (500 MHz, $\text{DMSO-}d_6$, 300 K) δ = 8.07 (d, J = 8.2 Hz, 1H, N-C-CH-CH), 7.96 (m, 1H, $\text{NH-CH}_2\text{-CH}_2$), 7.65 (d, J = 7.7 Hz, 1H, N-CH-C-C-CH), 7.52 (s, 1H, N-CH-C), 7.32 (t, J = 7.6 Hz, 1H, N-C-CH-

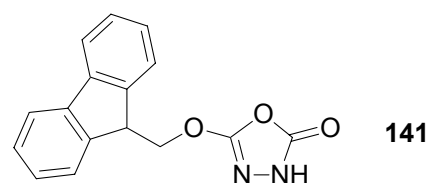
CH), 7.24 (t, $J = 7.3$ Hz, 3H, *m-CH* and N-CH-C-C-CH-CH), 7.17 (t, $J = 7.3$ Hz, 1H, *p-CH*), 7.12 (d, $J = 7.5$ Hz, 2H, *o-CH*), 3.48 (t, $J = 6.3$ Hz, 1H, NH-CH-CH₂), 3.25-3.31 (m, 2H, NH-CH₂-CH₂), 3.01 (dd, $J = 14.0$ Hz, $J = 5.3$ Hz, 1H, NH-CH-CHH), 2.80 (dd, $J = 14.5$ Hz, $J = 7.5$ Hz, 1H, NH-CH-CHH), 2.62 (t, $J = 7.3$ Hz, 2H, NH-CH₂-CH₂), 1.59 (s, 9H, CH₃); **MS** (ESI) m/z 159.1 (20), 291.2 (75), 308.1 (95), 352.1 (70), 408.1 (100) [M+H]⁺, 430.1 (35) [M+Na]⁺, 815.2 (15) [2M+H]⁺, 837.1 (20) [2M+Na]⁺; **Analytical HPLC** (5-90% in 30 min) $t_R = 21.18$ min.



***N*-[(9*H*-Fluoren-9-ylmethoxy)carbonyl]hydrazine (140)**^[392]

Boc-Hydrazine (10.0 g, 75.6 mmol) and DIPEA (12.95 mL, 75.6 mmol) were dissolved in dry CH₂Cl₂ (200 mL) and cooled to 0 °C. Then Fmoc-Cl (19.6 g, 75.8 mmol) in dry CH₂Cl₂ (100 mL) was added over a period of 30 min and the mixture was allowed to stir over night at room temperature. The organic phase was extracted with water (200 mL) and then reduced *in vacuo* to a volume of 100 mL. Trifluoroacetic acid (100 mL) was added carefully at 0 °C and the mixture was stirred for 1.5 hrs. Finally the product was precipitated by careful addition of saturated Na₂CO₃-solution (300 mL), drying yielded a colourless solid (18.02 g, 70.8 mmol, 94%).

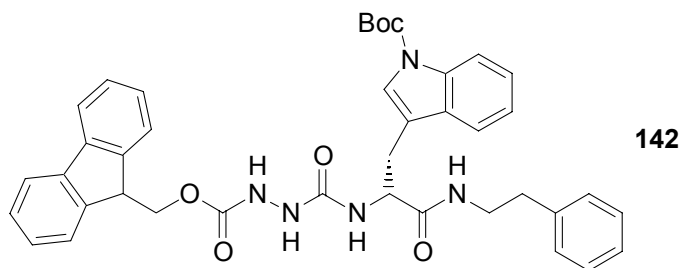
mp 150-153 °C; **¹H-NMR** (250 MHz, DMSO-*d*₆, 300 K) $\delta = 10.10$ (bs, 1H, NH), 9.60 (bs, 1H, NH), 7.89 (d, $J = 7.6$ Hz, 2H, CH₂-CH-C-C-CH), 7.70 (d, $J = 7.3$ Hz, 2H, CH₂-CH-C-CH), 7.42 (t, $J = 7.3$ Hz, 2H, CH₂-CH-C-CH-CH), 7.33 (t, $J = 7.4$ Hz, 2H, CH₂-CH-C-C-CH-CH), 4.48 (d, $J = 6.6$ Hz, 2H, CO-CH₂), 4.27 (t, $J = 6.7$ Hz, 1H, CO-CH₂-CH); **¹³C-NMR** (62.9 MHz, DMSO-*d*₆, 300 K) $\delta = 156.26, 143.59, 140.98, 127.96, 127.34, 125.33, 120.39, 67.00, 46.60$; **HRMS** (ESI-TOF) for C₁₅H₁₅N₂O₂ [M+H]⁺: 255.1134 (calcd 255.1119); **Analytical HPLC** (5-90% in 30 min) $t_R = 16.47$ min.



5-(9H-Fluoren-9-ylmethoxy)-1,3,4-oxadiazol-2(3H)-one (141)^[12,430,437]

A suspension of *N*-[(9*H*-fluoren-9-ylmethoxy)carbonyl]hydrazine (**140**) (1.49 g, 5.78 mmol), CH₂Cl₂ (60 mL) and saturated NaHCO₃-solution (60 mL) was stirred vigorously at 0 °C for 5 min, then stirring was stopped and the mixture was allowed to stand for 5 min. Then phosgene (1.89 M in toluene, 7.95 mL, 15.0 mmol) was added carefully to the lower organic phase by syringe and upon completion of the addition, stirring was continued. After 10 min water (20 mL) and CH₂Cl₂ (20 mL) were added, the phases were separated quickly and the aqueous phase was extracted with CH₂Cl₂ (50 mL). The combined organic phases were dried with Na₂SO₄, the solvent was removed *in vacuo*, drying yielded a colourless solid (1.35 g, 4.82 mmol, 83%).

mp 125 °C; ¹H NMR (250 MHz, CDCl₃, 300 K) δ = 8.72 (bs, 1H, NH), 7.77 (d, *J* = 7.5 Hz, 2H, CH₂-CH-C-C-CH), 7.59 (d, *J* = 7.4 Hz, 2H, CH₂-CH-C-CH), 7.42 (t, *J* = 7.1 Hz, 2H, CH₂-CH-C-CH-CH), 7.32 (t, *J* = 7.1 Hz, 2H, CH₂-CH-C-C-CH-CH), 4.49 (d, *J* = 7.8 Hz, 2H, CH₂-CH), 4.32-4.41 (m, 1H, CH₂-CH).

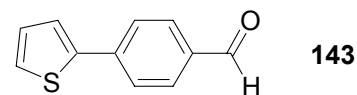


***N*1-(2-Phenylethyl)-(2*R*)-2-{[*N'*-((9*H*-fluoren-9-ylmethoxy)carbonyl)hydrazino]carboxamido}-3-[1-(*tert*-butoxycarbonyl)-3-indolyl]propanamide (142)**^[12,430,437]

tert-Butyl-3-{(2*R*)-2-amino-2-[1-(2-phenylethyl)carbamoyl]ethyl}-1*H*-1-indole-carboxylate (**139**) (500 mg, 1.23 mmol) and freshly prepared 5-(9*H*-fluoren-9-ylmethoxy)-1,3,4-oxadiazol-2(3*H*)-one (**141**) (515 mg, 1.84 mmol) were dissolved in dry DMF (20 mL) and the mixture was allowed to stir for 75 min at room temperature. Then the solvent was removed *in vacuo* using a liquid-nitrogen-cooled rotary

evaporator and the residue was chromatographed (chloroform/methanol, 20:1). Drying yielded a colourless solid (0.58 g, 0.84 mmol, 68%).

mp 135-137 °C; **TLC** R_f (chloroform/methanol, 20:1) = 0.27; **$^1\text{H-NMR}$** (500 MHz, DMSO- d_6 , 300 K) δ = 9.06 (bs, 1H, NH-NH), 8.13 (bs, 1H, NH-CH₂-CH₂), 7.98-8.01 (m, 2H, NH-NH and N-C-CH-CH), 7.89 (d, J = 7.1 Hz, 2H, CH₂-CH-C-C-CH), 7.68-7.73 (m, 2H, CH₂-CH-C-CH), 7.62 (d, J = 7.8 Hz, 1H, N-CH-C-C-CH), 7.46 (s, 1H, N-CH-C), 7.40-7.44 (m, 2H, CH₂-CH-C-C-CH-CH), 7.29-7.35 (m, 3H, CH₂-CH-C-CH-CH and N-C-CH-CH), 7.21-7.26 (m, 3H, *m*-CH and N-CH-C-C-CH-CH), 7.17 (t, J = 7.1 Hz, 1H, *p*-CH), 7.13 (d, J = 6.7 Hz, 2H, *o*-CH), 6.48 (d, J = 7.5 Hz, 1H, NH-CH-CH₂), 4.42-4.46 (m, 1H, NH-CH-CH₂), 4.22-4.34 (m, 3H, COO-CH₂-CH), 3.28 (m, 1H, NH-CHH-CH₂), 3.17 (m, 1H, NH-CHH-CH₂), 2.90-3.02 (m, 2H, NH-CH-CH₂), 2.62 (m, 2H, NH-CH₂-CH₂), 1.57 (s, 9H, CH₃); **HPLC-MS** (ESI) m/z 179.2 (10), 334.3 (10), 378.2 (10), 588.4 (10), 632.3 (25), 654.4 (35), 688.3 (80) [M+H]⁺, 710.4 (100) [M+Na]⁺, 1375.5 (40) [2M+H]⁺, 1397.5 (25) [2M+Na]⁺; **Analytical HPLC** (5-90% in 30 min) t_R = 30.44 min.

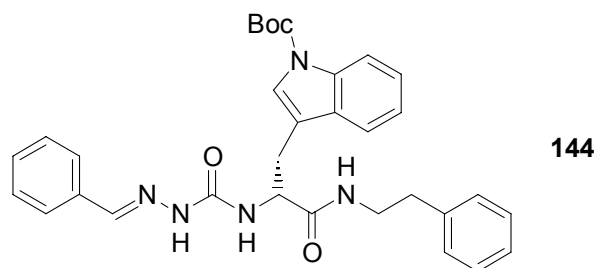


4-(2-Thienyl)benzaldehyde (143)^[458]

A stirred mixture of 4-bromobenzaldehyde (390 mg, 2.11 mmol), 2-thienyl boronic acid (300 mg, 2.34 mmol), powdered cesium fluoride (713 mg, 4.69 mmol) and Pd(PPh₃)₄ (81.1 mg, 3 mol percent, 70.2 μ mol) in DME (7.5 mL) was kept under argon while being heated at reflux for 20 hrs at 100 °C (oil bath). For workup, the solvent was removed *in vacuo*, chromatography of the residue (ethyl acetate/hexane, 1:5) afforded a yellow solid (350 mg, 1.86 mmol, 88%).

mp 73/74 °C; **TLC** R_f (ethyl acetate/hexane, 1:5) = 0.56; **$^1\text{H-NMR}$** (500 MHz, CDCl₃, 300 K) δ = 10.0 (s, 1H, CHO), 7.89 (d, J = 8.0 Hz, 2H, CHO-C-CH), 7.77 (d, J = 8.0 Hz, 2H, CHO-C-CH-CH), 7.47 (d, J = 3.6 Hz, 1H, S-CH), 7.40 (d, J = 4.7 Hz, 1H, S-CH-CH-CH), 7.14 (t, J = 4.2 Hz, 1H, S-CH-CH); **$^{13}\text{C-NMR}$** (125.7 MHz, CDCl₃, 300 K) δ = 191.43, 142.78, 140.19, 135.17, 130.48, 128.49, 126.93, 126.09, 125.06; **MS**

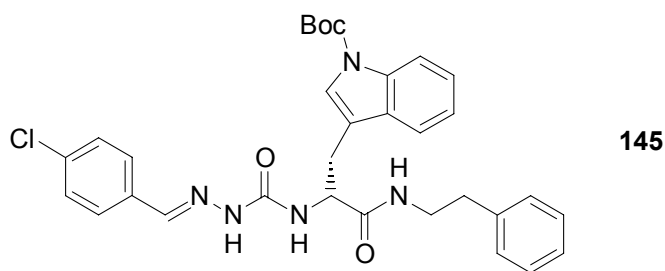
(EI) m/z 40.1 (8), 79.1 (8), 115.1 (45), 159.1 (20), 188.0 (100) $[M]^+$; **Analytical HPLC** (5-90% in 30 min) $t_R = 24.72$ min.



***N*1-(2-Phenylethyl)-(2*R*)-2- $\{[N'$ -(phenylmethylene)hydrazino]carboxamido $\}$ -3-[1-(*tert*-butoxycarbonyl)-3-indolyl]propanamide (**144**)**

*N*1-(2-Phenylethyl)-(2*R*)-2- $\{[N'$ -(phenylmethylene)hydrazino]carboxamido $\}$ -3-[1-(*tert*-butoxycarbonyl)-3-indolyl]propanamide (**144**) was prepared from *N*1-(2-phenylethyl)-(2*R*)-2- $\{[N'$ -(9*H*-fluoren-9-ylmethoxy)carbonyl]hydrazino]carboxamido $\}$ -3-[1-(*tert*-butoxycarbonyl)-3-indolyl]propanamide (**142**) (179 mg, 0.26 mmol) and benzaldehyde (55 mg, 0.52 mmol) according to general method 23 in a reaction time of 4 hrs. The residue was chromatographed using a gradient of ethyl acetate/hexane (1:1) to ethyl acetate/hexane (4:1), drying yielded a colourless, crystalline solid (120 mg, 0.217 mmol, 83%).

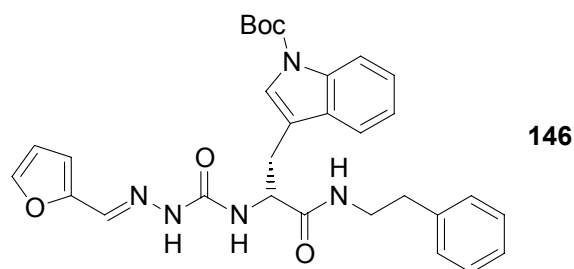
mp 102-104 °C; **TLC** R_f (ethyl acetate/hexane, 1:1) = 0.50; **$^1\text{H-NMR}$** (500 MHz, DMSO- d_6 , 300 K) δ = 10.49 (s, 1H, N-NH), 8.20 (t, $J = 5.5$ Hz, 1H, NH-CH₂-CH₂), 8.03 (d, $J = 8.2$ Hz, 1H, N-C-CH-CH), 7.85 (s, 1H, N-CH-C₆H₅), 7.71 (d, $J = 8.0$ Hz, 1H, N-CH-C-C-CH), 7.62 (d, $J = 7.5$ Hz, 2H, *o*-CH), 7.52 (s, 1H, N-CH-C), 7.37-7.42 (m, 3H, *m*-CH and *p*-CH), 7.31 (t, $J = 7.7$ Hz, 1H, N-C-CH-CH), 7.26 (t, $J = 7.5$ Hz, 2H, *m*-CH), 7.21 (t, $J = 7.5$ Hz, 1H, N-CH-C-C-CH-CH), 7.15-7.19 (m, 3H, *o*-CH and *p*-CH), 6.91 (d, $J = 8.4$ Hz, 1H, NH-CH-CH₂), 4.53 (m, 1H, NH-CH-CH₂), 3.31-3.34 (m, 1H, NH-CHH-CH₂), 3.22-3.27 (m, 1H, NH-CHH-CH₂), 3.14 (dd, $J = 14.3$ Hz, $J = 7.2$ Hz, 1H, NH-CH-CHH), 3.10 (dd, $J = 14.4$ Hz, $J = 5.2$ Hz, 1H, NH-CH-CHH), 2.69 (t, $J = 7.4$ Hz, 2H, NH-CH₂-CH₂), 1.53 (s, 9H, CH₃); **HPLC-MS** (ESI) m/z 498.3 (10), 554.3 (70) $[M+H]^+$, 576.4 (25) $[M+Na]^+$, 850.3 (30) $[(3M+K+H)/2]^{2+}$, 1107.4 (100) $[2M+H]^+$, 1129.4 (70) $[2M+Na]^+$, 1660.8 (10) $[3M+H]^+$, 1682.3 (20) $[3M+Na]^+$; **Analytical HPLC** (5-90% in 30 min) $t_R = 29.35$ min.



***N*1-(2-Phenylethyl)-(2*R*)-2-{[*N'*-(4-chlorophenylmethylene)hydrazino]carboxamido}-3-[1-(*tert*-butoxycarbonyl)-3-indolyl]propanamide (145)**

*N*1-(2-Phenylethyl)-(2*R*)-2-{[*N'*-(4-chlorophenylmethylene)hydrazino]carboxamido}-3-[1-(*tert*-butoxycarbonyl)-3-indolyl]propanamide (**145**) was prepared from *N*1-(2-phenylethyl)-(2*R*)-2-{[*N'*-((9*H*-fluoren-9-ylmethoxy)carbonyl)hydrazino]carboxamido}-3-[1-(*tert*-butoxycarbonyl)-3-indolyl]propanamide (**142**) (179 mg, 0.26 mmol) and 4-chlorobenzaldehyde (74 mg, 0.52 mmol) according to general method 23 in a reaction time of 18 hrs. The residue was chromatographed using a gradient of ethyl acetate/hexane (1:1) to ethyl acetate/hexane (4:1), drying yielded a colourless, crystalline solid (120 mg, 0.204 mmol, 78%).

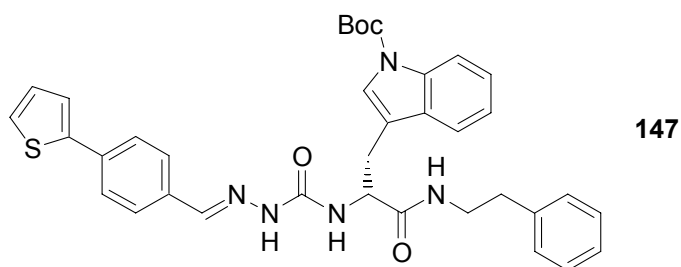
mp 140-142 °C; **TLC** R_f (ethyl acetate/hexane, 1:1) = 0.42; **¹H-NMR** (500 MHz, DMSO-*d*₆, 300 K) δ = 10.56 (s, 1H, N-NH), 8.20 (t, J = 5.5 Hz, 1H, NH-CH₂-CH₂), 8.03 (d, J = 8.2 Hz, 1H, N-C-CH-CH), 7.83 (s, 1H, N-CH-C₆H₄Cl), 7.70 (d, J = 7.9 Hz, 1H, N-CH-C-C-CH), 7.66 (d, J = 8.4 Hz, 2H, Cl-C-CH), 7.45 (d, J = 8.3 Hz, 2H, Cl-C-CH-CH), 7.30 (t, J = 7.6 Hz, 1H, N-C-CH-CH), 7.26 (t, J = 7.5 Hz, 2H, *m*-CH), 7.21 (t, J = 7.6 Hz, 1H, N-CH-C-C-CH-CH), 7.16-7.20 (m, 3H, *o*-CH and *p*-CH), 6.95 (d, J = 8.4 Hz, 1H, NH-CH-CH₂), 4.53 (m, 1H, NH-CH-CH₂), 3.34 (m, 1H, NH-CHH-CH₂), 3.25 (m, 1H, NH-CHH-CH₂), 3.11-3.13 (m, 2H, NH-CH-CH₂), 2.69 (t, J = 7.4 Hz, 2H, NH-CH₂-CH₂), 1.53 (s, 9H, CH₃); **MS** (ESI) m/z 532.2 (10), 588.3 (75) [M+H]⁺, 610.3 (10) [M+Na]⁺, 1175.3 (100) [2M+H]⁺, 1197.3 (15) [2M+Na]⁺, 1761.7 (10) [3M+H]⁺, 1784.1 (5) [3M+Na]⁺; **Analytical HPLC** (5-90% in 30 min) t_R = 31.09 min.



***N*1-(2-Phenylethyl)-(2*R*)-2-{[*N'*-(furan-2-ylmethylene)hydrazino]carboxamido}-3-[1-(*tert*-butoxycarbonyl)-3-indolyl]propanamide (146)**

*N*1-(2-Phenylethyl)-(2*R*)-2-{[*N'*-(furan-2-ylmethylene)hydrazino]carboxamido}-3-[1-(*tert*-butoxycarbonyl)-3-indolyl]propanamide (**146**) was prepared from *N*1-(2-phenylethyl)-(2*R*)-2-{[*N'*-((9*H*-fluoren-9-ylmethoxy)carbonyl)hydrazino]carboxamido}-3-[1-(*tert*-butoxycarbonyl)-3-indolyl]propanamide (**142**) (179 mg, 0.26 mmol) and furan-2-carbaldehyde (75 mg, 0.78 mmol) according to general method 23 in a reaction time of 2 d. The residue was chromatographed (ethyl acetate/hexane, 1:1), drying yielded a colourless, crystalline solid (100 mg, 0.184 mmol, 71%).

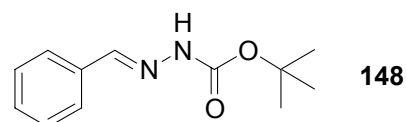
TLC R_f (ethyl acetate/hexane, 1:1) = 0.30; **$^1\text{H-NMR}$** (500 MHz, DMSO- d_6 , 300 K) δ = 10.47 (s, 1H, N-NH), 8.25 (s, 1H, NH-CH₂-CH₂), 8.03 (d, J = 8.0 Hz, 1H, N-C-CH-CH), 7.76 (s, 2H, C-O-CH and N-CH-C₄H₃O), 7.65 (d, J = 7.8 Hz, 1H, N-CH-C-C-CH), 7.47 (s, 1H, N-CH-C), 7.31 (t, J = 7.6 Hz, 1H, N-C-CH-CH), 7.15-7.27 (m, 6H, C₆H₅ and N-CH-C-C-CH-CH), 6.79 (s, 1H, O-C-CH-CH), 6.71 (d, J = 8.4 Hz, 1H, NH-CH-CH₂), 6.59 (s, 1H, O-C-CH-CH), 4.53 (m, 1H, NH-CH-CH₂), 3.30 (m, 1H, NH-CHH-CH₂), 3.22 (m, 1H, NH-CHH-CH₂), 3.07 (d, J = 5.7 Hz, 2H, CH-CH₂), 2.65 (t, J = 7.2 Hz, 2H, NH-CH₂-CH₂), 1.55 (s, 9H, CH₃); **MS** (ESI) m/z 510.3 (15), 544.3 (55) [M+H]⁺, 566.3 (50) [M+Na]⁺, 835.2 (25) [(3M+K+H)/2]²⁺, 1087.4 (45) [2M+H]⁺, 1109.5 (100) [2M+Na]⁺, 1630.3 (5) [3M+H]⁺, 1652.2 (20) [3M+Na]⁺; **Analytical HPLC** (5-90% in 30 min) t_R = 27.62 min.



***N*1-(2-Phenylethyl)-(2*R*)-2-{[*N*'-(4-(2-thienyl)phenylmethylene)hydrazino]carboxamido}-3-[1-(*tert*-butoxycarbonyl)-3-indolyl]propanamide (147)**

*N*1-(2-Phenylethyl)-(2*R*)-2-{[*N*'-(4-(2-thienyl)phenylmethylene)hydrazino]carboxamido}-3-[1-(*tert*-butoxycarbonyl)-3-indolyl]propanamide (**147**) was prepared from *N*1-(2-phenylethyl)-(2*R*)-2-{[*N*'-((9*H*-fluoren-9-ylmethoxy)carbonyl)hydrazino]carboxamido}-3-[1-(*tert*-butoxycarbonyl)-3-indolyl]propanamide (**142**) (100 mg, 0.146 mmol) and 4-(2-thienyl)benzaldehyde (**143**) (54.7 mg, 0.291 mmol) according to general method 23 in a reaction time of 4 d. The residue was purified by RP-HPLC (60-100% in 30 min), lyophilization yielded a colourless powder (44 mg, 0.069 mmol, 47%).

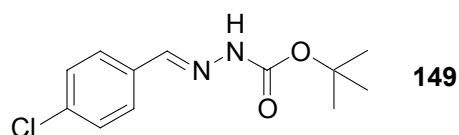
mp 188-191 °C; **¹H-NMR** (500 MHz, DMSO-*d*₆, 300 K) δ = 10.50 (s, 1H, N-NH), 8.18 (t, *J* = 5.6 Hz, 1H, NH-CH₂-CH₂), 8.01 (d, *J* = 8.5 Hz, 1H, N-C-CH-CH), 7.83 (s, 1H, N-CH-C₁₀H₇S), 7.64-7.70 (m, 5H, C₆H₄ and N-CH-C-C-CH), 7.57-7.58 (m, 2H, C₄HH₂S), 7.53 (s, 1H, N-CH-C), 7.30 (t, *J* = 7.6 Hz, 1H, N-C-CH-CH), 7.19-7.26 (m, 3H, *m*-CH and N-CH-C-C-CH-CH), 7.14-7.17 (m, 4H, *o*-CH and *p*-CH and C₄H₂HS), 6.91 (d, *J* = 8.4 Hz, 1H, NH-CH-CH₂), 4.48-4.52 (m, 1H, NH-CH-CH₂), 3.30-3.36 (m, 1H, NH-CHH-CH₂), 3.20-3.25 (m, 1H, NH-CHH-CH₂), 3.12 (dd, *J* = 7.9 Hz, *J* = 14.8 Hz, 1H, NH-CH-CHH), 3.08 (dd, *J* = 5.6 Hz, *J* = 14.8 Hz, 1H, NH-CH-CHH), 2.67 (t, *J* = 7.2 Hz, 2H, NH-CH₂-CH₂), 1.53 (s, 9H, CH₃); **HPLC-MS** (ESI) *m/z* 636.3 (75) [M+H]⁺, 658.4 (10) [M+Na]⁺, 1271.5 (100) [2M+H]⁺, 1293.5 (20) [2M+Na]⁺; **Analytical HPLC** (5-90% in 30 min) *t*_R = 32.00 min.



***N*²-(Phenylmethylene)hydrazinecarboxylic acid *tert*-butyl ester (148)**

*N*²-(Phenylmethylene)hydrazinecarboxylic acid *tert*-butyl ester (**148**) was synthesized according to general method 15 using benzaldehyde (2.4 g, 22.7 mmol). The precipitation was collected, drying yielded a colourless solid (4.1 g, 18.6 mmol, 82%).

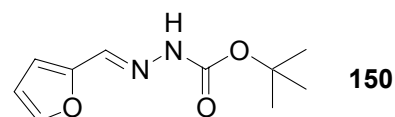
mp 187 °C; **TLC** R_f (ethyl acetate/hexane, 1:1) = 0.62; **¹H-NMR** (250 MHz, DMSO-*d*₆, 300 K) δ = 10.89 (bs, 1H, NH), 8.00 (s, 1H, N-CH), 7.60 (d, J = 7.6 Hz, 2H, *o*-CH), 7.39-7.42 (m, 3H, *m*-CH and *p*-CH), 1.47 (s, 9H, CH₃); **MS** (EI) m/z 41.2 (20), 57.2 (100), 120.1 (15), 147.0 (6), 164.0 (30), 220.0 (4) [M]⁺; **Analytical HPLC** (5-90% in 30 min) t_R = 22.03 min.



***N*²-(4-Chlorophenylmethylene)hydrazinecarboxylic acid *tert*-butyl ester (149)**

*N*²-(4-Chlorophenylmethylene)hydrazinecarboxylic acid *tert*-butyl ester (**149**) was synthesized according to general method 15 using 4-chloro-benzaldehyde (2.12 g, 15.1 mmol). The residue was chromatographed (ethyl acetate/hexane, 1:5), drying yielded a colourless solid (3.64 g, 14.3 mmol, 95%).

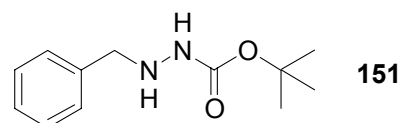
mp 170/171 °C; **TLC** R_f (ethyl acetate/hexane, 1:5) = 0.27; **¹H-NMR** (250 MHz, DMSO-*d*₆, 300 K) δ = 10.97 (bs, 1H, NH), 7.99 (s, 1H, N-CH), 7.63 (d, J = 8.6 Hz, 2H, Cl-C-CH), 7.47 (d, J = 8.6 Hz, 2H, Cl-C-CH-CH), 1.47 (s, 9H, CH₃); **MS** (EI) m/z 41.2 (20), 57.2 (100), 154.0 (10), 181.0 (5), 197.9 (20), 253.9 (5) [M]⁺; **Analytical HPLC** (5-90% in 30 min) t_R = 24.52 min.



***N'*-(Furan-2-ylmethylene)hydrazinecarboxylic acid *tert*-butyl ester (150)**

N'-(Furan-2-ylmethylene)hydrazinecarboxylic acid *tert*-butyl ester (**150**) was synthesized according to general method 15 using furan-2-carbaldehyde (4.3 g, 44.7 mmol). Drying yielded a colourless solid (9.0 g, 42.8 mmol, 96%).

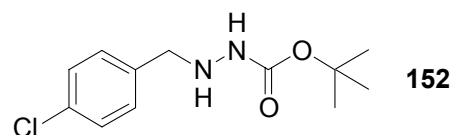
mp 158-160 °C; **TLC** R_f (ethyl acetate/hexane, 1:5) = 0.23; **$^1\text{H-NMR}$** (250 MHz, DMSO- d_6 , 300 K) δ = 10.84 (bs, 1H, NH), 7.89 (s, 1H, N-CH), 7.76 (d, J = 1.3 Hz, 1H, O-CH-CH), 6.76 (d, J = 3.1 Hz, 1H, O-C-CH), 6.56-6.58 (m, 1H, O-CH-CH), 1.46 (s, 9H, CH_3); **GC-MS** (EI) m/z 41.1 (30), 57.1 (100), 110.0 (35), 136.9 (8), 153.9 (15), 209.9 (8) $[\text{M}]^+$; **Analytical HPLC** (5-90% in 30 min) t_R = 18.49 min.



***N*-(*tert*-Butoxycarbonyl)-*N'*-(benzyl)hydrazine (151)**

N-(*tert*-Butoxycarbonyl)-*N'*-(benzyl)hydrazine (**138**) was synthesized from *N'*-(phenylmethylene)hydrazinecarboxylic acid *tert*-butyl ester (**135**) (1.5 g, 6.8 mmol) according to general method 16. Drying yielded a yellow oil (1.41 g, 6.3 mmol, 93%).

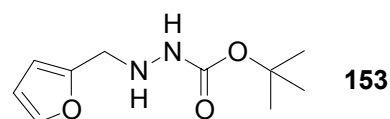
TLC R_f (ethyl acetate/hexane, 1:5) = 0.73; **$^1\text{H-NMR}$** (250 MHz, DMSO- d_6 , 300 K) δ = 8.24 (bs, 1H, NH-CO), 7.22-7.32 (m, 5H, C_6H_5), 4.71 (bs, 1H, NH- CH_2), 3.88 (s, 2H, NH- CH_2), 1.35 (s, 9H, CH_3); **GC-MS** (EI) m/z 41.1 (50), 57.1 (100), 91.1 (95), 106.0 (45), 122.0 (35), 149.0 (8), 165.9 (50), 222.0 (1) $[\text{M}]^+$; **Analytical HPLC** (5-90% in 30 min) t_R = 15.45 min.



***N*-(*tert*-Butoxycarbonyl)-*N'*-(4-chlorobenzyl)hydrazine (152)**

N-(*tert*-Butoxycarbonyl)-*N'*-(4-chlorobenzyl)hydrazine (**152**) was synthesized from *N'*-(4-chlorophenylmethylene)hydrazinecarboxylic acid *tert*-butyl ester (**149**) (1.5 g, 5.8 mmol) according to general method 16. The crude product was chromatographed (ethyl acetate/hexane, 1:4), drying yielded a colourless solid (1.05 g, 4.1 mmol, 71%).

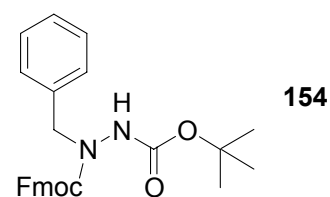
mp 77-82 °C; **TLC** R_f (ethyl acetate/hexane, 1:5) = 0.15; **$^1\text{H-NMR}$** (250 MHz, DMSO- d_6 , 300 K) δ = 8.23 (bs, 1H, NH-CO), 7.35 (m, 4H, C₆H₄Cl), 4.84 (bs, 1H, NH-CH₂), 3.85 (s, 2H, NH-CH₂), 1.37 (s, 9H, CH₃); **GC-MS** (CI) m/z 124.9 (10), 139.9 (10), 156.9 (60), 200.8 (100), 238.7 (2), 256.8 (2) [M+H]⁺; **Analytical HPLC** (5-90% in 30 min) t_R = 19.07 min.



***N*-(*tert*-Butoxycarbonyl)-*N'*-(2-furylmethyl)hydrazine (153)**

N-(*tert*-Butoxycarbonyl)-*N'*-(2-furylmethyl)hydrazine (**153**) was synthesized from *N'*-(furan-2-ylmethylene)hydrazinecarboxylic acid *tert*-butyl ester (**150**) (6.0 g, 28.7 mmol) according to general method 16. Drying yielded a colourless solid (5.37 g, 25.3 mmol, 88%).

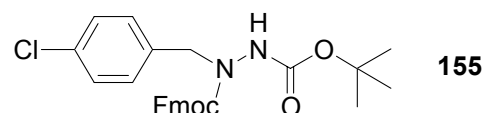
mp 53/54 °C; **TLC** R_f (ethyl acetate/hexane, 1:1) = 0.57; **$^1\text{H-NMR}$** (250 MHz, DMSO- d_6 , 300 K) δ = 8.25 (bs, 1H, NH-CO), 7.55 (s, 1H, O-CH-CH), 6.36-6.38 (m, 1H, O-C-CH), 6.24-6.28 (m, 1H, O-CH-CH), 4.68-4.73 (m, 1H, NH-CH₂), 3.83 (d, J = 9.5 Hz, 2H, NH-CH₂), 1.38 (s, 9H, CH₃); **GC-MS** (EI) m/z 41.2 (25), 57.1 (100), 81.1 (100), 96.1 (25), 112.1 (10), 156.0 (30), 212.0 (5) [M]⁺; **Analytical HPLC** (5-90% in 30 min) t_R = 14.35 min.



***N*-Benzyl-*N*-[(9*H*-fluorene-9-ylmethoxy)carbonyl]-*N'*-(*tert*-butoxycarbonyl)hydrazine (**154**)**

N-Benzyl-*N*-[(9*H*-fluorene-9-ylmethoxy)carbonyl]-*N'*-(*tert*-butoxycarbonyl)hydrazine (**154**) was prepared from *N*-(*tert*-butoxycarbonyl)-*N'*-(benzyl)hydrazine (**151**) (1.0 g, 4.49 mmol) according to general method 17. The residue was chromatographed (ethyl acetate/hexane, 1:2), drying yielded a colourless foam (1.95 g, 4.38 mmol, 98%).

TLC R_f (ethyl acetate/hexane, 1:3) = 0.47; **$^1\text{H-NMR}$** (250 MHz, DMSO- d_6 , 300 K) δ = 9.62 (bs, 1H, NH), 7.89 (d, J = 7.6 Hz, 2H, arom), 7.75 (d, J = 6.4 Hz, 1H, arom), 7.56 (m, 1H, arom), 7.28-7.43 (m, 8H, arom), 7.02 (m, 1H, arom), 4.15-4.65 (m, 5H, N- CH_2 and CO- CH_2 -CH), 1.44 (s, 9H, CH_3); **HPLC-MS** (ESI) m/z 167.0 (20), 179.1 (100), 467.1 (50) $[\text{M}+\text{Na}]^+$, 910.9 (15) $[2\text{M}+\text{Na}]^+$; **Analytical HPLC** (5-90% in 30 min) t_R = 27.95 min.

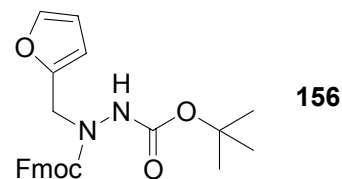


***N*-(4-Chlorobenzyl)-*N*-[(9*H*-fluorene-9-ylmethoxy)carbonyl]-*N'*-(*tert*-butoxycarbonyl)hydrazine (**155**)**

N-(4-Chlorobenzyl)-*N*-[(9*H*-fluorene-9-ylmethoxy)carbonyl]-*N'*-(*tert*-butoxycarbonyl)hydrazine (**155**) was prepared from *N*-(*tert*-butoxycarbonyl)-*N'*-(4-chlorobenzyl)hydrazine (**152**) (0.8 g, 3.12 mmol) according to general method 17. The residue was chromatographed (ethyl acetate/hexane, 1:2), drying yielded a colourless foam (1.37 g, 2.86 mmol, 92%).

mp 53-55 °C; **TLC** R_f (ethyl acetate/hexane, 1:1) = 0.78; **$^1\text{H-NMR}$** (250 MHz, DMSO- d_6 , 300 K) δ = 9.62 (s, 1H, NH), 7.89 (d, J = 7.3 Hz, 2H, arom), 7.74 (d, J = 6.7 Hz, 1H, arom), 7.56 (m, 1H, arom), 7.27-7.43 (m, 7H, arom), 6.99 (m, 1H, arom),

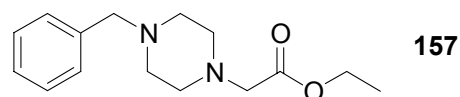
4.2-5.52 (m, 5H, N-CH₂ and CO-CH₂-CH), 1.43 (s, 9H, CH₃); **HPLC-MS** (ESI) *m/z* 179.2 (100), 200.9 (20), 501.1 (35) [M+Na]⁺, 978.8 (20) [2M+Na]⁺; **Analytical HPLC** (5-90% in 30 min) *t_R* = 28.82 min.



***N*-[(9*H*-Fluorene-9-ylmethoxy)carbonyl]-*N*-(2-furylmethyl)-*N'*-(*tert*-butoxycarbonyl)hydrazine (156)**

N-[(9*H*-Fluorene-9-ylmethoxy)carbonyl]-*N*-(2-furylmethyl)-*N'*-(*tert*-butoxycarbonyl)hydrazine (**156**) was prepared from *N*-(*tert*-butoxycarbonyl)-*N'*-(2-furylmethyl)hydrazine (**153**) (4.5 g, 21.2 mmol) according to general method 17. The residue was chromatographed (ethyl acetate/hexane, 1:1), drying yielded a colourless foam (6.6 g, 15.2 mmol, 72%).

TLC *R_f* (ethyl acetate/hexane, 1:3) = 0.54; **¹H-NMR** (250 MHz, DMSO-*d*₆, 300 K) δ = 9.57 (bs, 1H, NH), 7.90 (d, *J* = 7.5 Hz, 2H, arom), 7.58-7.72 (m, 3H, arom), 7.28-7.46 (m, 4H, arom), 6.39 (bs, 2H, arom), 4.22-4.51 (m, 5H, N-CH₂ and CO-CH₂-CH), 1.44 (s, 9H, CH₃); **HPLC-MS** (ESI) *m/z* 179.2 (100), 259.1 (65), 379.1 (40), 457.3 (85) [M+Na]⁺, 891.2 (25) [2M+Na]⁺; **Analytical HPLC** (5-90% in 30 min) *t_R* = 29.61 min.

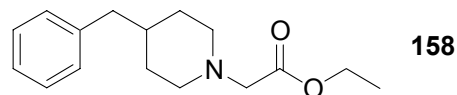


(4-Benzyl-piperazin-1-yl)acetic acid ethyl ester (157)

(4-Benzyl-piperazin-1-yl)acetic acid ethyl ester (**157**) was prepared according to general method 12 using 4-benzyl-piperazine (3.0 g, 17.0 mmol) and bromoacetic acid ethyl ester (2.84 g, 17.0 mmol). Drying yielded a colourless oil (4.09 g, 15.6 mmol, 92%).

TLC *R_f* (ethyl acetate/hexane, 1:1) = 0.50; **¹H-NMR** (250 MHz, DMSO-*d*₆, 300 K) δ = 7.28-7.39 (m, 5H, C₆H₅), 4.15 (q, *J* = 7.0 Hz, 2H, CH₂-CH₃), 3.52 (s, 2H, CH₂-C₆H₅), 3.25 (s, 2H, N-CH₂-CO), 2.59 (m, 4H, N-CH₂-CH₂), 2.45 (m, 4H, N-CH₂-CH₂),

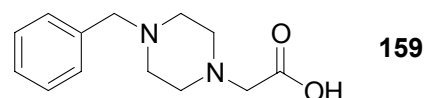
1.26 (t, $J = 7.0$ Hz, 3H, $\text{CH}_2\text{-CH}_3$); $^{13}\text{C-NMR}$ (62.9 MHz, $\text{DMSO-}d_6$, 300 K) $\delta = 169.702$ (CO), 138.141, 128.641, 127.989, 126.723, 62.092 ($\text{CH}_2\text{-C}_6\text{H}_5$), 59.621 (O- CH_2), 58.461 (N- $\text{CH}_2\text{-CO}$), 52.487 (N- $\text{CH}_2\text{-CH}_2$), 51.994 (N- $\text{CH}_2\text{-CH}_2$), 13.996 (CH_3); **HPLC-MS** (ESI) m/z 171.1 (35), 189.2 (20), 263.3 (100) $[\text{M}+\text{H}]^+$; **Analytical HPLC** (5-90% in 30 min) $t_R = 11.10$ min.



(4-Benzyl-piperidin-1-yl)acetic acid ethyl ester (158)

(4-Benzyl-piperidin-1-yl)acetic acid ethyl ester (**158**) was prepared according to general method 12 using 4-benzyl-piperidine (3.0 g, 17.1 mmol) and bromoacetic acid ethyl ester (2.86 g, 17.1 mmol). Drying yielded a colourless oil (4.02 g, 15.4 mmol, 90%).

TLC R_f (ethyl acetate/hexane, 1:1) = 0.64; $^1\text{H-NMR}$ (250 MHz, $\text{DMSO-}d_6$, 300 K) $\delta = 7.49\text{-}7.66$ (m, 5H, C_6H_5), 4.44 (q, $J = 7.0$ Hz, 2H, $\text{CH}_2\text{-CH}_3$), 3.51 (s, 2H, N- $\text{CH}_2\text{-CO}$), 3.17 (d, $J = 11.3$ Hz, 2H, N- $\text{CH}_2\text{-CH}_2$), 2.86 (d, $J = 6.4$ Hz, 2H, $\text{CH}_2\text{-C}_6\text{H}_5$), 2.45 (t, $J = 10.1$ Hz, 2H, N- $\text{CH}_2\text{-CH}_2$), 1.86-1.90 (m, 3H, CH and N- $\text{CH}_2\text{-CH}_2$), 1.63 (dd, $J = 11.9$ Hz, $J = 3.4$ Hz, 2H, N- $\text{CH}_2\text{-CH}_2$), 1.55 (t, $J = 7.0$ Hz, 3H, $\text{CH}_2\text{-CH}_3$); $^{13}\text{C-NMR}$ (62.9 MHz, $\text{DMSO-}d_6$, 300 K) $\delta = 169.823$ (CO), 140.135, 128.778, 127.906, 125.518, 59.492 (O- CH_2), 58.961 (N- $\text{CH}_2\text{-CO}$), 52.517 (N- $\text{CH}_2\text{-CH}_2$), 42.389 ($\text{CH}_2\text{-C}_6\text{H}_5$), 36.892 (CH), 31.623 (N- $\text{CH}_2\text{-CH}_2$), 13.951 (CH_3); **HPLC-MS** (ESI) m/z 188.2 (100), 234.2 (45), 262.2 (100) $[\text{M}+\text{H}]^+$; **Analytical HPLC** (5-90% in 30 min) $t_R = 16.12$ min.

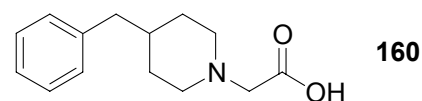


(4-Benzyl-piperazin-1-yl)acetic acid (159)

(4-Benzyl-piperazin-1-yl)acetic acid (**159**) was prepared from (4-benzyl-piperazin-1-yl)acetic acid ethyl ester (**157**) (1.0 g, 3.82 mmol) according to general method 14, drying yielded a colourless solid (0.89 g, quant).

mp 242-245 °C; **TLC** R_f (methanol) = 0.58; $^1\text{H-NMR}$ (500 MHz, $\text{DMSO-}d_6$, 300 K) $\delta = 7.68$ (m, 2H, arom), 7.44 (m, 3H, arom), 4.42 (s, 2H, $\text{CH}_2\text{-C}_6\text{H}_5$), 4.10 (s, 2H, N-

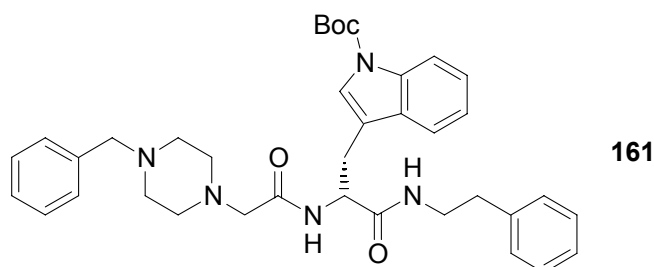
CH_2-CO), 3.5-3.7 (m, 4H, N- CH_2-CH_2), 3.46 (m, 4H, N- CH_2-CH_2); **GC-MS** (EI) m/z 38.1 (20), 91.1 (100), 119.1 (30), 132.1 (20), 146.1 (15), 189.1 (15), 234.1 (20) $[M]^+$; **Analytical HPLC** (5-90% in 30 min) $t_R = 7.64$ min.



(4-Benzyl-piperidin-1-yl)acetic acid (160)

(4-Benzyl-piperidin-1-yl)acetic acid (**160**) was prepared from (4-benzyl-piperidin-1-yl)acetic acid ethyl ester (**158**) (1.0 g, 3.82 mmol) according to general method 14, drying yielded a colourless solid (0.89 g, quant).

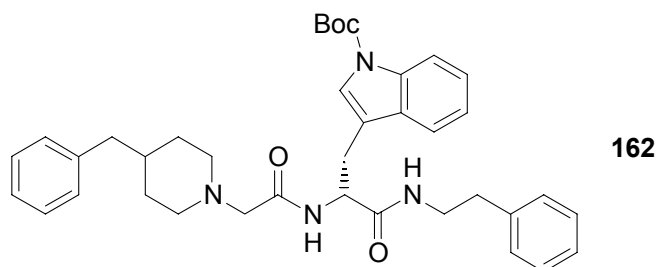
mp 250-252 °C; **TLC** R_f (methanol) = 0.71; **1H -NMR** (500 MHz, DMSO- d_6 , 300 K) δ = 7.26-7.29 (m, 2H, arom), 7.16-7.19 (m, 3H, arom), 3.63 (s, 2H, N- CH_2-CO), 3.39 (d, $J = 10.5$ Hz, 2H, N- CH_2-CH_2), 2.91 (m, 2H, $CH_2-C_6H_5$), 2.52 (t, $J = 7.2$ Hz, 2H, N- CH_2-CH_2), 1.66-1.75 (m, 3H, CH and N- CH_2-CH_2), 1.51-1.53 (m, 2H, N- CH_2-CH_2); **GC-MS** (EI) m/z 44.1 (10), 91.1 (15), 188.1 (100), 233.0 (5) $[M]^+$; **Analytical HPLC** (5-90% in 30 min) $t_R = 14.09$ min.



*N*1-(2-Phenylethyl)-(2*R*)-2-[[4-benzylpiperazino)methyl]carboxamido}-3-[1-(*tert*-butoxy carbonyl)-3-indolyl]propanamide (**161**)

*N*1-(2-Phenylethyl)-(2*R*)-2-[[4-benzylpiperazino)methyl]carboxamido}-3-[1-(*tert*-butoxy carbonyl)-3-indolyl]propanamide (**161**) was prepared from *tert*-butyl-3-{{(2*R*)-2-amino-2-[1-(2-phenylethyl)carbonyl]ethyl}-1*H*-1-indolecarboxylate (**139**) (150 mg, 0.368 mmol) and (4-benzyl-piperazin-1-yl)acetic acid (**159**) (86 mg, 0.368 mmol) according to general method 18 in a reaction time of 23 hrs. The residue was chromatographed (chloroform/methanol, 10:1), drying yielded a yellow oil (170 mg, 0.273 mmol, 74%).

TLC R_f (chloroform/methanol, 10:1) = 0.52; **$^1\text{H-NMR}$** (500 MHz, $\text{DMSO-}d_6$, 300 K) δ = 8.20 (t, J = 5.5 Hz, 1H, $\text{NH-CH}_2\text{-CH}_2$), 8.00 (d, J = 8.1 Hz, 1H, N-C-CH-CH), 7.72 (d, J = 8.5 Hz, 1H, NH-CH-CH_2), 7.63 (d, J = 7.8 Hz, 1H, N-CH-C-C-CH), 7.46 (s, 1H, N-CH-C), 7.22-7.31 (m, 9H, N-C-CH-CH and N-CH-C-C-CH-CH and $m\text{-CH}$ and C_6H_5), 7.16-7.18 (m, 3H, $o\text{-CH}$ and $p\text{-CH}$), 4.60-4.62 (m, 1H, NH-CH-CH_2), 3.36-3.44 (dd, J = 25.5 Hz, J = 13.5 Hz, 2H, $\text{NH-CH}_2\text{-C}_6\text{H}_5$), 3.29-3.36 (m, 1H, NH-CHH-CH_2), 3.21-3.27 (m, 1H, NH-CHH-CH_2), 3.04 (dd, J = 14.7 Hz, J = 5.2 Hz, 1H, NH-CH-CHH), 2.99 (dd, J = 14.7 Hz, J = 8.2 Hz, 1H, NH-CH-CHH), 2.73-2.93 (m, 2H, $\text{N-CH}_2\text{-CO}$), 2.20-2.33 (m, 8H, $\text{N-CH}_2\text{-CH}_2\text{-N}$), 1.56 (s, 9H, CH_3); **HPLC-MS** (ESI) m/z 189.1 (20), 568.3 (100), 624.3 (85) $[\text{M}+\text{H}]^+$, 646.3 (30) $[\text{M}+\text{Na}]^+$, 1269.3 (25) $[\text{2M}+\text{Na}]^+$; **Analytical HPLC** (5-90% in 30 min) t_R = 23.13 min.



***N*1-(2-Phenylethyl)-(2*R*)-2-[[4-benzylpiperidino)methyl]carboxamido}-3-[1-(*tert*-butoxy carbonyl)-3-indolyl]propanamide (**162**)**

*N*1-(2-Phenylethyl)-(2*R*)-2-[[4-benzylpiperidino)methyl]carboxamido}-3-[1-(*tert*-butoxy carbonyl)-3-indolyl]propanamide (**162**) was prepared from *tert*-butyl-3-[(2*R*)-2-amino-2-[1-(2-phenylethyl)carbamoyl]ethyl]-1*H*-1-indolecarboxylate (**139**) (150 mg, 0.368 mmol) and (4-benzyl-piperidin-1-yl)acetic acid (**160**) (86 mg, 0.368 mmol) according to general method 18 in a reaction time of 23 hrs. The residue was chromatographed (chloroform/methanol, 10:1), drying yielded a yellow oil (180 mg, 0.289 mmol, 79%).

TLC R_f (chloroform/methanol, 10:1) = 0.62; **$^1\text{H-NMR}$** (500 MHz, $\text{DMSO-}d_6$, 300 K) δ = 8.23 (t, J = 5.5 Hz, 1H, $\text{NH-CH}_2\text{-CH}_2\text{-C}_6\text{H}_5$), 8.03 (d, J = 8.5 Hz, 1H, N-C-CH-CH), 7.79 (bs, 1H, NH-CH-CH_2), 7.64 (d, J = 8.0 Hz, 1H, N-CH-C-C-CH), 7.47 (s, 1H, N-CH-C), 7.32 (t, J = 7.7 Hz, 1H, NH-C-CH-CH), 7.12-7.27 (m, 11H, N-CH-C-C-CH-CH and C_6H_5 and C_6H_5), 4.61-4.65 (m, 1H, NH-CH-CH_2), 3.30-3.40 (m, 1H,

NH-CHH-CH₂-C₆H₅), 3.23-3.28 (m, 1H, NH-CHH-CH₂-C₆H₅), 3.05 (dd, $J = 14.7$ Hz, $J = 5.2$ Hz, 1H, NH-CH-CHH), 2.99 (dd, $J = 14.6$ Hz, $J = 8.2$ Hz, 1H, NH-CH-CHH), 2.73-2.96 (m, 2H, N-CH₂-CO), 2.69 (t, $J = 7.2$ Hz, 2H, NH-CH₂-CH₂-C₆H₅), 2.65-2.73 (m, 1H, N-CHH-CH₂-CH), 2.47-2.53 (m, 1H, N-CHH-CH₂-CH), 2.44 (d, $J = 6.5$ Hz, 2H, CH-CH₂-C₆H₅), 1.80-2.0 (m, 2H, N-CHH-CH₂-CH), 1.58 (s, 9H, CH₃), 1.36-1.47 (m, 3H, N-CH₂-CHH-CH), 1.04-1.13 (m, 2H, N-CH₂-CHH-CH); **HPLC-MS** (ESI) m/z 188.1 (20), 567.3 (70), 623.3 (100) [M+H]⁺, 645.2 (25) [M+Na]⁺, 1245.2 (10) [2M+H]⁺, 1267.3 (40) [2M+Na]⁺; **Analytical HPLC** (5-90% in 30 min) $t_R = 25.49$ min.

8.3.2 Linear and Cyclic Peptide BRS-3 Agonists

Synthesis of linear peptides **4-13**, **23-31** and **40**, **41** was carried out using Rink Amide MBHA resin.^[307] Linear peptides **14-22**, **32-39** and **108-115** were synthesized on FMPE resin,^[310] which was reductively aminated with the corresponding amine and loaded with the appropriate Fmoc amino acid according to general method 1. Linear peptides **42-54** and **95-106** were synthesized on Sieber Amide resin.^[308] Peptides **55-57** and **107** were synthesized on TCP resin.^[309] The resin was loaded according to general method 2, Fmoc was removed according to general method 3. Chain extension was carried out either manually as described in chapter 8.1 or on a peptide synthesizer (*SyRoll*) using standard Fmoc protocols as depicted in general method 7. Peptide bonds were formed using activation according to general method 4. Cleavage from all resins was carried out using general method 8, except for Sieber Amide resin (general method 9). For preparation of peptides **58-94**, the linear sequence was synthesized on Sieber Amide resin, cleavage from solid support and deprotection were carried out according to general method 9. Then, cyclization via cysteine oxidation was carried out according to general method 10. The N-terminal free amine of peptides **43**, **45**, **47**, **49**, **51**, **53**, **57** and **96** was acetylated on solid support (general method 6). All peptides were purified by RP-HPLC, purity of the peptides was 95% or higher except for **17** (93%), **64** (94%), **76** (89%), **82** (91%), **85** (93%), **87** (93%), **88** (93%) and **99** (92%). Analytical data of peptides **4-115** is listed in Tables 8.1-8.13.

Table 8.1: Analytical data of peptides **4-13**.

no.	peptide	Σ	Analyt. HPLC		HPLC-MS (ESI) m/z
			grad	t_R [min]	
4	AQWAV β AHF-NIe-NH ₂	C ₅₁ H ₇₂ N ₁₄ O ₁₀	10-90%	11.10	1041.5 (68) [M+H] ⁺ , 1063.6 (100) [M+Na] ⁺ , 1079.3 (7) [M+K] ⁺
5	aQWAV β AHF-NIe-NH ₂	C ₅₁ H ₇₂ N ₁₄ O ₁₀	5-90%	15.09	1041.6 (100) [M+H] ⁺ , 1063.7 (26) [M+Na] ⁺
6	fAWAV β AHF-NIe-NH ₂	C ₅₅ H ₇₃ N ₁₃ O ₉	10-90%	12.50	1060.5 (68) [M+H] ⁺ , 1082.6 (100) [M+Na] ⁺ , 1098.4 (6) [M+K] ⁺
7	fQAAV β AHF-NIe-NH ₂	C ₄₉ H ₇₁ N ₁₃ O ₁₀	10-60%	15.55	1002.5 (46) [M+H] ⁺ , 1024.5 (100) [M+Na] ⁺ , 1040.3 (7) [M+K] ⁺
8	fQWAV β AHF-NIe-NH ₂	C ₅₇ H ₇₆ N ₁₄ O ₁₀	10-60%	17.83	1117.5 (58) [M+H] ⁺ , 1139.6 (100) [M+Na] ⁺ , 1155.4 (7) [M+K] ⁺
9	fQWAA β AHF-NIe-NH ₂	C ₅₅ H ₇₂ N ₁₄ O ₁₀	10-60%	14.98	1089.5 (52) [M+H] ⁺ , 1111.6 (100) [M+Na] ⁺ , 1127.4 (8) [M+K] ⁺
10	fQWAV β AHF-NIe-NH ₂	C ₅₇ H ₇₆ N ₁₄ O ₁₀	10-60%	18.20	1117.5 (100) [M+H] ⁺ , 1139.6 (100) [M+Na] ⁺ , 1155.4 (8) [M+K] ⁺
11	fQWAV β A β AF-NIe-NH ₂	C ₅₄ H ₇₄ N ₁₂ O ₁₀	10-60%	17.00	1034.5 (10), 1051.4 (68) [M+H] ⁺ , 1073.6 (100) [M+Na] ⁺ , 1089.3 (7) [M+K] ⁺
12	fQWAV β AHA-NIe-NH ₂	C ₅₁ H ₇₂ N ₁₄ O ₁₀	10-60%	15.55	1041.5 (76) [M+H] ⁺ , 1063.5 (100) [M+Na] ⁺ , 1079.3 (8) [M+K] ⁺
13	fQWAV β AHFA-NH ₂	C ₅₄ H ₇₀ N ₁₄ O ₁₀	10-60%	15.70	1075.5 (87) [M+H] ⁺ , 1097.5 (100) [M+Na] ⁺ , 1113.3 (10) [M+K] ⁺

Table 8.2: Analytical data of peptides **14-22**.

no.	peptide	Σ	Analyt. HPLC		HPLC-MS (ESI) m/z
			grad	t_R [min]	
14	AQWAVGHF-propylamide	$C_{47}H_{65}N_{13}O_9$	10-80%	14.40	956.4 (100) [M+H] ⁺ , 978.4 (78) [M+Na] ⁺ , 994 (10) [M+K] ⁺
15	aQWAVGHF-propylamide	$C_{47}H_{65}N_{13}O_9$	5-90%	15.41	956.6 (100) [M+H] ⁺ , 978.6 (31) [M+Na] ⁺
16	fAWAVGHF-propylamide	$C_{51}H_{66}N_{12}O_8$	10-80%	16.76	975.4 (100) [M+H] ⁺ , 997.4 (79) [M+Na] ⁺ , 1013.4 (7) [M+K] ⁺
17	fQAAVGHF-propylamide	$C_{45}H_{64}N_{12}O_9$	10-80%	12.99	917.4 (94) [M+H] ⁺ , 939.4 (100) [M+Na] ⁺ , 955 (14) [M+K] ⁺
18	fQWAVGHF-propylamide	$C_{53}H_{69}N_{13}O_9$	10-80%	14.94	1032.4 (100) [M+H] ⁺ , 1054.5 (87) [M+Na] ⁺ , 1070.3 (9) [M+K] ⁺
19	fQWAAGHF-propylamide	$C_{51}H_{65}N_{13}O_9$	10-80%	14.40	1004.4 (87) [M+H] ⁺ , 1026.4 (100) [M+Na] ⁺ , 1042.3 (12) [M+K] ⁺
20	fQWAVAHF-propylamide	$C_{54}H_{71}N_{13}O_9$	10-80%	15.73	1046.4 (94) [M+H] ⁺ , 1068.5 (100) [M+Na] ⁺ , 1084.3 (8) [M+K] ⁺
21	fQWAVGAF-propylamide	$C_{50}H_{67}N_{11}O_9$	10-80%	16.90	760.2 (14), 966.3 (80) [M+H] ⁺ , 988.4 (100) [M+Na] ⁺ , 1004.3 (10) [M+K] ⁺
22	fQWAVGHA-propylamide	$C_{47}H_{65}N_{13}O_9$	15-60%	12.39	956.4 (86) [M+H] ⁺ , 978.4 (100) [M+Na] ⁺ , 994 (10) [M+K] ⁺

Table 8.3: Analytical data of peptides **23-31**.

no.	peptide	Σ	Analyt. HPLC		HPLC-MS (ESI) m/z
			grad	t_R [min]	
23	FQWAV β AHF-Nle-NH ₂	C ₅₇ H ₇₆ N ₁₄ O ₁₀	20-80%	12.31	1117.4 (76) [M+H] ⁺ , 1139.5 (100) [M+Na] ⁺ , 1155.2 (9) [M+K] ⁺
24	f q WAV β AHF-Nle-NH ₂	C ₅₇ H ₇₆ N ₁₄ O ₁₀	20-80%	11.68	1117.4 (85) [M+H] ⁺ , 1139.4 (100) [M+Na] ⁺ , 1155.2 (12) [M+K] ⁺
25	fQWAV β AHF-Nle-NH ₂	C ₅₇ H ₇₆ N ₁₄ O ₁₀	20-80%	11.92	1117.4 (70) [M+H] ⁺ , 1139.4 (100) [M+Na] ⁺ , 1155.2 (12) [M+K] ⁺
26	fQW a V β AHF-Nle-NH ₂	C ₅₇ H ₇₆ N ₁₄ O ₁₀	20-80%	11.65	1117.4 (64) [M+H] ⁺ , 1139.5 (100) [M+Na] ⁺ , 1155.2 (12) [M+K] ⁺
27	fQW a v β AHF-Nle-NH ₂	C ₅₇ H ₇₆ N ₁₄ O ₁₀	20-80%	11.32	1117.3 (82) [M+H] ⁺ , 1139.4 (100) [M+Na] ⁺ , 1155.2 (15) [M+K] ⁺
28	fQWAV a HF-Nle-NH ₂	C ₅₇ H ₇₆ N ₁₄ O ₁₀	20-80%	12.21	1117.4 (100) [M+H] ⁺ , 1139.5 (100) [M+Na] ⁺ , 1155.3 (8) [M+K] ⁺
29	fQWAV β A h F-Nle-NH ₂	C ₅₇ H ₇₆ N ₁₄ O ₁₀	20-70%	12.42	1117.4 (72) [M+H] ⁺ , 1139.4 (100) [M+Na] ⁺ , 1155.2 (11) [M+K] ⁺
30	fQWAV β A H f-Nle-NH ₂	C ₅₇ H ₇₆ N ₁₄ O ₁₀	20-80%	12.60	1117.4 (82) [M+H] ⁺ , 1139.5 (100) [M+Na] ⁺ , 1155.2 (10) [M+K] ⁺
31	fQWAV β AHF- D -Nle-NH ₂	C ₅₇ H ₇₆ N ₁₄ O ₁₀	20-70%	14.11	1117.3 (76) [M+H] ⁺ , 1139.4 (100) [M+Na] ⁺ , 1155.2 (10) [M+K] ⁺

Table 8.4: Analytical data of peptides **32-39**.

no.	peptide	Σ	Analyt. HPLC		HPLC-MS (ESI) m/z
			grad	t_R [min]	
32	FQWAVGHF -propylamide	$C_{53}H_{69}N_{13}O_9$	20-55%	16.32	1032.3 (100) [M+H] ⁺ , 1054.4 (95) [M+Na] ⁺ , 1070.2 (8) [M+K] ⁺
33	fqWAVGHF -propylamide	$C_{53}H_{69}N_{13}O_9$	20-55%	15.34	1032.3 (100) [M+H] ⁺ , 1054.4 (91) [M+Na] ⁺ , 1070.2 (16) [M+K] ⁺
34	fQwAVGHF -propylamide	$C_{53}H_{69}N_{13}O_9$	20-55%	15.91	1032.3 (87) [M+H] ⁺ , 1054.4 (100) [M+Na] ⁺ , 1070.2 (12) [M+K] ⁺
35	fQWavGHF -propylamide	$C_{53}H_{69}N_{13}O_9$	20-55%	15.60	1032.2 (86) [M+H] ⁺ , 1054.3 (100) [M+Na] ⁺ , 1070.2 (16) [M+K] ⁺
36	fQWAVGHF -propylamide	$C_{53}H_{69}N_{13}O_9$	20-55%	15.29	1032.3 (42) [M+H] ⁺ , 1054.4 (100) [M+Na] ⁺ , 1070.2 (13) [M+K] ⁺
37	fQWAVaHF -propylamide	$C_{54}H_{71}N_{13}O_9$	20-55%	16.31	1046.3 (76) [M+H] ⁺ , 1068.4 (100) [M+Na] ⁺ , 1089 (12) [M+K] ⁺
38	fQWAVGhF -propylamide	$C_{53}H_{69}N_{13}O_9$	20-55%	14.73	1032.3 (82) [M+H] ⁺ , 1054.4 (100) [M+Na] ⁺ , 1070.2 (12) [M+K] ⁺
39	fQWAVGHf -propylamide	$C_{53}H_{69}N_{13}O_9$	20-80%	11.86	1032.3 (100) [M+H] ⁺ , 1054.4 (82) [M+Na] ⁺ , 1070.2 (8) [M+K] ⁺

Table 8.5: Analytical data of peptides **40-47**.

no.	peptide	Σ	Analyt. HPLC		HPLC-MS (ESI) m/z
			grad	t_R [min]	
40	fQWGV β AHF-Nle-NH ₂	C ₅₆ H ₇₄ N ₁₄ O ₁₀	20-70%	12.00	1103.4 (100) [M+H] ⁺ , 1125.4 (82) [M+Na] ⁺ , 1141.3 (9) [M+K] ⁺
41	fQWAVGHF-Nle-NH ₂	C ₅₆ H ₇₄ N ₁₄ O ₁₀	20-70%	12.82	1103.4 (100) [M+H] ⁺ , 1125.5 (75) [M+Na] ⁺ , 1141.3 (7) [M+K] ⁺
42	WAVGHF-Nle-NH ₂	C ₄₂ H ₅₇ N ₁₁ O ₇	20-70%	11.59	828.3 (81) [M+H] ⁺ , 850.4 (100) [M+Na] ⁺ , 866.2 (15) [M+K] ⁺
43	Ac-WAVGHF-Nle-NH ₂	C ₄₄ H ₅₉ N ₁₁ O ₈	20-65%	16.40	740.5 (10), 870.6 (100) [M+H] ⁺ , 892.6 (45) [M+Na] ⁺ , 908.5 (5) [M+K] ⁺
44	WAVAHF-Nle-NH ₂	C ₄₃ H ₅₉ N ₁₁ O ₇	20-70%	12.03	712.2 (10), 842.3 (91) [M+H] ⁺ , 864.4 (100) [M+Na] ⁺ , 880.3 (14) [M+K] ⁺
45	Ac-WAVAHF-Nle-NH ₂	C ₄₅ H ₆₁ N ₁₁ O ₈	20-80%	13.45	884.6 (100) [M+H] ⁺ , 906.7 (25) [M+Na] ⁺
46	WAV β AHF-Nle-NH ₂	C ₄₃ H ₅₉ N ₁₁ O ₇	20-70%	11.41	842.3 (80) [M+H] ⁺ , 864.4 (100) [M+Na] ⁺ , 880.3 (16) [M+K] ⁺
47	Ac-WAV β AHF-Nle-NH ₂	C ₄₅ H ₆₁ N ₁₁ O ₈	20-70%	14.87	607.3 (10), 754.4 (10), 884.5 (100) [M+H] ⁺ , 906.5 (67) [M+Na] ⁺

Table 8.6: Analytical data of peptides 48-57.

no.	peptide	Σ	Analyt. HPLC		HPLC-MS (ESI) m/z
			grad	t_R [min]	
48	WAVXHF-Nle-NH ₂	C ₄₄ H ₆₁ N ₁₁ O ₇	20-70%	11.42	856.3 (85) [M+H] ⁺ , 878.4 (100) [M+Na] ⁺ , 894 (10) [M+K] ⁺
49	Ac-WAVXHF-Nle-NH ₂	C ₄₆ H ₆₃ N ₁₁ O ₈	30-70%	9.63	624.1 (10), 768.5 (10), 881.7 (10), 898.6 (100) [M+H] ⁺ , 920.7 (62) [M+Na] ⁺ , 936.6 (10) [M+K] ⁺
50	wAVβAHF-Nle-NH ₂	C ₄₃ H ₅₉ N ₁₁ O ₇	20-70%	10.99	842.5 (42) [M+H] ⁺ , 864.6 (100) [M+Na] ⁺ , 880.5 (13) [M+K] ⁺
51	Ac-wAVβAHF-Nle-NH ₂	C ₄₅ H ₆₁ N ₁₁ O ₈	20-70%	15.35	462.0 (10), 607.3 (10), 754.5 (10), 867.5 (10), 884.5 (100) [M+H] ⁺ , 906.6 (64) [M+Na] ⁺ , 922.5 (10) [M+K] ⁺
52	WAVβAYF-Nle-NH ₂	C ₄₆ H ₆₁ N ₉ O ₈	20-70%	14.15	454.0 (12), 851.5 (10), 868.5 (100) [M+H] ⁺ , 890.6 (63) [M+Na] ⁺ , 906.5 (6) [M+K] ⁺
53	Ac-WAVβAYF-Nle-NH ₂	C ₄₈ H ₆₃ N ₉ O ₉	20-70%	18.57	475.1 (15), 633.2 (16), 893.4 (15), 932.6 (100) [M+Na] ⁺ , 948 (8) [M+K] ⁺
54	fQWAVβAYF-Nle-NH ₂	C ₆₀ H ₇₈ N ₁₂ O ₁₁	20-60%	18.14	866.6 (11), 1126.7 (10), 1143.7 (100) [M+H] ⁺ , 1165.8 (90) [M+Na] ⁺ , 1181.6 (10) [M+K] ⁺
55	fQWAVβAHF	C ₅₁ H ₆₄ N ₁₂ O ₁₀	15-70%	13.77	1005.6 (100) [M+H] ⁺ , 1027.6 (26) [M+Na] ⁺ , 1044 (10) [M+K] ⁺
56	WAVβAHF	C ₃₇ H ₄₇ N ₉ O ₇	20-70%	9.62	730.4 (100) [M+H] ⁺ , 752.5 (60) [M+Na] ⁺ , 768.5 (58) [M+K] ⁺
57	Ac-WAVβAHF	C ₃₉ H ₄₉ N ₉ O ₈	20-70%	13.09	772.5 (100) [M+H] ⁺ , 794.5 (25) [M+Na] ⁺ , 811.5 (13) [M+K] ⁺

X = γ -amino-butyric acid.

Table 8.7: Analytical data of peptides 58-67.

no.	peptide	Σ	Anal. HPLC		HPLC-MS (ESI) m/z [M+H] ⁺ (%), [M+Na] ⁺ (%), [M+K] ⁺ (%)
			grad	t _R [min]	
58	cyclo[6,14][Cys ^{6,14} ,β-Ala ¹¹ ,Phe ¹³]Bn(6-14)	C ₄₈ H ₆₄ N ₁₄ O ₁₀ S ₂	15-70%	12.52	1061.6 (100), 1083.6 (62), 1099.4 (15)
59	cyclo[6,14][D-Cys ⁶ ,β-Ala ¹¹ ,Phe ¹³ ,Cys ¹⁴]Bn(6-14)	C ₄₈ H ₆₄ N ₁₄ O ₁₀ S ₂	15-70%	12.27	1061.6 (100), 1083.6 (55), 1099.4 (10)
60	cyclo[6,14][Cys ⁶ ,β-Ala ¹¹ ,Phe ¹³ ,D-Cys ¹⁴]Bn(6-14)	C ₄₈ H ₆₄ N ₁₄ O ₁₀ S ₂	15-70%	11.47	1061.6 (100), 1083.6 (95), 1099.4 (18)
61	cyclo[6,14][D-Cys ^{6,14} ,β-Ala ¹¹ ,Phe ¹³]Bn(6-14)	C ₄₈ H ₆₄ N ₁₄ O ₁₀ S ₂	15-70%	11.77	1061.6 (100), 1083.6 (85), 1099.4 (12)
62	cyclo[7,14][D-Phe ⁶ ,Cys ^{7,14} ,β-Ala ¹¹ ,Phe ¹³]Bn(6-14)	C ₅₂ H ₆₅ N ₁₃ O ₉ S ₂	15-70%	14.40	1080.6 (100), 1102.6 (92), 1118.4 (12)
63	cyclo[7,14][D-Phe ⁶ ,D-Cys ⁷ ,β-Ala ¹¹ ,Phe ¹³ ,Cys ¹⁴]Bn(6-14)	C ₅₂ H ₆₅ N ₁₃ O ₉ S ₂	15-70%	14.39	1080.6 (100), 1102.6 (70), 1118.4 (10)
64	cyclo[7,14][D-Phe ⁶ ,Cys ⁷ ,β-Ala ¹¹ ,Phe ¹³ ,D-Cys ¹⁴]Bn(6-14)	C ₅₂ H ₆₅ N ₁₃ O ₉ S ₂	15-70%	14.93	1080.5 (92), 1102.6 (100), 1118.4 (10)
65	cyclo[7,14][D-Phe ⁶ ,D-Cys ^{7,14} ,β-Ala ¹¹ ,Phe ¹³]Bn(6-14)	C ₅₂ H ₆₅ N ₁₃ O ₉ S ₂	15-70%	16.32	1080.5 (100), 1102.6 (80), 1118.3 (10)
66	cyclo[9,14][D-Phe ⁶ ,Cys ^{9,14} ,β-Ala ¹¹ ,Phe ¹³]Bn(6-14)	C ₅₄ H ₆₈ N ₁₄ O ₁₀ S ₂	15-70%	15.55	1137.6 (100), 1159.6 (58), 1175.3 (9)
67	cyclo[9,14][D-Phe ⁶ ,D-Cys ⁹ ,β-Ala ¹¹ ,Phe ¹³ ,Cys ¹⁴]Bn(6-14)	C ₅₄ H ₆₈ N ₁₄ O ₁₀ S ₂	15-70%	13.98	1137.6 (85), 1159.6 (100), 1175.3 (15)

Table 8.8: Analytical data of peptides **68-77**.

no.	peptide	Σ	Analyt. HPLC		HPLC-MS (ESI) m/z [M+H] ⁺ (%), [M+Na] ⁺ (%), [M+K] ⁺ (%)
			grad	t_R [min]	
68	cyclo[9,14][D-Phe ⁶ ,Cys ⁹ , β -Ala ¹¹ ,Phe ¹³ ,D-Cys ¹⁴]Bn(6-14)	C ₅₄ H ₆₈ N ₁₄ O ₁₀ S ₂	15-70%	13.76	1137.6 (97), 1159.7 (100), 1175.3 (15)
69	cyclo[9,14][D-Phe ⁶ ,D-Cys ^{9,14} , β -Ala ¹¹ ,Phe ¹³]Bn(6-14)	C ₅₄ H ₆₈ N ₁₄ O ₁₀ S ₂	15-70%	17.24	1137.8 (85), 1159.8 (100), 1175.6 (15)
70	cyclo[10,14][D-Phe ⁶ ,Cys ^{10,14} , β -Ala ¹¹ ,Phe ¹³]Bn(6-14)	C ₅₂ H ₆₄ N ₁₄ O ₁₀ S ₂	15-70%	11.69	1109.6 (100), 1131.6 (95), 1147.4 (10)
71	cyclo[10,14][D-Phe ⁶ ,D-Cys ¹⁰ , β -Ala ¹¹ ,Phe ¹³ ,Cys ¹⁴]Bn(6-14)	C ₅₂ H ₆₄ N ₁₄ O ₁₀ S ₂	15-70%	11.08	1109.6 (50), 1131.6 (100), 1147.4 (12)
72	cyclo[10,14][D-Phe ⁶ ,Cys ¹⁰ , β -Ala ¹¹ ,Phe ¹³ ,D-Cys ¹⁴]Bn(6-14)	C ₅₂ H ₆₄ N ₁₄ O ₁₀ S ₂	15-70%	11.86	1109.6 (100), 1131.6 (82), 1147.4 (10)
73	cyclo[10,14][D-Phe ⁶ ,D-Cys ^{10,14} , β -Ala ¹¹ ,Phe ¹³]Bn(6-14)	C ₅₂ H ₆₄ N ₁₄ O ₁₀ S ₂	15-70%	13.71	1109.8 (78), 1131.9 (100), 1147.7 (17)
74	cyclo[6,12][Cys ^{6,12} , β -Ala ¹¹ ,Phe ¹³ ,Nle ¹⁴]Bn(6-14)	C ₄₈ H ₆₈ N ₁₂ O ₁₀ S ₂	15-70%	16.68	1037.8 (72), 1059.9 (100), 1075.7 (17)
75	cyclo[6,12][D-Cys ⁶ , β -Ala ¹¹ ,Cys ¹² ,Phe ¹³ ,Nle ¹⁴]Bn(6-14)	C ₄₈ H ₆₈ N ₁₂ O ₁₀ S ₂	15-70%	15.08	1037.8 (100), 1059.9 (52), 1075.7 (8)
76	cyclo[6,12][Cys ⁶ , β -Ala ¹¹ ,D-Cys ¹² ,Phe ¹³ ,Nle ¹⁴]Bn(6-14)	C ₄₈ H ₆₈ N ₁₂ O ₁₀ S ₂	15-70%	16.78	1037.4 (100), 1059.7 (92), 1075.3 (15)
77	cyclo[6,12][D-Cys ^{6,12} , β -Ala ¹¹ ,Phe ¹³ ,Nle ¹⁴]Bn(6-14)	C ₄₈ H ₆₈ N ₁₂ O ₁₀ S ₂	15-70%	16.11	1037.4 (100), 1059.6 (75), 1075.4 (12)

Table 8.9: Analytical data of peptides **78-85**.

no.	peptide	Σ	Analyt. HPLC		HPLC-MS (ESI) m/z [M+H] ⁺ (%), [M+Na] ⁺ (%), [M+K] ⁺ (%)
			grad	t _R [min]	
78	cyclo[7,12][D-Phe ⁶ ,Cys ^{7,12} ,β-Ala ¹¹ ,Phe ¹³ , Nle ¹⁴]Bn(6-14)	C ₅₂ H ₆₉ N ₁₁ O ₉ S ₂	15-70%	17.20	1056.6 (96), 1078.6 (100), 1094.5 (10)
79	cyclo[7,12][D-Phe ⁶ ,D-Cys ⁷ ,β-Ala ¹¹ ,Cys ¹² , Phe ¹³ ,Nle ¹⁴]Bn(6-14)	C ₅₂ H ₆₉ N ₁₁ O ₉ S ₂	15-70%	19.41	1056.6 (92), 1078.6 (100), 1094.5 (9)
80	cyclo[7,12][D-Phe ⁶ ,Cys ⁷ ,β-Ala ¹¹ ,D-Cys ¹² , Phe ¹³ ,Nle ¹⁴]Bn(6-14)	C ₅₂ H ₆₉ N ₁₁ O ₉ S ₂	15-70%	14.17	1056.5 (60), 1078.7 (100), 1094.5 (15)
81	cyclo[7,12][D-Phe ⁶ ,D-Cys ^{7,12} ,β-Ala ¹¹ , Phe ¹³ ,Nle ¹⁴]Bn(6-14)	C ₅₂ H ₆₉ N ₁₁ O ₉ S ₂	15-70%	18.84	1056.5 (100), 1078.7 (55), 1094.5 (6)
82	cyclo[9,12][D-Phe ⁶ ,Cys ^{9,12} ,β-Ala ¹¹ , Phe ¹³ ,Nle ¹⁴]Bn(6-14)	C ₅₄ H ₇₂ N ₁₂ O ₁₀ S ₂	15-70%	17.16	1113.6 (100), 1135.7 (52), 1151.5 (10)
83	cyclo[9,12][D-Phe ⁶ ,D-Cys ⁹ ,β-Ala ¹¹ ,Cys ¹² , Phe ¹³ ,Nle ¹⁴]Bn(6-14)	C ₅₄ H ₇₂ N ₁₂ O ₁₀ S ₂	15-70%	17.55	1113.7 (100), 1135.8 (62), 1151.5 (5)
84	cyclo[9,12][D-Phe ⁶ ,Cys ⁹ ,β-Ala ¹¹ ,D-Cys ¹² , Phe ¹³ ,Nle ¹⁴]Bn(6-14)	C ₅₄ H ₇₂ N ₁₂ O ₁₀ S ₂	15-70%	17.71	1113.5 (100), 1135.7 (40), 1151.5 (7)
85	cyclo[9,12][D-Phe ⁶ ,D-Cys ^{9,12} ,β-Ala ¹¹ , Phe ¹³ ,Nle ¹⁴]Bn(6-14)	C ₅₄ H ₇₂ N ₁₂ O ₁₀ S ₂	15-70%	17.97	1113.6 (100), 1135.7 (60), 1151.5 (12)

Table 8.10: Analytical data of peptides **86-94**.

no.	peptide	Σ	Analyt. HPLC		HPLC-MS (ESI) m/z	
			grad	t_R [min]	$[M+H]^+$ (%), $[M+Na]^+$ (%), $[M+K]^+$ (%)	$[M+K]^+$ (%)
86	cyclo[10,12][D-Phe ⁶ , Cys ^{10,12} , β -Ala ¹¹ , Phe ¹³ , Nle ¹⁴]Bn(6-14)	C ₅₂ H ₆₈ N ₁₂ O ₁₀ S ₂	15-70%	16.02	1085.6 (100), 1107.7 (61), 1123.4 (5)	
87	cyclo[10,12][D-Phe ⁶ , D-Cys ¹⁰ , β -Ala ¹¹ , Cys ¹² , Phe ¹³ , Nle ¹⁴]Bn(6-14)	C ₅₂ H ₆₈ N ₁₂ O ₁₀ S ₂	15-70%	16.22	1085.5 (100), 1107.6 (40), 1123.4 (5)	
88	cyclo[10,12][D-Phe ⁶ , Cys ¹⁰ , β -Ala ¹¹ , D-Cys ¹² , Phe ¹³ , Nle ¹⁴]Bn(6-14)	C ₅₂ H ₆₈ N ₁₂ O ₁₀ S ₂	15-70%	16.50	1085.5 (100), 1107.6 (35), 1123.3 (5)	
89	cyclo[10,12][D-Phe ⁶ , D-Cys ^{10,12} , β -Ala ¹¹ , Phe ¹³ , Nle ¹⁴]Bn(6-14)	C ₅₂ H ₆₈ N ₁₂ O ₁₀ S ₂	15-70%	16.11	1085.8 (100), 1107.9 (75), 1123.7 (12)	
90	cyclo[6,14][D-Cys ⁶ , Cys ¹⁴]Bn(6-14)	C ₄₄ H ₆₄ N ₁₄ O ₁₀ S ₂	15-70%	11.54	1013.8 (100), 1035.8 (83), 1051.7 (13)	
91	cyclo[6,14][D-Cys ⁶ , D-Ala ¹¹ , Cys ¹⁴]Bn(6-14)	C ₄₅ H ₆₆ N ₁₄ O ₁₀ S ₂	15-70%	12.03	1027.8 (67), 1049.9 (100), 1065.7 (15)	
92	cyclo[6,14][D-Cys ⁶ , Ala ¹¹ , Cys ¹⁴]Bn(6-14)	C ₄₅ H ₆₆ N ₁₄ O ₁₀ S ₂	15-70%	12.19	1027.8 (100), 1049.9 (85), 1065.7 (11)	
93	cyclo[6,14][D-Cys ⁶ , Ala ¹¹ , Phe ¹³ , Cys ¹⁴]Bn(6-14)	C ₄₈ H ₆₄ N ₁₄ O ₁₀ S ₂	15-70%	12.02	1061.7 (100), 1083.7 (72), 1099.5 (12)	
94	cyclo[6,14][D-Cys ⁶ , Phe ¹³ , Cys ¹⁴]Bn(6-14)	C ₄₇ H ₆₂ N ₁₄ O ₁₀ S ₂	15-70%	11.68	1047.7 (100), 1069.7 (81), 1085.6 (15)	

Table 8.11: Analytical data of peptides **95-101**.

no.	peptide	Σ	Analytical HPLC		HPLC-MS (ESI) m/z
			grad	t_R [min]	
95	fQwF-NH ₂	C ₃₄ H ₃₉ N ₇ O ₅	20-70%	13.22	276.1 (26), 351.1 (28), 462.2 (18), 626.3 (34) [M+H] ⁺ , 648.5 (100) [M+Na] ⁺ , 664.3 (16) [M+K] ⁺ , 1273.3 (14)
96	Ac-fQwF-NH ₂	C ₃₆ H ₄₁ N ₇ O ₆	5-90 %	17.99	690.5 (100) [M+Na] ⁺ , 706.3 (23) [M+K] ⁺
97	aQwF-NH ₂	C ₂₈ H ₃₅ N ₇ O ₅	5-90%	14.95	334.2 (20), 351.2 (36), 386.2 (20), 550.3 (17) [M+H] ⁺ , 572.4 (100) [M+Na] ⁺ , 588.3 (20) [M+K] ⁺
98	fAwF-NH ₂	C ₃₂ H ₃₆ N ₆ O ₄	5-90%	17.66	306.2 (10), 334.1 (15), 351.1 (20), 405.1 (15), 569.2 (22) [M+H] ⁺ , 591.3 (100) [M+Na] ⁺ , 607.2 (12) [M+K] ⁺ , 1159.0 (10)
99	fQaF-NH ₂	C ₂₆ H ₃₄ N ₆ O ₅	5-90%	12.00	276.1 (35), 347.2 (45), 511.3 (31) [M+H] ⁺ , 533.4 (100) [M+Na] ⁺ , 549.3 (16) [M+K] ⁺ , 1043.1 (17)
100	fQWA-NH ₂	C ₂₈ H ₃₅ N ₇ O ₅	10-80%	10.17	276.1 (46), 462.2 (12), 550.3 (24) [M+H] ⁺ , 572.4 (100) [M+Na] ⁺ , 588.2 (16) [M+K] ⁺ , 1121.2 (20)
101	FQwF-NH ₂	C ₃₄ H ₃₉ N ₇ O ₅	5-90%	16.35	276.1 (26), 351.1 (22), 462.2 (14), 626 (16) [M+H] ⁺ , 648.3 (100) [M+Na] ⁺ , 664.2 (15) [M+K] ⁺ , 1273.1 (10)

Table 8.12: Analytical data of peptides **102-108**.

no.	peptide	Σ	Analytical HPLC		HPLC-MS (ESI) m/z
			grad	t_R [min]	
102	fQWF-NH ₂	C ₃₄ H ₃₉ N ₇ O ₅	20-60%	13.24	276.1 (40), 351.1 (40), 462.2 (30), 626.3 (45) [M+H] ⁺ , 648.5 (100) [M+Na] ⁺ , 664.3 (15) [M+K] ⁺ , 1273.4 (20)
103	fQWf-NH ₂	C ₃₄ H ₃₉ N ₇ O ₅	20-70% ^a	10.21 ^a	276.1 (25), 351.1 (36), 462.2 (20), 626.3 (25) [M+H] ⁺ , 648.5 (100) [M+Na] ⁺ , 664.3 (10) [M+K] ⁺ , 1273.3 (10)
104	fQwf-NH ₂	C ₃₄ H ₃₉ N ₇ O ₅	20-70%	13.46	276.1 (35), 351.1 (25), 462.2 (22), 626.3 (26) [M+H] ⁺ , 648.5 (100) [M+Na] ⁺ , 664.3 (15) [M+K] ⁺ , 1273.3 (10)
105	fNwF-NH ₂	C ₃₃ H ₃₇ N ₇ O ₅	5-90%	15.96	262.0 (17), 351.1 (20), 448.1 (16), 612.2 (14) [M+H] ⁺ , 634.3 (100) [M+Na] ⁺ , 650.1 (9) [M+K] ⁺
106	f β AwF-NH ₂	C ₃₂ H ₃₆ N ₆ O ₄	5-90%	17.06	219.1 (17), 377.2 (15), 405.2 (18), 569.3 (28) [M+H] ⁺ , 591.4 (100) [M+Na] ⁺ , 607.2 (14) [M+K] ⁺ , 1159.0 (6)
107	fQwF	C ₃₄ H ₃₈ N ₆ O ₆	5-90%	16.52	276.0 (52), 352.1 (75), 462.2 (25), 627.2 (100) [M+H] ⁺ , 649.3 (53) [M+Na] ⁺ , 665.3 (45) [M+K] ⁺ , 1291.3 (20)
108	fQw- benzylamide	C ₃₂ H ₃₆ N ₆ O ₄	5-90%	16.33	276.1 (45), 294.1 (85), 569.3 (17) [M+H] ⁺ , 591.4 (100) [M+Na] ⁺ , 607.3 (8) [M+K] ⁺ , 1159.3 (10)

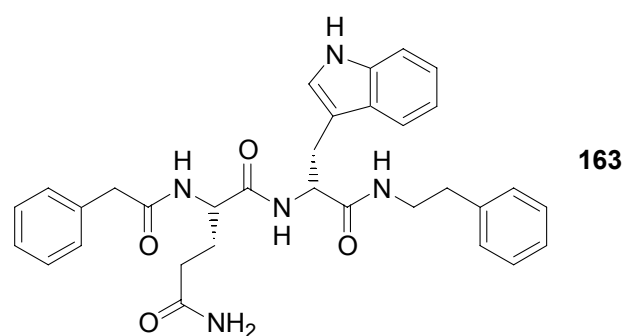
^a Detected on a HP 1100 System equipped with *Omnisrom* YMC ODS-A C₁₈ (125 mm \times 2.1 mm, 3 μ m, flow rate: 0.3 mL/min).

Table 8.13: Analytical data of peptides 109-115.

no.	peptide	Σ	Analyt. HPLC		HPLC-MS (ESI) m/z
			grad	t_R [min]	
109	fQw-1-(2-phenylethyl)amide	C ₃₃ H ₃₈ N ₆ O ₄	5-90%	17.11	276.1 (32), 308.1 (90), 583.3 (72) [M+H] ⁺ , 605.4 (100) [M+Na] ⁺ , 893.6 (13), 1165.2 (10) [2M+H] ⁺ , 1187.2 (40) [2M+Na] ⁺
110	fQw-1-[2-(3, 4-dimethoxyphenyl)ethyl]amide	C ₃₅ H ₄₂ N ₆ O ₆	5-90%	16.07	276.1 (23), 368.2 (46), 643.3 (35) [M+H] ⁺ , 665.4 (100) [M+Na] ⁺ , 1307.2 (15)
111	fQw-1-[2-(4-bromophenyl)ethyl]amide	C ₃₃ H ₃₇ BrN ₆ O ₄	5-90%	18.87	276.1 (60), 386.1 (45), 662 and 663.2 (65) [M+H] ⁺ , 682 and 683.3 (100) [M+Na] ⁺ , 700 and 701.2 (10) [M+K] ⁺ , 1345.0 (27)
112	fQw-1-[2-(2-pyridyl)ethyl]amide	C ₃₂ H ₃₇ N ₇ O ₄	5-90%	11.70	234.9 (16), 309.2 (17), 368.8 (11), 428.6 (10), 584.3 (7) [M+H] ⁺ , 606.4 (100) [M+Na] ⁺ , 622.3 (10) [M+K] ⁺
113	fQw-1-[(R)-(+)-β-methylphenylethyl]amide	C ₃₄ H ₄₀ N ₆ O ₄	5-90%	17.61	276.1 (30), 322.2 (82), 597.3 (55) [M+H] ⁺ , 619.4 (55) [M+Na] ⁺ , 635.3 (9) [M+K] ⁺ , 1215.3 (30)
114	fQw-1-[(S)-(-)-β-methylphenylethyl]amide	C ₃₄ H ₄₀ N ₆ O ₄	5-90%	17.81	276.1 (26), 322.2 (70), 597.3 (16) [M+H] ⁺ , 619.4 (100) [M+Na] ⁺ , 635.3 (7) [M+K] ⁺ , 1215.3 (12)
115	fQw-1-(2,2-diphenylethyl)amide	C ₃₉ H ₄₂ N ₆ O ₄	5-90%	19.79	384.2 (42), 659.3 (27) [M+H] ⁺ , 681.4 (100) [M+Na] ⁺ , 697 (7) [M+K] ⁺ , 1339.1 (15)

8.3.3 Peptidomimetic BRS-3 Agonists

Peptidomimetic BRS-3 agonists were synthesized in solution or on solid support. All compounds synthesized on solid support were synthesized on FMPE resin, loaded with 1-(2-phenylethyl)amine and Fmoc-D-Trp(Boc)-OH according to general method 1. Resin weights before and after loading (m_1 and m_2) and resin loading (l) are given in brackets. Yields are given with respect to the loaded resin.

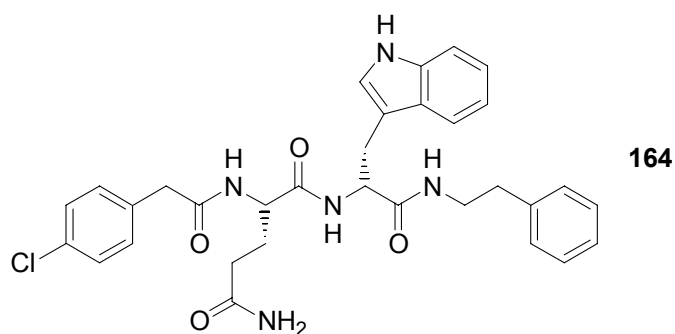


***N*1-((1*R*)-2-(1*H*-3-Indolyl)-1-[1-(2-phenylethyl)carbamoyl]ethyl)-(2*S*)-2-(benzyl-carboxamido)pentanediamide (163)**

*N*1-((1*R*)-2-(1*H*-3-Indolyl)-1-[1-(2-phenylethyl)carbamoyl]ethyl)-(2*S*)-2-(benzyl-carboxamido)pentanediamide (**163**) was synthesized on solid support ($m_1 = 100$ mg, $m_2 = 124$ mg, $l = 0.315$ mmol/g). Coupling of Fmoc-Gln(Trt)-OH (48 mg, 0.078 mmol) and phenylacetic acid (10.6 mg, 0.078 mmol), deprotection and cleavage from the resin were carried out according to general methods 3, 4, 7, and 8. HPLC purification and lyophilization yielded a colourless powder (11.1 mg, 0.020 mmol, 63%).

mp 226/227 °C; ¹H-NMR (500 MHz, DMSO-*d*₆, 300 K) $\delta = 10.77$ (s, 1H, NH-CH-C), 8.30 (d, $J = 7.1$ Hz, 1H, NH-CH-CH₂-CH₂), 8.18 (d, $J = 8.3$ Hz, 1H, NH-CH-CH₂), 7.95 (t, $J = 5.0$ Hz, 1H, NH-CH₂-CH₂), 7.55 (d, $J = 8.0$ Hz, 1H, NH-CH-C-C-CH), 7.31 (d, $J = 8.1$ Hz, 1H, NH-C-CH-CH), 7.23-7.27 (m, 6H, *o*-CH, *m*-CH), 7.16-7.19 (m, 2H, *p*-CH), 7.11 (d, $J = 7.5$ Hz, 2H, *o*-CH), 7.07 (s, 1H, NH-CH-C), 7.05 (t, $J = 7.7$ Hz, 1H, NH-C-CH-CH), 6.97 (t, $J = 7.2$ Hz, 1H, NH-CH-C-C-CH-CH), 6.72 (bs,

2H, CO-NH₂), 4.39-4.44 (m, 1H, NH-CH-CH₂), 4.15-4.21 (m, 1H, NH-CH-CH₂-CH₂), 3.47 (d, *J* = 6.0 Hz, 2H, CO-CH₂), 3.16-3.21 (m, 2H, NH-CH₂-CH₂), 3.11 (dd, *J* = 14.5 Hz, *J* = 4.9 Hz, 1H, NH-CH-CHH), 2.86 (dd, *J* = 14.7 Hz, *J* = 8.9 Hz, 1H, NH-CH-CHH), 2.57 (t, *J* = 8.0 Hz, 2H, NH-CH₂-CH₂), 1.92-2.00 (m, 1H, NH-CH-CH₂-CH₂), 1.85-1.92 (m, 1H, NH-CH-CH₂-CH₂), 1.69-1.77 (m, 1H, NH-CH-CH₂-CHH), 1.60-1.69 (m, 1H, NH-CH-CH₂-CHH); **HPLC-MS** (ESI) *m/z* 247.0 (25), 308.1 (70), 554.2 (60) [M+H]⁺, 576.4 (100) [M+Na]⁺, 850.0 (40), 1107.2 (20) [2M+H]⁺, 1129.2 (100) [2M+Na]⁺; **HRMS** (ESI-TOF) or C₃₂ H₃₅ N₅ O₄ [M+H]⁺: 554.2786 (calcd 554.2767); **Analytical HPLC** (5-90% in 30 min) *t*_R = 21.32 min (97.9% purity at 220 nm).

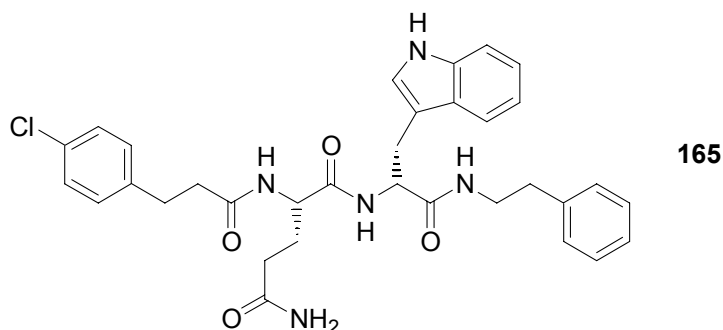


***N*1-((1*R*)-2-(1*H*-3-Indolyl)-1-[1-(2-phenylethyl)carbamoyl]ethyl)-(2*S*)-2-[(4-chlorobenzyl)carboxamido]pentanediamide (164)**

*N*1-((1*R*)-2-(1*H*-3-Indolyl)-1-[1-(2-phenylethyl)carbamoyl]ethyl)-(2*S*)-2-[(4-chlorobenzyl)carboxamido]pentanediamide (**164**) was synthesized on solid support (*m*₁ = 100 mg, *m*₂ = 128 mg, *l* = 0.357 mmol/g). Coupling of Fmoc-Gln(Trt)-OH (56 mg, 0.091 mmol) and 4-chlorophenylacetic acid (15.6 mg, 0.091 mmol), deprotection and cleavage from the resin were carried out according to general methods 3, 4, 7, and 8. HPLC purification and lyophilization yielded a colourless powder (6.3 mg, 0.011 mmol, 35%).

mp 219/220 °C; **¹H-NMR** (500 MHz, DMSO-*d*₆, 300 K) δ = 10.77 (s, 1H, NH-CH-C), 8.33 (d, *J* = 7.5 Hz, 1H, NH-CH-CH₂-CH₂), 8.19 (d, *J* = 9.0 Hz, 1H, NH-CH-CH₂), 7.94 (t, *J* = 5.0 Hz, 1H, NH-CH₂-CH₂), 7.55 (d, *J* = 7.5 Hz, 1H, NH-CH-C-C-CH), 7.29-7.32 (m, 3H, NH-C-CH-CH and Cl-C-CH), 7.23-7.26 (m, 4H, *m*-CH and Cl-C-CH-CH), 7.17 (t, *J* = 7.3 Hz, 1H, *p*-CH), 7.11 (d, *J* = 7.6 Hz, 2H, *o*-CH), 7.08 (s, 1H, NH-CH-C), 7.05 (t, *J* = 7.7 Hz, 1H, NH-C-CH-CH), 6.97 (t, *J* = 8.0 Hz, 1H, NH-CH-

C-C-CH-CH), 6.73 (bs, 2H, CO-NH₂), 4.39-4.44 (m, 1H, NH-CH-CH₂), 4.16-4.20 (m, 1H, NH-CH-CH₂-CH₂), 3.47 (d, *J* = 6.0 Hz, 2H, CO-CH₂), 3.16-3.21 (m, 2H, NH-CH₂-CH₂), 3.10 (dd, *J* = 14.3 Hz, *J* = 5.0 Hz, 1H, NH-CH-CHH), 2.86 (dd, *J* = 14.8 Hz, *J* = 8.5 Hz, 1H, NH-CH-CHH), 2.56 (t, *J* = 7.0 Hz, 2H, NH-CH₂-CH₂), 1.92-1.99 (m, 1H, NH-CH-CH₂-CH₂), 1.84-1.92 (m, 1H, NH-CH-CH₂-CH₂), 1.68-1.76 (m, 1H, NH-CH-CH₂-CHH), 1.60-1.68 (m, 1H, NH-CH-CH₂-CHH); **HPLC-MS** (ESI) *m/z* 308.1 (100), 588.2 (65) [M+H]⁺, 610.4 (35) [M+Na]⁺, 1175.1 (15) [2M+H]⁺, 1197.2 (30) [2M+Na]⁺; **HRMS** (ESI-TOF) for C₃₂H₃₄N₅O₄ Cl [M+H]⁺: 588.2382 (calcd 588.2378); **Analytical HPLC** (5-90% in 30 min) *t_R* = 22.62 min (99.7% purity at 220 nm).

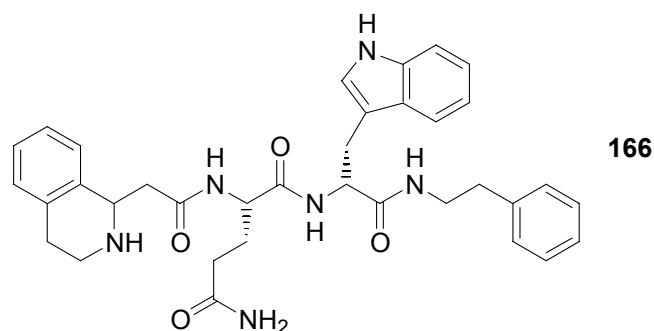


N1-{(1R)-2-(1H-3-Indolyl)-1-[1-(2-phenylethyl)carbamoyl]ethyl}-(2S)-2-[1-(2-(4-chlorophenyl)ethyl)carboxamido]pentanediamide (165)

N1-{(1R)-2-(1H-3-Indolyl)-1-[1-(2-phenylethyl)carbamoyl]ethyl}-(2S)-2-[1-(2-(4-chlorophenyl)ethyl)carboxamido]pentanediamide (**165**) was synthesized on solid support (*m*₁ = 78 mg, *m*₂ = 100 mg, *l* = 0.354 mmol/g). Coupling of Fmoc-Gln(Trt)-OH (43 mg, 0.070 mmol) and 3-(4-chlorophenyl)propionic acid (13.1 mg, 0.070 mmol), deprotection and cleavage from the resin were carried out according to general methods 3, 4, 7, and 8. HPLC purification and lyophilization yielded a colourless powder (16.8 mg, 0.028 mmol, 79%).

mp 213-215 °C; **¹H-NMR** (500 MHz, DMSO-*d*₆, 300 K) δ = 10.78 (s, 1H, NH-CH-C), 8.14 (d, *J* = 8.2 Hz, 1H, NH-CH-CH₂), 8.08 (d, *J* = 7.4 Hz, 1H, NH-CH-CH₂-CH₂), 7.99 (t, *J* = 5.8 Hz, 1H, NH-CH₂-CH₂), 7.55 (d, *J* = 8.5 Hz, 1H, NH-CH-C-C-CH), 7.28-7.32 (m, 3H, NH-C-CH-CH and Cl-C-CH), 7.26 (t, *J* = 7.4 Hz, 2H, *m*-CH), 7.21

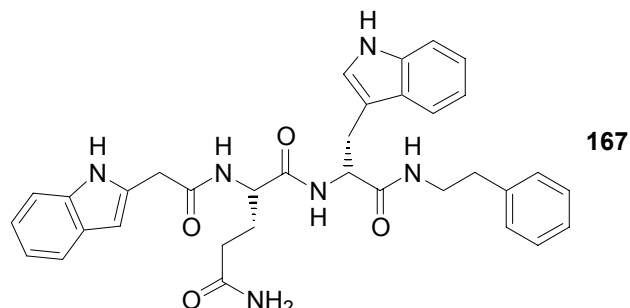
(d, $J = 8.0$ Hz, 2H, Cl-C-CH-CH), 7.18 (t, $J = 7.3$ Hz, 1H, *p*-CH), 7.15 (d, $J = 7.6$ Hz, 2H, *o*-CH), 7.08 (s, 1H, NH-CH-C), 7.05 (t, $J = 7.7$ Hz, 1H, NH-C-CH-CH), 6.97 (t, $J = 7.7$ Hz, 1H, NH-CH-C-C-CH-CH), 6.72 (bs, 2H, CO-NH₂), 4.39-4.45 (m, 1H, NH-CH-CH₂), 4.15-4.21 (m, 1H, NH-CH-CH₂-CH₂), 3.18-3.29 (m, 2H, NH-CH₂-CH₂), 3.11 (dd, $J = 14.4$ Hz, $J = 4.7$ Hz, 1H, NH-CH-CHH), 2.88 (dd, $J = 14.8$ Hz, $J = 8.8$ Hz, 1H, NH-CH-CHH), 2.79 (t, $J = 7.7$ Hz, 2H, CO-CH₂-CH₂), 2.64 (t, $J = 7.5$ Hz, 2H, NH-CH₂-CH₂), 2.34-2.46 (m, 2H, CO-CH₂-CH₂), 1.82-1.98 (m, 2H, NH-CH-CH₂-CH₂), 1.65-1.74 (m, 1H, NH-CH-CH₂-CHH), 1.55-1.65 (m, 1H, NH-CH-CH₂-CHH); **HPLC-MS** (ESI) m/z 308.1 (100), 602.2 (65) [M+H]⁺, 624.4 (30) [M+Na]⁺, 1203.2 (10) [2M+H]⁺, 1225.1 (30) [2M+Na]⁺; **HRMS** (ESI-TOF) for C₃₃H₃₆N₆O₄ [M+H]⁺: 602.2541 (calcd 602.2534); **Analytical HPLC** (5-90% in 30 min) $t_R = 22.58$ min (97.7% purity at 220 nm).



N1-[(1R)-2-(1H-3-Indolyl)-1-(phenethylcarbamoyl)ethyl]-[(2S)-2-[(1,2,3,4-tetrahydro-1-isoquinolinylmethyl)carboxamido]pentanediamide (166)

(166) was synthesized on solid support ($m_1 = 100$ mg, $m_2 = 126$ mg, $l = 0.336$ mmol/g). Coupling of Fmoc-Gln(Trt)-OH (52 mg, 0.085 mmol) and 2-{1-[1,2,3,4-tetrahydro-2-(9H-fluoren-9-ylmethoxy)carbonyl]isoquinolinyl}acetic acid (119) (35 mg, 0.085 mmol), deprotection and cleavage from the resin were carried out according to general methods 3, 4, 7, and 8. HPLC purification and lyophilization yielded a colourless powder (6.0 mg, 0.0099 mmol, 31%). According to the analytical HPLC chromatogram, the sample contained impurities. Further purification was not carried out.

HPLC-MS (ESI) m/z 308.1 (63), 609.3 (15) $[M+H]^+$, 631.3 (100) $[M+Na]^+$, 647.3 (10) $[M+K]^+$; 1239.3 (20) $[2M+Na]^+$; **HRMS** (ESI-TOF) for $C_{35}H_{40}N_6O_4$ $[M+H]^+$: 609.3179 (calcd 609.3189); **Analytical HPLC** (5-90% in 30 min) $t_R = 17.72$ min.

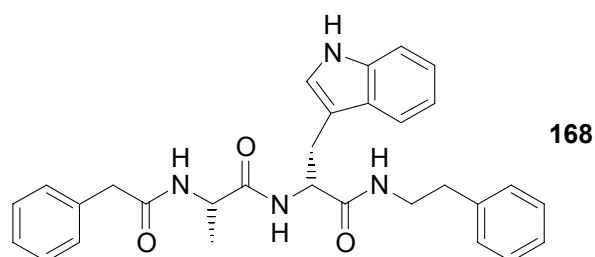


***N*1-{(1*R*)-2-(1*H*-3-Indolyl)-1-[1-(2-phenylethyl)carbamoyl]ethyl}-(2*S*)-2-[(1*H*-2-indolylmethyl)carboxamido]pentanediamide (167)**

*N*1-{(1*R*)-2-(1*H*-3-Indolyl)-1-[1-(2-phenylethyl)carbamoyl]ethyl}-(2*S*)-2-[(1*H*-2-indolylmethyl)carboxamido]pentanediamide (**167**) was synthesized on solid support ($m_1 = 78$ mg, $m_2 = 100$ mg, $l = 0.354$ mmol/g). Coupling of Fmoc-Gln(Trt)-OH (43 mg, 0.070 mmol) and (1*H*-indol-2-yl)acetic acid (**122**) (12.3 mg, 0.070 mmol), deprotection and cleavage from the resin were carried out according to general methods 3, 4, 7, and 8. HPLC purification and lyophilization yielded a colourless powder (6.6 mg, 0.011 mmol, 31%).

mp 195-201 °C; **¹H-NMR** (500 MHz, DMSO- d_6 , 300 K) $\delta = 10.86$ (s, 1H, NH-C), 10.76 (s, 1H, NH-C), 8.24 (d, $J = 7.5$ Hz, 1H, NH-CH-CH₂-CH₂), 8.21 (d, $J = 8.2$ Hz, 1H, NH-CH-CH₂), 7.96 (t, $J = 5.6$ Hz, 1H, NH-CH₂-CH₂), 7.55 (d, $J = 7.8$ Hz, 1H, NH-CH-C-C-CH), 7.39 (d, $J = 7.8$ Hz, 1H, NH-C-CH-C-CH), 7.29 (t, $J = 8.2$ Hz, 2H, C-NH-C-CH-CH and CH-NH-C-CH-CH), 7.22 (t, $J = 7.4$ Hz, 2H, *m*-CH), 7.14 (t, $J = 7.4$ Hz, 1H, *p*-CH), 7.06-7.08 (m, 3H, NH-CH-C and *o*-CH), 7.04 (t, $J = 8.0$ Hz, 1H, NH-C-CH-CH), 6.95-6.99 (m, 2H, NH-CH-C-C-CH-CH and NH-C-CH-CH), 6.90 (t, $J = 7.4$ Hz, 1H, NH-C-CH-C-CH-CH), 6.72 (bs, 2H, CO-NH₂), 6.20 (s, 1H, C-CH-C-NH), 4.41-4.45 (m, 1H, NH-CH-CH₂), 4.23-4.27 (m, 1H, NH-CH-CH₂-CH₂), 3.63 (d, $J = 3.4$ Hz, 2H, CO-CH₂-C₈H₆N), 3.13-3.24 (m, 2H, NH-CH₂-CH₂), 3.09 (dd, $J = 14.5$ Hz, $J = 5.4$ Hz, 1H, NH-CH-CHH), 2.86 (dd, $J = 14.5$ Hz, $J = 8.7$ Hz, 1H, NH-CH-

CHH), 2.56 (t, $J = 7.6$ Hz, 2H, NH-CH₂-CH₂), 1.87-2.01 (m, 2H, NH-CH-CH₂-CH₂), 1.71-1.78 (m, 1H, NH-CH-CH₂-CHH), 1.61-1.69 (m, 1H, NH-CH-CH₂-CHH); **HPLC-MS** (ESI) m/z 286.1 (20), 308.1 (25), 436.2 (20), 593.2 (100) [M+H]⁺, 908.6 (20), 1185.2 (40) [2M+H]⁺, 1207.2 (35) [2M+Na]⁺; **HRMS** (ESI-TOF) for C₃₄H₃₆N₆O₄ [M+H]⁺: 593.2888 (calcd 593.2876); **Analytical HPLC** (5-90 % in 30 min) $t_R = 21.62$ min (99.7% purity at 220 nm).

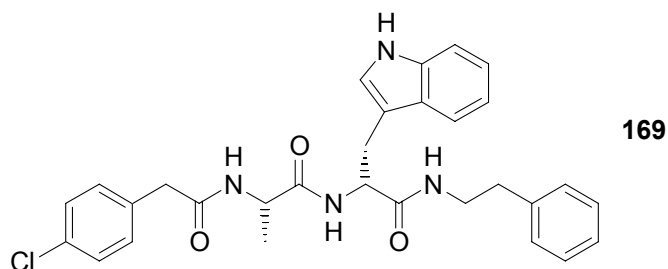


N1-(2-Phenylethyl)-(2R)-2-([(1S)-1-(benzylcarboxamido)ethyl]carboxamido)-3-(1H-3-indolyl)propanamide (168)

N1-(2-Phenylethyl)-(2R)-2-([(1S)-1-(benzylcarboxamido)ethyl]carboxamido)-3-(1H-3-indolyl)propanamide (**168**) was synthesized on solid support ($m_1 = 78$ mg, $m_2 = 100$ mg, $l = 0.354$ mmol/g). Coupling of Fmoc-Ala-OH (22 mg, 0.070 mmol) and phenylacetic acid (9.6 mg, 0.070 mmol), deprotection and cleavage from the resin were carried out according to general methods 3, 4, 7, and 8. HPLC purification and lyophilization yielded a colourless powder (12.6 mg, 0.025 mmol, 71%).

mp 205-207 °C; **¹H-NMR** (500 MHz, DMSO-*d*₆, 300 K) $\delta = 10.78$ (s, 1H, NH-CH-C), 8.24 (d, $J = 6.8$ Hz, 1H, NH-CH-CH₃), 8.18 (d, $J = 8.4$ Hz, 1H, NH-CH-CH₂), 8.00 (t, $J = 5.5$ Hz, 1H, NH-CH₂-CH₂), 7.57 (d, $J = 7.9$ Hz, 1H, NH-CH-C-C-CH), 7.31 (d, $J = 8.1$ Hz, 1H, NH-C-CH-CH), 7.23-7.27 (m, 6H, *o*-CH and *m*-CH), 7.16-7.19 (m, 2H, *p*-CH), 7.14 (d, $J = 7.5$ Hz, 2H, *o*-CH), 7.06 (s, 1H, NH-CH-C), 7.05 (t, $J = 7.7$ Hz, 1H, NH-C-CH-CH), 6.97 (t, $J = 7.3$ Hz, 1H, NH-CH-C-C-CH-CH), 4.38-4.43 (m, 1H, NH-CH-CH₂), 4.21-4.25 (m, 1H, NH-CH-CH₃), 3.45 (s, 2H, CO-CH₂), 3.19-3.24 (m, 2H, NH-CH₂-CH₂), 3.11 (dd, $J = 14.7$ Hz, $J = 4.6$ Hz, 1H, NH-CH-CHH), 2.84 (dd, $J = 14.6$ Hz, $J = 9.6$ Hz, 1H, NH-CH-CHH), 2.61 (t, $J = 7.6$ Hz, 2H, NH-CH₂-CH₂), 1.01 (d, $J = 7.0$ Hz, 3H, CH₃); **HPLC-MS** (ESI) m/z 159.1 (40), 291.2 (35), 308.1 (100), 497.2 (80) [M+H]⁺, 519.4 (55) [M+Na]⁺, 764.5 (20), 993.1 (10) [2M+H]⁺, 1015.2

(100) $[2M+Na]^+$; **HRMS** (ESI-TOF) for $C_{30}H_{32}N_4O_3$ $[M+H]^+$: 497.2566 (calcd 497.2553); **Analytical HPLC** (5-90% in 30 min) $t_R = 22.74$ min (99.9% purity at 220 nm).

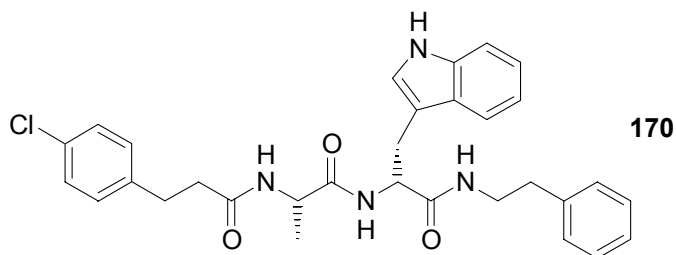


***N*1-(2-Phenylethyl)-(2*R*)-2-([(1*S*)-1-((4-chlorobenzyl)carboxamido)ethyl]carboxamido)-3-(1*H*-3-indolyl)propanamide (169)**

*N*1-(2-Phenylethyl)-(2*R*)-2-([(1*S*)-1-((4-chlorobenzyl)carboxamido)ethyl]carboxamido)-3-(1*H*-3-indolyl)propanamide (**169**) was synthesized on solid support ($m_1 = 78$ mg, $m_2 = 100$ mg, $l = 0.354$ mmol/g). Coupling of Fmoc-Ala-OH (22 mg, 0.070 mmol) and 4-chlorophenylacetic acid (12.1 mg, 0.070 mmol), deprotection and cleavage from the resin were carried out according to general methods 3, 4, 7, and 8. HPLC purification and lyophilization yielded a colourless powder (10.4 mg, 0.019 mmol, 54%).

mp 198-200 °C; **1H -NMR** (500 MHz, DMSO- d_6 , 300 K) $\delta = 10.78$ (s, 1H, NH-CH-C), 8.28 (d, $J = 6.8$ Hz, 1H, NH-CH-CH₃), 8.18 (d, $J = 8.4$ Hz, 1H, NH-CH-CH₂), 7.99 (t, $J = 5.5$ Hz, 1H, NH-CH₂-CH₂), 7.57 (d, $J = 7.9$ Hz, 1H, NH-CH-C-C-CH), 7.29-7.32 (m, 3H, NH-C-CH-CH and Cl-C-CH), 7.24-7.27 (m, 4H, *m*-CH and Cl-C-CH-CH), 7.18 (t, $J = 7.3$ Hz, 1H, *p*-CH), 7.13 (d, $J = 7.5$ Hz, 2H, *o*-CH), 7.07 (s, 1H, NH-CH-C), 7.05 (t, $J = 7.7$ Hz, 1H, NH-C-CH-CH), 6.97 (t, $J = 7.4$ Hz, 1H, NH-CH-C-C-CH-CH), 4.37-4.44 (m, 1H, NH-CH-CH₂), 4.20-4.26 (m, 1H, NH-CH-CH₃), 3.45 (s, 2H, CO-CH₂), 3.16-3.26 (m, 2H, NH-CH₂-CH₂), 3.11 (dd, $J = 14.7$ Hz, $J = 4.5$ Hz, 1H, NH-CH-CHH), 2.84 (dd, $J = 14.6$ Hz, $J = 9.6$ Hz, 1H, NH-CH-CHH), 2.60 (t, $J = 7.6$ Hz, 2H, NH-CH₂-CH₂), 1.00 (d, $J = 7.0$ Hz, 3H, CH₃); **HPLC-MS** (ESI) m/z 159.1 (30), 291.2 (25), 308.1 (65), 531.1 (100) $[M+H]^+$, 553.3 (20) $[M+Na]^+$, 816.4 (20), 1083.0 (55) $[2M+Na]^+$; **HRMS** (ESI-TOF) for $C_{30}H_{31}N_4O_3Cl$ $[M+H]^+$: 531.2139

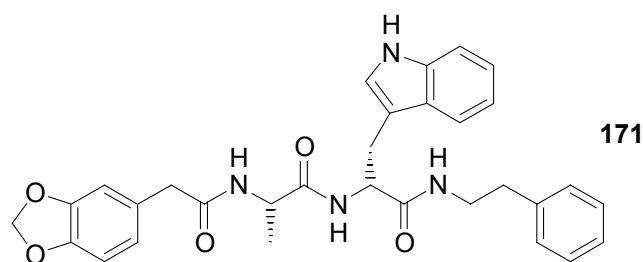
(calcd 531.2163); **Analytical HPLC** (5-90% in 30 min) $t_R = 24.15$ min (99.9% purity at 220 nm).



***N*1-(2-Phenylethyl)-(2*R*)-2-{[(1*S*)-1-(1-(2-(4-chlorophenyl)ethyl)carboxamido)ethyl]carboxamido}-3-(1*H*-3-indolyl)propanamide (170)**

*N*1-(2-Phenylethyl)-(2*R*)-2-{[(1*S*)-1-(1-(2-(4-chlorophenyl)ethyl)carboxamido)ethyl]carboxamido}-3-(1*H*-3-indolyl)propanamide (**170**) was synthesized on solid support ($m_1 = 78$ mg, $m_2 = 100$ mg, $l = 0.354$ mmol/g). Coupling of Fmoc-Ala-OH (22 mg, 0.070 mmol) and 3-(4-chlorophenyl)propionic acid (13.1 mg, 0.070 mmol), deprotection and cleavage from the resin were carried out according to general methods 3, 4, 7, and 8. HPLC purification and lyophilization yielded a colourless powder (10.2 mg, 0.019 mmol, 54%).

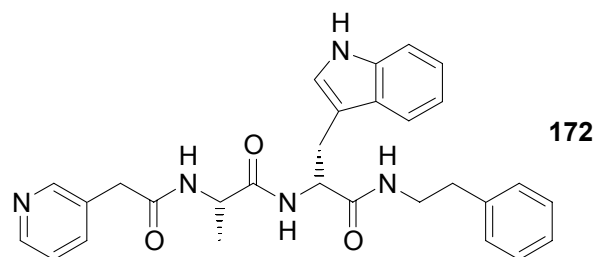
mp 214-217 °C; **¹H-NMR** (500 MHz, DMSO-*d*₆, 300K) $\delta = 10.78$ (s, 1H, NH-CH-C), 8.14 (d, $J = 8.5$ Hz, 1H, NH-CH-CH₂), 8.02-8.04 (m, 2H, NH-CH₂-CH₂ and NH-CH-CH₃), 7.57 (d, $J = 7.9$ Hz, 1H, NH-CH-C-C-CH), 7.24-7.32 (m, 5H, NH-C-CH-CH and *m*-CH and Cl-C-CH), 7.17-7.21 (m, 5H, *o*-CH and *p*-CH and Cl-C-CH-CH), 7.07 (s, 1H, NH-CH-C), 7.05 (t, $J = 7.5$ Hz, 1H, NH-C-CH-CH), 6.97 (t, $J = 7.4$ Hz, 1H, NH-CH-C-C-CH-CH), 4.39-4.43 (m, 1H, NH-CH-CH₂), 4.20-4.26 (m, 1H, NH-CH-CH₃), 3.22-3.29 (m, 2H, NH-CH₂-CH₂), 3.11 (dd, $J = 14.6$ Hz, $J = 4.5$ Hz, 1H, NH-CH-CHH), 2.86 (dd, $J = 14.6$ Hz, $J = 9.5$ Hz, 1H, NH-CH-CHH), 2.78 (t, $J = 7.7$ Hz, 2H, CO-CH₂-CH₂), 2.68 (t, $J = 7.5$ Hz, 2H, NH-CH₂-CH₂), 2.36-2.40 (m, 2H, CO-CH₂-CH₂), 0.97 (d, $J = 7.0$ Hz, 3H, CH₃); **HPLC-MS** (ESI) m/z 159.1 (40), 291.2 (30), 308.1 (100), 545.1 (95) [M+H]⁺, 567.4 (35) [M+Na]⁺, 837.3 (15), 1089.0 (30) [2M+H]⁺, 1111.0 (65) [2M+Na]⁺; **HRMS** (ESI-TOF) for C₃₁H₃₃N₄O₃Cl [M+H]⁺: 545.2327 (calcd 545.2319); **Analytical HPLC** (5-90% in 30 min) $t_R = 25.01$ min (98.0% purity at 220 nm).



***N*1-(2-Phenylethyl)-(2*R*)-2-{[(1*S*)-1-((1,3-benzodioxol-5-ylmethyl)carboxamido)ethyl]carboxamido}-3-(1*H*-3-indolyl)propanamide (171)**

*N*1-(2-Phenylethyl)-(2*R*)-2-{[(1*S*)-1-((1,3-benzodioxol-5-ylmethyl)carboxamido)ethyl]carboxamido}-3-(1*H*-3-indolyl)propanamide (**171**) was synthesized on solid support ($m_1 = 78$ mg, $m_2 = 100$ mg, $l = 0.354$ mmol/g). Coupling of Fmoc-Ala-OH (22 mg, 0.070 mmol) and 2-(1,3-benzodioxol-5-yl)acetic acid (12.8 mg, 0.070 mmol), deprotection and cleavage from the resin were carried out according to general methods 3, 4, 7, and 8. HPLC purification and lyophilization yielded a colourless powder (12.1 mg, 0.022 mmol, 62%).

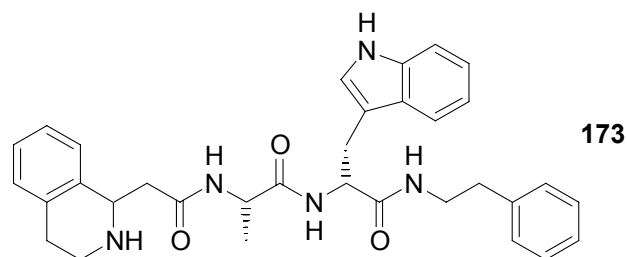
mp 211 °C; **¹H-NMR** (500 MHz, DMSO-*d*₆, 300 K) $\delta = 10.78$ (s, 1H, NH-CH-C), 8.17-8.19 (m, 2H, NH-CH-CH₂ and NH-CH-CH₃), 7.99 (t, $J = 5.5$ Hz, 1H, NH-CH₂-CH₂), 7.57 (d, $J = 7.9$ Hz, 1H, NH-CH-C-C-CH), 7.31 (d, $J = 8.1$ Hz, 1H, NH-C-CH-CH), 7.26 (t, $J = 7.5$ Hz, 2H, *m*-CH), 7.18 (t, $J = 7.3$ Hz, 1H, *p*-CH), 7.13 (d, $J = 7.5$ Hz, 2H, *o*-CH), 7.07 (s, 1H, NH-CH-C), 7.05 (t, $J = 7.7$ Hz, 1H, NH-C-CH-CH), 6.97 (t, $J = 7.4$ Hz, 1H, NH-CH-C-C-CH-CH), 6.81 (s, 1H, CO-CH₂-C-CH-C), 6.78 (d, $J = 7.9$ Hz, 1H, CO-CH₂-C-CH-CH), 6.68 (d, $J = 8.0$ Hz, 1H, CO-CH₂-C-CH-CH), 5.91 (s, 2H, O-CH₂-O), 4.38-4.43 (m, 1H, NH-CH-CH₂), 4.19-4.24 (m, 1H, NH-CH-CH₃), 3.35 (s, 2H, CO-CH₂-C₇H₅O₂), 3.18-3.27 (m, 2H, NH-CH₂-CH₂), 3.11 (dd, $J = 14.6$ Hz, $J = 4.5$ Hz, 1H, NH-CH-CHH), 2.83 (dd, $J = 14.6$ Hz, $J = 9.7$ Hz, 1H, NH-CH-CHH), 2.61 (t, $J = 7.6$ Hz, 2H, NH-CH₂-CH₂), 0.99 (d, $J = 7.0$ Hz, 3H, CH₃); **HPLC-MS** (ESI) m/z 159.1 (45), 291.1 (40), 308.1 (95), 541.2 (55) [M+H]⁺, 563.3 (60) [M+Na]⁺, 1103.1 (100) [2M+Na]⁺; **HRMS** (ESI-TOF) for C₃₁H₃₂N₄O₅ [M+H]⁺: 541.2452 (calcd 541.2451); **Analytical HPLC** (5-90% in 30 min) $t_R = 22.38$ min (99.7% purity at 220 nm).



***N*1-(2-Phenylethyl)-(2*R*)-2-[[[(1*S*)-1-((3-pyridyl)methylcarboxamido)ethyl]carboxamido]-3-(1*H*-3-indolyl)propanamide (172)**

*N*1-(2-Phenylethyl)-(2*R*)-2-[[[(1*S*)-1-((3-pyridyl)methylcarboxamido)ethyl]carboxamido]-3-(1*H*-3-indolyl)propanamide (**172**) was synthesized solid support ($m_1 = 78$ mg, $m_2 = 100$ mg, $l = 0.354$ mmol/g). Coupling of Fmoc-Ala-OH (22 mg, 0.070 mmol) and 3-pyridylacetic acid (12.3 mg, 0.070 mmol), deprotection and cleavage from the resin were carried out according to general methods 3, 4, 7, and 8. HPLC purification and lyophilization yielded a colourless powder (13.2 mg, 0.027 mmol, 76%).

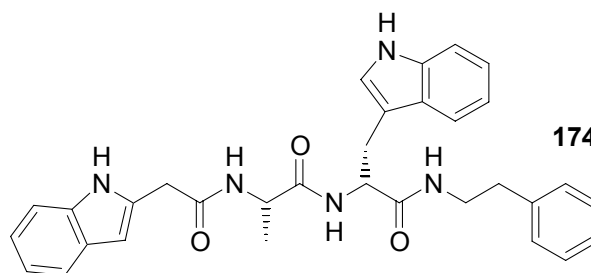
mp 95-97 °C; **¹H-NMR** (500 MHz, DMSO-*d*₆, 300 K) $\delta = 10.78$ (s, 1H, NH-CH-C), 8.57-8.59 (m, 2H, N-CH-CH and N-CH-C), 8.40 (d, $J = 7.0$ Hz, 1H, NH-CH-CH₃), 8.20 (d, $J = 8.4$ Hz, 1H, NH-CH-CH₂), 7.97-8.01 (m, 2H, NH-CH₂-CH₂ and N-CH-C-CH), 7.57 (d, $J = 7.8$ Hz, 2H, NH-CH-C-C-CH and N-CH-CH), 7.31 (d, $J = 8.1$ Hz, 1H, NH-C-CH-CH), 7.26 (t, $J = 7.5$ Hz, 2H, *m*-CH), 7.18 (t, $J = 7.2$ Hz, 1H, *p*-CH), 7.13 (d, $J = 7.5$ Hz, 2H, *o*-CH), 7.07 (s, 1H, NH-CH-C), 7.05 (t, $J = 7.7$ Hz, 1H, NH-C-CH-CH), 6.97 (t, $J = 7.4$ Hz, 1H, NH-CH-C-C-CH-CH), 4.04-4.45 (m, 1H, NH-CH-CH₂), 4.23-4.29 (m, 1H, NH-CH-CH₃), 3.61 (s, 2H, CO-CH₂-C₅H₄N), 3.18-3.28 (m, 2H, NH-CH₂-CH₂), 3.09 (dd, $J = 14.6$ Hz, $J = 4.7$ Hz, 1H, NH-CH-CHH), 2.84 (dd, $J = 14.6$ Hz, $J = 9.6$ Hz, 1H, NH-CH-CHH), 2.60 (t, $J = 7.5$ Hz, 2H, NH-CH₂-CH₂), 1.01 (d, $J = 7.1$ Hz, 3H, CH₃); **HPLC-MS** (ESI) m/z 159.1 (75), 191.0 (45), 291.1 (60), 308.1 (80), 377.1 (30), 498.2 (85) [M+H]⁺, 520.3 (40) [M+Na]⁺, 995.1 (5) [2M+H]⁺, 1017.1 (100) [2M+Na]⁺; **HRMS** (ESI-TOF) for C₂₉H₃₁N₅O₃ [M+H]⁺: 498.2495 (calcd 498.2505); **Analytical HPLC** (5-90% in 30 min) $t_R = 15.52$ min (99.7% purity at 220 nm).



***N*1-(2-Phenylethyl)-(2*R*)-2-[[[(1*S*)-1-((1,2,3,4-tetrahydro-1-isoquinolinyl)methylcarboxamido)ethyl]carboxamido]-3-(1*H*-3-indolyl)propanamide (173)**

*N*1-(2-Phenylethyl)-(2*R*)-2-[[[(1*S*)-1-((1,2,3,4-tetrahydro-1-isoquinolinyl)methylcarboxamido)ethyl]carboxamido]-3-(1*H*-3-indolyl)propanamide (173) was synthesized on solid support ($m_1 = 78$ mg, $m_2 = 100$ mg, $l = 0.354$ mmol/g). Coupling of Fmoc-Ala-OH (22 mg, 0.070 mmol) and 2-{1-[1,2,3,4-tetrahydro-2-(9*H*-fluoren-9-ylmethoxy)carbonyl]isoquinolinyl}acetic acid (119) (29 mg, 0.070 mmol), deprotection and cleavage from the resin were carried out according to general methods 3, 4, 7, and 8. HPLC purification and lyophilization yielded a colourless powder (4.7 mg, 0.0085 mmol, 24%). The compound shows cis/trans-isomerie in a ratio of 1:1.08.

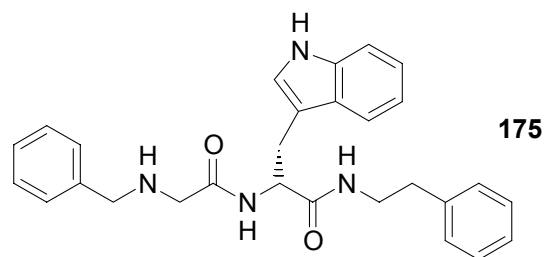
mp 110-113 °C; **¹H-NMR** (500 MHz, DMSO-*d*₆, 300 K) $\delta = 10.78$ (s, 1H, NH-CH-C), 8.80 and 9.21 (bs, 1H, CH₂-NH-CH), 8.39 and 8.45 (d, $J = 7.5$ Hz, 1H, NH-CH-CH₃), 8.21 and 8.23 (d, $J = 8.5$ Hz, 1H, NH-CH-CH₂), 8.10 (s, 1H, NH-CH₂-CH₂-C₆H₅), 7.60 (d, $J = 7.8$ Hz, 1H, C-NH-CH-C-C-CH), 7.31 (d, $J = 8.1$ Hz, 1H, NH-C-CH-CH), 7.15-7.28 (m, 9H, C₆H₅ and NH-CH-C₆H₄), 7.08 (s, 1H, C-NH-CH-C), 7.05 (t, $J = 7.6$ Hz, 1H, CH-NH-C-CH-CH), 6.97 (t, $J = 7.5$ Hz, 1H, C-NH-CH-C-C-CH-CH), 4.77-4.82 (m, 1H, NH-CH-CH₂-CO), 4.46-4.52 (m, 1H, NH-CH-CH₂-C₈H₆N), 4.33-4.44 (m, 1H, NH-CH-CH₃), 3.40-3.48 (m, 1H, CH-NH-CHH-CH₂), 3.27-3.36 (m, 2H, CH-NH-CHH-CH₂ and NH-CHH-CH₂-C₆H₅), 3.17-3.24 (m, 1H, NH-CHH-CH₂-C₆H₅), 2.81-3.08 (m, 6H, CH-NH-CH₂-CH₂ and NH-CH-CH₂-CO and NH-CH-CH₂-C₈H₆N), 2.64 (t, $J = 7.5$ Hz, 2H, NH-CH₂-CH₂-C₆H₅), 0.94 and 1.02 (d, $J = 7.0$ Hz, 3H, CH₃); **HPLC-MS** (ESI) m/z 159.1 (15), 300.1 (10), 308.2 (30), 421.2 (10), 552.3 (15) [M+H]⁺, 574.3 (100) [M+Na]⁺, 1125.2 (20) [2M+Na]⁺; **HRMS** (ESI-TOF) for C₃₃H₃₇N₅O₃ [M+H]⁺: 552.2959 (calcd 552.2975); **Analytical HPLC** (5-90% in 30 min) $t_R = 18.91$ min.



***N*1-(2-Phenylethyl)-(2*R*)-2-[[[(1*S*)-1-((1*H*-2-indolyl)methylcarboxamido)ethyl]-carboxamido]-3-(1*H*-3-indolyl)propanamide (174)**

*N*1-(2-Phenylethyl)-(2*R*)-2-[[[(1*S*)-1-((1*H*-2-indolyl)methylcarboxamido)ethyl]-carboxamido]-3-(1*H*-3-indolyl)propanamide (174) was synthesized on solid support ($m_1 = 78$ mg, $m_2 = 100$ mg, $l = 0.354$ mmol/g). Coupling of Fmoc-Ala-OH (22 mg, 0.070 mmol) and (1*H*-indol-2-yl)acetic acid (122) (12.3 mg, 0.070 mmol), deprotection and cleavage from the resin were carried out according to general methods 3, 4, 7, and 8. HPLC purification and lyophilization yielded a colourless powder (5.8 mg, 0.011 mmol, 31%).

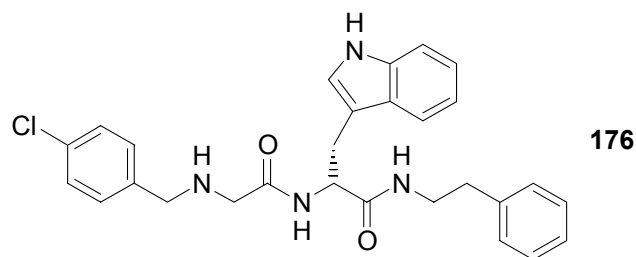
mp 188-193 °C; **$^1\text{H-NMR}$** (500 MHz, DMSO- d_6 , 300 K) $\delta = 10.86$ (s, 1H, NH-C), 10.76 (s, 1H, NH-C), 8.20 (d, $J = 8.5$ Hz, 1H, NH-CH-CH₂), 8.17 (d, $J = 7.1$ Hz, 1H, NH-CH-CH₃), 8.01 (t, $J = 5.5$ Hz, 1H, NH-CH₂-CH₂), 7.56 (d, $J = 8.1$ Hz, 1H, NH-CH-C-C-CH), 7.38 (d, $J = 7.8$ Hz, 1H, NH-C-CH-C-CH), 7.29 (t, $J = 9.1$ Hz, 2H, C-NH-C-CH-CH and CH-NH-C-CH-CH), 7.22 (t, $J = 7.4$ Hz, 2H, *m*-CH), 7.15 (t, $J = 7.4$ Hz, 1H, *p*-CH), 7.11 (d, $J = 7.6$ Hz, 2H, *o*-CH), 7.06 (s, 1H, NH-CH-C), 7.04 (t, $J = 7.6$ Hz, 1H, NH-C-CH-CH), 6.94-6.99 (m, 2H, NH-CH-C-C-CH-CH and NH-C-CH-CH), 6.90 (t, $J = 7.0$ Hz, 1H, NH-C-CH-C-CH-CH), 6.19 (s, 1H, C-CH-C-NH), 4.41-4.45 (m, 1H, NH-CH-CH₂), 4.26-4.31 (m, 1H, NH-CH-CH₃), 3.60 (d, $J = 3.5$ Hz, 2H, CO-CH₂-C₈H₆N), 3.15-3.29 (m, 2H, NH-CH₂-CH₂), 3.08 (dd, $J = 14.6$ Hz, $J = 4.8$ Hz, 1H, NH-CH-CHH), 2.84 (dd, $J = 14.4$ Hz, $J = 9.5$ Hz, 1H, NH-CH-CHH), 2.61 (t, $J = 7.6$ Hz, 2H, NH-CH₂-CH₂), 1.00 and 1.01 (s, 3H, CH₃); **HPLC-MS** (ESI) m/z 229.0 (25), 308.1 (45), 379.2 (40), 536.2 (100) [M+H]⁺, 558.4 (40) [M+Na]⁺, 823.0 (25), 1071.2 (70) [2M+H]⁺, 1093.2 (75) [2M+Na]⁺; **HRMS** (ESI-TOF) for C₃₂H₃₃N₅O₃ [M+H]⁺: 536.2661 (calcd 536.2662); **Analytical HPLC** (5-90% in 30 min) $t_R = 23.55$ min (97.7% purity at 220 nm).



***N*1-(2-Phenylethyl)-(2*R*)-2-([(benzyl)amino]methylcarboxamido)-3-(1*H*-3-indol-yl)propanamide (175)**

*N*1-(2-Phenylethyl)-(2*R*)-2-([(benzyl)amino]methylcarboxamido)-3-(1*H*-3-indol-yl)propanamide (**175**) was synthesized on solid support ($m_1 = 78$ mg, $m_2 = 100$ mg, $l = 0.354$ mmol/g). Coupling of 2-{benzyl-[(9*H*-fluoren-9-ylmethoxy)carbonyl]amino} acetic acid (**131**) (27 mg, 0.070 mmol), deprotection and cleavage from the resin were carried out according to general methods 3, 4, 7, and 8. HPLC purification and lyophilization yielded a colourless powder (9.8 mg, 0.022 mmol, 62%).

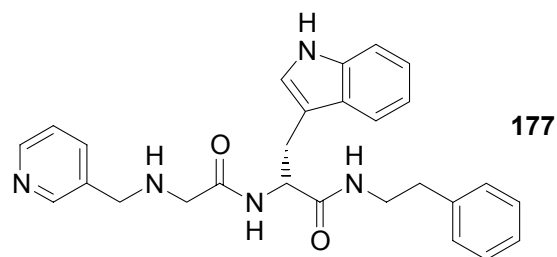
mp 107-109 °C; **¹H-NMR** (500 MHz, DMSO-*d*₆, 300 K) $\delta = 10.82$ (s, 1H, NH-CH-C), 9.11 (bs, 1H, NH-CH₂-CO), 8.69 (d, $J = 8.1$ Hz, 1H, NH-CH-CH₂), 8.24 (m, 1H, NH-CH₂-CH₂), 7.62 (d, $J = 7.9$ Hz, 1H, NH-CH-C-C-CH), 7.38-7.43 (m, 5H, C₆H₅), 7.32 (d, $J = 8.1$ Hz, 1H, NH-C-CH-CH), 7.26 (t, $J = 7.4$ Hz, 2H, *m*-CH), 7.18 (t, $J = 7.2$ Hz, 1H, *p*-CH), 7.16 (d, $J = 7.4$ Hz, 2H, *o*-CH), 7.10 (s, 1H, NH-CH-C), 7.06 (t, $J = 7.4$ Hz, 1H, NH-C-CH-CH), 6.98 (t, $J = 7.5$ Hz, 1H, NH-CH-C-C-CH-CH), 4.57 (q, $J = 5.7$ Hz, 1H, NH-CH), 4.02 (m, 2H, NH-CH₂-C₆H₅), 3.63-3.66 (m, 1H, NH-CH₂-CO), 3.53-3.56 (m, 1H, NH-CH₂-CO), 3.27-3.34 (m, 1H, NH-CH₂-CH₂), 3.20-3.26 (m, 1H, NH-CH₂-CH₂), 3.04 (dd, $J = 14.5$ Hz, $J = 5.1$ Hz, 1H, NH-CH-CHH), 2.86 (dd, $J = 14.5$ Hz, $J = 9.0$ Hz, 1H, NH-CH-CHH), 2.64 (t, $J = 7.5$ Hz, 2H, NH-CH₂-CH₂); **HPLC-MS** (ESI) m/z 159.1 (35), 291.2 (60), 308.2 (100), 455.2 (45) [M+H]⁺, 477.4 (30) [M+Na]⁺, 931.2 (60) [2M+Na]⁺; **HRMS** (ESI-TOF) for C₂₈H₃₀N₄O₂ [M+H]⁺: 455.2452 (calcd 455.2447); **Analytical HPLC** (5-90% in 30 min) $t_R = 19.00$ min (97.6% purity at 220 nm).



***N*1-(2-Phenylethyl)-(2*R*)-2-[[4-chlorobenzyl]amino]methylcarboxamido}-3-(1*H*-3-indolyl)propanamide (176)**

*N*1-(2-Phenylethyl)-(2*R*)-2-[[4-chlorobenzyl]amino]methylcarboxamido}-3-(1*H*-3-indolyl)propanamide (**176**) was synthesized on solid support ($m_1 = 78$ mg, $m_2 = 100$ mg, $l = 0.354$ mmol/g). Coupling of 2-{4-chlorobenzyl-[(9*H*-fluoren-9-ylmethoxy)carbonyl]amino}acetic acid (**132**) (29.8 mg, 0.070 mmol), deprotection and cleavage from the resin were carried out according to general methods 3, 4, 7, and 8. HPLC purification and lyophilization yielded a colourless powder (11 mg, 0.022 mmol, 62%).

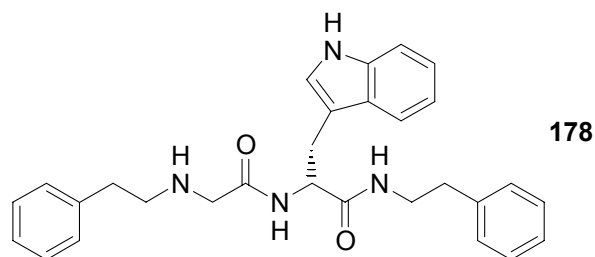
mp 138-140 °C; **¹H-NMR** (500 MHz, DMSO-*d*₆, 300 K) $\delta = 10.82$ (s, 1H, NH-CH-C), 9.13 (bs, 1H, NH-CH₂-CO), 8.68 (d, $J = 8.2$ Hz, 1H, NH-CH-CH₂), 8.25 (m, 1H, NH-CH₂-CH₂), 7.61 (d, $J = 7.9$ Hz, 1H, NH-CH-C-C-CH), 7.49 (d, $J = 8.2$ Hz, 2H, Cl-C-CH), 7.41 (d, $J = 8.1$ Hz, 2H, Cl-C-CH-CH), 7.32 (d, $J = 8.1$ Hz, 1H, NH-C-CH-CH), 7.26 (t, $J = 7.4$ Hz, 2H, *m*-CH), 7.18 (t, $J = 7.3$ Hz, 1H, *p*-CH), 7.16 (d, $J = 7.5$ Hz, 2H, *o*-CH), 7.10 (s, 1H, NH-CH-C), 7.06 (t, $J = 7.3$ Hz, 1H, NH-C-CH-CH), 6.97 (t, $J = 7.5$ Hz, 1H, NH-CH-C-C-CH-CH), 4.57 (q, $J = 5.8$ Hz, 1H, NH-CH), 4.03 (m, 2H, NH-CH₂-C₆H₄Cl), 3.62-3.67 (m, 1H, NH-CH₂-CO), 3.51-3.56 (m, 1H, NH-CH₂-CO), 3.26-3.34 (m, 1H, NH-CH₂-CH₂), 3.19-3.26 (m, 1H, NH-CH₂-CH₂), 3.04 (dd, $J = 14.5$ Hz, $J = 5.1$ Hz, 1H, NH-CH-CHH), 2.86 (dd, $J = 14.5$ Hz, $J = 9.0$ Hz, 1H, NH-CH-CHH), 2.64 (t, $J = 7.5$ Hz, 2H, NH-CH₂-CH₂); **HPLC-MS** (ESI) m/z 159.1 (30), 291.2 (50), 308.1 (100), 489.2 (60) [M+H]⁺, 511.4 (10) [M+Na]⁺, 999.1 (30) [2M+Na]⁺; **HRMS** (ESI-TOF) for C₂₈H₂₉N₄O₂Cl [M+H]⁺: 489.2055 (calcd 489.2057); **Analytical HPLC** (5-90% in 30 min) $t_R = 20.15$ min (99.5% purity at 220 nm).



***N*1-(2-Phenylethyl)-(2*R*)-2-[(3-pyridyl)methylamino]methylcarboxamido}-3-(1*H*-3-indolyl)propanamide (177)**

*N*1-(2-Phenylethyl)-(2*R*)-2-[(3-pyridyl)methylamino]methylcarboxamido}-3-(1*H*-3-indolyl)propanamide (**177**) was synthesized on solid support ($m_1 = 78$ mg, $m_2 = 100$ mg, $l = 0.354$ mmol/g). Coupling the TFA-salt of 2-{pyridine-3-ylmethyl-[(9*H*-fluorene-9-ylmethoxy)carbonyl]amino}acetic acid (**133**) (35.4 mg, 0.070 mmol), deprotection and cleavage from the resin were carried out according to general methods 3, 4, 7, and 8. HPLC purification and lyophilization yielded a colourless powder (6.6 mg, 0.014 mmol, 40%).

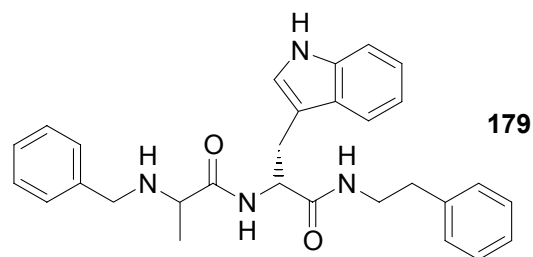
mp 89-93 °C; **¹H-NMR** (500 MHz, DMSO-*d*₆, 300 K) $\delta = 10.82$ (s, 1H, NH-CH-C), 9.20 (bs, 1H, NH-CH₂-CO), 8.71 (d, $J = 8.0$ Hz, 1H, NH-CH-CH₂), 8.59-8.62 (m, 2H, N-CH-C and N-CH-CH), 8.26 (t, $J = 5.5$ Hz, 1H, NH-CH₂-CH₂), 7.83 (d, $J = 8.0$ Hz, 1H, N-CH-C-CH), 7.62 (d, $J = 8.0$ Hz, 1H, NH-CH-C-C-CH), 7.46 (dd, $J = 7.9$ Hz, $J = 4.7$ Hz, 1H, N-CH-CH), 7.32 (d, $J = 8.0$ Hz, 1H, NH-C-CH-CH), 7.26 (d, $J = 7.4$ Hz, 2H, *m*-CH), 7.18 (t, $J = 7.2$ Hz, 1H, *p*-CH), 7.16 (d, $J = 7.5$ Hz, 2H, *o*-CH), 7.11 (s, 1H, NH-CH-C), 7.06 (t, $J = 7.0$ Hz, 1H, NH-C-CH-CH), 6.98 (t, $J = 7.0$ Hz, 1H, NH-CH-C-C-CH-CH), 4.57 (q, $J = 6.0$ Hz, 1H, NH-CH), 4.09 (m, 2H, NH-CH₂-C₅H₄N), 3.69-3.75 (m, 1H, NH-CHH-CO), 3.57-3.64 (m, 1H, NH-CHH-CO), 3.27-3.35 (m, 1H, NH-CHH-CH₂), 3.19-3.27 (m, 1H, NH-CHH-CH₂), 3.05 (dd, $J = 14.9$ Hz, $J = 5.2$ Hz, 1H, NH-CH-CHH), 2.87 (dd, $J = 14.6$ Hz, $J = 8.8$ Hz, 1H, NH-CH-CHH), 2.64 (t, $J = 7.1$ Hz, 2H, NH-CH₂-CH₂); **HPLC-MS** (ESI) m/z 159.1 (15), 291.2 (35), 308.2 (40), 456.2 (100) [M+H]⁺, 478.4 (10) [M+Na]⁺, 703.1 (20), 911.0 (15) [2M+H]⁺, 933.1 (40) [2M+Na]⁺; **HRMS** (ESI-TOF) for C₂₇H₂₉N₅O₂ [M+H]⁺: 456.2387 (calcd 456.2400); **Analytical HPLC** (5-90% in 30 min) $t_R = 15.58$ min (99.6% purity at 220 nm).



***N*1-(2-Phenylethyl)-(2*R*)-2-[[1-(2-phenylethyl)amino]methylcarboxamido]-3-(1*H*-3-indolyl)propanamide (178)**

*N*1-(2-Phenylethyl)-(2*R*)-2-[[1-(2-phenylethyl)amino]methylcarboxamido]-3-(1*H*-3-indolyl)propanamide (**178**) was synthesized on solid support ($m_1 = 78$ mg, $m_2 = 100$ mg, $l = 0.354$ mmol/g). Coupling of 2-[[1-(2-phenylethyl)-[(9*H*-fluoren-9-yl-methoxy)carbonyl]amino]acetic acid (**134**) (28.3 mg, 0.070 mmol), deprotection and cleavage from the resin were carried out according to general methods 3, 4, 7, and 8. HPLC purification and lyophilization yielded a colourless powder (2.7 mg, 0.0058 mmol, 16%).

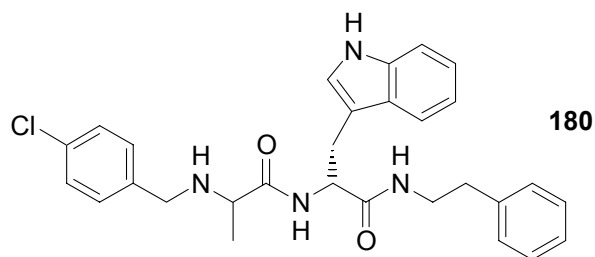
mp 197-199 °C; **¹H-NMR** (500 MHz, DMSO-*d*₆, 300 K) $\delta = 10.82$ (s, 1H, NH-CH-C), 8.79 (bs, 1H, NH-CH₂-CO), 8.74 (d, $J = 8.5$ Hz, 1H, NH-CH-CH₂), 8.26 (t, $J = 5.5$ Hz, 1H, NH-CH₂-CH₂), 7.62 (d, $J = 8.0$ Hz, 1H, NH-CH-C-C-CH), 7.31-7.34 (m, 3H, NH-C-CH-CH and *m*-CH), 7.25-7.28 (m, 3H, *p*-CH and *m*-CH), 7.19-7.21 (m, 3H, *p*-CH and *o*-CH), 7.16 (d, $J = 7.6$ Hz, 2H, *o*-CH), 7.12 (s, 1H, NH-CH-C), 7.05 (t, $J = 7.5$ Hz, 1H, NH-C-CH-CH), 6.98 (t, $J = 7.5$ Hz, 1H, NH-CH-C-C-CH-CH), 4.58 (q, $J = 5.5$ Hz, 1H, NH-CH), 3.73-3.79 (m, 1H, NH-CHH-CO), 3.62-3.67 (m, 1H, NH-CHH-CO), 3.29-3.34 (m, 1H, NH-CHH-CH₂), 3.20-3.25 (m, 1H, NH-CHH-CH₂), 3.04-3.08 (m, 3H, NH-CH-CHH and CH₂-NH-CH₂-CH₂), 2.84-2.92 (m, 3H, NH-CH-CHH and CH₂-NH-CH₂-CH₂), 2.64 (t, $J = 7.4$ Hz, 2H, NH-CH₂-CH₂); **HPLC-MS** (ESI) m/z 159.1 (20), 291.1 (40), 308.1 (90), 469.2 (100) [M+H]⁺, 491.3 (25) [M+Na]⁺, 507.2 (15) [M+K]⁺, 722.6 (10), 959.1 (50) [2M+Na]⁺; **HRMS** (ESI-TOF) for C₂₉H₃₂N₄O₂ [M+H]⁺: 469.2604 (calcd 469.2604); **Analytical HPLC** (5-90% in 30 min) $t_R = 19.50$ min (97.9% purity at 220 nm).



***N*1-(2-Phenylethyl)-(2*R*)-2-[[1-(benzylamino)ethyl]carboxamido]-3-(1*H*-3-indolyl)propanamide (179)**

*N*1-(2-Phenylethyl)-(2*R*)-2-[[1-(benzylamino)ethyl]carboxamido]-3-(1*H*-3-indolyl)propanamide (**179**) was prepared from *tert*-butyl-3-{(2*R*)-2-amino-2-[1-(2-phenylethyl)carbamoyl]ethyl}-1*H*-1-indolecarboxylate (**139**) (0.30 g, 0.736 mmol) and 2-{benzyl-[(9*H*-fluoren-9-ylmethoxy)carbonyl]amino}propanoic acid (**135**) (0.295 g, 0.735 mmol) according to general method 19 in a reaction time of 1 hr. The residue was chromatographed (ethyl acetate/ hexane, 1:1) and then fully deprotected according to the general methods 21 and, subsequently without intermediate purification, 20. The product was finally chromatographed (ethyl acetate), lyophilization yielded a colourless powder (0.25 g, 0.534 mmol, 73%). The ratio of the two isomers was determined from the NMR-integrals of the CH₃ group as 1:1.52.

mp 100-105 °C; **TLC** *R_f* (ethyl acetate) = 0.34; **¹H-NMR** (500 MHz, DMSO-*d*₆, 300 K) δ = 10.83 and 10.85 (s, 1H, NH-CH-C), 9.1 (m, 1H, NH-CH-CH₃), 8.74-8.78 (m, 1H, NH-CH-CH₂), 8.27 and 8.34 (t, *J* = 5.6 Hz, 1H, NH-CH₂-CH₂), 7.63 and 7.68 (d, *J* = 7.8 Hz, 1H, NH-CH-C-C-CH), 7.17-7.21 and 7.24-7.33 and 7.33-7.37 and 7.40-7.43 (m, 11H, C₆H₅ and C₆H₅ and N-C-CH-CH), 7.09 and 7.14 (s, 1H, NH-CH-C), 6.96-7.07 (m, 2H, NH-C-CH-CH and NH-CH-C-C-CH-CH), 4.62-4.68 (m, 1H, NH-CH-CH₂), 3.98-4.01 (m, 1H, NH-CHH-C₆H₅), 3.76-3.78 (m, 1H, NH-CH-CH₃), 3.61-3.67 and 3.41-3.43 (m, 1H, NH-CHH-C₆H₅), 3.34-3.39 (m, 1H, NH-CHH-CH₂), 3.26-3.30 (m, 1H, NH-CHH-CH₂), 3.05-3.09 (m, 1H, NH-CH-CHH), 2.84-2.93 (m, 1H, NH-CH-CHH), 2.67-2.72 (m, 2H, NH-CH₂-CH₂), 1.11 and 1.34 (d, *J* = 6.9 Hz, 3H, CH₃); **HPLC-MS** (ESI) *m/z* 291.2 (30), 308.1 (100), 469.2 (95) [M+H]⁺, 491.4 (10) [M+Na]⁺, 937.2 (15) [2M+H]⁺, 959.2 (55) [2M+Na]⁺; **HRMS** (ESI-TOF) for C₂₉H₃₂N₄O₂ [M+H]⁺: 469.2595 (calcd 469.2604); **Analytical HPLC** (5-90% in 30 min) *t_R* = 19.05 and 19.34 (98.7% purity at 220 nm).

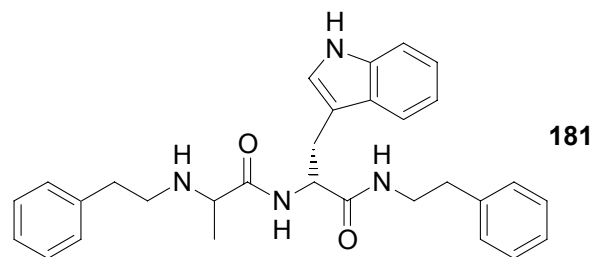


***N*1-(2-Phenylethyl)-(2*R*)-2-[[1-((4-chlorobenzyl)amino)ethyl]carboxamido]-3-(1*H*-3-indolyl)propanamide (180)**

*N*1-(2-Phenylethyl)-(2*R*)-2-[[1-((4-chlorobenzyl)amino)ethyl]carboxamido]-3-(1*H*-3-indolyl)propanamide (**180**) was prepared from *tert*-butyl-3-{(2*R*)-2-amino-2-[1-(2-phenylethyl)carbamoyl]ethyl}-1*H*-1-indolecarboxylate (**139**) (0.30 g, 0.736 mmol) and 2-{4-chlorobenzyl-[(9*H*-fluoren-9-ylmethoxy)carbonyl]amino}propanoic acid (**136**) (0.32 g, 0.734 mmol) according to general method 19 in a reaction time of 1 hr. The residue was chromatographed (ethyl acetate/ hexane, 1:1) and then fully deprotected according to the general methods 21 and, subsequently without intermediate purification, 20. The product was finally chromatographed (ethyl acetate), lyophilization yielded a colourless powder (320 mg, 0.637 mmol, 87%). The ratio of the two isomers was determined from the NMR-integrals of the CH₃ group as 1:1.24.

mp 107-110 °C; **TLC** *R_f* (ethyl acetate) = 0.24; **¹H-NMR** (500 MHz, DMSO-*d*₆, 300 K) δ = 10.85 and 10.83 (s, 1H, NH-CH-C), 9.2 (m, 1H, NH-CH-CH₃), 8.72 and 8.77 (d, *J* = 8.5 Hz, 1H, NH-CH-CH₂), 8.28 and 8.34 (t, *J* = 5.5 Hz, 1H, NH-CH₂-CH₂), 7.68 and 7.63 (d, *J* = 7.7 Hz, 1H, NH-CH-C-C-CH), 7.17-7.20 and 7.24-7.33 and 7.40-7.50 (m, 10H, C₆H₅ and C₆H₄Cl and NH-C-CH-CH), 7.09 and 7.15 (s, 1H, NH-CH-C), 6.96-7.07 (m, 2H, NH-C-CH-CH and NH-CH-C-C-CH-CH), 4.61-4.69 (m, 1H, NH-CH-CH₂), 3.98-4.02 (m, 1H, NH-CHH-C₆H₄Cl), 3.75 (m, 1H, NH-CH-CH₃), 3.60-3.67 and 3.39-3.43 (m, 1H, NH-CHH-C₆H₄Cl), 3.34-3.38 (m, 1H, NH-CHH-CH₂), 3.24-3.29 (m, 1H, NH-CHH-CH₂), 3.05-3.08 (m, 1H, NH-CH-CHH), 2.85-2.92 (m, 1H, NH-CH-CHH), 2.67-2.71 (m, 2H, NH-CH₂-CH₂), 1.33 and 1.10 (d, *J* = 6.9 Hz, 3H, CH₃); **HPLC-MS** (ESI) *m/z* 291.2 (30), 308.1 (100), 503.2 (35) [M+H]⁺, 525.4 (15) [M+Na]⁺, 1027.1 (20) [2M+Na]⁺; **HRMS** (ESI-TOF) for C₂₉H₃₁N₄O₂Cl [M+H]⁺:

503.2218 (calcd 503.2214); **Analytical HPLC** (5-90% in 30 min) $t_R = 20.16$ min and 20.52 min (99.6% purity at 220 nm).

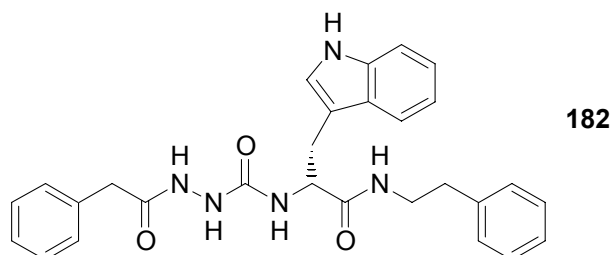


***N*1-(2-Phenylethyl)-(2*R*)-2-{[1-(1-(2-phenylethyl)amino)ethyl]carboxamido}-3-(1*H*-3-indolyl)propanamide (181)**

*N*1-(2-Phenylethyl)-(2*R*)-2-{[1-(1-(2-phenylethyl)amino)ethyl]carboxamido}-3-(1*H*-3-indolyl)propanamide (**181**) was prepared from *tert*-butyl-3-{(2*R*)-2-amino-2-[1-(2-phenylethyl)carbamoyl]ethyl}-1*H*-1-indolecarboxylate (**139**) (0.30 g, 0.737 mmol) and 2-{1-(2-phenylethyl)-[(9*H*-fluoren-9-ylmethoxy)carbonyl]amino}propanoic acid (**137**) (0.305 g, 0.737 mmol) according to general method 19 in a reaction time of 1 hr. The residue was chromatographed (ethyl acetate/ hexane, 1:1) and then fully deprotected according to the general methods 21 and subsequently without intermediate purification, 20. The product was finally chromatographed (ethyl acetate), lyophilization yielded a colourless powder (230 mg, 0.477 mmol, 65%). The ratio of the two isomers was determined from the NMR-integrals of the CH₃ group as 1:1.59.

mp 89-91 °C; **TLC** R_f (ethyl acetate) = 0.15; **¹H-NMR** (500 MHz, DMSO-*d*₆, 300 K) $\delta = 10.83$ and 10.79 (s, 1H, NH-CH-C), 8.88 (m, 1H, NH-CH-CH₃), 8.77 (m, 1H, NH-CH-CH₂), 8.24 and 8.32 (t, $J = 5.4$ Hz, 1H, NH-CH₂-CH₂), 7.63 (d, $J = 7.8$ Hz, 1H, NH-CH-C-C-CH), 7.15 - 7.18 and 7.21 - 7.28 and 7.29 - 7.33 (m, 11H, NH-C-CH-CH and C₆H₅ and C₆H₅), 7.04 - 7.12 (m, 2H, NH-C-CH-CH and NH-CH-C), 6.94 - 7.00 (m, 1H, NH-CH-C-C-CH-CH), 4.59 - 4.64 (m, 1H, NH-CH), 3.82 - 3.86 (m, 1H, CH-CH₃), 3.29 - 3.35 (m, 1H, NH-CHH-CH₂), 3.22 - 3.30 (m, 1H, NH-CHH-CH₂), 2.75 - 3.09 (m, 6H, NH-CH-CH₂ and CH-NH-CH₂-CH₂), 2.66 (t, $J = 7.2$ Hz, 2H, NH-CH₂-CH₂), 1.35 and 1.12 (d, $J = 6.9$ Hz, 3H, CH₃); **HPLC-MS** (ESI) m/z 291.2 (30), 308.1 (100), 362.1 (35), 483.3 (95) [M+H]⁺, 505.4 (30) [M+Na]⁺, 987.2 (50) [2M+Na]⁺; **HRMS** (ESI-

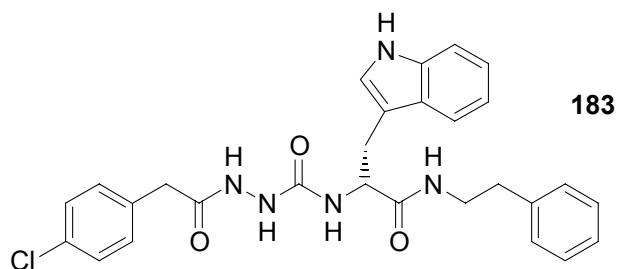
TOF) for $C_{30}H_{34}N_4O_2$ $[M+H]^+$: 483.2759 (calcd 483.2760); **Analytical HPLC** (5-90% in 30 min) $t_R = 19.76$ min and 20.05 min (96.1% purity at 220 nm).



***N*1-(2-Phenylethyl)-(2*R*)-2-{[*N*'-(benzoyl)hydrazino]carboxamido}-3-(1*H*-3-indolyl)propanamide (182)**

*N*1-(2-Phenylethyl)-(2*R*)-2-{[*N*'-(benzoyl)hydrazino]carboxamido}-3-(1*H*-3-indolyl)propanamide (**182**) was synthesized on solid support ($m_1 = 78$ mg, $m_2 = 100$ mg, $l = 0.354$ mmol/g). Coupling of 5-(9*H*-fluoren-9-ylmethoxy)-1,3,4-oxadiazol-2(3*H*)-one (**141**) (30.5 mg, 0.108 mmol) was carried out according to general method 11, coupling of phenylacetic acid (9.5 mg, 0.070 mmol), deprotection and cleavage from the resin were carried out according to general methods 3, 4, 7, and 8. HPLC purification and lyophilization yielded a colourless powder (2.6 mg, 0.0054 mmol, 15%).

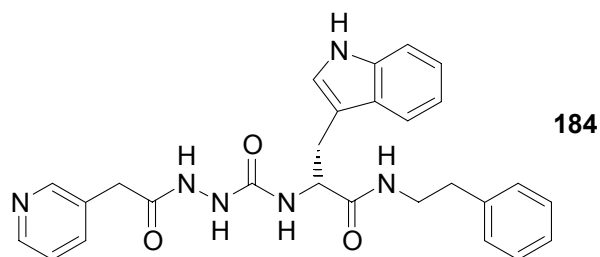
mp 109-114 °C; **1H -NMR** (500 MHz, DMSO- d_6 , 300 K) $\delta = 10.79$ (s, 1H, NH-CH-C), 9.80 (s, 1H, NH-NH), 7.95-8.00 (m, 2H, NH-CH₂-CH₂ and NH-NH), 7.51 (d, $J = 7.9$ Hz, 1H, NH-CH-C-C-CH), 7.30 (d, $J = 8.2$ Hz, 1H, NH-C-CH-CH), 7.23-7.28 (m, 6H, *o*-CH, *m*-CH), 7.19-7.22 (m, 1H, *p*-CH), 7.16 (t, $J = 7.1$ Hz, 1H, *p*-CH), 7.13 (d, $J = 7.5$ Hz, 2H, *o*-CH), 7.02-7.04 (m, 2H, NH-CH-C and NH-C-CH-CH), 6.95 (t, $J = 7.5$ Hz, 1H, NH-CH-C-C-CH-CH), 6.36 (d, $J = 8.0$ Hz, 1H, NH-CH-CH₂), 4.36 (q, $J = 6.6$ Hz, 1H, NH-CH), 3.41 (s, 2H, CO-CH₂), 3.14-3.29 (m, 2H, NH-CH₂-CH₂), 3.01 (dd, $J = 14.6$ Hz, $J = 5.7$ Hz, 1H, NH-CH-CHH), 2.91 (dd, $J = 14.5$ Hz, $J = 7.5$ Hz, 1H, NH-CH-CHH), 2.58 (t, $J = 7.1$ Hz, 2H, NH-CH₂-CH₂); **HPLC-MS** (ESI) m/z 334.3 (25), 484.3 (90) $[M+H]^+$, 506.4 (20) $[M+Na]^+$, 745.2 (20), 967.4 (100) $[2M+H]^+$, 989.4 (40) $[2M+Na]^+$; **HRMS** (ESI-TOF) for $C_{28}H_{29}N_5O_3$ $[M+H]^+$: 484.2347 (calcd 484.2349); **Analytical HPLC** (5-90% in 30 min) $t_R = 21.07$ min (98.6% purity at 220 nm).



***N*1-(2-Phenylethyl)-(2*R*)-2-{[*N*'-(4-chlorobenzoyl)hydrazino]carboxamido}-3-(1*H*-3-indolyl)propanamide (183)**

*N*1-(2-Phenylethyl)-(2*R*)-2-{[*N*'-(4-chlorobenzoyl)hydrazino]carboxamido}-3-(1*H*-3-indolyl)propanamide (**183**) was synthesized on solid support ($m_1 = 78$ mg, $m_2 = 100$ mg, $l = 0.354$ mmol/g). Coupling of 5-(9*H*-fluoren-9-ylmethoxy)-1,3,4-oxadiazol-2(3*H*)-one (**141**) (30.5 mg, 0.108 mmol) was carried out according to general method 11, coupling of 4-chlorophenylacetic acid (12 mg, 0.070 mmol), deprotection and cleavage from the resin were carried out according to general methods 3, 4, 7, and 8. HPLC purification and lyophilization yielded a colourless powder (3.0 mg, 0.0058 mmol, 16%).

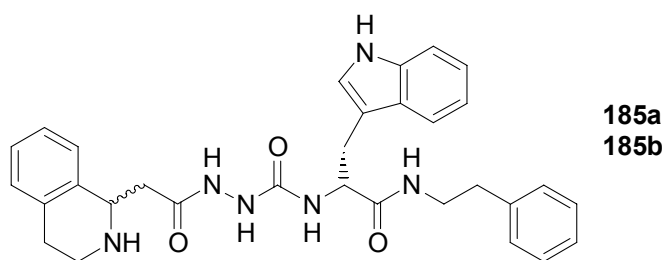
mp 195/196 °C; **¹H-NMR** (500 MHz, DMSO-*d*₆, 300 K) $\delta = 10.79$ (s, 1H, NH-CH-C), 9.81 (s, 1H, NH-NH), 8.00 (s, 1H, NH-NH), 7.94 (bs, 1H, NH-CH₂-CH₂), 7.51 (d, $J = 7.9$ Hz, 1H, NH-CH-C-C-CH), 7.23-7.34 (m, 7H, *m*-CH and C₆H₄Cl and NH-C-CH-CH), 7.17 (t, $J = 7.3$ Hz, 1H, *p*-CH), 7.13 (d, $J = 7.5$ Hz, 2H, *o*-CH), 7.02-7.05 (m, 2H, NH-CH-C and NH-C-CH-CH), 6.95 (t, $J = 7.5$ Hz, 1H, NH-CH-C-C-CH-CH), 6.38 (d, $J = 8.1$ Hz, 1H, NH-CH), 4.36 (q, $J = 6.7$ Hz, 1H, NH-CH), 3.42 (s, 2H, CO-CH₂), 3.16-3.24 (m, 2H, NH-CH₂-CH₂), 3.01 (dd, $J = 14.9$ Hz, $J = 5.6$ Hz, 1H, NH-CH-CHH), 2.91 (dd, $J = 14.5$ Hz, $J = 7.5$ Hz, 1H, NH-CH-CHH), 2.58 (t, $J = 7.5$ Hz, 2H, NH-CH₂-CH₂); **HPLC-MS** (ESI) m/z 334.2 (40), 518.2 (100) [M+H]⁺, 540.2 (30) [M+Na]⁺, 1035.3 (65) [2M+H]⁺; **HRMS** (ESI-TOF) for C₂₈H₂₈N₅O₃Cl [M+H]⁺: 518.1951 (calcd 518.1959); **Analytical HPLC** (5-90% in 30 min) $t_R = 22.50$ min (99.5% purity at 220 nm).



***N*1-(2-Phenylethyl)-(2*R*)-2-{[*N*'-(2-(3-pyridyl)ethanoyl)hydrazino]carboxamido}-3-(1*H*-3-indolyl)propanamide (184)**

*N*1-(2-Phenylethyl)-(2*R*)-2-{[*N*'-(2-(3-pyridyl)ethanoyl)hydrazino]carboxamido}-3-(1*H*-3-indolyl)propanamide (**184**) was synthesized on solid support ($m_1 = 78$ mg, $m_2 = 100$ mg, $l = 0.354$ mmol/g). Coupling of 5-(9*H*-fluoren-9-ylmethoxy)-1,3,4-oxadiazol-2(3*H*)-one (**141**) (30.5 mg, 0.108 mmol) was carried out according to general method 11, coupling of 3-pyridylacetic acid (12 mg, 0.070 mmol), deprotection and cleavage from the resin were carried out according to general methods 3, 4, 7, and 8. HPLC purification and lyophilization yielded a colourless powder (4.5 mg, 0.0093 mmol, 26%).

mp 116-120 °C; **¹H-NMR** (500 MHz, DMSO-*d*₆, 300 K) $\delta = 10.79$ (s, 1H, NH-CH-C), 9.89 (s, 1H, NH-NH), 8.63 (s, 1H, N-CH-C), 8.61 (d, $J = 5.0$ Hz, 1H, N-CH-CH), 8.02-8.04 (m, 2H, NH-NH and N-CH-C-CH), 7.96 (bs, 1H, NH-CH₂-CH₂), 7.63 (dd, $J = 7.3$ Hz, $J = 5.8$ Hz, 1H, N-CH-CH), 7.51 (d, $J = 7.9$ Hz, 1H, NH-CH-C-C-CH), 7.30 (d, $J = 8.2$ Hz, 1H, NH-C-CH-CH), 7.25 (t, $J = 7.6$ Hz, 2H, *m*-CH), 7.17 (t, $J = 7.4$ Hz, 1H, *p*-CH), 7.13 (d, $J = 7.5$ Hz, 2H, *o*-CH), 7.02-7.04 (m, 2H, NH-CH-C and NH-C-CH-CH), 6.95 (t, $J = 8.0$ Hz, 1H, NH-CH-C-C-CH-CH), 6.44 (d, $J = 8.1$ Hz, 1H, NH-CH), 4.32-4.36 (m, 1H, NH-CH), 3.59 (s, 2H, CO-CH₂-C₅H₄N), 3.22-3.26 (m, 1H, NH-CHH-CH₂), 3.15-3.19 (m, 1H, NH-CHH-CH₂), 3.01 (dd, $J = 14.4$ Hz, $J = 5.6$ Hz, 1H, NH-CH-CHH), 2.91 (dd, $J = 14.6$ Hz, $J = 7.4$ Hz, 1H, NH-CH-CHH), 2.58 (t, $J = 7.5$ Hz, 2H, NH-CH₂-CH₂); **HPLC-MS** (ESI) m/z 152.1 (40), 185.2 (30), 334.3 (30), 485.3 (100) [M+H]⁺, 507.3 (70) [M+Na]⁺, 523.3 (10) [M+Na]⁺, 969.3 (20) [2M+H]⁺, 991.4 (50) [2M+Na]⁺, 1007.5 (20) [2M+K]⁺; **HRMS** (ESI-TOF) for C₂₇H₂₈N₆O₃ [M+H]⁺: 485.2298 (calcd 485.2301); **Analytical HPLC** (5-90 % in 30 min) $t_R = 15.96$ min (99.3 % purity at 220 nm).



***N*1-(2-Phenylethyl)-(2*R*)-2-{[*N*'-(2-(1,2,3,4-tetrahydro-1-isoquinolinyl)ethanoyl)hydrazino]carboxamido}-3-(1*H*-3-indolyl)propanamide (185)**

*N*1-(2-Phenylethyl)-(2*R*)-2-{[*N*'-(2-(1,2,3,4-tetrahydro-1-isoquinolinyl)ethanoyl)hydrazino]carboxamido}-3-(1*H*-3-indolyl)propanamide (**185**) was synthesized on solid support ($m_1 = 78$ mg, $m_2 = 100$ mg, $l = 0.354$ mmol/g). Coupling of 5-(9*H*-fluoren-9-ylmethoxy)-1,3,4-oxadiazol-2(3*H*)-one (**141**) (30.5 mg, 0.108 mmol) was carried out according to general method 11, coupling of 2-{1-[1,2,3,4-tetrahydro-2-(9*H*-fluoren-9-ylmethoxy)carbonyl]isoquinolinyl}acetic acid (**119**) (29 mg, 0.070 mmol), deprotection and cleavage from the resin were carried out according to general methods 3, 4, 7, and 8. The two isomers, **185a** and **185b** were separated by HPLC, lyophilization yielded colourless powders (**185a**: 1.6 mg, 0.0029 mmol, 8%, **185b**: 0.9 mg, 0.0017 mmol, 5%).

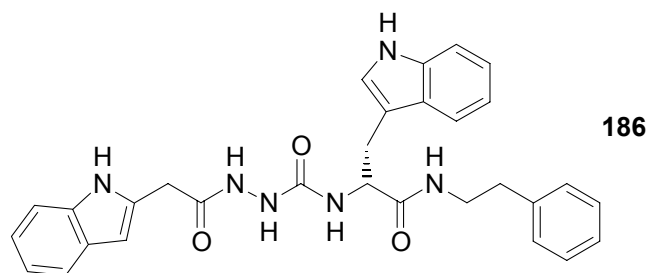
Spectroscopical data for **185a**:

mp 105-110 °C; **¹H-NMR** (500 MHz, DMSO-*d*₆, 300 K) $\delta = 10.79$ (s, 1H, C-NH-CH-C), 9.94 (s, 1H, NH-NH), 8.75 and 9.25 (bs, 1H, CH₂-NH-CH), 8.12 (s, 1H, NH-NH), 8.04 (t, $J = 5.5$ Hz, 1H, NH-CH₂-CH₂-C₆H₅), 7.54 (d, $J = 7.5$ Hz, 1H, NH-CH-C-CH), 7.31 (d, $J = 8.0$ Hz, 1H, NH-C-CH-CH), 7.17-7.26 (m, 7H, NH-CH-C₆H₄ and *m*-CH and *p*-CH), 7.14 (d, $J = 7.4$ Hz, 2H, *o*-CH), 7.05 (s, 1H, NH-CH-C), 7.04 (t, $J = 7.7$ Hz, 1H, NH-C-CH-CH), 6.96 (t, $J = 7.0$ Hz, 1H, NH-CH-C-C-CH-CH), 6.49 (d, $J = 8.0$ Hz, 1H, NH-CH-CH₂-C₈H₆N), 4.75-4.84 (m, 1H, CH-CH₂-CO), 4.35-4.39 (m, 1H, NH-CH-CO), 3.31-3.48 (m, 2H, NH-CH₂-CH₂), 3.24-3.28 (m, 1H, NH-CHH-CH₂-C₆H₅), 3.16-3.20 (m, 1H, NH-CHH-CH₂-C₆H₅), 2.87-3.01 (m, 6H, NH-CH₂-CH₂ and NH-CH-CH₂-CO and NH-CH-CH₂-C₈H₆N), 2.59 (t, $J = 7.5$ Hz, 2H, NH-CH₂-CH₂-C₆H₅); **HPLC-MS** (ESI) m/z 308.2 (20), 539.3 (45) [M+H]⁺, 561.3 (100)

$[M+Na]^+$, 577.2 (15) $[M+K]^+$, 1077.3 (10) $[2M+H]^+$, 1099.3 (40) $[2M+Na]^+$, 1115.4 (15) $[2M+K]^+$; **HRMS** (ESI-TOF) for $C_{31}H_{34}N_6O_3$ $[M+H]^+$: 539.2764 (calcd 539.2771); **Analytical HPLC** (5-90% in 30 min) t_R = 18.08 min (94% purity at 220 nm).

Spectroscopical data for **185b**:

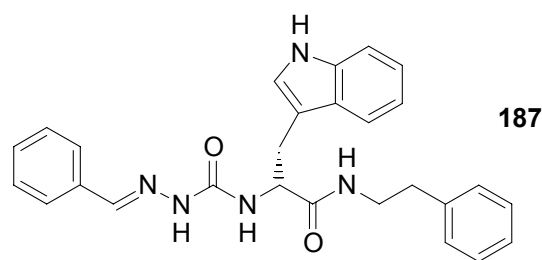
mp 120-123 °C; **1H -NMR** (500 MHz, DMSO- d_6 , 300 K) δ = 10.79 (s, 1H, C-NH-CH-C), 9.95 (s, 1H, NH-NH), 8.78 and 9.26 (bs, 1H, NH), 8.12 (s, 1H, NH-NH), 8.03 (t, J = 5.8 Hz, 1H, NH-CH₂-CH₂-C₆H₅), 7.54 (d, J = 7.7 Hz, 1H, NH-CH-C-C-CH), 7.31 (d, J = 8.1 Hz, 1H, NH-C-CH-CH), 7.17-7.26 (m, 7H, NH-CH-C₆H₄ and *m*-CH and *p*-CH), 7.14 (d, J = 7.3 Hz, 2H, *o*-CH), 7.03-7.05 (m, 2H, NH-CH-C and NH-C-CH-CH), 6.95 (t, J = 7.0 Hz, 1H, NH-CH-C-C-CH-CH), 6.49 (d, J = 8.2 Hz, 1H, NH-CH-CH₂-C₈H₆N), 4.80-4.86 (m, 1H, CH-CH₂-CO), 4.37 (q, J = 3.6 Hz, 1H, NH-CH-CH₂-C₈H₆N), 3.31-3.48 (m, 2H, NH-CH₂-CH₂), 3.22-3.28 (m, 1H, NH-CHH-CH₂-C₆H₅), 3.15-3.20 (m, 1H, NH-CHH-CH₂-C₆H₅), 2.87-3.05 (m, 6H, NH-CH₂-CH₂ and NH-CH-CH₂-CO and NH-CH-CH₂-C₈H₆N), 2.59 (t, J = 7.5 Hz, 2H, NH-CH₂-CH₂-C₆H₅); **HPLC-MS** (ESI) m/z 308.2 (20), 539.3 (30) $[M+H]^+$, 561.3 (100) $[M+Na]^+$, 577.3 (15) $[M+K]^+$, 1099.3 (25) $[2M+Na]^+$; **HRMS** (ESI-TOF) for $C_{31}H_{34}N_6O_3$ $[M+H]^+$: 539.2768 (calcd 539.2771); **Analytical HPLC** (5-90% in 30 min) t_R = 18.10 min (98.6% purity at 220 nm).



***N*1-(2-Phenylethyl)-(2*R*)-2-{[*N*'-(2-(1*H*-2-indolyl)ethanoyl)hydrazino]carboxamido}-3-(1*H*-3-indolyl)propanamide (186)**

*N*1-(2-Phenylethyl)-(2*R*)-2-{[*N*'-(2-(1*H*-2-indolyl)ethanoyl)hydrazino]carboxamido}-3-(1*H*-3-indolyl)propanamide (**186**) was synthesized on solid support ($m_1 = 78$ mg, $m_2 = 100$ mg, $l = 0.354$ mmol/g). Coupling of 5-(9*H*-fluoren-9-ylmethoxy)-1,3,4-oxadiazol-2(3*H*)-one (**141**) (30.5 mg, 0.108 mmol) was carried out according to general method 11, coupling of (1*H*-indol-2-yl)acetic acid (**122**) (12.3 mg, 0.070 mmol), deprotection and cleavage from the resin were carried out according to general methods 3, 4, 7, and 8. HPLC purification and lyophilization yielded a colourless powder (5.7 mg, 0.011 mmol, 31%).

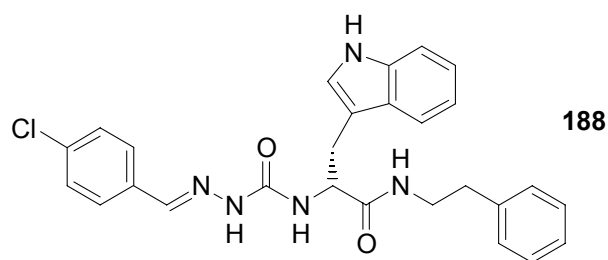
mp 109-115 °C; **¹H-NMR** (500 MHz, DMSO-*d*₆, 300 K) $\delta = 10.92$ (s, 1H, *NH*-C), 10.79 (s, 1H, *NH*-C), 9.80 (s, 1H, *NH*-NH), 8.04 (s, 1H, *NH*-NH), 7.97 (bs, 1H, *NH*-CH₂-CH₂), 7.52 (d, $J = 7.9$ Hz, 1H, *NH*-CH-C-*CH*), 7.40 (d, $J = 7.7$ Hz, 1H, *NH*-C-CH-C-*CH*), 7.30 (d, $J = 8.0$ Hz, 2H, *CH*-*NH*-C-*CH* and C-*NH*-C-*CH*), 7.24 (t, $J = 7.4$ Hz, 2H, *m*-*CH*), 7.16 (t, $J = 7.3$ Hz, 1H, *p*-*CH*), 7.12 (d, $J = 7.5$ Hz, 2H, *o*-*CH*), 6.90-7.05 (m, 5H, C-*CH*-*NH* and *CH*-*NH*-C-*CH*-*CH*-*CH* and C-*NH*-C-*CH*-*CH*-*CH*), 6.45 (d, $J = 8.0$ Hz, 1H, *NH*-CH-CH₂), 6.23 (s, 1H, C-*CH*-C-*NH*), 4.36-4.40 (m, 1H, *NH*-*CH*-CH₂), 3.60 (s, 2H, CO-CH₂-C₆H₅N), 3.15-3.26 (m, 2H, CH₂-CH₂-C₆H₅), 3.02 (dd, $J = 14.5$ Hz, $J = 5.7$ Hz, 1H, *NH*-*CH*-*CHH*), 2.91 (dd, $J = 14.6$ Hz, $J = 7.4$ Hz, 1H, *NH*-*CH*-*CHH*), 2.58 (t, $J = 7.4$ Hz, 2H, CH₂-CH₂-C₆H₅); **HPLC-MS** (ESI) m/z 366.1 (30), 523.2 (100) [*M*+*H*]⁺, 545.3 (25) [*M*+*Na*]⁺, 803.6 (20), 1045.2 (90) [*2M*+*H*]⁺, 1067.2 (40) [*2M*+*Na*]⁺; **HRMS** (ESI-TOF) for C₃₀H₃₀N₆O₃ [*M*+*H*]⁺: 523.2444 (calcd 523.2458); **Analytical HPLC** (5-90% in 30 min) $t_R = 22.31$ min (98.7% purity at 220 nm).



***N*1-(2-Phenylethyl)-(2*R*)-2-{[*N*'-(phenylmethylene)hydrazino]carboxamido}-3-(1*H*-3-indolyl)propanamide (187)**

*N*1-(2-Phenylethyl)-(2*R*)-2-{[*N*'-(phenylmethylene)hydrazino]carboxamido}-3-(1*H*-3-indolyl)propanamide (**187**) was prepared from *N*1-(2-phenylethyl)-(2*R*)-2-{[*N*'-(phenylmethylene)hydrazino]carboxamido}-3-[1-(*tert*-butoxycarbonyl)-3-indolyl]propanamide (**144**) (120 mg, 0.217 mmol) according to general method 21. Lyophilization yielded a colourless powder (62 mg, 0.137 mmol, 63%).

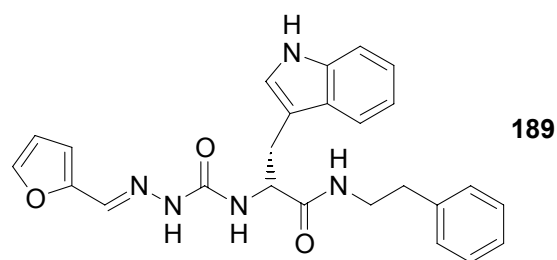
mp 183 °C; **¹H-NMR** (500 MHz, DMSO-*d*₆, 300 K) δ = 10.85 (s, 1H, NH-CH-C), 10.43 (s, 1H, N-NH), 8.06 (t, *J* = 5.5 Hz, 1H, NH-CH₂), 7.81 (s, 1H, N-CH-C₆H₅), 7.60 (d, *J* = 7.9 Hz, 1H, NH-CH-C-C-CH), 7.54 (d, *J* = 7.4 Hz, 2H, *o*-CH), 7.36-7.41 (m, 3H, *m*-CH and *p*-CH), 7.32 (d, *J* = 8.1 Hz, 1H, NH-C-CH-CH), 7.25 (t, *J* = 7.5 Hz, 2H, *m*-CH), 7.14-7.19 (m, 3H, *o*-CH and *p*-CH), 7.11 (s, 1H, NH-CH-C), 7.05 (t, *J* = 7.4 Hz, 1H, NH-C-CH-CH), 6.94 (t, *J* = 7.5 Hz, 1H, NH-CH-C-C-CH-CH), 6.72 (d, *J* = 8.0 Hz, 1H, NH-CH), 4.44 (q, *J* = 7.4 Hz, 1H, NH-CH-CH₂), 3.27-3.35 (m, 1H, NH-CHH-CH₂), 3.19-3.27 (m, 1H, NH-CHH-CH₂), 3.11 (d, *J* = 6.4 Hz, 2H, NH-CH-CH₂), 2.66 (t, *J* = 7.4 Hz, 2H, NH-CH₂-CH₂); **HPLC-MS** (ESI) *m/z* 454.2 (30) [M+H]⁺, 476.2 (100) [M+Na]⁺, 700.0 (75), 929.1 (100) [2M+Na]⁺; **HRMS** (ESI-TOF) for C₂₇H₂₇N₅O₂ [M+H]⁺: 454.2246 (calcd 454.2243); **Analytical HPLC** (5-90% in 30 min) *t*_R = 23.49 min (94.3% purity at 220 nm).



***N*1-(2-Phenylethyl)-(2*R*)-2-{[*N*'-(4-chlorophenylmethylene)hydrazino]carboxamido}-3-(1*H*-3-indolyl)propanamide (188)**

*N*1-(2-Phenylethyl)-(2*R*)-2-{[*N*'-(4-chlorophenylmethylene)hydrazino]carboxamido}-3-(1*H*-3-indolyl)propanamide (**188**) was prepared from *N*1-(2-phenylethyl)-(2*R*)-2-{[*N*'-(4-chlorophenylmethylene)hydrazino]carboxamido}-3-[1-(*tert*-butoxycarbonyl)-3-indolyl]propanamide (**145**) (120 mg, 0.204 mmol) according to general method 21. Lyophilization yielded a colourless powder (56 mg, 0.115 mmol, 56%).

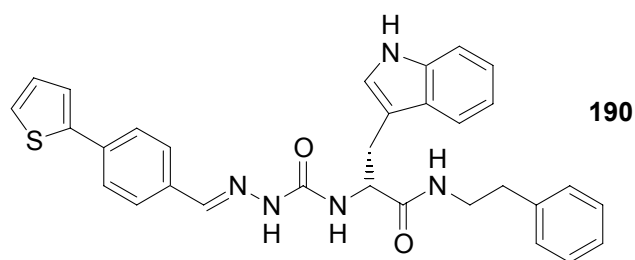
mp 173-175 °C; **¹H-NMR** (500 MHz, DMSO-*d*₆, 300 K) δ = 10.85 (s, 1H, NH-CH-C), 10.51 (s, 1H, N-NH), 8.05 (t, *J* = 5.5 Hz, 1H, NH-CH₂), 7.79 (s, 1H, N-CH-C₆H₄Cl), 7.59 (d, *J* = 8.0 Hz, 1H, NH-CH-C-C-CH), 7.56 (d, *J* = 8.4 Hz, 2H, Cl-C-CH), 7.46 (d, *J* = 8.3 Hz, 2H, Cl-C-CH-CH), 7.33 (d, *J* = 8.1 Hz, 1H, NH-C-CH-CH), 7.25 (t, *J* = 7.5 Hz, 2H, *m*-CH), 7.15-7.18 (m, 3H, *o*-CH and *p*-CH), 7.11 (s, 1H, NH-CH-C), 7.05 (t, *J* = 7.4 Hz, 1H, NH-C-CH-CH), 6.94 (t, *J* = 7.5 Hz, 1H, NH-CH-C-C-CH-CH), 6.73 (d, *J* = 8.0 Hz, 1H, NH-CH-CH₂), 4.43 (q, *J* = 7.5 Hz, 1H, NH-CH-CH₂), 3.27-3.35 (m, 1H, NH-CHH-CH₂), 3.19-3.27 (m, 1H, NH-CHH-CH₂), 3.11 (d, *J* = 6.2 Hz, 2H, NH-CH-CH₂), 2.66 (t, *J* = 7.5 Hz, 2H, NH-CH₂-CH₂); **HPLC-MS** (ESI) *m/z* 339.1 (30), 488.2 (60) [M+H]⁺, 510.3 (100) [M+Na]⁺, 752.0 (80), 997.2 (75) [2M+Na]⁺; **HRMS** (ESI-TOF) for C₂₇H₂₆N₅O₂Cl [M+H]⁺: 488.1859 (calcd 488.1853); **Analytical HPLC** (5-90% in 30 min) *t*_R = 25.18 min (98.1% purity at 220nm).



N1-(2-Phenylethyl)-(2R)-2-{[N'-(furan-2-ylmethylene)hydrazino]carboxamido}-3-(1H-3-indolyl)propanamide (189)

N1-(2-Phenylethyl)-(2R)-2-{[N'-(furan-2-ylmethylene)hydrazino]carboxamido}-3-(1H-3-indolyl)propanamide (189) was prepared from *N1-(2-phenylethyl)-(2R)-2-{[N'-(furan-2-ylmethylene)hydrazino]carboxamido}-3-[1-(tert-butoxycarbonyl)-3-indolyl]propanamide (146)* (100 mg, 0.184 mmol) according to general method 21. Lyophilization yielded a colourless powder (46 mg, 0.104 mmol, 57%).

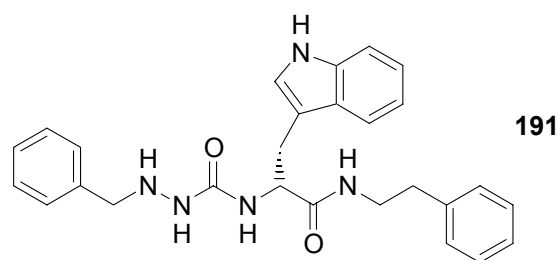
mp 100/101 °C; **¹H-NMR** (500 MHz, DMSO-*d*₆, 300 K) δ = 10.82 (s, 1H, NH-CH-C), 10.41 (s, 1H, N-NH), 8.09 (t, *J* = 5.5 Hz, 1H, NH-CH₂), 7.76 (s, 1H, C-O-CH), 7.73 (s, 1H, N-CH-C₄H₃O), 7.55 (d, *J* = 7.9 Hz, 1H, NH-CH-C-C-CH), 7.30 (d, *J* = 8.1 Hz, 1H, NH-C-CH-CH), 7.25 (t, *J* = 7.4 Hz, 2H, *m*-CH), 7.14-7.17 (m, 3H, *o*-CH and *p*-CH), 7.07 (s, 1H, NH-CH-C), 7.03 (t, *J* = 7.4 Hz, 1H, NH-C-CH-CH), 6.93 (t, *J* = 7.5 Hz, 1H, NH-CH-C-C-CH-CH), 6.74 (d, *J* = 3.2 Hz, 1H, O-C-CH-CH), 6.58-6.60 (m, 2H, NH-CH-CH₂ and O-C-CH-CH), 4.45 (q, *J* = 6.8 Hz, 1H, NH-CH-CH₂), 3.24-3.31 (m, 1H, NH-CHH-CH₂), 3.17-3.24 (m, 1H, NH-CHH-CH₂), 3.02-3.10 (m, 2H, NH-CH-CH₂), 2.62 (t, *J* = 7.4 Hz, 2H, NH-CH₂-CH₂); **HPLC-MS** (ESI) *m/z* 444.2 (30) [M+H]⁺, 466.3 (65) [M+Na]⁺, 685.1 (90), 909.2 (100) [2M+Na]⁺, 1352.1 (15) [3M+Na]⁺; **HRMS** (ESI-TOF) for C₂₅H₂₅N₅O₃ [M+H]⁺: 444.2036 (calcd 444.2036); **Analytical HPLC** (5-90% in 30 min) *t*_R = 22.07 min (93.2% purity at 220 nm).



***N*1-(2-Phenylethyl)-(2*R*)-2-{[*N'*-(4-(2-thienyl)phenylmethylene)hydrazino]carboxamido}-3-(1*H*-3-indolyl)propanamide (190)**

*N*1-(2-Phenylethyl)-(2*R*)-2-{[*N'*-(4-(2-thienyl)phenylmethylene)hydrazino]carboxamido}-3-(1*H*-3-indolyl)propanamide (**190**) was prepared from *N*1-(2-phenylethyl)-(2*R*)-2-{[*N'*-(4-(2-thienyl)phenylmethylene)hydrazino]carboxamido}-3-[1-(*tert*-butoxycarbonyl)-3-indolyl]propanamide (**147**) (40 mg, 0.063 mmol) according to general method 21. Lyophilization yielded a colourless powder (25 mg, 0.047 mmol, 74%).

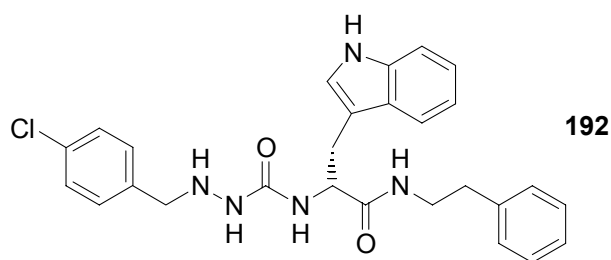
mp 219-221 °C; **¹H-NMR** (500 MHz, DMSO-*d*₆, 300 K) δ = 10.87 (s, 1H, NH-CH-C), 10.48 (s, 1H, N-NH), 8.06 (t, *J* = 5.5 Hz, 1H, NH-CH₂-CH₂), 7.81 (s, 1H, N-CH-C₁₀H₇S), 7.69 (d, *J* = 8.2 Hz, 2H, CH-CH-C-C₄H₃S), 7.57-7.61 (m, 5H, NH-CH-C-C-CH and CH-C-C₄H₃S and C₄HH₂S), 7.33 (d, *J* = 8.1 Hz, 1H, NH-C-CH-CH), 7.25 (t, *J* = 7.5 Hz, 2H, *m*-CH), 7.16-7.18 (m, 4H, *o*-CH and *p*-CH and C₄H₂HS), 7.13 (s, 1H, NH-CH-C), 7.06 (t, *J* = 7.7 Hz, 1H, NH-C-CH-CH), 6.95 (t, *J* = 7.5 Hz, 1H, NH-CH-C-C-CH-CH), 6.74 (d, *J* = 7.9 Hz, 1H, NH-CH-CH₂), 4.43 (q, *J* = 7.7 Hz, 1H, NH-CH-CH₂), 3.27-3.34 (m, 1H, NH-CHH-CH₂), 3.20-3.27 (m, 1H, NH-CHH-CH₂), 3.12 (d, *J* = 6.4 Hz, 2H, NH-CH-CH₂), 2.66 (t, *J* = 7.4 Hz, 2H, NH-CH₂-CH₂); **HPLC-MS** (ESI) *m/z* 387.0 (25), 536.1 (100) [M+H]⁺, 558.2 (20) [M+Na]⁺, 822.9 (30), 1070.9 (50) [2M+H]⁺, 1093.0 (30) [2M+Na]⁺; **HRMS** (ESI-TOF) for C₃₁H₂₉N₅O₂S [M+H]⁺: 536.2120 (calcd 536.2120); **Analytical HPLC** (5-90% in 30 min) *t*_R = 26.61 min (98.5% purity at 220 nm).



***N*1-(2-Phenylethyl)-(2*R*)-2- {[*N'*-(benzyl)hydrazino]carboxamido}-3-(1*H*-3-indol-yl)propanamide (**191**)**

*N*1-(2-Phenylethyl)-(2*R*)-2- {[*N'*-(benzyl)hydrazino]carboxamido}-3-(1*H*-3-indol-yl)propanamide (**191**) was prepared from *N*-benzyl-*N*-[(9*H*-fluorene-9-ylmethoxy)carbonyl]-*N'*-(*tert*-butoxycarbonyl)hydrazine (**154**) (0.24 g, 0.54 mmol) and *tert*-butyl-3-{(2*R*)-2-amino-2-[1-(2-phenylethyl)carbonyl]ethyl}-1*H*-1-indolecarboxylate (**139**) (0.22 g, 0.54 mmol) according to general method 22. Lyophilization yielded a colourless powder (34.2 mg, 0.075 mmol, 14%).

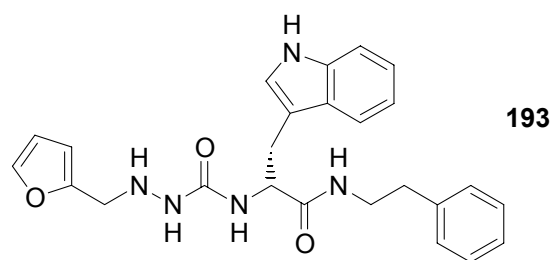
mp 81-84 °C; **¹H-NMR** (500 MHz, CDCl₃, 300 K) δ = 8.13 (s, 1H, NH), 7.56 (d, J = 7.9 Hz, 1H, NH-CH-C-C-CH), 7.34 (d, J = 8.1 Hz, 1H, NH-C-CH-CH), 7.16-7.29 (m, 9H, NH-C-CH-CH and *m*-CH and *p*-CH and C₆H₅), 7.11 (t, J = 7.1 Hz, 1H, NH-CH-C-C-CH-CH), 6.94-6.95 (m, 3H, *o*-CH and NH-CH-C), 6.88 (bs, 1H, NH-CH), 5.99 (bs, 1H, NH), 4.43 (q, J = 6.5 Hz, 1H, NH-CH-CH₂), 3.91 (bs, 2H, NH-CH₂-C₆H₅), 3.34-3.42 (m, 1H, NH-CHH-CH₂), 3.16-3.24 (m, 1H, NH-CHH-CH₂), 3.14 (dd, J = 14.0 Hz, J = 5.5 Hz, 1H, NH-CH-CHH), 3.07 (dd, J = 14.3 Hz, J = 7.4 Hz, 1H, NH-CH-CHH), 2.45-2.59 (m, 2H, NH-CH₂-CH₂); **HPLC-MS** (ESI) m/z 307.1 (20), 456.1 (45) [M+H]⁺, 478.3 (45) [M+Na]⁺, 703.0 (100), 911.0 (15) [2M+H]⁺, 933.0 (90) [2M+Na]⁺, 995.1 (15), 1387.9 (15) [3M+Na]⁺; **HRMS** (ESI-TOF) for C₂₇H₂₉N₅O₂ [M+H]⁺: 456.2403 (calcd 456.2400); **Analytical HPLC** (5-90% in 30 min) t_R = 21.09 min (98.3% purity at 220 nm).



***N*1-(2-Phenylethyl)-(2*R*)-2- {[*N'*-(4-chlorobenzyl)hydrazino]carboxamido}-3-(1*H*-3-indolyl)propanamide (192)**

*N*1-(2-Phenylethyl)-(2*R*)-2- {[*N'*-(4-chlorobenzyl)hydrazino]carboxamido}-3-(1*H*-3-indolyl)propanamide (**192**) was prepared from *N*-(4-chlorobenzyl)-*N*-[(9*H*-fluoren-9-ylmethoxy)carbonyl]-*N'*-(*tert*-butoxycarbonyl)hydrazine (**155**) (0.30 g, 0.63 mmol) and *tert*-butyl-3- {(2*R*)-2-amino-2-[1-(2-phenylethyl)carbonyl]ethyl}-1*H*-1-indole carboxylate (**139**) (0.26 g, 0.63 mmol) according to general method 22. Lyophilization yielded a colourless powder (26.8 mg, 0.055 mmol, 9%).

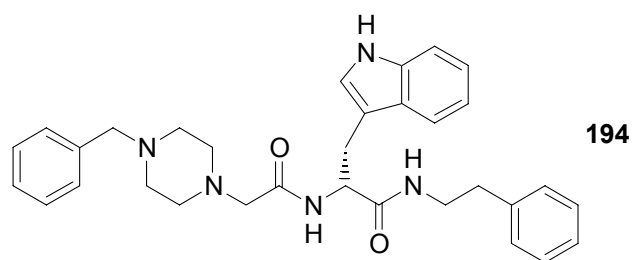
mp 75-80 °C; **¹H-NMR** (500 MHz, ACN-*d*₃, 300 K) δ = 9.74 (bs, 1H, NH), 7.91 (d, *J* = 7.7 Hz, 1H, NH-CH-C-C-CH), 7.98 (d, *J* = 8.1 Hz, 1H, NH-C-CH-CH), 7.74-7.83 (m, 5H, *m*-CH and *p*-CH and Cl-C-CH), 7.71 (t, *J* = 7.4 Hz, 1H, NH-C-CH-CH), 7.66-7.69 (m, 4H, *o*-CH and Cl-C-CH-CH), 7.62 (t, *J* = 7.5 Hz, 1H, NH-CH-C-C-CH-CH), 7.58 (s, 1H, NH-CH-C), 6.99 (bs, 1H, NH-CH), 6.89 (bs, 1H, NH-CH₂-CH₂), 4.87 (q, *J* = 6.9 Hz, 1H, NH-CH-CH₂), 4.34 (bs, 2H, NH-CH₂-C₆H₄Cl), 3.87-3.94 (m, 1H, NH-CHH-CH₂), 3.76-3.82 (m, 1H, NH-CHH-CH₂), 3.66 (d, *J* = 6.2 Hz, 2H, NH-CH-CH₂), 3.17 (t, *J* = 7.3 Hz, 2H, NH-CH₂-CH₂); **HPLC-MS** (ESI) *m/z* 490.1 (70) [M+H]⁺, 512.3 (50) [M+Na]⁺, 754.8 (100), 978.9 (25) [2M+H]⁺, 1001.0 (90) [2M+Na]⁺, 1063.1 (20); **HRMS** (ESI-TOF) for C₂₇H₂₈N₅O₂Cl [M+H]⁺: 490.2006 (calcd 490.2010); **Analytical HPLC** (5-90% in 30 min) *t*_R = 23.01 min (98.7% purity at 220 nm).



***N*1-(2-Phenylethyl)-(2*R*)-2- {[*N*'-(2-furylmethyl)hydrazino]carboxamido}-3-(1*H*-3-indolyl)propanamide (193)**

*N*1-(2-Phenylethyl)-(2*R*)-2- {[*N*'-(2-furylmethyl)hydrazino]carboxamido}-3-(1*H*-3-indolyl)propanamide (**193**) was prepared from *N*-[(9*H*-fluoren-9-ylmethoxy)carbonyl]-*N*-(2-furylmethyl)-*N*'-(*tert*-butoxycarbonyl)hydrazine (**156**) (0.30 g, 0.69 mmol) and *tert*-butyl-3-{(2*R*)-2-amino-2-[1-(2-phenylethyl)carbamoyl]ethyl}-1*H*-1-indolecarboxylate (**139**) (0.28 g, 0.69 mmol) according to general method 22. Lyophilization yielded a colourless powder (65.1 mg, 0.146 mmol, 21%).

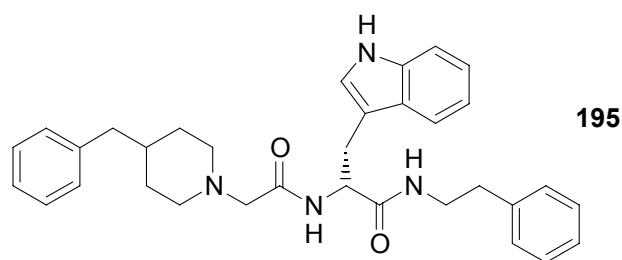
mp 59-62 °C; **¹H-NMR** (500 MHz, ACN-*d*₃, 300 K) δ = 9.72 (s, 1H, NH), 8.14 (d, *J* = 7.9 Hz, 1H, NH-CH-C-C-CH), 7.97 (d, *J* = 8.3 Hz, 1H, NH-C-CH-CH), 7.95 (s, 1H, C-O-CH), 7.82 (t, *J* = 7.5 Hz, 2H, *m*-CH), 7.76 (t, *J* = 7.2 Hz, 1H, *p*-CH), 7.70 (t, *J* = 7.4 Hz, 1H, NH-C-CH-CH), 7.67 (d, *J* = 7.5 Hz, 2H, *o*-CH), 7.62 (t, *J* = 7.6 Hz, 1H, NH-CH-C-C-CH-CH), 7.60 (s, 1H, NH-CH-C), 7.05 (bs, 2H, NH-CH-CH₂, and NH-CH₂-CH₂), 6.89 (s, 1H, O-C-CH-CH), 6.80 (s, 1H, O-C-CH), 4.89 (q, *J* = 6.8 Hz, 1H, NH-CH-CH₂), 4.41 (bs, 2H, NH-CH₂-C₄H₃O), 3.82-3.92 (m, 2H, NH-CH₂-CH₂), 3.68 (dd, *J* = 14.5 Hz, *J* = 5.9 Hz, 1H, NH-CH-CHH), 3.64 (dd, *J* = 14.0 Hz, *J* = 7.7 Hz, 1H, NH-CH-CHH), 3.17 (t, *J* = 7.0 Hz, 2H, NH-CH₂-CH₂); **HPLC-MS** (ESI) *m/z* 446.2 (30) [M+H]⁺, 468.3 (65) [M+Na]⁺, 688.0 (80), 913.1 (100) [2M+Na]⁺; **HRMS** (ESI-TOF) for C₂₅H₂₇N₅O₃ [M+H]⁺: 446.2196 (calcd 446.2192); **Analytical HPLC** (5-90% in 30 min) *t*_R = 21.51 min (98.6% purity at 220 nm).



***N*1-(2-Phenylethyl)-(2*R*)-2-[[4-benzylpiperazino)methyl]carboxamido}-3-(1*H*-3-indolyl)propanamide (194)**

*N*1-(2-Phenylethyl)-(2*R*)-2-[[4-benzylpiperazino)methyl]carboxamido}-3-(1*H*-3-indolyl)propanamide (**194**) was prepared from *N*1-(2-phenylethyl)-(2*R*)-2-[[4-benzylpiperazino)methyl]carboxamido}-3-[1-(*tert*-butoxycarbonyl)-3-indolyl]propanamide (**161**) (170 mg, 0.273 mmol) according to general method 21. Lyophilization yielded a colourless powder (97 mg, 0.185 mmol, 68%).

mp 67-70 °C; **¹H-NMR** (500 MHz, CDCl₃, 300 K) δ = 8.40 (s, 1H, NH-CH-C), 7.60 (d, J = 7.9 Hz, 1H, NH-CH-C-C-CH), 7.55 (d, J = 7.5 Hz, 1H, NH-CH-CH₂), 7.43-7.49 (m, 3H, *m*-CH and *p*-CH), 7.34-7.37 (m, 3H, *o*-CH and NH-C-CH-CH), 7.23-7.27 (m, 2H, *m*-CH), 7.19 (t, J = 7.2 Hz, 2H, NH-C-CH-CH and *p*-CH), 7.13 (t, J = 7.5 Hz, 1H, NH-CH-C-C-CH-CH), 7.05 (d, J = 7.4 Hz, 2H, *o*-CH), 6.96 (s, 1H, NH-CH-C), 6.26 (s, 1H, NH-CH₂-CH₂), 4.68 (q, J = 7.5 Hz, 1H, NH-CH-CH₂), 4.03 (dd, J = 23.8 Hz, J = 12.9 Hz, 2H, NH-CH₂-C₆H₅), 3.48-3.55 (m, 1H, NH-CHH-CH₂), 3.38-3.45 (m, 1H, NH-CHH-CH₂), 3.23 (dd, J = 14.8 Hz, J = 7.4 Hz, 1H, NH-CH-CHH), 3.14 (dd, J = 14.8 Hz, J = 7.2 Hz, 1H, NH-CH-CHH), 3.08 (m, 2H, N-CH₂-CO), 2.70 (t, J = 6.9 Hz, 2H, NH-CH₂-CH₂-C₆H₅), 2.61-2.75 (m, 8H, N-CH₂-CH₂-N); **HPLC-MS** (ESI) m/z 189.1 (75), 524.4 (100) [M+H]⁺, 546.5 (20) [M+Na]⁺, 562.4 (15) [M+K]⁺, 1069.4 (25) [2M+Na]⁺; **HRMS** (ESI-TOF) for C₃₂H₃₇N₅O₂ [M+H]⁺: 524.3026 (calcd 524.3026); **Analytical HPLC** (5-90% in 30 min) t_R = 18.73 min (99.7% purity at 220 nm).



***N*1-(2-Phenylethyl)-(2*R*)-2-[[4-(benzylpiperidino)methyl]carboxamido]-3-(1*H*-3-indolyl)propanamide (195)**

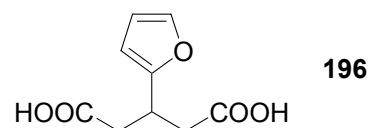
*N*1-(2-Phenylethyl)-(2*R*)-2-[[4-(benzylpiperidino)methyl]carboxamido]-3-(1*H*-3-indolyl)propanamide (**195**) was prepared from *N*1-(2-phenylethyl)-(2*R*)-2-[[4-(benzylpiperidino)methyl]carboxamido]-3-[1-(*tert*-butoxycarbonyl)-3-indolyl]propanamide (**162**) (180 mg, 0.289 mmol) according to general method 21. Lyophilization yielded a colourless powder (109 mg, 0.209 mmol, 72%).

mp 73-75 °C; **¹H-NMR** (500 MHz, DMSO-*d*₆, 300 K) δ = 10.84 (s, 1H, NH-CH-C), 8.81 (d, *J* = 8.3 Hz, 1H, NH-CH-CH₂), 8.25 (t, *J* = 5.2 Hz, 1H, NH-CH₂-CH₂), 7.61 (d, *J* = 7.7 Hz, 1H, NH-CH-C-C-CH), 7.14-7.31 (m, 11H, N-C-CH-CH and C₆H₅ and C₆H₅), 7.09 (s, 1H, NH-CH-C), 7.02 (t, *J* = 7.3 Hz, 1H, NH-C-CH-CH), 6.96 (t, *J* = 6.9 Hz, 1H, NH-CH-C-C-CH-CH), 4.60 (q, *J* = 6.9 Hz, 1H, NH-CH-CH₂), 3.81 (d, *J* = 15.2 Hz, 1H, N-CHH-CO), 3.67 (d, *J* = 13.1 Hz, 1H, N-CHH-CO), 3.21-3.34 (m, 3H, NH-CH₂-CH₂ and N-CHH-CH₂-CH), 3.06 (dd, *J* = 14.4 Hz, *J* = 4.9 Hz, 1H, NH-CH-CHH), 2.97-2.93 (m, 3H, NH-CH-CHH and N-CHH-CH₂-CH), 2.59-2.67 (m, 3H, NH-CH₂-CH₂ and N-CHH-CH₂-CH), 2.46-2.48 (m, 2H, CH-CH₂-C₆H₅), 1.57-1.70 (m, 3H, N-CH₂-CHH-CH and CH-CH₂-C₆H₅), 1.32-1.46 (m, 2H, N-CH₂-CHH-CH); **HPLC-MS** (ESI) *m/z* 188.1 (70), 523.3 (100) [M+H]⁺, 803.7 (20), 1045.1 (20) [2M+H]⁺, 1067.3 (40) [2M+Na]⁺; **HRMS** (ESI-TOF) for C₃₃H₃₈N₄O₂ [M+H]⁺: 523.3070 (calcd 523.3073); **Analytical HPLC** (5-90% in 30 min) *t*_R = 21.30 (99.8% purity at 220 nm).

8.4 $\alpha\beta 3$ Integrin Antagonists

8.4.1 Solution-Phase Synthesis of Building Blocks

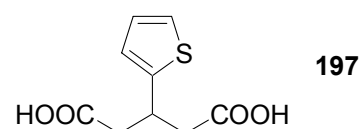
Synthesis of the $\alpha\beta 3$ antagonists (chapter 8.4.2) was carried out using the building blocks described below and, additionally, 5-(9*H*-fluoren-9-ylmethoxy)-3*H*-[1,3,4]oxadiazol-2-one (**141**) and 2-{1-[1,2,3,4-tetrahydro-2-(9*H*-fluoren-9-ylmethoxy)carbonyl]isoquinolinyl}acetic acid (**119**), which were described earlier in chapter 8.3.1.



3-(Furan-2-yl)glutaric acid (**196**)

3-(Furan-2-yl)glutaric acid (**196**) was prepared from 2-furylcarboxaldehyde (7.68 g, 80 mmol) and ethylacetoacetate (20.6 g, 158.4 mmol) according to general method 24. Saponification of the intermediate product, a viscous oil, yielded the desired product as a crystalline, colourless solid (4.46 g, 22.5 mmol, 28%).

mp 130 °C; **¹H-NMR** (250 MHz, DMSO-*d*₆, 300 K) δ = 7.48-7.50 (m, 1H, C-O-CH), 6.30-6.32 (m, 1H, O-CH-CH), 6.09 (d, *J* = 3.2 Hz, 1H, O-C-CH), 3.52 (m, 1H, CH₂-CH-CH₂), 2.56 (d, *J* = 7.1 Hz, 4H, CH₂-CH-CH₂); **¹³C-NMR** (62.9 MHz, DMSO-*d*₆, 300 K) δ = 172.86 (COOH), 156.57 (O-C-CH), 141.79 (C-O-CH), 110.53 (O-CH-CH), 105.18 (O-C-CH), 37.99 (CH₂-CH-CH₂), 31.82 (CH₂-CH-CH₂); **Analytical HPLC** (5-90% in 30 min) *t*_R = 11.75 min.

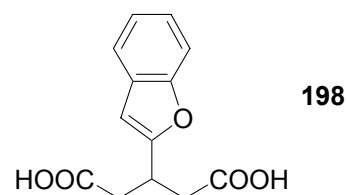


3-(Thiophene-2-yl)glutaric acid (**197**)

3-(Thiophene-2-yl)glutaric acid (**197**) was prepared from 2-thiophenecarbaldehyde (8.97 g, 80 mmol) and ethylacetoacetate (20.6 g, 158.4 mmol) according to general method 24. Saponification of the intermediate product, a crystalline solid

(13.32 g, mp 100 °C), yielded the desired product as a brown solid (8.07 g, 37.7 mmol, 47%).

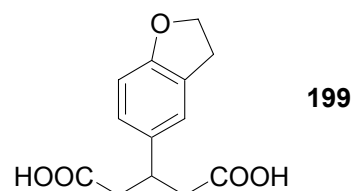
mp 115/116 °C; **¹H-NMR** (250 MHz, DMSO-*d*₆, 300 K) δ = 7.28-7.31 (m, 1H, C-S-CH), 6.89-6.93 (m, 2H, S-C-CH-CH), 3.71 (m, 1H, CH₂-CH-CH₂), 2.48-2.72 (m, 4H, CH₂-CH-CH₂); **¹³C-NMR** (62.9 MHz, DMSO-*d*₆, 300 K) δ = 172.77 (COOH), 146.99 (S-C); 126.89, 124.17, 123.89, 41.25 (CH₂-CH-CH₂), 33.47 (CH₂-CH-CH₂); **Analytical HPLC** (5-90% in 30 min) t_R = 13.17 min.



3-(Benzofuran-2-yl)glutaric acid (198)

3-(Benzofuran-2-yl)glutaric acid (**198**) was prepared from 2-benzofuryl-carboxaldehyde (4.82 g, 33 mmol) and ethylacetoacetate (8.52 g, 65.5 mmol) according to general method 24. Saponification of the intermediate product, a colourless solid (5.89 g, mp 132 °C), yielded the desired product as a colourless solid (3.68 g, 14.8 mmol, 45%).

mp 139/140 °C; **¹H-NMR** (250 MHz, DMSO-*d*₆, 300 K) δ = 7.44-7.55 (m, 2H, O-C-CH-CH-CH-CH), 7.14-7.26 (m, 2H, O-C-CH-CH-CH), 6.61 (s, 1H, O-C-CH-C), 3.67 (m, 1H, CH₂-CH-CH₂), 2.67 (d, J = 9.4 Hz, 4H, CH₂-CH-CH₂); **¹³C-NMR** (62.9 MHz, DMSO-*d*₆, 300 K) δ = 172.69 (COOH), 159.99, 154.12, 128.51, 123.83, 122.94, 120.88, 111.05 (O-C-CH-CH), 102.27 (O-C-CH-C), 37.66 (CH₂-CH-CH₂), 32.24 (CH₂-CH-CH₂); **Analytical HPLC** (5-90% in 30 min) t_R = 16.79 min.

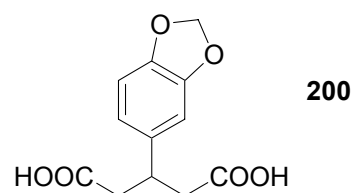


3-(2,3-Dihydrobenzo[*b*]furan-5-yl)glutaric acid (199)

3-(2,3-Dihydrobenzo[*b*]furan-5-yl)glutaric acid (**199**) was prepared from 2,3-dihydrobenzo[*b*]furan-5-carbaldehyde (2.0 g, 13.5 mmol) and ethylacetoacetate (3.47

g, 26.7 mmol) according to general method 24. Saponification of the intermediate product, a crystalline solid (1.77 g, mp 145 °C), yielded the desired product as a colourless solid (1.35 g, 5.4 mmol, 40%).

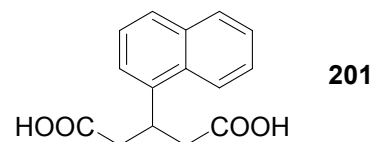
mp 144 °C; **¹H-NMR** (250 MHz, DMSO-*d*₆, 300 K) δ = 7.65 (m, 1H, C-CH-C), 7.47-7.50 (m, 1H, C-CH-CH-C-O), 7.17 (d, *J* = 8.2 Hz, 1H, C-CH-CH-C-O), 5.00 (t, *J* = 8.8 Hz, 2H, O-CH₂-CH₂), 3.85-3.91 (m, 1H, CH₂-CH-CH₂), 3.65 (t, *J* = 8.6 Hz, 2H, O-CH₂-CH₂); **¹³C-NMR** (62.9 MHz, DMSO-*d*₆, 300 K) δ = 173.08 (COOH), 158.47 (O-C), 135.46, 127.17, 127.00, 124.18, 108.58, 70.94 (O-CH₂-O), 37.71 (CH₂-CH-CH₂), 29.33 (CH₂-CH-CH₂); **Analytical HPLC** (5-90% in 30 min) *t*_R = 13.42 min.



3-(1,3-Benzodioxole-5-yl)glutaric acid (200)

3-(1,3-Benzodioxole-5-yl)glutaric acid (**200**) was prepared from 1,3-benzodioxole-5-carboxaldehyde (25.0 g, 166.5 mmol) and ethylacetoacetate (42.1 g, 323.7 mmol) according to general method 24. Saponification of the intermediate product, a colourless solid (41.9 g), yielded the desired product as a colourless solid (19.3 g, 76.5 mmol, 46%).

mp 171 °C; **¹H-NMR** (250 MHz, DMSO-*d*₆, 300 K) δ = 6.87 (s, 1H, C-CH-C-O), 6.79 (d, *J* = 7.9 Hz, 1H, C-CH-CH-C-O), 6.70 (d, *J* = 8.0 Hz, 1H, C-CH-CH-C-O), 5.95 (s, 2H, O-CH₂-O), 3.35 (m, 1H, CH₂-CH-CH₂), 2.41-2.65 (m, 4H, CH₂-CH-CH₂); **Analytical HPLC** (10-90% in 30 min) *t*_R = 11.85 min.

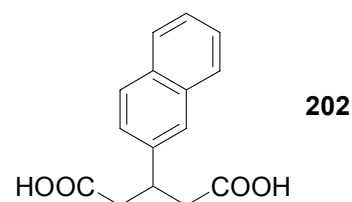


3-(Naphth-1-yl)glutaric acid (201)

3-(Naphth-1-yl)glutaric acid (**201**) was prepared from 1-naphthylcarboxaldehyde (6.24 g, 40 mmol) and ethylacetoacetate (10.35 g, 79.5 mmol) according to general

method 24. Saponification of the intermediate product, a viscous oil, yielded the desired product as a slightly yellow solid (1.54 g, 5.96 mmol, 15%).

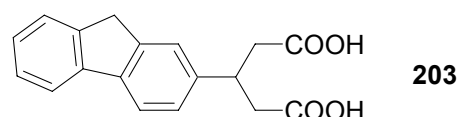
mp 193/194 °C; **¹H-NMR** (250 MHz, DMSO-*d*₆, 300 K) δ = 8.20 (d, *J* = 8.3 Hz, 1H, 8-*H*), 7.91 (d, *J* = 7.9 Hz, 1H, 5-*H*), 7.78 (d, *J* = 7.4 Hz, 1H, 4-*H*), 7.45-7.61 (m, 4H, 2-*H* and 3-*H* and 6-*H* and 7-*H*), 4.38 (m, 1H, CH₂-CH-CH₂), 2.75 (d, *J* = 7.2 Hz, 4H, CH₂-CH-CH₂); **¹³C-NMR** (62.9 MHz, DMSO-*d*₆, 300 K) δ = 173.16 (COOH), 139.78, 133.80, 131.22, 128.97, 127.06, 126.36, 125.76, 125.73, 123.44, 123.32, 40.09 (CH₂-CH-CH₂), 32.44 (CH₂-CH-CH₂); **Analytical HPLC** (5-90% in 30 min) *t*_R = 17.49 min.



3-(Naphth-2-yl)glutaric acid (202)

3-(Naphth-2-yl)glutaric acid (**202**) was prepared from 2-naphthylcarboxaldehyde (5.7 g, 36.5 mmol) and ethylacetoacetate (9.47 g, 72.8 mmol) according to general method 24. Saponification of the intermediate product, a slightly yellow solid (9.98 g, mp 155-157 °C), yielded the desired product as a slightly yellow solid (4.1 g, 15.9 mmol, 44%).

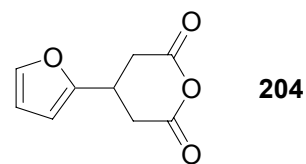
mp 176/177 °C; **¹H-NMR** (250 MHz, DMSO-*d*₆, 300 K) δ = 12.09 (bs, 1H, COOH), 7.82-7.87 (m, 3H, 4-*H* and 5-*H* and 8-*H*), 7.75 (s, 1H, C-CH-C), 7.45-7.49 (m, 3H, 3-*H* and 6-*H* and 7-*H*), 3.59 (m, 1H, CH₂-CH-CH₂), 2.58-2.79 (m, 4H, CH₂-CH-CH₂); **Analytical HPLC** (5-90% in 30 min) *t*_R = 17.03 min.



3-(9H-Fluoren-2-yl)glutaric acid (203)

3-(9H-Fluoren-2-yl)glutaric acid (**203**) was prepared from 9H-2-fluorene-carbaldehyde (5.0 g, 25.7 mmol) and ethylacetoacetate (6.7 g, 51.5 mmol) according to general method 24. Saponification of the intermediate product, a crystalline solid (8.5

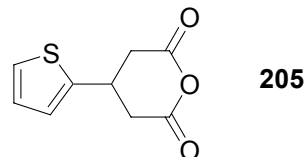
g, mp 188-190 °C), yielded the desired product as a colourless solid (5.0 g, 16.9 mmol, 66%).



3-(Furan-2-yl)glutaric acid anhydride (204)

3-(Furan-2-yl)glutaric acid anhydride (**204**) was prepared from 3-(furan-2-yl)glutaric acid (**196**) (2.7 g, 13.6 mmol) according to general method 25. The residue was chromatographed, drying yielded colourless crystals (2.09 g, 11.6 mmol, 85%).

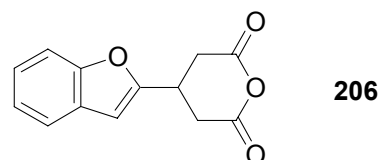
mp 102 °C; **TLC** R_f (CH₂Cl₂/ethyl acetate, 20:1) = 0.79; **¹H-NMR** (250 MHz, DMSO-*d*₆, 300 K) δ = 7.59-7.61 (m, 1H, C-O-CH), 6.39-6.41 (m, 1H, O-CH-CH), 6.25-6.27 (m, 1H, O-C-CH), 3.66 (m, 1H, CH₂-CH-CH₂), 2.92-3.16 (m, 4H, CH₂-CH-CH₂); **¹³C-NMR** (62.9 MHz, DMSO-*d*₆, 300 K) δ = 167.05 (CO), 154.08 (O-C-CH), 142.85 (C-O-CH), 110.75 (O-CH-CH), 105.96 (O-C-CH), 34.07 (CH₂-CH-CH₂), 27.52 (CH₂-CH-CH₂); **Analytical HPLC** (5-90% in 30 min) t_R = 16.58 min.



3-(Thiophene-2-yl)glutaric acid anhydride (205)

3-(Thiophene-2-yl)glutaric acid anhydride (**205**) was prepared from 3-(thiophene-2-yl)glutaric acid (**197**) (5.5 g, 25.7 mmol) according to general method 25. The residue was chromatographed, drying yielded a colourless solid (3.24 g, 16.5 mmol, 64%).

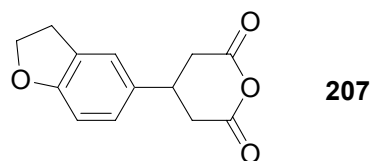
mp 95 °C; **TLC** R_f (CH₂Cl₂/ethyl acetate, 20:1) = 0.75; **¹H-NMR** (250 MHz, DMSO-*d*₆, 300 K) δ = 7.43-7.45 (m, 1H, C-S-CH), 6.99-7.02 (m, 1H, S-C-CH-CH), 3.85 (m, 1H, CH₂-CH-CH₂), 2.98-3.19 (m, 4H, CH₂-CH-CH₂); **¹³C-NMR** (62.9 MHz, DMSO-*d*₆, 300 K) δ = 166.94 (CO), 144.35 (S-C), 127.40, 125.05, 124.49, 37.07 (CH₂-CH-CH₂), 29.04 (CH₂-CH-CH₂); **Analytical HPLC** (5-90% in 30 min) t_R = 18.10 min.



3-(Benzofuran-2-yl)glutaric acid anhydride (206)

3-(Benzofuran-2-yl)glutaric acid anhydride (**206**) was prepared from 3-(benzofuran-2-yl)glutaric acid (**198**) (2.6 g, 10.5 mmol) according to general method 25. The desired product precipitated upon cooling, drying yielded colourless crystals (1.86 g, 8.1 mmol, 77%).

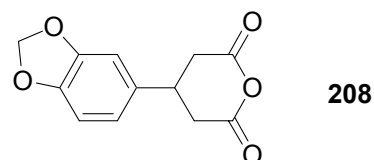
mp 166/167 °C; **¹H-NMR** (250 MHz, DMSO-*d*₆, 300 K) δ = 7.50-7.60 (m, 2H, O-C-CH-CH-CH-CH), 7.19-7.32 (m, 2H, O-C-CH-CH-CH), 6.76 (s, 1H, O-C-CH-C), 3.88 (m, 1H, CH₂-CH-CH₂), 3.06-3.28 (m, 4H, CH₂-CH-CH₂); **¹³C-NMR** (62.9 MHz, DMSO-*d*₆, 300 K) δ = 166.89 (CO), 157.35, 154.34, 128.03, 124.46, 123.24, 121.23, 111.17 (O-C-CH-CH), 102.94 (O-C-CH-C), 33.78 (CH₂-CH-CH₂), 27.98 (CH₂-CH-CH₂); **Analytical HPLC** (5-90% in 30 min) t_R = 21.69 min.



3-(2,3-Dihydrobenzo[*b*]furan-5-yl)glutaric acid anhydride (207)

3-(2,3-Dihydrobenzo[*b*]furan-5-yl)glutaric acid anhydride (**207**) was prepared from 3-(2,3-dihydrobenzo[*b*]furan-5-yl)glutaric acid (**199**) (1.05 g, 4.2 mmol) according to general method 25. The residue was chromatographed, drying yielded a yellow solid (0.72 g, 3.1 mmol, 69%).

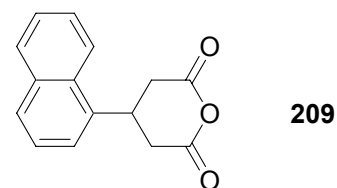
mp 136/137 °C; **TLC** R_f (CH₂Cl₂/ethyl acetate, 20:1) = 0.58; **¹H-NMR** (250 MHz, DMSO-*d*₆, 300 K) δ = 7.14 (m, 1H, C-CH-C), 6.95-6.99 (m, 1H, C-CH-CH-C-O), 6.71 (d, J = 8.2 Hz, 1H, C-CH-CH-C-O), 4.49 (t, J = 8.7 Hz, 2H, O-CH₂-CH₂), 3.40-3.53 (m, 1H, CH₂-CH-CH₂), 3.14 (t, J = 8.7 Hz, 2H, O-CH₂-CH₂), 2.85-3.05 (m, 4H, CH₂-CH-CH₂); **¹³C-NMR** (62.9 MHz, DMSO-*d*₆, 300 K) δ = 167.66 (CO), 159.04 (O-C), 132.82, 128.02, 126.29, 123.52, 109.09, 71.14 (O-CH₂), 36.82, 32.60, 29.24.



3-(1,3-Benzodioxole-5-yl)glutaric acid anhydride (208)

3-(1,3-Benzodioxole-5-yl)glutaric acid anhydride (**208**) was prepared from 3-(1,3-benzodioxole-5-yl)glutaric acid (**200**) (4.0 g, 15.9 mmol) according to general method 25. The desired product precipitated upon cooling, drying yielded a colourless solid (3.1 g, 13.2 mmol, 84%).

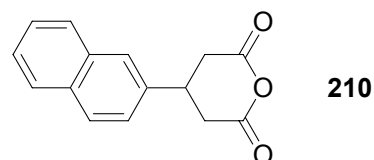
mp 184 °C; **¹H-NMR** (250 MHz, DMSO-*d*₆, 300 K) δ = 6.90-6.91 (m, 1H, C-CH-C-O), 6.87 (d, *J* = 8.0 Hz, 1H, C-CH-CH-C-O), 6.70-6.74 (m, 1H, C-CH-CH-C-O), 5.98 (s, 2H, CH₂-O-CH₂), 3.47 (m, 1H, CH₂-CH-CH₂), 2.86-3.06 (m, 4H, CH₂-CH-CH₂); **Analytical HPLC** (5-90% in 30 min) *t*_R = 18.87 min.



3-(Naphth-1-yl)glutaric acid anhydride (209)

3-(Naphth-1-yl)glutaric acid anhydride (**209**) was prepared from 3-(naphth-1-yl)glutaric acid (**201**) (1.35 g, 5.2 mmol) according to general method 25. The desired product precipitated upon cooling, drying yielded a colourless solid (0.85 g, 3.5 mmol, 63%).

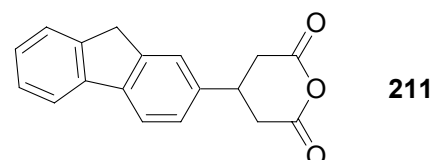
mp 162 °C; **¹H-NMR** (250 MHz, DMSO-*d*₆, 300 K) δ = 8.25 (d, *J* = 8.1 Hz, 1H, 8-*H*), 7.95 (d, *J* = 7.1 Hz, 1H, 5-*H*), 7.86 (d, *J* = 8.1 Hz, 1H, 4-*H*), 7.48-7.62 (m, 3H, 3-*H* and 6-*H* and 7-*H*), 7.41 (d, *J* = 7.1 Hz, 1H, 2-*H*), 4.48 (m, 1H, CH₂-CH-CH₂), 3.00-3.22 (m, 4H, CH₂-CH-CH₂); **¹³C-NMR** (62.9 MHz, DMSO-*d*₆, 300 K) δ = 167.73 (CO), 137.00, 133.69, 130.88, 129.02, 127.88, 126.76, 126.14, 125.82, 123.20, 122.72, 36.35 (CH₂-CH-CH₂), 28.47 (CH₂-CH-CH₂); **Analytical HPLC** (5-90% in 30 min) *t*_R = 23.40 min.



3-(Naphth-2-yl)glutaric acid anhydride (210)

3-(Naphth-2-yl)glutaric acid anhydride (**210**) was prepared from 3-(naphth-2-yl)glutaric acid (**202**) (3.9 g, 15.1 mmol) according to general method 25. The desired product precipitated upon cooling, drying yielded a colourless solid (2.5 g, 10.4 mmol, 69%).

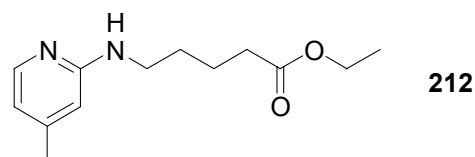
mp 194-196 °C; **¹H-NMR** (250 MHz, DMSO-*d*₆, 300 K) δ = 7.88-7.94 (m, 3H, 4-*H* and 5-*H* and 8-*H*), 7.78 (s, 1H, C-*CH*-C), 7.48-7.55 (m, 3H, 3-*H* and 6-*H* and 7-*H*), 3.75 (m, 1H, CH₂-*CH*-CH₂), 3.03-3.24 (m, 4H, CH₂-*CH*-CH₂); **Analytical HPLC** (5-90% in 30 min) t_R = 22.64 min.



3-(9*H*-Fluoren-2-yl)glutaric acid anhydride (211)

3-(9*H*-Fluoren-2-yl)glutaric acid anhydride (**211**) was prepared from 3-(9*H*-fluoren-2-yl)glutaric acid (**203**) (5.0 g, 16.9 mmol) according to general method 25. The desired product precipitated upon cooling, drying yielded a colourless solid (3.4 g, 12.2 mmol, 72%).

mp 239-242 °C; **Analytical HPLC** (5-90% in 30 min) t_R = 23.79 min.

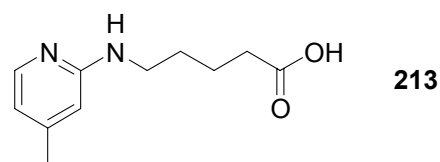


5-[*N*-(4-Methylpyridine-2-yl)amino]pentanoic acid ethyl ester (212)

5-Bromopentanoic acid ethyl ester (33.03 g, 25 mL, 158 mmol) and 2-amino-4-methylpyridine (32.9 g, 304 mmol) were refluxed over night at 130 °C (oil bath temperature). After cooling down to room temperature, saturated NaHCO₃-solution

(100 mL) was added to the reaction mixture, which was then extracted with diethyl ether (5×100 mL). The combined organic phases were dried over MgSO_4 and the solvent was removed *in vacuo*. The residue was submitted to flash chromatography (ethyl acetate/hexane, 1:1, 2 L; 3:2, 1 L; 7:3, 1 L; 4:1, 1 L), drying yielded a colourless solid (16.7 g, 70.7 mmol, 45%).

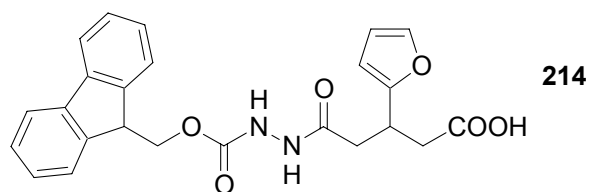
mp 41-43 °C; **TLC** R_f (ethyl acetate/hexane, 1:1) = 0.26; **$^1\text{H-NMR}$** (250 MHz, $\text{DMSO-}d_6$, 300 K) δ = 7.90 (d, J = 5.3 Hz, 1H, N-CH-CH), 6.38 (d, J = 5.2 Hz, 1H, N-C-CH), 6.17 (s, 1H, N-CH-CH), 4.51 (bs, 1H, NH), 4.11 (q, J = 7.2 Hz, 2H, O-CH₂-CH₃), 3.25 (q, J = 6.3 Hz, 2H, NH-CH₂), 2.33 (t, J = 7.0 Hz, 2H, CH₂-CO), 2.21 (s, 3H, C-CH₃), 1.60-1.80 (m, 4H, NH-CH₂-CH₂-CH₂), 1.23 (t, J = 7.0 Hz, 2H, O-CH₂-CH₃); **Analytical HPLC** (5-90% in 30 min) t_R = 13.58 min.



5-[N-(4-Methylpyridine-2-yl)amino]pentanoic acid (213)

5-[N-(4-Methylpyridine-2-yl)amino]pentanoic acid ethyl ester (**212**) (16.7 g, 70.7 mmol) was dissolved in methanol (20 mL), treated with 2 M aqueous NaOH (71 mL, 141 mmol) and stirred at room temperature over night. Then the solvent was removed *in vacuo* and the remaining solid was thoroughly extracted with CHCl_3 (500 mL) and excess of DIPEA. The filtrate was evaporated, drying yielded a colourless solid (3.92 g, 18.8 mmol, 27 %).

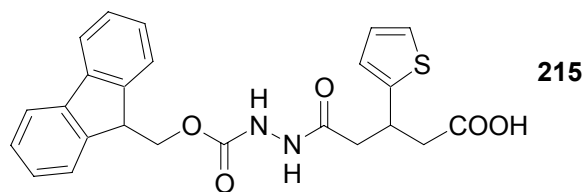
mp 138-140 °C; **$^1\text{H-NMR}$** (250 MHz, $\text{DMSO-}d_6$, 300 K) δ = 7.79 (d, J = 5.2 Hz, 1H, NH), 6.26-6.30 (m, 2H, arom), 6.22 (s, 1H, arom), 3.17 (dt, J = 5.8 Hz, 2H, NH-CH₂), 2.21 (t, J = 7.0 Hz, 2H, CH₂-CH₂-CO), 2.11 (s, 3H, CH₃), 1.41-1.58 (m, 4H, NH-CH₂-CH₂-CH₂); **$^{13}\text{C-NMR}$** (62.9 MHz, $\text{DMSO-}d_6$, 300 K) δ = 174.6 (COOH), 159.3, 147.3, 146.8, 113.1, 107.9, 40.5, 33.7, 28.8, 22.4, 20.8; **HRMS** (ESI-TOF) for $\text{C}_{11}\text{H}_{17}\text{N}_2\text{O}_2$ $[\text{M}+\text{H}]^+$: 209.1293 (calcd 209.1290); **Analytical HPLC** (5-90 % in 30 min) t_R = 9.83 min.



5-[*N'*-(9*H*-Fluoren-9-ylmethoxycarbonyl)hydrazino]-5-oxo-3-(furan-2-yl)pentanoic acid (214)

5-[*N'*-(9*H*-Fluoren-9-ylmethoxycarbonyl)hydrazino]-5-oxo-3-(furan-2-yl)pentanoic acid (**214**) was prepared from 3-(furan-2-yl)glutaric acid anhydride (**204**) (0.6 g, 3.3 mmol) and *N*-[(9*H*-fluoren-9-ylmethoxy)carbonyl]hydrazine (**140**) (0.85 g, 3.3 mmol) according to general method 26. The residue was chromatographed, drying yielded a colourless solid foam (1.13 g, 2.6 mmol, 79%).

mp 143/144 °C; **TLC** R_f (ethyl acetate/hexane/acetic acid, 2:1:1%) = 0.30; **¹H-NMR** (250 MHz, DMSO-*d*₆, 300 K) δ = 9.80 (s, 1H, NH-NH), 9.26 (s, 1H, NH-NH), 7.89 (d, J = 7.3 Hz, 2H, arom), 7.71 (d, J = 7.3 Hz, 2H, arom), 7.50 (s, 1H, O-CH-CH), 7.29-7.44 (m, 4H, arom), 6.32-6.33 (m, 1H, O-CH-CH), 6.09-6.12 (m, 1H, O-C-CH), 4.20-4.34 (m, 3H, CH-CH₂-O), 3.51-3.60 (m, 1H, CH₂-CH-CH₂), 2.36-2.68 (m, 4H, CH₂-CH-CH₂); **HPLC-MS** (ESI) m/z 195.1 (25), 435.1 (65) [M+H]⁺, 457.4 (50) [M+Na]⁺, 473.3 (12) [M+K]⁺, 671.5 (50), 869.2 (100) [2M+H]⁺, 891.3 (87) [2M+Na]⁺, 907.4 (47) [2M+K]⁺, 1105.6 (35), 1303.1 (37) [3M+H]⁺; **HRMS** (ESI-TOF) for C₂₄H₂₃N₂O₆ [M+H]⁺: 435.1565 (calcd 435.1556); **Analytical HPLC** (5-90% in 30 min) t_R = 21.88 min.

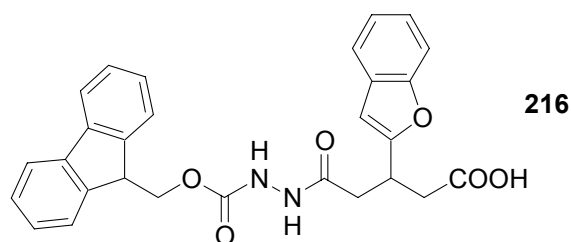


5-[*N'*-(9*H*-Fluoren-9-ylmethoxycarbonyl)hydrazino]-5-oxo-3-(thiophene-2-yl)pentanoic acid (215)

5-[*N'*-(9*H*-Fluoren-9-ylmethoxycarbonyl)hydrazino]-5-oxo-3-(thiophene-2-yl)pentanoic acid (**215**) was prepared from 3-(thiophene-2-yl)glutaric acid anhydride

(**205**) (0.7 g, 3.6 mmol) and *N*-[(9*H*-fluoren-9-ylmethoxy)carbonyl]hydrazine (**140**) (0.91 g, 3.6 mmol) according to general method 26. The residue was chromatographed, drying yielded a colourless solid foam (1.3 g, 2.9 mmol, 81%).

mp 86/87 °C; **TLC** R_f (ethyl acetate/hexane/acetic acid, 2:1:1%) = 0.33; **¹H-NMR** (250 MHz, DMSO-*d*₆, 300 K) δ = 9.77 (s, 1H, *NH-NH*), 9.25 (s, 1H, *NH-NH*), 7.88 (d, J = 7.4 Hz, 2H, arom), 7.71 (d, J = 7.0 Hz, 2H, arom), 7.31-7.44 (m, 5H, arom), 6.89 (m, 2H, S-CH-CH-CH), 4.23-4.33 (m, 3H, CH-CH₂-O), 3.78 (m, 1H, CH₂-CH-CH₂), 2.47-2.78 (m, 4H, CH₂-CH-CH₂); **HPLC-MS** (ESI) m/z 179.2 (25), 433.1 (15), 451.1 (42) [M+H]⁺, 473.3 (52) [M+Na]⁺, 489.2 (15) [M+K]⁺, 695.5 (50), 901.2 (50) [2M+H]⁺, 923.2 (100) [2M+Na]⁺, 939.3 (55) [2M+K]⁺, 1145.4 (15), 1351.1 (10) [3M+H]⁺, 1373.2 (30) [3M+Na]⁺, 1389.3 (20) [3M+K]⁺; **HRMS** (ESI-TOF) for C₂₄H₂₃N₂O₅S [M+H]⁺: 451.1339 (calcd 451.1328); **Analytical HPLC** (5-90% in 30 min) t_R = 22.10 min.

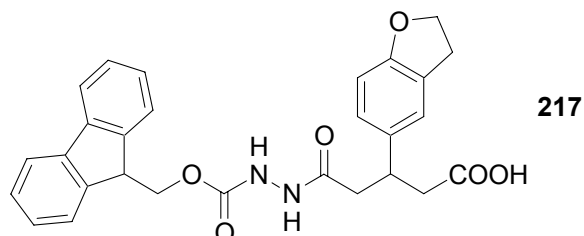


5-[*N'*-(9*H*-Fluoren-9-ylmethoxycarbonyl)hydrazino]-5-oxo-3-(benzofuran-2-yl)pentanoic acid (**216**)

5-[*N'*-(9*H*-Fluoren-9-ylmethoxycarbonyl)hydrazino]-5-oxo-3-(benzofuran-2-yl)pentanoic acid (**216**) was prepared from 3-(benzofuran-2-yl)glutaric acid anhydride (**206**) (0.7 g, 3.0 mmol) and *N*-[(9*H*-fluoren-9-ylmethoxy)carbonyl]hydrazine (**140**) (0.77 g, 3.0 mmol) according to general method 26. The residue was chromatographed, drying yielded a colourless solid foam (1.1 g, 2.3 mmol, 77%).

mp 167 °C; **TLC** R_f (ethyl acetate/hexane/acetic acid, 2:1:1%) = 0.24; **¹H-NMR** (250 MHz, DMSO-*d*₆, 300 K) δ = 9.85 (s, 1H, *NH-NH*), 9.27 (s, 1H, *NH-NH*), 7.88 (d, J = 7.4 Hz, 2H, arom), 7.71 (d, J = 7.4 Hz, 2H, arom), 7.15-7.54 (m, 8H, arom), 6.61 (s, 1H, O-C-CH), 4.24-4.34 (m, 3H, CH-CH₂-O), 3.64-3.75 (m, 1H, CH₂-CH-CH₂), 2.53-

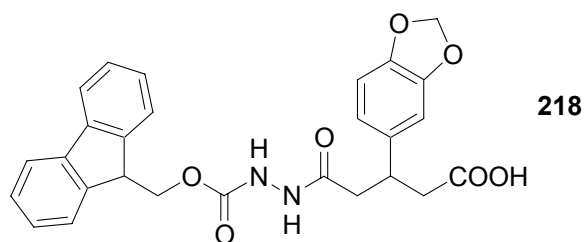
2.78 (m, 4H, $CH_2-CH-CH_2$); **HPLC-MS** (ESI) m/z 179.2 (45), 245.2 (35), 289.1 (25), 307.1 (25), 467.1 (15), 485.2 (77) $[M+H]^+$, 507.4 (55) $[M+Na]^+$, 523.3 (40) $[M+K]^+$, 746.7 (70), 969.3 (100) $[2M+H]^+$, 991.4 (90) $[2M+Na]^+$, 1007.4 (73) $[2M+K]^+$, 1230.8 (20), 1453.2 (30) $[3M+H]^+$; **HRMS** (ESI-TOF) for $C_{28}H_{25}N_2O_6$ $[M+H]^+$: 485.1718 (calcd 485.1713); **Analytical HPLC** (5-90% in 30 min) $t_R = 24.16$ min.



5-[*N'*-(9*H*-Fluoren-9-ylmethoxycarbonyl)hydrazino]-5-oxo-3-(2,3-dihydrobenzo [*b*]furan-5-yl)pentanoic acid (217)

5-[*N'*-(9*H*-Fluoren-9-ylmethoxycarbonyl)hydrazino]-5-oxo-3-(2,3-dihydrobenzo [*b*]furan-5-yl)pentanoic acid (**217**) was prepared from 3-(2,3-dihydrobenzo [*b*]furan-5-yl)glutaric acid anhydride (**207**) (0.35 g, 1.5 mmol) and *N*-[(9*H*-fluoren-9-ylmethoxy) carbonyl]hydrazine (**140**) (0.38 g, 1.5 mmol) according to general method 26. The residue was chromatographed, drying yielded a colourless solid foam (0.6 g, 1.2 mmol, 80%).

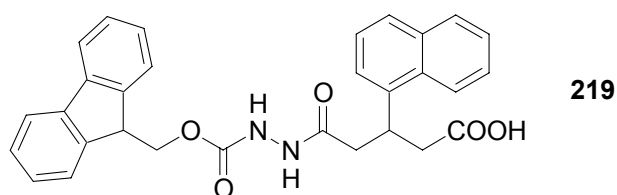
mp 161/162 °C; **TLC** R_f (ethyl acetate/hexane/acetic acid) = 0.26; **¹H-NMR** (250 MHz, DMSO- d_6 , 300 K) $\delta = 9.68$ (s, 1H, *NH-NH*), 9.20 (s, 1H, *NH-NH*), 7.89 (d, $J = 7.4$ Hz, 2H, arom), 7.71 (d, $J = 7.0$ Hz, 2H, arom), 7.29-7.44 (m, 4H, arom), 7.08 (s, 1H, O-C-C-*CH*-C), 6.93 (d, $J = 8.0$ Hz, 1H, C-*CH*-*CH*-C-O), 6.63 (d, $J = 7.7$ Hz, 1H, C-*CH*-*CH*-C-O), 4.46 (t, $J = 8.4$ Hz, 2H, O- CH_2-CH_2), 4.25-4.32 (m, 3H, *CH-CH_2*-O), 3.40 (m, 1H, $CH_2-CH-CH_2$), 3.11 (t, $J = 8.0$ Hz, 2H, O- CH_2-CH_2), 2.36-2.71 (m, 4H, $CH_2-CH-CH_2$); **HPLC-MS** (ESI) m/z 179.2 (25), 247.2 (28), 291.0 (11), 469.1 (19), 487.2 (55) $[M+H]^+$, 509.4 (57) $[M+Na]^+$, 525.3 (35) $[M+K]^+$, 749.7 (76) $[(3M+K+H)/2]^{2+}$, 768.7 (14), 973.3 (72) $[2M+H]^+$, 995.4 (100) $[2M+Na]^+$, 1011.5 (85) $[2M+K]^+$, 1235.8 (33), 1459.3 (10) $[3M+H]^+$, 1481.3 (20) $[3M+Na]^+$, 1497.6 (22) $[3M+K]^+$; **HRMS** (ESI-TOF) for $C_{28}H_{27}N_2O_6$ $[M+H]^+$: 487.1868 (calcd 487.1869); **Analytical HPLC** (5-90% in 30 min) $t_R = 22.23$ min.



5-[*N'*-(9*H*-Fluoren-9-ylmethoxycarbonyl)hydrazino]-5-oxo-3-(1,3-benzodioxole-5-yl)pentanoic acid (218)

5-[*N'*-(9*H*-Fluoren-9-ylmethoxycarbonyl)hydrazino]-5-oxo-3-(1,3-benzodioxole-5-yl)pentanoic acid (**218**) was prepared from 3-(1,3-benzodioxole-5-yl)glutaric acid anhydride (**208**) (1.0 g, 4.3 mmol) and *N*-[(9*H*-fluoren-9-ylmethoxy)carbonyl]hydrazine (**140**) (1.1 g, 4.3 mmol) according to general method 26. The residue was chromatographed, drying yielded a yellow solid foam (2.0 g, 4.1 mmol, 95%).

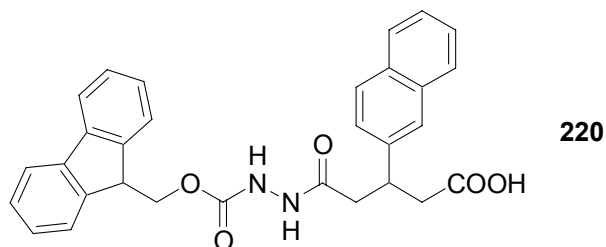
mp 100 °C; **HPLC-MS** (ESI) *m/z* 179.2 (42), 249.1 (54), 293.0 (30), 471.0 (26), 489.0 (76) [M+H]⁺, 511.2 (76) [M+Na]⁺, 527.1 (37) [M+K]⁺, 752.3 (27), 977.0 (94) [2M+H]⁺, 999.0 (100) [2M+Na]⁺, 1015.1 (70) [2M+K]⁺, 1486.8 (14) [3M+Na]⁺; **HRMS** (ESI-TOF) for C₂₇H₂₅N₂O₇ [M+H]⁺: 489.1688 (calcd 489.1662); **Analytical HPLC** (5-90% in 30 min) *t_R* = 20.82 min.



5-[*N'*-(9*H*-Fluoren-9-ylmethoxycarbonyl)hydrazino]-5-oxo-3-(naphth-1-yl)pentanoic acid (219)

5-[*N'*-(9*H*-Fluoren-9-ylmethoxycarbonyl)hydrazino]-5-oxo-3-(naphth-1-yl)pentanoic acid (**219**) was prepared from 3-(naphth-1-yl)glutaric acid anhydride (**209**) (0.51 g, 2.1 mmol) and *N*-[(9*H*-fluoren-9-ylmethoxy)carbonyl]hydrazine (**140**) (0.54 g, 2.1 mmol) according to general method 26. The residue was chromatographed, drying yielded a colourless solid foam (0.85 g, 1.7 mmol, 81%).

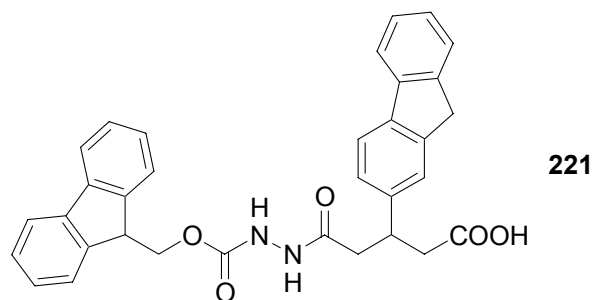
mp 208 °C; **¹H-NMR** (250 MHz, DMSO-*d*₆, 300 K) δ = 9.85 (s, 1H, NH-NH), 9.26 (s, 1H, NH-NH), 8.24 (d, *J* = 8.3 Hz, 1H, arom), 7.87-7.93 (m, 3H, arom), 7.70-7.80 (m, 3H, arom), 7.29-7.62 (m, 8H, arom), 4.24-4.41 (m, 4H, CH-CH₂-O and CH₂-CH-CH₂), 2.53-2.84 (m, 4H, CH₂-CH-CH₂); **HPLC-MS** (ESI) *m/z* 179.2 (60), 241.2 (22), 255.2 (27), 495.3 (60) [M+H]⁺, 517.5 (90) [M+Na]⁺, 533.3 (76) [M+K]⁺, 761.8 (48) (3M+K+Na)/2]²⁺, 780.7 (15), 989.4 (64) [2M+H]⁺, 1011.5 (92) [2M+Na]⁺, 1027.5 (100) [2M+K]⁺, 1256.1 (14), 1483.4 (10) [3M+H]⁺, 1505.6 (10) [3M+Na]⁺, 1521.6 (10) [3M+K]⁺; **HRMS** (ESI-TOF) for C₃₀H₂₇N₂O₅ [M+H]⁺: 495.1893 (calcd 495.1920); **Analytical HPLC** (5-90% in 30 min) *t*_R = 24.14 min.



5-[*N'*-(9*H*-Fluoren-9-ylmethoxycarbonyl)hydrazino]-5-oxo-3-(naph-2-yl)pentanoic acid (**220**)

5-[*N'*-(9*H*-Fluoren-9-ylmethoxycarbonyl)hydrazino]-5-oxo-3-(naph-2-yl)pentanoic acid (**220**) was prepared from 3-(naph-2-yl)glutaric acid anhydride (**210**) (0.72 g, 3.0 mmol) and *N*-[(9*H*-fluoren-9-ylmethoxy)carbonyl]hydrazine (**140**) (0.76 g, 3.0 mmol) according to general method 26. The residue was chromatographed, drying yielded a colourless solid foam (1.1 g, 2.2 mmol, 73%).

mp 101-103°C; **TLC** *R*_f (ethyl acetate/hexane/acetic acid, 2:1:1%) = 0.26; **¹H-NMR** (250 MHz, DMSO-*d*₆, 300 K) δ = 12.03 (bs, 1H, COOH), 9.76 (s, 1H, NH-NH), 9.21 (s, 1H, NH-NH), 7.29-7.90 (m, 15H, arom), 4.23-4.33 (m, 3H, CH-CH₂-O), 3.67 (m, 1H, CH₂-CH-CH₂), 2.60-2.78 (m, 4H, CH₂-CH-CH₂); **MS** (ESI) *m/z* 179.1 (31), 241.1 (24), 255.1 (40), 299.0 (27), 477.0 (12), 495.0 (60) [M+H]⁺, 517.3 (36) [M+Na]⁺, 533.1 (25) [M+K]⁺, 989.0 (100) [2M+H]⁺, 1011.1 (52) [2M+Na]⁺, 1027.1 (44) [2M+K]⁺; **HRMS** (ESI-TOF) for C₃₀H₂₇N₂O₅ [M+H]⁺: 495.1893 (calcd 495.1920); **Analytical HPLC** (5-90% in 30 min) *t*_R = 23.45 min.



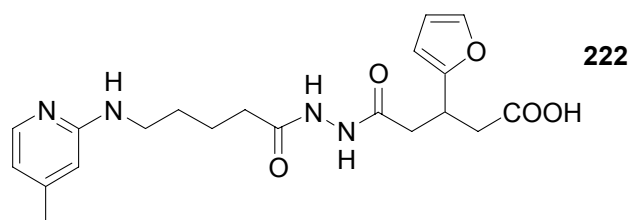
5-[*N'*-(9*H*-Fluoren-9-ylmethoxycarbonyl)hydrazino]-5-oxo-3-(9*H*-fluoren-2-yl)pentanoic acid (221)

5-[*N'*-(9*H*-Fluoren-9-ylmethoxycarbonyl)hydrazino]-5-oxo-3-(9*H*-fluoren-2-yl)pentanoic acid (**221**) was prepared from 3-(9*H*-fluoren-2-yl)glutaric acid anhydride (**211**) (1.0 g, 3.6 mmol) and *N*-[(9*H*-fluoren-9-ylmethoxy)carbonyl]hydrazine (**140**) (0.91 g, 3.6 mmol) according to general method 26. The residue was chromatographed, drying yielded a colourless solid foam (1.2 g, 2.3 mmol, 64%).

mp 130 °C; **¹H-NMR** (250 MHz, DMSO-*d*₆, 300 K) δ = 9.72 (s, 1H, NH-NH), 9.20 (s, 1H, NH-NH), 7.21-7.89 (m, 15H, arom), 4.22-4.32 (m, 3H, CH-CH₂-O), 3.55 (m, 1H, CH₂-CH-CH₂), 2.37-2.81 (m, 4H, CH₂-CH-CH₂); **MS** (ESI) *m/z* 179.1 (38), 279.1 (46), 293.1 (66), 337.0 (20), 515.0 (16), 533.0 (70) [M+H]⁺, 555.3 (36) [M+Na]⁺, 571.1 (43) [M+K]⁺, 1065.0 (100) [2M+H]⁺, 1103.1 (38) [2M+K]⁺; **HRMS** (ESI-TOF) for C₃₃H₂₉N₂O₅ [M+H]⁺: 533.2111 (calcd 533.2076); **Analytical HPLC** (5-90% in 30 min) *t*_R = 24.65 min.

8.4.2 Peptidomimetic $\alpha\text{v}\beta\text{3}$ Integrin Antagonists

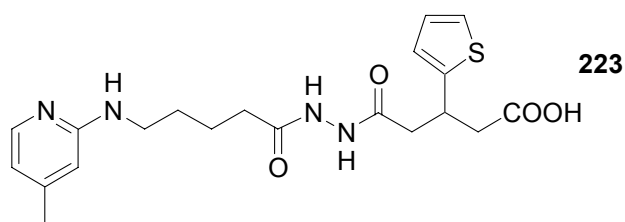
Peptidomimetic $\alpha\text{v}\beta\text{3}$ antagonists were synthesized on solid support (TCP resin). Resin weights before and after loading (m_1 and m_2) and resin loading (l) are given in brackets. Yields are given with respect to the loaded resin.



5-{*N'*-[5-(4-Methylpyridine-2-ylamino)pentanoyl]hydrazino}-3-(furan-2-yl)-5-oxopentanoic acid (**222**)

TCP resin was loaded with 5-[*N'*-(9*H*-fluoren-9-ylmethoxycarbonyl)hydrazino]-5-oxo-3-(furan-2-yl)pentanoic acid (**214**) (0.27 g, 0.62 mmol) according to general method 2 ($m_1 = 430$ mg, $m_2 = 600$ mg, $l = 0.71$ mmol/g). Fmoc-deprotection and coupling of 5-[*N*-(4-methylpyridine-2-yl)amino]pentanoic acid (**213**) (177 mg, 0.85 mmol) were carried out according to general methods 3 and 5, cleavage from the resin was carried out according to general method 8. RP-HPLC purification and lyophilization yielded a colourless, solid resin (13.8 mg, 0.0342 mmol, 8%).

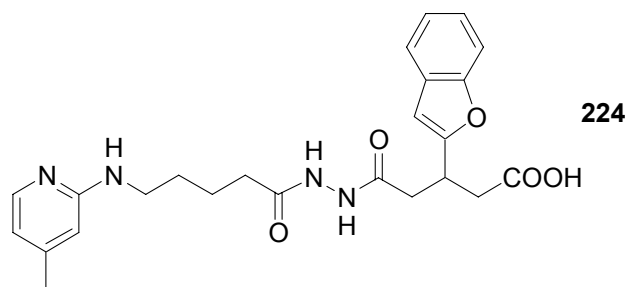
mp 69-72 °C; **¹H-NMR** (500 MHz, DMSO-*d*₆, 300 K) $\delta = 12.22$ (bs, 1H, COOH), 9.80 (s, 1H, NH-NH), 9.73 (s, 1H, NH-NH), 8.41 (bs, 1H, NH-CH₂), 7.81 (d, $J = 6.0$ Hz, 1H, N-CH), 7.50 (s, 1H, CH-O), 6.80 (s, 1H, N-C-CH), 6.68 (d, $J = 6.0$ Hz, 1H, N-CH-CH), 6.33 (s, 1H, CH-CH-O), 6.12 (s, 1H, CH-CH-CH-O), 3.56 (m, 1H, CH₂-CH-CH₂), 3.27 (m, 2H, NH-CH₂), 2.64 (dd, $J = 15.9$ Hz, $J = 5.1$ Hz, 1H, CH₂-CH-CH₂), 2.49-2.54 (m, 2H, CH₂-CH-CH₂), 2.40 (dd, $J = 14.7$ Hz, $J = 7.7$ Hz, 1H, CH₂-CH-CH₂), 2.31 (s, 3H, CH₃), 2.16 (m, 2H, CH₂-CH₂-CO), 1.59 (m, 4H, CH₂-CH₂-CH₂-CO); **MS** (ESI) m/z 191.2 (100), 223.2 (48), 385.4 (28), 403.3 (96) [M+H]⁺, 441.2 (25) [M+K]⁺, 865.2 (21) [2M-H+2K]⁺; **HRMS** (ESI-TOF) for C₂₀H₂₇N₄O₅ [M+H]⁺: 403.1947 (calcd 403.1981); **Analytical HPLC** (5-90% in 30 min) $t_R = 11.53$ min (95% purity at 220 nm).



5-{*N'*-[5-(4-Methylpyridine-2-ylamino)pentanoyl]hydrazino}-3-(thiophene-2-yl)-5-oxopentanoic acid (**223**)

TCP resin was loaded with 5-[*N'*-(9*H*-fluoren-9-ylmethoxycarbonyl)hydrazino]-5-oxo-3-(thiophene-2-yl)pentanoic acid (**215**) (0.29 g, 0.64 mmol) according to general method 2 ($m_1 = 474$ mg, $m_2 = 600$ mg, $l = 0.51$ mmol/g). Fmoc-deprotection and coupling of 5-[*N*-(4-methylpyridine-2-yl)amino]pentanoic acid (**213**) (127 mg, 0.61 mmol) were carried out according to general methods 3 and 5, cleavage from the resin was carried out according to general method 8. RP-HPLC purification and lyophilization yielded a colourless powder (38.0 mg, 0.0907 mmol, 30%).

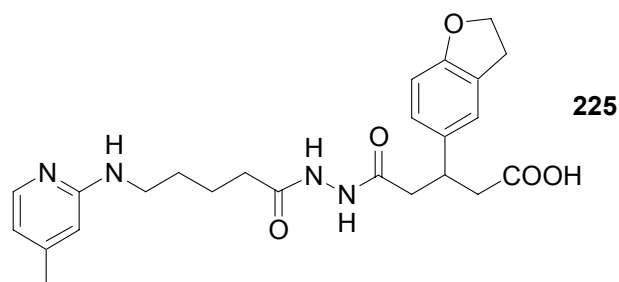
mp 67-72 °C; **¹H-NMR** (500 MHz, DMSO-*d*₆, 300 K) $\delta = 12.19$ (bs, 1H, COOH), 9.79 (s, 1H, NH-NH), 9.71 (s, 1H, NH-NH), 8.49 (bs, 1H, NH-CH₂), 7.80 (m, 1H, N-CH), 7.30 (m, 1H, S-CH), 6.89-6.91 (m, 2H, arom), 6.81 (s, 1H, arom), 6.69 (m, 1H, N-CH-CH), 3.77 (m, 1H, CH₂-CH-CH₂), 3.27 (m, 2H, NH-CH₂), 2.72-2.78 (m, 1H, CH₂-CH-CH₂), 2.49 (m, 3H, CH₂-CH-CH₂), 2.32 (s, 3H, CH₃), 2.15 (m, 2H, CH₂-CH₂-CO), 1.58 (m, 4H, CH₂-CH₂-CH₂-CO); **HPLC-MS** (ESI) m/z 191.2 (97), 223.2 (47), 401.3 (23), 419.3 (100) [M+H]⁺, 441.3 (6) [M+Na]⁺, 457.2 (5) [M+K]⁺; **HRMS** (ESI-TOF) for C₂₀H₂₇N₄O₄S [M+H]⁺: 419.1731 (calcd 419.1753); **Analytical HPLC** (5-90% in 30 min) $t_R = 11.75$ min (94% purity at 220 nm).



5-{*N'*-[5-(4-Methylpyridine-2-ylamino)pentanoyl]hydrazino}-3-(benzo[*b*]furan-2-yl)-5-oxopentanoic acid (224)

TCP resin was loaded with 5-[*N'*-(9*H*-fluoren-9-ylmethoxycarbonyl)hydrazino]-5-oxo-3-(benzofuran-2-yl)pentanoic acid (**216**) (0.31 g, 0.64 mmol) was loaded on the resin according to general method 2 ($m_1 = 480$ mg, $m_2 = 600$ mg, $l = 0.45$ mmol/g). Fmoc-deprotection and coupling of 5-[*N*-(4-methylpyridine-2-yl)amino]pentanoic acid (**213**) (112 mg, 0.54 mmol) were carried out according to general methods 3 and 5, cleavage from the resin was carried out according to general method 8. RP-HPLC purification and lyophilization yielded a colourless powder (39.4 mg, 0.087 mmol, 32%).

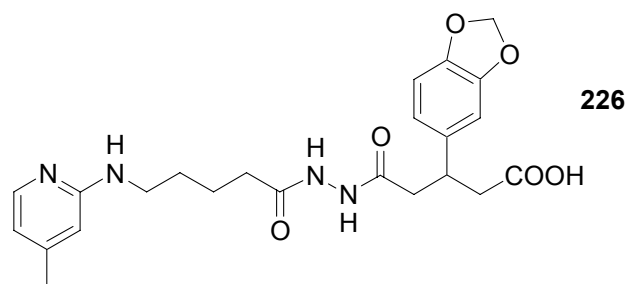
mp 112-114 °C; **¹H-NMR** (500 MHz, DMSO-*d*₆, 300 K) $\delta = 12.31$ (bs, 1H, COOH), 9.85 (s, 1H, NH-NH), 9.72 (s, 1H, NH-NH), 8.48 (bs, 1H, NH-CH₂), 7.80 (m, 1H, N-CH), 7.53 (d, $J = 6.8$ Hz, 1H, O-C-(CH)₃-CH), 7.48 (d, $J = 8.0$ Hz, 1H, O-C-CH-CH), 7.19-7.23 (m, 2H, O-C-CH-(CH)₂), 6.81 (s, 1H, N-C-CH), 6.69 (m, 1H, N-CH-CH), 6.61 (s, 1H, O-C-CH-C), 3.71 (m, 1H, CH₂-CH-CH₂), 3.27 (m, 2H, NH-CH₂), 2.63-2.74 (m, 3H, CH₂-CH-CH₂), 2.53-2.55 (m, 1H, CH₂-CH-CH₂), 2.31 (s, 3H, CH₃), 2.15 (m, 2H, CH₂-CH₂-CO), 1.58 (m, 4H, CH₂-CH₂-CH₂-CO); **MS** (ESI) m/z 191.2 (56), 223.2 (26), 453.3 (100) [M+H]⁺, 491.3 (15) [M+K]⁺, 943.3 (13) [2M+K]⁺, 965.4 (10) [2M-H+K+Na]⁺; **HRMS** (ESI-TOF) for C₂₄H₂₉N₄O₅ [M+H]⁺: 453.2159 (calcd 453.2138); **Analytical HPLC** (5-90% in 30 min) $t_R = 14.92$ min (96% purity at 220 nm).



5-{*N'*-[5-(4-Methylpyridine-2-ylamino)pentanoyl]hydrazino}-3-(2,3-dihydrobenzo[*b*]furan-5-yl)-5-oxopentanoic acid (225)

TCP resin was loaded with 5-[*N'*-(9*H*-fluoren-9-ylmethoxycarbonyl)hydrazino]-5-oxo-3-(2,3-dihydrobenzo[*b*]furan-5-yl)pentanoic acid (**217**) (0.28 g, 0.57 mmol) according to general method 2 ($m_1 = 420$ mg, $m_2 = 600$ mg, $l = 0.66$ mmol/g). Fmoc-deprotection and coupling of 5-[*N*-(4-methylpyridine-2-yl)amino]pentanoic acid (**213**) (165 mg, 0.79 mmol) were carried out according to general methods 3 and 5, cleavage from the resin was carried out according to general method 8. RP-HPLC purification and lyophilization yielded a colourless powder (10.8 mg, 0.0237 mmol, 6%).

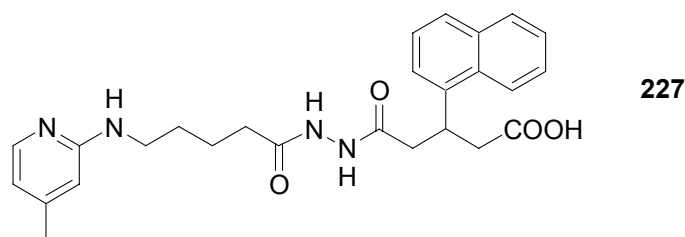
mp 75-80 °C; **¹H-NMR** (500 MHz, DMSO-*d*₆, 300 K) $\delta = 11.92$ (bs, 1H, COOH), 9.69 (s, 1H, NH-NH), 9.67 (s, 1H, NH-NH), 8.44 (bs, 1H, NH-CH₂), 7.80 (d, $J = 6.4$ Hz, N-CH), 7.08 (s, 1H, C-CH-C-O), 6.92 (d, $J = 8.1$ Hz, 1H, CH-CH-C-CH₂-CH₂-O), 6.81 (s, 1H, N-C-CH), 6.70 (d, $J = 6.4$ Hz, 1H, N-CH-CH), 6.63 (d, $J = 8.2$ Hz, 1H, CH-CH-C-CH₂-CH₂-O), 4.47 (t, $J = 8.6$ Hz, 2H, CH₂-CH₂-O), 3.36-3.43 (m, 1H, CH₂-CH-CH₂), 3.26-3.28 (m, 2H, NH-CH₂), 3.12 (t, $J = 8.6$ Hz, 2H, CH₂-CH₂-O), 2.67 (dd, $J = 15.5$ Hz, $J = 5.6$ Hz, 1H, CH₂-CH-CHH), 2.36-2.47 (m, 3H, CH₂-CH-CHH), 2.32 (s, 3H, CH₃), 2.14 (m, 2H, CH₂-CH₂-CO), 1.58 (m, 4H, CH₂-CH₂-CH₂-CO); **HPLC-MS** (ESI) m/z 191.1 (100), 223.1 (55), 437.2 (15), 455.2 (54) [M+H]⁺, 477.2 (6) [M+Na]⁺; **HRMS** (ESI-TOF) for C₂₄H₃₁N₄O₅ [M+H]⁺: 455.2310 (calcd 455.2294); **Analytical HPLC** (5-90% in 30 min) $t_R = 12.44$ min (95% purity at 220 nm).



5-{*N'*-[5-(4-Methylpyridine-2-ylamino)pentanoyl]hydrazino}-3-(1,3-benzodioxole-5-yl)-5-oxopentanoic acid (226)

TCP resin was loaded with 5-[*N'*-(9*H*-fluoren-9-ylmethoxycarbonyl)hydrazino]-5-oxo-3-(1,3-benzodioxole-5-yl)pentanoic acid (**218**) (0.35 g, 0.72 mmol) according to general method 2 ($m_1 = 525$ mg, $m_2 = 700$ mg, $l = 0.55$ mmol/g). Fmoc-deprotection and coupling of 5-[*N*-(4-methylpyridine-2-yl)amino]pentanoic acid (**213**) (160 mg, 0.77 mmol) were carried out according to general methods 3 and 5, cleavage from the resin was carried out according to general method 8. RP-HPLC purification and lyophilization yielded a colourless powder (103.9 mg, 0.228 mmol, 59%).

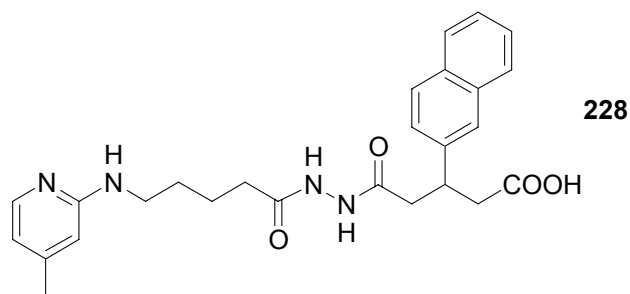
mp 85-90 °C; **¹H-NMR** (500 MHz, DMSO-*d*₆, 300 K) $\delta = 9.70$ (s, 1H, NH-NH), 9.67 (s, 1H, NH-NH), 8.53 (bs, 1H, NH-CH₂), 7.81 (m, 1H, N-CH), 6.78-6.83 (m, 3H, N-CH-CH and CH-CH-C-O and C-CH-C-O), 6.67-6.71 (m, 2H, N-CH-CH and CH-CH-C-O), 5.96 (s, 2H, O-CH₂-O), 3.36-3.43 (m, 1H, CH₂-CH-CH₂), 3.28 (m, 2H, NH-CH₂), 2.63-2.69 (m, 1H, CH₂-CH-CHH), 2.35-2.50 (m, 3H, CH₂-CH-CHH), 2.33 (s, 3H, CH₃), 2.14 (m, 2H, CH₂-CH₂-CO), 1.58 (m, 4H, CH₂-CH₂-CH₂-CO); **HPLC-MS** (ESI) m/z 191.1 (100), 223.1 (60), 439.2 (15), 457.2 (90) [M+H]⁺, 479.2 (10) [M+Na]⁺; 934.9 (15) [2M+Na]⁺; **HRMS** (ESI-TOF) for C₂₃H₂₉N₄O₆ [M+H]⁺: 457.2052 (calcd 457.2087); **Analytical HPLC** (5-90% in 30 min) $t_R = 12.44$ min (96% purity at 220 nm).



5-{*N'*-[5-(4-Methylpyridine-2-ylamino)pentanoyl]hydrazino}-3-(naphth-1-yl)-5-oxopentanoic acid (**227**)

TCP resin was loaded with 5-[*N'*-(9*H*-fluoren-9-ylmethoxycarbonyl)hydrazino]-5-oxo-3-(naphth-1-yl)pentanoic acid (**219**) (0.29 g, 0.59 mmol) according to general method 2 ($m_1 = 435$ mg, $m_2 = 600$ mg, $l = 0.60$ mmol/g). Fmoc-deprotection and coupling of 5-[*N*-(4-methylpyridine-2-yl)amino]pentanoic acid (**213**) (150 mg, 0.72 mmol) were carried out according to general methods 3 and 5, cleavage from the resin was carried out according to general method 8. RP-HPLC purification and lyophilization yielded a colourless powder (79.8 mg, 0.173 mmol, 48%).

mp 90-95 °C; **¹H-NMR** (500 MHz, DMSO-*d*₆, 300 K) $\delta = 12.09$ (bs, 1H, COOH), 9.83 (s, 1H, NH-NH), 9.69 (s, 1H, NH-NH), 8.51 (bs, 1H, NH-CH₂), 8.21 (d, $J = 7.7$ Hz, 1H, 9-*H*), 7.92 (d, $J = 7.7$ Hz, 1H, 6-*H*), 7.72-7.82 (m, 2H, N-CH and 4-*H*), 7.47-7.58 (m, 4H, 2-*H*, 3-*H*, 7-*H*, 8-*H*), 6.82 (s, 1H, N-C-CH), 6.70 (d, $J = 5.3$ Hz, 1H, N-CH-CH), 4.35-4.43 (m, 1H, CH₂-CH-CH₂), 3.27 (m, 2H, NH-CH₂), 2.74-2.85 (m, 2H, CH₂-CH-CH₂), 2.58-2.65 (m, 1H, HHC-CH-CH₂), 2.49-2.55 (m, 1H, HHC-CH-CH₂), 2.32 (s, 3H, CH₃), 2.14 (m, 2H, CH₂-CH₂-CO), 1.59 (m, 4H, CH₂-CH₂-CH₂-CO); **HPLC-MS** (ESI) m/z 191.1 (100), 223.1 (62), 445.3 (15), 463.2 (83) [M+H]⁺, 485.2 (8) [M+Na]⁺; **HRMS** (ESI-TOF) for C₂₆H₃₁N₄O₄ [M+H]⁺: 463.2308 (calcd 463.2345); **Analytical HPLC** (5-90% in 30 min) $t_R = 14.57$ min (94% purity at 220 nm).

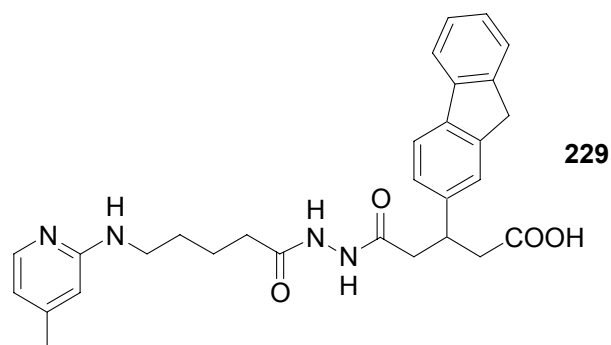


228

5-{*N'*-[5-(4-Methylpyridine-2-ylamino)pentanoyl]hydrazino}-3-(naphth-2-yl)-5-oxopentanoic acid (228)

TCP resin was loaded with 5-[*N'*-(9*H*-fluoren-9-ylmethoxycarbonyl)hydrazino]-5-oxo-3-(naphth-2-yl)pentanoic acid (**220**) (0.31 g, 0.63 mmol) according to general method 2 ($m_1 = 465$ mg, $m_2 = 600$ mg, $l = 0.49$ mmol/g). Fmoc-deprotection and coupling of 5-[*N*-(4-methylpyridine-2-yl)amino]pentanoic acid (**213**) (122 mg, 0.59 mmol) were carried out according to general methods 3 and 5, cleavage from the resin was carried out according to general method 8. RP-HPLC purification and lyophilization yielded a colourless powder (43.4 mg, 0.0938 mmol, 32%).

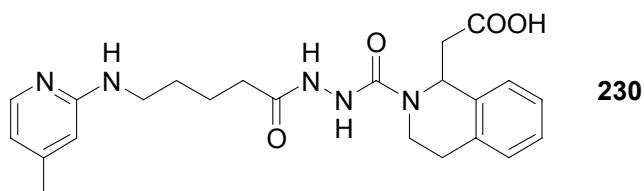
mp 92-95 °C; **¹H-NMR** (500 MHz, DMSO-*d*₆, 300 K) $\delta = 9.76$ (s, 1H, NH-NH), 9.65 (s, 1H, NH-NH), 8.52 (bs, 1H, NH-CH₂), 7.82-7.86 (m, 3H, 4-*H*, 6-*H*, 9-*H*), 7.80 (d, $J = 6.5$ Hz, 1H, N-CH), 7.73 (s, 1H, 1-*H*), 7.43-7.49 (m, 3H, 3-*H*, 7-*H*, 8-*H*), 6.82 (s, 1H, N-C-CH), 6.70 (d, $J = 6.5$ Hz, 1H, N-CH-CH), 3.62-3.71 (m, 1H, CH₂-CH-CH₂), 3.26 (m, 2H, NH-CH₂), 2.80 (dd, $J = 15.8$ Hz, $J = 5.4$ Hz, 1H, CH₂-CH-CHH), 2.64 (dd, $J = 15.9$ Hz, $J = 9.7$ Hz, 1H, CH₂-CH-CHH), 2.56 (d, $J = 7.5$ Hz, 2H, CH₂-CH-CH₂), 2.32 (s, 3H, CH₃), 2.13 (m, 2H, CH₂-CH₂-CO), 1.57 (m, 4H, CH₂-CH₂-CH₂-CO); **MS** (ESI) m/z 191.1 (100), 223.1 (63), 445.3 (20), 463.2 (68) [M+H]⁺, 501.2 (10) [M+K]⁺; **HRMS** (ESI-TOF) for C₂₆H₃₁N₄O₄ [M+H]⁺: 463.2307 (calcd 463.2345); **Analytical HPLC** (5-90% in 30 min) $t_R = 15.23$ min (91% purity at 220 nm).



5-{*N'*-[5-(4-Methylpyridine-2-ylamino)pentanoyl]hydrazino}-3-(9*H*-fluoren-2-yl)-5-oxopentanoic acid (**229**)

TCP resin was loaded with 5-[*N'*-(9*H*-fluoren-9-ylmethoxycarbonyl)hydrazino]-5-oxo-3-(9*H*-fluoren-2-yl) pentanoic acid (**221**) (0.32 g, 0.6 mmol) according to general method 2 ($m_1 = 450$ mg, $m_2 = 600$ mg, $l = 0.50$ mmol/g). Fmoc-deprotection and coupling of 5-[*N*-(4-methylpyridine-2-yl)amino]pentanoic acid (**213**) (125 mg, 0.60 mmol) were carried out according to general methods 3 and 5, cleavage from the resin was carried out according to general method 8. RP-HPLC purification and lyophilization yielded a colourless powder (34.7 mg, 0.0693 mmol, 23%).

mp 92-94 °C; **¹H-NMR** (500 MHz, DMSO-*d*₆, 300 K) $\delta = 9.75$ (s, 1H, NH-NH), 9.67 (s, 1H, NH-NH), 8.41 (bs, 1H, NH-CH₂), 7.84 (d, $J = 7.5$ Hz, 1H, N-CH), 7.77-7.80 (m, 2H, CH-CH-CH-CH-C-CH₂ and C-CH-CH-C-C-CH₂), 7.56 (d, $J = 7.4$ Hz, 1H, CH-CH-CH-CH-C-CH₂), 7.46 (s, 1H, C-CH-C-CH₂), 7.36 (t, $J = 7.4$ Hz, 1H, CH-CH-CH-CH-C-CH₂), 7.25-7.30 (m, 2H, C-CH-CH-C-C-CH₂ and CH-CH-CH-CH-C-CH₂), 6.80 (s, 2H, N-C-CH), 6.68 (d, $J = 6.4$ Hz, 1H, N-CH-CH), 3.87 (s, 2H, C-CH₂-C), 3.53-3.57 (m, 1H, CH₂-CH-CH₂), 3.25-3.27 (m, 2H, NH-CH₂), 2.76 (dd, $J = 15.8$ Hz, $J = 5.4$ Hz, 1H, CH₂-CH-CHH), 2.58 (dd, $J = 16.1$ Hz, $J = 9.7$ Hz, 1H, CH₂-CH-CHH), 2.50-2.52 (m, 2H, CH₂-CH-CH₂), 2.31 (s, 3H, CH₃), 2.13 (m, 2H, CH₂-CH₂-CO), 1.58 (m, 4H, CH₂-CH₂-CH₂-CH₂-CO); **HPLC-MS** (ESI) m/z 191.2 (100), 223.1 (72), 501.2 (80) [M+H]⁺, 539.1 (12) [M+K]⁺; **HRMS** (ESI-TOF) for C₂₉H₃₃N₄O₄ [M+H]⁺: 501.2510 (calcd 501.2502); **Analytical HPLC** (5-90% in 30 min) $t_R = 16.86$ min (94% purity at 220 nm).



1-(Acet-2-yl)-2-{*N'*-[5-(4-methylpyridine-2-ylamino)pentanoyl]hydrazino}carboxy-1,2,3,4-tetrahydroisochinoline (230)

TCP resin was loaded with 2-{1-[1,2,3,4-tetrahydro-2-(9*H*-fluoren-9-ylmethoxy)carbonyl]isoquinolinyl}acetic acid (**119**) (0.48 g, 1.16 mmol) according to general method 2 ($m_1 = 0.84$ g, $m_2 = 1.0$ g, $l = 0.426$ mmol/g). Fmoc-deprotection and coupling of freshly prepared 5-(9*H*-fluoren-9-ylmethoxy)-3*H*-[1,3,4]oxadiazol-2-one (**141**) (385 mg, 1.32 mmol) were carried out according to general methods 3 and 11, coupling of 5-[*N*-(4-methylpyridine-2-yl)amino]pentanoic acid (**213**) (177 mg, 0.852 mmol) according to general method 5, cleavage from the resin was carried out according to general method 8. RP-HPLC purification (10-80% in 30 min) and lyophilization yielded a colourless powder (3.0 mg, 0.00542 mmol, 1.3%).

mp 103-109 °C; **¹H-NMR** (500 MHz, DMSO-*d*₆, 300 K) $\delta = 8.81$ (bs, 1H, NH-NH), 8.44 (bs, 1H, NH-NH), 8.25 (d, $J = 6.5$ Hz, 1H, N-CH-CH), 7.74-7.77 (m, 4H, arom), 7.34 (s, 1H, N-C-CH), 7.21 (d, $J = 6.4$ Hz, 1H, N-CH-CH), 6.06-6.07 (m, 1H, N-CH), 4.46-4.52 (m, 1H, CH-CH₂), 3.82-3.93 (m, 3H, NH-CH₂ and CH-CH₂), 3.47-3.57 (m, 2H, N-CH₂-CH₂), 3.30-3.40 (m, 2H, N-CH₂-CH₂), 2.94 (s, 3H, CH₃), 2.79-2.84 (m, 2H, CH₂-CO), 2.23-2.35 (m, 4H, CH₂-CH₂-CH₂-CO); **MS** (ESI) m/z 191.2 (8), 249.1 (100), 440.1 (30) [M+H]⁺, 462.1 (8) [M+Na]⁺, 478.1 (10) [M+K]⁺, 901.0 (2) [2M+Na]⁺, 917.1 (3) [2M+K]⁺, 939.1 (4) [2M-H+Na+K]⁺, 945.1 (4); **HRMS** (ESI-TOF) for C₂₃H₃₀N₅O₄ [M+H]⁺: 440.2273 (calcd 440.2298); **Analytical HPLC** (5-90% in 30 min) $t_R = 14.69$ min (92.7% purity at 220 nm).

8.5 Biological Evaluation

8.5.1 Molecular Cloning, Transfection and Cell Culture

The cDNA of the human BRS-3 receptor (Acc. L08893), of the human NMB receptor (Acc. M73482) and of the human GRP receptor (Acc. M73481) was kindly provided by James Battey, Ph.D. (NIDCD, NIH, USA) to *Solvay Pharmaceuticals GmbH* (Hannover, Germany). The cDNA was cut out of pGEM4 (*Promega*, Madison, USA), in case of BRS-3 and GRP with Eco RI, in case of NMB with Eco RI and Bam HI and cloned into the expression vector pcDNA3.1(-) (*Invitrogen*, Carlsbad, California).

For transfection, CHO-K1 cells (*Molecular Devices*, Sunnyvale, California), stably transfected with the expression vector RD-HGA16 of the human G α 16-protein (Acc. M63904), were seeded into 24-well plates (2×10^4 cells/well) and cultured over night under sterile conditions in a humidified Nuair incubator from *Zapf* (Sarstedt, Germany) at 37 °C and 5% CO₂ in Nut.Mix.F-12 (Ham) with Glutamax-I medium (*GibcoBRL*, Paisley, Scotland) supplemented with 10% fetal calf serum (inactivated at 56 °C for 1 hr, origin: South America, *GibcoBRL*), 0.025 mg/mL gentamicin (*GibcoBRL*) and 0.2 mg/mL hygromycin B (*GibcoBRL*). The next day, cells were transfected with 12 μ L of a 0.3 μ g/ μ L receptor's DNA solution using the 'Effectene Transfection Reagent' from *Qiagen* (Hilden, Germany) according to the manufacturer's instruction.^[510] One day after transfection the medium was changed. From now on, cells were cultured under sterile conditions (37 °C, 5% CO₂) in Nut.Mix.F-12 (Ham) with Glutamax-I medium (*GibcoBRL*, Paisley, Scotland) supplemented with 10% fetal calf serum (*GibcoBRL*), 0.025 mg/mL gentamicin (*GibcoBRL*), 0.2 mg/mL hygromycin B (*GibcoBRL*) and 0.5 mg/mL geneticin (*GibcoBRL*). For cell test optimization, cells with the highest receptor expression rate were selected. Therefore, transfected cells were diluted 1:30000 with the above described medium and transferred into 96-well plates. After incubation (37 °C, 5% CO₂) over night, wells containing a single cell were chosen and cells were cultivated in 24-well plates, then 25 mL- and finally 250 mL *Costar* plastic flasks (*Corning*, NY,

USA). Then receptor expression was assessed by determination of the EC₅₀-value of the corresponding endogenous ligand, NMB (**2**) for NMB-R, GRP (**3**) for GRP-R, or [D-Phe⁶,β-Ala¹¹,Phe¹³,Nle¹⁴]Bn(6-14) (**1**) for BRS-3, respectively.

Selected cells were stored in aliquots of 1.8 mL (1 x 10⁶ cells/mL) medium in 10% DMSO (v/v) at -80 °C. For cultivation, aliquots were warmed up to 37 °C, transferred into a *Costar* plastic flask (225 mL) from *Corning* (NY, USA) and diluted with 50 mL of supplemented medium. The medium was exchanged after 30 min of cultivation. Every following 1 to 3 days the medium was removed, the adherent cells (40-95% confluency) were washed with *PBS Dulbecco's* (*GibcoBRL*) and then separated from the flask bottom by treatment with trypsin-EDTA (*GibcoBRL*) for 2 min at 37 °C. For further cultivation, cells were transferred into a new plastic flask with fresh medium. For FLIPR measurements, cells were seeded into *Costar* 96-well assay plates (clear bottom with lid, *Corning*) at a density of 1.2 x 10⁴ cells/well.

8.5.2 FLIPR (Fluorometric Imaging Plate Reader) Assay

CHO cells were cultivated 18-24 hrs in *Costar* 96-well assay plates (*Corning*) until they were confluent. Probenecid solution was prepared fresh every day, at a stock concentration of 250 mM. Therefore, probenecid (710 mg, 2.5 mmol) from *Sigma* (Seelze) was dissolved in 1 N NaOH (5 mL) and diluted with HBSS without phenol red (*GibcoBRL*) with 20 mM HEPES (*PAA Laboratories GmbH*, Linz, Austria). A stock solution (2 mM) of fluorescent calcium indicator dye Fluo4 (*Molecular Probes*, OR, USA) was prepared from Fluo4 (1 mg) solubilized in DMSO (440 μL) and stored at -20 °C. Immediately before use an aliquot of dye stock solution (22 μL) was mixed with an equal volume of 20% (w/v) pluronic acid F-127 (*Sigma*, Seelze) in DMSO. Then the cells were loaded for 45-60 min (37 °C, 5% CO₂) with 100 μL loading medium prepared from HBSS without phenol red (42 mL) with 60 mM HEPES and aliquots of stock solutions of probenecid (420 μL), Fluo4 (22 μL) and pluronic acid (22 μL). The cells were washed three times with 100 μL of HBSS with 20 mM HEPES and 2.5 mM probenecid in a Denley cell-washer (*Labsystems*). After

the final wash, a 100 μL residual volume remained on the cells in each of the 96 well. Peptides were dissolved in DMSO as 10 mM stock solutions and diluted with HBSS with 20 mM HEPES into 96-well plates from *Greiner* (Frickenhausen, Germany). The highest concentration applied for measurements usually was 33 μM , in some cases as low as 1 μM . Well-to-well dilutions were 1:2, 1:3, 1:4 or 1:10 into 8 or 16 different wells depending on compound and receptor. For reference, each ligand microplate contained [D-Phe⁶, β -Ala¹¹,Phe¹³,Nle¹⁴]Bn(6-14) (**1**) (*Polypeptide Laboratories*, Wolfenbüttel), in case of measurements on BRS-3, NMB (**2**) (*Bachem*, Heidelberg) in case of NMB-R and GRP (**3**) (*Bachem*, Heidelberg) in case of GRP-R. The FLIPR (*Molecular Devices*, Sunnyvale, California) was programmed to measure background fluorescence during 30 sec in 6 sec intervals. Then 50 μL from each well of the ligand microplate were transferred to the cell plate and fluorescence change in counts was recorded during 100 sec in 1 sec intervals and in 6 sec intervals during the last 42 sec. From each well the maximum of fluorescence change was exported to *Excel* (*Microsoft*) and normalized with the value of the reference compound at a concentration of maximal response, usually 16 μM . Dose response curves and EC₅₀-values were calculated using *Graphpad Prism* (Version 3.00, *Graphpad Software*).

8.5.3 FLIPR Antagonist Experiment

The FLIPR was programmed to measure background fluorescence during 60 sec in 6 sec intervals. Then fluorescence change in counts was recorded during 100 sec in 1 sec intervals and 50 μL from each well of the microplate containing the potential antagonists and the known antagonists [D-Phe¹²]Bn (*Bachem*), [D-Phe⁶,Leu¹³,p-chloro-Phe¹⁴]Bn(6-14) (*Bachem*) and [D-Phe⁶,Leu-NHEt¹³,desMet¹⁴]Bn(6-14) (*Bachem*) were transferred to the cell plate after 12 sec.^[232,459,460] The highest concentration of the potential and known antagonist applied for the measurements was 10 μM , well-to-well dilutions were 1:3. Then fluorescence was measured during 210 sec in 6 sec intervals. In the subsequent 100 sec, measurements were carried out every 1 sec. After 37 sec, 50 μL of a solution containing the agonist, NMB for NMB-R and

GRP for GRP-R was transferred to each well of the cell plate. The concentration of the agonists in each well was 1 μM for NMB and 0.5 μM for GRP. Finally fluorescence was measured during 120 sec dissected in 6 sec intervals.

9 Literature

- [1] E. Fischer, *Ber. Dtsch. Chem. Ges.* **1894**, 27, 2985-2993.
- [2] A. L. Hopkins, C. R. Groom, *Nat. Rev. Drug Dis.* **2002**, 1, 727-730.
- [3] G. Wess, M. Urmann, B. Sickenberger, *Angew. Chem. Int. Ed.* **2001**, 40, 3341-3350.
- [4] R. B. Merrifield, *J. Am. Chem. Soc.* **1963**, 85, 2149-2154.
- [5] A. Furka, F. Sebestyén, M. Asgedom, G. Dibó, *Int. J. Pept. Protein Res.* **1991**, 37, 487-493.
- [6] A. Furka, *notariially certified document file no. 36237/1982*, Budapest **1982**.
- [7] R. A. Houghten, *Proc. Natl. Acad. Sci. USA* **1985**, 82, 5131-5135.
- [8] R. A. Houghten, C. Pinilla, S. E. Blondelle, J. R. Appel, C. T. Dooley, J. H. Cuervo, *Nature* **1991**, 354, 84-86.
- [9] K. S. Lam, M. Lebl, V. Krchnak, *Chem. Rev.* **1997**, 97, 411-448.
- [10] K. Burgess, A. I. Liaw, N. Wang, *J. Med. Chem.* **1994**, 37, 2985-2987.
- [11] K. S. Lam, S. E. Salmon, E. M. Hersh, V. J. Hruby, W. M. Kazmierski, R. J. Knapp, *Nature* **1991**, 354, 82-84.
- [12] C. Gibson, G. A. G. Sulyok, D. Hahn, S. L. Goodman, G. Hölzemann, H. Kessler, *Angew. Chem. Int. Ed.* **2001**, 40, 165-169.
- [13] K. D. Janda, *Proc. Natl. Acad. Sci. USA* **1994**, 91, 10779-10785.
- [14] P. Eckes, *Angew. Chem. Int. Ed.* **1994**, 33, 1573-1575.
- [15] H. M. Geysen, R. H. Meloen, S. J. Barteling, *Proc. Natl. Acad. Sci. USA* **1984**, 81, 3998-4002.
- [16] H. M. Geysen, S. J. Rodda, T. J. Mason, *Mol. Immunol.* **1986**, 23, 709-715.
- [17] S. V. Ley, I. R. Baxendale, *Nat. Rev. Drug Dis.* **2002**, 1, 573-586.
- [18] H.-J. Boehm, G. Klebe, H. Kubinyi, *Wirkstoffdesign*, Spektrum Verlag, Heidelberg, Berlin, **1996**.
- [19] W. Rogalski, *Handbook of Experim. Pharmacol.* **1985**, 78, 179-316.
- [20] L. Wessjohann, *Angew. Chem. Int. Ed.* **1997**, 36, 715-718.
- [21] M. Suffness, *Ann. Rep. Med. Chem.* **1993**, 28, 305-314.

- [22] G. R. Pettit, Y. Kamano, C. L. Herald, Y. Fujii, H. Kizu, M. R. Boyd, F. E. Boettner, D. L. Doubek, J. M. Schmidt, J.-C. Chapuis, C. Michel, *Tetrahedron* **1993**, *49*, 9151-9170.
- [23] G. Domagk, *Ann. N. Y. Acad. Sci.* **1957**, *69*, 380-384.
- [24] T. Mander, *Drug Discovery Today* **2000**, *5*, 223-225.
- [25] H. D. Kleinert, S. H. Rosenberg, W. R. Baker, H. H. Stein, V. Klinghofer, J. Barlow, K. Spina, J. Polakowski, P. Kovar *et al.*, *Science* **1992**, *257*, 1940-1943.
- [26] M. A. Zaman, S. Oparil, D. A. Calhoun, *Nat. Rev. Drug Dis.* **2002**, *1*, 621-636.
- [27] P. Y. S. Lam, P. K. Jadhav, C. J. Eyermann, C. N. Hodge, Y. Ru, L. T. Bachelier, O. M. J. Meek, M. M. Rayner, *Science* **1994**, *263*, 380-384.
- [28] G. V. De Lucca, P. Y. S. Lam, *Drugs of the Future* **1998**, *23*, 987-994.
- [29] K. Palczewski, T. Kumasaka, T. Hori, C. A. Behnke, H. Motoshima, B. A. Fox, T. Le, I. D. C. Teller, T. Okada, R. E. Stenkamp, M. Yamamoto, M. Miyano, *Science* **2000**, *289*, 739-745.
- [30] R. E. Stenkamp, D. C. Teller, K. Palczewski, *ChemBioChem* **2002**, *3*, 967-967.
- [31] J. Antel, *Curr. Opinion Drug Dis. Develop.* **1999**, *2*, 224-233.
- [32] S. Flohr, M. Kurz, E. Kostenis, A. Brkovich, A. Fournier, T. Klabunde, *J. Med. Chem.* **2002**, *45*, 1799-1805.
- [33] L. Yiang, S. C. Berk, S. P. Rohrer, R. T. Mosley, L. Guo, D. J. Underwood, B. H. Arison, E. T. Birzin, E. C. Hayes, S. W. Mitra, R. P. Parmar, K. Cheng, T.-J. Wu, B. S. Butler, F. Foor, A. Pasternak, J. M. Schaeffer, A. A. Patchett, *Proc. Natl. Acad. Sci. USA* **1998**, *95*, 10836-10841.
- [34] S. P. Rohrer, E. T. Birzin, R. T. Mosley, S. C. Berk, S. M. Hutchins, D.-M. Shen, Y. Xiong, E. C. Hayes, R. M. Parmar, F. Foor, S. W. Mitra, S. J. Degrado, M. Shu, J. M. Klopp, S.-J. Cai, A. Blake, W. W. S. Chan, A. Pasternak, L. Yang, A. A. Patchett, R. G. Smith, K. T. Chapman, J. M. Schaeffer, *Science* **1998**, *282*, 737-740.
- [35] D. C. Horwell, W. Howson, D. C. Rees, *Drug Des. Discov.* **1994**, *12*, 63-75.
- [36] D. C. Horwell, *Trends Biotechnol.* **1995**, *13*, 132-134.
- [37] P. S. Farmer, E. J. Ariens, *Trends Pharmacol. Sci.* **1982**, *3*, 362-365.

- [38] R. Schwyzer, *Trends Pharmacol. Sci.* **1980**, *3*, 327-331.
- [39] P. S. Farmer, in *Drug Design*, E. J. Ariens, ed., Academic Press, New York, **1980**, pp. 119-143.
- [40] G. W. Bemis, M. A. Murcko, *J. Med. Chem.* **1996**, *39*, 2887-2893.
- [41] B. R. Neustadt, E. M. Smith, N. Lindo, T. Nechuta, A. Bronnenkant, A. Wu, L. Armstrong, C. Kumar, *Bioorg. Med. Chem. Lett.* **1998**, *8*, 2395-2398.
- [42] L. A. Thompson, J. A. Ellman, *Chem. Rev.* **1996**, *96*, 555-600.
- [43] T. Klabunde, G. Hessler, *ChemBioChem* **2002**, *3*, 928-944.
- [44] J. Caldwell, I. Gardner, N. Swales, *Toxicol. Pathol.* **1995**, *23*, 102-114.
- [45] A. P. Li, *Drug Discovery Today* **2001**, *6*, 357-366.
- [46] P. J. Eddershaw, A. P. Beresford, M. K. Bayliss, *Drug Discovery Today* **2000**, *5*, 409-414.
- [47] D. E. Johnson, G. H. I. Wolfgang, *Drug Discovery Today* **2000**, *5*, 445-454.
- [48] C. Hansch, T. Fujita, *J. Am. Chem. Soc.* **1964**, *86*, 1616-1626.
- [49] Present software packages, which can be used for the calculation of cLogP values *e.g.* are *Sybyl 6.8* from *Tripos Inc.* or the *BioByte cLogP 4.0 estimator*, as implemented in the *Daylight Chemical Information System v. 4.71*.
- [50] C. A. Lipinski, F. Lombardo, B. W. Dominy, P. J. Feeney, *Adv. Drug. Del. Rev.* **1997**, *23*, 3-25.
- [51] D. F. Veber, S. R. Johnson, H.-Y. Cheng, B. R. Smith, K. W. Ward, K. D. Kopple, *J. Med. Chem.* **2002**, *45*, 2615-2623.
- [52] J. G. Topliss, *J. Med. Chem.* **1972**, *15*, 1006-1011.
- [53] F. Yoshida, J. G. Topliss, *J. Med. Chem.* **2000**, *43*, 2575-2585.
- [54] R. D. Cramer, D. E. Patterson, J. D. Bunce, *J. Am. Chem. Soc.* **1988**, *110*, 5959-5967.
- [55] T. H. Ji, M. Grossmann, I. Ji, *J. Biol. Chem.* **1998**, *273*, 17299-17302.
- [56] J. Drews, *Science* **2000**, *287*, 1960-1963.
- [57] Source: IMS Health, Fairfield, CT, USA, **2001**.
- [58] J. M. Stadel, S. Wilson, D. J. Bergsma, *Trends Pharmacol. Sci.* **1997**, *18*, 430-437.

- [59] S. Wilson, D. J. Bergsma, J. K. Chambers, A. I. Muir, K. G. M. Fantom, C. Ellis, P. R. Murdock, N. C. Herrity, J. M. Stadel, *Br. J. Pharmacol.* **1998**, *125*(7), 1387-1392.
- [60] S. J. Dowell, *Drug Discovery Today* **2001**, *6*, 884-886.
- [61] International Human Genome Sequencing Consortium, *Nature* **2001**, *409*, 860-921.
- [62] J. C. Venter *et al.*, *Science* **2001**, *291*, 1304-1351.
- [63] A. D. Howard, G. McAllister, S. D. Feighner, Q. Liu, R. P. Nargund, *Trends Pharmacol. Sci.* **2001**, *22*, 132-140.
- [64] J. Wess, *Pharmacol. Ther.* **1998**, *80*, 231-264.
- [65] M. Laburthe, A. Covineau, P. Gaudin, J.-J. Maoret, C. Rouyer-Fessard, P. Nicole, *Ann. NY Acad. Sci.* **1996**, *805*, 94-111.
- [66] Y. Kubo, T. Miyashita, Y. Murata, *Science* **1998**, *279*, 1722-1725.
- [67] K. Takahashi, K. Tsuchida, Y. Tanabe, M. Masu, S. Nakanishi, *J. Biol. Chem.* **1993**, *268*, 19341-19345.
- [68] O. P. Ernst, F. J. Bartl, *ChemBioChem* **2002**, *3*, 968-974.
- [69] Z.-L. Lu, J. W. Saldanha, E. C. Hulme, *Trends Pharmacol. Sci.* **2002**, *23*, 140-146.
- [70] T. Otaka, I. Le Trong, B. A. Fox, C. A. Behnke, R. E. Stenkamp, K. Palczewski, *J. Struct. Biol.* **2000**, *130*, 73-80.
- [71] T. Otaka, K. Takeda, T. Kouyama, *Photochem. Photobiol.* **1998**, *67*, 495-499.
- [72] V. M. Unger, P. A. Hargrave, J. M. Baldwin, G. F. X. Schertler, *Nature* **1997**, *389*, 203-206.
- [73] J. M. Baldwin, G. F. X. Schertler, V. M. Unger, *J. Mol. Biol.* **1997**, *272*, 144-164.
- [74] O. P. Ernst, C. K. Meyer, E. P. Marin, P. Henklein, W.-Y. Fu, T. P. Sakmar, K. P. Hofmann, *J. Biol. Chem.* **2000**, *275*, 1937-1943.
- [75] E. P. Marin, A. G. Krishna, T. A. Zvyaga, J. Isele, F. Siebert, T. P. Sakmar, *J. Biol. Chem.* **2000**, *275*, 1930-1936.
- [76] B. Koenig, A. Arendt, J. H. McDowell, M. Kahlert, P. A. Hargrave, K. P. Hofmann, *Proc. Natl. Acad. Sci. USA* **1989**, *86*, 6878-6882.

- [77] E. Pebay-Peyroula, G. Rummel, J. Rosenbusch, E. Landau, *Science* **1997**, *277*, 1676-1681.
- [78] V. Unger, P. Hargrave, J. Baldwin, G. Schertler, *Nature* **1997**, *389*, 203-206.
- [79] T. Mizobe, M. Mervyn Maze, V. Lam, S. Suryanarayana, B. Kobilka, *J. Biol. Chem.* **1996**, *271*, 2387-2389.
- [80] C. D. Strader, I. S. Sigal, R. A. F. Dixon, *FASEB J.* **1989**, *3*, 1825-1832.
- [81] C. D. Strader, T. M. Fong, M. R. Tota, D. Underwood, *Annu. Rev. Biochem.* **1994**, *63*, 101-132.
- [82] M. R. Tota, M. R. Candelore, R. A. Dixon, C. D. Strader, *Trends Pharmacol. Sci.* **1991**, *12*, 4-6.
- [83] T. Mirzadegan, F. Diehl, B. Ebi, S. Bhakta, I. Polski, D. McCarley, M. Mulkins, G. S. Weatherhead, J. M. Lapierre, J. Dankwardt, D. Morgans, R. Wilhelm, K. Jarnagin, *J. Biol. Chem.* **2000**, *275*, 25562-25571.
- [84] S. Moro, C. Hoffmann, K. A. Jacobsen, *Biochemistry* **1999**, *38*, 3498-3507.
- [85] S. Moro, D. P. Guo, E. Camainoni, J. L. Boyer, T. K. Harden, K. A. Jacobsen, *J. Med. Chem.* **1998**, *41*, 1456-1466.
- [86] T. W. Schwartz, M. M. Rosenkilde, *Trends Pharmacol. Sci.* **1996**, *17*, 213-216.
- [87] S. Zoffmann, U. Gether, T. W. Schwartz, *FEBS Lett.* **1993**, *336*, 506-510.
- [88] T. W. Schwartz, *Curr. Opin. Biotechnol.* **1994**, *5*, 434-444.
- [89] T. W. Schwartz, U. Gether, H. T. Schambye, S. A. Hjorth, *Curr. Pharmaceut. Design* **1995**, *1*, 325-342.
- [90] Y. Li, M. Marnerakis, E. R. Stimson, J. E. Maggio, *J. Biol. Chem.* **1995**, *270*, 1213-1220.
- [91] S. A. Alla, U. Qwitterer, S. Grigoriev, A. Maidhof, M. Haasemann, K. Jarnagin, W. Mueller-Estel, *J. Biol. Chem.* **1996**, *271*, 1748-1755.
- [92] A. De Lean, J. M. Stadel, R. J. Lefkowitz, *J. Biol. Chem.* **1980**, *255*, 7108-7117.
- [93] P. Samana, S. Cotecchia, T. Costa, R. J. Lefkowitz, *J. Biol. Chem.* **1993**, *268*, 4625-4636.
- [94] R. J. Lefkowitz, S. Cotecchia, P. Samana, T. Costa, *Trends Pharmacol. Sci.* **1993**, *14*, 303-307.

- [95] T. Costa, A. Herz, *Proc. Natl. Acad. Sci. USA* **1989**, *86*, 7321-7325.
- [96] A. Christopoulos, *Nat. Rev. Drug Dis.* **2002**, *1*, 198-210.
- [97] P. B. Hedlund, M. J. Carson, J. G. Sutcliffe, E. A. Thomas, *Biochem. Pharmacol.* **1999**, *58*, 1807-1813.
- [98] E. A. Thomas, M. J. Carson, M. J. Neal, J. G. Sutcliffe, *Proc. Natl. Acad. Sci. USA* **1997**, *94*, 14115-14119.
- [99] A. B. Fawzi, D. MacDonald, L. L. Benbow, A. Smith-Torhan, H. Zhang, B. C. Weig, G. Ho, D. Tulshian, M. E. Linder, M. P. Graziano, *Mol. Pharmacol.* **2001**, *59*, 30-37.
- [100] F. Y. Carroll, A. Stolle, P. M. Beart, A. Voerste, I. Brabet, F. Mauler, C. Joly, H. Antonicek, J. Bockaert, T. Mueller, J. P. Pin, L. Prezeau, *Mol. Pharmacol.* **2001**, *59*, 965-973.
- [101] T. A. Spalding, C. Trotter, N. Skjaerbaek, T. L. Messier, E. A. Currier, E. S. Burstein, D. Li, U. Hacksell, M. R. Brann, *Mol. Pharmacol.* **2002**, *61*, 1297-1302.
- [102] S. Lazareno, A. Popham, N. J. M. Birdsall, *Mol. Pharmacol.* **2000**, *58*, 194-207.
- [103] T. Nanevicz, L. Wang, M. Chen, M. Ishii, S. R. Coughlins, *J. Biol. Chem.* **1996**, *271*, 702-706.
- [104] D. T. Chalmers, D. P. Behan, *Nat. Rev. Drug Dis.* **2002**, *1*, 103-110.
- [105] P. G. Strange, *Trends Pharmacol. Sci.* **2002**, *23*, 89-95.
- [106] T. Kenakin, *Nat. Rev. Drug Dis.* **2002**, *1*, 103-110.
- [107] U. Gether, B. K. Kobilka, *J. Biol. Chem.* **1998**, *273*, 17979-17982.
- [108] A. Scheer, F. Fanelli, T. Costa, P. G. de Benedetti, S. Cotecchia, *EMBO J.* **1996**, *15*, 3566-3578.
- [109] L. A. Devi, *Trends Pharmacol. Sci.* **2001**, *22*, 532-537.
- [110] S. R. George, B. F. O'Dowd, S. P. Lee, *Nat. Rev. Drug Dis.* **2002**, *1*, 808-820.
- [111] M. I. Simon, M. P. Strathmann, N. Gautam, *Science* **1991**, *252*, 802-808.
- [112] H. E. Hamm, *J. Biol. Chem.* **1998**, *273*, 669-672.
- [113] M. P. Strathmann, M. I. Simon, *Proc. Natl. Acad. Sci. USA* **1991**, *88*, 5582-5586.

- [114] T. T. Amatruda, D. A. Steele, V. Z. Slepak, M. I. Simon, *Proc. Natl. Acad. Sci. USA* **1991**, *88*, 5587-5591.
- [115] S. Offermanns, M. I. Simons, *J. Biol. Chem.* **1995**, *270*, 15175-15180.
- [116] www.moldev.com
- [117] E. Kostenis, *Trends Pharmacol. Sci.* **2001**, *22*, 560-564.
- [118] B. R. Conklin, Z. Farfel, K. D. Lustig, D. Julius, H. R. Bourne, *Nature*, **1993**, *363*, 274-276.
- [119] B. R. Conklin, P. Herzmark, S. Ishida, T. A. Voyno-Yasenetskaya, Y. Sun, Z. Farfel, H. R. Bourne, *Mol. Pharmacol.* **1996**, *50*, 885-890.
- [120] G. Milligan, S. Rees, *Trends Pharmacol. Sci.* **1999**, *20*, 118-124.
- [121] D. G. Lambright, J. Sondek, A. Bohm, N. P. Skiba, H. E. Hamm, P. B. Sigler, *Nature* **1996**, *379*, 311-319.
- [122] L. Stryer, *Biochemistry*, W. H. Freeman Company, New York, **1995**.
- [123] D. G. Lambright, J. P. Noel, H. E. Hamm, P. B. Siegler, *Nature* **1994**, *369*, 621-628.
- [124] J. Sondek, A. Bohm, D. G. Lambright, H. E. Hamm, P. B. Siegler, *Nature* **1996**, *379*, 369-374.
- [125] M. I. Simon, M. P. Strathmann, N. Gautam, *Science* **1991**, *252*, 802-808.
- [126] L. A. Birnbaumer, *Rev. Pharmac. Toxicol.* **1990**, *30*, 675-705.
- [127] Y. Kaziro, H. Itoh, T. Kozasa, M. Nakafuku, T. A. Satoh, *Rev. Biochem.* **1991**, *60*, 349-400.
- [128] H. G. Dohlmann, J. Thorner, M. G. Caron, R. J. Lefkowitz, *Rev. Biochem.* **1991**, *60*, 653-688.
- [129] B. W. Koenig, *ChemBioChem* **2002**, *3*, 975-980.
- [130] H. Bourne, *Curr. Opin. Cell Biol.* **1997**, *9*, 134-142.
- [131] S. R. Sprang, *Annu. Rev. Biochem.* **1997**, *66*, 639-678.
- [132] R. E. West, J. Moss, M. Vaughan, T. Liu, T. Y. Liu, *J. Biol. Chem.* **1985**, *260*, 14428-14430.
- [133] K. A. Sullivan, R. T. Miller, S. B. Masters, B. Beiderman, W. Heideman, H. R. Bourne, *Nature* **1987**, *330*, 758-760.
- [134] J. P. Hirsch, C. Dietzel, J. Kurjan, *Genes Dev.* **1991**, *5*, 467-474.

- [135] W. F. Simonds, P. K. Goldsmith, J. Codina, C. G. Unson, A. M. Spiegel, *Proc. Natl. Acad. Sci. USA* **1989**, *86*, 7809-7813.
- [136] S. Gutowski, A. Smrcka, L. Nowak, D. Wu, M. Simon, P. C. Sternweis, *J. Biol. Chem.* **1991**, *266*, 20519-20524.
- [137] A. Shenker, P. Goldsmith, C. G. Unson, A. M. Spiegel, *J. Biol. Chem.* **1991**, *266*, 9309-9313.
- [138] H. E. Hamm, D. Deretic, A. Arendt, P. A. Hargrave, B. Koenig, K. P. Hofmann, *Science* **1988**, *241*, 832-835.
- [139] O. G. Kisselev, M. V. Ermolaeva, N. Gautam, *J. Biol. Chem.* **1994**, *269*, 21399-21402.
- [140] O. G. Kisselev, C. K. Meyer, M. Heck, O. P. Ernst, K. P. Hofmann, *Proc. Natl. Acad. Sci. USA* **1999**, *96*, 4898-4903.
- [141] O. G. Kisselev, J. Kao, J. W. Ponder, Y. C. Fann, N. Gautam, G. R. Marshall, *Proc. Natl. Acad. Sci. USA* **1998**, *95*, 4270-4275.
- [142] E. A. Dratz, J. E. Furstenau, C. G. Lambert, D. L. Thireault, H. Rarick, T. Schepers, S. Pakhlevanians, H. E. Hamm, *Nature* **1993**, *363*, 276-280.
- [143] B. W. Koenig, D. C. Mitchell, S. Koenig, S. Grzesiek, B. J. Litman, A. Bax, *J. Biomol. NMR* **2000**, *16*, 121-125.
- [144] B. W. Koenig, G. Kontaxis, D. C. Mitchell, J. M. Louis, B. J. Litman, A. Bax, *J. Mol. Biol.* **2002**, *322*, 441-461.
- [145] S. Nishimura, J. Sasaki, H. Kandori, T. Matsuda, Y. Fukada, A. Maeda, *Biochemistry*, **1996**, *35*, 13267-13271.
- [146] S. Nishimura, H. Kandori, A. Maeda, *Biochemistry*, **1998**, *37*, 15816-15824.
- [147] F. Bartl, E. Ritter, K. P. Hofmann, *FEBS Lett.* **2000**, *473*, 259-264.
- [148] R. R. Franke, B. Koenig, T. P. Sakmar, H. G. Khorana, K. P. Hofmann, *Science* **1990**, *250*, 123-125.
- [149] E. Kostenis, B. R. Conklin, J. Wess, *Biochemistry* **1997**, *36*, 1487-1495.
- [150] M. J. Berridge, *Nature* **1993**, *361*, 315-325.
- [151] Y. Nishizuka, *Science* **1992**, *258*, 607-614.
- [152] P. C. Sternweis, A. V. Smrcka, *Trends Biochem. Sci.* **1992**, *17*, 502-506.

- [153] J. Krupinski, F. Coussen, H. A. Bakalyar, W. J. Tang, P. G. Feinstein, K. Orth, C. Slaughter, R. R. Reed, A. G. Gilman, *Science* **1989**, *244*, 1558-1564.
- [154] R. Taussig, A. G. Gilman, *J. Biol. Chem.* **1995**, *270*, 1-4.
- [155] R. J. Lefkowitz, *J. Biol. Chem.* **1998**, *273*, 18677-18680.
- [156] A.-H. Maehle, C.-R. Pruell, R. F. Halliwell, *Nat. Rev. Drug Dis.* **2002**, *1*, 637-641.
- [157] A. Marchese, S. R. George, L. F. Kolakowski, K. R. Lynch, B. F. O'Dowd, *Trends Pharmacol. Sci.* **1999**, *20*, 370-375.
- [158] F. Libert, G. Vassart, M. Parmentier, *Curr. Opin. Cell Biol.* **1991**, *8*, 218-223.
- [159] O. Civelli, *FEBS Letters* **1998**, *430*, 55-58.
- [160] O. Civelli, R. Reinscheid, H.-P. Nothacker, *Brain Res.* **1999**, *848*, 63-65.
- [161] O. Civelli, H.-P. Nothacker, Y. Saito, Z. Wang, S. Lin, , R. Renscheid, *Trends Neurosci.* **2001**, *24*, 230-237.
- [162] R. K. Renscheid, H.-P. Nothacker, A. Bourson, A. Ardati, R. A. Henningsen, J. R. Bunzow, D. K. Grandy, H. Langen, F. J. Monsma, O. Civelli, *Science* **1995**, *270*, 792-794.
- [163] T. Sakurai, A. Amemiya, M. Ishii, I. Matsuzaki, R. M. Chemelli, H. Tanaka, S. C. Williams, J. A. Richardson, G. P. Kozlowski, S. Shelagh, J. R. S. Arch, R. E. Buckingham, A. C. Haynes, S. A. Carr, R. S. Annan, D. E. McNulty, W.-S. Liu, J. A. Terrett, N. A. Elshourbagy, D. J. Bergsma, M. Yanagisawa, *Cell* **1998**, *92*, 573-585.
- [164] L. Lin, J. Faraco, R. Li, H. Kadotani, W. Rogers, X. Lin, X. Qiu, P. J. de Jong, S. Nishino, E. Mignot, *Cell* **1999**, *98*, 365-376.
- [165] S. Hinuma, Y. Habata, R. Fujii, Y. Kawamata, M. Hosoya, S. Fukusumi, C. Kitada, Y. Masuo, T. Asano, H. Matsumoto, M. Sekiguchi, T. Kurokawa, O. Nishimura, H. Onda, M. Fujino, *Nature* **1998**, *393*, 272-276.
- [166] Y. Habata, R. Fujii, M. Hosoya, S. Fukusumi, Y. Kawamata, S. Hinuma, C. Kitada, N. Nishizawa, S. Murosaki, T. Kurokawa, H. Onda, K. Tatemoto, M. Fujino, *Biochem. Biophys. Acta* **1999**, *1452*, 25-35.
- [167] M. Kojima, H. Hosada, Y. Date, M. Nakazato, H. Matsuo, K. Kangawa, *Nature* **1999**, *402*, 656-660.

- [168] Y. Saito, H.-P. Nothacker, Z. Wang, S. Lin, F. Leslie, O. Civelli, *Nature*, **1999**, *400*, 265-269.
- [169] R. S. Ames, H. M. Sarau, J. K. Chambers, R. N. Willette, N. V. Aiyar, A. M. Romanic, C. S. Loudon, J. J. Foley, C. F. Sauermelch, R. W. Coatney, Z. Ao, J. Disa, S. D. Holmes, J. M. Stadel, J. D. Martin, W. S. Liu, G. I. Glover, S. Wilson, D. E. McNulty, C. E. Ellis, N. A. Elshourbagy, U. Shabon, J. J. Trill, D. W. Hay, E. H. Ohlstein, D. J. Bergsma, S. A. Douglas, *Nature* **1999**, *401*, 282-286.
- [170] H.-P. Nothacker, Z. Wang, A. M. McNeill, Y. Saito, S. Merten, B. O'Dowd, S. P. Duckles, O. Civelli, *Nat. Cell Biol.* **1999**, *1*, 383-385.
- [171] M. Mori, T. Sugo, M. Abe, Y. Shimomura, M. Kurihara, C. Kitada, K. Kikuchi, Y. Shintani, T. Kurokawa, H. Onda, O. Nishimura, M. Fujino, *Biochem. Biophys. Res. Comm.* **1999**, *265*, 123-129.
- [172] Q. Liu, S. S. Pong, Z. Zeng, Q. Zhang, A. D. Howard, D. L. Williams, M. Davidoff, R. Wang, C. P. Austin, T. P. Austin, T. P. McDonald, C. Bai, S. R. George, J. F. Evans, C. T. Caskey, *Biochem. Biophys Res. Comm.* **1999**, *266*, 174-178.
- [173] M. Kojima, R. Haruno, M. Nakazato, Y. Date, N. Murakami, R. Hanada, H. Matsuo, K. Kangawa, *Biochem. Biophys. Res. Comm.* **2000**, *276*, 435-438.
- [174] Nature insight „Functional genomics“, *Nature* **2000**, *405*, 819-867.
- [175] G. Milligan, J. H. White, *Trends Pharmacol. Sci.* **2001**, *22*, 513-518.
- [176] S. Huang, *Nat. Biotechnol.* **2000**, *18*, 471-472.
- [177] R. Aebersold, L. E. Hood, J. D. Watts, *Nat. Biotechnol.* **2000**, *18*, 359.
- [178] T. Haga, G. Berstein, *G-Protein-Coupled-Receptors*, CRC Press, Boca Raton, **1999**.
- [179] I. Bronstein, J. Fortin, P. E. Stanley, G. S. A. B. Stewart, L. J. Kricka, *Anal. Biochem.* **1994**, *219*, 169-181.
- [180] K. V. Wood, *Curr. Opin. Biotechnol.* **1995**, *6*, 50-58.
- [181] C. Stratowa, A. Himmler, A. P. Czernilofsky, *Curr. Opin. Biotechnol.* **1995**, *6*, 574-581.
- [182] C. Roelant, W. Scheirer, D. A. Burns, *Biotechniques* **1996**, *20*, 914-917.

- [183] M. Chalfie, Y. Tu, G. Euskirchen, W. W. Ward, D. C. Prasher, *Science* **1994**, *263*, 802-805.
- [184] H. Braeuner-Osborne, M. R. Brann, *Europ. J. Pharmacol.* **1996**, *295*, 93-102.
- [185] T. L. Messier, C. M. Dorman, H. Brauner-Osborne, D. Eubanks, M. R. Bann, *Pharmacol. Toxicol.* **1995**, *76*, 308-311.
- [186] E. S. Burnstein, H. Brauner-Osborne, T. A. Spalding, B. R. Conklin, M. R. Bann, *J. Neurochem.* **1997**, *68*, 525-533.
- [187] M. Pausch, *Trends Biotechnol.* **1997**, *15*, 487-494.
- [188] I. Erlenbach, E. Kostenis, C. Schmidt, C. Sarradeil-Le Gal, D. Raufaste, M. E. Dumont, M. H. Pausch, J. Wess, *J. Biol. Chem.* **2001**, *276*, 29382-29392.
- [189] Y. Fang, A. G. Frutos, J. Lahiri, *ChemBioChem* **2002**, *3*, 987-991.
- [190] Y. Fang, A. G. Frutos, J. Lahiri, *J. Am. Chem. Soc.* **2002**, *124*, 2394-2395.
- [191] A. Anastasi, V. Erspamer, M. Bucci, *Experientia* **1971**, *27*, 166-167.
- [192] E. R. Spindel, *Trends Neurosci.* **1986**, *9*, 130-133.
- [193] G. F. Erspamer, C. Severini, V. Erspamer, P. Melchiorri, G. Delle Fave, T. Nakajima, *Regul. Pept.* **1988**, *21*, 1-11.
- [194] M. Broccardo, G. Falconieri Erspamer, P. Melchiorri, L. Negri, R. De Castiglione, *Br. J. Pharmacol.* **1975**, *55*, 221-227.
- [195] T. J. McDonald, H. Jornvall, G. Nilsson, M. Vagne, M. Ghatei, S. R. Bloom, *Biochem. Biophys. Res. Commun.* **1979**, *90*, 227-233.
- [196] E. R. Spindel, W. W. Chin, J. Price, L. H. Rees, G. M. Besser, J. F. Habener, *Proc. Natl. Acad. Sci. USA* **1984**, *81*, 5699-5703.
- [197] N. Minamino, K. Kangawa, H. Matsuo, *Biochem. Biophys. Res. Commun.* **1983**, *114*, 541-548.
- [198] A.-M. Lebacqz-Verheyden, J. Trepel, E. A. Sausville, J. F. Battey, *Handbook of Experimental Pharmacology*, M. Sporn, A. Roberts, eds., Springer Verlag, Berlin, **1990**, p. 71-124.
- [199] B. Schjoldager, S. S. Poulsen, P. Schmidt, D. H. Coy, J. J. Hplst, *Am. J. Physiol.* **1991**, *260*, 577-585.

- [200] M. A. Ghatei, R. T. Jung, J. C. Stevenson, C. J. Hillyard, T. E. Adrian, Y. C. Lee, N. D. Christofides, D. L. Sarson, K. Mashiter, *J. Clin. Endocrinol. Metab.* **1982**, *54*, 980-985.
- [201] J. E. Rivier, M. R. Brown, *Biochemistry* **1978**, *17*, 1766-1771.
- [202] H. Okhi-Hamazaki, Y. Sakai, K. Kamata, H. Ogura, S. Okuyama, K. Watase, K. Yamada, K. Wada, *J. Neurosci.* **1999**, *19*, 948-954.
- [203] Y. Santo-Yamada, K. Yamada, K. Wada, *Physiol. Behav.* **2001**, *74*, 139-143.
- [204] S. Itoh, A. Takashima, T. Itoh, T. Morimoto, *Jpn. J. Physiol.* **1994**, *44*, 271-281.
- [205] Z. Merali, J. McIntosh, H. Anisman, *Neuropeptides* **1999**, *33*, 376-386.
- [206] E. E. Ladenheim, J. E. Taylor, D. H. Coy, T. S. Carrigan, A. Wohn, T. H. Moran, *Am. J. Physiol.* **1997**, *272*, 433-437.
- [207] L. L. Hampton, E. E. Ladenheim, M. Akeson, J. M. Way, H. C. Weber, V. E. Sutcliff, R. T. Jensen, L. J. Wine, H. Arnheiter, J. F. Battey, *Proc. Natl. Acad. Sci. USA* **1998**, *95*, 3188-3192.
- [208] Z. Merali, C. A. Merchant, J. N. Crawley, D. H. Coy, P. Heinz-Erian, R. T. Jensen, T. W. Moody, *Synapse* **1988**, *2*, 282-287.
- [209] K. Yamada, E. Wada, Y. Santo-Yamada, K. Wada, *Europ. J. Pharmacol.* **2002**, *440*, 281-290.
- [210] J. Gibbs, D. J. Fauser, E. A. Rowe, B. J. Rolls, E. T. Rolls, S. P. Maddison, *Nature* **1979**, *282*, 208-210.
- [211] D. N. Carney, F. Cuttitta, T. W. Moody, J. D. Minna, *Cancer Res.* **1987**, *47*, 821-825.
- [212] F. Cuttitta, N. Carney, J. Mulshine, T. W. Moody, J. Fedorko, A. Fischler, J. D. Minna, *Nature* **1985**, *316*, 823-826.
- [213] M. C. Lee, R. T. Jensen, D. H. Coy, T. W. Moody, *Mol. Cell. Neurosci.* **1990**, *1*, 161-167.
- [214] E. E. Ladenheim, R. T. Jensen, S. A. Mantey, P. R. McHugh, T. H. Moran, *Brain Res.* **1990**, *537*, 233-240.
- [215] T. von Schrenck, P. Heinz-Erian, T. Moran, S. A. Mantey, J. D. Gardner, R. T. Jensen, *Am. J. Physiol.* **1989**, *256*, 747-758.

- [216] T. von Schrenck, L. H. Wang, D. H. Coy, M. L. Villanueva, S. Mantey, R. T. Jensen, *Am. J. Physiol.* **1990**, *259*, 468-473.
- [217] E. E. Ladenheim, R. T. Jensen, S. A. Mantey, J. E. Taylor, D. H. Coy, T. H. Moran, *Europ. J. Pharmacol.* **1993**, *235*, 121-125.
- [218] P. Vigne, E. Feolde, C. Van Renterghem, J. P. Breittmayer, C. Frelin, *Eur. J. Biochem.* **1995**, *233*, 414-418.
- [219] J. Battey, E. Wada. *Trends Neurosci.* **1991**, *14*, 524-528.
- [220] E. Wada, J. Way, H. Shapira, K. Kusano, A. Lebacq-Verheyden, D. H. Coy, R. T. Jensen, J. F. Battey, *Neuron* **1991**, *6*, 421-430.
- [221] J. F. Battey, J. M. Way, M. H. Corjay, H. Shapira, K. Kusano, R. Harkins, J. Wu, T. Slattery, E. Mann, R. Feldman, *Proc. Natl. Acad. Sci. USA* **1991**, *88*, 395-399.
- [222] S. A. Mantey, H. C. Weber, E. Sainz, M. Akeson, R. R. Ryan, T. K. Pradhan, R. P. Searles, E. R. Spindel, J. F. Battey, D. H. Coy, R. T. Jensen, *J. Biol. Chem.* **1997**, *272*, 26062-26071.
- [223] Z. Fathi, M. H. Corjay, H. Shapira, E. Wada, R. Benya, R. Jensen, J. Viallet, E. A. Sausville, J. F. Battey, *J. Biol. Chem.* **1993**, *268*, 5979-5984.
- [224] V. Gorbulev, A. Akhundova, H. Büchner, F. Fahrenholz, *Eur. J. Biochem.* **1992**, *208*, 405-410.
- [225] S. R. Nagalla, B. J. Barry, K. C. Creswick, P. Eden, J. T. Taylor, E. R. Spindel, *Proc. Natl. Acad. Sci. USA* **1995**, *92*, 6205-6209.
- [226] T. Katsuno, T. K. Pradhan, R. R. Ryan, S. A. Mantey, W. Hou, P. J. Donohue, M. A. Akeson, E. R. Spindel, J. F. Battey, D. H. Coy, R. T. Jensen, *Biochemistry* **1999**, *38*, 7307-7320.
- [227] R. T. Jensen, D. H. Coy, *Trends Pharmacol. Sci.* **1991**, *12*, 13-19.
- [228] R. T. Jensen, S. W. Jones, K. Folkers, J. D. Gardner, *Nature* **1984**, *309*, 61-63.
- [229] P. J. Woll, E. Rozengurt, *Proc. Natl. Acad. Sci. USA* **1988**, *85*, 1859-1863.
- [230] Z. A. Saeed, S. C. Huang, D. H. Coy, N. Y. Jiang, P. Heinz-Erian, S. Mantey, J. D. Gardner, R. T. Jensen, *Pept.* **1989**, *10*, 597-603.
- [231] D. H. Coy, P. H. Erian, N.-Y. Jiang, Y. Sasaki, J. Taylor, J.-P. Moreau, W. T. Wolfrey, J. D. Gardner, R. T. Jensen, *J. Biol. Chem.* **1988**, *263*, 5056-5060.

- [232] D. H. Coy, J. E. Taylor, N. Y. Jiang, S. H. Kim, L. H. Wang, S. C. Huang, J. P. Moreau, R. T. Jensen, *Pept.: Chem., Struct. Biol., Proc. Am. Pept. Symp.*, 11th (1990), Meeting date 1989, J. E. Rivier, G. R. Marshall, eds., ESCOM, Leiden, 1990, p. 65-67.
- [233] D. H. Coy, J. E. Taylor, N.-Y. Jiang, S. H. Kim, L.-H. Wang, S. C. Huang, J.-P. Moreau, J. D. Gardner, R. T. Jensen, *J. Biol. Chem.* **1989**, *264*, 14691-14697.
- [234] J. J. Leban, A. Landavazo, J. D. McDermed, E. J. Diliberto, M. Jansen, B. Stockstill, F. C. Kull, *J. Med. Chem.* **1994**, *37*, 439-445.
- [235] E. Chiotellis, B. Nock, T. Maina, *Europ. Pat. Appl.* **2002**, EP1181936.
- [236] M. Llinares, C. Devin, O. Chaloin, J. Azay, A.-M. Noel-Artis, N. Bernad, J.-A. Fehrentz, J. Martinez, *J. Peptide Res.* **1999**, *53*, 275-283.
- [237] L.-H. Wang, D. H. Coy, J. E. Taylor, N.-Y. Jiang, S. H. Kim, J.-P. Moreau, S. C. Huang, S. A. Mantey, H. Frucht, R. T. Jensen, *Biochemistry* **1990**, *29*, 616-622.
- [238] L.-H. Wang, D. H. Coy, J. E. Taylor, N.-Y. Jiang, J.-P. Moreau, S. C. Huang, H. Frucht, B. M. Haffar, R. T. Jensen, *J. Biol. Chem.* **1990**, *265*, 15695-15703.
- [239] D. C. Heimbrook, M. E. Boyer, V. M. Garsky, N. L. Balishin, D. M. Kiefer, A. Oliff, M. W. Riemen, *J. Biol. Chem.* **1988**, *263*, 7016-7019.
- [240] D. C. Heimbrook, W. S. Saari, N. L. Balishin, A. Friedman, K. S. Moore, M. W. Riemen, D. M. Kiefer, N. S. Rotberg, J. W. Wallen, A. Oliff, *J. Biol. Chem.* **1989**, *264*, 11258-11262.
- [241] W. S. Saari, D. C. Heimbrook, A. Friedman, T. W. Fisher, A. Oliff, *Biochem. Biophys. Res. Commun.* **1989**, *165*, 114-117.
- [242] S. A. Mantey, D.H. Coy, T. K. Pradhan, H. Igarashi, I. M. Rizo, L. Shen, W. Hou, S. Hocart, R. T. Jensen, *J. Biol. Chem.* **2001**, *276*, 9219-9229.
- [243] D. H. Coy, N.-Y. Jiang, S. H. Kim, J.-P. Moreau, J.-T. Lin, H. Frucht, J.-M. Qian, L.-W. Wang, R. T. Jensen, *J. Biol. Chem.* **1991**, *266*, 16441-16447.
- [244] J. J. Leban, F. C. Kull, A. Landavazo, B. Stockstill, J. D. McDermed, *Proc. Natl. Acad. Sci. USA* **1993**, *90*, 1922-1926.
- [245] D. Erne, R. Schwyzer, *Biochemistry* **1987**, *26*, 6316-6319.

- [246] D. C. Horwell, W. Howson, D. Naylor, S. Osborne, R. D. Pinnock, G. S. Ratcliffe, N. Suman-Chauhan, *Int. J. Pept. Prot. Res.* **1996**, *48*, 522-531.
- [247] M. Cristau, C. Devin, C. Oiry, O. Chaloin, M. Amblard, N. Bernard, A. Heitz, J.-A. Fehrentz, J. Martinez, *J. Med. Chem.* **2000**, *43*, 2356-2361.
- [248] J.-T. Lin, D. H. Coy, S. A. Mantey, R. T. Jensen, *J. Pharmacol. Exp. Ther.* **1995**, *275*, 285-295.
- [249] M. Orbuch, J. E. Taylor, D. H. Coy, J. E. Mrozinski, S. A. Mantey, J. F. Battey, J. P. Moreau, R. T. Jensen, *Mol. Pharmacol.* **1993**, *44*, 841-850.
- [250] J. J. Valentine, S. Nakanishi, D. L. Hageman, R. M. Snider, R. W. Spencer, F. J. Vinick, *Bioorg. Med. Chem. Lett.* **1992**, *2*, 333-338.
- [251] S. Mihara, M. Hara, M. Nakamura, K. Sakurawi, K. Tokura, M. Fujimoto, T. Fukai, T. Nomura, *Biochem. Biophys. Res. Commun.* **1995**, *213*, 594-599.
- [252] D. C. Horwell, *Lett. Pept. Sci.* **1998**, *5*, 115-116.
- [253] J. M. Eden, M. D. Hall, M. Higginbottom, D. C. Horwell, W. Howson, J. Hughes, R. E. Jordan, R. A. Lewthwaite, K. Martin, A. T. McKnight, J. C. O'Toole, R. D. Pinnock, M. C. Pritchard, N. Suman-Chauhan, S. C. Williams, *Bioorg. Med. Chem. Lett.* **1996**, *6*, 2617-2622.
- [254] V. Ashwood, V. Brownhill, M. Higginbottom, D. C. Horwell, J. Hughes, R. A. Lewthwaite, A. T. McKnight, R. D. Pinnock, M. C. Pritchard, N. Suman-Chauhan, C. Webb, S. C. Williams, *Bioorg. Med. Chem. Lett.* **1998**, *8*, 2589-2594.
- [255] M. I. Gonzalez, M. Higginbottom, R. D. Pinnock, M. C. Pritchard, H. T. Stock, *PTC Int. Appl.* **2002**, *WO 0240022*.
- [256] D. C. Horwell, A. Beeby, C. R. Clark, J. Hughes, *J. Med. Chem.* **1987**, *30*, 729-732.
- [257] D. H. Horwell, J. Hughes, J. C. Hunter, M. C. Pritchard, R. S. Richardson, E. Roberts, G. N. Woodruff, *J. Med. Chem.* **1991**, *34*, 404-414.
- [258] P. R. Boden, M. Higginbottom, D. R. Hill, D. C. Horwell, J. Hughes, D. C. Rees, E. Roberts, L. Singh, N. Suman-Chauhan, G. N. Woodruff, *J. Med. Chem.* **1993**, *36*, 552-565.

- [259] L. Singh, M. J. Field, D. R. Hill, D. C. Horwell, A. T. McKnight, E. Roberts, K. W. Tang, G. N. Woodruff, *Eur. J. Pharmacol.* **1995**, *286*, 185-191.
- [260] B. K. Trivedi, J. K. Padia, A. Holmes, S. Rose, D. S. Wright, J. P. Hinton, M. C. Pritchard, J. M. Eden, C. Kneen, L. Webdale, N. Suman-Chauhan, P. Boden, L. Singh, M. J. Field, D. Hill, *J. Med. Chem.* **1998**, *41*, 38-45.
- [261] V. A. Ashwood, M. J. Field, D.C. Horwell, C. Julien-Larose, R. A. Lewthwaite, S. McCleary, M. C. Pritchard, J. Raphy, L. Singh, *J. Med. Chem.* **2001**, *44*, 2276-2285.
- [262] S. Boyle, S. Guard, M. Higginbottom, D. C. Horwell, W. Howson, A. T. McKnight, K. Martin, M. C. Pritchard, J. O'Toole, J. Raphy, D. C. Rees, E. Roberts, K. J. Watling, G. Woodruff, J. Hughes, *Bioorg. Med. Chem. Lett.* **1994**, *2*, 357-370.
- [263] S. Boyle, S. Guard, J. Hodgson, D. C. Horwell, W. Howson, J. Hughes, A. T. McKnight, K. Martin, M. C. Pritchard, K. J. Watling, *Bioorg. Med. Chem.* **1994**, *2*, 101-113.
- [264] C. A. Maggi, R. Patacchini, S. Giuliani, A. Giachetti, *Eur. J. Pharmacol.* **1993**, *234*, 83-90.
- [265] P. Boden, J. M. Eden, J. Hodgson, D. C. Horwell, J. Hughes, A. T. McKnight, R. A. Lewthwaite, M. C. Pritchard, J. Raphy, K. Meecham, G. S. Ratcliffe, N. Suman-Chauhan, G. N. Woodruff, *J. Med. Chem.* **1996**, *39*, 1664-1675.
- [266] P. Boden, J. M. Eden, J. Hodgson, D. C. Horwell, M. C. Pritchard, J. Raphy, N. Suman-Chauhan, *Bioorg. Med. Chem. Lett.* **1995**, *5*, 1773-1778.
- [267] A. Janecka, M. Zubrzycka, T. Janecki, *J. Pept. Res.* **2001**, *58*, 91-107.
- [268] A. Pasternak, Y. Pan, D. Marino, P. E. Sanderson, R. Mosley, S. P. Rohrer, E. T. Birzin, S.-E. Wu Huskey, T. Jacks, K. D. Schlem, K. Cheng, J. M. Schaeffer, A. A. Patchett, L. Yang, *Bioorg. Med. Chem. Lett.* **1999**, *9*, 491-496.
- [269] S. R. Vigna, A. S. Giraud, A. H. Soll, J. H. Walsh, P. W. Mantyn, *Ann. N. Y. Acad. Sci.* **1988**, *547*, 131-137.
- [270] V. Gorbulev, A. Akhundova, K. H. Grzeschick, F. Fahrenholz, *FEBS Lett.* **1994**, *340*, 260-264.

- [271] H. Okhi-Hamazaki, E. Wada, K. Matsui, K. Wada, *Brain Res.* **1997**, *762*, 165-172.
- [272] H.-P. Lammerich, A. Busmann, C. Kutzleb, M. Wendland, P. Seiler, C. Berger, P. Eickelmann, M. Meyer, W.-G. Fossmann, E. Maronde, *PTC Int. Appl.* **2002**, *WO 02063305*.
- [273] H. Okhi-Hamazaki, K. Watase, K. Yamamoto, H. Ogura, M. Yamano, K. Yamada, H. Maeno, J. Imaki, S. Kikuyama, E. Wada, K. Wada. *Nature* **1997**, *390*, 165-169.
- [274] K. Yamada, E. Wada, J. Imaki, H. Ohki-Hamazaki, K. Wada, *Physiol. Behav.* **1999**, *66*, 863-867.
- [275] K. Hotta, Y. Matsukawa, M. Nishida, K. Kotani, M. Takahashi, H. Kuriyama, T. Nakamura, K. Wada, S. Yamashita, T. Funahashi, Y. Matsuzawa, *Horm. Metabol. Res.* **2000**, *32*, 33-34.
- [276] M. A. DeMichele, A. L. Davis, J. D. Hunt, R. J. Landreneau, J. M. Siegfried, *Am. J. Respir. Cell Mol. Biol.* **1994**, *11*, 66-74.
- [277] M. Toi-Scott, C. L. Jones, M. A. Kane, *Lung Cancer* **1996**, *15*, 341-354.
- [278] H. Kiaris, A. V. Schally, A. Nagy, B. Sun, P. Armatis, K. Szepeshazi, *Br. J. Cancer* **1999**, *81*, 966-971.
- [279] B. Sun, A. V. Schally, G. Halmos, *Regul. Pept.* **2000**, *90*, 77-84.
- [280] D. Smart, P. Strijbos, *PTC Int. Appl.* **2001**, *WO 0168120*.
- [281] J. M. Wu, D. E. Nitecki, S. Biancalana, R. I. Feldman, *Mol. Pharmacol.* **1996**, *50*, 1355-1363.
- [282] T. K. Pradhan, T. Katsuno, J. E. Taylor, S. H. Kim, R. R. Ryan, S. A. Mantey, P. J. Donohue, H. C. Weber, E. Sainz, J. F. Battey, D. H. Coy, R. T. Jensen, *Eur. J. Pharmacol.* **1998**, *343*, 275-287.
- [283] R. R. Ryan, H. C. Weber, W. Hou, E. Sainz, S. A. Mantey, J. F. Battey, D. H. Coy, R. T. Jensen, *J. Biol. Chem.* **1998**, *273*, 13613-13624.
- [284] M. Akeson, E. Sainz, S. A. Mantey, R. T. Jensen, J. F. Battey, *J. Biol. Chem* **1997**, *272*, 17405-17409.
- [285] R. R. Ryan, H. C. Weber, S. A. Mantey, W. Hou, M. E. Hilburger, T. K. Pradhan, D. H. Coy, R. T. Jensen, *J. Pharmacol. Exp. Ther.* **1998**, *287*,

- 366-380.
- [286] R. R. Ryan, T. Katsuno, S. A. Mantey, T. P. Pradhan, H. C. Weber, J. F. Battey, R. T. Jensen, *J. Pharmacol. Exp. Ther.* **1999**, *290*, 1202-1211.
- [287] J.-T. Lin, D. H. Coy, S. A. Mantey, R. T. Jensen, *Eur. J. Pharmacol.* **1995**, *294*, 55-69.
- [288] Y. Lin, X. Jian, Z. Lin, G. S. Kroog, S. Mantey, R. T. Jensen, J. Battey, J. Northup, *J. Pharmacol. Exp. Ther.* **2000**, *294*, 1053-1062.
- [289] P. J. Donohue, E. Sainz, M. Akeson, G. S. Kroog, S. A. Mantey, J. F. Battey, R. T. Jensen, J. K. Northup, *Biochemistry* **1999**, *38*, 9366-9372.
- [290] K. Tokita, S. J. Hocart, T. Katsuno, S. A. Mantey, D. H. Coy, R. T. Jensen, *J. Biol. Chem.* **2001**, *276*, 495-504.
- [291] E. Sainz, M. Akeson, S. A. Mantey, R. T. Jensen, J. F. Battey, *J. Biol. Chem.* **1998**, *273*, 15927-15932.
- [292] J. G. Darker, S. J. Brough, J. Heath, D. Smart, *J. Peptide Sci.* **2001**, *7*, 598-605.
- [293] T. Curtius, *J. Prakt. Chem.* **1881**, *24*, 239.
- [294] E. Fischer, *Chem. Ber.* **1902**, *35*, 1095.
- [295] F. Hofmeister, *Ergeb. Physiol. Biol. Chem. Exp. Pharmacol.* **1902**, *1*, 759.
- [296] E. Fischer, *Chem. Ber.* **1906**, *39*, 530.
- [297] J. A. McLaren, *Aust. J. Chem.* **1958**, *11*, 360-365.
- [298] M. Bergmann, L. Zervas, *Chem. Ber.* **1932**, *65*, 1192-1201.
- [299] G. Barany, R. B. Merrifield, *J. Am. Chem. Soc.* **1977**, *99*, 7363-7365.
- [300] M. Bodanszky, V. du Vigneaud, *Nature* **1959**, *183*, 1324-1325.
- [301] R. Schwyzer, H. Kappeler, *Helv. Chim. Acta* **1963**, *46*, 1550-1572.
- [302] E. Atherton, R. C. Sheppard, *Solid Phase Peptide Synthesis: A Practical Approach*, IRL Press, Oxford, **1989**.
- [303] G. B. Fields, R. L. Noble, *Int. J. Pept. Protein Res.* **1990**, *35*, 161-214.
- [304] C. Chan, D. White, *Fmoc solid phase peptide synthesis: a practical approach*, Oxford University Press, Oxford, **2000**.
- [305] L. A. Carpino, G. Y. Han, *J. Am. Chem. Soc.* **1970**, *92*, 5748-5749.
- [306] L. A. Carpino, G. Y. Han, *J. Org. Chem.* **1972**, *37*, 3404-3409.
- [307] H. Rink, *Tetrahedron Lett.* **1987**, *28*, 3787-3790.

- [308] P. Sieber, *Tetrahedron Lett.* **1987**, 28, 2107-2110.
- [309] K. Barlos, D. Gatos, J. Kallitsis, G. Papaphotius, P. Sotiriu, W. Yao, W. Schaefer, *Tetrahedron Lett.* **1989**, 30, 3943-3946.
- [310] A. Floersheimer, B. Riniker, *Pept.* **1990**, *Proc. Eur. Pept. Symp.*, 21th (1991), Meeting Date 1990. E. Giralt, D. Andreu, eds., ESCOM, Leiden, 1990, 131.
- [311] L. A. Carpino, B. J. Cohen, K. E. Stephens, S. Y. Sadat-Aalae, J.-H. Tien, D. C. Langridge, *J. Org. Chem.* **1986**, 51, 3734-3736.
- [312] L. A. Carpino, D. Sadat-Aalae, H. G. Chao, R. H. DeSelms, *J. Am. Chem. Soc.* **1990**, 112, 9651-9652.
- [313] H. Chantrenne, *Nature* **1947**, 160, 603-604.
- [314] J. Kovacs, L. Kisfaludy, M. Q. Ceprini, *J. Am. Chem. Soc.* **1967**, 89, 183-184.
- [315] J. C. Sheehan, G. P. Hess, *J. Am. Chem. Soc.* **1955**, 77, 1067-1068.
- [316] M. Bodanszky, *Principles of Peptide Synthesis*, Springer Verlag, Berlin, **1984**.
- [317] F. Albericio, J. M. Bofill, A. El-Faham, S. A. Kates, *J. Org. Chem.* **1998**, 63, 9678-9683.
- [318] V. Dourtoglou, B. Gross, V. Lambropoulou, C. Zioudrou, *Synthesis* **1984**, 7, 572-4.
- [319] J. M. Humphrey, A. R. Chamberlin, *Chem. Rev.* **1997**, 97, 2243-2266.
- [320] J. Coste, D. Le-Nguyen, *Tetrahedron Lett.* **1990**, 31, 205-208.
- [321] B. Castro, J. R. Dormoy, G. Evin, C. Selve, *Tetrahedron Lett.* **1975**, 16, 1219-1222.
- [322] V. Dourtoglou, J.-C. Ziegler, B. Gross, *Tetrahedron Lett.* **1978**, 19, 1269-1272.
- [323] R. Knorr, A. Trzeciak, W. Bannwarth, D. Gillessen, *Tetrahedron Lett.* **1989**, 30, 1927-1930.
- [324] W. König, R. Geiger, *Chem. Ber.* **1970**, 103, 788-798.
- [325] W. König, R. Geiger, *Chem. Ber.* **1970**, 103, 2024-2033.
- [326] L. A. Carpino, *J. Am. Chem. Soc.* **1993**, 115, 4397-4398.
- [327] Y. Han, F. Albericio, G. Barany, *J. Org. Chem.* **1997**, 62, 4307-4312.
- [328] L. A. Carpino, A. El-Faham, *J. Org. Chem.* **1994**, 59, 695-698.
- [329] C. G. Fields, G. B. Fields, *Tetrahedron Lett.* **1993**, 34, 6661-6664.
- [330] N. A. Solé, G. Barany, *J. Org. Chem.* **1992**, 57, 5399-5403.

- [331] P. White, *Pept.: Chem. Biol., Proc. Am. Pept. Symp.*, 12th, **1992**, Meeting date 1991, 537-8.
- [332] B. Dörner, P. White, *Pept.* **1998**, *Proc. Eur. Pept. Symp.*, 25th (1999), Meeting Date 1998. S. Bajusz, F. Hudecz, eds., Akadémiai Kiadó, Budapest, 1999, 90.
- [333] J.-P. Xiong, T. Stehle, R. Zhang, A. Joachimiak, M. Frech, S. L. Goodman, M. A. Arnaout, *Science* **2002**, 296, 151-155.
- [334] H. Kessler, H. Matter, G. Gemmecker, H.-J. Diehl, C. Isernia, S. Mronga, *Int. J. Pept. Prot. Res.* **1994**, 43, 47-61.
- [335] M. S. Lim, E. R. Johnston, C. A. Kettner, *J. Med. Chem.* **1993**, 36, 1831-1838.
- [336] H. Kessler, *Angew. Chem. Int. Ed.* **1982**, 21, 512-523.
- [337] R. Haubner, D. Finsinger, H. Kessler, *Angew. Chem. Int. Ed.* **1997**, 3, 1374-89.
- [338] H. Kessler, in V. Claassen (Ed.): *Trends in Drug Research, Vol. 13*, Elsevier Science Publisher **1990**, p. 73-84.
- [339] D. H. Coy, N. Y. Jiang, S. H. Kim, J. P. Moreau, J. T. Lin, S. Mantey, R. T. Jensen, *Pept.: Chem. Biol., Proc. Am. Pept. Symp.*, 12th, **1992**, Meeting date 1991, 40-1.
- [340] J. Boer, D. Gottschling, A. Schuster, M. Semmrich, B. Holzmann, H. Kessler, *J. Med. Chem.* **2001**, 44, 2586-2592.
- [341] G. Byk, D. Halle, I. Zeltser, G. Bitan, Z. Selinger, C. Gilon, *J. Med. Chem.* **1996**, 39, 3174-3178.
- [342] M. Bürgle, M. Koppitz, C. Riemer, H. Kessler, B. König, U. H. Weidle, J. Kellermann, F. Lottspeich, H. Graeff, M. Schmitt, L. Goretzki, U. Reuning, O. G. Wilhelm, V. Magdolen, *Biol. Chem.* **1997**, 378, 231-237.
- [343] V. Magdolen, M. Bürgle, N. Arroyo De Prada, N. Schmiedeberg, C. Riemer, F. Schroeck, J. Kellermann, K. Degitz, O. G. Wilhelm, M. Schmitt, H. Kessler, *Biol. Chem.* **2001**, 382, 1197-1205.
- [344] N. Schmiedeberg, M. Schmitt, C. Roelz, V. Truffault, M. Sukopp, M. Bürgle, O. G. Wilhelm, W. Schmalix, V. Magdolen, H. Kessler, *J. Med. Chem.* **2002**, 45, 4984-4994.
- [345] E. Ruoslahti, M. D. Pierschbacher, *Science* **1987**, 238, 491-497.

- [346] M. J. Briskin, L. Rott, E. C. Butcher, *J. Immunol.* **1996**, *156*, 719-726.
- [347] J. L. Viney, S. Joenes, H. H. Chiu, B. Lagrimas, M. E. Renz, L. G. Presta, D. Jackson, K. J. Hillan, S. Lew, S. Fong, *J. Immunol.* **1996**, *157*, 2488-2497.
- [348] L. Osborn, C. Vassallo, B. G. Browning, R. Tizard, D. O. Haskard, C. D. Benjamin, I. Dougas, T. Kirchhausen, *J. Cell. Biol.* **1994**, *124*, 601-608.
- [349] M. E. Renz, H. H. Chiu, S. Jones, J. Fox, K. J. Kim, L. G. Presta, S. Fong, *J. Cell. Biol.* **1994**, *125*, 1395-1406.
- [350] R. H. Vonderheide, T. F. Tedder, T. A. Springer, D. E. Staunton, *J. Cell. Biol.* **1994**, *125*, 215-222.
- [351] E. Y. Jones, K. Harlos, M. J. Bottomley, R. C. Robinson, P. C. Driscoll, R. M. Edwards, J. M. Clements, T. J. Dudgeon, D. I. Stuart, *Nature* **1995**, *373*, 539-544.
- [352] J. H. Wang, R. B. Pepinsky, T. Stehle, J. H. Liu, M. Karpusas, B. Browning, L. Osborn, *Proc. Natl. Acad. Sci. USA* **1995**, *92*, 5714-5718.
- [353] A. Komoriya, L. J. Green, M. Mervic, S. S. Yamada, K. M. Yamada, M. J. Humphries, *J. Biol. Chem.* **1991**, *266*, 15075-15079.
- [354] E. A. Wayner, N. L. Kovach, *J. Cell Biol.* **1992**, *116*, 489-497.
- [355] M. D. Pierschbacher, E. Ruoslahti, *J. Biol. Chem.* **1987**, *262*, 7294-7298.
- [356] M. Kurz, *Doctoral Thesis* **1991**, Technical University Munich.
- [357] C. Riemer, *Doctoral Thesis* **1999**, Technical University Munich.
- [358] R. Schweyzer, P. Sieber, B. Goroup, *Chimia* **1958**, *12*, 90-91.
- [359] H. Kessler, P. Kondor, *Chem. Ber.* **1979**, *112*, 3541-3551.
- [360] H. Kessler, G. Hölzemann, *Liebigs Ann. Chem.* **1981**, *11*, 2028-2044.
- [361] R. Haubner, *Doctoral Thesis* **1995**, Technical University Munich.
- [362] J. Boer, *Doctoral Thesis* **2000**, Technical University Munich.
- [363] J. F. Reichwein, B. Wels, J. A. W. Kruijtzter, C. Versluis, R. M. J. Liskamp, *Angew. Chem. Int. Ed.* **1999**, *38*, 3684-3687.
- [364] B. C. Wilkes, V. J. Hruby, A. M. Castrucci, W. C. Sherbrooke, M. E. Hadley, *Science* **1984**, *224*, 1111-1113.
- [365] M. Froimowitz, V. J. Hruby, *Int. J. Pept. Prot. Res.* **1989**, *34*, 88-96.

- [366] J. L. Krstenansky, T. J. Owen, S. H. Buck, K. A. Hagaman, L. R. Mclean, *Proc. Natl. Acad. Sci. USA* **1989**, *86*, 4377-4381.
- [367] N. Schmiedeberg, *Doctoral Thesis* **2002**, Technical University Munich.
- [368] M. Bürgle, *Doctoral Thesis* **1998**, Technical University Munich.
- [369] D. A. Pearson, M. Blanchette, M. L. Baker, C. A. Guindon, *Tetrahedron Lett.* **1989**, *30*, 2739-2742.
- [370] H. Franzen, L. Grehn, U. Ragnarsson, *J. Chem. Soc., Chem. Commun.* **1984**, 1699-1700.
- [371] J. P. Tam, *Int. J. Pept. Prot. Res.* **1987**, *29*, 421-431.
- [372] J. A. Camarero, E. Giralt, D. Andreu, *Tetrahedron Lett.* **1995**, *36*, 1137-1140.
- [373] R. Volkmer-Engert, C. Landgraf, J. Schneider-Mergener, *J. Pept. Res.* **1998**, *51*, 365-369.
- [374] B. Kamber, A. Hartmann, K. Eisler, B. Riniker, H. Rink, P. Sieber, W. Rittel, *Helv. Chim. Acta* **1980**, *63*, 899-915.
- [375] P. Sieber, B. Kamber, B. Riniker, W. Rittel, *Helv. Chim. Acta* **1980**, *63*, 2358-2363.
- [376] N. Fujii, T. Wanatabe, A. Otaka, K. Bessho, I. Yamamoto, T. Noda, H. Yajima, *Chem. Pharm. Bull.* **1987**, *35*, 4769-4776.
- [377] S. N. McCurdy, *Pept. Res.* **1989**, *2*, 147-152.
- [378] E. V. Kudryavtseva, M. V. Sidorova, M. V. Ovchinnikov, Z. D. Bespalova, V. N. Bushuev, *J. Pept. Res.* **1997**, *49*, 52-58.
- [379] J. P. Tam, C.-R. Wu, W. Liu, J.-W. Zhang, *J. Am. Chem. Soc.* **1991**, *113*, 6657-6662.
- [380] A. Otaka, T. Koide, A. Shide, N. Fujii, *Tetrahedron Lett.* **1991**, *32*, 1223-1226.
- [381] J. C. Spetzler, M. Meldal, *Lett. Pept. Sci.* **1996**, *3*, 327-332.
- [382] H. Tamamura, T. Ishihara, H. Oyake, M. Imai, A. Otaka, T. Ibuka, R. Arakaki, H. Nakashima, T. Murakami, M. Waki, A. Matsumoto, N. Yamamoto, N. Fujii, *J. Chem. Soc., Perkin Trans. 1*, **1998**, 495-500.
- [383] B. Hargittai, G. Barany, *J. Pept. Res.* **1999**, *54*, 468-479.
- [384] D. Weber, C. Berger, T. Heinrich, P. Eickelmann, J. Antel, H. Kessler, *J. Pept. Sci.* **2002**, *8*, 461-475.

- [385] A. G. Beck-Sickinger, P. Weber, *Kombinatorische Methoden in Chemie und Biologie*, Spektrum Verlag, Heidelberg, Berlin, **1999**.
- [386] J. R. Wyatt, T. A. Vickers, J. L. Roberson, R. W. Buckheit, T. Klimkait, E. Debaets, P. W. Davis, B. Rayner, J. L. Imbach, D. J. Ecker, *Proc. Natl. Acad. Sci. USA* **1994**, *91*, 1356-1360.
- [387] R. Gretler, E. Askitoglu, H. Kühne, M. Hesse, *Helv. Chim. Acta* **1978**, *6*, 1730-1755.
- [388] J. C. Pelletier, M. P. Cava, *Synthesis* **1987**, *5*, 474-477.
- [389] A. Mai, M. Artico, G. Sbardella, S. Massa, E. Novellino, G. Greco, A. G. Loi, E. Tramontano, M. E. Marongiu, P. La Colla, *J. Med. Chem.* **1999**, *42*, 619-627.
- [390] C. J. Moody, F. Rahimtoola, *J. Chem. Soc., Perkin Trans. 1* **1990**, 673-679.
- [391] C. L. Slemon, L. C. Hellwig, J.-P. Ruder, E. W. Hoskins, D. B. MacLean, *Can. J. Chem.* **1981**, *59*, 3055-3060.
- [392] D. Gottschling, *Doctoral Thesis* **2001**, Technical University Munich.
- [393] A. A. Aroyan, M. S. Kramer, *Chem. Abstr.* **1971**, *75*, 49022w.
- [394] Y. Oikawa, K. Sugano, O. Yonemitsu, *J. Org. Chem.* **1978**, *43*, 2087-2088.
- [395] T. Sommerfeld, D. Seebach, *Angew. Chem. Int. Ed.* **1995**, *34*, 553-554.
- [396] C. Gennari, C. Longari, S. Ressel, B. Salom, A. Mielgo, *Eur. J. Org. Chem.* **1998**, 945-959.
- [397] P. A. Bartlett, C. K. Marlowe, *Science* **1987**, *235*, 569-571.
- [398] K. Burgess, D. S. Linthicum, H. Shin, *Angew. Chem. Int. Ed.* **1995**, *34*, 907-909.
- [399] K. Burgess, J. Ibarzo, D. S. Linthicum, D. H. Russell, H. Shin, A. Shitangkoon, R. Totani, A. J. Zhang, *J. Am. Chem. Soc.* **1997**, *119*, 1556-1564.
- [400] S. M. Hutchins, K. T. Chapman, *Tetrahedron Lett.* **1995**, *36*, 2583-2586.
- [401] S. M. Hutchins, K. T. Chapman, *Tetrahedron Lett.* **1994**, *35*, 4055-4058.
- [402] Y. Sasaki, W. A. Murphy, M. L. Heiman, V. A. Lance, D. H. Coy, *J. Med. Chem.* **1987**, *30*, 1162-1166.
- [403] J. M. Qian, D. H. Coy, N. Y. Jiang, J. D. Gardner, R. T. Jensen, *J. Biol. Chem.* **1989**, *264*, 16667-16671.

- [404] R. J. Simon, R. S. Kania, R. N. Zuckermann, V. D. Huebner, D. A. Jewell, S. Banville, S. Ng, L. Wang, S. Rosenberg, C. K. Marlowe, D. C. Spellmeyer, R. Tan, A. D. Frankel, D. V. Santi, P. A. Bartlett, *Proc. Nat. Acad. Sci. USA* **1992**, *89*, 9367-9371.
- [405] R. N. Zuckermann, J. M. Kerr, S. B. H. Kent, W. H. Moos, *J. Am. Chem. Soc.* **1992**, *114*, 10646-10647.
- [406] H. Kessler, *Angew. Chem. Int. Ed.* **1993**, *32*, 543-544.
- [407] R. Ruijtenbeek, J. A. Kruijtzter, W. van der Wiel, M. J. E. Fischer, M. Redegeld, R. M. J. Liskamp, F. P. Nijkamp, *ChemBioChem* **2001**, *2*, 171-179.
- [408] T.-A. Tran, R.-H. Mattern, M. Afargan, O. Amitay, O. Ziv, B. A. Morgan, E. Taylor, D. Hoyer, M. Goodman, *J. Med. Chem.* **1998**, *41*, 2679-2685.
- [409] D. C. Horwell, *Spec. Publ. R. Soc. Chem.* **1988**, *65*, 62-72.
- [410] F. Hamy, E. R. Felder, G. Heizmann, J. Lazdins, F. Aboul-ela, G. Varani, J. Karns, T. Klimkait, *Proc. Natl. Acad. Sci. USA* **1997**, *94*, 3548-3553.
- [411] J. T. Nguyen, C. W. Turck, F. E. Cohen, R. N. Zuckermann, W. A. Lim, *Science* **1998**, *282*, 2088-2092.
- [412] S. M. Miller, R. J. Simon, S. Ng, R. N. Zuckermann, J. M. Kerr, W. H. Moos, *Bioorg. Med. Chem. Lett.* **1994**, *4*, 2657-2662.
- [413] R. N. Zuckermann, E. J. Martin, D. C. Spellmeyer, G. B. Stauber, K. R. Shoemaker, J. M. Kerr, G. M. Figliozzi, D. A. Goff, M. A. Siani, R. J. Simon, S. C. Banville, E. G. Brown, L. Wang, L. S. Richter, W. H. Moos, *J. Med. Chem.* **1994**, *37*, 2678-2685.
- [414] J. A. W. Kruijtzter, R. M. J. Liskamp, *Tetrahedron Lett.* **1995**, *36*, 6969-6972.
- [415] J. A. W. Kruijtzter, L. J. F. Hofmeyer, W. Heerma, C. Versluis, R. M. J. Liskamp, *Chem. Eur. J.* **1998**, *4*, 1570-1580.
- [416] J. M. Kerr, S. C. Banville, R. N. Zuckermann, *J. Am. Chem. Soc.* **1993**, *115*, 2529-2531.
- [417] A. J. Speziale, E. G. Jaworski, *J. Org. Chem.* **1960**, *25*, 728-732.
- [418] H. C. Stewart, *Austr. J. Chem.* **1961**, *14*, 654-656.
- [419] M. Dechantsreiter, H. Kessler, M. Bernd, B. Kutscher, T. Beckers, *Ger. Offen.* **2000**, *DE 19941248 A1*, 32 pp.

- [420] M. Dechantsreiter, *Doctoral Thesis* **1998**, Technical University of Munich.
- [421] J. Gante, *Synthesis* **1989**, *6*, 405-413.
- [422] H. J. Hess, W. T. Moreland, G. D. Laubach, *J. Am. Chem. Soc.* **1963**, *85*, 4040-4041.
- [423] J. Gante, W. Lautsch, *Chem. Ber.* **1964**, *97*, 983-988.
- [424] C. H. Reynolds, R. E. Hormann, *J. Am. Chem. Soc.* **1996**, *118*, 9395-9401.
- [425] F. André, G. Boussard, D. Bayeul, C. Didierjean, A. Aubry, M. Marraud, *J. Pept. Res.* **1997**, *49*, 556-562.
- [426] F. André, A. Vicherat, G. Boussard, A. Aubry, M. Marraud, *J. Pept. Res.* **1997**, *50*, 372-381.
- [427] H.-J. Lee, I.-A. Anh, S. Ro, K.-H. Choi, Y.-S. Choi, K.-B. Lee, *J. Pept. Res.* **2000**, *56*, 35-46.
- [428] A. S. Dutta, M. B. Giles, *J. Chem. Soc. Perkin 1* **1976**, 244-248.
- [429] C. J. Gray, J. C. Ireson, R. C. Parker, *Tetrahedron Lett.* **1977**, *33*, 739-743.
- [430] C. Gibson, S. L. Goodman, D. Hahn, G. Hölzemann, H. Kessler, *J. Org. Chem.* **1999**, *64*, 7388-7394.
- [431] H. Han, K. D. Janda, *J. Am. Chem. Soc.* **1996**, *118*, 2539-2544.
- [432] M. Quibell, W. G. Turnell, T. Johnson, *J. Chem. Soc., Perkin Trans. 1* **1993**, 2843-2849.
- [433] M. Liley, T. Johnson, *Tetrahedron Lett.* **2000**, *41*, 3983-3985.
- [434] F. André, M. Marraud, T. Tsouloufīs, S. J. Tzartos, G. Boussard, *J. Pept. Sci.* **1997**, *3*, 429-441.
- [435] C. Frochot, R. Vanderesse, A. Driou, G. Linden, M. Marraud, M. T. Cung, *Lett. Pept. Sci.* **1997**, *4*, 219-225.
- [436] A. S. Dutta, B. J. A. Furr, M. B. Giles, *J. Chem. Soc. Perkin 1* **1979**, 379-388.
- [437] G. A. G. Sulyok, C. Gibson, S. L. Goodman, G. Hölzemann, M. Wiesner, H. Kessler, *J. Med. Chem.* **2001**, *44*, 1938-1950.
- [438] G. Bold, A. Fässler, H.-G. Capraro, R. Cozens, T. Klimkait, J. Lazdins, J. Mestan, B. Poncioni, J. Rösel, D. Stover, M. Tintelnot-Blomley, F. Acemoglu, W. Beck, E. Boss, M. Eschbach, T. Hürlimann, E. Masso, S. Roussel, K. Ucci-Stoll, D. Wyss, M. Lang, *J. Med. Chem.* **1998**, *41*, 3387-3401.

- [439] J. Magrath, R. H. Abeles, *J. Med. Chem.* **1992**, *35*, 4279-4283.
- [440] J. C. Powers, R. Boone, D. L. Carroll, B. F. Gupton, C.-M. Kam, N. Nishino, M. Sakamoto, P. M. Tuhy, *J. Biol. Chem.* **1984**, *259*, 4288-4294.
- [441] R. Zhang, J. P. Durkin, W. T. Windsor, *Bioorg. Med. Chem. Lett.* **2002**, *12*, 1005-1008.
- [442] G. Witherell, *Curr. Opinion Invest. Drugs* **2001**, *2*, 340-347.
- [443] D.-K. Shin, H.-J. Lee, K.-B. Lee, Y.-S. Choi, C.-J. Yoon, S. Ro, *Pept. , Proc. Am. Pept. Symp., 17th (2001)*, Meeting date 2001, M. Lebl, R. A. Houghten, eds., Kluwer, Dordrecht, **2001**, p. 583-584.
- [444] H.-J. Lee, K.-H. Choi, I.-A. Anh, S. Ro, H. G. Jang, Y.-S. Choi, K.-B. Lee, *J. Mol. Struct.* **2001**, *569*, 43-54.
- [445] S. Ro, H.-J. Lee, I.-A. Anh, D. K. Shin, K.-B. Lee, C.-J. Yoon, Y.-S. Choi, *Bioorg. Med. Chem.* **2001**, *9*, 1834-1841.
- [446] A. S. Dutta, J. S. Morley, *J. Chem. Soc., Perkin Trans. 1* **1975**, *17*, 1712-1720.
- [447] N. I. Ghali, D. L. Venton, *J. Org. Chem.* **1981**, *46*, 5413-5414.
- [448] R. Calabretta, C. Giordano, C. Gallina, V. Morea, V. Consalvi, R. Scandurra, *Eur. J. Med. Chem.* **1995**, *30*, 931-941.
- [449] C. J. Gray, M. Quibell, K.-L. Jiang, N. Baggett, *Synthesis* **1991**, *2*, 141-146.
- [450] J. H. Biel, A. E. Drukker, T. F. Mitchell, E. P. Sprengeler, P. A. Nuhfer, A. C. Conway, A. Horita, *J. Am. Chem. Soc.* **1959**, *81*, 2805.
- [451] T. K. Hansen, *Tetrahedron Lett.* **1999**, *40*, 9119-9120.
- [452] J. Gante, M. Krug, G. Lauterbach, R. Weitzel, W. Hiller, *J. Pept. Sci.* **1995**, *2*, 201-206.
- [453] J. Wermuth, *Doctoral Thesis* **1996**, Technical University Munich.
- [454] J. S. Schmitt, *Doctoral Thesis* **1998**, Technical University Munich.
- [455] C. J. Gray, M. Quibell, N. Baggett, T. Hammerle, *Int. J. Peptide Protein Res.* **1992**, *40*, 351-362.
- [456] G. Sulyok, *Doctoral Thesis* **2001**, Technical University Munich.
- [457] C. Gibson, *Doctoral Thesis* **2000**, Technical University Munich.
- [458] S. W. Wright, D. L. Hageman, L. D. McClure, *J. Org. Chem.* **1994**, *59*, 6095-6097.

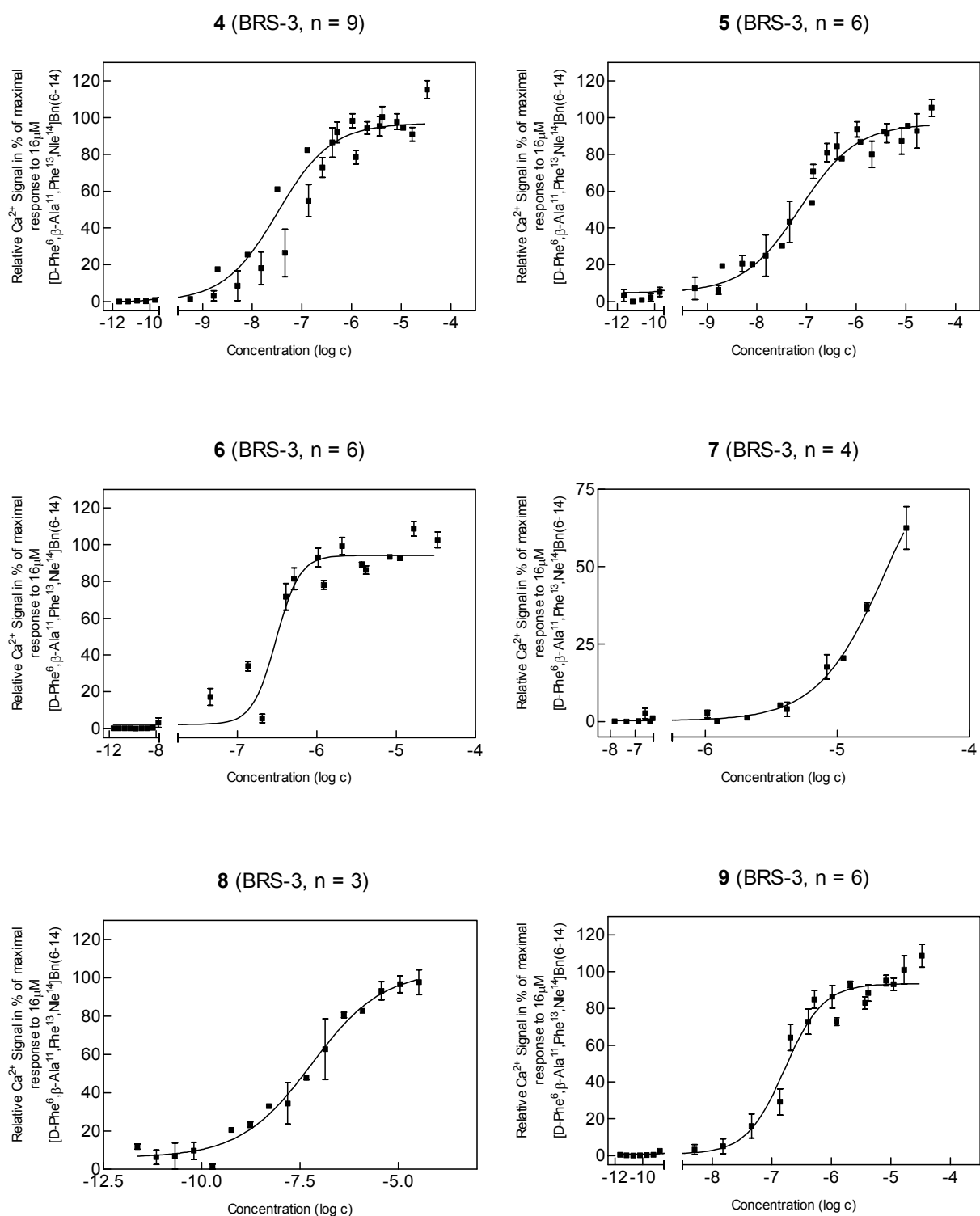
- [459] P. Heinz-Erian, D. H. Coy, M. Tamura, S. W. Jones, J. Gardner, R. T. Jensen, *Am. J. Physiol.* **1987**, *252*, G439-G442.
- [460] F. Thomas, F. Arvelo, E. Antoine, M. Jacrot, M. F. Poupon, *Cancer Res.* **1992**, *52*, 4872-4877.
- [461] M. J. Humphries, *Biochem. Soc. Trans.* **2000**, *28*, 311-340.
- [462] S. M. Albelda, C. A. Buck, *FASEB J.* **1990**, *4*, 2868-2880.
- [463] J. Travis, *Science* **1993**, *260*, 906-908.
- [464] R. O. Hynes, *Cell* **1992**, *69*, 11-25.
- [465] K. M. Yamada, B. Geiger, *Curr. Opin. Cell. Biol.* **1997**, *9*, 76-85.
- [466] S. Dedhar, *Curr. Opin. Hematol.* **1999**, *6*, 37-43.
- [467] J. A. Eble, in *Integrin-Ligand Interaction*, J. A. Eble, ed., Springer Verlag, Heidelberg, **1997**, pp. 1-40.
- [468] T. A. Springer, *Nature* **1990**, *346*, 425-434.
- [469] M. Pfaff, in *Integrin-Ligand Interaction*, J. A. Eble, ed., Springer Verlag, Heidelberg, **1997**, pp. 101-121.
- [470] E. F. Plow, T. A. Haas, L. Zhang, J. Loftus, J. W. Smith, *J. Biol. Chem.* **2000**, *275*, 21785-21788.
- [471] J. Samanen, Z. Jonak, D. Rieman, T.-L. Yue, *Curr. Pharm. Des.* **1997**, *3*, 545-584.
- [472] R. O. Hynes, *Nature Med.* **2002**, *8*, 918-921.
- [473] P. C. Brooks, R. A. F. Clark, D. A. Cheresh, *Science* **1994**, *264*, 569-571.
- [474] B. P. Eliceiri, D. A. Cheresh, *Curr. Opin. Cell Biol.* **2001**, *13*, 563-568.
- [475] A. M. P. Montgomery, R. A. Reisfeld, D. A. Cheresh, *Proc. Natl. Acad. Sci. USA* **1994**, *91*, 8856-8860.
- [476] E. Ruoslahti, J. C. Reed, *Cell* **1994**, *77*, 477-478.
- [477] B. A. Crippes, V. W. Englemann, S. L. Settle, J. Delarco, R. L. Ornberg, M. H. Helfrich, M. A. Horton, G. A. Nickols, *Endocrinology* **1996**, *137*, 918-924.
- [478] M. Kantlehner, P. Schaffner, D. Finsinger, J. Meyer, A. Jonczyk, B. Diefenbach, B. Nies, G. Hölzemann, S. L. Goodman, H. Kessler, *ChemBioChem* **2000**, *1*, 107-114.

- [479] J.-P. Xiong, T. Stehle, B. Diefenbach, R. Zhang, R. Dunker, D. L. Scott, A. Joachimiak, S. L. Goodman, M. A. Arnaout, *Science* **2001**, *294*, 339-345.
- [480] A. P. Mould, A. Komoriya, K. M. Yamada, M. J. Humphries, *J. Biol. Chem.* **1991**, *266*, 3579-3585.
- [481] J.-O. Lee, L. Anne-Bankston, M. A. Arnaout, R. C. Liddington, *Structure* **1995**, *3*, 1333-1340.
- [482] J.-O. Lee, P. Rieu, M. A. Arnaout, R. Liddington, *Cell* **1994**, *80*, 631-638.
- [483] D. J. Rees, E. S. Ades, S. J. Singer, R. O. Hynes, *Nature* **1990**, *347*, 685-689.
- [484] A. P. Gilmore, K. Burridge, *Nature* **1995**, *373*, 197.
- [485] R. P. Johnson, S. W. Craig, *Nature* **1995**, *373*, 261-264.
- [486] C. A. Otey, F. M. Pavalko, K. Burridge, *J. Cell Biol.* **1990**, *111*, 721-729.
- [487] G. Hoelzemann, *IDrugs* **2001**, *4*, 72-81.
- [488] R. M. Scarborough, *Curr. Med. Chem.* **1999**, *6*, 971-981.
- [489] R. M. Keenan, W. H. Miller, L. S. Barton, W. E. Bondinell, R. D. Cousins, D. F. Eppley, S.-M. Hwang, C. Kwon, M. A. Lago, T. T. Nguyen, B. R. Smith, I. N. Uzinskas, C. C. K. Yuan, *Bioorg. Med. Chem. Lett.* **1999**, *9*, 1801-1806.
- [490] W. H. Miller *et al.*, *Bioorg. Med. Chem. Lett.* **1999**, *9*, 1807-1812.
- [491] A. Peyman, V. Wehner, J. Knolle, H. U. Stilz, G. Breipohl, K.-H. Scheunemann, D. Carniato, J.-M. Ruxer, J. F. Gourvest, T. R. Gadek, S. Bondary, *Bioorg. Med. Chem. Lett.* **2000**, *10*, 179-182.
- [492] M. S. Smyth, J. Rose, M. M. Mehrotra, J. Heath, G. Ruther, T. Schotten, J. Serogy, D. Volkots, A. Pandey, R. M. Scarborough, *Bioorg. Med. Chem. Lett.* **2001**, *11*, 1289-1292.
- [493] M. M. Mehrotra, J. A. Heath, J. W. Rose, M. S. Smyth, J. Seerogy, D. L. Volkots, G. Ruther, T. Schotten, L. Alaimo, G. Park, A. Pandey, R. M. Scarborough, *Bioorg. Med. Chem. Lett.* **2002**, *12*, 1103-1107.
- [494] R. S. Meissner, J. J. Perkins, L. T. Duong, G. D. Hartman, W. F. Hofman, J. R. Huff, N. C. Ihle, C.-T. Leu, R. M. Nagy, A. Naylor-Olsen, G. A. Rodan, S. B. Rodan, D. B. Whitman, G. A. Wesolowski, M. E. Duggan, *Bioorg. Med. Chem. Lett.* **2002**, *12*, 25-29.
- [495] A. Manaka, M. Sato, M. Aoki, M. Tanaka, T. Ikeda, Y. Toda, Y. Yamane, S.

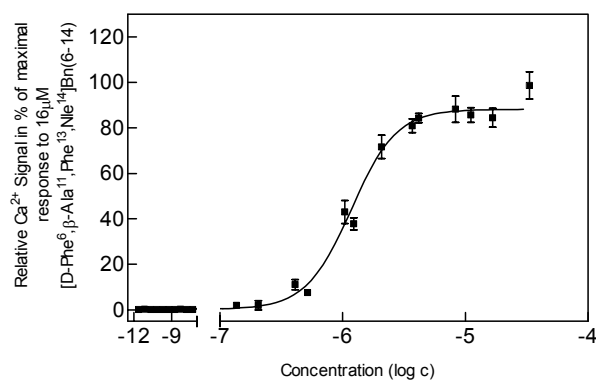
- Nakaike, *Bioorg. Med. Chem. Lett.* **2001**, *11*, 1031-1035.
- [496] A. L. Rockwell, M. Rafalski, W. J. Pitts, D. G. Batt, J. J. Petraitis, W. F. DeGrado, S. Mousa, P. K. Jadhav, *Bioorg. Med. Chem. Lett.* **1999**, *9*, 937-942.
- [497] A. E. Adang, H. Lucas, A. P. de Man, R. A. Engh, P. D. Grootenhuis, *Bioorg. Med. Chem. Lett.* **1998**, *8*, 3603-3608.
- [498] M. E. Duggan, L. T. Duong, J. E. Fisher, T. G. Hamill, W. F. Hoffman, J. R. Huff, N. C. Ihle, C.-T. Leu, R. M. Nagy, J. J. Perkins, S. B. Rodan, G. Wesolowski, D. B. Whitman, A. E. Zartman, G. A. Rodan, G. D. Hartman, *J. Med. Chem.* **2000**, *43*, 3736-3745.
- [499] W. H. Miller, R. M. Keenan, R. N. Willette, M. W. Lark, *Drug Discovery Today* **2000**, *5*, 397-408.
- [500] A. Giannis, F. Rübsam, *Angew. Chem.* **1997**, *109*, 606-609.
- [501] M. Miyashita, M. Akamatsu, Y. Hayashi, T. Ueno, *Bioorg. Med. Chem. Lett.* **2000**, *10*, 859-863.
- [502] J. Perregaard, E. K. Moltzen, E. Meier, C. Sanchez, *J. Med. Chem.* **1995**, *38*, 1998-2008.
- [503] N. L. Allinger, S. Greenberg, *J. Am. Chem. Soc.* **1959**, *81*, 5733-5736.
- [504] A. C. Cope, H. L. Holmes, H. O. House, *Org. React.* **1957**, *9*, 107-331.
- [505] I. McCall, G. R. Proctor, L. Purdie, *J. Chem. Soc. (C)* **1970**, 1126-1128.
- [506] R. F. Naylor, *J. Chem. Soc.* **1947**, 1106-1108.
- [507] P. J. Coleman, B. C. Askew, J. H. Hutchinson, D. B. Whitman, J. J. Perkins, G. D. Hartman, G. A. Rodan, C.-T. Leu, T. Prueksaritanont, C. Fernandez-Metzler, K. M. Merkle, R. Lynch, S. B. Rodan, M. E. Duggan, *Bioorg. Med. Chem. Lett.* **2002**, *12*, 2463-2465.
- [508] K. M. Brashear, C. A. Hunt, B. T. Kucer, M. E. Duggan, G. T. Hartman, G. A. Rodan, S. B. Rodan, C.-T. Leu, T. Prueksaritanont, C. Fernandez-Metzler, A. Barrish, C. F. Homnick, J. H. Hutchinson, P. J. Coleman, *Bioorg. Med. Chem. Lett.* **2002**, *12*, 3483-3486.
- [509] P. J. Coleman *et al.*, *Bioorg. Med. Chem. Lett.* **2002**, *12*, 31-34.
- [510] The Quiagen Effectene Transfection Reagent Handbook. Quiagen, Hilden, Germany, **2001**, 13-14.

10 Appendix

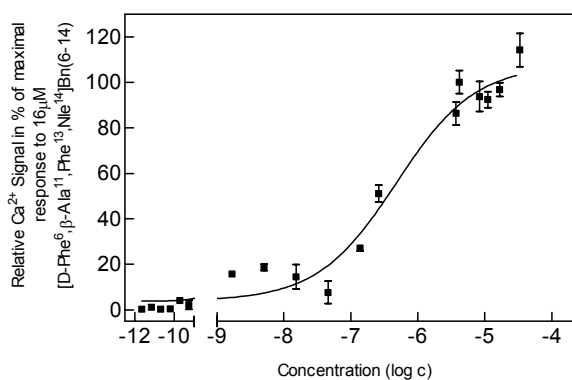
10.1 Alascan of [D-Phe⁶,β-Ala¹¹,Phe¹³,Nle¹⁴]Bn(6-14) (**1**). Dose response curves (BRS-3) of peptides **4-13** (Table 4.2) (n = number of independent dose response measurements).



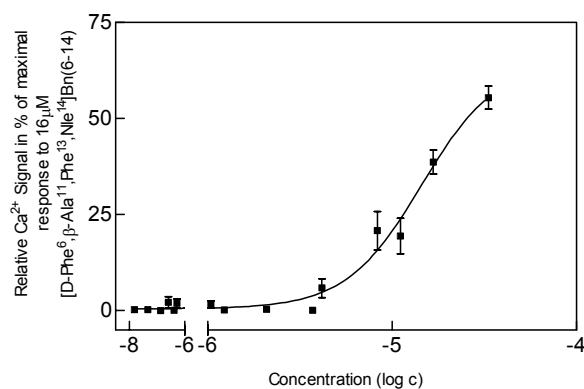
10 (BRS-3, n = 8)



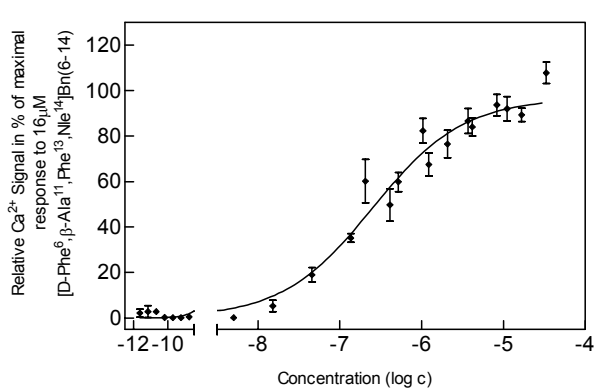
11 (BRS-3, n = 6)



12 (BRS-3, n = 6)

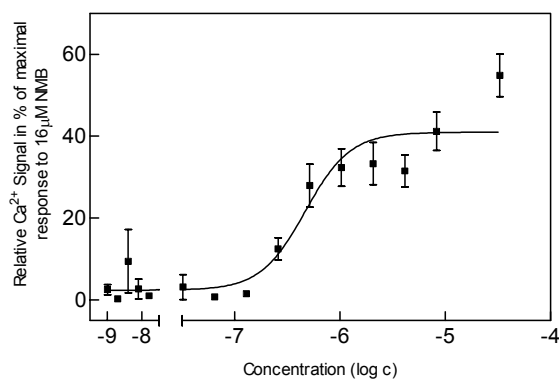


13 (BRS-3, n = 6)

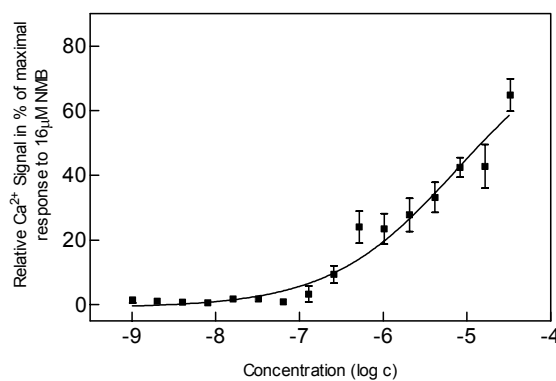


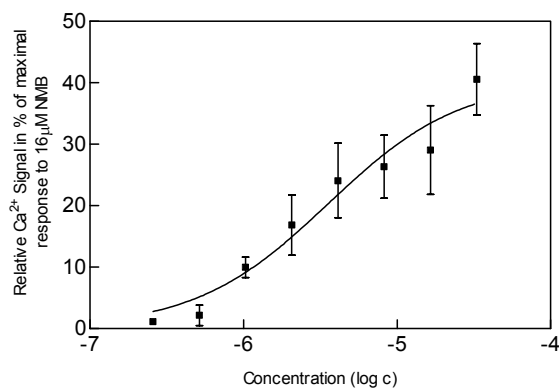
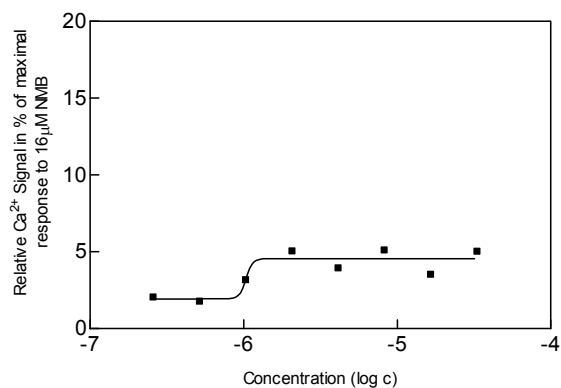
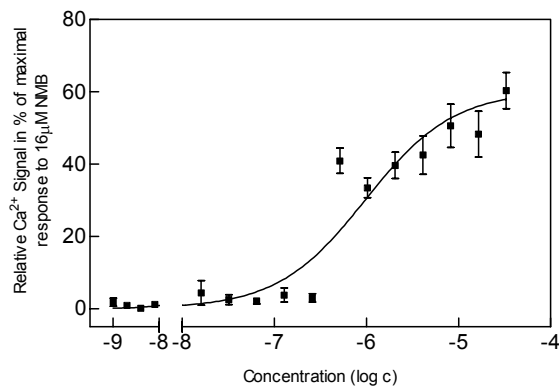
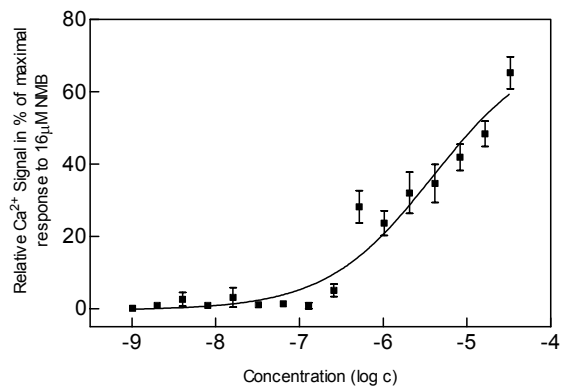
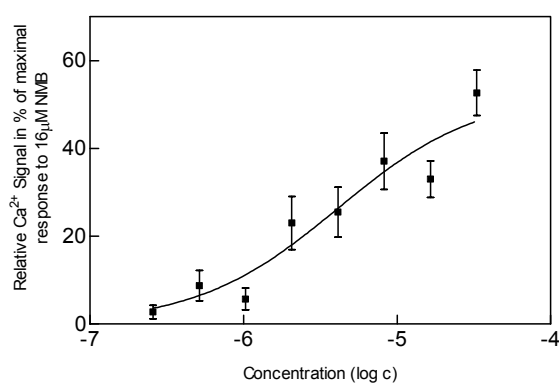
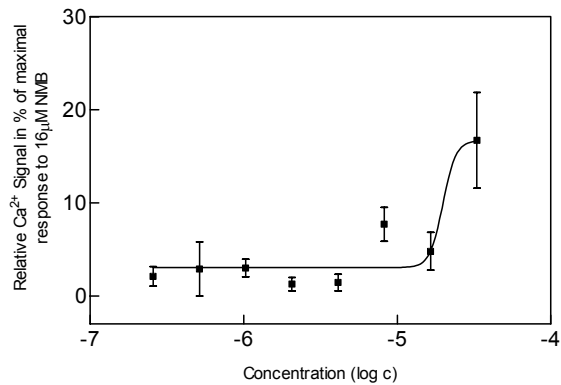
10.2 Alascan of $[D\text{-Phe}^6,\beta\text{-Ala}^{11},\text{Phe}^{13},\text{Nle}^{14}]\text{Bn}(6\text{-}14)$ (**1**). Dose response curves (NMB-R) of peptides **4-13** (Table 4.2).

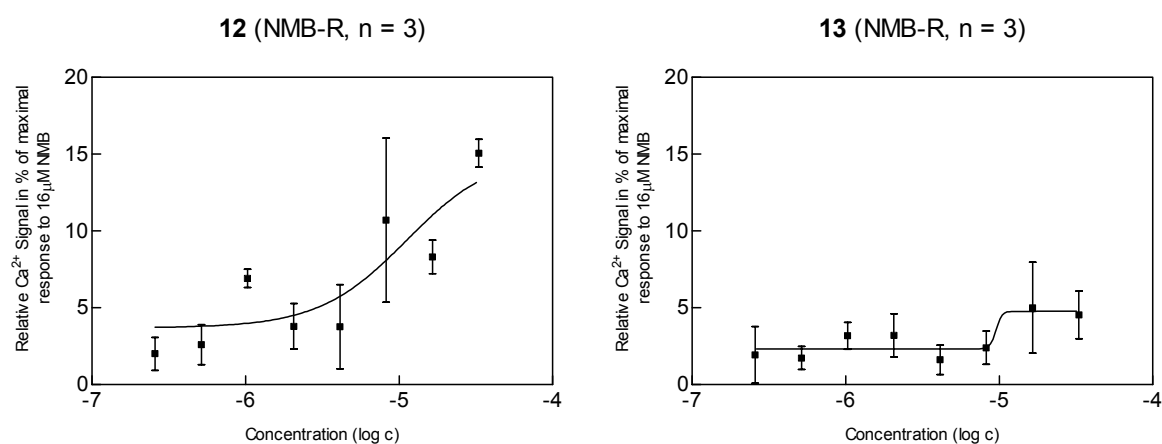
4 (NMB-R, n = 5)



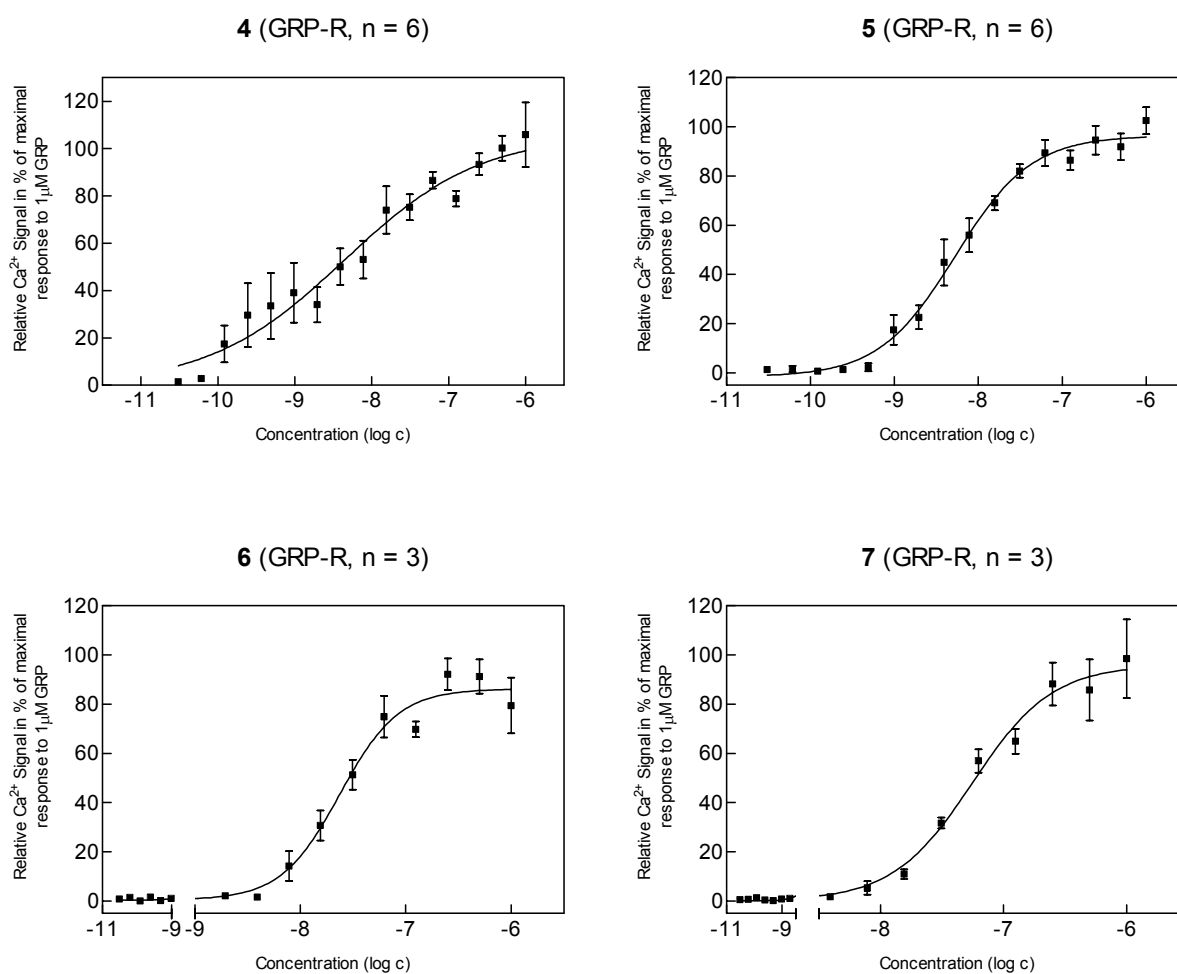
5 (NMB-R, n = 5)

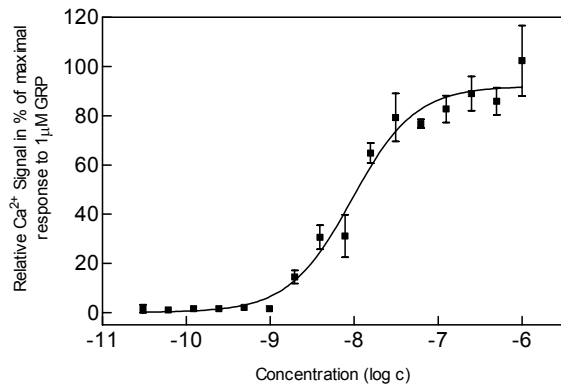
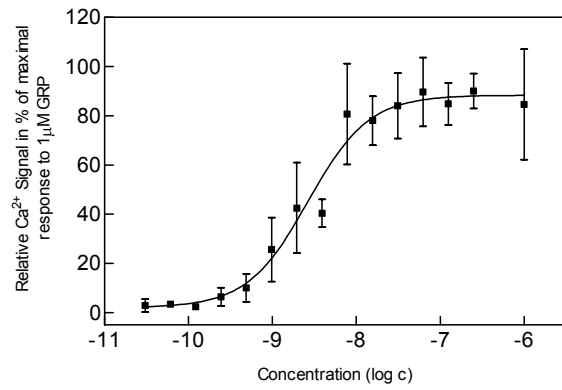
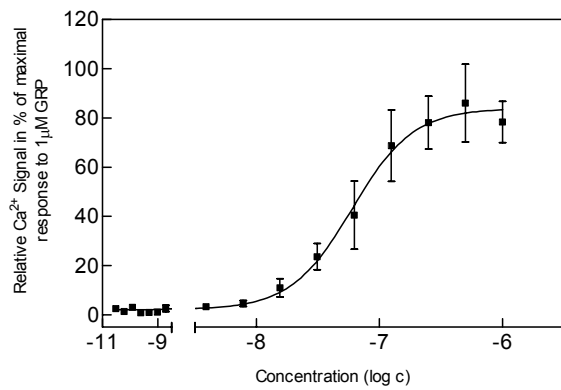
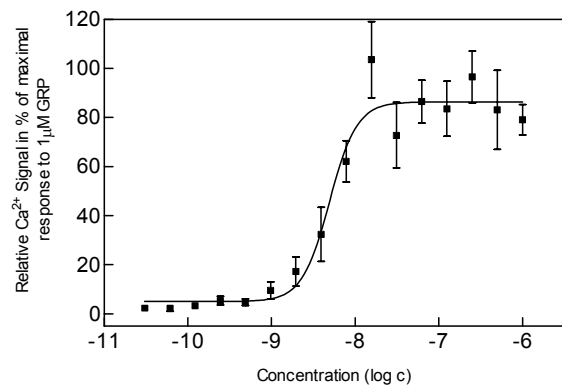
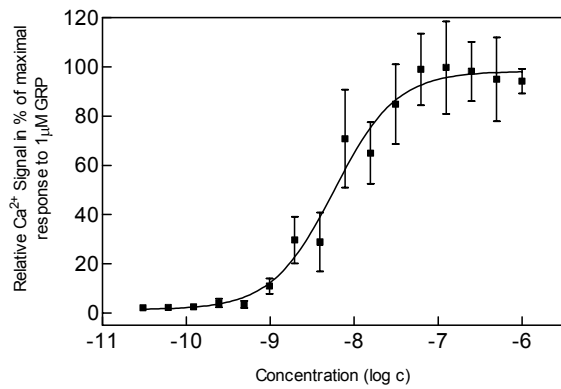
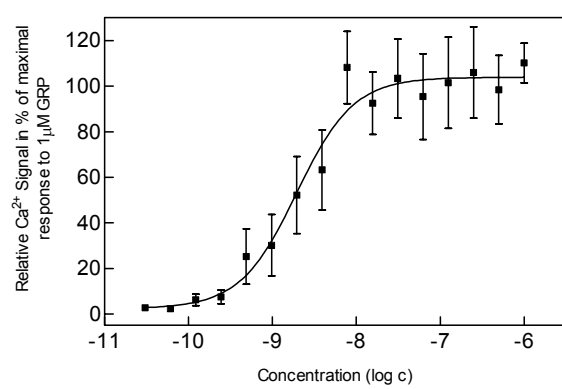


6 (NMB-R, n = 3)**7 (NMB-R, n = 3)****8 (NMB-R, n = 5)****9 (NMB-R, n = 5)****10 (NMB-R, n = 3)****11 (NMB-R, n = 3)**

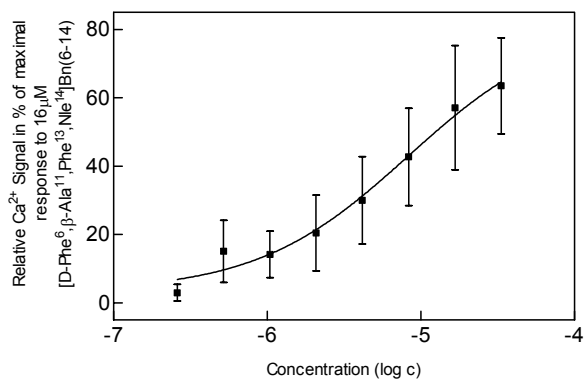
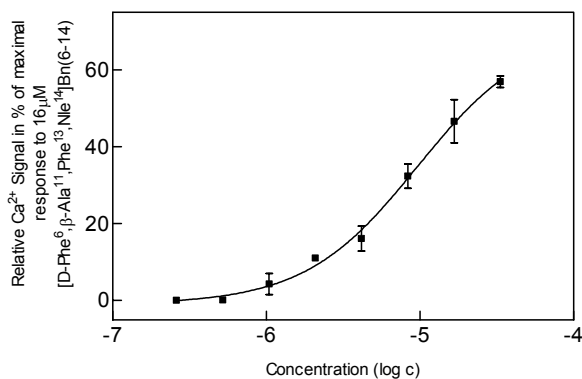
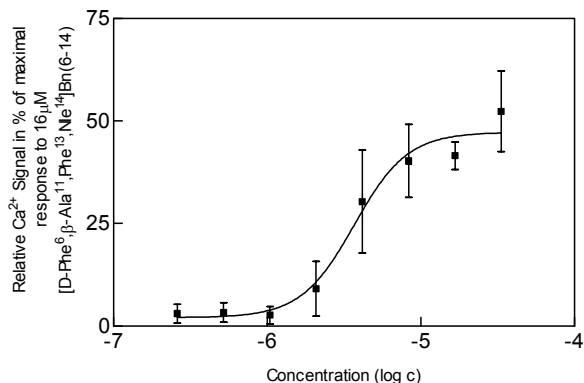
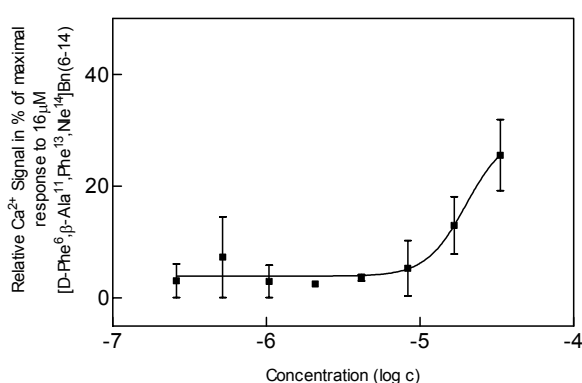
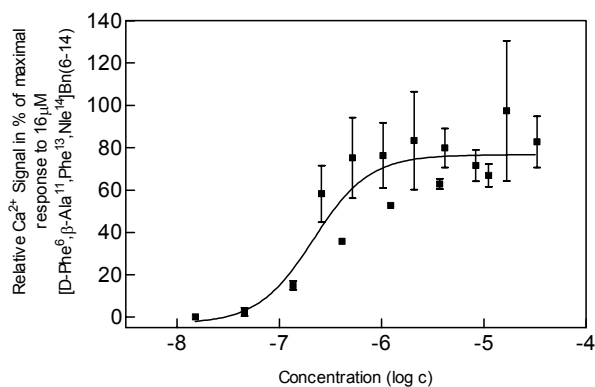
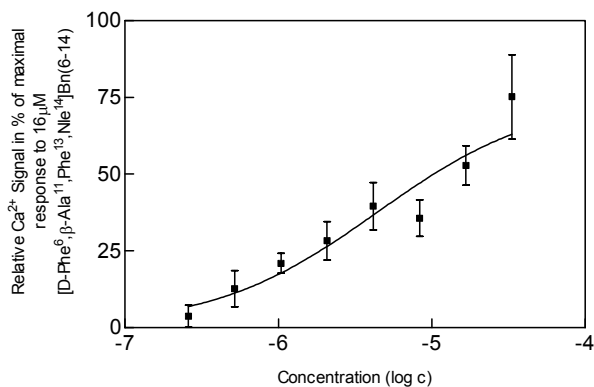


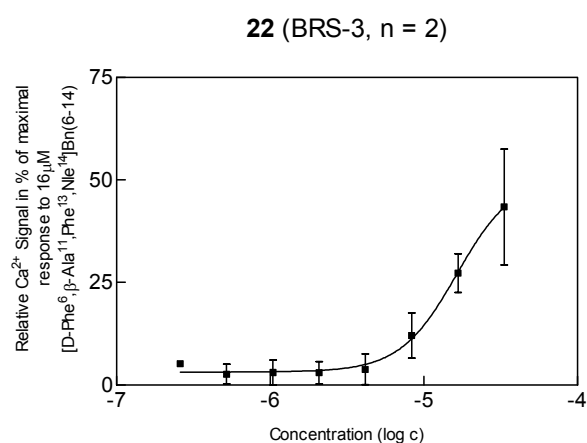
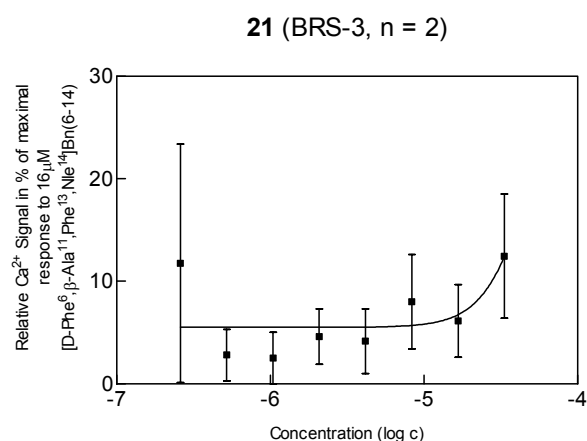
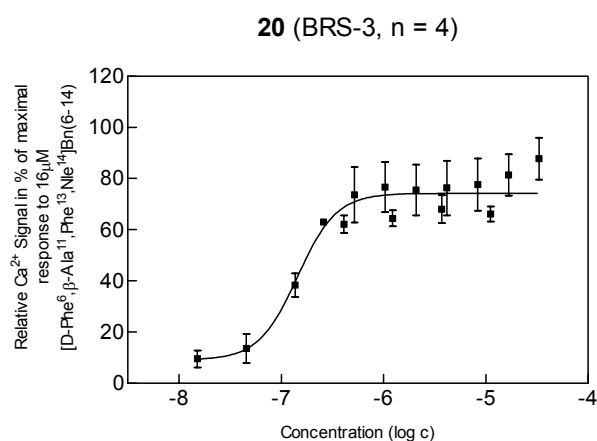
10.3 Alascan of [D-Phe⁶,β-Ala¹¹,Phe¹³,Nle¹⁴]Bn(6-14) (**1**). Dose response curves (GRP-R) of peptides **4-13** (Table 4.2).



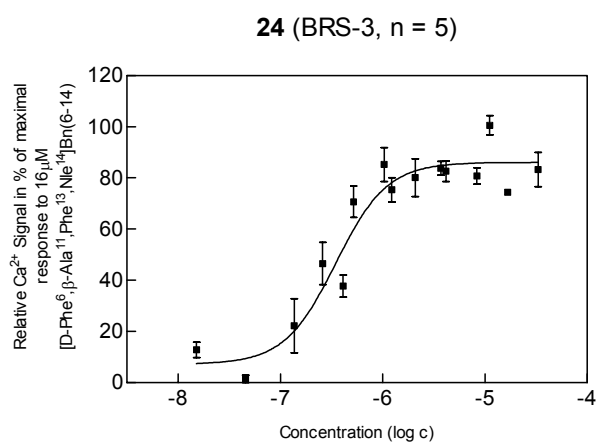
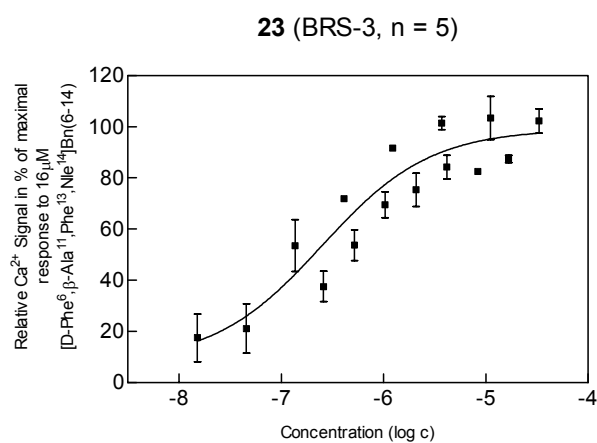
8 (GRP-R, n = 3)**9** (GRP-R, n = 3)**10** (GRP-R, n = 3)**11** (GRP-R, n = 3)**12** (GRP-R, n = 3)**13** (GRP-R, n = 3)

10.4 Alascan of [D-Phe⁶,Phe¹³]Bn(6-13) propylamide. Dose response curves (BRS-3) of peptides 14-22 (Table 4.3).

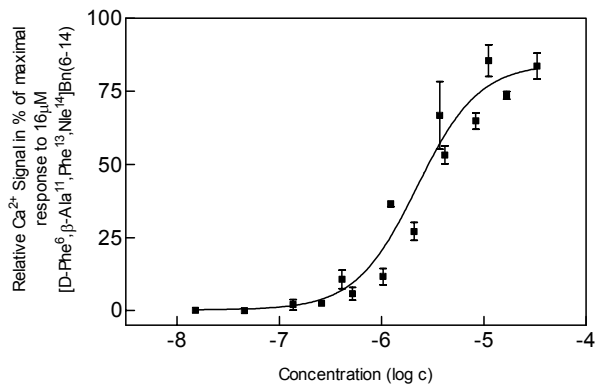
14 (BRS-3, n = 4)**15** (BRS-3, n = 2)**16** (BRS-3, n = 2)**17** (BRS-3, n = 2)**18** (BRS-3, n = 4)**19** (BRS-3, n = 2)



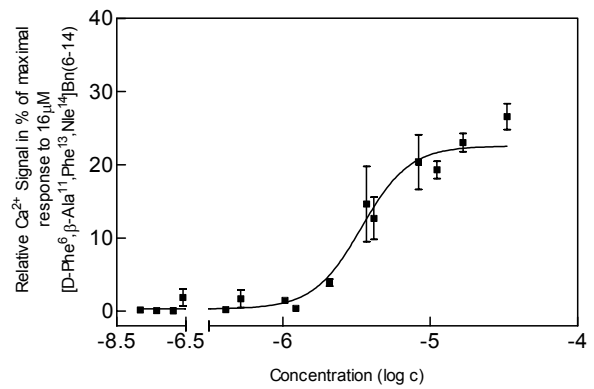
10.5 D-amino acid scan of [D-Phe⁶,β-Ala¹¹,Phe¹³,Nle¹⁴]Bn(6-14) (**1**). Dose response curves (BRS-3) of peptides **23-31** (Table 4.4).



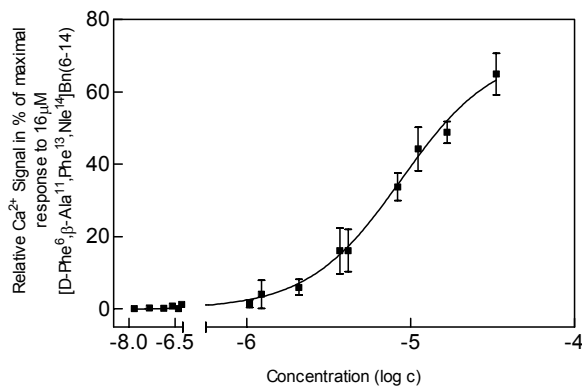
25 (BRS-3, n = 5)



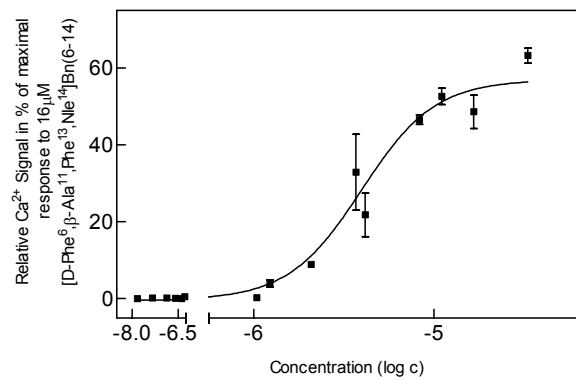
26 (BRS-3, n = 5)



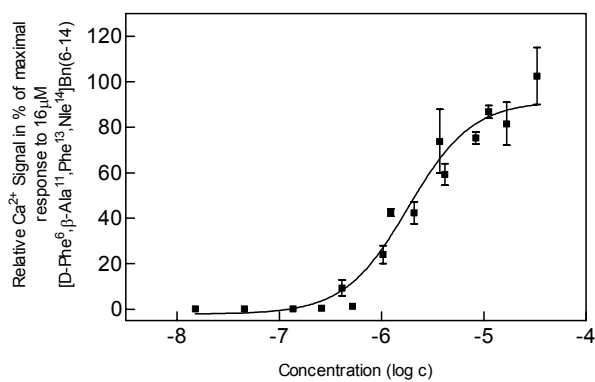
27 (BRS-3, n = 5)



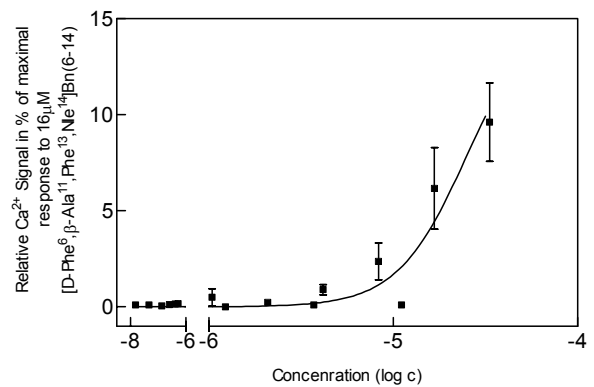
28 (BRS-3, n = 5)

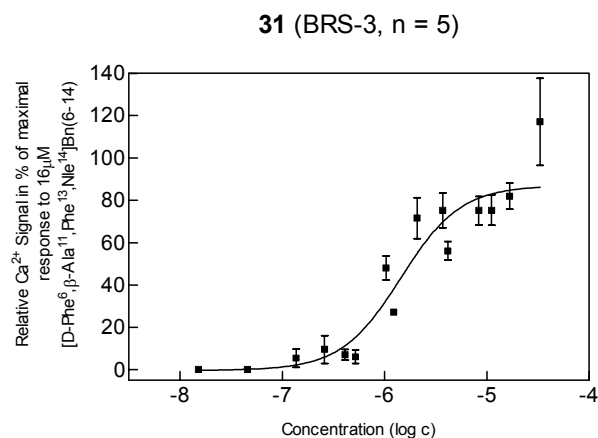


29 (BRS-3, n = 5)

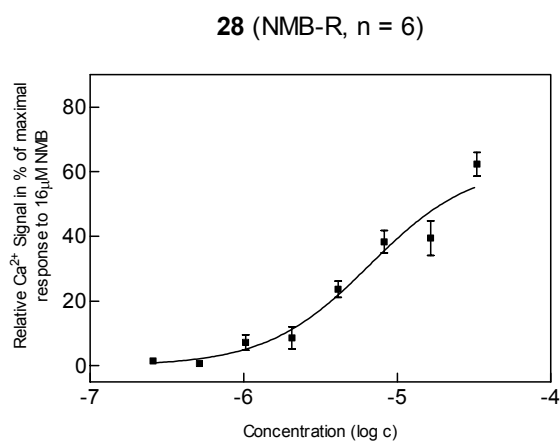
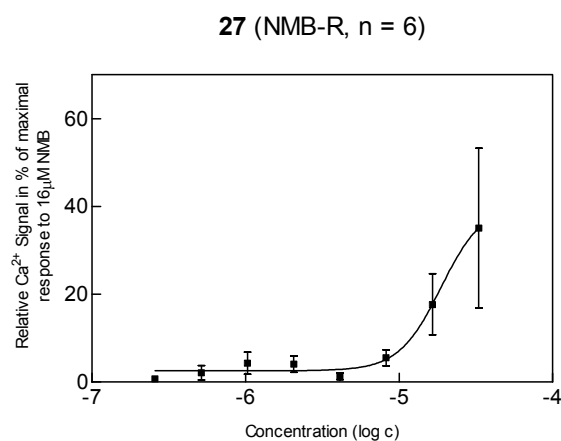
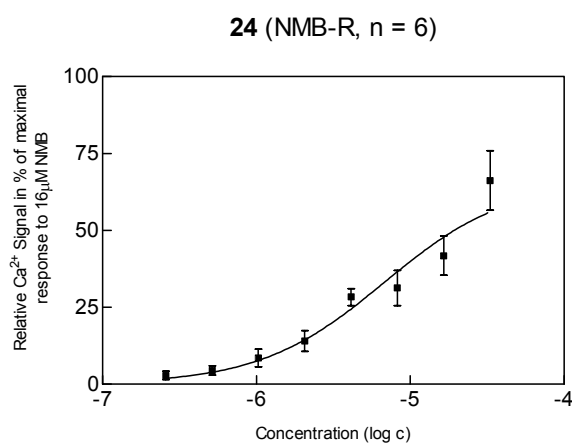
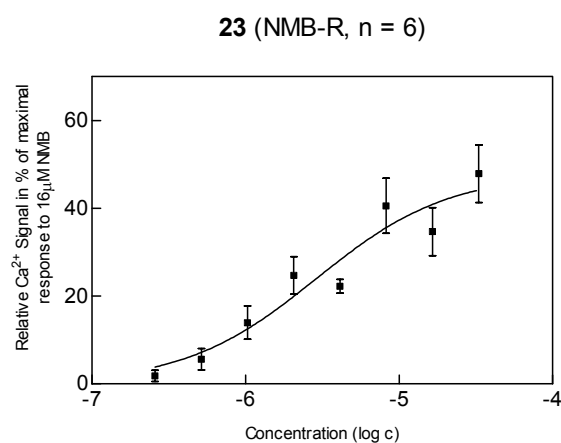


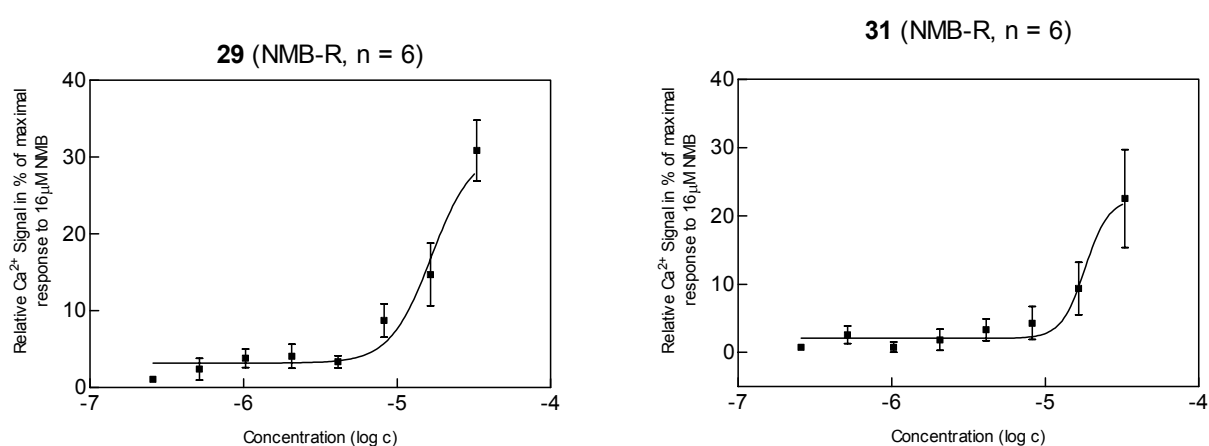
30 (BRS-3, n = 5)



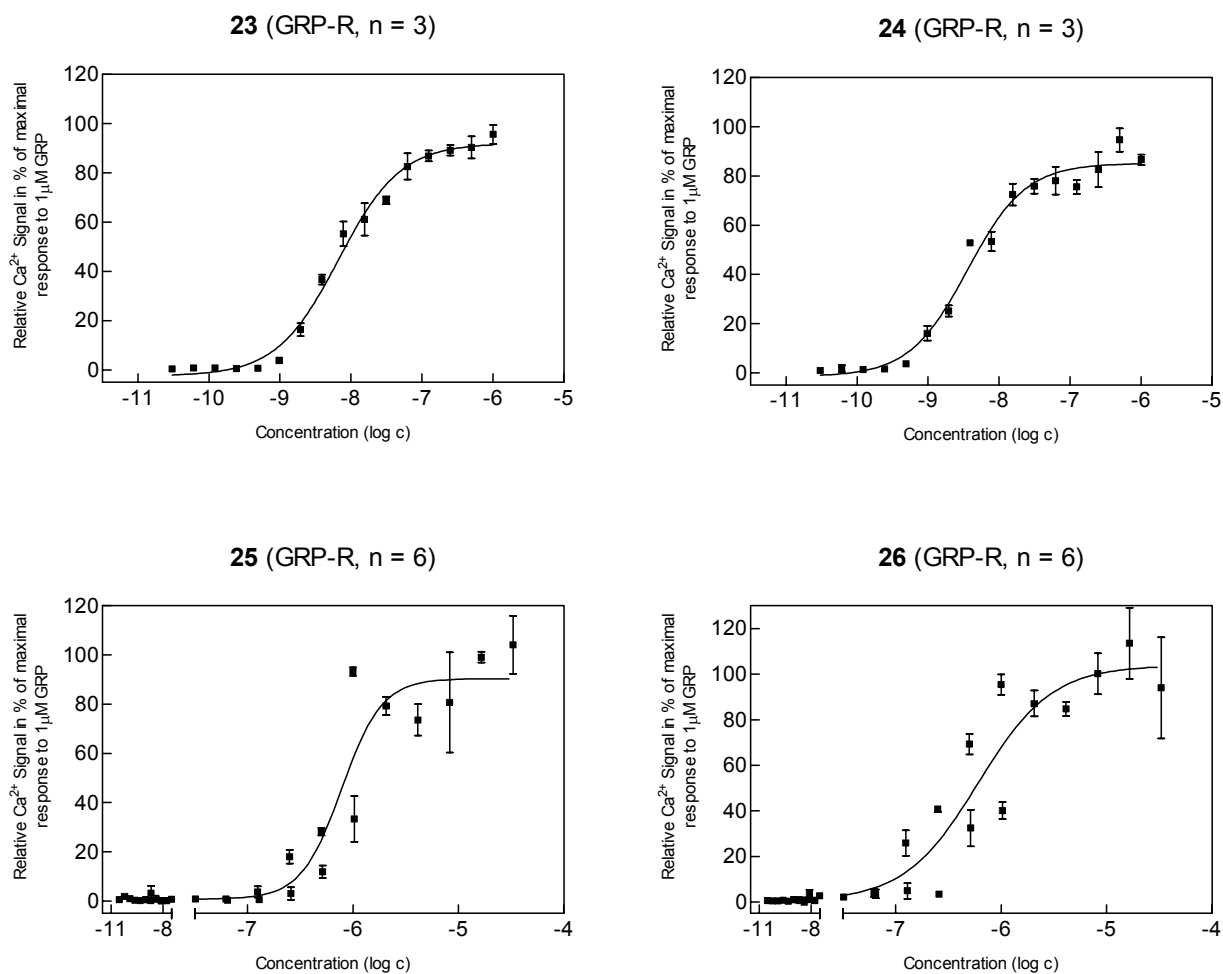


10.6 D-amino acid scan of [D-Phe⁶, β -Ala¹¹,Phe¹³,Nle¹⁴]Bn(6-14) (**1**). Dose response curves (NMB-R) of peptides **23**, **24**, **27-29**, **31** (Table 4.4).

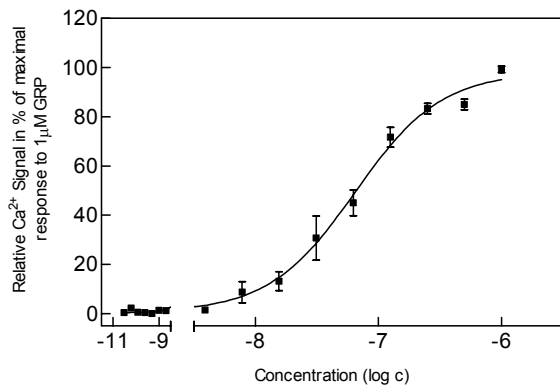




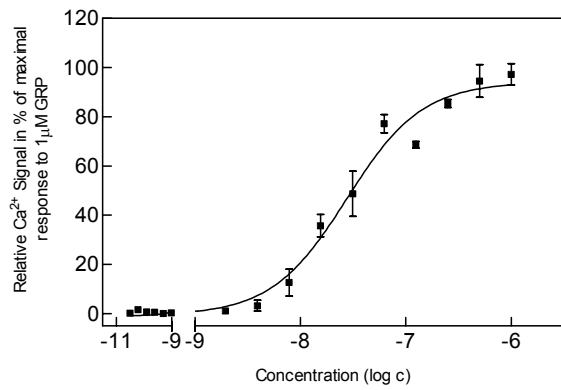
10.7 D-amino acid scan of [D-Phe⁶,β-Ala¹¹,Phe¹³,Nle¹⁴]Bn(6-14) (**1**). Dose response curves (GRP-R) of peptides **23-31** (Table 4.4).



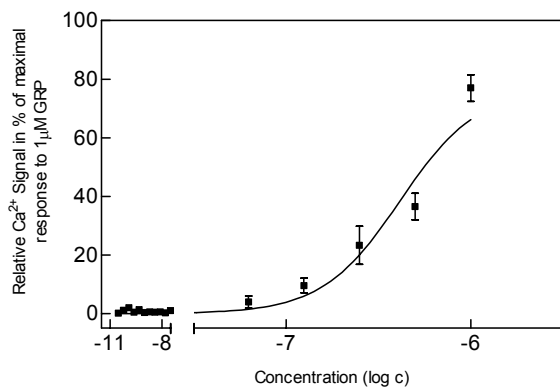
27 (GRP-R, n = 3)



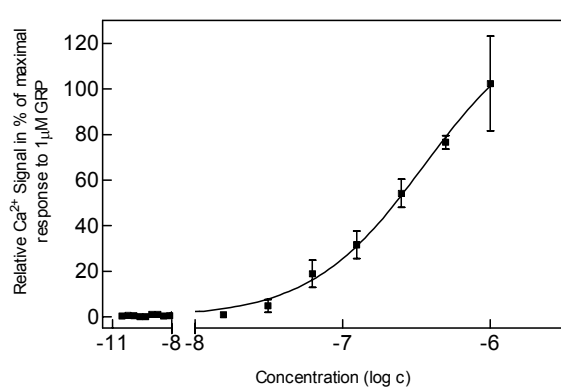
28 (GRP-R, n = 3)



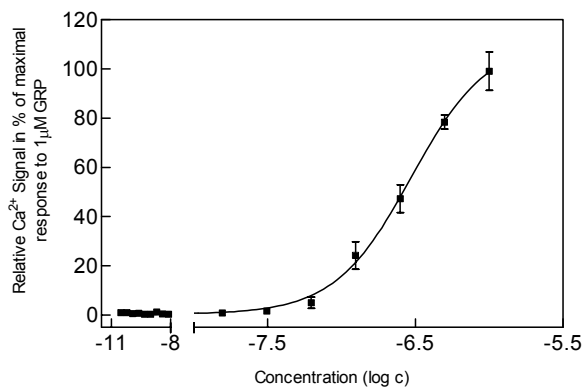
29 (GRP-R, n = 3)



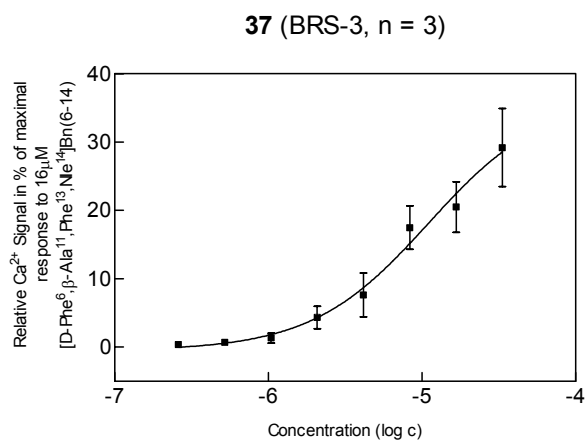
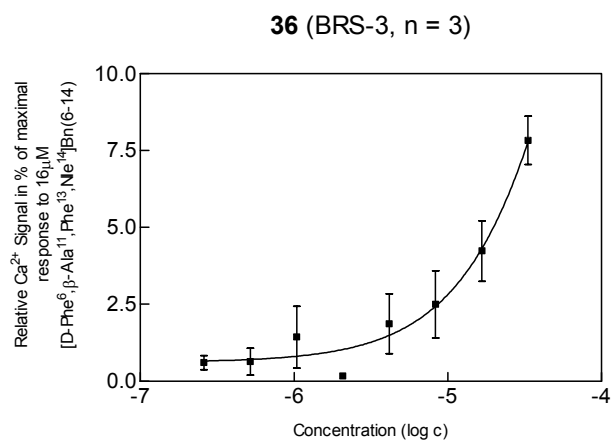
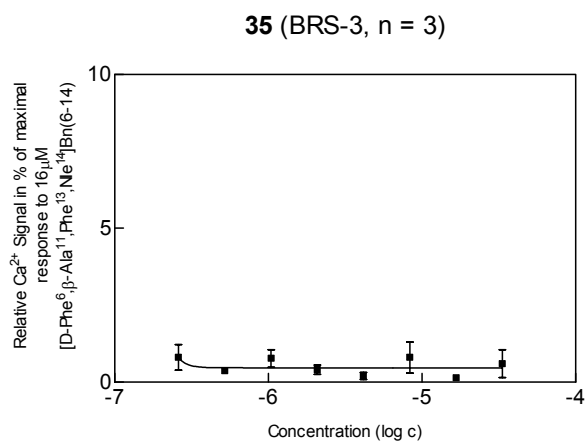
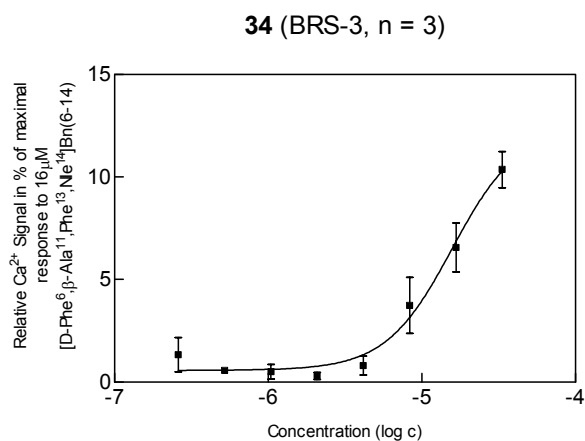
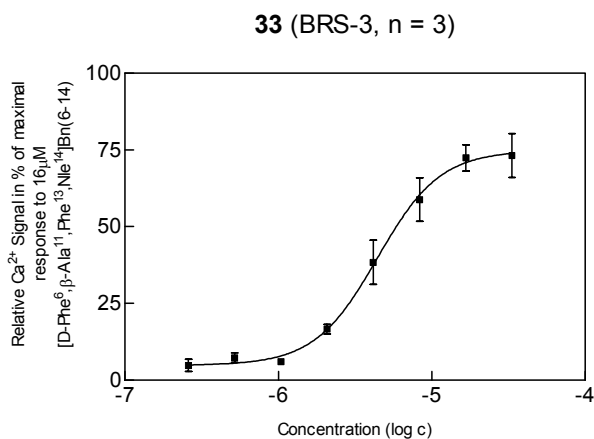
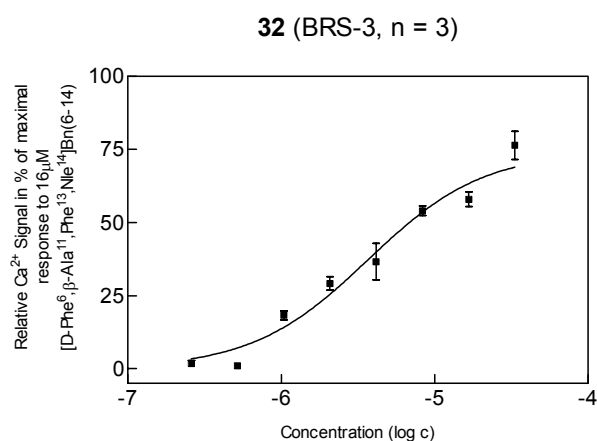
30 (GRP-R, n = 3)



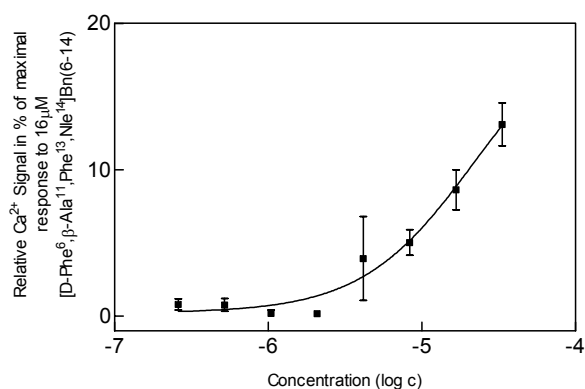
31 (GRP-R, n = 3)



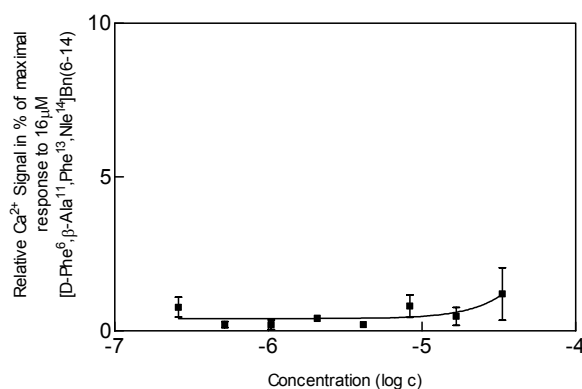
10.8 D-amino acid scan of [D-Phe⁶,Phe¹³]Bn(6-13) propylamide. Dose response curves (BRS-3) of peptides 32-39 (Table 4.5).



38 (BRS-3, n = 3)

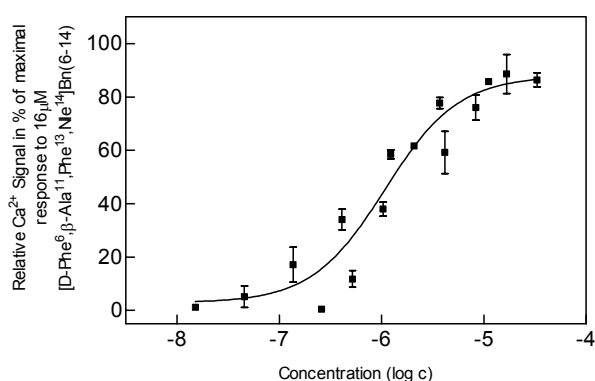


39 (BRS-3, n = 3)

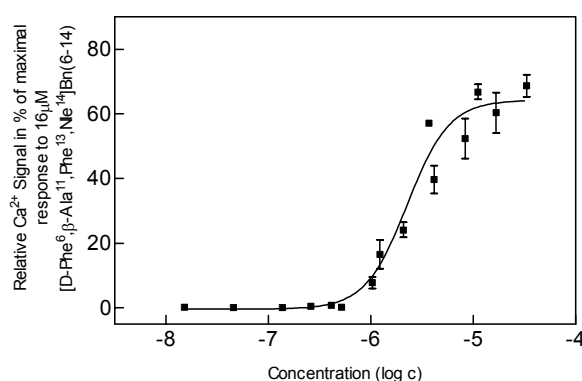


10.9 Analogues of [D-Phe⁶,β-Ala¹¹,Phe¹³,Ne¹⁴]Bn(6-14) (**1**) with N-terminal and/or C-terminal deleted amino acids, individual amino acids are substituted and the N-terminus is acetylated. Dose response curves (BRS-3) of peptides **40-57** (Tables 4.6 and 4.7).

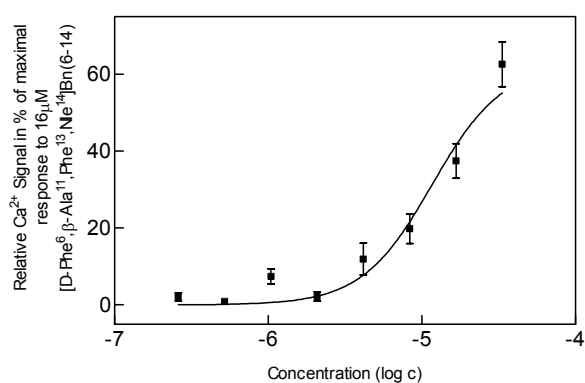
40 (BRS-3, n = 5)



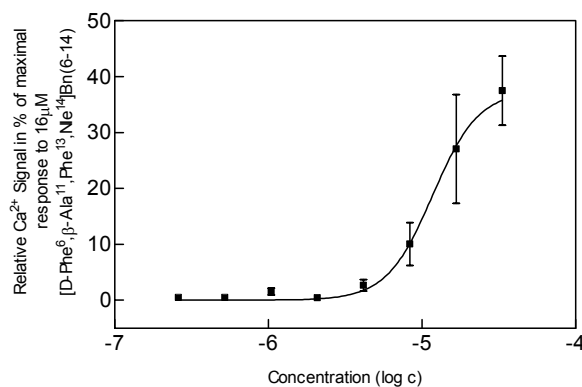
41 (BRS-3, n = 5)



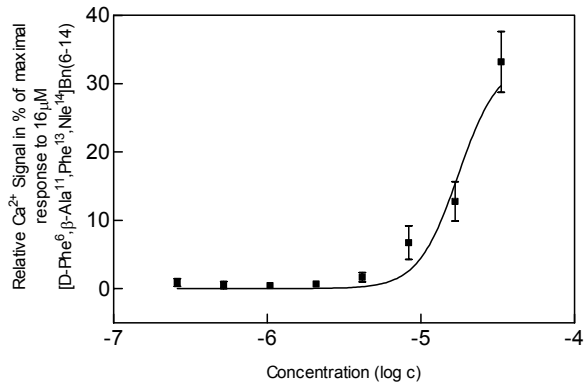
42 (BRS-3, n = 3)



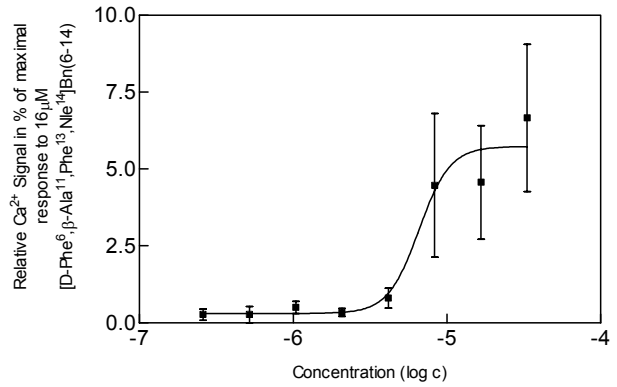
43 (BRS-3, n = 3)



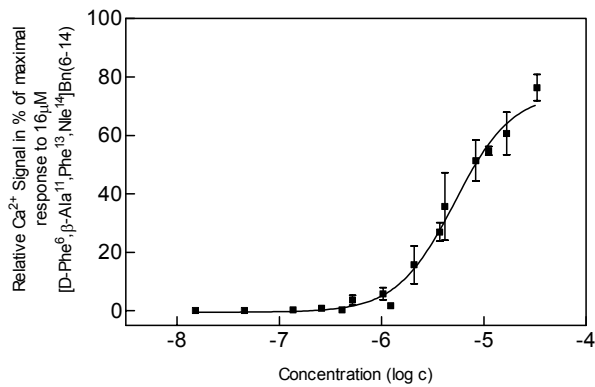
44 (BRS-3, n = 3)



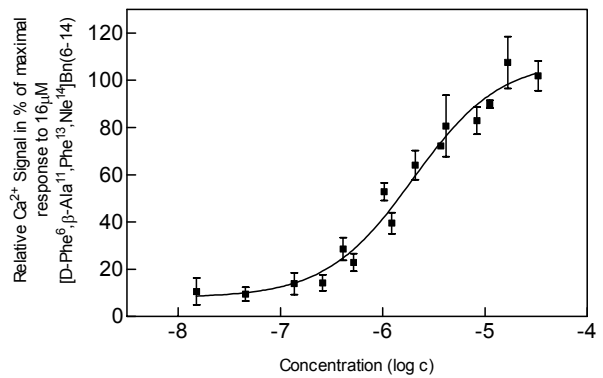
45 (BRS-3, n = 3)



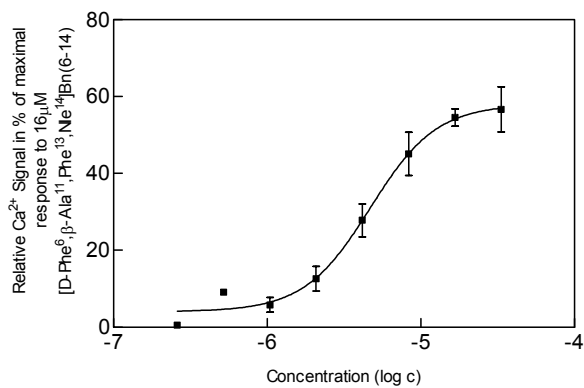
46 (BRS-3, n = 5)



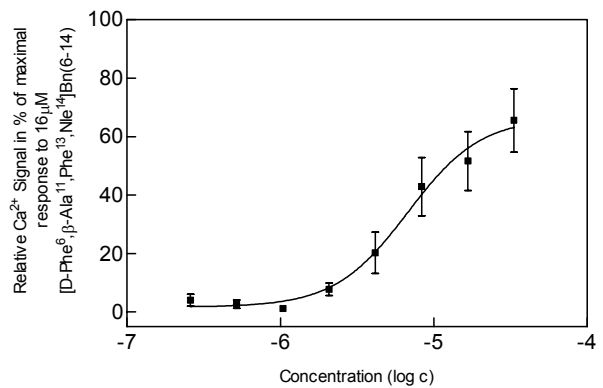
47 (BRS-3, n = 5)



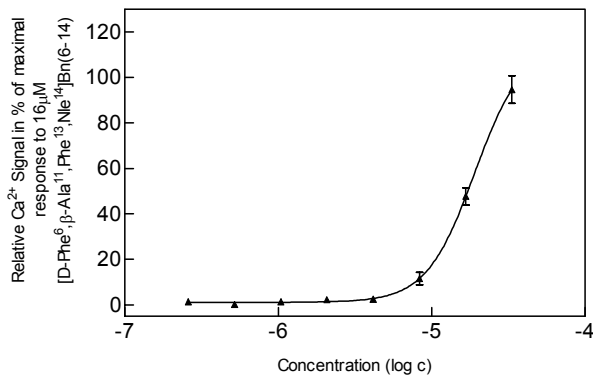
48 (BRS-3, n = 3)



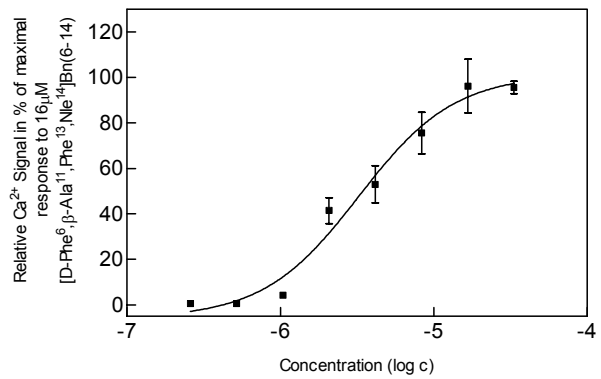
49 (BRS-3, n = 3)



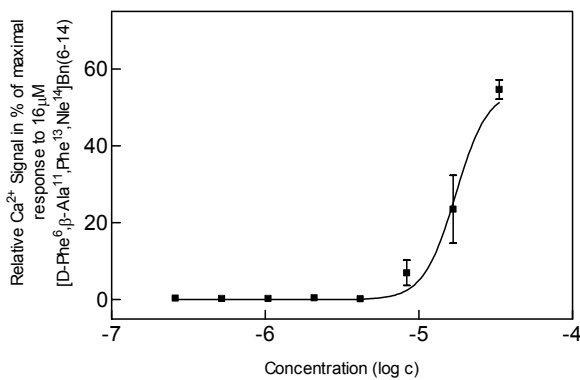
50 (BRS-3, n = 3)



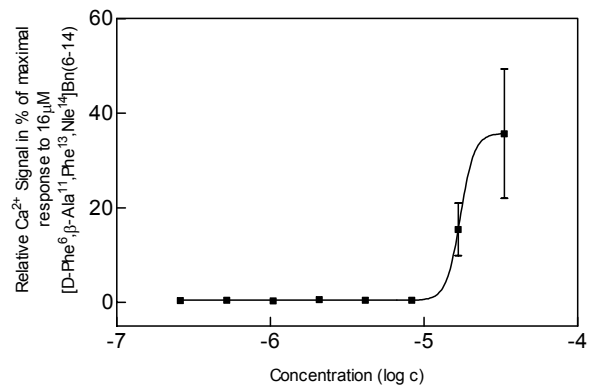
51 (BRS-3, n = 3)



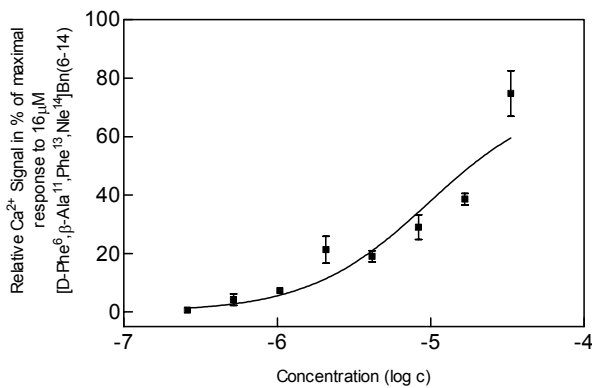
52 (BRS-3, n = 3)



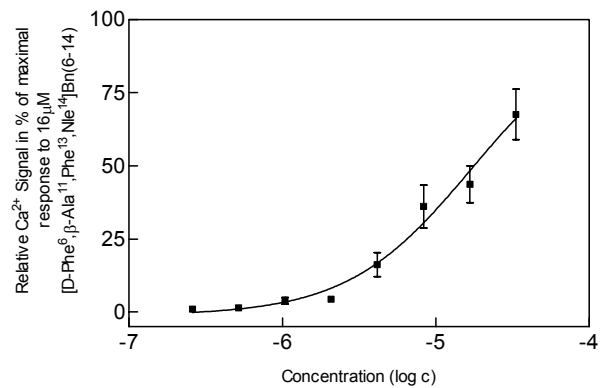
53 (BRS-3, n = 3)

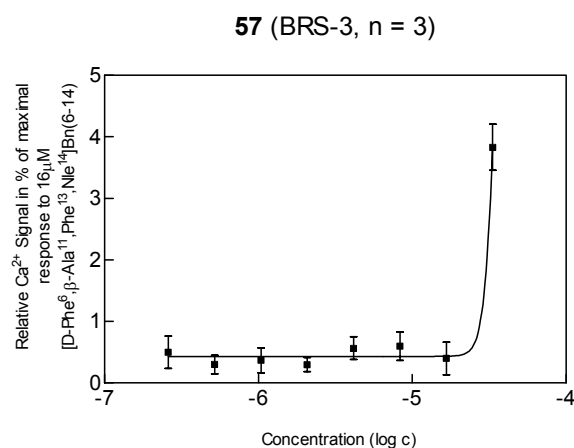
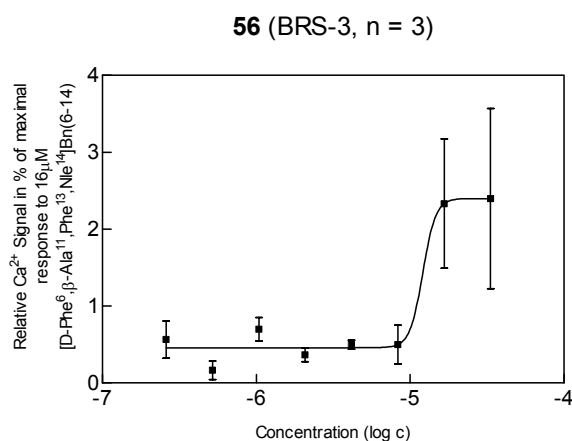


54 (BRS-3, n = 3)

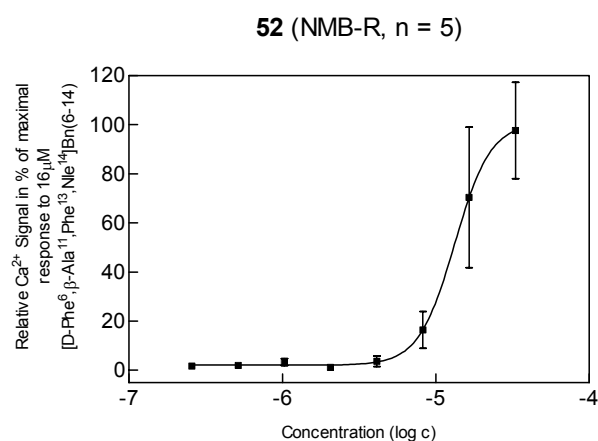
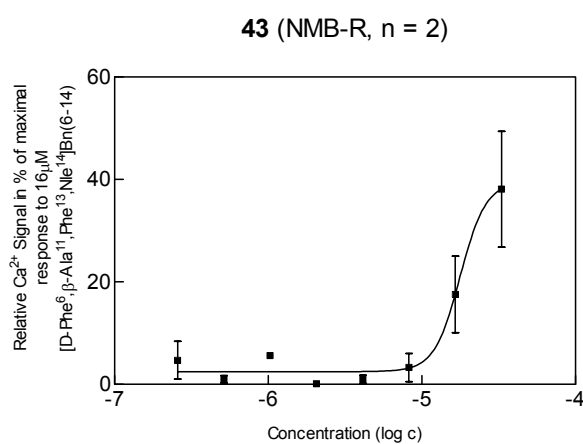
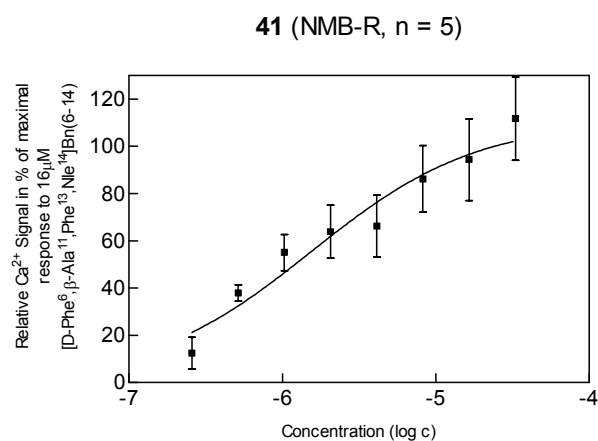
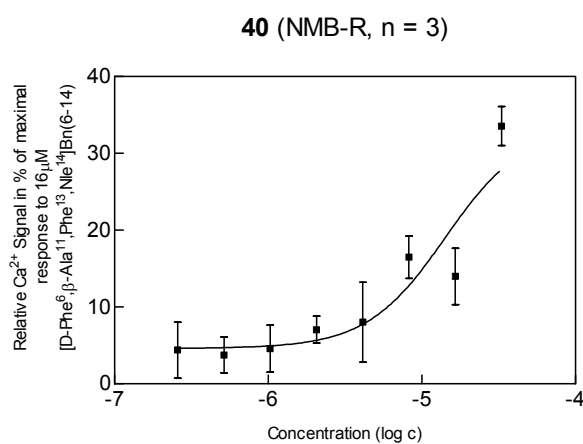


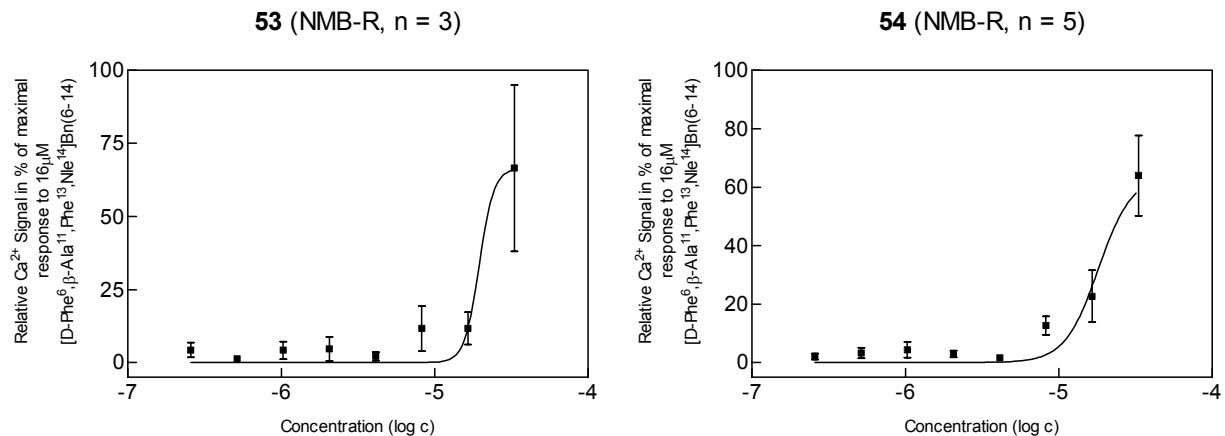
55 (BRS-3, n = 3)



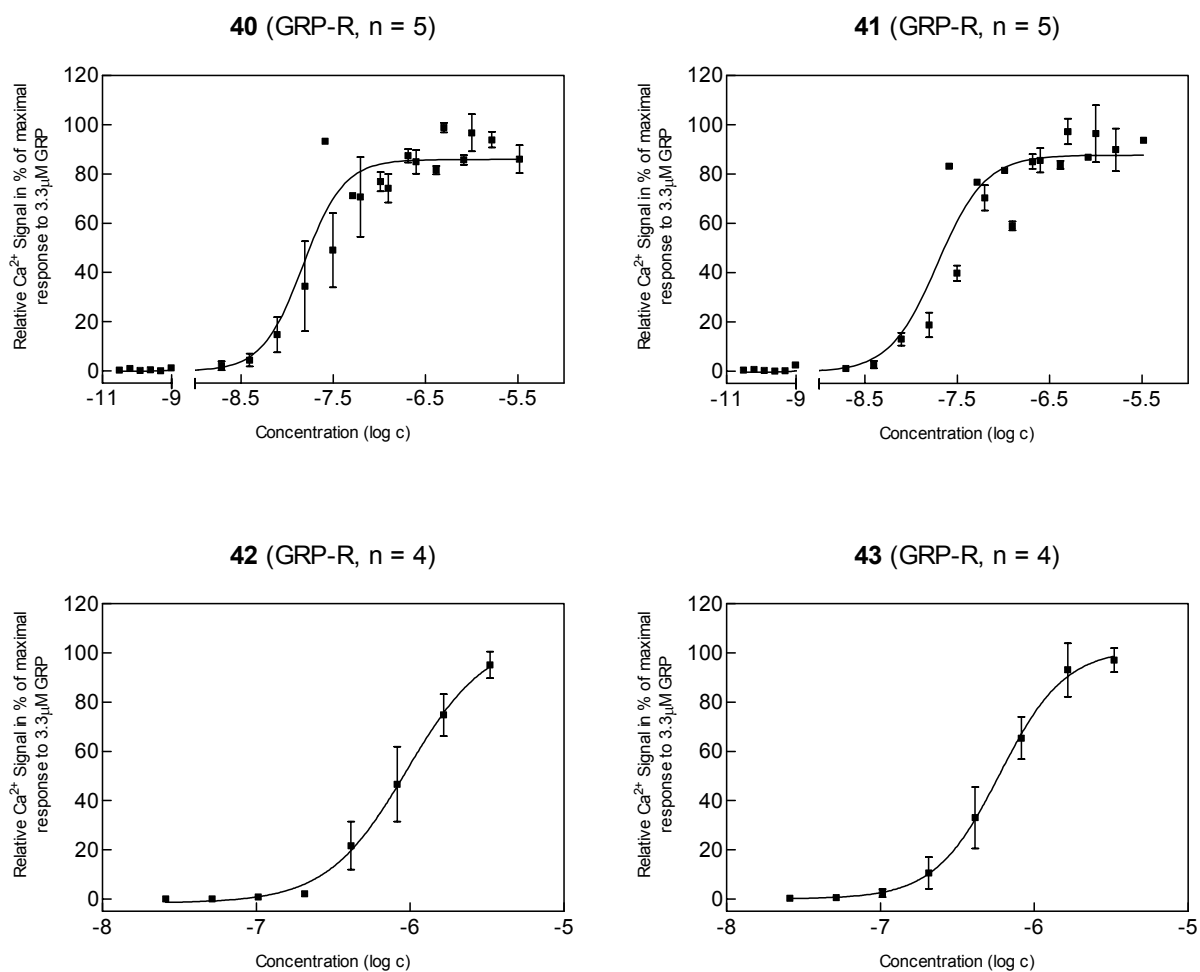


10.10 Analogues of [D-Phe⁶,β-Ala¹¹,Phe¹³,Nle¹⁴]Bn(6-14) (**1**) with N-terminal and/or C-terminal deleted amino acids, individual amino acids are substituted and the N-terminus is acetylated. Dose response curves (NMB-R) of peptides **40**, **41**, **43**, **52-54** (Tables 4.6 and 4.7).

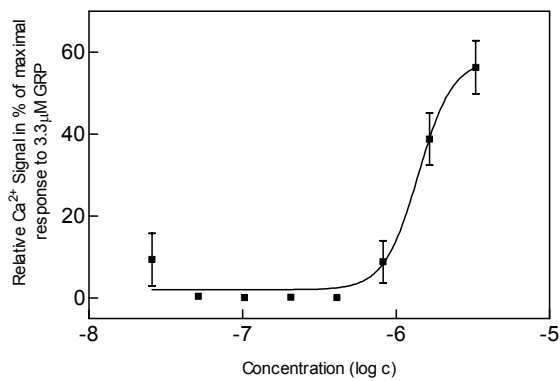




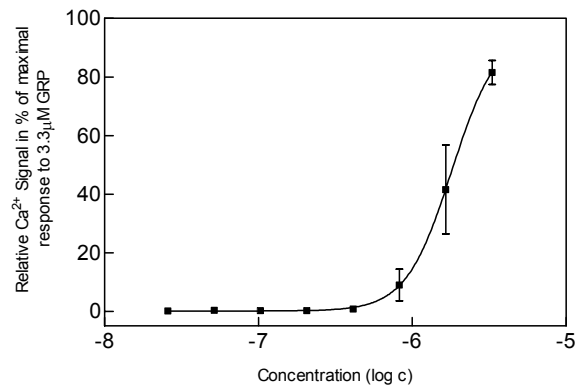
10.11 Analogues of $[D\text{-Phe}^6,\beta\text{-Ala}^{11},\text{Phe}^{13},\text{Nle}^{14}]\text{Bn}(6\text{-}14)$ with N-terminal and/or C-terminal deleted amino acids, individual amino acids are substituted and the N-terminus is acetylated. Dose response curves (GRP-R) of peptides **40-55** (Tables 4.6 and 4.7).



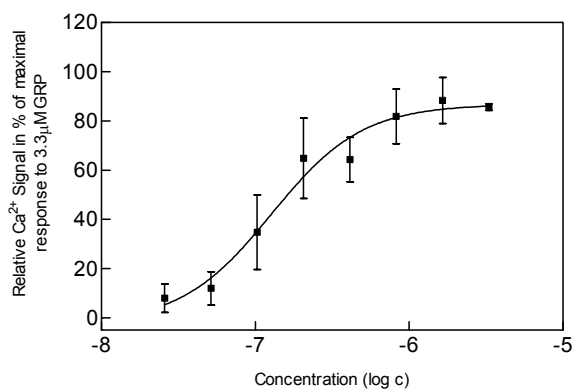
44 (GRP-R, n = 4)



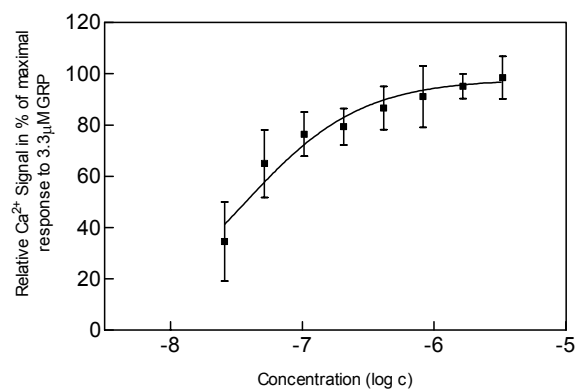
45 (GRP-R, n = 4)



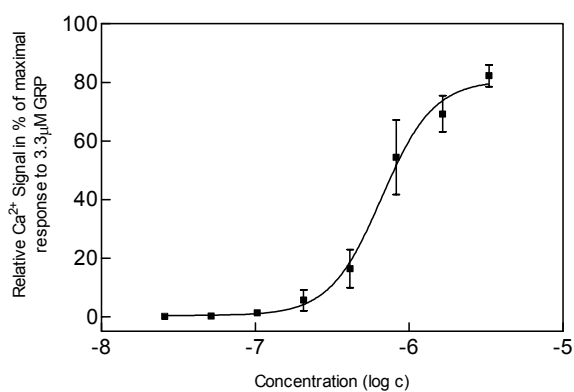
46 (GRP-R, n = 4)



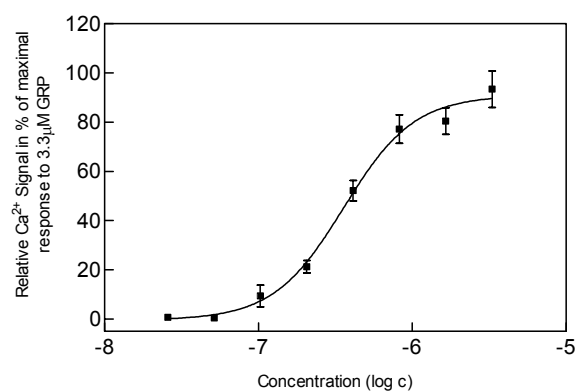
47 (GRP-R, n = 4)



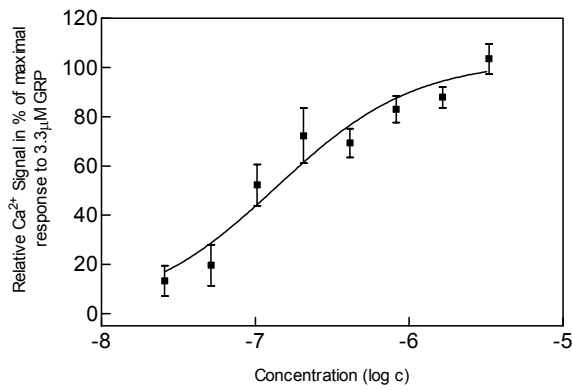
48 (GRP-R, n = 4)



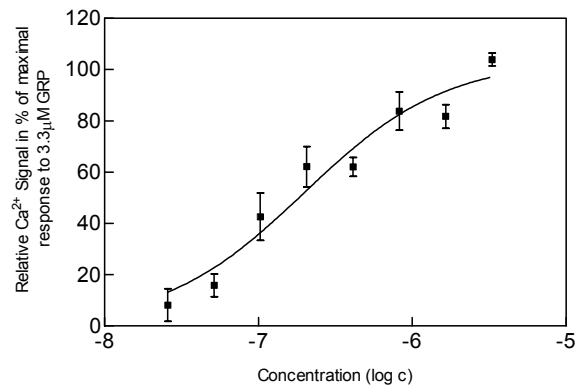
49 (GRP-R, n = 4)



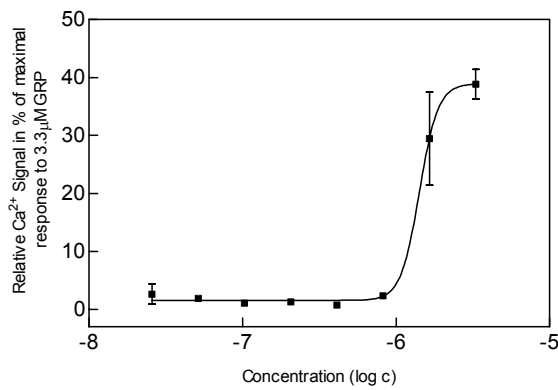
50 (GRP-R, n = 4)



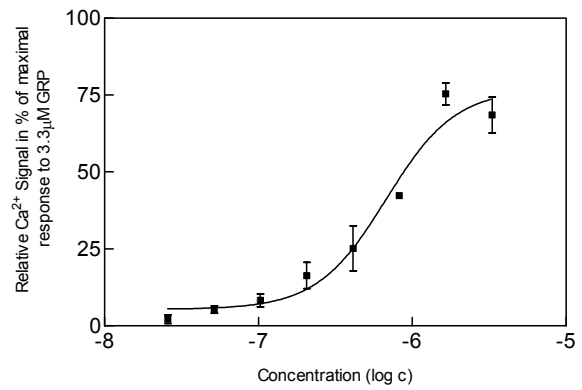
51 (GRP-R, n = 4)



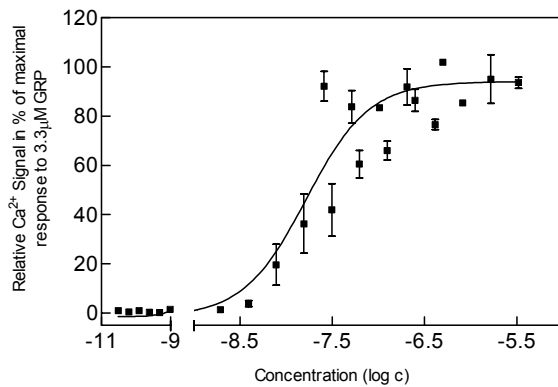
52 (GRP-R, n = 2)



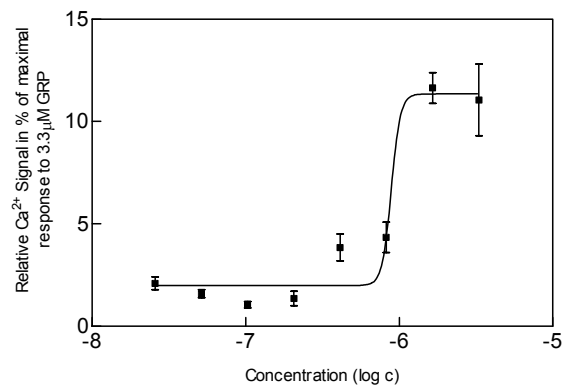
53 (GRP-R, n = 2)

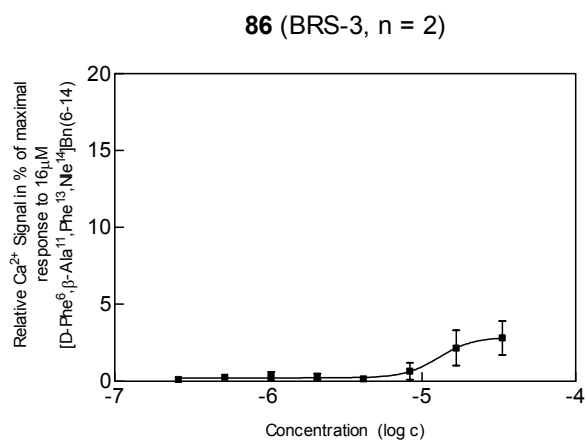
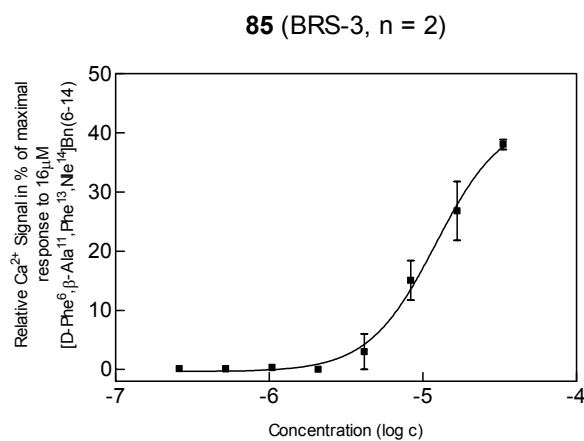
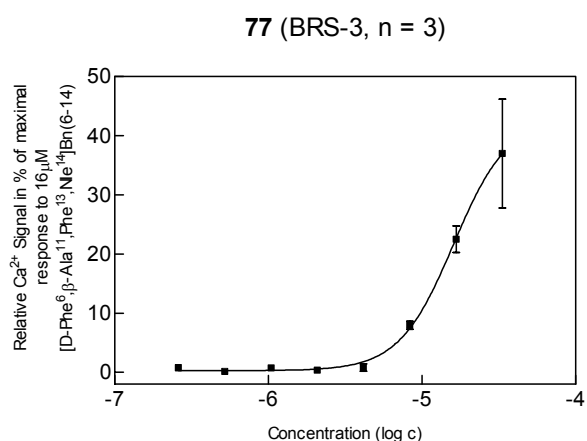
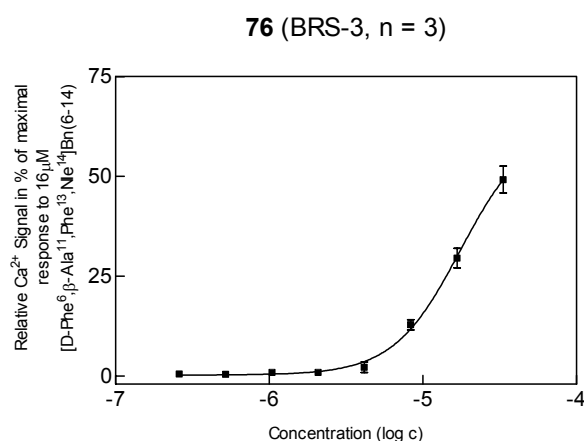
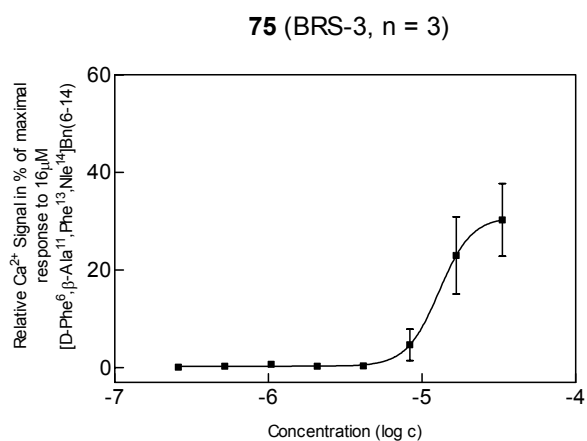
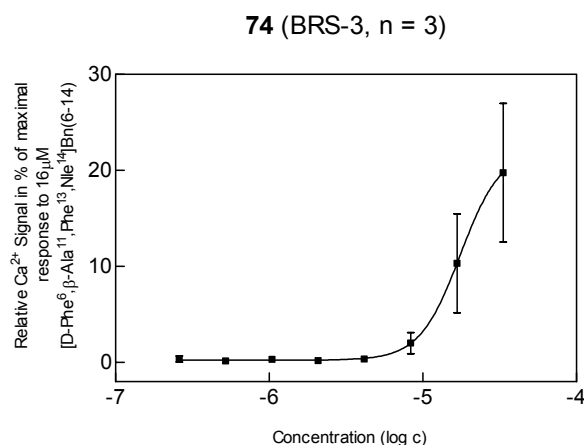


54 (GRP-R, n = 5)

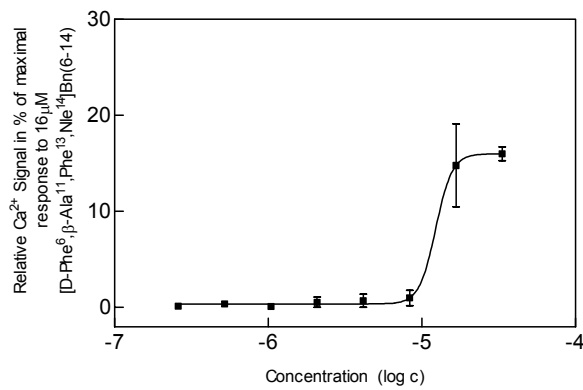


55 (GRP-R, n = 2)



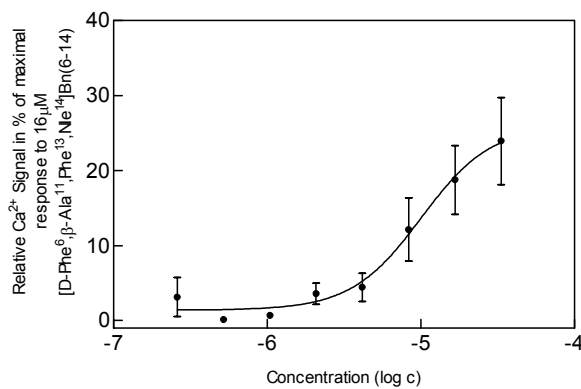
10.12 Disulfide bridged cyclic analogues of [D-Phe⁶,β-Ala¹¹,Phe¹³,Nle¹⁴]Bn(6-14)(1). Dose response curves (BRS-3) of peptides **74-77** and **85-87** (Table 4.8).

87 (BRS-3, n = 2)

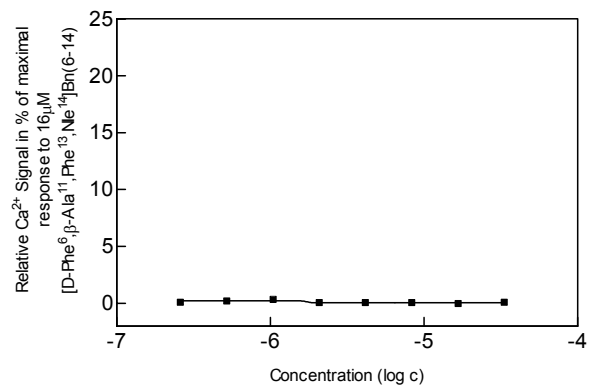


10.13 Tetrapeptide mini-library and analogues in which individual amino acids were substituted. Dose response curves (BRS-3) of peptides 95-107 (Table 4.9).

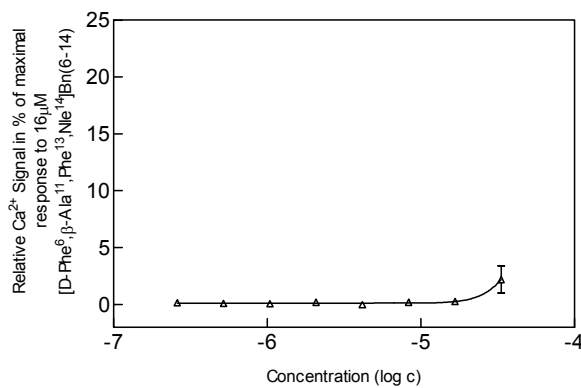
95 (BRS-3, n = 5)



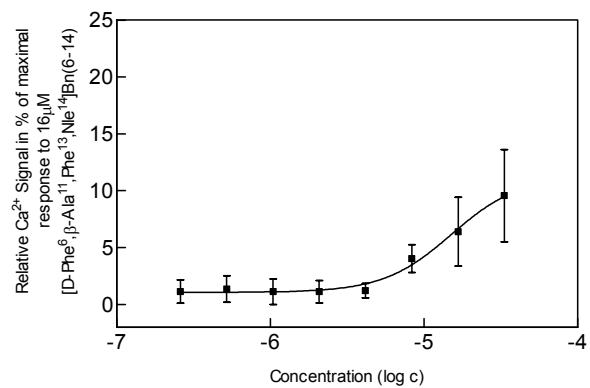
96 (BRS-3, n = 2)



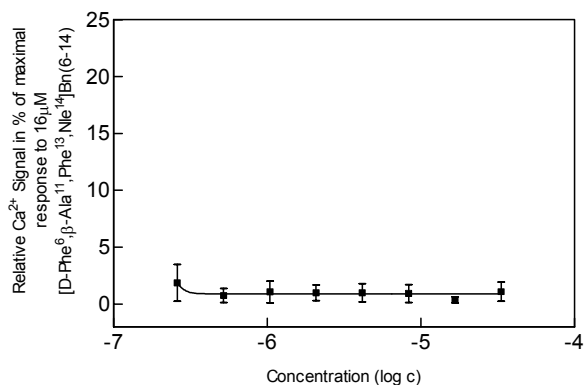
97 (BRS-3, n = 2)



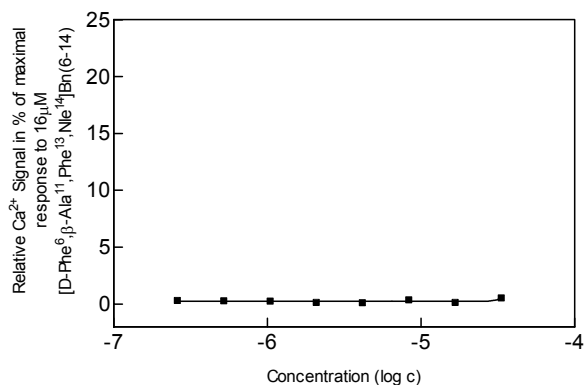
98 (BRS-3, n = 3)



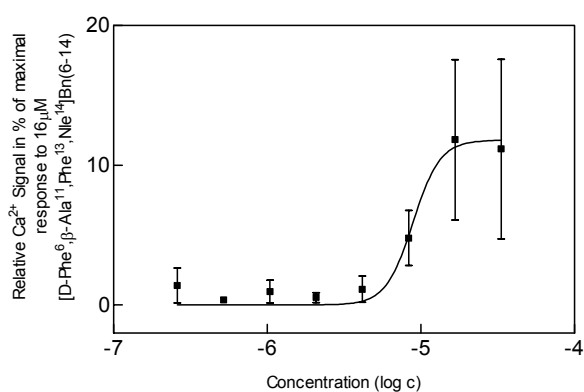
99 (BRS-3, n = 3)



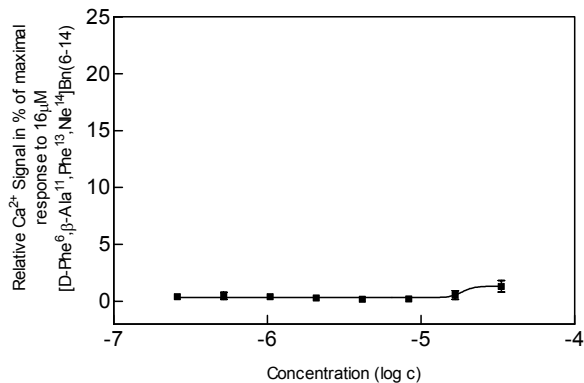
100 (BRS-3, n = 5)



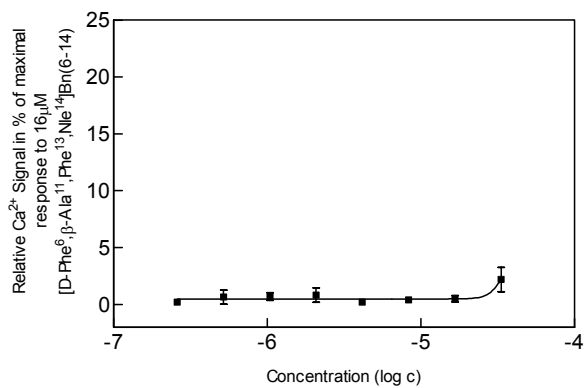
101 (BRS-3, n = 3)



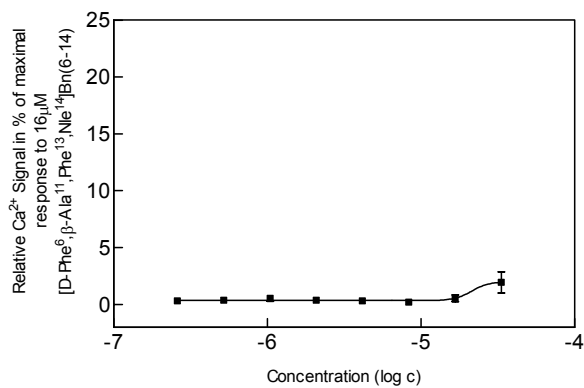
102 (BRS-3, n = 5)



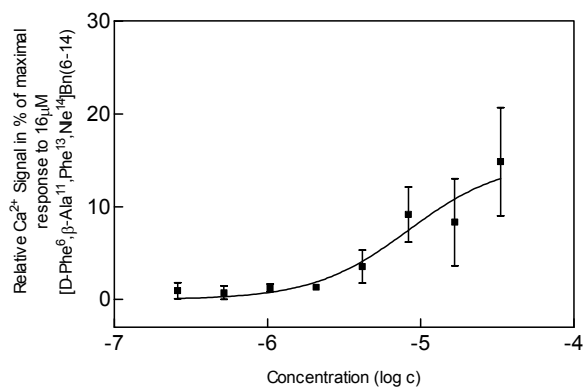
103 (BRS-3, n = 5)



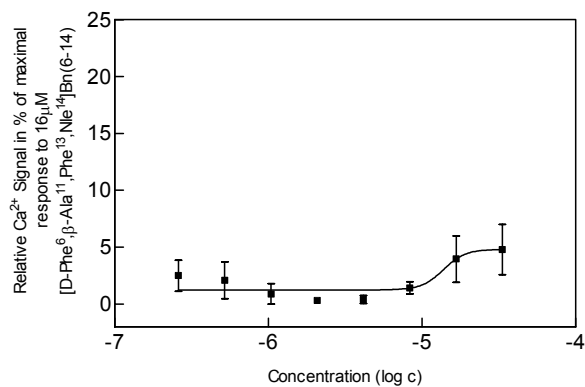
104 (BRS-3, n = 5)



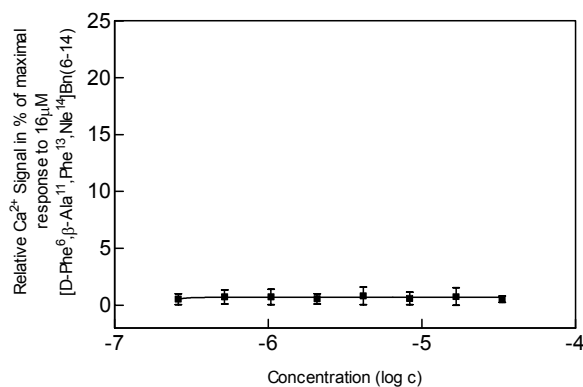
105 (BRS-3, n = 3)



106 (BRS-3, n = 3)

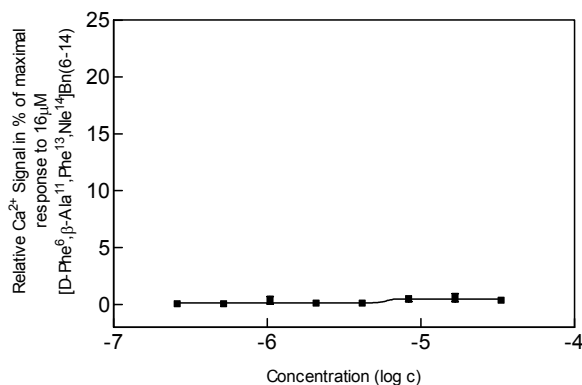


107 (BRS-3, n = 3)

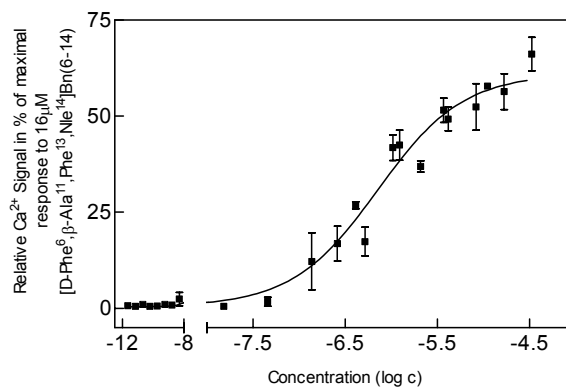


10.14 C-terminally modified analogues of **95**. Dose response curves (BRS-3) of peptides **108-115** (Table 4.10).

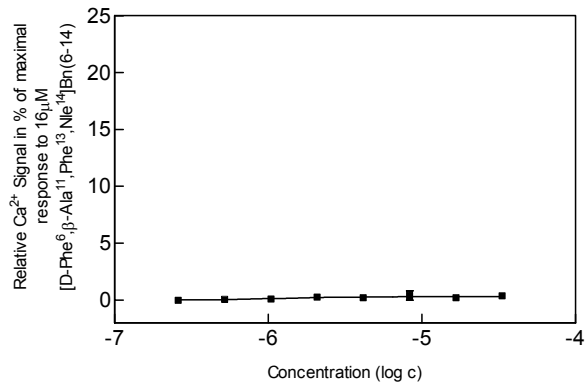
108 (BRS-3, n = 3)



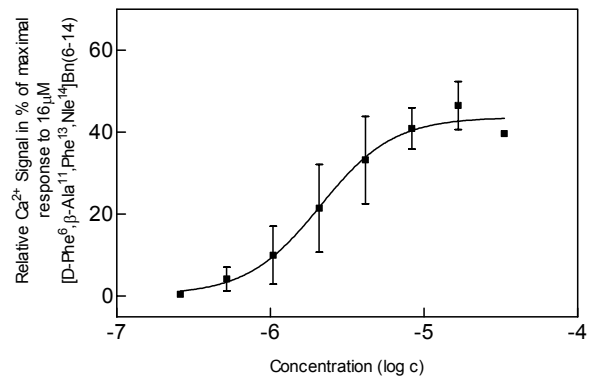
109 (BRS-3, n = 5)



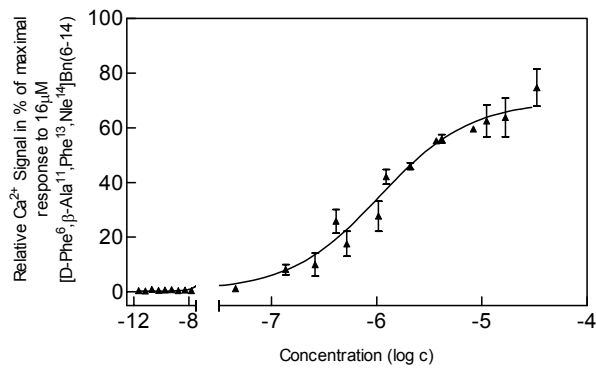
110 (BRS-3, n = 3)



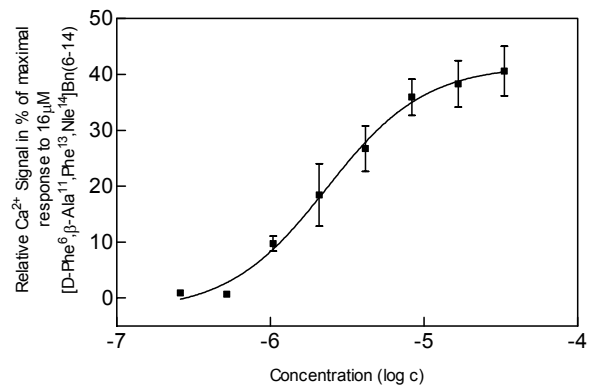
111 (BRS-3, n = 3)



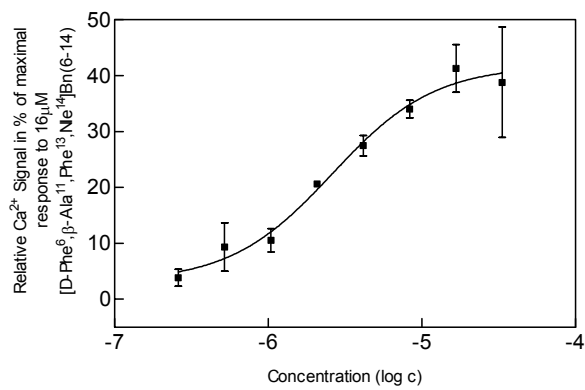
112 (BRS-3, n = 5)



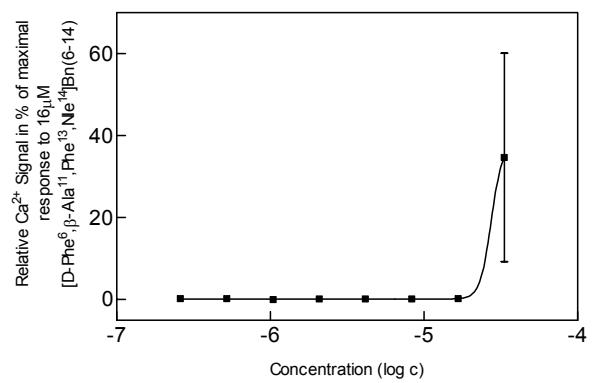
113 (BRS-3, n = 3)



114 (BRS-3, n = 3)

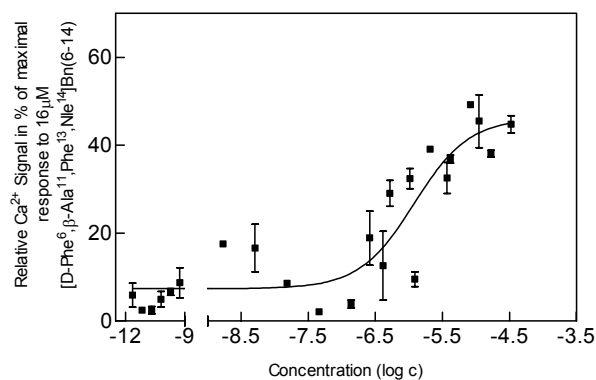


115 (BRS-3, n = 2)

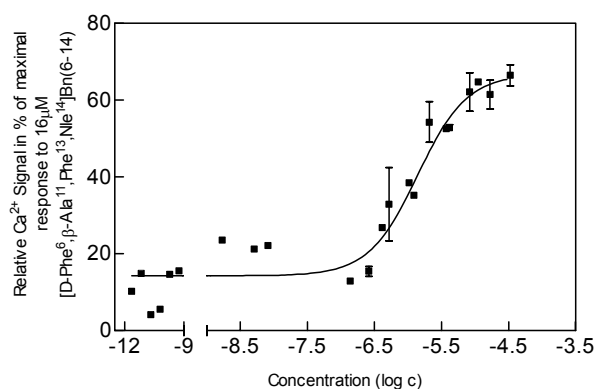


10.15 Analogues of **109** with N-terminally deleted aminofunction and additionally with Gln replaced by Ala. Dose response curves (BRS-3) of compounds **163-174** (Table 4.11).

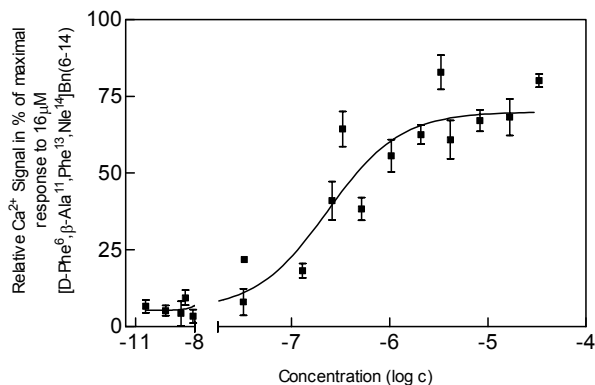
163 (BRS-3, n = 4)



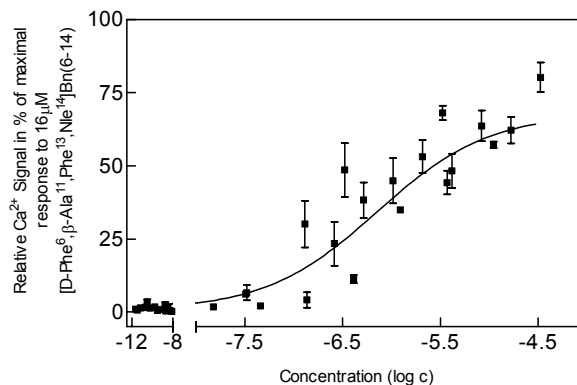
164 (BRS-3, n = 4)



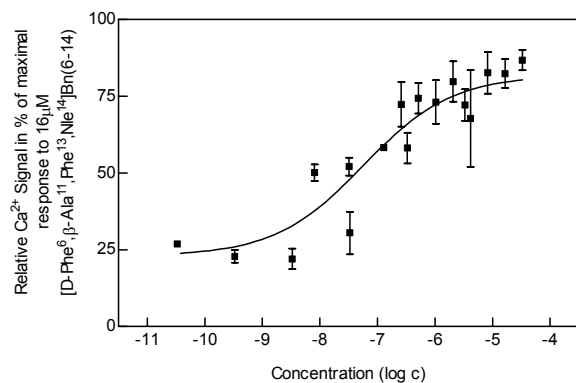
165 (BRS-3, n = 7)



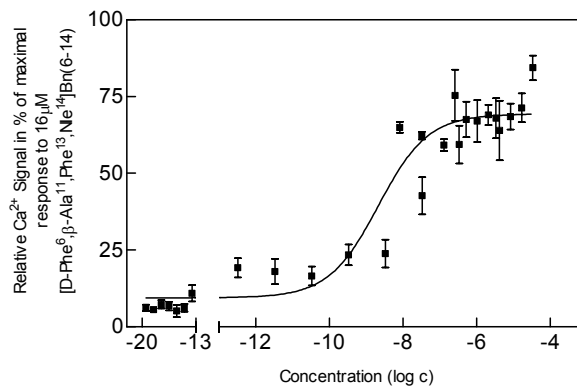
166 (BRS-3, n = 11)



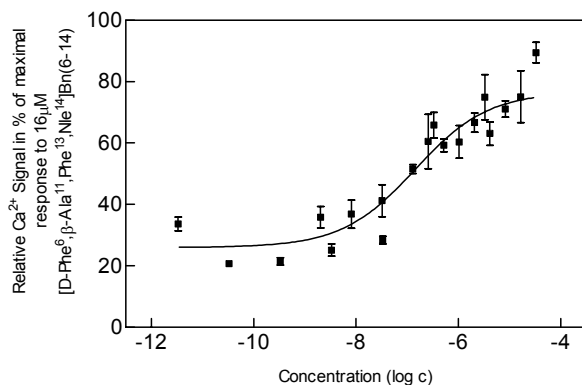
167 (BRS-3, n = 7)



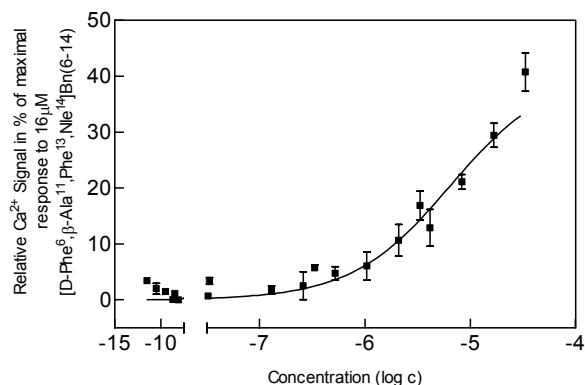
168 (BRS-3, n = 11)



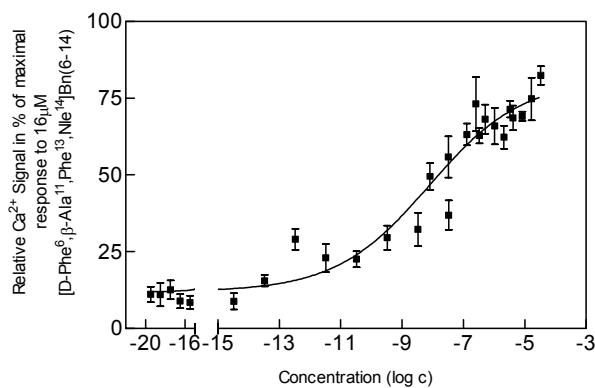
169 (BRS-3, n = 7)



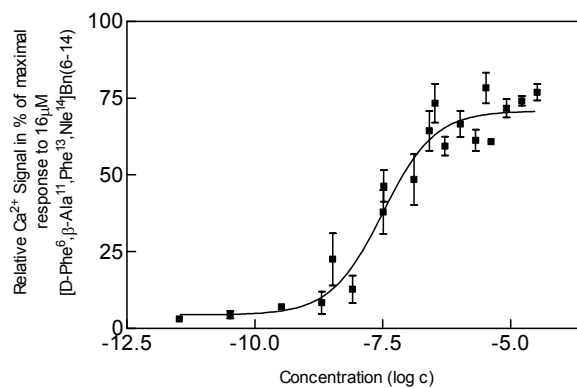
170 (BRS-3, n = 7)



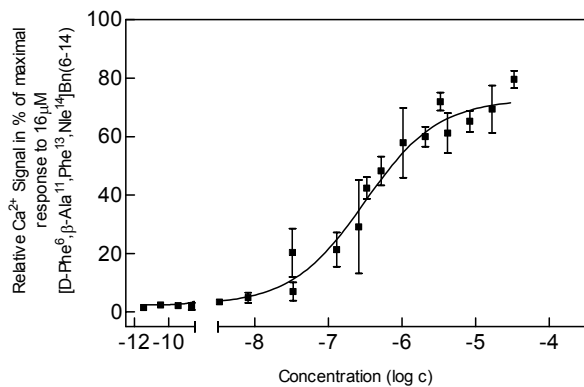
171 (BRS-3, n = 11)



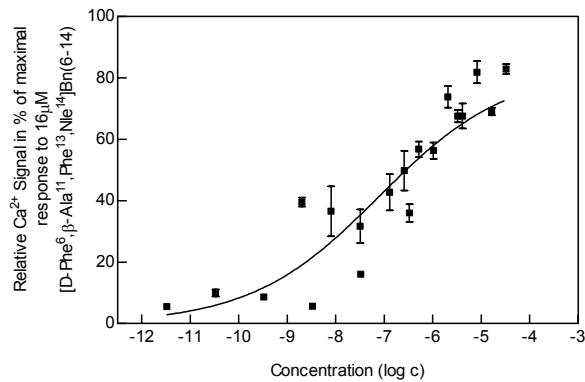
172 (BRS-3, n = 7)



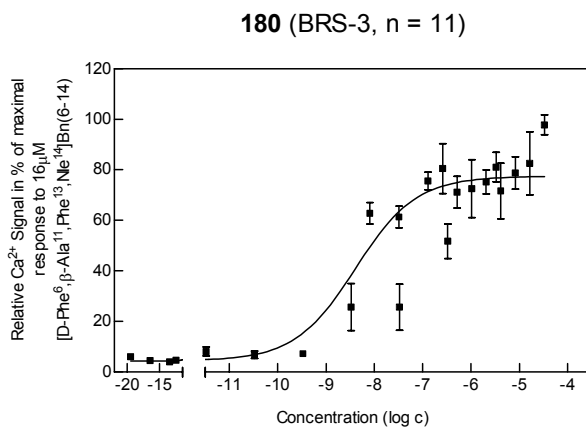
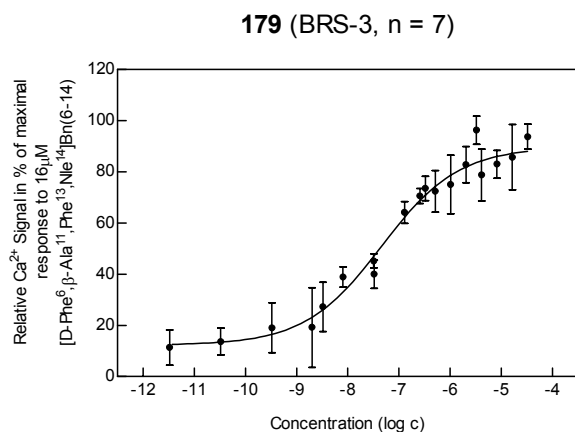
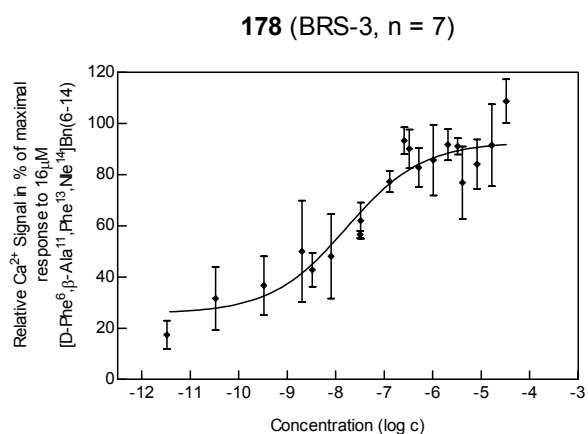
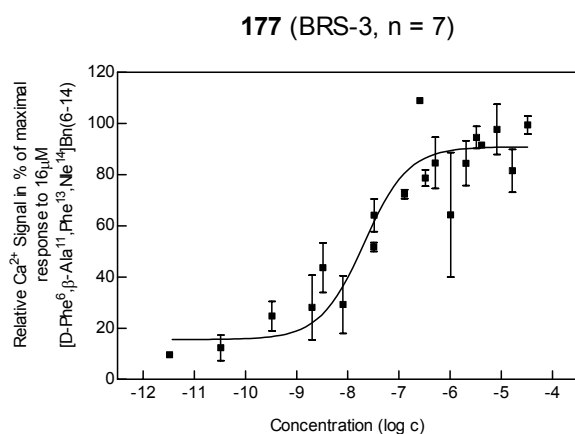
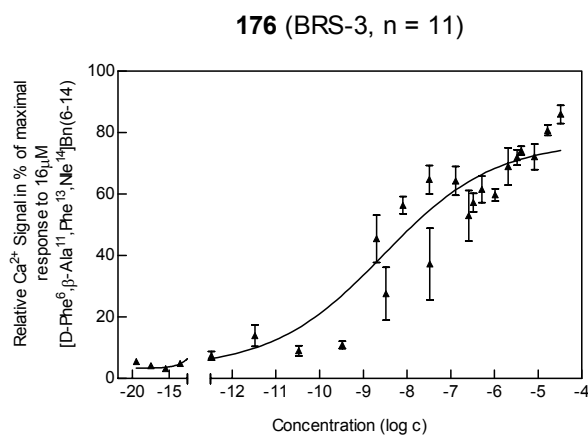
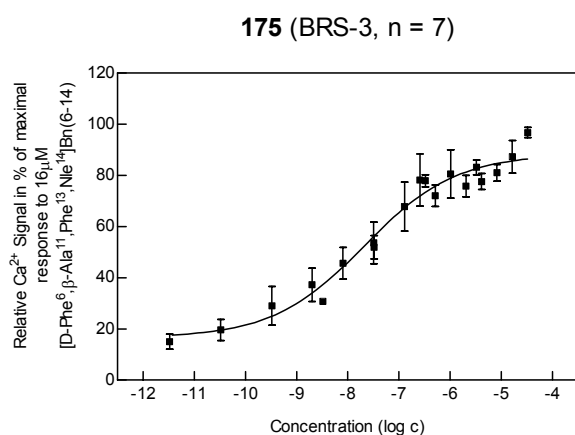
173 (BRS-3, n = 7)

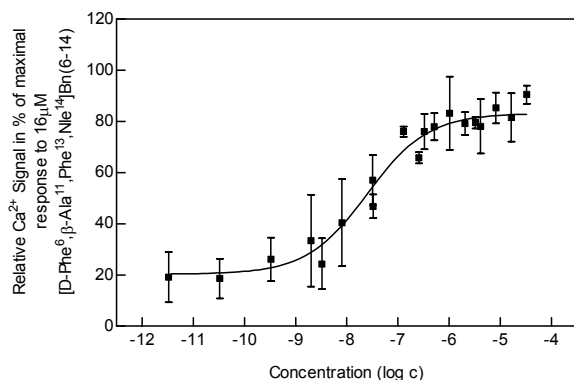
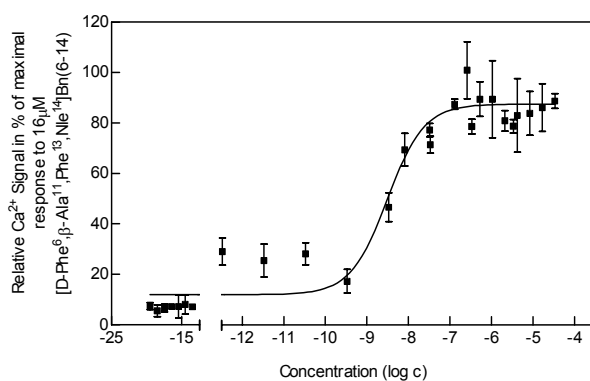
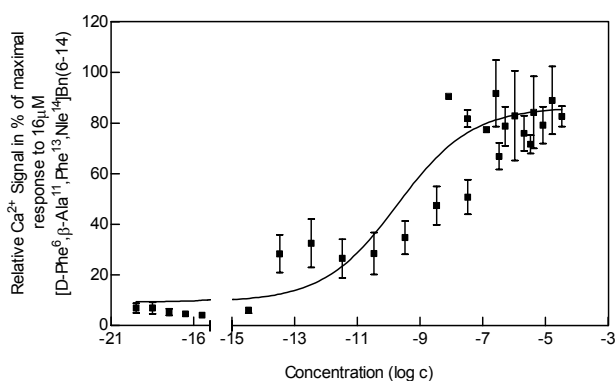
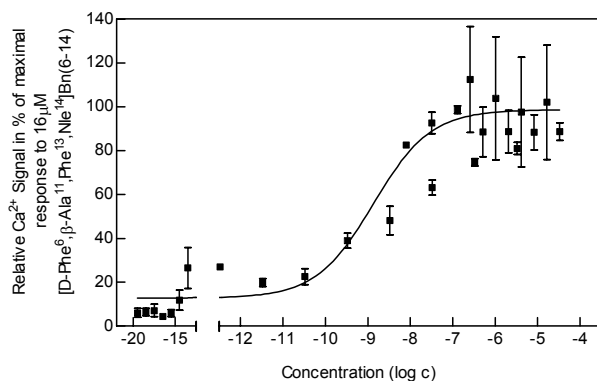
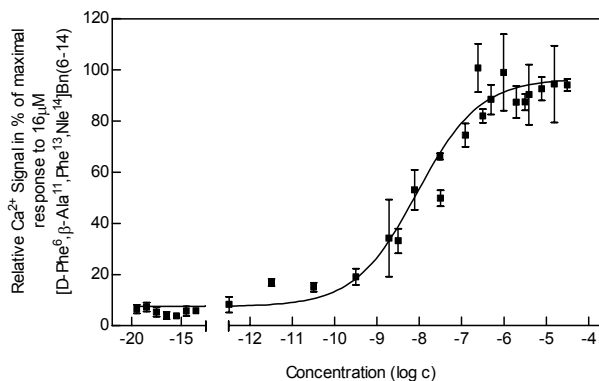


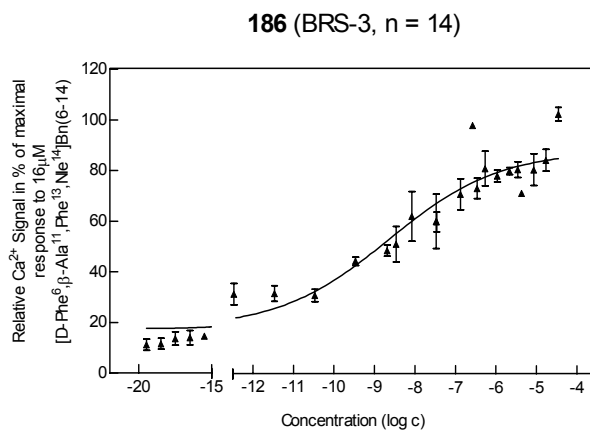
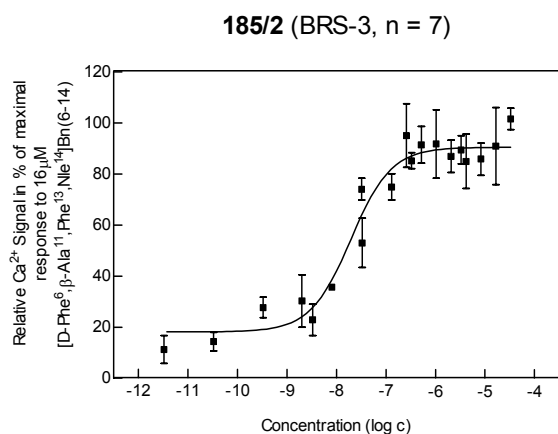
174 (BRS-3, n = 7)



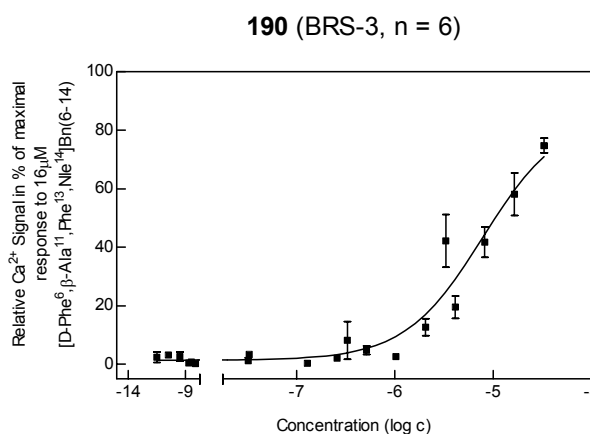
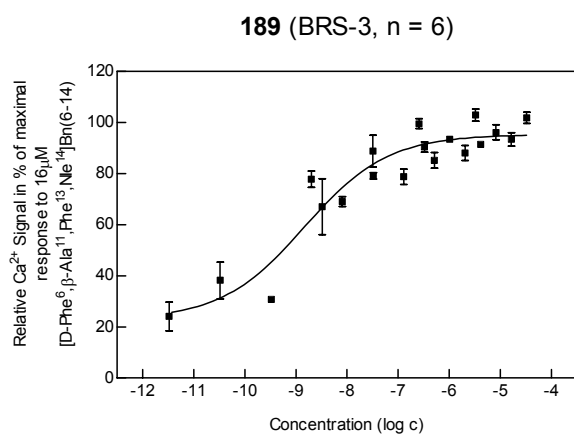
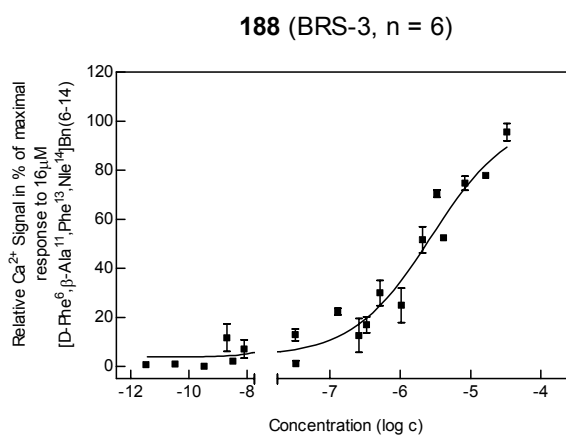
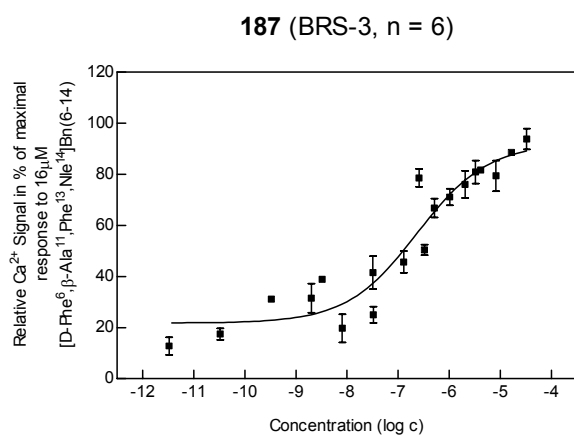
10.16 Analogues of **109** containing peptide monomer building blocks and *N*-arylated 2-aminopropionic acid building blocks. Dose response curves (BRS-3) of compounds **175-181** (Table 4.12).

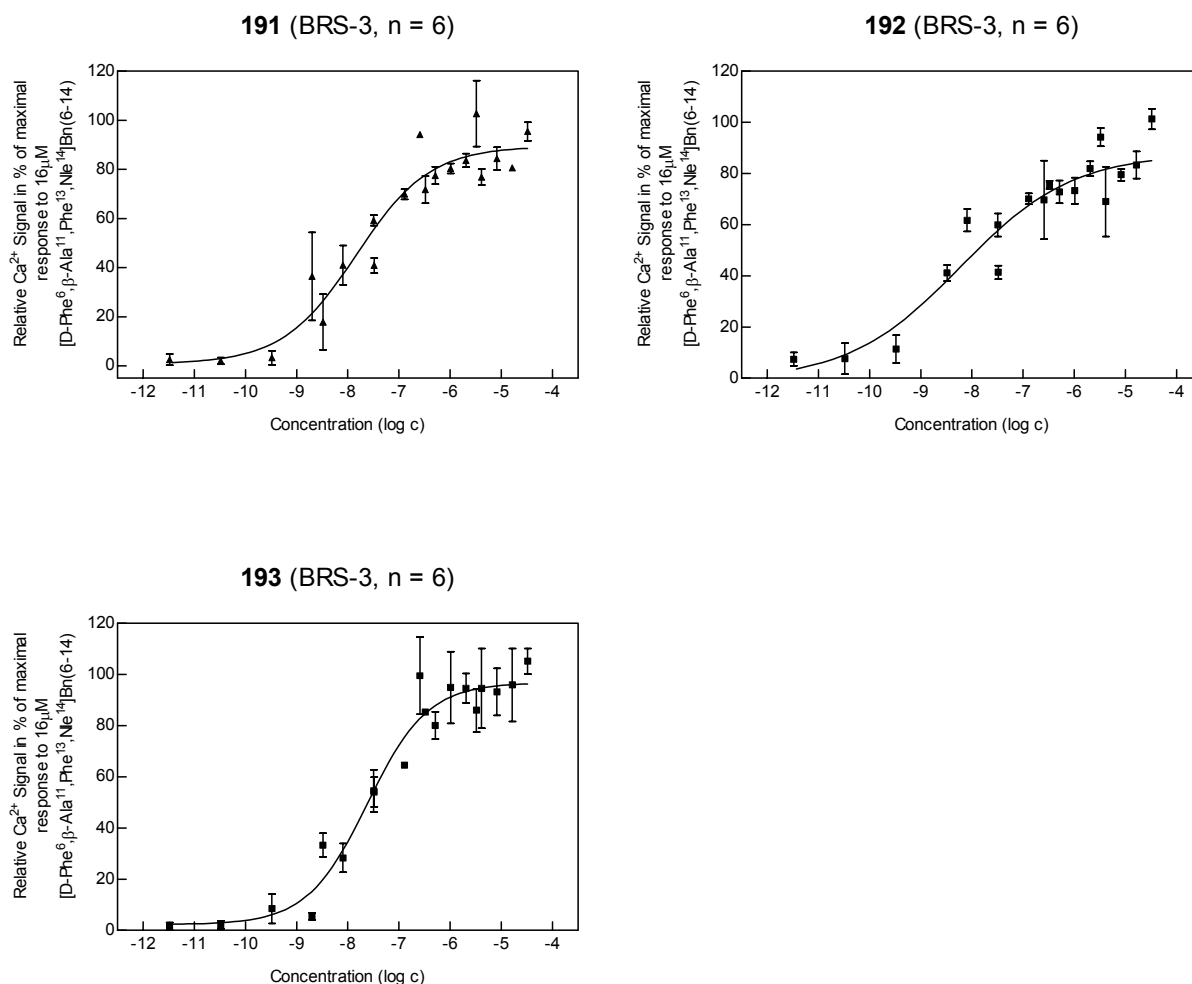
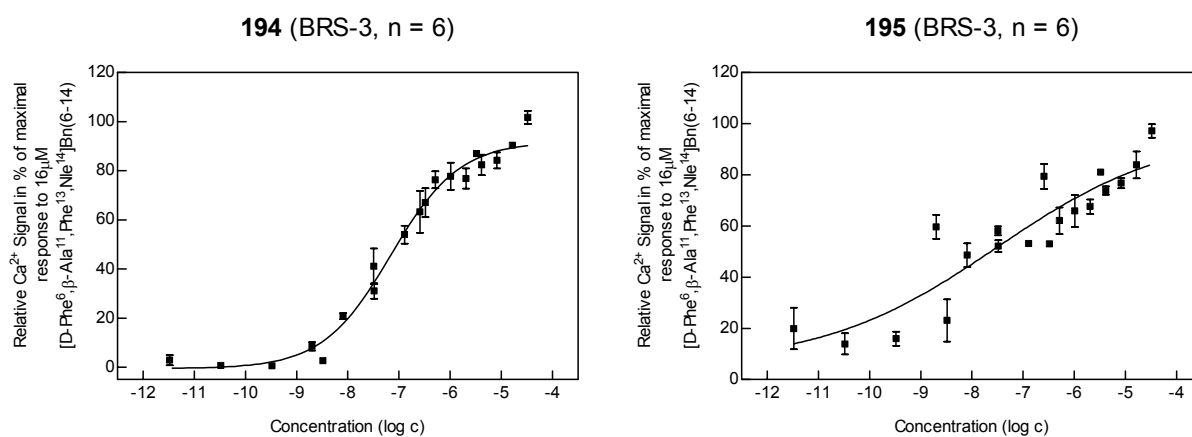


181 (BRS-3, n = 7)**10.17** Dose response curves (BRS-3) of azapeptides **182-185** (Table 4.13).**182** (BRS-3, n = 11)**183** (BRS-3, n = 11)**184** (BRS-3, n = 11)**185/1** (BRS-3, n = 11)

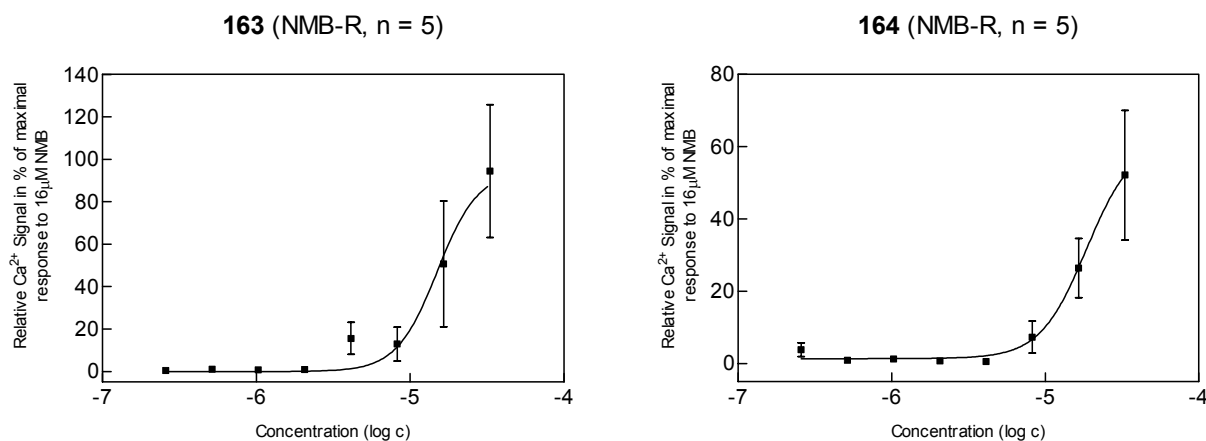


10.18 Dose response curves (BRS-3) of semicarbazones **187-190** (Table 4.14).



10.19 Dose response curves (BRS-3) of semicarbazides **191-193** (Table 4.15).**10.20** Dose response curves (BRS-3) of compounds **194** and **195** (Table 4.16).

10.21 Analogues of **109** with N-terminally deleted aminofunction. Dose response curves (NMB-R) of compounds **163** and **164** (Table 4.11).



10.22 Dose response curves (GRP-R) of tetrapeptide **95** and analogues of **109** with N-terminally deleted aminofunction, compounds **163** and **164** (Tables 4.9 and 4.11).

